frontiers | Research Topics

Innate and adaptive immunity against tuberculosis infection: Diagnostics, vaccines, and therapeutics

Edited by
Zhidong Hu, Lanbo Shi, Jianping Xie and Xiao-Yong Fan

Published in
Frontiers in Immunology

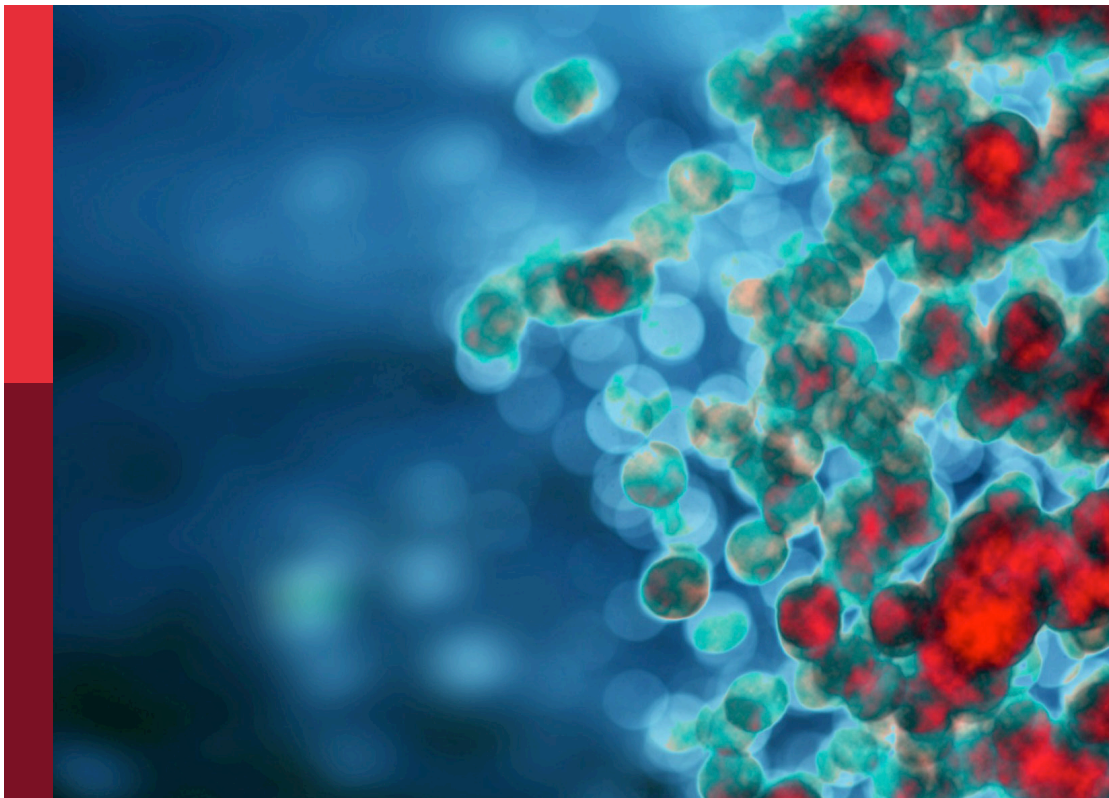

ISSN 1664-8714
ISBN 978-2-8325-4416-7
DOI 10.3389/978-2-8325-4416-7

About Frontiers

Frontiers is more than just an open access publisher of scholarly articles: it is a pioneering approach to the world of academia, radically improving the way scholarly research is managed. The grand vision of Frontiers is a world where all people have an equal opportunity to seek, share and generate knowledge. Frontiers provides immediate and permanent online open access to all its publications, but this alone is not enough to realize our grand goals.

Frontiers journal series

The Frontiers journal series is a multi-tier and interdisciplinary set of open-access, online journals, promising a paradigm shift from the current review, selection and dissemination processes in academic publishing. All Frontiers journals are driven by researchers for researchers; therefore, they constitute a service to the scholarly community. At the same time, the *Frontiers journal series* operates on a revolutionary invention, the tiered publishing system, initially addressing specific communities of scholars, and gradually climbing up to broader public understanding, thus serving the interests of the lay society, too.

Dedication to quality

Each Frontiers article is a landmark of the highest quality, thanks to genuinely collaborative interactions between authors and review editors, who include some of the world's best academicians. Research must be certified by peers before entering a stream of knowledge that may eventually reach the public - and shape society; therefore, Frontiers only applies the most rigorous and unbiased reviews. Frontiers revolutionizes research publishing by freely delivering the most outstanding research, evaluated with no bias from both the academic and social point of view. By applying the most advanced information technologies, Frontiers is catapulting scholarly publishing into a new generation.

What are Frontiers Research Topics?

Frontiers Research Topics are very popular trademarks of the *Frontiers journals series*: they are collections of at least ten articles, all centered on a particular subject. With their unique mix of varied contributions from Original Research to Review Articles, Frontiers Research Topics unify the most influential researchers, the latest key findings and historical advances in a hot research area.

Find out more on how to host your own Frontiers Research Topic or contribute to one as an author by contacting the Frontiers editorial office: frontiersin.org/about/contact

Innate and adaptive immunity against tuberculosis infection: Diagnostics, vaccines, and therapeutics

Topic editors
Zhidong Hu — Fudan University, China
Lanbo Shi — Rutgers University, Newark, United States
Jianping Xie — Southwest University, China
Xiao-Yong Fan — Fudan University, China

Citation
Hu, Z., Shi, L., Xie, J., Fan, X.-Y., eds. (2024). *Innate and adaptive immunity against tuberculosis infection: Diagnostics, vaccines, and therapeutics*. Lausanne: Frontiers Media SA. doi: 10.3389/978-2-8325-4416-7

Table of contents

05 Editorial: Innate and adaptive immunity against tuberculosis infection: diagnostics, vaccines, and therapeutics
Zhidong Hu, Lanbo Shi, Jianping Xie and Xiao-Yong Fan

08 Utility of recombinant fusion protein ESAT6-CFP10 skin test for differential diagnosis of active tuberculosis: A prospective study
Yuan Yuan, Lu Xia, Qiaoyu Wu, Xuhui Liu and Shuihua Lu

16 Single-cell profiling reveals distinct immune response landscapes in tuberculous pleural effusion and non-TPE
Xinting Yang, Jun Yan, Yu Xue, Qing Sun, Yun Zhang, Ru Guo, Chaohong Wang, Xuelian Li, Qingtao Liang, Hangyu Wu, Chong Wang, Xinlei Liao, Sibo Long, Maike Zheng, Rongrong Wei, Haoran Zhang, Yi Liu, Nanying Che, Laurence Don Wai Luu, Junhua Pan, Guirong Wang and Yi Wang

32 Recombinant BCG expressing the LTAK63 adjuvant increased memory T cells and induced long-lasting protection against *Mycobacterium tuberculosis* challenge in mice
Lázaro Moreira Marques-Neto, Monalisa Martins Trentini, Alex Issamu Kanno, Dunia Rodriguez and Luciana Cezar de Cerqueira Leite

43 Outlook for CRISPR-based tuberculosis assays now in their infancy
Zhen Huang, Guoliang Zhang, Christopher J. Lyon, Tony Y. Hu and Shuihua Lu

52 Bridging the gaps to overcome major hurdles in the development of next-generation tuberculosis vaccines
Hongmin Kim, Han-Gyu Choi and Sung Jae Shin

76 Advances in protein subunit vaccines against tuberculosis
Ying Zhang, Jin-chuan Xu, Zhi-dong Hu and Xiao-yong Fan

90 "Spotting" *Mycobacterium bovis* infection in leopards (*Panthera pardus*) – novel application of diagnostic tools
Rachiel Gumbo, Wynand J. Goosen, Peter E. Buss, Lin-Mari de Klerk-Lorist, Konstantin Lyashchenko, Robin M. Warren, Paul D. van Helden, Michele A. Miller and Tanya J. Kerr

100 The functional response of human monocyte-derived macrophages to serum amyloid A and *Mycobacterium tuberculosis* infection
Malwina Kawka, Renata Płocińska, Przemysław Płociński, Jakub Pawełczyk, Marcin Słomka, Justyna Gatkowska, Katarzyna Dzitko, Bożena Dziadek and Jarosław Dziadek

118 Divergent proinflammatory immune responses associated with the differential susceptibility of cattle breeds to tuberculosis
Rishi Kumar, Sripratyusha Gandham, Avi Rana, Hemanta Kumar Maity, Uttam Sarkar and Bappaditya Dey

130 Immunological effects of the PE/PPE family proteins of *Mycobacterium tuberculosis* and related vaccines
Fangzheng Guo, Jing Wei, Yamin Song, Baiqing Li, Zhongqing Qian, Xiaojing Wang, Hongtao Wang and Tao Xu

147 Cargoes of exosomes function as potential biomarkers for *Mycobacterium tuberculosis* infection
Nan Wang, Yongliang Yao, Yingfen Qian, Dewen Qiu, Hui Cao, Huayuan Xiang and Jianjun Wang

160 Alterations of lipid-related genes during anti-tuberculosis treatment: insights into host immune responses and potential transcriptional biomarkers
Nguyen Ky Phat, Nguyen Tran Nam Tien, Nguyen Ky Anh, Nguyen Thi Hai Yen, Yoon Ah Lee, Hoang Kim Tu Trinh, Kieu-Minh Le, Sangzin Ahn, Yong-Soon Cho, Seongoh Park, Dong Hyun Kim, Nguyen Phuoc Long and Jae-Gook Shin

177 Immunogenicity of PE18, PE31, and PPE26 proteins from *Mycobacterium tuberculosis* in humans and mice
María García-Bengoa, Emil Joseph Vergara, Andy C. Tran, Lorenzo Bossi, Andrea M. Cooper, John E. Pearl, Tufária Mussá, Maren von Köckritz-Blickwede, Mahavir Singh and Rajko Reljic

195 Inflammatory immune profiles associated with disease severity in pulmonary tuberculosis patients with moderate to severe clinical TB or anemia
Senait Ashenafi, Marco Giulio Loreti, Amsalu Bekele, Getachew Aseffa, Wondwossen Amogne, Endale Kassa, Getachew Aderaye and Susanna Brighenti

212 Reanalysis and validation of the transcriptional pleural fluid signature in pleural tuberculosis
Raquel da Silva Corrêa, Thyago Leal-Calvo, Thiago Thomaz Mafort, Ana Paula Santos, Janaína Leung, Roberta Olmo Pinheiro, Rogério Rufino, Milton Ozório Moraes and Luciana Silva Rodrigues

frontiers | Frontiers in Immunology

TYPE Editorial
PUBLISHED 23 January 2024
DOI 10.3389/fimmu.2024.1366976

OPEN ACCESS

EDITED AND REVIEWED BY
Ian Marriott,
University of North Carolina at Charlotte,
United States

*CORRESPONDENCE
Zhidong Hu
huzhidong@fudan.edu.cn
Xiao-Yong Fan
xyfan008@fudan.edu.cn

RECEIVED 08 January 2024
ACCEPTED 16 January 2024
PUBLISHED 23 January 2024

CITATION
Hu Z, Shi L, Xie J and Fan X-Y (2024) Editorial: Innate and adaptive immunity against tuberculosis infection: diagnostics, vaccines, and therapeutics.
Front. Immunol. 15:1366976.
doi: 10.3389/fimmu.2024.1366976

Editorial: Innate and adaptive immunity against tuberculosis infection: diagnostics, vaccines, and therapeutics

Zhidong Hu[1]*, Lanbo Shi[2], Jianping Xie[3] and Xiao-Yong Fan[1]*

[1]Shanghai Public Health Clinical Center & Shanghai Institute of Infectious Disease and Biosecurity, Fudan University, Shanghai, China, [2]Public Health Research Institute, New Jersey Medical School, Rutgers Biomedical and Health Sciences, Rutgers, The State University of New Jersey, Newark, NJ, United States, [3]Chongqing Municipal Key Laboratory of Karst Environment, School of Life Sciences, Southwest University, Chongqing, China

KEYWORDS

tuberculosis, innate immunity, adaptive immunity, diagnostics, therapeutics, vaccines

Editorial on the Research Topic

Innate and adaptive immunity against tuberculosis infection: diagnostics, vaccines, and therapeutics

Tuberculosis (TB) remains one of the major causes of infectious disease mortality to this day. According to the latest "Global Tuberculosis Report" released by WHO, there were 10.6 million new cases and 1.3 million deaths in 2022 (1). Thus, TB remains the world's most lethal infectious disease, only being surpassed by COVID-19 during the 2019-2021 pandemic.

TB is caused by the acid-fast bacillus *Mycobacterium tuberculosis* (*Mtb*), which was identified by Robert Koch in 1882. One of the fundamental pillars to reduce the spread of *Mtb* infection is accurate and rapid diagnostics. The current TB diagnostics include culture, smear, GeneXpert MTB/RIF (Xpert), interferon-gamma release assays (IGRAs), imaging examination, etc. However, the traditional detection of growth in bacterial cultures is time-consuming; the sensitivity of acid-fast staining-based smear diagnostic is low; Xpert is expensive and impractical for widespread clinical use in developing countries although it is rapid and sensitive; IGRAs cannot distinguish between asymptomatic latent TB infection and active TB disease; and the specificity of imaging examination is low (2–4). Thus, the diagnosis of TB remains challenging. In this editorial, firstly, we introduce a Research Topic that include a number of studies that investigated novel diagnostic methods in the diagnosis of TB and several review papers that focused on different topics and indicated directions for future research.

The antigens ESAT-6/CFP10 (EC), which are *Mtb*-specific proteins and are absent in BCG strains, have been widely used as *Mtb*-specific stimulators in IGRA diagnosis. In a prospective cohort study, Yuan et al. enrolled 357 patients to evaluate the sensitivity and specificity of this EC skin test, which was performed by intradermal injection of recombinant EC proteins. Their data showed that the sensitivity and specificity of the EC skin test for patients were 71.52% and 65.45%, based on the clinical reference standards. Phat et al. investigated the expression of lipid-related genes during anti-TB chemotherapy through a targeted and knowledge-based approach, to evaluate the potential use of lipid-

related genes as prognostic biomarkers of treatment responses. Their data showed that transcriptomic signatures of lipid-related genes were associated with the immune responses, and might be useful for treatment prognosis and TB diagnosis. Ashenafi et al. explored the peripheral inflammatory immune profiles of different TB patient sub-groups based on disease severity, anemia, and radiological performance of lung diseases. The Bio-Plex Magpix multiplex assays were used to detect cytokines in plasma and cell culture supernatants from whole blood stimulation with the EC antigens that were used in the IGRA assay. Their data suggest that inflammatory immune profiles were related to the clinical disease severity, and the top-ranked inflammatory mediators might be used as biomarkers of TB disease severity and treatment monitoring.

Gumbo et al. evaluated the performance of currently available immunological assays, including QFT, tuberculin skin test (TST), and Xpert Ultra, on detecting *M. bovis* infection in leopards (*Panthera pardus*), an African big cat population. Their preliminary results showed that TST might be a suitable tool to identify *M. bovis*-infected leopards, and the Xpert Ultra provided rapid detection of infected leopards. Corrêa et al. selected a set of candidate genes previously described to be associated with pulmonary TB and evaluated their transcriptional signatures in clinical samples from a Brazilian cohort of pleural TB patients. As a result, three genes (*CARD17*, *GBP2*, and *C1QB*) showed promise in discriminating pleural TB from other causes of exudative pleural effusion.

Wang et al. summarized the current studies demonstrating the functions of exosomes, including miRNA, circRNA, and protein, in *Mtb* infection, and discussed the potential values of exosomes as biomarkers to be used in TB diagnosis and treatment monitoring. The potential usage of exosomes in blood-based diagnostics of TB is anticipated but will need to be optimized in future studies. Another review written by Huang et al. systematically reviewed the development and clinical evaluation of proposed CRISPR-based technology in TB diagnostics, and they gave constructive suggestions on improving sample pretreatment, method development, and clinical validation of the current assays to enhance their development and translation. The booming development of CRISPR-based technology has the potential to overcome the weaknesses of current TB diagnostics and simplify sample collection by using blood or fecal specimens to give accurate results.

As the only licensed TB vaccine, immunization of *M. bovis* Bacille Calmette-Guérin (BCG) in infancy offers protection against the aggressive childhood forms of the disease including meningeal and miliary TB (5). However, its protective efficacy against TB diseases ranges from 0% to 80% in adolescents and adults (6), leading to increased morbidity among these populations (7). Thus, the lack of an optimal TB vaccine is believed to be one of the crucial barriers to global TB control, and a more effective TB vaccine is required, particularly in adolescents and adults (8). In this editorial, secondly, we summarized several studies/reviews that investigated/summarized next-generation vaccine design against TB, which aims to accelerate TB vaccine research.

Kim et al. systematically described five hurdles they think should be overcome to develop more effective TB vaccines, and then discussed the current knowledge gaps between preclinical and clinical studies regarding peripheral versus tissue-resident immune responses, different individual conditions, and correlates of protection (COP) findings. Finally, they proposed that the recent discoveries on TB risk/susceptibility-related factors could be utilized as novel biomarkers or COP, for better evaluating/predicting vaccine-induced protection against *Mtb* infection, which will facilitate the novel TB vaccine development process. Zhang et al. summarized recent progress in subunit protein vaccines against TB research. The development of bioinformatics and structural biology techniques has greatly facilitated the screening and optimization of protective *Mtb* antigens during the past decades, and the design of multistage subunit vaccines containing multiple antigens in different growth stages of *Mtb* will somewhat overcome the shorting comings of limited antigen numbers in subunit vaccines.

The development of novel adjuvants will further improve the immunogenicity of subunit vaccines. The family of proteins Pro-Glu motif-containing (PE) and Pro-Pro-Glu motif-containing (PPE) account for as much as 10% of the genome of *Mtb*, which has been found to play crucial roles in pathogenesis and persistent infection. Guo et al. reviewed the immunological regulation effects of PE/PPE proteins and the development of PE/PPE family proteins-based novel TB vaccines, including protein-based, virus vector-based, and recombinant BCG vaccines. The current studies suggest that the PE/PPE family of proteins is a highly active and promising recent area research of for TB vaccines. García-Bengoa et al. explored the immunogenicity and protection efficacy against *Mtb* infection of three PE/PPE proteins, PE18, PE31, and PPE26. As a result, all three proteins are immunoreactive in TB patients, IGRA-positive latent infected close contacts, and BCG-vaccinated healthy controls. The three antigens also induced antigen-specific T-cell immune responses and antibody responses in PBMCs and bronchoalveolar lavage in murine models. However, these antigens did not show protection in a low-dose murine aerosol *Mtb* infection model. Marques-Neto et al. evaluated a recombinant BCG vaccine encoding LTAK63 (an adjuvant that genetically detoxified a derivative of the subunit A from *E. coli* heat-labile toxin) in murine models. Their data showed that this novel vaccine induced robust and long-term Th1/Th17 T-cell immune response in the draining lymph nodes and the lungs, which was responsible for the increased protection post-*Mtb* infection six months after immunization.

As an intracellular bacterium, *Mtb* colonizes inside cells, thus, the host inflammatory and adaptive cellular immune responses, as well as the basic cellular physiologic mechanisms play important roles in the establishment of *Mtb* infection and progression of TB diseases (9, 10). In this editorial, thirdly, we summarized several studies that focus on deciphering host immune profiles against *Mtb* infection which might facilitate the anti-TB host-directed therapeutics research.

Tuberculous pleural effusion (TPE) is characterized by an influx of immune cells to the pleural space and was regarded as an appropriate platform for dissecting complex tissue responses against *Mtb* infection. Yang et al. employed a single-cell RNA

sequencing study using ten pleural fluid samples from six patients with TPE and four without TPE including two from patients with transudative pleural effusion and two from patients with malignant pleural effusion, and a distinct local immune response was observed. During the process of *Mtb* infection, the levels of major acute phase protein serum amyloid A (SAA), increase up to 100-fold in the pleural fluids. However, the stimulating effects of SAA on macrophages that have not yet been in contact with mycobacteria have not been discovered yet. Kawka et al. evaluated the functional responses of human monocyte-derived macrophages under elevated SAA conditions using RNA-seq assays. Their data suggest that the presence of SAA during *Mtb* infection elevates the innate (MHC-I engagement of natural killer cells) and adaptive (MHC-I through peptides presented to cytotoxic T cells and MHC-II) immune responses induced by macrophages. Kumar et al. found that the incidence of bovine TB reactors is higher in crossbred than indigenous cattle in India, which was associated with several innate immunological factors. Their data provided a reason for adopting an appropriate crossbreeding policy that balances production and disease-resistance traits for sustainable livestock farming.

Taken together, these manuscripts published within this Research Topic provide novel information on the innate and adaptive immunity against TB infection. With more advanced knowledge, we are hopeful that more accurate diagnostics and more effective vaccines/therapeutics against *Mtb* infection will be achieved in the near future.

Author contributions

ZH: Conceptualization, Writing – original draft, Writing – review & editing. LS: Conceptualization, Writing – review & editing. JX: Conceptualization, Writing – review & editing. X-YF: Conceptualization, Writing – review & editing.

Funding

The author(s) declare financial support was received for the research, authorship, and/or publication of this article. National Natural and Science Foundation of China (82171739, 82171815, 32394014), National Key Research and Development Program of China (2021YFC2301503, 2022YFC2302900), and Shanghai Municipal Health Bureau (2022XD060).

Acknowledgments

We are thankful to the authors who submitted their articles to support this Research Topic.

Conflict of interest

The authors declare that the research was conducted in the absence of any commercial or financial relationships that could be construed as a potential conflict of interest.

The author(s) declared that they were an editorial board member of Frontiers, at the time of submission. This had no impact on the peer review process and the final decision.

Publisher's note

References

1. WHO. *World health organization global tuberculosis report*. (2023). World Health Organization. Available at: https://www.who.int/publications/i/item/9789240083851

2. Kontsevaya I, Cabibbe AM, Cirillo DM, DiNardo AR, Frahm N, Gillespie SH, et al. Update on the diagnosis of tuberculosis. *Clin Microbiol Infect* (2023) S1198-743X(23):00340-3.

3. Palanivel J, Sounderrajan V, Thangam T, Rao SS, Harshavardhan S, Parthasarathy K. Latent tuberculosis: challenges in diagnosis and treatment, perspectives, and the crucial role of biomarkers. *Curr Microbiol* (2023) 80(12):392.

4. Graciaa DS, Schechter MC, Fetalvero KB, Cranmer LM, Kempker RR, Castro KG. Updated considerations in the diagnosis and management of tuberculosis infection and disease: integrating the latest evidence-based strategies. *Expert Rev Anti Infect Ther* (2023) 21(6):595–616.

5. Trunz BB, Fine P, Dye C. Effect of BCG vaccination on childhood tuberculous meningitis and miliary tuberculosis worldwide: a meta-analysis and assessment of cost-effectiveness. *Lancet* (2006) 367(9517):1173–80.

6. Mangtani P, Abubakar I, Ariti C, Beynon R, Pimpin L, Fine PE, et al. et al: Protection by BCG vaccine against tuberculosis: a systematic review of randomized controlled trials. *Clin Infect Dis* (2014) 58(4):470–80.

7. Andersen P, Doherty TM. The success and failure of BCG - implications for a novel tuberculosis vaccine. *Nat Rev Microbiol* (2005) 3 (8):656–62.

8. Hu Z, Lu SH, Lowrie DB, Fan XY. Research advances for virus-vectored tuberculosis vaccines and latest findings on tuberculosis vaccine development. *Front Immunol* (2022) 13:895020.

9. Chandra P, Grigsby SJ, Philips JA. Immune evasion and provocation by Mycobacterium tuberculosis. *Nat Rev Microbiol* (2022) 20(12):750–66.

10. Flynn JL, Chan J. Immune cell interactions in tuberculosis. *Cell* (2022) 185 (25):4682–702.

frontiers | Frontiers in Immunology

TYPE Original Research
PUBLISHED 25 April 2023
DOI 10.3389/fimmu.2023.1162177

OPEN ACCESS

EDITED BY
Jianping Xie,
Southwest University, China

REVIEWED BY
Wei Sha,
Tongji University School of Medicine, China
Yu Pang,
Beijing Chest Hospital, Capital Medical University, China

*CORRESPONDENCE
Xuhui Liu
liuxuhui666@126.com
Shuihua Lu
lushuihua66@126.com

†These authors have contributed equally to this work

SPECIALTY SECTION
This article was submitted to Microbial Immunology, a section of the journal Frontiers in Immunology

RECEIVED 09 February 2023
ACCEPTED 29 March 2023
PUBLISHED 25 April 2023

CITATION
Yuan Y, Xia L, Wu Q, Liu X and Lu S (2023) Utility of recombinant fusion protein ESAT6-CFP10 skin test for differential diagnosis of active tuberculosis: A prospective study.
Front. Immunol. 14:1162177.
doi: 10.3389/fimmu.2023.1162177

Utility of recombinant fusion protein ESAT6-CFP10 skin test for differential diagnosis of active tuberculosis: A prospective study

Yuan Yuan[1†], Lu Xia[2†], Qiaoyu Wu[3†], Xuhui Liu[2*] and Shuihua Lu[2*]

[1]Shanghai Public Health Clinical Center, Fudan University, Shanghai, China, [2]National Clinical Research Center for Infectious Diseases, The Third People's Hospital of Shenzhen, The Second Affiliated Hospital of Southern University of Science and Technology, Shenzhen, Guangdong, China, [3]Bengbu Medical College, School of Life Science, Bengbu, Anhui, China

Background: The recombinant mycobacterium tuberculosis fusion protein ESAT6-CFP10 skin test (ECST) is a novel test for tuberculosis (TB) infection; however, its accuracy in active tuberculosis (ATB) remains uncertain. This study aimed to evaluate the accuracy of ECST in the differential diagnosis of ATB for an early real-world assessment.

Methods: This prospective cohort study recruited patients suspected of ATB in Shanghai Public Health Clinical Center from January 2021 to November 2021. The diagnostic accuracy of the ECST was evaluated under the gold standard and composite clinical reference standard (CCRS) separately. The sensitivity, specificity, and corresponding confidence interval of ECST results were calculated, and subgroup analyses were conducted.

Results: Diagnostic accuracy was analyzed using data from 357 patients. Based on the gold standard, the sensitivity and specificity of the ECST for patients were 72.69% (95%CI 66.8%-78.5%) and 46.15% (95%CI 37.5%-54.8%), respectively. Based on the CCRS, the sensitivity and specificity of the ECST for patients were 71.52% (95%CI 66.4%-76.6%) and 65.45% (95%CI 52.5%-78.4%), respectively. The consistency between the ECST and the interferon-γ release (IGRA) test is moderate (Kappa = 0.47).

Conclusion: The ECST is a suboptimum tool for the differential diagnosis of active tuberculosis. Its performance is similar to IGRA, an adjunctive diagnostic test for diagnosing active tuberculosis.

Clinical trial registration: http://www.chictr.org.cn, identifier ChiCTR20000 36369.

KEYWORDS

tuberculosis, ESAT6-CFP10 skin test, IGRA, diagnostic accuracy, coherence

1 Introduction

In 2021, ~10.6 million people worldwide were newly infected with tuberculosis (TB), whereas the number of newly diagnosed TB was only 6.4 million (1). To achieve the World Health Organization's goal of ending TB by 2035, it is essential to screen and diagnose TB. Until now, the detection methods for diagnosing TB are limited. Tuberculin skin test (TST) and interferon-γrelease (IGRA) test are the main methods for screening TB; TST has poor specificity and IGRA is expensive and requires specialized laboratory conditions. Therefore, a new diagnostic method with high specificity and low cost is urgently needed.

Recombinant *Mycobacterium tuberculosis* fusion protein ESAT6-CFP10 (EC) skin test was made from the recombinant *Mycobacterium tuberculosis* fusion protein obtained by *Escherichiacoli* after fermentation, isolation, and purification (2, 3). Compared with the IGRA test, the ESAT6-CFP10 skin test (ECST) is performed by intradermal injection of recombinant ESAT6-CFP10 antigen. The EC test solves the false-positive problem after BCG vaccination and combined the advantages of the TST and the high specificity of IGRA detection. At present, EC (trade name: YiKa) has obtained the national first-class new drug and completed clinical trials on April 23, 2021.

The sensitivity, specificity, and safety of diagnostic reagents are concerns in clinical diagnosis. The sensitivity, specificity, and safety of ECST were evaluated by phase I, II, and III clinical trials before marketing. However, phase III clinical trial participants were strictly screened and did not include those with underlying diseases and comorbidities. Owing to the lack of ECST results in TB patients with comorbidities, this study aimed to evaluate the accuracy and safety of the ECST in tertiary hospitals to assess its value in the diagnosis of ATB and provide data support for the subsequent large-scale post marketing re-evaluation.

2 Methods

2.1 Study design and participants

A prospective cohort study was conducted in Shanghai Public Health Clinical Center from January 2021 to November 2021. All participants suspected pulmonary TB (PTB) were consecutively recruited from inpatient services. Including routine laboratory examinations, each participant would receive IGRA (T-SPOT.TB. Oxford, UK.) and ECST. The results were compared by statistical analysis. The primary outcome of this study was a comparison of the diagnostic accuracy of ECST and T-SPOT.TB assays for active TB. The secondary outcomes included the consistency between the two assays, the diagnostic yields in different subgroups, and the safety of ECST.

2.2 Study procedure

From January to November 2021, the accuracy of the ECST was evaluated in the Tuberculosis Department of Shanghai Public Health Clinical Center. All participants underwent an IGRA test and then an ECST (Figure 1). The transverse and longitudinal diameters of skin erythema and/or induration at the injection site were measured in millimeters at different time points. Skin erythema was defined as visible red discoloration of the skin at the injection site, and induration was measured by palpation of the forearm. Systemic and local adverse events were recorded within 72 h of injection. Systemic and local adverse events, such as rash, pain, and itching, and adverse reactions such as anaphylactic shock, local tissue ulcer, local necrosis and liquefaction, systemic allergic rash, systemic urticaria, and allergic purpura, were observed and recorded. An adverse event was defined as any adverse event in a patient who underwent the ECST.

2.3 Statistical analysis

ECST results were expressed as the number of millimeters of the transverse and longitudinal diameters of erythema or induration at the forearm injection site at 48–72 h after the ECST injection. The results were based on the redness or induration, and the average diameter of the reaction (sum of the horizontal and vertical diameters divided by 2) was not less than 5 mm. Those with blisters, necrosis, and lymphangitis were strongly positive.

IBM SPSS Statistics version 26.0 (IBM Corp., Armonk, NY, USA) was used as a statistical tool. The clinical diagnosis results and bacteriological results were taken as reference standards to calculate the sensitivity and specificity of the EC reagent and IGRA detection, draw the ROC curve, and assess the consistency between the ECST and the IGRA test. The chi-square test was used to compare categorical variables, and the t-test was used to analyze continuous variables. 95% Confidence intervals were calculated based on bilateral distribution. All statistical tests were two-tailed, with $P < 0.05$ as the significant difference.

2.4 Case definitions and inclusion/exclusion criteria

Active PTB patients were diagnosed in concordance with the diagnostic standard by the National Health Commission of the People's Republic of China (4), The following criteria will increase the possibility for making a PTB diagnosis: (1) house-hold tuberculosis contact in the prior 3 months, (2) fever or cough for more than two weeks, weight loss or failure to gain weight in the previous 3 months, (3) a positive tuberculin skin test or interferon-γ release assay result, (4) a chest radiograph suggestive of TB. (5) effective anti-tuberculosis treatment, (6) smear positive on respiratory tract specimen with/without positive culture or xpert assay. Patients who met the above criteria were bacteriologically confirmed TB, patients who met 1-5 criteria except the sixth criterion were clinically diagnosed TB. Microbiological reference standard of PTB was defined as the gold standard.

Suspected pulmonary TB cases were defined as those who aroused a suspicion of pulmonary TB but for whom a clinical diagnosis and decisions were not made.

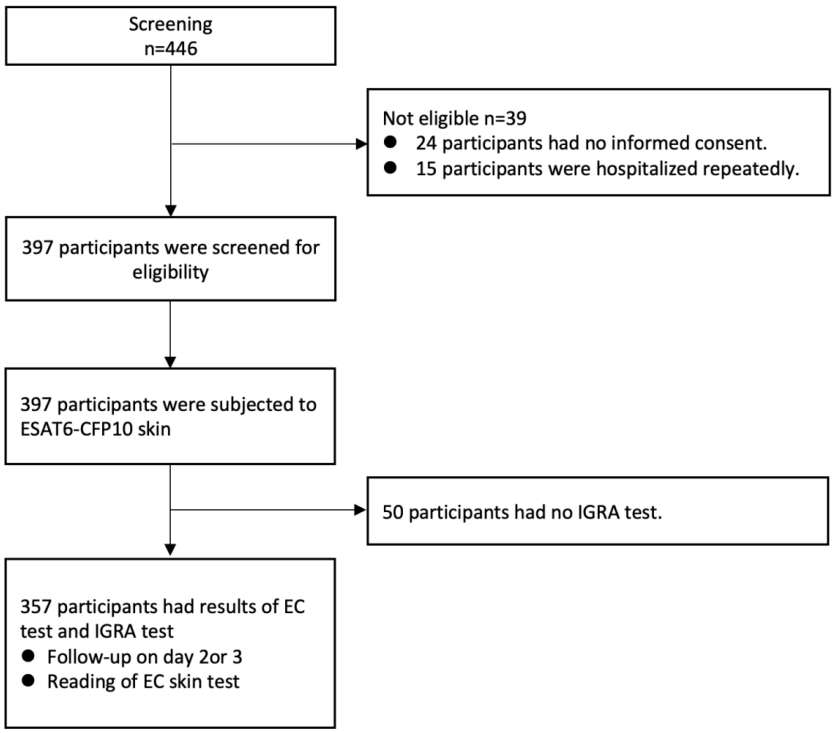

FIGURE 1
Study flow diagram.

Non-TB is a patient who does not meet the criteria for the clinically diagnosed tuberculosis.

The inclusion criteria were as follows: (1) age > 6 months, (2) suspected tuberculosis, and (3) willing to provide written informed consent.

The exclusion criteria were as follows: (1) pregnancy or lactation, (2) children with congenital immunodeficiency, (3) HIV infection, (4) live vaccination or biological agent within 4 weeks, (5) previous mental illness or cognitive dysfunction, and (6) other circumstances that the researcher considered unsuitable for the experiment.

3 Results

3.1 Participant characteristics

A total of 446 patients were screened for this study, excluding 24 who were unwilling to sign the informed consent form, 15 with repeated admissions, and 50 without IGRA test results. All the enrolled patients were suspected TB, and 50 of them did not have IGRA test results. These 50 patients were TST-positive and did not want to be tested for IGRA. A total of 357 patients underwent the EC skin and IGRA tests, of which 302 were clinically diagnosed with TB and 55 were not diagnosed with TB. There were 247 male and 110 female patients. The youngest and older patients were 2 and 94 years old, respectively. The mean age was 51.50 and 54.00 years old in the TB and non-TB groups, respectively, and no significant difference was noted between the two groups (P = 0.96). The mean body mass index values of the two groups were 20.87 and 20.78 kg/m^2, respectively, and no significant difference was found between the two groups (P = 0.13) (Table 1).

3.2 Sensitivity and specificity of the ECST

Based on the gold standard, 227 patients comprised the TB group and 130 made up the non-TB group. The sensitivity of the ECST was 72.69% (66.8%-78.5%), the specificity was 46.15% (37.5%-54.8%), and the AUC_{EC} was 0.59. The sensitivity and specificity of IGRA were 86.34% (81.8%-90.8%) and 36.15% (27.8%-44.5%), respectively, and the AUC_{IGRA} was 0.61 (Table 2).

Based on composite clinical reference standard (CCRS), 302 patients had TB and 55 patients do not have TB. The sensitivity of the ECST was 71.52% (66.4%–76.6%), the specificity was 65.45% (52.5%-78.4%), and the AUC_{EC} was 0.69. The sensitivity and specificity of the IGRA test were 85.10% (81.1%–89.1%) and 60.00% (46.6%-73.4%), respectively, and the AUC_{IGRA} was 0.73 (Table 3, Figure 2).

3.3 Subgroup analysis

In the baseline analysis, a history of TB was statistically different between the TB group and the non-TB group (Table 1). After the subgroup analysis, the sensitivity of the ECST was 72.73% (66.7%–77.7%), the specificity was 73.17% (59.0%-87.3%), and the AUC_{EC} was 0.73. The sensitivity and specificity of the IGRA test were

TABLE 1 Clinical characteristics of the participants in the tuberculosis and non-tuberculosis groups.

	TB (N = 302)	Non-TB (N = 55)	P value
Age, years (IQR)	51.50 (31.0–65.0)	54.00(27.00-68.00)	0.96
Female, sex, n. (%)	96(31.79)	14(25.5)	0.35
BMI, mean (kg/m^2)	20.87 ± 3.52	20.78 ± 4.19	0.13
Cancer, n. (%)	8 (2.64)	3 (5.45)	0.49
Hypertension, n. (%)	62 (20.53)	9 (16.36)	0.48
Diabetes, n (%)	57 (18.87)	9(16.40)	0.66
Hyperlipemia, n (%)	6 (1.98)	2 (3.64)	0.79
Liver disease, n (%)	46 (15.23)	11 (20.00)	0.38
Nephropathy, n (%)	22 (7.28)	6 (10.91)	0.52
Anemia, n (%)	25 (8.28)	4 (7.27)	1.00
Connective tissue disease, n. (%)	6 (1.98)	1 (1.82)	1.00
Bacteriological diagnosed tuberculosis, n(%)	161	5	0.00
Extrapulmonary tuberculosis	69	0(0.00)	0.00
Pass infected tuberculosis n. (%)	4 (0.01)	14(25.5)	0.00

TABLE 2 Comparison of the accuracy of the ECST and IGRA tests in patients with bacteriological diagnosed tuberculosis.

	Result	TB (n)	Not TB (n)	Sensitivity (%)	95%CI	Specificity (%)	95%CI	AUC
ECST	+	165	70	72.69	66.8-78.5	46.15	37.5-54.8	0.59
	–	62	60					
IGRA	+	196	83	86.34	81.8-90.8	36.15	27.8-44.5	0.61
	–	31	47					

TABLE 3 Comparison of the accuracy of the ECST and IGRA tests in patients with clinically diagnosed tuberculosis.

	Result	TB (n)	Not TB (n)	Sensitivity (%)	95% CI	Specificity (%)	95%CI	AUC
ECST	+	216	19	71.52	66.4–76.6	65.45	52.5-78.4	0.69
	–	86	36					
IGRA	+	257	22	85.10	81.1–89.1	60.00	46.6-73.4	0.73
	–	45	33					

85.57% (81.6%–89.6%) and 68.29% (53.4%-83.2%), respectively, and the AUC_{IGRA} was 0.77 (Table 4).

Considering that patient age may affect the sensitivity and specificity of the EC skin and IGRA tests, analyses of different age groups were performed. The sensitivity and specificity of the ECST were 88.00% and 72.73%, in patients aged 0–18 years, 77.44% and 73.33% in patients aged 19–52 years, 68.57% and 72.73% in patients aged 52–65 years, and 58.11% and 50.00% in patients aged 65–94 years, respectively (Table 5). The sensitivity and specificity of the IGRA test were 88.00% and 81.82% for patients aged 0–18 years, 90.98% and 53.33% for patients aged 19–52 years, 81.43% and 54.55% for those aged 52–65 years, and 77.03% and 55.56% for those aged 65–94 years, respectively (Table 6). The ROC curves were drawn for participants of different ages (Figure 3), 36 patients were between 0 and 18 years old, and the AUC_{EC} and AUC_{IGRA} were 0.80 and 0.85, respectively. Moreover, 148 patients were 19–52 years old, and the AUC_{EC} and AUC_{IGRA} were 0.75 and 0.72, respectively. In addition, 81 patients were 52–65 years old, and the AUC_{EC} and AUC_{IGRA} were 0.71 and 0.68, respectively. There were 92 patients aged 65–94, and the AUC_{EC} and AUC_{IGRA} were 0.54 and 0.66, respectively (Tables 5, 6).

10.3389/fimmu.2023.1162177

TABLE 4 Comparison of the accuracy of ECST and IGRA tests in newly diagnosed TB.

	Result	TB(n)	Not TB(n)	Sensitivity (%)	95%CI	Specificity (%)	95%CI	AUC
ECST	+	224	11	72.73	67.7–77.7	73.17	59.0-87.3	0.73
	–	84	30					
IGRA	+	255	13	85.57	81.6–89.6	68.29	53.4-83.2	0.77
	–	43	28					

TABLE 5 Comparison of the accuracy of the ECST in patients of different ages with clinically diagnosed tuberculosis.

ECST	Result	TB (n)	Not TB (n)	Sensitivity (%)	95% CI	Specificity (%)	95%CI	AUC
0–18	+	22	3	88.00	74.3–101.7	72.73	41.3-104.1	0.80
	–	3	8					
19–52	+	103	4	77.44	70.2–84.6	73.33	48.0-98.7	0.75
	–	30	11					
52–65	+	48	3	68.57	57.4–79.7	72.73	41.3–104.1	0.71
	–	22	8					
65–94	+	43	9	58.11	46.6–69.6	50.00	24.4-75.6	0.54
	–	31	9					

TABLE 6 Comparison of the accuracy of IGRA test in patients of different ages with clinically diagnosed tuberculosis.

IGRA	Result	TB (n)	Not TB (n)	Sensitivity (%)	95% CI	Specificity (%)	95% CI	AUC
0–18	+	22	2	88.00	74.3–101.7	81.82	54.6-109.0	0.85
	–	3	9					
19–52	+	121	7	90.98	86.0–95.9	53.33	24.7-81.9	0.72
	–	12	8					
52–65	+	57	5	81.43	72.1–90.8	54.55	19.5–89.6	0.68
	–	13	6					
65–94	+	57	8	77.03	67.2–86.8	55.56	30.1-81.0	0.66
	–	17	10					

3.4 Consistency of EC skin and IGRA tests

In all patients, the kappa value of the ECST and the IGRA test was 0.47. Consistency analysis was conducted for patients with TB at different sites, and the kappa values were 0.29 and0.54 in patients with TB and simple extrapulmonary TB, respectively. The kappa values of different age groups were 0.66, 0.46, 0.40 and 0.35.

3.5 Safety evaluation of the ECST

Grade 3 and 4 adverse reactions were not observed. A total of 33 (9.24%) patients had grade 1–2 adverse reactions, and the most common complaints were pain and pruritus at the injection site. Among them, 18 were men and 15 were women. Local adverse reactions occurred in two children, 14 patients aged 19–44 years, 16 patients aged 45–74 years, and 1 patient aged >74 years.

4 Discussion

In China, suspected pulmonary TB patients with complex conditions, comorbidities, and uncertain diagnoses often seek treatment in tertiary hospitals. Since China is an area with high prevalence of *Mycobacterium tuberculosis*, the proportion of people with *Mycobacterium tuberculosis* infection among non-TB patients

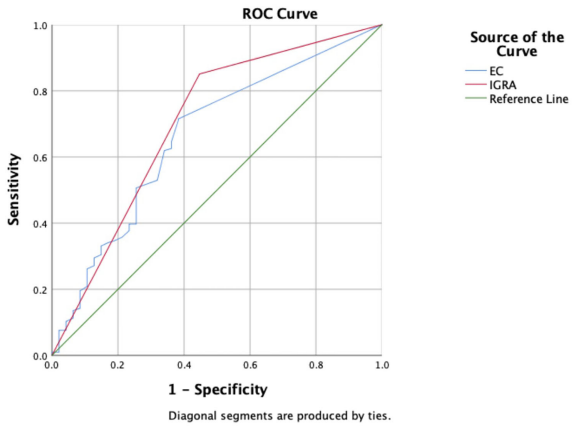

FIGURE 2
Receiver operating characteristic curves of the ECST and IGRA tests in patients with clinically diagnosed tuberculosis.

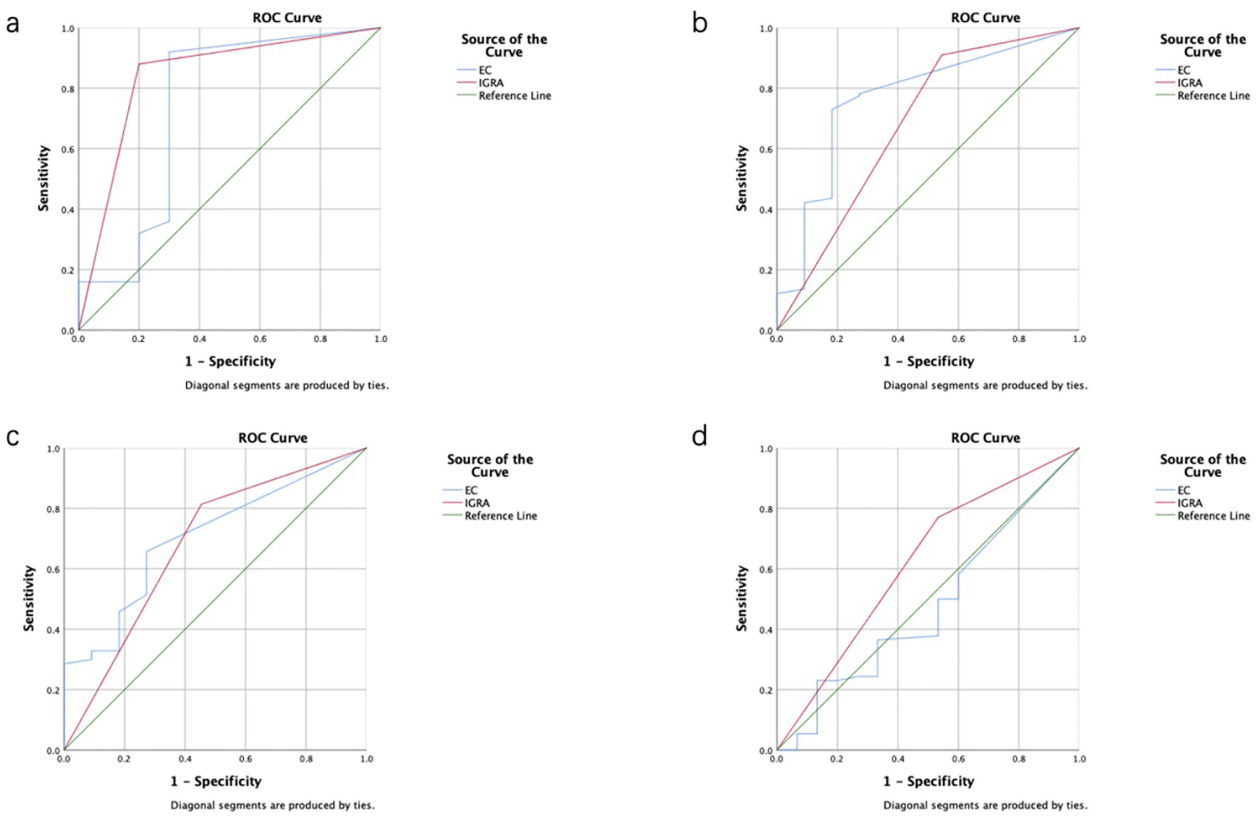

FIGURE 3
Receiver operating characteristic (ROC) curves of the ECST and IGRA tests in patients of different ages. **(A)** ROC curves for EC skin and IGRA tests in patients aged 0–18 years. **(B)** ROC curves for EC skin and IGRA tests in patients aged 19–52 years. **(C)** ROC curves for EC skin and IGRA tests in patients aged 52–65 years. **(D)** ROC curves for EC skin and IGRA tests in patients aged 65–94 years.

may be as high as 20%. If the patient is combined with immunocompromised status or other special diseases, such as silicosis, end-stage renal disease, HIV infection, etc., the risk of tuberculosis infection will be even higher. These patients may yield positive ECST results despite no active TB, theoretically. Therefore, we tested the differential diagnostic value of ECST in an environment with many interfering factors (a real-world setting), and this can be viewed as a stress testing of ECST. In this study, all patients underwent ECST. In a previous phase III clinical trial, we demonstrated the consistency and safety of ECST in healthy

individuals and patients with TB. In the present clinical trial, we focused on evaluating the accuracy of ECST in the differential diagnosis of active TB in tertiary specialized hospitals.

The study showed no significant difference in the sensitivity of ECST among patients with bacteriological diagnosed TB (72.69%), clinically diagnosed TB (71.52%), and newly diagnosed TB (72.73%). Meanwhile, the specificity of ECST in clinical diagnosis was 65.45%; however, in the subgroup, the specificity of the ECST in newly diagnosed TB was 73.17%, which indicated that the diagnostic efficacy was higher after excluding TB history. The specificity of the IGRA test in this trial was comparable, i.e., 60.00% vs. 68.29%, which is similar to the result of a previous study in which the specificity of the IGRA test was lower in patients with a history of TB than in patients without a history of it (21% [9%–39%] vs. 63% [55%–71%], P = 0.001) (5).

The sensitivity and specificity of Diaskintest were 78.1%–88.9% and 92.1%–96.4% (6, 7), and that of C-Tb were 73.9% (95% CI 67.8–79.3) and 99.3%, respectively (8, 9). The ECST produced by Anhui Zhifeilong Koma Biological Co., Ltd., showed a sensitivity of 87.5% (77.8%–97.2%) and specificity of 98.4% (95.4%–99.7%) in a phase II b clinical trial (10). In a phase III clinical trial, the 48-h sensitivity and specificity of ECST were 90.85% and 89.83%, respectively (11). The sensitivity and specificity of this test were 71.52% and 65.45%, respectively. The factors that affect the results of skin tests include product type, quality, and dose. Infection was related to the immune status, age, and physical strength of the vaccinated participants. Moreover, it is related to the inoculation technique by the medical staff and the evaluation technique of the results. The positive rate of ECST in this study was low because both stage II and stage III were RCTS, and highly homogeneous participants were selected through a series of nanoscale criteria. Patients who had a challenging diagnosis and had more underlying diseases were found in tertiary specialized hospitals. In this study, most of the hospitalized patients were not first-time patients, and most of them have atypical TB, or multidrug-resistant TB, which is difficult to diagnose. Even though all patients had TB, large individual differences exist and many had complicated diseases. In this study, the patients mainly had 3–5 diseases, 235 (65.8%) were >45 years old, 71 (19.9%) had hypertension, 66 (18.5%) had diabetes, and 28 (7.84%) had kidney disease among common diseases.

In the present study, the AUC value of the ECST was close to that of the IGRA test (0.59 vs. 0.61), indicating little difference in accuracy. However, the kappa value was only 0.47, indicating that the critical value of the ECST set at 5 mm in tertiary specialized hospitals may not be appropriate and should be further evaluated. In a phase IIb trial, the consistency of EC skin and IGRA tests was good, possibly because the left forearm of IIb received 0.1 mL of TB-PPD, and the right forearm received 0.5 μg/0.1 mL or 1.0 μg/0.1mL in the ECST; however, only 0.1 mL was injected in this trial. The low AUC and kappa values may be attributed to the different doses of the antigen injected.

In this study, 61 (15.7%) patients had EC-negative and IGRA-positive findings, including 45/61 (73.8%) patients aged >45 years, possibly due to aging or immunosuppression, which is consistent with the conclusion that accuracy decreases with age in the subpopulation. The IGRA detection in the present study also showed a similar trend, consistent with the conclusion in previous studies that the sensitivity of IGRA detection in patients with immunocompromised status was lower than that in patients with normal immune function (53% [29%–76%] vs. 83% [67%–92%], P = 0.045). Therefore, for patients of different ages and different underlying diseases, especially those with low immunity, 5 mm as the threshold value may be too general. We also found elder age had obviously impact on ECST rather than IGRA. By comparing the results at all ages, the sensitivity of ECST decreased from 88% to 58.11%, while the sensitivity of IGRA detection decreased by only 11%. Age may be an influencing factor. This result may also be due to the small sample size in the sub group analysis. what's more, the specificity of IGRA detection was only 55.56%, which may also be due to the sample size. Clinical trials with larger sample sizes will be needed to verify this conclusion.

This study has some limitations. First, immunological test results may be affected before and after treatment. In real-world tests, auxiliary diagnosis is usually performed before treatment or within 2 weeks after treatment. TB screening is recommended at the first test or 3 months after the first test. Second, the patients in this study lacked a TB treatment history for evaluation. Third, as patients aged <65 years were included in phases II and III, patients aged >65 years in the present study were not well compared with previous studies. Fourth, this study did not record in detail whether the patient had received TST at the first hospital and whether there was an enhancement effect after receiving the ECST again. Fifth, the experiment was conducted in the TB department, where most patients had TB; thus, the proportions of the TB and non-TB groups were unreasonable. The diagnostic accuracy and safety of ECST in tertiary specialized hospitals are average; thus, follow-up studies with larger populations are needed.

5 Conclusion

The ECST is a suboptimum tool for the differential diagnosis of active tuberculosis. Its performance is similar to IGRA, an adjunctive diagnostic test for diagnosing active tuberculosis.

Data availability statement

The original contributions presented in the study are included in the article/supplementary material. Further inquiries can be directed to the corresponding authors.

Ethics statement

This trial was conducted in compliance with the Declaration of Helsinki and principles of Good Clinical Practice. The studies involving human participants were reviewed and approved by the ethics committee of Shanghai Public Health Clinical Center

(No.2020-S121-01). Written informed consent to participate in this study was provided by the participants' legal guardian/next of kin.

Author contributions

SL, XL, and LX conceived and designed the study. YY and QW were involved in data analysis and collection. YY drafted and wrote the article and all authors provided critical revisions. All authors contributed to the article and approved the submitted version.

Funding

The work was funded by the Special Fund for Science and Technology Innovation of Guangdong (No. 2020B1111170014), the Shenzhen Fund for Guangdong Provincial High-level Clinical Key Specialties (No. SZGSP010), Shenzhen Natural Science Foundation (No. JCYJ20220530163212027), the Shenzhen Clinical Research Center for Tuberculosis (No. 20210617141509001), the Special Fund of Shenzhen Central-leading-local Scientific and Technological Foundation (No. LCYX20220620105200001).

Acknowledgments

We thank participants from the Shanghai Public Health Clinical Center, without whom this study may not be accomplished. The authors are grateful to Guozhi Wang for helpful discussion on topics related to this work.

Conflict of interest

The authors declare that the research was conducted in the absence of any commercial or financial relationships that could be construed as a potential conflict of interest.

Publisher's note

All claims expressed in this article are solely those of the authors and do not necessarily represent those of their affiliated organizations, or those of the publisher, the editors and the reviewers. Any product that may be evaluated in this article, or claim that may be made by its manufacturer, is not guaranteed or endorsed by the publisher.

References

1. World Health Organization. *Global tuberculosis report 2022*. World Health Organization (2022).

2. Berthet FX, Rasmussen PB, Rosenkrands I, Andersen P, Gicquel B. A mycobacterium tuberculosis operon encoding ESAT-6 and a novel low-molecular-mass culture filtrate protein (CFP-10). *Microbiol (Reading Engl)* (1998) 144:3195–203. doi: 10.1099/00221287-144-11-3195

3. van Pinxteren LA, Ravn P, Agger EM, Pollock J, Andersen P. Diagnosis of tuberculosis based on the two specific antigens ESAT-6 and CFP10. *Clin Diagn Lab Immunol* (2000) 7:155–60. doi: 10.1128/CDLI.7.2.155-160.2000

4. National Health and Family Planning Commission of the People's Republic of China. *WS 288-2017 tuberculosis diagnosis*. (2017).

5. Meyssonnier V, Guihot A, Chevet K, Veziris N, Assoumou L, Bourgarit A, et al. Performance of QuantiFERON for the diagnosis TB[J]. *Med Mal Infect* (2012) 42:579–84. doi: 10.1016/j.medmal.2012.08.003

6. Pankratova L, Kazimirova N, Volchkova I, Zlatorev A. Experience of using diaskintest in adult patients with tuberculosis and non-tuberculosis respiratory diseases in a regional TB hospital. *Eur Respir J* (2013) 42:P2787.

7. Nikitina IY, Karpina NL, Kasimceva OV, Gergert VY, Ergeshov A, Lyadova IV. Comparative performance of QuantiFERON-TB gold versus skin test with tuberculosis recombinant allergen (Diaskintest) among patients with suspected pulmonary tuberculosis in Russia. *Int J Infect Dis* (2019) 86:18–24. doi: 10.1016/j.ijid.2019.06.014

8. Hoff ST, Peter JG, Theron G, Pascoe M, Tingskov PN, Aggerbeck H, et al. Sensitivity of c-Tb: a novel RD-1-specific skin test for the diagnosis of tuberculosis infection. *Eur Respir J* (2016) 47:919–28. doi: 10.1183/13993003.01464-2015

9. Aggerbeck H, Giemza R, Joshi P, Tingskov PN, Hoff ST, Boyle J, et al. Randomised clinical trial investigating the specificity of a novel skin test (C-Tb) for diagnosis of m tuberculosis infection. *PloS One* (2013) 8:e64215. doi: 10.1371/journal.pone.0064215

10. Xu M, Lu W, Li T, Li J, Du W, Wu Q, et al. Sensitivity, specificity and safety of a novel skin test (ESAT6-CFP10) for tuberculosis infection in China: randomized, blinded, self-controlled, parallel-group phase 2b trials. *Clin Infect Dis* (2022) 74 (4):668–77. doi: 10.1093/cid/ciab472

11. Zhang H, Wang L, Li F, Lu S, Xia J. Induration or erythema diameter not less than 5 mm as results of recombinant fusion protein ESAT6-CFP10 skin test for detecting m tuberculosis infection. *BMC Infect Dis* (2020) 20:685. doi: 10.1186/s12879-020-05413-9

frontiers | Frontiers in Immunology

TYPE Original Research
PUBLISHED 26 June 2023
DOI 10.3389/fimmu.2023.1191357

OPEN ACCESS

EDITED BY
Lu Huang,
University of Arkansas for Medical Sciences,
United States

REVIEWED BY
Gopinath Venugopal,
University of Arkansas for Medical Sciences,
United States
Fergal Joseph Duffy,
Center for Infectious Disease Research,
United States

*CORRESPONDENCE
Yi Wang
wildwolf0101@163.com
Guirong Wang
wangguirong1230@ccmu.edu.cn
Junhua Pan
panjunhua999@sina.com
Laurence Don Wai Luu
laurence.luu@uts.edu.au
Xinting Yang
yl-14t@163.com

†These authors have contributed equally to this work

RECEIVED 22 March 2023
ACCEPTED 30 May 2023
PUBLISHED 26 June 2023

CITATION
Yang X, Yan J, Xue Y, Sun Q, Zhang Y, Guo R, Wang C, Li X, Liang Q, Wu H, Wang C, Liao X, Long S, Zheng M, Wei R, Zhang H, Liu Y, Che N, Luu LDW, Pan J, Wang G and Wang Y (2023) Single-cell profiling reveals distinct immune response landscapes in tuberculous pleural effusion and non-TPE. *Front. Immunol.* 14:1191357. doi: 10.3389/fimmu.2023.1191357

Single-cell profiling reveals distinct immune response landscapes in tuberculous pleural effusion and non-TPE

Xinting Yang[1*†], Jun Yan[2†], Yu Xue[3†], Qing Sun[4], Yun Zhang[1], Ru Guo[1], Chaohong Wang[2], Xuelian Li[1], Qingtao Liang[1], Hangyu Wu[5], Chong Wang[5], Xinlei Liao[2], Sibo Long[2], Maike Zheng[2], Rongrong Wei[6], Haoran Zhang[6], Yi Liu[6], Nanying Che[6], Laurence Don Wai Luu[7*], Junhua Pan[8*], Guirong Wang[2*] and Yi Wang[9*]

[1]Tuberculosis Department, Beijing Chest Hospital, Capital Medical University, Beijing, China, [2]Department of Clinical Laboratory, Beijing Chest Hospital, Capital Medical University, Beijing Tuberculosis and Thoracic Tumor Institute, Beijing, China, [3]Department of Emergency, Beijing Chest Hospital, Capital Medical University, Beijing, China, [4]National Clinical Laboratory on Tuberculosis, Beijing Key Laboratory for Drug-Resistant Tuberculosis Research, Beijing Chest Hospital, Capital Medical University, Beijing Tuberculosis and Thoracic Tumor Institute, Beijing, China, [5]Heart Center, Beijing Chest Hospital, Capital Medical University, Beijing, China, [6]Biobank, Beijing Chest Hospital, Capital Medical University, Beijing, China, [7]School of Life Sciences, University of Technology Sydney, Sydney, Australia, [8]Beijing Chest Hospital, Capital Medical University, Beijing, China, [9]Experimental Research Center, Capital Institute of Pediatrics, Beijing, China

Background: Tuberculosis (TB) is caused by *Mycobacterium tuberculosis* (*Mtb*) and remains a major health threat worldwide. However, a detailed understanding of the immune cells and inflammatory mediators in *Mtb*-infected tissues is still lacking. Tuberculous pleural effusion (TPE), which is characterized by an influx of immune cells to the pleural space, is thus a suitable platform for dissecting complex tissue responses to *Mtb* infection.

Methods: We employed singe-cell RNA sequencing to 10 pleural fluid (PF) samples from 6 patients with TPE and 4 non-TPEs including 2 samples from patients with TSPE (transudative pleural effusion) and 2 samples with MPE (malignant pleural effusion).

Result: Compared to TSPE and MPE, TPE displayed obvious difference in the abundance of major cell types (e.g., NK, CD4+T, Macrophages), which showed notable associations with disease type. Further analyses revealed that the CD4 lymphocyte population in TPE favored a Th1 and Th17 response. Tumor necrosis factors (TNF)-, and XIAP related factor 1 (XAF1)-pathways induced T cell apoptosis in patients with TPE. Immune exhaustion in NK cells was an important feature in TPE. Myeloid cells in TPE displayed stronger functional capacity for phagocytosis, antigen presentation and IFN-γ response, than TSPE and MPE. Systemic elevation of inflammatory response genes and pro-inflammatory cytokines were mainly driven by macrophages in patients with TPE.

Conclusion: We provide a tissue immune landscape of PF immune cells, and revealed a distinct local immune response in TPE and non-TPE (TSPE and MPE). These findings will improve our understanding of local TB immunopathogenesis and provide potential targets for TB therapy.

KEYWORDS

Mycobacterium tuberculosis, tuberculosis, tuberculous pleural effusion, ScRNA-seq, local immune response

Introduction

Tuberculosis (TB) is caused by *Mycobacterium tuberculosis* and it is one of the leading causes of deaths worldwide. Globally, an estimated 9.9 million people contracted TB in 2020 with 16% corresponding to extrapulmonary forms (1). Tuberculous pleurisy is the second most common form of extrapulmonary TB as well as the main cause of pleural effusion in many countries (1, 2). The pathogenesis of tuberculous pleurisy involves intricate cellular and humoral immune responses (3, 4). Host defense against TB involves infiltration of peripheral blood mononuclear cells (PBMC) into the pleural space (5). This leads to accumulation of immune cells such as lymphocytes and myeloid cells, in the tuberculous pleural fluid (6). As a result, tuberculous pleurisy provides a good model to study the correlates of protective immune responses at the site of infection. However, the mechanism of localized immune response in the pleural fluid remains elusive.

Based on its pathogenesis, pleural effusion can be divided into transudative or exudative pleural effusion. Transudative pleural effusion (TSPE) is caused by systemic factors such as congestive heart failure and liver cirrhosis (7). Exudative pleural effusion is mostly caused by diseased pleural surfaces, such as tuberculous pleural effusion (TPE) and malignant pleural effusion (MPE) (8). Although TPE and MPE are both characterized as lymphocyte-predominant exudates (9, 10), other immune cells such as macrophages, neutrophils and dendritic cells are also present (11). Immune responses dominate depending on different types of pleural effusions. Thus, understanding the heterogeneity, exhaustion, migration and various functional capacity (e.g., effector functions, phagocytosis and antigen presentation) of immune cells in the pleural fluid (PF) from TPE will provide crucial insights into host anti-*Mtb* responses at the tissue level.

Cai Y et al. (12) previously described the local T cell immune landscape in TPE. In Cai's report, they provide key insights into the spectrum of T cell heterogeneity at TPE. However, TB is a complex inflammatory disease with involvement of various immune cell types besides T cells. Their interactions determine the outcome of TB infection (13). Currently, a comprehensive study into how various immune cells interact and the immune response landscape in *Mtb*-infected tissues (e.g., TPE) is still lacking. Additionally, little is known about the immune features of TPE compared to other pleural effusion like TSPE and MPE.

Single-cell RNA sequencing (scRNA-seq) is a powerful tool for dissecting the immune response and analyzing various cell populations, including cells in complex microenvironments (14, 15). To understand the complex host response to TB and reveal the distinct features among PFs, we performed scRNA-seq to obtain an unbiased and comprehensive visualization of immune responses in pleural fluid mononuclear cells (PFMC) from patients with TSPE, MPE and TPE. Our analysis provides a high-resolution immunological landscape of PFMCs in TPE and reveals distinct response signatures between TPE, TSPE and MPE, facilitating a comprehensive understanding of protective and pathogenic immune responses in patients with TPE.

Results

Single-cell transcriptional profiling of pleural fluid mononuclear cells

Here, we aimed to reveal the immune landscape in pleural fluid (PF) from patients with tuberculous pleural effusion (TPE). We collected fresh PF samples from six patients with TPE before anti-TB treatment (Figure 1A). Four fresh PF samples (non-TPE samples), including two samples from patients with malignant pleural effusion (MPE) and two samples from patients with transudative pleural effusion (TSPE), were used for comparative analysis (Figure 1A). Thus, the 10 patients were classified into three clinical conditions: tuberculous pleural effusion (TB, n=6), transudative pleural effusion (CO, n=2) and malignant pleural effusion (CT, n=2). The clinical features and laboratory findings of enrolled patients are provided in Table S1. We then performed scRNA-seq on these samples (Figure 1A). After filtering (see Methods), a total of 70,034 cell transcriptomes was retained across the ten patients, with an average of 5977 unique molecular identifiers (UMIs), representing 2097 genes (Figures 1B, S1).

Following graph-based clustering of uniform manifold approximation and projection (UMAP), cells were manually annotated based on RNA expression and distribution of canonical cell-type or cell-subtype markers (Figures S2, S3). We identified nine major cell-types (CD4: CD4+T cells; B: B cells; PB: plasma cells; CD8: CD8+T cells; MAIT: mucosal-associated invariant T cells; NK: natural killer cells; DCs: dendritic cells; Mono:

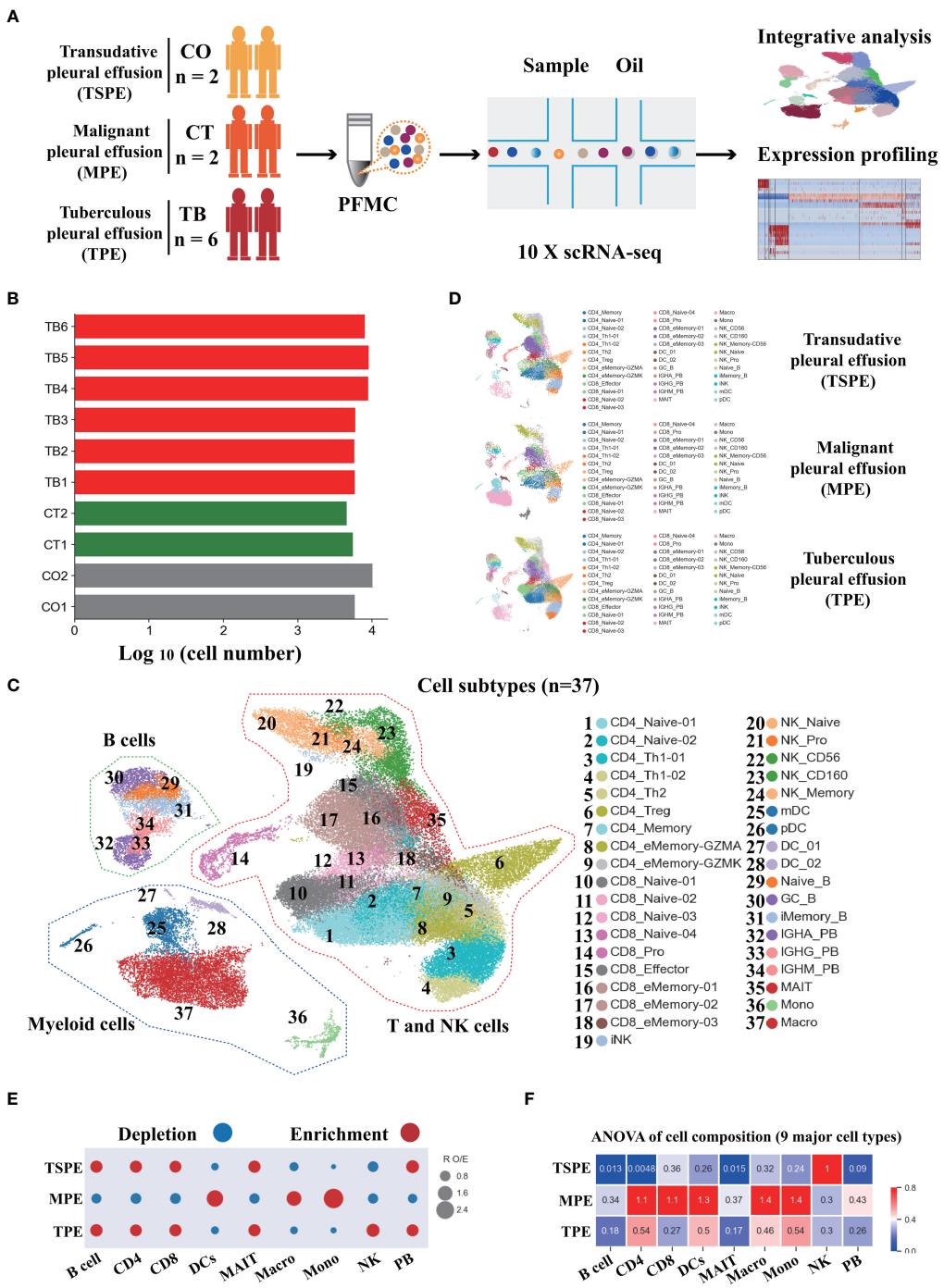

FIGURE 1
Study design and overall results of single-cell transcriptional profiling of PFs from participants. **(A)** Schematic diagram of the overall study design. 10 subjects, including 2 patients with transudative pleural effusion (TSPE), 2 patients with malignant pleural effusion (MPE) and 6 patients with tuberculous pleural effusion (TPE). **(B)** Bar plot shows the $\log_{10}$ transformed cell number of each sample. Red represents the 6 patients with TPE, grey represents the 2 patients with TSPE, and green represents the 2 patients with MPE. **(C)** The clustering result of 37 cell subtypes from 10 individuals. Each point represents one single cell, colored according to cell type. **(D)** The UMAP projection of the 37 cell subtypes in each of the three conditions. Cells are colored by the 37 cell subtypes. **(E)** Disease preference of major cell clusters estimated by $R_{O/E}$. **(F)** Heatmap for q values of ANOVA for disease severity.

monocytes; Macro: macrophages), and 37 subtypes following sub-clustering. These cells covered various immune cell types in the respiratory system (Figures 1C, D, S2, 3; Tables S2–7). Most of the cell-subtypes were identified in multiple TB patients, suggesting common immune characteristics in TB patients (Figure S5).

We determined the compositional changes of major immune cell types in PF. Among PFMCs, 43.25%, 26.58%, 8.8%, 6.55%, 2.45% and 12.28% were CD4, CD8, NK, B, MAIT and myeloid cells (DCs, Mono and Macro), respectively. Compared to TSPE and MPE, multiple immune cells from PFMCs were obviously altered in

TPE. We observed a significant decrease of NK cells in TPE relative to TSPE, and a relative expansion of $CD4^+$T, B and PB cells (Figures 1E, S4). In contrast, the relative abundance of DCs, Mono and Macro significantly increased in MPE compared to TPE (Figures 1E, S4). We also observed a decreased proportion of CD4, B, PB and CD8 in MPE compared to TPE (Figures 1E, S4). These data indicate that the level of major immune cells in TPE patients (e.g., NK, Mono, Macro) are distinct from non-TPE patients and might be a promising biomarker to diagnose or differentiate TPE from non-TPE.

Activation of the Th1 and Th17 response as well as T cell apoptosis in patients with TPE

Subtyping indicated a high level of diversity within T cells (CD4, CD8 and MAIT), with 19 different subsets identified (Figure 1C, S3, S6). All T cell subtypes were present in TPE, TSPE and MPE, although the relative percentages varied in a disease-dependent manner (Figure S6). Among the 19 different subtypes, we defined 9 subtypes of CD4 T cells, 9 subtypes of CD8 T cells, and an additional cluster of MAIT cells (Figures S6A, B; Tables S3, 4). We next defined CD4 T and CD8 T subsets according to their expression of classical subtype-specific marker genes and subtype-specific gene expression patterns (Table S3; Figures S2B, C, S3A, B). For CD4 T cells, we annotated two naïve CD4 T cell subtypes (CD4_Naïve-01 and CD4_Naïve-02), one CD4_Memory subset (CD4_Memory), two Th1 subtypes (CD4_Th1-01 and CD4_Th1-02), two effector memory subsets (CD4_eMemory-GZMA and CD4_eMemory-GZMK), one CD4 regulatory subtype and one Th2 subtypes (CD4_Treg) (Figures S2B, S7A, and Table S3). We observed a relative expansion of four CD4 T subsets (CD4_Naïve-01, CD4_Naïve-02, CD4_Memory and CD4_Th1-02) in patients with TPE compared with patients with TPE and MPE, while a decreased proportion of CD4_Th1-01 and CD_eMemory-GZMA were found in patients with TPE (Figure S6). Furthermore, CD4 T cells in patients with TPE were enriched with activation genes such as CD69 and IFNG (Figures S7A, S7C). Likewise, we also annotated 9 subtypes of CD8 T cells, including four naïve CD8 T cell subclusters (CD8_Naïve-01, CD8_Naïve-02, CD8_Naïve-03 and CD8_Naïve-04), one proliferative CD8 T subclusters (CD8_Pro) and 3 effector memory subclusters (CD8_eMemory-01, CD8_eMemory-02 and CD8_eMemory-03) (Figures 1D, S2C, S3B, S7B; Table S4). Particularly, CD8 T cell types in patients with TPE were enriched with activation gene CD69 (Figures S7B, C).

Among the CD4 T cell subtypes, Th1 cells (CD4_Th1-01 and CD4_Th1-01) are thought to play crucial role in combating *Mtb* infection by secreting important cytokines (e.g., IFN-γ and TNF). We observed that CD4 T cells were enriched in Th1 gene signatures (e.g., TBX21, GNLY, BHLHE40, IFNG) in patients with TPE (Figure 2A). Consistently, we also found that the expression of IFN-γ in Th1 cells was significantly higher in patients with TPE than in patients with TSPE and MPE (Figure 2B). This implies that Th1 cells in TPE are capable of producing high levels of IFN-γ. These data suggest that the CD4 T cell population in TPE was skewed towards a Th1 response, which is consistent with previous reports (16, 17). Additionally, a CD8 T cell subtype (CD8_Pro) displayed significantly higher expression of IFN-γ in patients with TPE (Figure 2B), suggesting that proliferative CD8 T cells might be another source of IFN-γ in TB patients. Besides IFN-γ, TNF also plays an import role in granuloma formation and controlling *Mtb* infection by generating reactive nitrogen intermediates together with IFN-γ (18). Therefore, this study also examined its expression in Th1 cells but it was not significantly upregulated in patients with TPE compared to patients with TSPE and MPE (Figure S7D). In addition, CD4 T cells in patients with TPE were enriched in Th17 signature gene such as CCR6, RORA, RORC, IRF4, STAT3 and IL23R, indicating activation of the Th17 response (Figure 2A). The above results suggest that CD4 population in TPE favored a Th1 and Th17 response.

In addition to the production of cytokines, T cells, especially effector T cells, can release cytotoxic molecules (e.g., perforins, granzymes) to directly kill *Mtb*, cause apoptosis of target cells and lead to immunopathology (19). Therefore, we used a cytotoxicity score to evaluate the cytotoxic state of each effector T cell subtype across three conditions. Patients with TPE had the lowest cytotoxicity sores in the effector T cell subsets (Figure 2C) whereas patients with transudative PE had the highest cytotoxicity score in the effector CD 8 T cell subsets. For patients with malignant PE, they had the highest cytotoxicity score for effector CD4 T cell subsets (Figure S7E). Consistent with these results, patients with TPE displayed lower expression of cytotoxic genes than patients with transudative and malignant PE, with the exception of GNLY (Figure S7F). These results indicate that effector T cells from patients with TPE might have lower cytotoxicity.

In *Mtb* infection, CD4 and CD8 T cells are exposed to persistent *Mtb* antigens, and this scenario might lead to deterioration of CD4 and CD8 T cell function: a state named "exhaustion". Thus, we tested whether TPE patients with exposure to persistent *Mtb* antigen had exhaustion in CD4 and CD8 T cells. According to the expression of exhaustion response genes and exhaustion markers, we defined an exhaustion response score and used this score to evaluate the exhaustion state of each activated T cell subset. Our scRNA-seq analysis suggested that, at the bulk level, activated T cells in TPE did not exhibit higher exhaustion scores compared to TSPE and MPE (Figure 2D). We also did not observe any exhausted T cells in PF from TPE (Figure S8A). In addition, we also did not find that activated T cells in PF from TPE highly expressed typical inhibitory molecules (e.g., PDCD1, LAG3, HAVCR2) (Figure S8B). These suggest that CD4 and CD8 T cells in PF from TPE might not undergo exhaustion.

Apoptosis is an important component of pathogen-induced cell death (20). We next investigated the expression of genes in apoptosis-related XAF1, TNF and FAS pathways. XAF1 is involved in pro-apoptotic responses and forms a positive feedback loop with IRF1 to initiate cell apoptosis under stress (21). Through post-translational modification, XAF1 is able to enhance TP53-mediated cell apoptosis (22). The expression of genes related to XAF1-mediated cell apoptosis, including XAF1, IRF1, TP53, BCL2L11, and CASP3, were investigated (Figures S8C,

D). The expression of XAF1 and IRF1 were significantly increased in T cells from patients with TPE compared to patients with TSPE and MPE (Figure 2E). Expression of XAF1 was increased in all T cell subsets in patients with TPE, while IRF1, TP53, BCL2L11, and CASP3 displayed different patterns in different T cell subsets (Figures S8C, D). In addition to the XAF1-mediated apoptosis pathway, the expression of genes in other apoptosis-associated pathways, including TNF- and Fas-mediated apoptosis, were also analyzed in T cells. The expression of TNFSF10 and its receptor TNFRSF10B were upregulated in T cells from patients with TPE relative to patients with TSPE and MPE (Figure 2F). Another TNF pathway gene, TNFRSF25, was also increased in T cells of patients with TPE. For the FAS pathway, the expression of FAS, FASLG, FADD, TRADD and CASP8 were notably decreased in T cells of patients with TPE (Figure 2F). Taken together, these results support the hypothesis that patients with TPE might have increased T-cell apoptosis due to upregulated genes associated with the XAF1- and TNF-apoptosis pathways.

We also examined the migration state of T cells in patients with TPE using a migration scoring system (Figure 2G). T cells in patients with TPE did not exhibit a stronger migration score compared to patients with TSPE and MPE. In contrast, T cells from patients with TSPE likely underwent migration as they had the highest migration score (Figure 2G).

NK cell exhaustion observed in patients with TPE

Six NK cell subclusters were observed in our scRNA-data including immature NK cells (iNK), naïve NK (NK_naïve), NK_CD56, NK_CD160, memory NK (NK_Memory-CD56) and proliferative NK cells. (Figures 1D, S2D, S3C, S9). Besides immature NK cells, the other five NK subclusters in patients with TPE showed high expression of activation and/or cytotoxic genes. This includes naïve NK cells (GNLY, GZMB, PRF1, KLRD1, CTSW), NK_CD56

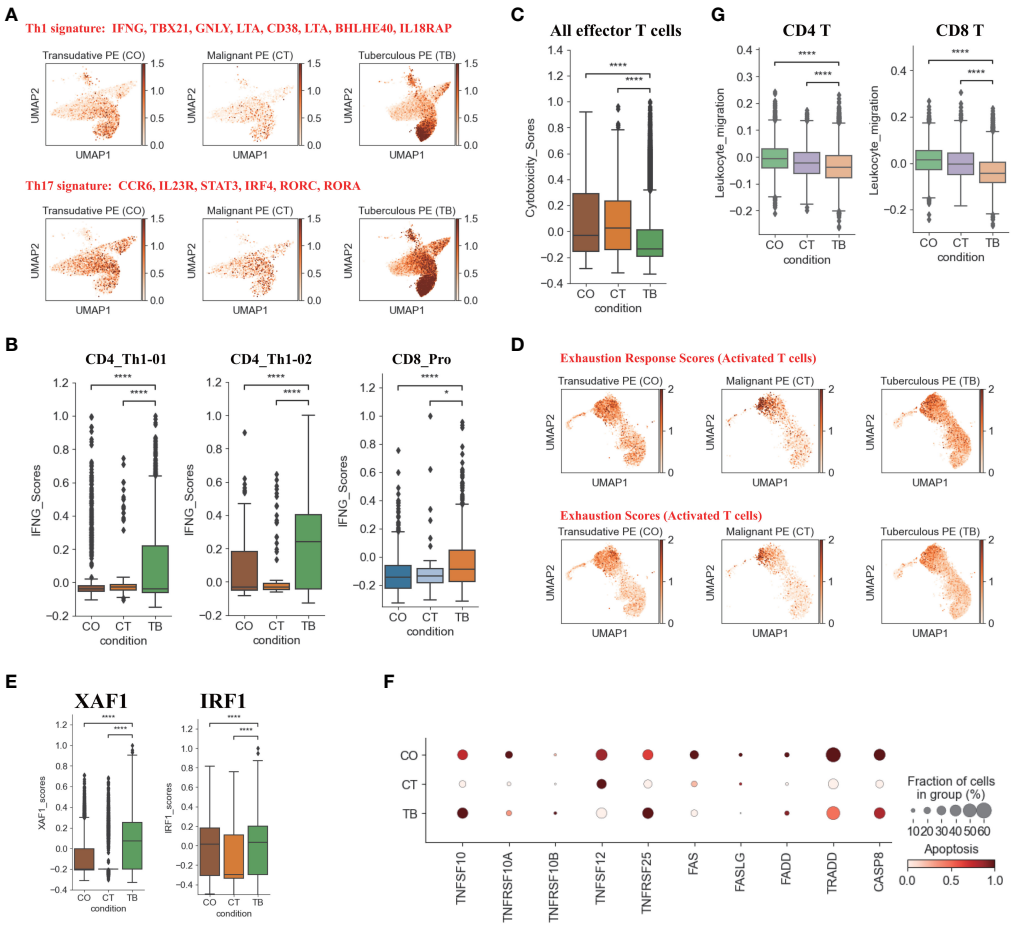

FIGURE 2
Characterization of gene expression differences in CD4$^+$ and CD8$^+$T cells across three conditions. **(A)** UMAP plots of mean gene expression from Th1 (Top) and Th17 (Bottom) gene signatures, split by condition. **(B)** Box plots showing the IFNG expression in CD4_Th1-01, CD4_Th1-02 and CD8_Pro subset per condition. **(C)** Box plots showing the cytotoxicity scores in effector T cells across different conditions. **(D)** UMAP plots of exhaustion response scores and exhaustion scores in activated T cells, split by condition. **(E)** Box plots showing XAF1 and IRF1 expression in T cells across each condition. **(F)** Dot plots showing the expression of selected apoptosis-associated genes in T cells across each condition. **(G)** Box plots of leukocyte migration scores in T cells across different conditions. Student's T-test was applied to test significance in **(B,C, E, G)** *p<0.05, ****p<0.0001.

(LAG3, BHLHE40, S100A11 and CTSW), NK_CD160 (PRF1, GNLY, GZMK, KLRB1, CTSW, CST7), memory NK cells (LAG3, KLRK1, S100A11, CTSW, KLRD1, KLRK1) and NK_Pro (GNLY, GZMA, GZMB, NKG7, CTSW, etc.) (Figures 1D, 3A, S2D, S9; Table S5).These data indicate the presence of an activated NK cell response as a distinct feature in patients with TPE. Three NK cell subclusters (iNK, NK_naïve and NK_Pro) had an increased trend in patients with TPE, while a decrease trend was observed for NK_CD56, NK_CD160 and NK_Memory-CD56 (Figure S9F). In addition, we found that NK cells from patients with TPE had high expression of tissue-resident NK (rNK) cell markers such as CD69, CXL1 and XCL2, but low expression of circulating NK cell markers (cNK) (FCGR3A, FGFBP2 and SPON2) (Figure 3A). In contrast, NK cells from transudative PE had high expression of cNK markers (Figures 3A, S10A). This suggests a predominance of rNK cells in TPE and a predominance of cNK cells in transudative PE.

We then applied PAGA (partition-based graph abstraction) to analyze the global connectivity and potential trajectory topology in the NK cell state transitions. Our data revealed that several nodes showed the high connectivity between NK cell subclusters, implying that these nodes represent potential trans-differentiation bridges (Figure 3B). The proliferative NK subcluster (NK_Pro) seemed to be an intermediate state, which connected immature and naïve NK cells to all other subclusters (NK_Memory-CD56, NK_CD56 and NK_CD160). In addition, we also observed high connectivity between NK_Memory-CD56 and NK_CD56 and between NK_Memory-CD56 and NK_CD160 (Figure 3B). This suggests that NK_Pro might serve as an intermediate subcluster, which could be valuable for therapeutic strategies targeting this intermediate state.

Similar to Th1 cells, the NK cells also can produce anti-*Mtb*-associated cytokines (e.g., IFN-γ and TNF). IFN-γ and TNF in NK cells were significantly downregulated in TPE comparing to TSPE, but upregulated relative to MPE (Figure 3C). Furthermore, NK cells, which contribute to anti-*Mtb* host defense through cell-related cytotoxicity, exhibited lower cytotoxicity scores in TPE compared to TSPE, with the lowest cytotoxic score in MPE (Figure S10B). These data results suggest that

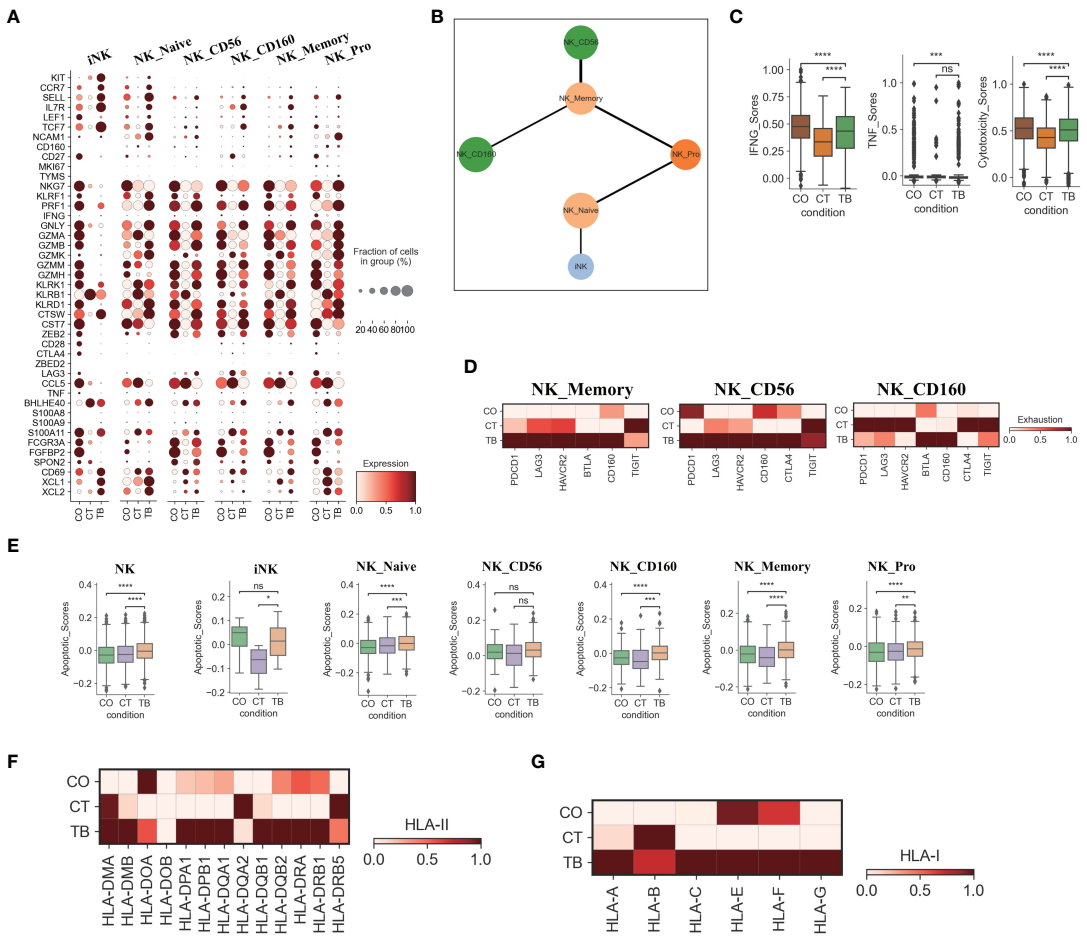

FIGURE 3
Characterization of gene expression differences in NK cells across three conditions. **(A)** Dot plots showing the expression of selected genes in each NK cell subtype per condition. **(B)** PAGA analysis of NK cell pseudo-time: the associated cell type is shown. **(C)** Box plots of the expression of IFNG, TNF and cytotoxicity scores in NK cells per condition. **(D)** Heatmap plots of the expression of selected exhaustion associated genes in NK_memory, NK_CD56 and NK_CD160 cells per condition. **(E)** Box plots showing the apoptotic scores in NK cells and subtypes per condition. **(F)** Heatmap plots of HLA-II molecules in NK cells per condition. **(G)** Heatmap plots of HLA-I molecules in NK cells per condition. Student's T-test was applied to test significance in **(A-E)**. *p<0.05, **p<0.01, ***p<0.001, ****p<0.0001, ^{ns}p>0.05.

lower levels of IFN-γ, TNF and cytotoxicity scores in NK cells from patients with TPE may lead to ineffective immune response to *Mtb* infection. Furthermore, the dysfunctional NK response in patients with TPE and MPE might be related to immune exhaustion, and thus we sought to explore the potential sources of NK exhaustion in patients with TPE.

We observed a significant increase in expression of exhaustion response genes and exhaustion markers in NK_Memory, NK_CD56 and NK_CD160 cells from patients with TPE (Figure S10C). This includes high expression of multiple inhibitory receptors such as PDCD1, LAG3, HAVCR2, BTLA, CD160, CTLA4 and TIGIT (Figure 3D). In contrast, patients with TSPE displayed the lowest exhaustion response scores and exhaustion scores in these three NK subclusters (Figure S10C). These results indicate that NK_Memory, NK_CD56 and NK_160 cells might be functionally impaired in patients with TPE.

We also further investigated the apoptosis and migration of NK cells. Significant activation of apoptosis pathways were observed in NK cells from TPE, with four subsets (NK_Naive, NK_CD160, NK_Memory and NK_Pro) exhibiting higher apoptotic scores in patients with TPE than patients with TSPE and MPE (Figure 3E). Genes associated with the XAF1-, TNF- and Fas-apoptosis pathways (e.g., TNFSF10, FADD, XAF1 and CASP8) were upregulated in NK cells from patients with TPE, suggesting that these pathways might cause the increased NK cell apoptosis observed in patients with TPE. This study did not find significant activation of NK migration in TPE relative to TSPE and MPE (Figure S10E), implying that NK cells in TPE did not undergo migration. In addition, we observed that genes encoding HLA class II molecules (e.g., HLA-DMB, HLA-DPA1, HLA-DPB1) and HLA Class I (HLA-A, HLA-C and HLA-G) were highly expressed in NK cells from patients with TPE compared to patients with transudative

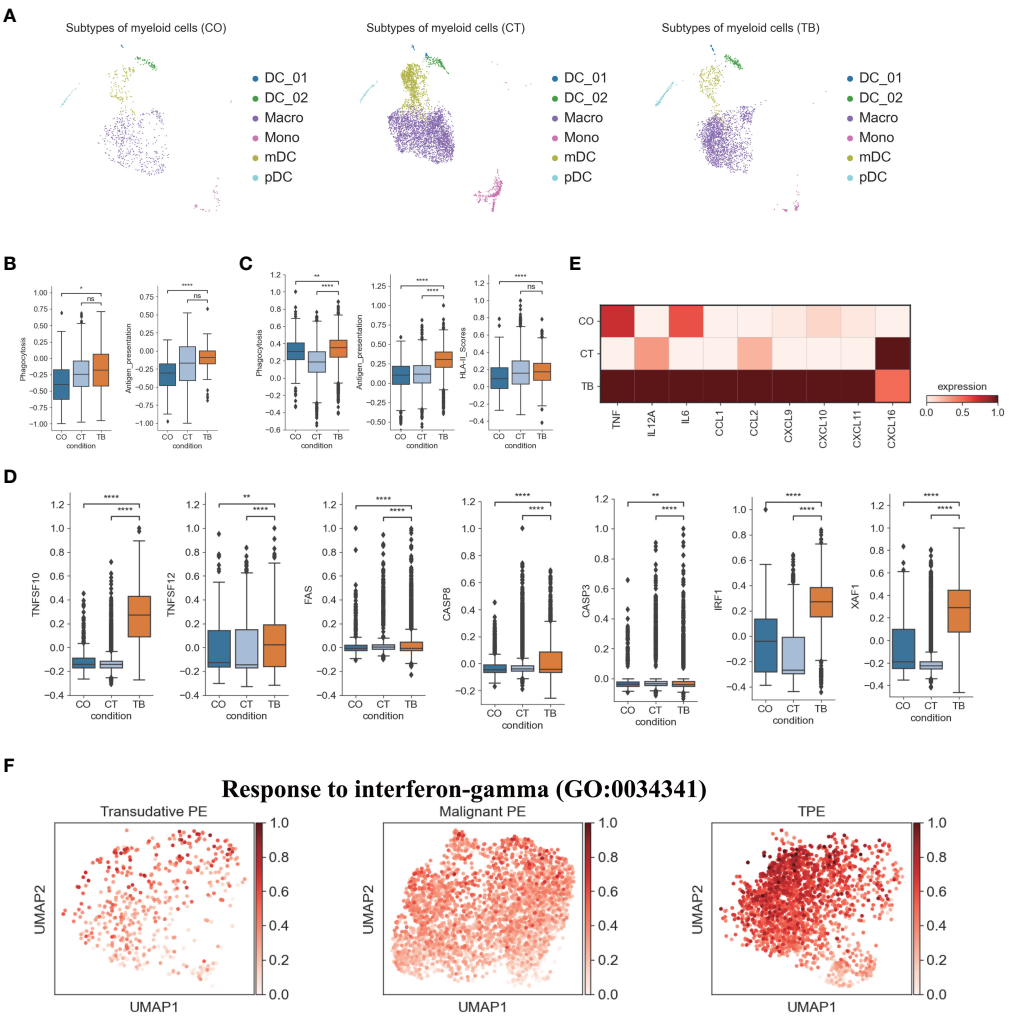

FIGURE 4
Characterization of gene expression differences in myeloid cells across three conditions. **(A)** The UMAP projection of the 6 myeloid cell subtypes across three conditions. Cells are colored by the 6 myeloid cell subtypes. **(B)** Box plots showing the phagocytosis and antigen presentation scores in monocytes across three conditions. **(C)** Box plots showing the phagocytosis, antigen presentation and HLA-II molecule scores in macrophages across three conditions. **(D)** Box plots of the expression of apoptosis-related genes in macrophages across three conditions. **(E)** Heatmap showing the expression of selected genes in macrophages across three conditions. **(F)** UMAP plots showing mean gene expression of interferon-gamma response gene signatures in macrophages, split by condition. Student's T-test was applied to test significance in **(B–D)**. *p<0.05, **p<0.01, ****p<0.0001, ^{ns}p>0.05.

and malignant PE (Figures 3F, G). The upregulation of HLA class II molecules is important for various pathways (e.g., promote crosstalk between NK cells and DCs).

Features of myeloid cells in patients with TPE

Transcriptome analysis of myeloid cells identified 4 DC subsets, 1 monocyte subset and 1 macrophage subset (Figures 4A, 1D, S11B, S11; Table S6). pDCs play an important role in microbial sensing and secrete type I interferons (IFNs) in response to microbial infection (4). Our scRNA-seq analysis found that pDCs from TPE highly expressed microbial recognition receptors like TLR7 and TLR9, and interferon production-related genes such as IRF1, IRF7, IRF8, PACSIN1 and DERL3 (Figure S11B). IRF1 and IRF5 are important for expression of type I IFNs in DCs and had high expression in pDCs from TPE (Figure S11B). CCR7, as a key chemokine receptor in pDCs, is upregulated upon exposure to TLR ligands, and we observed increased expression of CCR7 in TEP relative to transudative and malignant PE (Figure S11B). In addition, the percentage of pDCs was significantly increased in patients with TPE compared to patients with TSPE and MPE (Figure S11). These results suggests that pDCs in TPE may be involved in anti-*Mtb* response.

In contrast, the percentage of mDCs was significantly decreased in TPE relative to TSPE and MPE, and comprised of ~10% of all myeloid cells in TPE (Figure S11). However, mDC from TPE had relative low expression of the Fc epsilon receptor gene FCER1A. This may reflect variation in mDC states between different PFs. mDC, which specializes in antigen processing, play a crucial role in the interface between innate and adaptive immunity. Our analysis suggests that mDCs from TPE had a relatively high expression of HLA-DR molecules, which are essential for antigen presentation (Figure S11B). In addition, the high expression of these HLA class II genes validated that the mDCs cluster was activated. In addition, genes involved in mDCs development such as RELB, RBPJ, IRF2 and IRF4, were highly expressed in mDCs from TPE (Figure S11B). Genes associated with neutrophil activation were expressed at high levels in mDCs from TPE, while genes related to the proinflammatory response such as CCL3, CCL5 and CXCL8 were expressed at lower levels in mDCs from TPE compared to TSPE and MPE (Figure S11B). These data showed that mDCs from TPE might also have a positive role in anti-*Mtb*, and a minor contribution to the proinflammatory response. In addition to mDC and pDC, we observed two subsets corresponding to DC1 (DC_01: CLEC9A, CADM1, CAMK2D) and DC5 (DC_02: LYZ, PPP1R14A) dendritic cell types defined previously (Figures 1, S11) (23). Similar to the results observed in mDCs, DC_01 and DC_02 had a relatively high expression genes associated with HLA-DR molecules, neutrophil activation and DCs development (Figure S11B), implying that these DC subsets may also contribute to anti-*Mtb*.

We also investigated TPE-related differences in monocyte composition. Comparing the relative cell proportions in patients with TSPE and MPE, we observed a notable decrease in monocytes in patients with TPE (Figure S11). This cluster highly expressed S100A family genes (e.g., S100A8, S100A9) in patients with TPE and MPE, which are characteristic markers of human myeloid-derived suppressor cells (24). This suggests that monocytes may contribute to immune paralysis in TB and tumor patients (Figure S11B). In addition, monocytes from TPE had relatively high expression of cell proliferation genes (e.g., EIF5A), IFN-inducible genes (e.g., ISG15, MX1, MX2), antigen presenting genes (e.g., HLA-DRA, HLA-DQA1, HLA-DPB1, CD74) and component 1q genes (e.g., C1QA, C1QB and C1QC) (Figure S11B), suggesting that monocytes might play an important role in anti-TB infection. In particular, monocytes from TPE indicated greater functional capacity, including phagocytosis and antigen presentation, than TSPE and TPE (Figures 4B, S12A), as evidenced by the high expression of phagocytosis-related genes and HLA-II components (Figure S12A).

We also identified a macrophage subset (Macro: LYZ, CST3, CD68, CD163) (Figures 1D, S11B), which had a notable increase in patients with TPE relative to patients with TSPE and MPE (Figure S11). Macrophages can engulf *Mtb* through a series of membrane invagination, budding and fusion events, leading to the formation of the phagosome (25). Thus, we first analyzed the phagocytosis capacity of macrophages, and found that macrophages in patients with TPE indicated greater phagocytosis capacity than patients with TSPE and MPE (Figure 4C). We observed significant increased expression of phagocytosis-associated genes (e.g., ARF6, RAC2, PRKCE, VAV2) in macrophages from TPE (Figure S12B). After phagocytosis, macrophages can deliver these materials for antigen processing and presentation to activate T cells and the adaptive immune response against *Mtb*. Hence, we also investigated the antigen presentation capacity of macrophages, and observed that macrophages from TPE exhibited higher antigen presentation capacity than TSPE and MPE (Figure 4C). Compared to TSPE and MPE, macrophages from TPE highly expressed antigen presentation-associated genes (e.g., CITA, RFX5, B2M, HLA-F, HLA-DQA2, TAP1) (Figure S12C). MHC class II molecules, which play an important role in antigen presentation, were significantly upregulated in macrophages from TPE relative to TSPE and MPE (Figures 4C, S12C). Furthermore, macrophage apoptosis, which releases apoptotic vesicles carrying *Mtb* antigens to *Mtb*-uninfected DCs, can result in more effective antigen presentation (26). Genes associated with the TNF-, Fas- and XAF1-apoptosis pathways (e.g., TNFSF10, TNFSF12, FAS, CASP8, XAF1) were upregulated in macrophages from patients with TPE, suggesting an increase in macrophage apoptosis in patients with TPE (Figures 4D, S12E). In addition, the activation of macrophages can result in secretion and production of various cytokines and chemokines, which attracts NK, T cells, neutrophils, and more DC and macrophages to the *Mtb*-infection site. Genes encoding cytokines and chemokines (TNF, CCL1, CCL2, CXCL9, etc) were upregulated in patients with TPE compared to patients with transudative and malignant PE (Figure 4E). To further examine the anti-*Mtb* immune responses of macrophages, we also investigated the expression of genes belonging to the Gene Ontology (GO) biological process term: response to interferon (IFN)-gamma in macrophages. We found that response to IFN-γ was significantly upregulated in macrophages from TPE compared

to transudative and malignant PE (Figures 4F, S12D). These results indicate that macrophages in patients with TPE displayed strong anti-*Mtb* response.

Features of B cells in patients with TPE

A comprehensive analysis of both cellular and humoral immunity could contribute to a better understanding of the immune response to TB. Currently, less is known about the role of B cell-mediated immunity in protection against *Mtb*-infection. Therefore, we analyzed the scRNA-seq result of B cells in the immune response to *Mtb*. A total of 6 B cell subclusters were identified according to classical B cell markers including Naïve B cell (Naïve_B), Germinal center B cell (GB_B), Intermediate transition Memory B cell (iMemory_B), IGHA expressing plasma cell (IGHA_PB), IGHM expressing plasma cell (IGHM_PB) and IGHB expressing plasma cell (IGHG_PB) (Figures 1, S2, S13; Table S7). We then examined the compositional changes of the 6 categories of B cells in PE. Naïve_B, GB_B and iMemory_B did not show significant changes among patients with TPE, TSPE and MPE (Figure S13). However, plasma cell clusters may be associated with different PE conditions. Using pseudo-time analysis, we observed that plasma cells appeared to be derived from memory state B cell (iMemory_B) (Figure S14A). The percentage of IGHM_PB and IGHG_PB reached ~15% and showed an increased trend in patients with TPE (Figure S13). In contrast, for IGHA-PB, it was highest in patients with malignant PE, reaching ~20% (Figure S13). These data suggest that increased IGHM and IGHG plasma cells appears to be a feature of TPE.

Next, we examined the transcriptomic changes of B and PB cells (Figures 5, S13) in TPE, TSPE and MPE. Plasma cells highly expressed genes encoding the constant regions of immunoglobulin G1 (IgG1), IGHA1, IGHG2, IGHG4 and IGHM (Figure 5A), indicating their function in the secretion of antigen-specific antibodies. Plasma cells from TPE had a higher expression of Ig signature genes (IGHG1, IGHG2, IGHG3, IGHG4, IGHA1, IGHA2, IGHM) than TSPE and TPE (Figure 5B). Naïve_B from TPE were also enriched with key activation genes (e.g., CD69, IL21R, PAX5, BACH2 and HLA-DRA, etc.) (Figure 5C). Likewise, GC_B and iMemory_B also highly expressed their activation markers in TPE (GC_B for CD69, MKI67, HLA-DRB1, BACH2, and iMemory_B for TBX21, XBP1, IRF4, HLA-DRA) (Figure 5C). These results suggest that B/plasma cell-activation-associated pathways, such as somatic hypermutation, class switching, expansion and antibody production, were enriched in patients with TPE, implying that B/plasma cells from TPE may be activated for immune response to TB.

Previous reports have documented that B cell cytokines play an important in modulating T cell responses against intracellular bacteria while this has not been investigated in *Mtb* infection (27). We examined the key genes encoding representative cytokines in B cells, which are involved in T cell differentiation, expansion, and anti-*Mtb* response. Our data indicate that B cells from TPE were enriched with IL6, IL10, IL-12A and TNF (Figure S14B). Additionally, B cells are able to capture and internalize antigens via surface immunoglobulins, and then present these antigens on their surface as MHC II:peptide complexes to CD4 cells (especially to prime naïve CD4 T cells) (28). Thus, we analyzed the antigen presentation capacity of B cells in PF, and found that all B cell subsets from TPE displayed significantly higher antigen presenting capacity than transudative and malignant PE (Figures 5D, S14C). B cells from TPE highly expressed various presentation-associated genes (e.g., LGMN, CIITA, PFX5, TAP2, PSME1, TAP1, etc.) (Figure S14D). MHC molecules, especially MHC II, were significantly upregulated in B cells from TPE relative to TSPE and MPE (Figure 5E). These findings indicate that B cells from TPE might contribute to protection against *Mtb*-infection. In addition, we observed that apoptosis-associated genes (e.g. FAS, XAF1, TNFSF10, etc.) were upregulated in TPE compared to TSPE and MPE, implying that B cells in TPE likely underwent apoptosis (Figure 5F).

Macrophages are the main drives of inflammation in TPE

We next explored the potential sources of cytokine production in TPE. Using the reported inflammatory response genes and cytokine genes (Table S9) (15), we defined an inflammatory score and a cytokine score. Both scores were then used to assess the potential contribution to inflammation for each cell type. Macrophages were identified with significantly higher inflammatory and cytokine scores based on our scRNA-seq data from TPE samples (Figures 6A, B, S15A). This suggests that macrophages might be major sources of inflammation in TPE. Although the percentage of macrophages only reached ~ 3% in TPE (Figure 1E), the inflammatory and cytokine scores of macrophages reached 90% in TPE (Figure 6C) and were significantly higher than other cells (Figure 6D), further validating this cell type as inflammatory cells. In addition, five cell types, including B, CD8, MAIT, PB and NK cells, had higher inflammatory scores in TPE but their cytokine scores showed no difference compared to TSPE and MPE (Figure S15A). This suggest that these cell types may also contribute to inflammation response in TPE.

We then investigated the inflammatory signatures for pro-inflammatory macrophages in TPE. Our scRNA-seq data showed that macrophages in TPE had high expression of various pro-inflammatory cytokines (e.g., CCL2, CCL3, CXCL3, CCL8, IL1B, etc.) (Figures 6E, F, S15B) indicating various mechanisms leading to inflammation. The top 15 most highly expressed proinflammatory cytokines contributed to ~90% of the cytokine score (Figure 6D), highlighting the central role of these cytokines in driving inflammation in TPE (Figures 6E, S15B). Macrophages from TPE expressed significantly higher levels of these top 15 cytokines relative to other cells (e.g., B, CD4, CD8, NKs, etc.), further confirming their role as the major contributors to inflammation in TPE (Figure S15B). In addition, we observed significant elevated

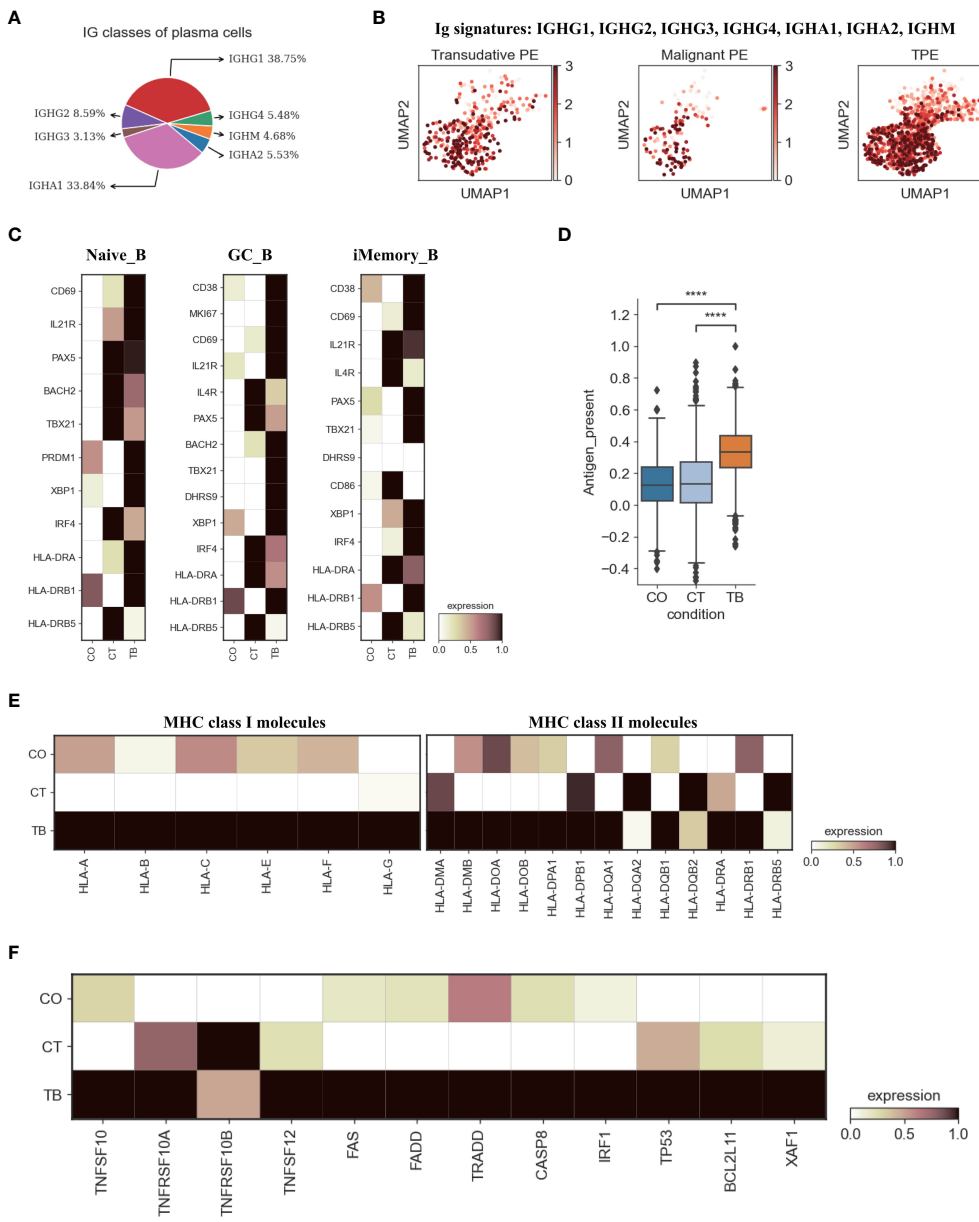

FIGURE 5
Characterization of gene expression differences in B cells across three conditions. **(A)** Proportion of heavy chain classes identified in plasma cells. **(B)** UMAP plots of mean gene expression from Ig signature genes in plasma cells, split by condition. **(C)** Heatmap showing the expression of selected B cell activation-associated genes in Naïve_B, GC_B and iMemory_B cell subset per condition. **(D)** Box plot showing the antigen presentation scores in B cells across three conditions. **(E)** Heatmap showing expression of HLA-I and HLA-II molecules in B cells across three conditions. **(F)** Heatmap of the expression of apoptosis-related genes in B cells across three conditions. Student's T-test was applied to test significance in **(D)** ****p<0.0001.

expression of inflammatory and cytokine genes in macrophages from TPE relative to TSPE and TPE (Figures S15C, D). Taken together, these findings illustrate that macrophages-driven inflammatory might be a distinct feature of TPE.

We reasoned that the systematic inflammatory response in patients with TPE may be related to the cross-talk between macrophages and other cells via secreting diverse pro-inflammatory cytokines such as those identified in the top 15. To investigate this, we examined the ligand-receptor pairing patterns between the hyper-inflammatory cell type (macrophages) and non-inflammatory cell types in TPE samples (Figures 6G, H). The interactions between macrophages and other cells appeared to display significant alterations (Figure 6G). Macrophages in TPE exhibited stronger interactions with DCs, monocytes and MAIT cells (Figure 6G). The interactions of macrophages with other cells mainly relied on CCR1, CCR2, CCR5, CCR3, CXCR3 and ACKR2 (Figures 6G, H). Interestingly, DCs cells in TPE expressed CCR1, CCR5 and CCR3, which can receive multiple cytokine stimuli generated by macrophages. Likewise, MAIT cells expressed CCR1, CCR5, CXCR3 and DPP4 while monocytes expressed CCR3,

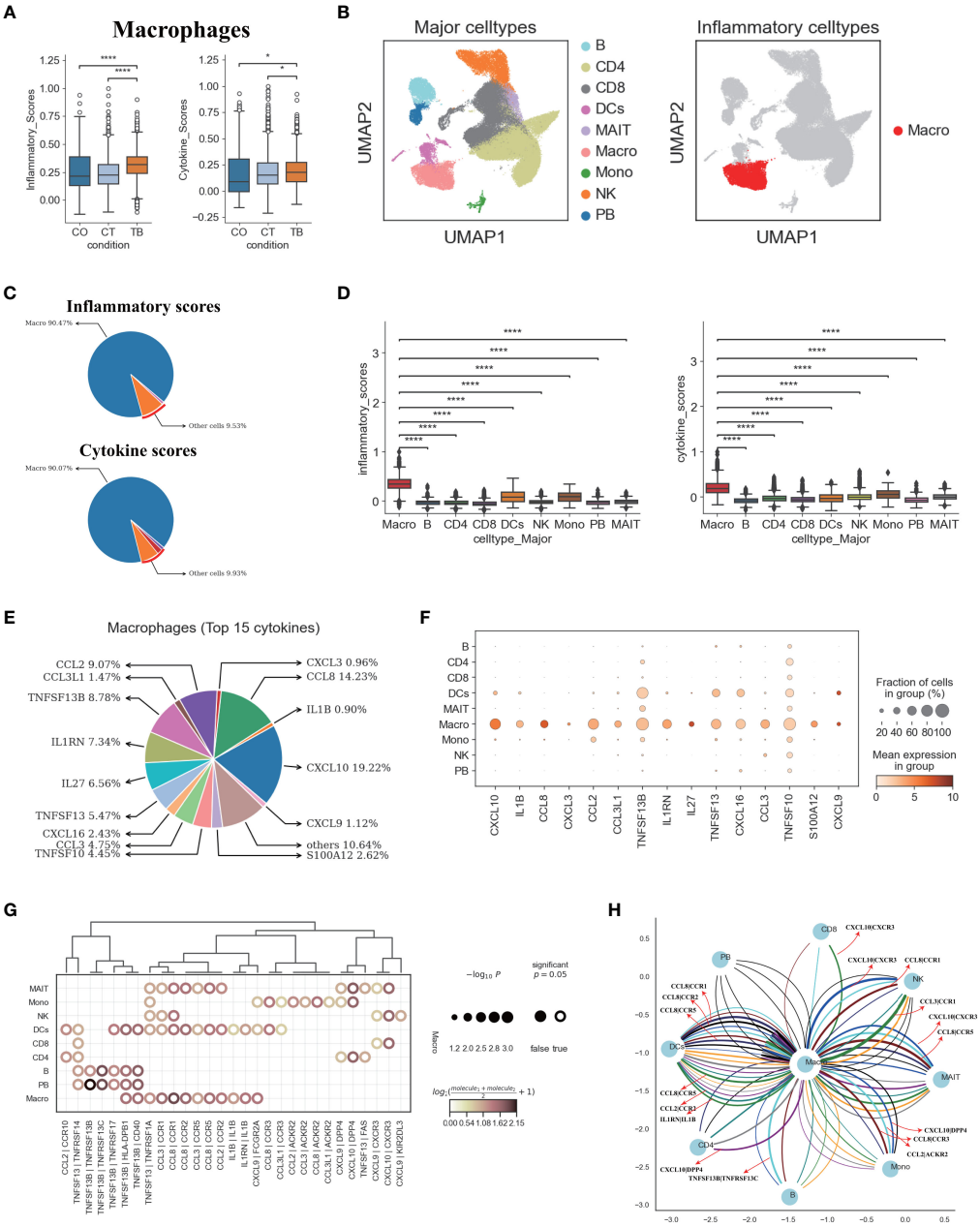

FIGURE 6
Macrophages in TPE as key cellular sources for inflammatory cytokines **(A)** Box plots of the inflammatory and cytokine scores in macrophage across three conditions. Student's T-test was applied to test significance. *p<0.05, ****p<0.0001. **(B)** UMAP plots of PFMCs colored by: major cell types (Left panel) and inflammatory cell type (Right panel). **(C)** Pie charts showing the relative percentage contribution of each cell type to the inflammatory score (Top panel) and cytokine score (Bottom panel). **(D)** Box plots of inflammatory scores (Left panel) and cytokine scores (Right panel) in nine major cell types. **(E)** Pie charts showing the relative percentage contribution of each pro-inflammatory cytokine in macrophages from TPE. **(F)** Dot plot showing the expression of selected pro-inflammatory cytokines in TPE across nine major cell types. **(G)** Dot plot of the interactions between macrophages and other immune cell types in patients with TPE. P values are indicated by the circle sizes, as shown in the scale on the right. **(H)** Macrophage-other immune cell interaction network in patients with TPE. Interactions with P values <0.05 are shown. Representative ligand-receptor interactions between macrophages and other immune cell types are marked.

ACKR2 and DPP4, which can also receive multiple cytokine stimuli yielded from macrophages (Figures 6G, H). Furthermore, we observed that macrophages in TPE also could interact with itself using CCR1, CCR2, CCR5 and IL1B (Figures 6G, H). Taken together, these results illustrate the molecular basis for potential cell-cell interactions in TPE at the local site of infection in TB patients.

Discussion

Tuberculosis (TB) caused by *Mtb* infection continues to be a severe threat to human health. Therefore, it is important to understand disease mechanisms, including mechanisms orchestrating local immune responses to *Mtb*, to effectively control this disease globally. Due to a lack of comprehensive data

about the immune landscape in tissues, our understanding of disease mechanisms in TB is limited. The use of TPE is advantageous as it reflects the localized immune response to TB. Therefore, this study was the first to map the entire immune landscape, comprising of T-cells, NK cells, B cells and myeloid cells, to dissect the potential immune responses related to TPE and determine the potential sources of the inflammation in TPE.

By analyzing 78900 cells from TPE, MPE and TSPE, we identified 9 major cell-types and 37 subtypes, covering various immune cells in PF (Figures 1, S1–S4). Thus, this information-rich data enabled reliable analysis of these cell types or subtypes at different resolution. The proportion of different immune cells in PF were successfully defined and the compositional change for each was determined. Notably, various myeloid clusters, including DCs, monocytes and macrophages, were more enriched in MPE than TPE and TSPE (Figure 1E) suggesting that this might be a distinct characteristic of MPE and may be used as valuable biomarkers for differentiating MPE and TPE. In contrast, $CD4^+$T and $CD8^+$T cells were significantly increased in TPE relative to MPE, which can be used as other biomarkers to further differentiate MPE and TPE (Figure 1E). Additionally, $CD4^+$T, B and PB cells were more enriched in TPE than TSPE while NK cells were significantly decreased (Figure 1E). These changes may be a promising biomarker for differentiating TPE and TSPE. Taken together, our scRNA-Seq data suggest that the relative abundance of immune cells in PF could be valuable for diagnosing TPE, and differentiating TPE from MPE and TSPE.

For T cells, our analysis suggested a high level of heterogeneity within T cell compartments among PFs. Previous reports have demonstrated that the T cell population in PF from TPE supports a Th1 response, with high levels of IFN-γ (29, 30). In our report, we identified two Th1 subtypes, including CD2_Th1-01 (immature Th1 cell) and CD4_Th1-02 (mature Th1 cell). TPE had a significantly higher proportion of CD4-Th1-02 cells than MPE and TSPE, which might be consistent with a phenomenon called "compartmentalization", resulting in the paucibacillary nature in TPE and low yield in *Mtb* culture (11, 17). We found the two Th1 subtypes showed markedly higher IFNG expression in TPE compared to MPE and TSPE. This suggests higher production of IFN-γ in TPE. IFN-γ is required to activate macrophages and kill *Mtb* by promoting phagosomal maturation and production of reactive oxygen and nitrogen intermediates (26). In addition to the high expression of IFNG, the Th1 subtypes in TPE also displayed higher Th1 signatures (e.g., TBX21, GNLY, CXCR3, CD38, LTA, etc.), suggesting a Th1 response in TPE that is consistent with previous studies (29, 30). Moreover, we found that the two Th1 subtypes also highly expressed activation genes (e.g., CD69) and cytotoxic genes (e.g., GZMA, GZMK), suggesting that these two subtypes are likely multifunctional. In addition to the Th1 response, our data also supports a Th17 response in TPE, which may be related to protective immunity against TB.

We also identified two effector CD4 sub-clusters (CD4_eMemory-GZMA and CD4_eMemory-GZMK) in PF (including TPE) that shared similar gene expression characteristics with effector CD8 T sub-clusters (GZMA, GZMK, GZMM, KLRB1). These CD4 sub-clusters have not previously been identified in TPE. It has been hypothesized that these CD4 T effector clusters (especially effector memory CD4 T cells), possibly produced through repeated antigen stimulation, might play an important protective role against infectious diseases (e.g., *Mtb*) (31, 32). Although effector CD4 cells have been thought to employ various mechanisms to kill their target cells (33), the exact molecular mechanisms and their role in anti-*Mtb* remains unclear. Therefore, further studies should examine what role these effector CD4 T cells play in TB.

Growing evidence indicates that CD8 T cells play key roles in preventing and controlling *Mtb* infection through various granzymes (34, 35). Previous reports suggested that granzymes (e.g., GZMB) were able to directly kill *Mtb* in the presence of granulysin, via various mechanisms (36). In our report, we found that different CD8 T subclusters in TPE exhibited different phenotypes from those seen in MPE and TSPE. Effector CD8 T cells from TPE had the lowest cytotoxicity score and lower expression of cytotoxicity-related genes relative to TSPE and MPE. This suggests that effector CD8 T cell subclusters in TPE may have limited roles in anti-*Mtb*. Previous studies have demonstrated that low T cell responses are related to cell exhaustion and apoptosis (37, 38). Consistently, we found that XAF1 and TNF pathways were involved in CD8 T cell apoptosis in TPE, especially for effector CD8 T cells. Genes associated with the XAF1 and TNF pathways displayed higher expression in CD8 T cells from TPE than those from TSPE and MPE, potentially contributing to the low effector CD8 T cell response in TPE.

NK cells are recruited early to the site of infection and have an important role in amplifying the antimicrobial immune response to TB. By PAGA analysis, we confirmed that NK_Pro, as a proliferative subcluster, was an intermediate state. NK_Pro was connected to all other NK subtypes, indicating that this subtype might be valuable for therapeutic strategies targeting this intermediate NK subcluster. Unexpected, a dysfunctional NK response was found in TPE relative to TSPE and MPE, evidenced by low expression of cytokines and cytotoxicity-related genes. Our further analysis suggested that NK cell exhaustion and apoptosis may be the potential reason for the dysfunctional NK response in TPE. NK cells in TPE had high expression of multiple inhibitory receptors (e.g., PCDC1, LAG3, TIGIT, etc.). Similar to CD8 T cells, NK cells in TPE also showed a high apoptotic state, as genes associated with the XAF1, TNF and FAS pathways were upregulated in NK cells from TPE. These factors may result in functional impairment of NK cells in TPE.

Myeloid cells are an important component of the innate immune system for controlling and preventing *Mtb*. Myeloid cells including DCs, macrophages and monocytes in TPE showed stronger functional capacity for phagocytosis, antigen presentation and IFN-γ response as well as higher expression of HLA molecules, illustrating their effective role in anti-*Mtb*. Phagocytosis of *Mtb* by macrophages results in the formation of the phagosome and through a series of vesicle trafficking events, Mtb antigens are distributed through antigen processing and presentation pathways (25). Antigen-loaded MHC class II molecules are then shuttled to the plasma membrane to activate T cells and adaptive immune response against *Mtb*. In addition to

macrophages, DCs also connect the adaptive and innate immune response through their role in capturing, processing and presenting antigens. Our findings show that macrophages and DCs in TPE had higher expression of HLA molecules and genes associated with phagocytosis and antigen presentation relative to TSPE and MPE, implying that these myeloid cells might provide the protective response to *Mtb* at the local site of infection. Interestingly, increased apoptosis of macrophages was also observed in TPE which may promote the release of *Mtb* antigen carrying vesicles. These vesicles can then be taken up by nearby DCs resulting in cross priming to further induce a protective response against *Mtb*. Additionally, our study observed that "response to IFN-γ" pathway in macrophages was significantly upregulated. IFN-γ is important for activating macrophages to kill engulfed *Mtb* via various mechanisms such as phagosome-lysosome fusion and generation of reactive oxygen and nitrogen intermediates (25, 39). This data indicate that myeloid cells in TPE may generate a protective response against *Mtb*.

Increasing evidence indicate that B cells and humoral immunity can modulate the immune response to various intracellular microbes, including *Mtb*, by producing cytokines and affecting T cell responses (40). B cells can present antigens to T cells with high efficiency by capturing and internalizing antigens via surface immunoglobulins. These antigens are then processed and presented on the surface as peptide:MHC class II complexes. Interestingly, B cells from TPE showed stronger antigen presenting capacity and had higher MHC II expression than B cells from TSPE and MPE, thus supporting their role as APCs that can prime T cells in TPE. We found that B cells from TPE might be activated due to the high expression of various activation genes. In addition, we observed that B cells in TPE highly expressed a wide variety of cytokines like IL6, IL10, IL-12A and TNF, which might influence the development of T cell-mediated immune response to *Mtb*. However, the detailed functions of B cell-derived cytokines in TPE remain to be evaluated. Our observations from TPE suggest that B cells may modulate the local immune response to *Mtb*.

In our attempt to explore the cellular origins of potential inflammatory cytokines, our data suggests that macrophages might be the major sources for these cytokines in TPE. This cell cluster might contribute to pro-inflammatory reaction via enhanced expression of pro-inflammatory cytokines such as CXCL10, CCL8, CCL2, TNFSF13B, IL1RN, CCL3, TNFSF13, etc. We found that hyper-inflammatory macrophages expressed multiple pro-inflammatory cytokines, highlighting potentially different mechanisms leading to the pro-inflammatory response in patients with TPE. In addition, potential cross-talk between macrophages and other cells were identified from our scRNA-seq data, as shown in Figures 6G, H. Targeting this crosstalk could be a potential strategy for controlling inflammation in future studies.

Conclusion

Our comprehensive scRNA-seq dataset which covered three PFs (TPE, TSPE and MPE) revealed unique immune features in TPE that were not previously adequately appreciated. This data offers an important resource and crucial insights in revealing the localized immune response to TPE and potentially assist in the development of new effective therapeutics against *Mtb* infection.

Methods

Study design and participants

Adults with pleural effusion were prospectively recruited and sampled at Beijing Chest Hospital (Beijing, China). Enrolled participants had been administered anti-TB drug for ≤3 days in the past 6 months, had a detailed medical record and presented a minimum of 50 mL pleural fluid volume. According to Light's criteria (41), pleural effusion was divided into exudative and transudative. For pleural TB cases, the inclusion criteria were: (1) Bacteriological evidence provided by culture, Xpert or PCR from pleural effusion; or (2) diagnosed as active pleural TB by a physician according to clinical findings, thoracoscopic reports and radiologic imaging. The exclusion criteria were: (1) had malignant tumors; (2) undergoing immunosuppressive therapy; (3) pregnant.

Sample collection

Supplementary Table 1 summarizes the characteristics of participants included in our study. Fresh PF samples from 2 patients with TSPE, 2 patients with MPE and 6 patients with TPE were immediately subjected to PFMCs isolation using standard density gradient centrifugation. Cell viability was measured using the Countstar cell viability detection kit. The cell viability was >90% for each sample and thus underwent cell encapsulation to generate 5' gene expression profiles. Amplified cDNA was generated using a commercial emulsion-based microfluidic platform (Chromium 10x) and this cDNA was used for to prepare the single cell RNA-seq libraries.

Single cell RNA library preparation and sequencing

The single cell RNA library preparation and sequencing was performed by NoveIBio Co., Ltd. (Shanghai) and as described in our previous studies (15, 42).

Quantification and Statistical analysis

Single-cell RNA-seq data analysis

Single cell RNA-seq data was processed as previously described (15, 42). Briefly, the kallisto/bustools (kb v0.24.4) pipeline was used to generate the raw and filtered gene expression matrices. The anndata (ad) (v0.7.6) and scanpy (sc) (v1.7.2) packages in python (v3.8.10) were then used to analyze the filtered feature, barcode and matrix files. Potential doublets and low-quality cells were filtered and gene expression matrix were then normalized by library size to

10,000 reads per cell as described in Wang et al. (4, 42). The sc.pp.highly_variable_genes function was used to select the consensus set of 1,500 most highly-variable genes (HVGs) and prioritize gene features in the data with high cell-to-cell variations as previously described (43).

Immune cell clustering and annotations

The sc.tl.louvain function was used to perform unsupervised clustering of cells at different resolutions. Using the neighborhood relations of cells, clustering consisted of two rounds: the first round (Louvain resolution = 2.0) identified 9 major cell types ($CD4^+$ T cells, $CD8^+$ T cells, MAIT cells, NK cells, B cells, plasma B cells, monocyte cells, dendritic cells, and macrophages) while the second round (with Louvain resolution 2.0) subdivided CD4+/CD8+ T, B, NK and DC cells into sub-clusters which represented distinct immune cell lineages within each major cell type. Each subset was confirmed by 1) manually matching canonical marker genes and 2) matching subset-specific signature genes using the sc.tl.rank_genes_groups function. Cluster annotation was also performed by manually matching canonical cell marker genes with subset-specific signature genes. Canonical marker genes and subset-specific signatures genes are provided in the main text and supplementary tables (Tables S2–S7).

Cell state scores for immune cell subtypes

Defined gene sets for the were used to define and compare the overall activation level/physiological activity of cell clusters. The inflammatory response, pro-inflammatory cytokine and exhaustion response gene sets were collected from previous studies (15, 42). The leukocyte migration gene set (GO:0050900) and response to interferon-gamma (GO:0034341) were collected from MsigDB and previous studies (44–46). The cytotoxicity score was defined using 17 cytotoxicity-associated genes (*PRF1*, *IFNG*, *GNLY*, *NKG7*, *GZMA*, *GZMB*, *GZMH*, *GZMK*, *GZMM*, *KLRK1*, *KLRB1*, *KLRD1*, *FCGR3A*, *FGFBP2*, *ZEB2*, *CTSW* and *CST7*). The phagocytosis score was defined using 25 phagocytosis-related genes (ARF6, CDC42, ARPC4, PIK3R2, WASF2, ARPC1A, ARPC2, MARCKSL1, RAC2, CFL1, RPS6KB2, PRKCE, MARCKS, VAV2, DNM2, PIK3CG, FCGR3A, VASP, ARPC3, HCK, LYN, DOCK2, PLCG2, ARPC5, PTPRC). The antigen presentation score was defined using 36 antigen presentation-related genes (LGMN, CIITA, HLA-DMB, RFX5, HLA-DMA, NFYC, CTSL, IFI30, B2M, HLA-E, TAP2, PSME1, PSME2, HLA-F, HLA-C, HSP90AB1, HSPA8, HLA-DOA, CD74, HLA-DQA2, HLA-DQB1, HLA-DRA, HLA-DRB1, HLA-DRB5, HLA-DPA1, HLA-DQA1, HLA-DPB1, HSPA4, CALR, HSP90AA1, HLA-A, PDIA3, CTSB, PSME3, HLA-B, TAP1, CD4). The exhaustion response score and exhaustion score were defined using exhaustion response genes and exhaustion markers, respectively (Table S8). The migration score was defined using LEUKOCYTE MIGRATION Pathway (GO:0050900).The Scanpy sc.tl.score_genes function was used to calculate the cell state scores, which was defined as the average expression of genes from these predefined gene sets with respect to the reference genes. Comparison of the cell state scores between different groups were statistically assessed using t-test.

Statistics

Statistical analysis and visualizations were performed in python and R and are provided with the results in the main text, in the figure legends or in the above Methods sections. The following symbols are used to indicate statistical significance for all figures: ns: $p > 0.05$; *$p <= 0.05$; **$p <= 0.01$; ***$p <= 0.001$; ****$p <= 0.0001$

Code availability

Experimental protocols and pipelines used in this study follow the 10X Genomics and Scanpy official websites. Analysis steps, functions and parameters are described in detail in the Methods section. Custom scripts used to analyze data are available upon reasonable request.

Software and algorithms

Software	SOURCE	IDENTIFIER
annadata	pypi	https://github.com/theislab/anndata
CellRanger v6.1.1	10x Genomics	http://10xgenomics.com
ggplot	bioconductor	https://ggplot2.tidyverse.org
ggpubr	bioconductor	https://github.com/kassambara/ggpubr
gseapy-0.10.7	pypi	https://pypi.org/project/gseapy
harmonypy	pypi	https://github.com/slowkow/harmonypy
kallistobustools-0.24.4	pypi	https://github.com/pachterlab/kb_python Modular, efficient and constant-memory single-cell RNA-seq preprocessing. *Nat Biotechnol* 39, 813–818 (2021).
scanpy v1.7.2	bioconda	https://github.com/theislab/scanpy
scirpy v0.7.0	bioconda	https://github.com/icbi-lab/scirpy
scrublet v0.2.3	pypi	https://github.com/swolock/scrublet
statannot	pypi	https://pypi.org/project/statannot

Data availability statement

The data presented in the study are deposited in the OMIX repository, accession number OMIX004145.

Ethics statement

Ethics approval for this study was obtained from the Beijing Chest Hospital ethics committee (ethical approval No. YNLX-2022-

005). Written informed consent was acquired from each participant. The patients/participants provided their written informed consent to participate in this study.

Author contributions

YW conceived the study. YW and GW designed the study. YW, GW, JP and LL supervised this project. XY, JY, YX, QS, YZ, RG, CHW, XuL, QL, HW, CW, XiL, SL, MZ, RW, HZ, YL and NC performed the experiments. XY, YW, GW and JP contributed the reagents, materials, and analysis tools. YW performed the software. YW, XY, GW and LL analyze the data; YW drafted the original paper. YW, LL revised and edited this paper. LL, JP, GW and YW reviewed the paper. All authors read and approved the final manuscript.

Funding

This work was supported by grants from National Key Research and Development Program of China (Grant Nos. 2021YFC2301101, 2021YFC2301102), Capital's Funds for Health Improvement and Research (2022-1G-2162), Beijing Public Health Experts Project (2022-3-040), Key Project of the Department of Science and Technology, Beijing, China (Grant Nos.D181100000418003, Z191100006619078). National Natural Science Foundation of China (82100011), LL was supported by a UTS Chancellor's Postdoctoral Research Fellowship.

Acknowledgments

We thank all the participants. We thank for the Biological samples and data resource supported by Biobank of Beijing Chest Hospital. We gratefully acknowledge the participation of Beijing Digitf Biotechnology Co., Ltd. (Beijing) for the support of data analysis, Tongyuan Gene Co., Ltd. (Qingdao) for the support of cloud computing platform, and NoveIBio Co., Ltd. (Shanghai) for construction of single cell sequencing Library, and thanks Dr. Yunke Li (Beijing Digitf Biotechnology) and Pengwei Hou (NoveIBio) and Chao Wang (NoveIBio) for their contribution.

Conflict of interest

The authors declare that the research was conducted in the absence of any commercial or financial relationships that could be construed as a potential conflict of interest.

Publisher's note

All claims expressed in this article are solely those of the authors and do not necessarily represent those of their affiliated organizations, or those of the publisher, the editors and the reviewers. Any product that may be evaluated in this article, or claim that may be made by its manufacturer, is not guaranteed or endorsed by the publisher.

Supplementary material

The Supplementary Material for this article can be found online at: https://www.frontiersin.org/articles/10.3389/fimmu.2023.1191357/full#supplementary-material

References

1. Antonangelo L, Faria CS, Sales RK. Tuberculous pleural effusion: diagnosis & management. *Expert Rev Respir Med* (2019) 13(8):747–59. doi: 10.1080/17476348.2019.1637737

2. Jia N, Wang C, Liu X, Huang X, Xiao F, Fu J, et al. A CRISPR-Cas12a-based platform for ultrasensitive rapid highly specific detection of mycobacterium tuberculosis in clinical application. *Front Cell Infection Microbiol* (2023) 13. doi: 10.3389/fcimb.2023.1192134

3. Wang Y, Huang X, Li F, Jia X, Jia N, Fu J, et al. Serum-integrated omics reveal the host response landscape for severe pediatric community-acquired pneumonia. *Crit Care* (2023) 27(1):1–17. doi: 10.1186/s13054-023-04378-w

4. Wang Y, Sun Q, Zhang Y, Li X, Liang Q, Guo R, et al. Systemic immune dysregulation in severe tuberculosis patients revealed by a single-cell transcriptome atlas. *J Infection* (2023) 86(5):421–38. doi: 10.1016/j.jinf.2023.03.020

5. Jalapathy KV, Prabha C, Das SD. Correlates of protective immune response in tuberculous pleuritis. *FEMS Immunol Med Microbiol* (2004) 40(2):139–45. doi: 10.1016/S0928-8244(03)00303-1

6. Zeng J, Song Z, Cai X, Huang S, Wang W, Zhu Y, et al. Tuberculous pleurisy drives marked effector responses of gammadelta, CD4+, and CD8+ T cell subpopulations in humans. *J Leukoc Biol* (2015) 98(5):851–7. doi: 10.1189/jlb.4A0814-398RR

7. Cartin-Ceba R, Krowka MJ. Pulmonary complications of portal hypertension. *Clin Liver Dis* (2019) 23(4):683–711. doi: 10.1016/j.cld.2019.06.003

8. Ferreiro L, Porcel JM, Bielsa S, Toubes ME, Alvarez-Dobano JM, Valdes L. Management of pleural infections. *Expert Rev Respir Med* (2018) 12(6):521–35. doi: 10.1080/17476348.2018.1475234

9. Ruan SY, Chuang YC, Wang JY, Lin JW, Chien JY, Huang CT, et al. Revisiting tuberculous pleurisy: pleural fluid characteristics and diagnostic yield of mycobacterial culture in an endemic area. *Thorax* (2012) 67(9):822–7. doi: 10.1136/thoraxjnl-2011-201363

10. Egan AM, McPhillips D, Sarkar S, Breen DP. Malignant pleural effusion. *QJM* (2014) 107(3):179–84. doi: 10.1093/qjmed/hct245

11. Mitra DK, Sharma SK, Dinda AK, Bindra MS, Madan B, Ghosh B. Polarized helper T cells in tubercular pleural effusion: phenotypic identity and selective recruitment. *Eur J Immunol* (2005) 35(8):2367–75. doi: 10.1002/eji.200525977

12. Cai Y, Wang Y, Shi C, Dai Y, Li F, Xu Y, et al. Single-cell immune profiling reveals functional diversity of T cells in tuberculous pleural effusion. *J Exp Med* (2022) 219(3): e20211777. doi: 10.1084/jem.20211777

13. Esaulova E, Das S, Singh DK, Choreno-Parra JA, Swain A, Arthur L, et al. The immune landscape in tuberculosis reveals populations linked to disease and latency. *Cell Host Microbe* (2021) 29(2):165–178 e168. doi: 10.1016/j.chom.2020.11.013

14. Szabo PA, Levitin HM, Miron M, Snyder ME, Senda T, Yuan J, et al. Single-cell transcriptomics of human T cells reveals tissue and activation signatures in health and disease. *Nat Commun* (2019) 10(1):4706. doi: 10.1038/s41467-019-12464-3

15. Wang Y, Wang X, Luu LDW, Li J, Cui X, Yao H, et al. Single-cell transcriptomic atlas reveals distinct immunological responses between COVID-19 vaccine and natural SARS-CoV-2 infection. *J Med Virol* (2022) 94(11):5304–24. doi: 10.1002/jmv.28012

16. da Cunha Lisboa V, Ribeiro-Alves M, da Silva Corrêa R, Ramos Lopes I, Mafort TT, Santos AP, et al. Predominance of Th1 immune response in pleural effusion of patients with tuberculosis among other exudative etiologies. *J Clin Microbiol* (2019) 58 (1):e00927–19. doi: 10.1128/JCM.00927-19

17. Sharma SK, Mitra DK, Balamurugan A, Pandey RM, Mehra NK. Cytokine polarization in miliary and pleural tuberculosis. *J Clin Immunol* (2002) 22(6):345–52. doi: 10.1023/A:1020604331886

18. Cavalcanti YVN, Brelaz MCA, JKdAL N, JC F. Pereira VRA. Role of TNF-alpha, IFN-gamma, and IL-10 in the development of pulmonary tuberculosis. *Pulmonary Med* (2012) 2012:745483. doi: 10.1155/2012/745483

19. Prezzemolo T, Guggino G, La Manna MP, Di Liberto D, Dieli F, Caccamo N. Functional signatures of human CD4 and CD8 T cell responses to mycobacterium tuberculosis. *Front Immunol* (2014) 5:180. doi: 10.3389/fimmu.2014.00180

20. Elmore S. Apoptosis: a review of programmed cell death. *Toxicologic Pathol* (2007) 35(4):495–516. doi: 10.1080/01926230701320337

21. Jeong S-I, Kim J-W, Ko K-P, Ryu B-K, Lee M-G, Kim H-J, et al. XAF1 forms a positive feedback loop with IRF-1 to drive apoptotic stress response and suppress tumorigenesis. *Cell Death Dis* (2018) 9(8):1–16. doi: 10.1038/s41419-018-0867-4

22. Zou B, Chim CS, Pang R, Zeng H, Dai Y, Zhang R, et al. XIAP-associated factor 1 (XAF1), a novel target of p53, enhances p53-mediated apoptosis via post-translational modification. *Mol Carcinog* (2012) 51(5):422–32. doi: 10.1002/mc.20807

23. Villani A-C, Satija R, Reynolds G, Sarkizova S, Shekhar K, Fletcher J, et al. Single-cell RNA-seq reveals new types of human blood dendritic cells, monocytes, and progenitors. *Science* (2017) 356(6335):eaah4573. doi: 10.1126/science.aah4573

24. Zhao F, Hoechst B, Duffy A, Gamrekelashvili J, Fioravanti S, Manns MP, et al. S100A9 a new marker for monocytic human myeloid-derived suppressor cells. *Immunology* (2012) 136(2):176–83. doi: 10.1111/j.1365-2567.2012.03566.x

25. Pieters J. Mycobacterium tuberculosis and the macrophage: maintaining a balance. *Cell Host Microbe* (2008) 3(6):399–407. doi: 10.1016/j.chom.2008.05.006

26. Dheda K, Schwander SK, Zhu B, Van Zyl-Smit RN, Zhang Y. The immunology of tuberculosis: from bench to bedside. *Respirology* (2010) 15(3):433–50. doi: 10.1111/j.1440-1843.2010.01739.x

27. Chan J, Mehta S, Bharrhan S, Chen Y, Achkar JM, Casadevall A, et al. The role of b cells and humoral immunity in mycobacterium tuberculosis infection. In: *Seminars in immunology: 2014*. Elsevier (2014). p. 588–600.

28. Divangahi M. *The new paradigm of immunity to tuberculosis*. New York: Springer (2013).

29. Seiscento M, Vargas F, Acencio M, Teixeira L, Capelozzi V, Sales R, et al. Pleural fluid cytokines correlate with tissue inflammatory expression in tuberculosis. *Int J tuberculosis Lung Dis* (2010) 14(9):1153–8.

30. Hooper CE, Lee YG, Maskell NA. Interferon-gamma release assays for the diagnosis of TB pleural effusions: hype or real hope? *Curr Opin pulmonary Med* (2009) 15(4):358–65. doi: 10.1097/MCP.0b013e32832bcc4e

31. Casazza JP, Betts MR, Price DA, Precopio ML, Ruff LE, Brenchley JM, et al. Acquisition of direct antiviral effector functions by CMV-specific CD4+ T lymphocytes with cellular maturation. *J Exp Med* (2006) 203(13):2865–77. doi: 10.1084/jem.20052246

32. Brown DM, Dilzer AM, Meents DL, Swain SL. CD4 T cell-mediated protection from lethal influenza: perforin and antibody-mediated mechanisms give a one-two punch. *J Immunol* (2006) 177(5):2888–98. doi: 10.4049/jimmunol.177.5.2888

33. Brown DM, Kamperschroer C, Dilzer AM, Roberts DM, Swain SL. IL-2 and antigen dose differentially regulate perforin- and FasL-mediated cytolytic activity in antigen specific CD4+ T cells. *Cell Immunol* (2009) 257(1-2):69–79. doi: 10.1016/j.cellimm.2009.03.002

34. Woodworth JS, Wu Y, Behar SM. Mycobacterium tuberculosis-specific CD8+ T cells require perforin to kill target cells and provide protection *in vivo*. *J Immunol* (2008) 181(12):8595–603. doi: 10.4049/jimmunol.181.12.8595

35. Lewinsohn DA, Heinzel AS, Gardner JM, Zhu L, Alderson MR, Lewinsohn DM. Mycobacterium tuberculosis-specific CD8+ T cells preferentially recognize heavily infected cells. *Am J Respir Crit Care Med* (2003) 168(11):1346–52. doi: 10.1164/rccm.200306-837OC

36. Dotiwala F, Sen Santara S, Binker-Cosen AA, Li B, Chandrasekaran S, Lieberman J. Granzyme b disrupts central metabolism and protein synthesis in bacteria to promote an immune cell death program. *Cell* (2017) 171(5):1125–1137.e1111. doi: 10.1016/j.cell.2017.10.004

37. Hirsch CS, Toossi Z, Vanham G, Johnson JL, Peters P, Okwera A, et al. Apoptosis and T cell hyporesponsiveness in pulmonary tuberculosis. *J Infect Dis* (1999) 179(4):945–53. doi: 10.1086/314667

38. Hirsch CS, Johnson JL, Okwera A, Kanost RA, Wu M, Peters P, et al. Mechanisms of apoptosis of T-cells in human tuberculosis. *J Clin Immunol* (2005) 25(4):353–64. doi: 10.1007/s10875-005-4841-4

39. Mihret A. The role of dendritic cells in mycobacterium tuberculosis infection. *Virulence* (2012) 3(7):654–9. doi: 10.4161/viru.22586

40. Kozakiewicz L, Phuah J, Flynn J, Chan J. The role of B cells and humoral immunity in Mycobacterium tuberculosis infection. *Adv Exp Med Biol* (2013) 783:225–50. doi: 10.1007/978-1-4614-6111-1_12

41. Light RW, Macgregor MI, Luchsinger PC, Ball WCJr. Pleural effusions: the diagnostic separation of transudates and exudates. *Ann Intern Med* (1972) 77(4):507–13. doi: 10.7326/0003-4819-77-4-507

42. Wang Y, Wang X, Jia X, Li J, Fu J, Huang X, et al. Influenza vaccination features revealed by a single-cell transcriptome atlas. *J Med Virol*. (2023) 95(1):e28174. doi: 10.1002/jmv.28174

43. Ren X, Wen W, Fan X, Hou W, Su B, Cai P, et al. COVID-19 immune features revealed by a large-scale single-cell transcriptome atlas. *Cell* (2021) 184(7):1895–1913.e1819. doi: 10.1016/j.cell.2021.01.053

44. Wilk AJ, Rustagi A, Zhao NQ, Roque J, Martínez-Colón GJ, McKechnie JL, et al. A single-cell atlas of the peripheral immune response in patients with severe COVID-19. *Nat Med* (2020) 26(7):1070–6. doi: 10.1038/s41591-020-0944-y

45. Zhang J-Y, Wang X-M, Xing X, Xu Z, Zhang C, Song J-W, et al. Single-cell landscape of immunological responses in patients with COVID-19. *Nat Immunol* (2020) 21(9):1107–18. doi: 10.1038/s41590-020-0762-x

46. Lee JS, Park S, Jeong HW, Ahn JY, Choi SJ, Lee H, et al. Immunophenotyping of COVID-19 and influenza highlights the role of type I interferons in development of severe COVID-19. *Sci Immunol* (2020) 5(49):eabd1554. doi: 10.1126/sciimmunol.abd1554

frontiers | Frontiers in Immunology

TYPE Original Research
PUBLISHED 13 July 2023
DOI 10.3389/fimmu.2023.1205449

OPEN ACCESS

EDITED BY
Jianping Xie,
Southwest University, China

REVIEWED BY
Laurence Don Wai Luu,
Univesity of Technology Sydney, Australia
Suraj P. Parihar,
Univesity of Cape Town, South Africa

*CORRESPONDENCE
Luciana Cezar de Cerqueira Leite
luciana.leite@butantan.gov.br

RECEIVED 13 April 2023
ACCEPTED 29 June 2023
PUBLISHED 13 July 2023

CITATION
Marques-Neto LM, Trentini MM, Kanno AI, Rodriguez D and Leite LCdC (2023) Recombinant BCG expressing the LTAK63 adjuvant increased memory T cells and induced long-lasting protection against *Mycobacterium tuberculosis* challenge in mice.
Front. Immunol. 14:1205449.
doi: 10.3389/fimmu.2023.1205449

Recombinant BCG expressing the LTAK63 adjuvant increased memory T cells and induced long-lasting protection against *Mycobacterium tuberculosis* challenge in mice

Lázaro Moreira Marques-Neto, Monalisa Martins Trentini, Alex Issamu Kanno, Dunia Rodriguez and Luciana Cezar de Cerqueira Leite*

Laboratório de Desenvolvimento de Vacinas, Instituto Butantan, São Paulo, Brazil

Vaccine-induced protection against *Mycobacterium tuberculosis (Mtb)* is usually ascribed to the induction of Th1, Th17, and $CD8^+$ T cells. However, protective immune responses should also involve other immune cell subsets, such as memory T cells. We have previously shown improved protection against *Mtb* challenge using the rBCG-LTAK63 vaccine (a recombinant BCG strain expressing the LTAK63 adjuvant, a genetically detoxified derivative of the A subunit from *E. coli* heat-labile toxin). Here we show that mice immunized with rBCG-LTAK63 exhibit a long-term (at least until 6 months) polyfunctional Th1/Th17 response in the draining lymph nodes and in the lungs. This response was accompanied by the increased presence of a diverse set of memory T cells, including central memory, effector memory and tissue-resident memory T cells. After the challenge, the T cell phenotype in the lymph nodes and lungs were characterized by a decrease in central memory T cells, and an increase in effector memory T cells and effector T cells. More importantly, when challenged 6 months after the immunization, this group demonstrated increased protection in comparison to BCG. In conclusion, this work provides experimental evidence in mice that the rBCG-LTAK63 vaccine induces a persistent increase in memory and effector T cell numbers until at least 6 months after immunization, which correlates with increased protection against *Mtb*. This improved immune response may contribute to enhance the long-term protection.

KEYWORDS

tuberculosis, recombinant BCG, long-term protection, adjuvant, vaccine

1 Introduction

Tuberculosis (TB) is one of the deadliest infectious diseases in the world, responsible for more than 1.3 million deaths in 2021 (1). BCG is the only licensed vaccine against TB, providing protection against severe forms of TB, especially in children. However, as protection wanes, young individuals and adults exhibit variable protection and are more susceptible to pulmonary tuberculosis (2). Given BCG's excellent safety record, adjuvant properties (heterologous protection), and effectiveness in newborns, several vaccines in development against TB seek to improve BCG's protection (3–6). In this sense, the vaccine should confer durable protection and induce a prompt and robust immune response against the bacteria in the lungs (the primary site of infection). Therefore, the generation of memory subsets is one of the main goals sought to improve TB vaccines (7, 8).

Classically, the Th1 cells (specially IFN-γ^+ or polyfunctional cells producing IFN-γ, IL-2 and/or TNF-α) have been considered the most important correlates of protection for TB vaccines. As vaccine development progressed in the field, Th17 and $CD8^+$ T cells were also considered important cell populations to induce protective responses (9). In mice, immunization with BCG preferentially induces effector T cells and effector memory T cells (TEM - $CD4^+CD44^+CD62^-$) and not central memory T cells (TCM - $CD4^+CD44^+CD62^+$). The effector T cells have an immediate effect but are believed to be vulnerable to exhaustion from chronic infection and continuous exposure to mycobacteria, contrary to TCMs. Another recombinant BCG vaccine, VPM1002 (BCGΔ*ureC*::*hly*) which is in phase III clinical trials, demonstrates that part of its protection against TB is related to an enhancement of the TCM population (10).

Beyond TCM and TEM, tissue-resident memory T cells (TRM - $KLRG1^-PD\text{-}1^+$) have also been described as cell subsets involved in protection against TB. KLRG1 and PD-1 are considered important prognosis biomarkers (8, 11). TRM is a memory T cell subset that has a long lifespan in non-lymphoid tissues; they have low body recirculation capacity, but rapidly migrate through the resident organ parenchyma and differentiate into effector cells upon stimulation. In tuberculosis, the pulmonary TRMs were shown to quickly migrate into the lung after adoptive transfer and protect against *Mtb* infection (12–15). The development of TRM, however, was only achieved when BCG was used through the mucosal route, with intradermal/subcutaneous immunization failing to induce this cell population (8, 10). Finally, the level of T cell differentiation (reduced expression of KLRG1 marker, as well as the presence of the inhibitor marker PD-1) can indicate increased IL-2 producer cells that help to maintain effector T cell populations, as well as being less sensitive to exhaustion and apoptosis in chronic infection (12, 16, 17).

The LTK63 is a genetically detoxified *E. coli* heat-labile enterotoxin mutant that exhibits a potent mucosal adjuvanticity. It has been shown that LTK63 can activate several components of the immune response, including the recruitment and activation of neutrophils, NK cells, macrophages, dendritic cells, and B and T cells (18). We have previously developed a recombinant BCG (rBCG) strain expressing the subunit A of LTK63 as an adjuvant (named rBCG-LTAK63). Immunization of mice with rBCG-LTAK63 increased innate and adaptive immune responses and improved the protection against *Mtb* challenge in comparison to BCG (19, 20). Here, we show that the immunization of mice with rBCG-LTAK63 enhances the generation of polyfunctional T cells, TCM, and TEM cells. Six months after immunization, these cells are still in higher numbers. At this time point, mice immunized with rBCG-LTAK63 when challenged with *Mtb*, displayed increased protection as compared with BCG.

2 Materials and methods

2.1 Animals and immunization

Specific-pathogen-free female BALB/c mice (4–8 weeks old), from Instituto Butantan – Central Animal Facility, were maintained in ABSL-2 racks fitted with a HEPA-filtered air intake and exhaust system. They were kept at the animal care facility of the Laboratório de Desenvolvimento de Vacinas, with water and food provided *ad libitum*. The temperature was maintained from 20–24°C, relative humidity of 40–70%, and a 12 h light/dark cycle. This study was carried out in strict accordance with the Guide for the Care and Use of Laboratory Animals of the Committee of SBCAL (Sociedade Brasileira de Ciência em Animais de Laboratório) recommendations and was approved by the Animal Research Ethical Committee of Instituto Butantan (number: 3435250619).

The rBCG-LTAK63 strain used in this work was previously described (20). BCG or rBCG-LTAK63 were grown in Middlebrook 7H9 (Difco, Detroit, MI, USA) supplemented with 10% of OADC (oleic acid-albumin-dextrose-catalase; BBL, Cockeysville, MD, USA), 0.5% glycerol and 0.05% Tween 80 (7H9-OADC) or plated on Middlebrook 7H10 agar supplemented with 0.5% glycerol and OADC (7H10-OADC).

To evaluate long-term immune response and protection, groups of mice (n=5) were immunized with BCG or rBCG-LTAK63 ($1x10^6$ CFU/100 µL) resuspended in phosphate-buffered saline (PBS- 137 mM NaCl, 2.7 mM KCl, 8 mM Na_2HPO_4, and 2 mM KH_2PO_4) and administered subcutaneously in the back of the animals.

2.2 Intranasal infection with *Mtb*

The intranasal infection was performed as described by Logan et al. (2008) (21). A frozen vial of *Mycobacterium tuberculosis* H37Rv (kept at -80°C) was thawed, and the inoculum was adjusted to $1.25x10^4$ CFU/mL with PBS. Ninety and 180 days after immunization, the groups of mice were intranasally challenged with the *Mtb* suspension (500 CFU/40 µL in one nostril). To confirm the bacterial load used, a single mouse from each group was euthanized at day 1 post-inoculation, and the lung homogenates were plated on 7H11-OADC agar. To determine protection, thirty days after infection, animals were euthanized, and the anterior and mediastinal right-lung lobes were collected, homogenized, and plated on 7H11-OADC agar. The bacterial load

was determined by counting the CFU numbers after 14-21 days of incubation at 37°C.

2.3 Cellular immune responses in draining lymph nodes and lungs

Flow cytometry analysis for specific effector T cell and memory T cell were performed as described in previous protocols (22, 23). Briefly, 90 and 180 days after the immunization, axillar draining lymph nodes and lung lobes were collected. Draining lymph nodes were prepared as single-cell suspensions using 70-µm cell strainers (BD Biosciences), and the cells were resuspended in RPMI-1640 medium supplemented with 10% fetal calf serum, 0.15% sodium bicarbonate, 1% L-glutamine and 1% nonessential amino acids.

Lung lobes were digested with DNAse IV (30 µg/mL) and collagenase III (0.7 mg/mL) for 30 min at 37°C. The digested lungs were prepared as single-cell suspensions using 70-µm cell strainers and erythrocytes lysed using an RBC lysing solution (0.15 M NH_4Cl, 10 mM $KHCO_3$). For both organs, viable cells were counted in a Neubauer chamber using Tripan Blue (0.2%), and cell concentration was adjusted to 1×10^6 cells/mL. All reagents were purchased from Sigma-Aldrich®, Merck KGaA, St. Louis, MO, USA.

Cells were plated in 96-well plates (CellWells™) and stimulated with 10 µg of BCG CFP (*"culture filtrate protein"*, a proteinaceous supernatant of a BCG grown in Sauton medium for 14 days and concentrated through a 5,000 MWCO filter), ConA (positive control) or left unstimulated and incubated at 37°C and 5% CO_2 for 4 h. Then, monensin (3 µM; eBioscience) was added and cultures were further incubated for another 4 h. Cells were then treated with 0.1% sodium azide (Sigma-Aldrich) in PBS for 30 min at room temperature and centrifuged at 400 x g for 15 min. The cellular phenotype was determined by permeabilization with Perm Fix/Perm Wash (BD Pharmingen) and incubation for 30 min with the following conjugated antibodies: TNF-α-FITC (clone MP6-XT22), IFN-γ-PE (clone XMG1.2), CD4-PerCP (clone RM4-5), CD44-APCcy7 (clone IM7), IL-17-BV421 (clone TC11-18H10), CD62L-FITC (clone MEL-14), PD-1-PE (clone J43), KLRG1-APC (clone 2F1).

Cell acquisition of 70,000 (draining lymph nodes) and 200,000 (lungs) total events per sample was performed using a BD FACS Canto II flow cytometer and data analyzed using FlowJo™ v10 Software (BD Life Sciences).

The $CD4^+$ effector T cell population was characterized as to expression of IFN-γ, TNF-α and/or IL-17, either as single, double, or triple-positive cells. Memory T cell population was characterized as: naïve ($CD4^+CD44^-CD62L^+$), central memory (TCM-$CD4^+CD44^+CD62L^+$), effector memory (TEM-$CD4^+CD44^+CD62L^-$), and tissue resident memory (TRM-$CD4^+PD\text{-}1^+KLRG1^-$) cells.

The gating strategy for all memory T cell subsets is shown in Supplementary Materials. Supplementary Figure 1 depicts gating for naïve/TEM/TCM (Supplementary Figure 1A) and an example of analysis in the lymph node for each group in both time points (Figure 1B). Supplementary Figure 2 shows gating for TRM (Supplementary Figure 2A) and an example of analysis in the lungs for each group in both time points (Figure 2B). Supplementary Figure 3 displays an example of lymph nodes analysis, based on FMO of a single functional T cell, producing IFN-γ (Supplementary Figure 3A), TNF-α (Supplementary Figure 3B), or IL-17 (Supplementary Figure 3C). Cytokine events were background corrected based on this FMO.

The number of cells in each organ was quantified by multiplying the percentage of cells in each gate by the number of live cells counted in the Neubauer chamber.

2.4 Statistical analysis

Results were tabulated using the software GraphPad Prism 9 (GraphPad, La Jolla, CA, USA). The violin plot was plotted in Origin (Pro), Version Number (2022b – OriginLab Corporation, Northampton, MA, USA). The differences between groups were assessed using one-way ANOVA. Differences in p values < 0.05 were considered statistically significant. All biological experiments were performed at least twice, repeating the immunization and assessments of immune response and protection".

3 Results

3.1 rBCG-LTAK63 improves Th1, Th17, memory T cells, and protection, 90 days after immunization

Protection against TB is correlated with an increased Th1/Th17 cytokine response observed at the time of challenge (Figure 1A). In agreement, here we show that mice immunized with rBCG-LTAK63 displayed a general increase in the Th1 and Th17 cell populations. At 90 days after immunization, there was an increase of a diverse milieu of $CD4^+$ T cells expressing TNF-α, IFN-γ and IL-17 either alone or in combination (double and triple polyfunctional cells) in draining lymph nodes and lungs (Figures 1B, C).

In the lymph nodes, rBCG-LTAK63 immunization induced an increased percentage of $CD4^+$ single TNF-α and IL-17-producing cells, and combinations of double TNF-α, IFN-γ, and IL-17-producing cells at 90 days. The most significant differences in terms of percentage and in the difference as compared to BCG were in $CD4^+TNF\text{-}\alpha^+$ single positive, $CD4^+IFN\text{-}\gamma^+IL\text{-}17^+$ (double positive), and the triple polyfunctional T cells (Figure 1B). In the lungs as the target organ, the single $CD4^+$ T cells producing IFN-γ and TNF-α, and the double polyfunctional T cells were also increased as compared to BCG. In this case, the largest differences were seen with the $CD4^+IFN\text{-}\gamma^+$ and the triple positive $CD4^+TNF\text{-}\alpha^+IFN\text{-}\gamma^+IL\text{-}17^+$ T cells (Figure 1C).

Regarding the numbers of polyfunctional T cells in the lymph node, the triple positive $CD4^+TNF\text{-}\alpha^+IFN\text{-}\gamma^+IL\text{-}17^+$ T cells showed the largest difference compared to BCG (Figure 1C). In the lungs, the double positive $CD4^+TNF\text{-}\alpha^+IL\text{-}17^+$ T cells were in larger numbers in the rBCG-LTAK63-immunized animals as compared to the BCG group, with a corresponding decrease in the numbers of $CD4^+IFN\text{-}\gamma^+IL\text{-}17^+$ T cells (Figure 1D).

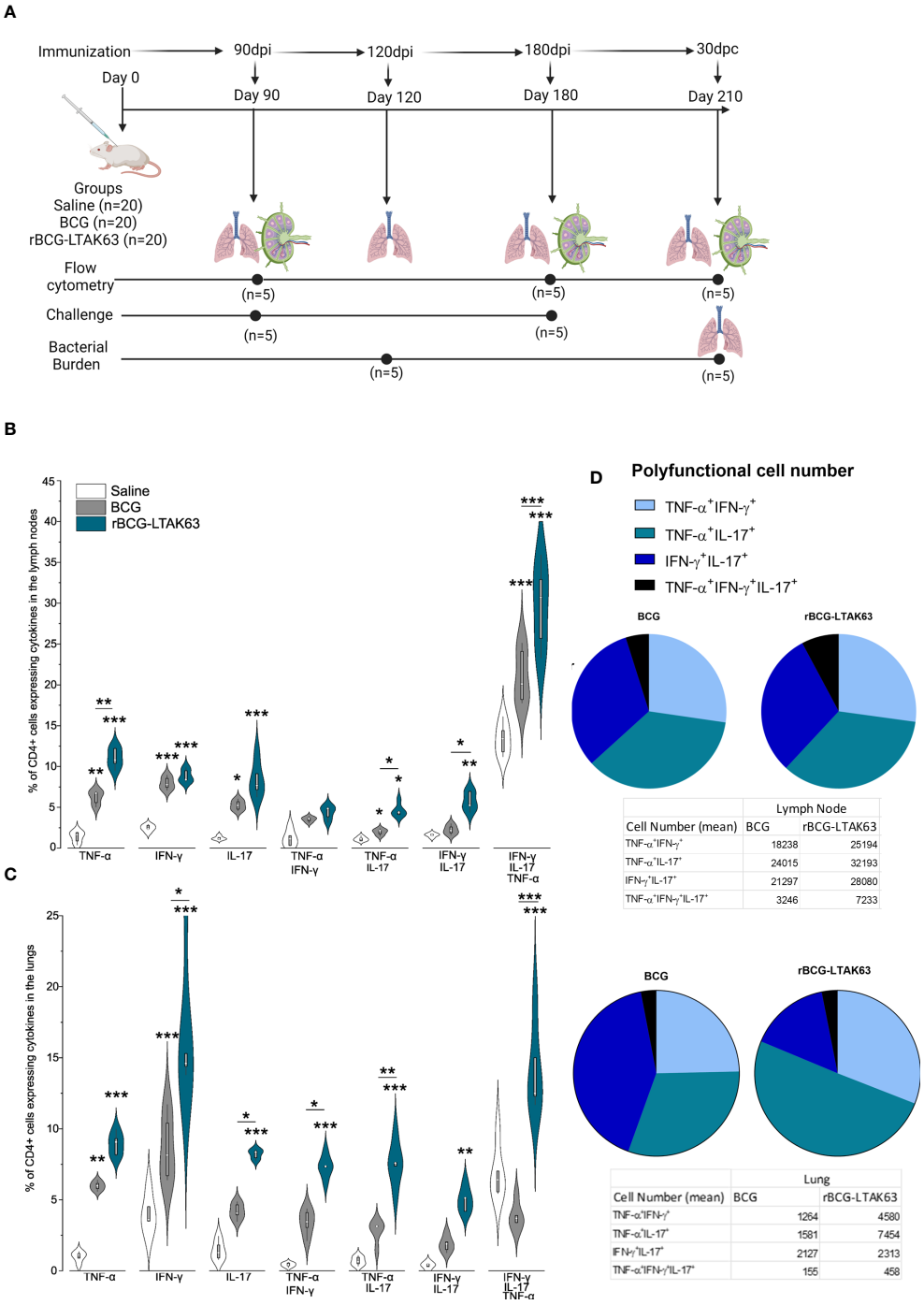

FIGURE 1
Increased induction of Th1, Th17, and polyfunctional cells in the draining lymph nodes and lungs of rBCG-LTAK63-immunized mice, 90 days after immunization. **(A)** Experimental design of the long-term immune response and protection performed. Created with BioRender.com. Twenty animals were immunized on day 0 with wild-type BCG or rBCG-LTAK63 or mock saline (n=20 per group). Immune responses were evaluated 90 and 180 days after immunization (n=5 per group). Challenges were performed 90 and 180 days after immunization and the protection was evaluated 30 days later (n=5 per group). In the last challenge evaluation (210 days after immunization) the immune response was also measured. Groups of BALB/c mice (n=5/group) were subcutaneously immunized with wild-type BCG or rBCG-LTAK63, and control groups received saline. Axillary lymph nodes **(B)** and lungs **(C)** were collected at 90 days after immunization and cellular suspensions were re-stimulated with CFP (culture filtrate proteins) to evaluate the presence of $CD4^+$ single and polyfunctional effector T cell subsets. Violin plots with box whiskers represent the data distribution, median and outliers. **(D)** The pie charts depict the number of polyfunctional cells in evaluated organs. (*) Represents the statistical comparison between groups (*$p \leq 0.05$, **$p \leq 0.01$, ***$p \leq 0.001$). Differences were considered statistically significant when $p \leq 0.05$ as compared to saline or BCG group (one-way ANOVA). The (*) above violin plots indicated comparison with the saline control and the (*) bar showed all other group comparisons. The figure shows a representative of two independent experiments.

Since an increased presence of effector $CD4^+$ T cells was observed until 90 days after the immunization with rBCG-LTAK63, we assessed vaccine-induced memory T cells in the draining lymph nodes and lungs of immunized mice. In the lymph nodes, mice immunized with rBCG-LTAK63 displayed a tendency to decrease the naïve T cell population and significantly increased TCM and TEM cells as compared to BCG (Figure 2A). In the lungs, the same tendency was observed; in this case, rBCG-LTAK63 immunization displayed significantly larger percentages of the TCM and TEM cell populations. There was a trend to an increase in TRM in rBCG-LTAK63-immunized animals as compared to the saline group; however, this increase was not significant (p value 0.17) (Figure 2B).

We had previously shown that rBCG-LTAK63-immunization induces protection against *Mtb* challenge in the intratracheal model of infection, 90 days after immunization (20). Hence, we here confirmed protection against *Mtb* challenge using the intranasal model, 90 days after immunization with rBCG-LTAK63. Animals were administered 500 CFU of *M. tuberculosis* H37Rv intranasally and the bacterial load in the lungs was measured thirty days after the challenge. Also in the intranasal infection model, rBCG-LTAK63 immunization induces better protection than BCG, reducing the bacillary load by more than two logs as compared to the non-immunized group and one log as compared to BCG (Figure 2C).

3.2 The protective immune response induced by rBCG-LTAK63 immunization is maintained for up to 180 days after immunization

To determine if the enhanced TEM and TCM cells at 90 days could increase the duration of protection, mice were immunized subcutaneously with 10^6 CFU (BCG or rBCG-LTAK63), and we assessed TEM and TCM generation, and protection against challenge 180 days later. At 180 days, the $CD4^+$ T cells expressing TNF-α, IFN-γ, or IL-17 remained at higher levels in rBCG-LTAK63-immunized animals in comparison to the BCG group in both organs (Figures 3A, B). In the lymph nodes, only $CD4^+$TNF-α^+IL-17^+ double positive is present at a higher level (Figure 3A), while in the lungs, $CD4^+$TNF-α^+IL-17^+, $CD4^+$IFN-γ^+IL-17^+ double positives are increased, together with the triple-positive T cells (Figure 3B).

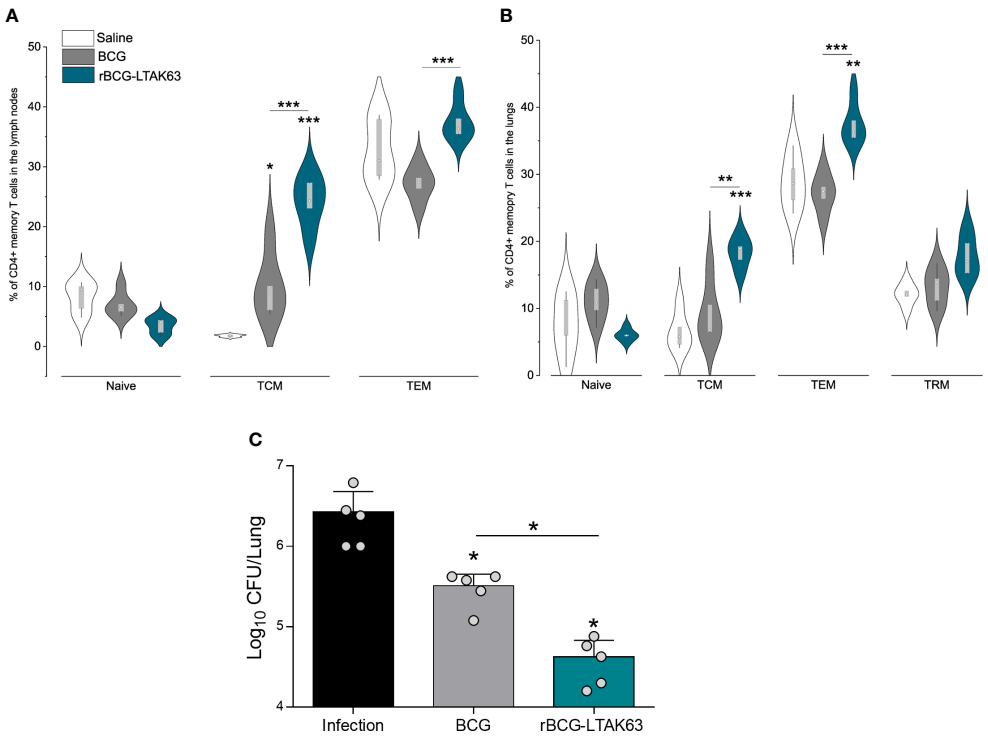

FIGURE 2
Generation of memory T cells and protection of mice immunized with rBCG-LTAK63, 90 days after immunization. BALB/c mice (n=5/group) were immunized with either BCG or rBCG-LTAK63 (10^6 CFU); control groups received saline. Lymph node and lung cells were isolated after 90 days and were *in vitro* re-stimulated with CFP to evaluate memory T cell subsets. Memory T cells were characterized as naïve T cells ($CD4^+CD44^-CD62L^+$), central memory T cells (TCM-$CD4^+CD44^+CD62L^+$), effector memory T cells (TEM - $CD4^+CD44^+CD62L^-$) present in the lymph nodes **(A)** and lungs **(B)** of immunized animals. Tissue-resident memory T cells were characterized as $CD4^+PD\text{-}1^+KLRG\text{-}1^-$ in the animal's lungs **(B)**. Violin plots with box whiskers represent the data distribution, median, and outliers. **(C)** Immunized and control animals were challenged intranasally with 500 CFU of *M. tuberculosis* H37Rv 90 days after immunization, and the lung bacillary load was assessed 30 days after infection. (*) Displays the statistical comparison between groups (*$p \leq 0.05$, **$p \leq 0.01$, ***$p \leq 0.001$). Differences were considered statistically significant when $p \leq 0.05$ as compared to the saline or BCG group (one-way ANOVA). Bars represent mean ± S.D. The (*) above violin plots indicated comparisons with the saline control and the (*) bar showed all other group comparisons. The figure shows a representative of two independent experiments.

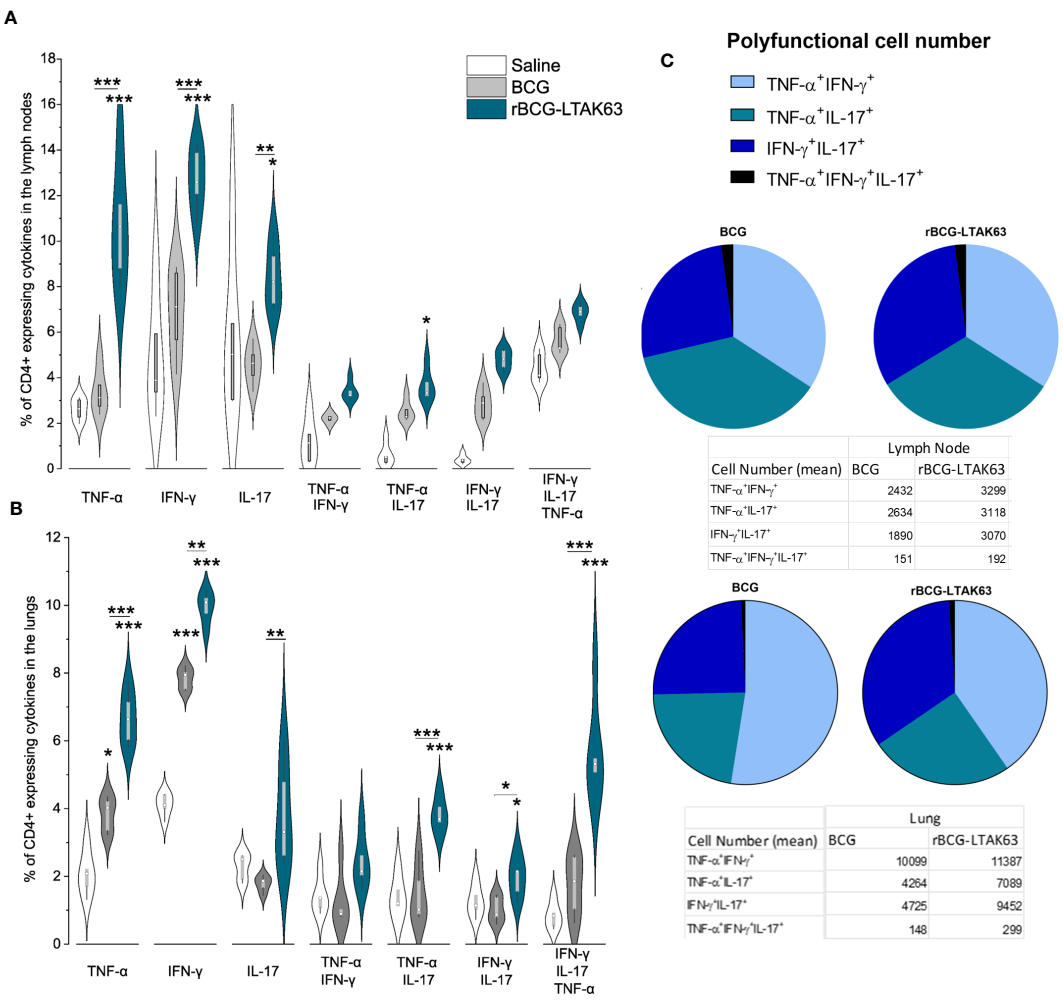

	Lymph Node	
Cell Number (mean)	BCG	rBCG-LTAK63
TNF-α+IFN-γ+	2432	3299
TNF-α+IL-17+	2634	3118
IFN-γ+IL-17+	1890	3070
TNF-α+IFN-γ+IL-17+	151	192

	Lung	
Cell Number (mean)	BCG	rBCG-LTAK63
TNF-α+IFN-γ+	10099	11387
TNF-α+IL-17+	4264	7089
IFN-γ+IL-17+	4725	9452
TNF-α+IFN-γ+IL-17+	148	299

FIGURE 3
Increased induction of Th1, Th17, and polyfunctional cells in the draining lymph nodes and lungs of rBCG-LTAK63-immunized mice, 180 days after immunization. Groups of BALB/c mice (n=5/group) were subcutaneously immunized with BCG or rBCG-LTAK63; the control group received saline. Axillary lymph nodes **(A)** and lungs **(B)** were collected at 180 days after immunization and cellular suspensions were re-stimulated with CFP (culture filtrate proteins) to evaluate the presence of $CD4^+$ effector T cell subsets. Violin plots with box whiskers represent the data distribution, median, and outliers. **(C)** The pie chart depicts the number of polyfunctional cells in evaluated organs. (*) Displays the statistical comparison between groups (*$p \leq 0.05$, **$p \leq 0.01$, ***$p \leq 0.001$). Differences were considered statistically significant when $p \leq 0.05$ as compared to saline or BCG group (one-way ANOVA). The (*) above violin plots indicated comparison with the saline control and the (*) bar showed all other group comparisons. The figure shows a representative of two independent experiments.

Regarding the number of polyfunctional T cells in the lymph node, the double positive $CD4^+IFN\text{-}\gamma^+IL\text{-}17^+$ T cells displayed the largest difference compared to BCG (Figure 3C). In the lungs, the double positive $CD4^+TNF\text{-}\alpha^+IFN\text{-}\gamma^+$ T cells were in larger numbers in both groups, but the $CD4^+IFN\text{-}\gamma^+IL\text{-}17^+$ T cells were higher in the rBCG-LTAK63 group (Figure 3C).

An increase in TEM cell populations occurs in both organs at 180 days after rBCG-LTAK63 immunization, while there is no alteration of TEM in BCG groups (Figures 4A, B). Only rBCG-LTAK63 showed a higher percentage of TCM in the draining lymph node, as compared to BCG (Figure 4A). There is also an increase in TRM cells in the lungs of rBCG-LTAK63-immunized animals (Figure 4B).

In terms of protection, even after 180 days, rBCG-LTAK63 immunization sustained higher protection against intranasal challenge with *Mtb*, reducing the bacillary load in the animals' lungs by nearly two logs (Figure 4C).

3.3 Challenge with *Mtb* induces TEM differentiation and Th1/Th17 recall in animals immunized with rBCG-LTAK63

Mice were immunized with BCG or rBCG-LTAK63, challenged with *Mtb* 180 days later, and the memory cells (naive, TCM, and TEM) were examined using flow cytometry 30 days later. TEM response in infected animal lymph nodes was higher in animals immunized with rBCG-LTAK63 than in those only infected (Figure 5A). In the lungs, TEM was higher in rBCG-LTAK63 group than in both the BCG and infected groups (Figure 5B).

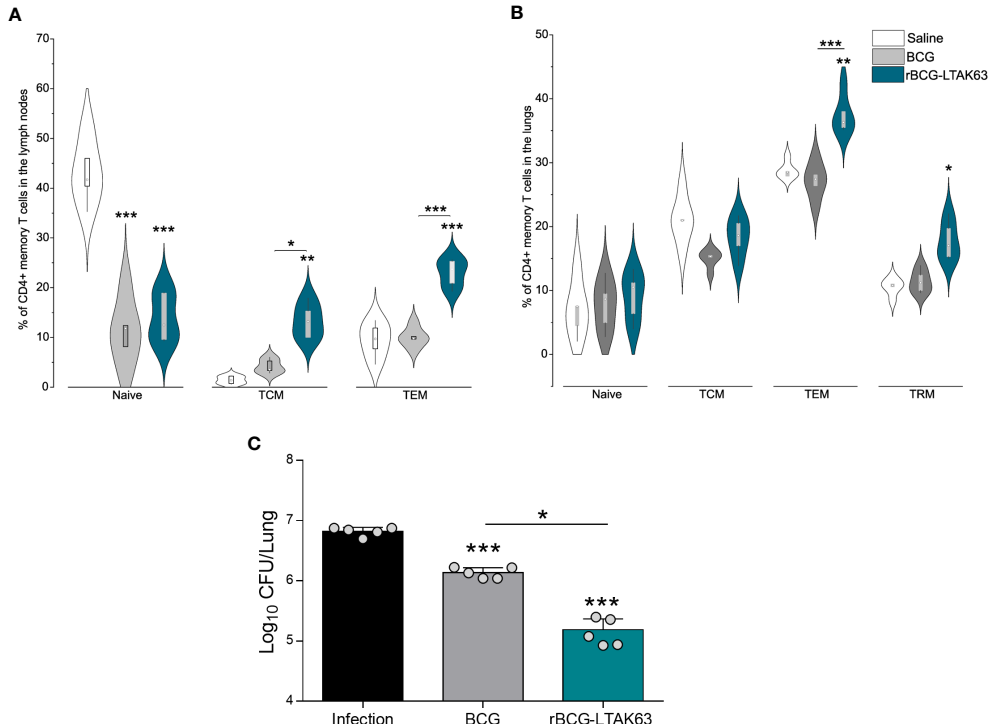

FIGURE 4
Generation of memory T cells and protection of mice immunized with rBCG-LTAK63, 180 days after immunization. BALB/c mice (n=5/group) were immunized with either BCG or rBCG-LTAK63 (10^6 CFU); the control group received saline. Lymph node and lung cells were isolated after 180 days and *in vitro* re-stimulated with CFP to evaluate memory T cell subsets. **(A)** Memory T cells were characterized as naïve T cells ($CD4^+CD44^-CD62L^+$), central memory T cells (TCM-$CD4^+CD44^+CD62L^+$), effector memory T cells (TEM-$CD4^+CD44^+CD62L^-$) present in the lymph nodes **(A)** and lungs **(B)** of immunized animals. Tissue-resident memory T cells were characterized as $CD4^+PD\text{-}1^+KLRG\text{-}1^-$ in the animal's lungs **(B)**. Violin plots with box whiskers represent the data distribution, median and outliers. **(C)** Animals were challenged intranasally with 500 CFU of *Mycobacterium tuberculosis* H37Rv 180 days after immunization, and the lung bacillary load was assessed 30 days after infection. (*) Displays the statistical comparison between groups (*$p \leq 0.05$, **$p \leq 0.01$, ***$p \leq 0.001$). Differences were considered statistically significant when $p \leq 0.05$ as compared to saline or BCG group (one-way ANOVA). Bars represent mean ± S.D. The (*) above violin plots indicated comparison with the saline control and the (*) bar showed all other group comparisons. The figure shows a representative of two independent experiments.

TCM population showed no significant difference between groups in both organs as compared to BCG.

The increase in the TEM population in the infected animal's lungs indicates a possible differentiation from TCM into TEM and further into effector cells. Therefore, we also evaluated the Th1 and Th17 responses. The infection with *Mtb* increases $CD4^+TNF\text{-}\alpha^+$, $CD4^+IFN\text{-}\gamma^+$, and $CD4^+IL\text{-}17^+$ in the lymph nodes of rBCG-LTAK63 immunized animals (Figure 5C), while in the lungs, there was a drastic difference in $CD4^+IFN\text{-}\gamma^+$, and $CD4^+IL\text{-}17^+$, when compared with BCG (Figure 5D).

Finally, we compared the cell population dynamics across all time points during a longer period of immunization and infection. Regardless of the vaccine used, we can see that after a long period of immunization (180 dpi - before challenge), there is a tendency to decrease in all populations studied, most notably in the lungs of animals (Figure 6). Following infection, there is a decrease in the population of TCM cells in both organs and a considerable increase in the TEM cells in the lungs of the animals immunized with rBCG-LTAK63 (Figures 6G–J). At the same time, there is an increase in the TNF-α (6B) and IL-17 (6F) producing $CD4^+$ T cells in the lungs of the rBCG-LTAK63 group, but they remain stable in the BCG group.

4 Discussion

In this study, we show that immunization with rBCG-LTAK63 produces a broader range of effector cells than BCG. It also stimulates the production of more memory cells, primarily TCM. This leads to superior and longer-lasting protection against *Mycobacterium tuberculosis*. To obtain protection against TB, several $CD4^+$ T cell subsets should be induced by immunization. Initially, Th1 and Th17 are the main effector cells associated with protection (24). Together, pre-existent TCM, after antigen re-exposure or infection, differentiates into TEM and then into Th1 or Th17 cells that migrate and exert their effector functions in infected tissues. A proportion of these T cells subsequently remain in the lung as TRM and constitute an efficient frontline defense in the organ. These also can turn into Th1/Th17 effector cells, or rapidly recruit new effector cells after infection. In a chronic infection like *Mtb*, the longevity of the immune response and its resistance to continuous antigen exposure without exhaustion, is of equal importance. Hence, cells with lower expression of KLRG1 play a central role, because their proliferative potential can maintain the T cells in the tissue as the infection lasts (8, 25).

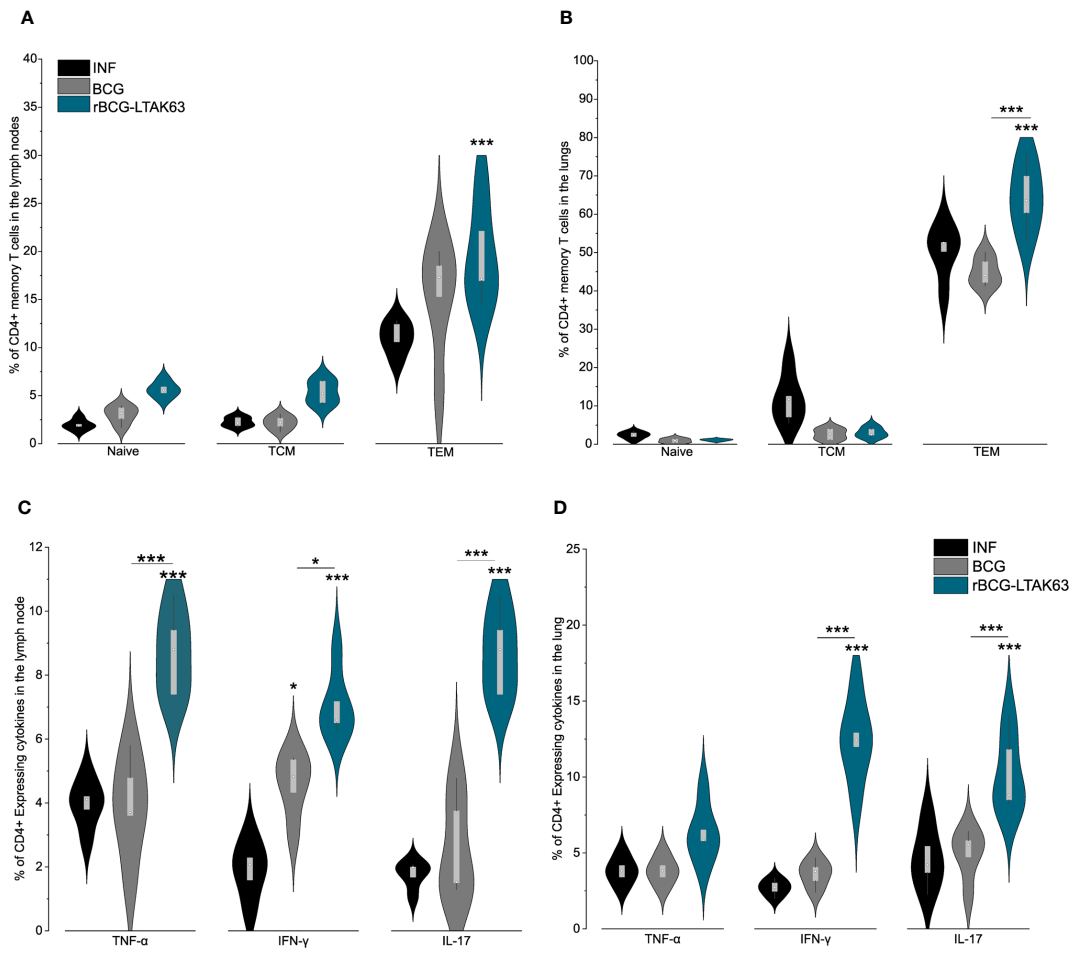

FIGURE 5
rBCG-LTAK63 induces higher effector and effector memory T cell after infection. BALB/c mice (n=5/group) were immunized with either BCG or rBCG-LTAK63 (10^6 CFU); the control group received saline. Animals were challenged intranasally with 500 CFU of *Mycobacterium tuberculosis* H37Rv 180 days after immunization; lymph nodes and lung cells were isolated 30 days after infection. Memory T cells were characterized as naïve T cells ($CD4^+CD44^-CD62L^+$), central memory T cells (TCM-$CD4^+CD44^+CD62L^+$), effector memory T cells (TEM - $CD4^+CD44^+CD62L^-$) present in the lymph nodes **(A)** and lungs **(B)** of immunized animals. The lymph nodes **(C)** and lung **(D)** cells were isolated 30 days after infection to evaluate the presence of $CD4^+$ effector T cell subsets. Violin plots with box whiskers represent the data distribution, median, and outliers. (*) Displays the statistical comparison between groups (*$p \leq 0.05$, ***$p \leq 0.001$). Differences were considered statistically significant when $p \leq 0.05$ as compared to infection or BCG (one-way ANOVA). The (*) above violin plots indicated comparison with the saline control and the (*) bar showed all other group comparisons. The figure shows a representative of two independent experiments.

The protective mechanism(s) of polyfunctional $CD4^+$ T cells induced by vaccines or natural infection are still unknown. However, it has been considered that cells that express multiple effector functions may be more effective at controlling *Mtb* infection than cells that produce a single cytokine. We had previously shown that rBCG-LTAK63 elicited an increased protective response (as compared with BCG) when immunized mice were challenged with H37Rv or a highly virulent Beijing strain (intratracheally) at 90 days after immunization (20). Here we confirmed the previous results in an intranasal challenge model and show that when immunized mice were challenged after 180 days, this improved protection is maintained (Figures 2, 4). Immunization with rBCG-LTAK63 increases Th1 and Th17 single and polyfunctional responses in the lymph node and lungs, for up to 180 days, in contrast to BCG. This long-term protective response is directly associated with the production of Th1 responses, which activate macrophages, stimulate phagocytosis, phagosome maturation, nitrogen reactive production, and improve antigen presentation (26). At the same time, Th17 cells mediate antibacterial and pro-inflammatory responses, contributing to the generation of protective immune responses and memory cells, and support Th1 cell reactivity by down-regulating IL-10 and up-regulating IL-12 production. These responses can protect against tuberculosis infection in the absence of a Th1 response (27, 28).

We have previously demonstrated that intraperitoneal inoculation of rBCG-LTAK63 induced increased recruitment of $CD4^+$ lymphocytes (19). Moreover, *in vitro* studies with human macrophages demonstrated that rBCG-LTAK63 upregulated interferon-inducible, antimicrobial, and inflammatory cytokines, and induced tissue repair genes when compared to BCG. Specifically, rBCG-LTAK63-infected macrophages produced higher levels of inflammatory cytokines including IL-12(p70),

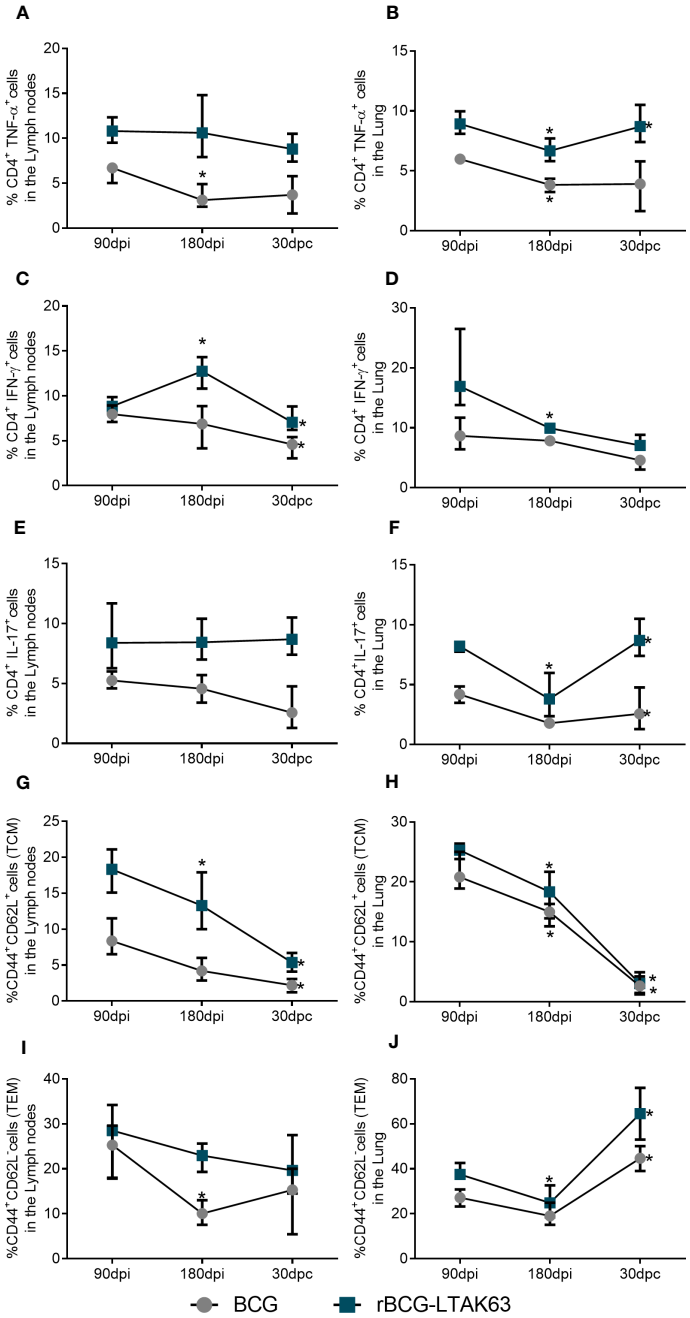

FIGURE 6
Dynamics of the T cell population show increased TEM and effector T cells after *Mtb* challenge in the lungs of rBCG-LTAK63 immunized animals. Evolution of the cell populations of immunized animals at 90 days (90dpi) and 180 days after immunization (180 dpi), and 30 days after challenge (30dpc): $CD4^+TNF\text{-}\alpha^+$ T cells in lymph nodes **(A)** and lungs **(B)**; $CD4^+IFN\text{-}\gamma^+$ T cells in lymph nodes **(C)** and lungs **(D)**; $CD4^+IL\text{-}17^+$ T cells in lymph nodes **(E)** and lungs **(F)**; TCM ($CD4^+CD44^+CD62L^+$) cell populations in lymph nodes **(G)** and lungs **(H)**; TEM ($CD4^+CD44^+CD62L^-$) in the lymph nodes **(I)** and lungs **(J)**. Bars represent ± S.D. *Statistical difference ($p \leq 0.05$) as compared to the prior timepoint in two-way ANOVA test.

TNF-α, and IL-15 (29). Our work demonstrates that immunization with rBCG-LTAK63 induces TCM cells in the lymphoid organ (Figure 2), as well as TRM cells in the lungs (Figure 4). IL-15 (together with IL-7 and IL-2) plays a crucial function in memory T cell development and homeostasis and may explain the TRM and TEM generation. However, the TCM generation seems to be IL-15 independent, and the mechanism by which rBCG-LTAK63 induces TCM is still unknown (30–32). In the TCM and TEM cell population study, it was demonstrated that rBCG-LTAK63 enhances the TCM response and, as expected, this response is maintained in the lymphoid organ while also increased in the animal's lungs. This improvement is one of the most auspicious characteristics of rBCG-LTAK63 described here. In adoptive transfer studies, TCM generated by VPM1002 immunization was demonstrated to be partly responsible for its increased protection (10).

After the infection, it is expected that the TCM cells differentiate into TEM cells, which migrate from the lymphoid organ to the lungs (3). TCM are not different between the recombinant vaccine and wild-type BCG, while TEM cells are increased in the lungs after infection (Figures 5, 6). This can indicate a possible differentiation of TCM into TEM. Differentiation of TEM will induce an increase in effector T cells (Th1/Th17), and we can see this enhancement in lymph node $CD4^+TNF\text{-}\alpha^+/CD4^+IFN\text{-}\gamma^+/CD4^+IL\text{-}17^+$, and in the lungs $CD4^+IFN\text{-}\gamma^+/CD4^+IL\text{-}17^+$ (Figure 6). Our previous work showed that rBCG-LTAK63 reduces NF-κB, IL-12, IFN-γ, TNF-α, and IL-17 after challenge while increasing TGF-β (20). Our results differ from the previous one, most likely due to the method used. In that case, cytokine production was evaluated using RNA transcription, which measures the total cytokine expressed in the tissue. The reduction in total inflammatory cytokine production correlates with the decrease in CFU and in the inflammation area. Here we show the increase in specific T-cell response, which agrees with the later paper that showed an increase in $CD4^+TNF\text{-}\alpha^+$ cells in animals immunized with rBCG-LTAK63, fifteen days after H37Rv infection (19).

The long-term protection induced against tuberculosis can be associated with other memory T cells such as the TRM cells; KLRG-1/PD-1 marked T cells are one of the most prominent subsets (16, 17). TRM cells are non-lymphoid tissue memory cells that were shown to be induced in BCG only when the vaccine is intranasally delivered (15, 33). They are considered to be highly protective against tuberculosis (14, 33). Here, the immunization with BCG or rBCG-LTAK63 was performed subcutaneously. Surprisingly, rBCG-LTAK63 improved the generation of TRM (Figure 4), which reaches statistical significance at 180 days after immunization. Again, this can be associated to IL-15 production, which also plays an important role in TRM generation and maintenance (30). It is important to observe that a limitation to this study subset is in the characterization of the TRM population. While the expression of PD-1+ KLRG1- has been used as a marker for TRM, these cells can also be found in the vasculature, BAL, and parenchyma. Therefore, in order to confirm that these are actually lung tissue resident cells, we could include CXCR3 as a marker *in vitro* or perform *in vivo* CD45 labeling.

The T CD8 cell populations did not reveal any significant differences between BCG and rBCG-LTAK63 (data not shown). The genetically detoxified LTKA63 protein does not display the same toxicity as LTA, which is an adenylyl cyclase activator; however, LTKA63 maintains part of the adjuvanticity of the original protein. Since neither LTA nor LTAK63 produce cross-presentation, phagosome scape, or any other CD8-inducing function, it was not expected that rBCG-LTAK63 would have this effect. It is important to note that here we do not explore the influence of rBCG-LTAK63 on crucial cell populations involved in tuberculosis protection and protective immunity development (i.e., dendritic cells, monocytes, macrophages), and we use a single gender and mouse strain (34, 35). The next stages should address these limitations using mice strains with diverse tuberculosis susceptibility (e.g., CBA, C3HeB/FeJ, DBA/2, and 129SvJ), different animal genders, and evaluating other possible processes associated with the rBCG-LTAK63 protective effect.

Overall, our findings show that rBCG-LTAK63 immunization increased the levels of several memory T cell subsets, which correlates with the longer-lasting protection observed against challenge. These findings suggest that rBCG-LTAK63 can induce a more durable and stable immune response and protection, which could address some of the current BCG vaccine issues.

Data availability statement

The raw data supporting the conclusions of this article will be made available by the authors, without undue reservation.

Ethics statement

The animal study was reviewed and approved by 3435250619.

Author contributions

LM-N, MT, DR, AK, and LL conceived and designed the experiments; MT and LM-N performed the experiments and collected data; LM-N, MT, DR, AK, and LL processed and analyzed the data; LM-N, MT, AK, and LL wrote the manuscript, and all authors critically revised the manuscript.

Funding

We acknowledge the support from FAPESP (Projects 2017/24832-6, 2019/06454-0 and 2019/02305-0) and Fundação Butantan.

Conflict of interest

LL has a patent application on the use of rBCG-LTAK63 as a vaccine against *Mtb*.

The remaining authors declare that the research was conducted in the absence of any commercial or financial relationships that could be construed as a potential conflict of interest.

Publisher's note

Supplementary material

The Supplementary Material for this article can be found online at: https://www.frontiersin.org/articles/10.3389/fimmu.2023.1205449/full#supplementary-material

References

1. World Heath Organization. *Global tuberculosis report 2022*. Geneva: World Health Organization (2022). Licence: CC BY-NC-SA 3.0 IGO.

2. Harding E. WHO global progress report on tuberculosis elimination. *Lancet Respir Med* (2020) 8:19. doi: 10.1016/S2213-2600(19)30418-7

3. Angelidou A, Diray-Arce J, Conti MG, Smolen KK, van Haren SD, Dowling DJ, et al. BCG As a case study for precision vaccine development: lessons from vaccine heterogeneity, trained immunity, and immune ontogeny. *Front Microbiol* (2020) 11:332. doi: 10.3389/fmicb.2020.00332

4. Lalor MK, Floyd S, Gorak-Stolinska P, Ben-Smith A, Weir RE, Smith SG, et al. BCG Vaccination induces different cytokine profiles following infant BCG vaccination in the UK and Malawi. *J Infect Dis* (2011) 204:1075–85. doi: 10.1093/infdis/jir515

5. Garly ML, Martins CL, Balé C, Baldé MA, Hedegaard KL, Gustafson P, et al. BCG Scar and positive tuberculin reaction associated with reduced child mortality in West Africa. a non-specific beneficial effect of BCG? *Vaccine* (2003) 21:2782–90. doi: 10.1016/s0264-410x(03)00181-6

6. Roth A, Jensen H, Garly ML, Djana Q, Martins CL, Sodemann M, et al. Low birth weight infants and Calmette-Guérin bacillus vaccination at birth: community study from Guinea-Bissau. *Pediatr Infect Dis J* (2004) 23:544–50. doi: 10.1097/01.inf.0000129693.81082.a0

7. Tonaco MM, Moreira JD, Nunes FFC, Loures CMG, Souza LR, Martins JM, et al. Evaluation of profile and functionality of memory T cells in pulmonary tuberculosis. *Immunol Lett* (2017) 192:52–60. doi: 10.1016/j.imlet.2017.10.014

8. Henao-Tamayo M, Ordway DJ, Orme IM. Memory T cell subsets in tuberculosis: what should we be targeting? *Tuberculosis* (2014) 94:455–61. doi: 10.1016/j.tube.2014.05.001

9. de Martino M, Lodi L, Galli L, Chiappini E. Immune response to Mycobacterium tuberculosis: a narrative review. *Front Pediatr* (2019) 7:350. doi: 10.3389/fped.2019.00350

10. Vogelzang A, Perdomo C, Zedler U, Kuhlmann S, Hurwitz R, Gengenbacher M, et al. Central memory CD4+ T cells are responsible for the recombinant Bacillus Calmette-Guérin ΔureC::hly vaccine's superior protection against tuberculosis. *J Infect Dis* (2014) 210:1928–37. doi: 10.1093/infdis/jiu347

11. Counoupas C, Triccas JA. The generation of T-cell memory to protect against tuberculosis. *Immunol Cell Biol* (2019) 97:656–63. doi: 10.1111/imcb.12275

12. Lindenstrøm T, Knudsen NPH, Agger EM, Andersen P. Control of chronic Mycobacterium tuberculosis infection by CD4 KLRG1– IL-2–secreting central memory cells. *J Immunol* (2013) 190:6311–9. doi: 10.4049/jimmunol.1300248

13. Yang Q, Zhang M, Chen Q, Chen W, Wei C, Qiao K, et al. Cutting edge: characterization of human tissue-resident memory T cells at different infection sites in patients with tuberculosis. *J Immunol* (2020) 204:2331 LP – 2336. doi: 10.4049/jimmunol.1901326

14. Ogongo P, Porterfield JZ, Leslie A. Lung tissue resident memory T-cells in the immune response to Mycobacterium tuberculosis. *Front Immunol* (2019) 10:992. doi: 10.3389/fimmu.2019.00992

15. Perdomo C, Zedler U, Kühl AA, Lozza L, Saikali P, Sander LE, et al. Mucosal BCG vaccination induces protective lung-resident memory T cell populations against tuberculosis. *MBio* (2016) 7:e01686-16. doi: 10.1128/mBio.01686-16

16. Hu Z, Zhao H-M, Li C-L, Liu X-H, Barkan D, Lowrie DB, et al. The role of KLRG1 in human CD4+ T-cell immunity against tuberculosis. *J Infect Dis* (2018) 217:1491–503. doi: 10.1093/infdis/jiy046

17. Boer MC, van Meijgaarden KE, Goletti D, Vanini V, Prins C, Ottenhoff THM, et al. KLRG1 and PD-1 expression are increased on T-cells following tuberculosis-treatment and identify cells with different proliferative capacities in BCG-vaccinated adults. *Tuberculosis* (2016) 97:163–71. doi: 10.1016/j.tube.2015.11.008

18. Tritto E, Muzzi A, Pesce I, Monaci E, Nuti S, Galli G, et al. The acquired immune response to the mucosal adjuvant LTK63 imprints the mouse lung with a protective signature. *J Immunol* (2007) 179:5346–57. doi: 10.4049/jimmunol.179.8.5346

19. Carvalho Dos Santos C, Rodriguez D, Kanno Issamu A, Cezar De Cerqueira Leite L, Pereira Nascimento I. Recombinant BCG expressing the LTAK63 adjuvant induces increased early and long-term immune responses against mycobacteria. *Hum Vaccin Immunother* (2020) 16:673–83. doi: 10.1080/21645515.2019.1669414

20. Nascimento IP, Rodriguez D, Santos CC, Amaral EP, Rofatto HK, Junqueira-Kipnis AP, et al. Recombinant BCG expressing LTAK63 adjuvant induces superior protection against Mycobacterium tuberculosis. *Sci Rep* (2017) 7:2109. doi: 10.1038/s41598-017-02003-9

21. Logan KE, Gavier-Widen D, Hewinson RG, Hogarth PJ. Development of a Mycobacterium bovis intranasal challenge model in mice. *Tuberculosis* (2008) 88:437–43. doi: 10.1016/j.tube.2008.05.005

22. Junqueira-Kipnis AP, de Oliveira FM, Trentini MM, Tiwari S, Chen B, Resende DP, et al. Prime-boost with Mycobacterium smegmatis recombinant vaccine improves protection in mice infected with Mycobacterium tuberculosis. *PloS One* (2013) 8: e78639. doi: 10.1371/journal.pone.0078639

23. Neto LMM, Zufelato N, de Sousa-Júnior AA, Trentini MM, da Costa AC, Bakuzis AF, et al. Specific T cell induction using iron oxide based nanoparticles as subunit vaccine adjuvant. *Hum Vaccin Immunother* (2018) 14:2786–801. doi: 10.1080/21645515.2018.1489192

24. Cooper AM. Cell-mediated immune responses in tuberculosis. *Annu Rev Immunol* (2009) 27:393–422. doi: 10.1146/annurev.immunol.021908.132703

25. Bull NC, Kaveh DA, Garcia-Pelayo MC, Stylianou E, McShane H, Hogarth PJ. Induction and maintenance of a phenotypically heterogeneous lung tissue-resident CD4+ T cell population following BCG immunisation. *Vaccine* (2018) 36:5625–35. doi: 10.1016/j.vaccine.2018.07.035

26. Lyadova IV, Panteleev AV. Th1 and Th17 cells in tuberculosis: protection, pathology, and biomarkers. *Mediators Inflammation* (2015) 2015:854507. doi: 10.1155/2015/854507

27. Wozniak TM, Saunders BM, Ryan AA, Britton WJ. Mycobacterium bovis BCG-specific Th17 cells confer partial protection against Mycobacterium tuberculosis infection in the absence of gamma interferon. *Infect Immun* (2010) 78:4187–94. doi: 10.1128/IAI.01392-09

28. Gallegos AM, van Heijst JWJ, Samstein M, Su X, Pamer EG, Glickman MS. A gamma interferon independent mechanism of CD4 T cell mediated control of M. tuberculosis infection *in vivo*. *PloS Pathog* (2011) 7:e1002052. doi: 10.1371/journal.ppat.1002052

29. dos Santos CC, Walburg KV, van Veen S, Wilson LG, Trufen CEM, Nascimento IP, et al. Recombinant BCG-LTAK63 vaccine candidate for tuberculosis induces an inflammatory profile in human macrophages. *Vaccines* (2022) 10:831. doi: 10.3390/vaccines10060831

30. Strutt TM, Dhume K, Finn CM, Hwang JH, Castonguay C, Swain SL, et al. IL-15 supports the generation of protective lung-resident memory CD4 T cells. *Mucosal Immunol* (2018) 11:668–80. doi: 10.1038/mi.2017.101

31. Surh CD, Boyman O, Purton JF, Sprent J. Homeostasis of memory T cells. *Immunol Rev* (2006) 211:154–63. doi: 10.1111/j.0105-2896.2006.00401.x

32. Picker LJ, Reed-Inderbitzin EF, Hagen SI, Edgar JB, Hansen SG, Legasse A, et al. IL-15 induces CD4 effector memory T cell production and tissue emigration in nonhuman primates. *J Clin Invest* (2006) 116(6):1514–24. doi: 10.1172/JCI27564

33. Aguilo N, Alvarez-Arguedas S, Uranga S, Marinova D, Monzón M, Badiola J, et al. Pulmonary but not subcutaneous delivery of BCG vaccine confers protection to tuberculosis-susceptible mice by an interleukin 17-dependent mechanism. *J Infect Dis* (2016) 213:831–9. doi: 10.1093/infdis/jiv503

34. Nieuwenhuizen NE, Zyla J, Zedler U, Bandermann S, Abu Abed U, Brinkmann V, et al. Weaker protection against tuberculosis in BCG-vaccinated male 129 S2 mice compared to females. *Vaccine* (2021) 39:7253–64. doi: 10.1016/j.vaccine.2021.09.039

35. Kurtz SL, Rossi AP, Beamer GL, Gatti DM, Kramnik I, Elkins KL. The diversity outbred mouse population is an improved animal model of vaccination against tuberculosis that reflects heterogeneity of protection. *mSphere* (2020) 5:10.1128. doi: 10.1128/msphere.00097-20

frontiers | Frontiers in Immunology

TYPE Review
PUBLISHED 03 August 2023
DOI 10.3389/fimmu.2023.1172035

OPEN ACCESS

EDITED BY
Xiao-Yong Fan,
Fudan University, China

REVIEWED BY
Jin Wang,
Shanghai Tolo Biotechnology Company Limited, China
Wei Sha,
Tongji University School of Medicine, China
Michel Drancourt,
Aix-Marseille Université, France

*CORRESPONDENCE
Zhen Huang
huang.zhen@outlook.com
Shuihua Lu
lushuihua66@126.com

RECEIVED 23 February 2023
ACCEPTED 03 July 2023
PUBLISHED 03 August 2023

CITATION
Huang Z, Zhang G, Lyon CJ, Hu TY and Lu S (2023) Outlook for CRISPR-based tuberculosis assays now in their infancy. *Front. Immunol.* 14:1172035. doi: 10.3389/fimmu.2023.1172035

Outlook for CRISPR-based tuberculosis assays now in their infancy

Zhen Huang[1]*, Guoliang Zhang[1], Christopher J. Lyon[2,3], Tony Y. Hu[2,3] and Shuihua Lu[1]*

[1]National Clinical Research Center for Infectious Disease, Shenzhen Third People's Hospital, Shenzhen, Guangdong, China, [2]Center for Cellular and Molecular Diagnostics, Tulane University School of Medicine, New Orleans, LA, United States, [3]Department of Biochemistry and Molecular Biology, Tulane University School of Medicine, New Orleans, LA, United States

Tuberculosis (TB) remains a major underdiagnosed public health threat worldwide, being responsible for more than 10 million cases and one million deaths annually. TB diagnosis has become more rapid with the development and adoption of molecular tests, but remains challenging with traditional TB diagnosis, but there has not been a critical review of this area. Here, we systematically review these approaches to assess their diagnostic potential and issues with the development and clinical evaluation of proposed CRISPR-based TB assays. Based on these observations, we propose constructive suggestions to improve sample pretreatment, method development, clinical validation, and accessibility of these assays to streamline future assay development and validation studies.

KEYWORDS

tuberculosis, diagnosis, CRISPR, point-of-care, challenge and outlook

Abbreviations: *Mtb*, *mycobacterium tuberculosis*; TB, tuberculosis; DR, drug-resistant; HIV, human immunodeficiency virus; PCR, polymerase chain reaction; Xpert, GeneXpert MTB/RIF; CRISPR, clustered regularly interspaced short palindromic repeats; NA, nucleic acid; SNP, single-nucleotide polymorphisms; POC, point-of-care; NTM, nontuberculous mycobacteria; NAA, nucleic acid amplification; RPA, recombinase polymerase amplification; LAMP, loop-mediated isothermal amplification; RR, rifampicin resistance; RRDR, rifampicin resistance-determining region; SARS–CoV–2, severe acute respiratory syndrome coronavirus 2; QUADAS, quality assessment of diagnostic accuracy studies; PAM, protospacer adjacent motif sequence.

1 Introduction

It is estimated that one-quarter of the world population is infected with *Mycobacterium tuberculosis* (*Mtb*), and about 10 millions of these individuals develop tuberculosis (TB) annually, with more than 1 million TB-related deaths per year (1). Further, the global burden of TB and drug-resistant TB (DR-TB) has increased by 4.5% and 3% over the past year (1), deviating from the anticipated reduction rates required to meet the current schedule of the "End TB" strategy (2).

Early and accurate diagnosis of TB is critical for TB eradication efforts (3), but TB diagnosis remains challenging, and >35% of the estimated global TB cases are undiagnosed by current efforts (1, 4). This includes cases missed by insensitive sputum microbiology assays and immunoassays (5, 6), individuals who have difficulty producing diagnostic sputum samples (children, people living with HIV, extrapulmonary TB cases, or certain neurological impairments, including Dementia and Parkinson's disease) (7–11), people living in remote high TB burden areas (4), and individuals infected with DR strain who have not undergone DR screening (1). Invasive (e.g., bronchoalveolar lavage or gastric aspirate) (12) and non-invasive (e.g., stool) (13) samples can be used as additional complementary specimens to improve pulmonary TB diagnosis in Patients that have difficulty producing expectorated sputum, while additional invasive biopsies are often required to diagnose extrapulmonary TB. However, these samples versus sputum may exhibit reduced diagnostic sensitivity and be more variable and difficult to obtain.

Research is ongoing to develop new TB biomarkers and detection technologies to enhance TB diagnosis. The application of new tools has accelerated the discovery of TB biomarkers, revealing many pathogen-derived biomarkers such as nucleic acids (*Mtb* DNA and RNA) and antigens (whole bacilli, cell components, or metabolites), as well as host-derived markers and signatures including antibodies, cytokines and chemokines, transcriptomic, proteomic and metabolic markers, and hematological effectors (14). However, only a small fraction (4%, 44/1008) of the biomarker candidates screened to date have shown diagnostic value in validation studies, and only a sputum-based PCR test for *Mtb* DNA (e.g., GeneXpert MTB/RIF, Xpert) is endorsed and promoted worldwide by the WHO for TB diagnosis (14). Xpert can rapidly diagnose TB with high sensitivity, and identify the most common form of initial drug resistance, when used to analyze sputum with high *Mtb* levels (15), but has poor diagnostic accuracy with low *Mtb* concentration (paucibacillary) samples (16) and for extrapulmonary TB (17). Its high cost also limits its accessibility in remote areas, which may explain why Xpert has not increased global TB detection rates (18). There is a pressing need for more efficient TB diagnostic tests, as described in the WHO target product profile (14, 19), which should employ easy-to-use techniques and sensitively detect or quantify TB-specific biomarkers in non-sputum samples to rapidly diagnose TB and respond to treatment.

Clustered regularly interspaced short palindromic repeats (CRISPR) sequence-specific cleavage activity provides a useful means to overcome challenges associated with TB diagnosis. CRISPR/Cas complexes utilize a short guide RNA to bind a specific target sequence, which activates their cis-cleavage activity to cut this target sequence and can also induce a trans-cleavage activity that cuts non-specific sequences while bound to its target sequence. This trans-cleavage activity can be used to repeatedly cleavage an abundant reporter oligonucleotide in proportion to the abundance of the target sequence for signal amplification (20, 21). CRISPR/Cas activity can thus be used to detect low copy number targets that differ by single-nucleotide polymorphisms (SNPs) (22, 23) to accurately detect trace nucleic acid (NA) or non-NA targets (24, 25) in complex clinical samples, including SNPs associated with microbial DR (26). CRISPR systems call also be easily integrated into portable platforms suitable for point-of-care (POC) testing (27–29). These features provide the opportunity to create CRISPR diagnostic platforms for cross-over the barriers of TB finding.

Several groups have realized the potential of CRISPR-based assays to overcome weaknesses associated with current tests employed for TB diagnosis (30–43). However, their studies largely ignore the drawbacks and challenges of CRISPR-based TB (CRISPR-TB) assays for methodology development and clinical validation studies, as these applications are still in their infancy. Here, we systematically reviewed current CRISPR-TB assays to identify their weakness, describe potential barriers to their future adoption, and propose steps that should be taken to enhance the development and translation of these assays.

2 Summary of current CRISPR-TB assay research

Fourteen studies have employed CRISPR to diagnose TB, identify DR-*Mtb* strains, and distinguish *Mtb* from nontuberculous mycobacteria (NTM) species that may produce similar symptoms but require different treatments (Figures 1A, S1). Most of these studies were published after 2019, indicating the recent nature of most of the interest in using CRISPR assays for TB diagnosis.

2.1 CRISPR-TB assay methodologies

Most reported assays still adhere to the original design paradigm of CRISPR assays, where CRISPR-based signal amplification is performed after an exponential nucleic acid amplification (NAA) step (21, 44, 45). This assay design detects trace levels of target NA sequences in clinical specimens to yield high analytical sensitivity (30, 34, 36, 41), but can prolong run times (> 1 h) (32, 33, 36, 39, 40, 43) (Figure 1A) and increase the risk of cross-contamination if amplified target NA sequences are transferred to separate CRISPR reactions. Most of these CRISPR assays employ recombinase polymerase amplification (RPA) or loop-mediated isothermal amplification (LAMP)-based isothermal amplification reactions for NAA to avoid the need for a thermocycler, which can facilitate the development of POC

A

No.	Target	NAA	Cas	Steps	Output	Qualitative/ quantitative	Time (min)*	LOD (copy/test)#	Scope$	Clinical specimen	Ref.
1	16S rRNA	PCR	dCas 9	Two	Fluorescent	Qualitative	UR	1	Diagnosis	No	30
2	IS6110	RPA	Cas12a	Two	Fluorescent	Qualitative	~ 50	12.5	Diagnosis	Yes	31
3	rpoB	PCR	Cas12a	Two	Fluorescent	Qualitative	~ 120	1.6×10^5	Typing	Yes (strain)	32
4	IS1081	RPA	Cas12a	Two	Fluorescent	Qualitative	~ 120	2700	Diagnosis	Yes	33
5	IS6110	RPA	Cas12a	Two	Fluorescent	Qualitative	> 40	1	Diagnosis	Yes	34
6	rpsl	RPA	Cas12a	Two	Fluorescent	Qualitative	> 45	UR	DR screen	Yes (strain)	35
7	IS6110	LAMP	Cas12b	Two	Fluorescent	Qualitative	> 80	2.6	Diagnosis	Yes	36
8	IS6110	LAMP	Cas12a	Two	Fluorescent/strip	Qualitative	> 45	10	Diagnosis	Yes	37
9	rpoB	PCR	Cas 9	Two	Fluorescent	Qualitative	~ 60	UR	DR screen	No	38
10	gyrA	PCR	Cas13a	Two	Fluorescent	Qualitative	> 80	1 copy/μL##	DR screen	Yes (strain)	39
11	16S rRNA	-	Cas 9	One	Electrochemical	Quantitative	~ 150	30 CFU/mL##	Diagnosis	No	40
12	IS6110	PCR/ RPA	Cas12a	Two	Fluorescent/strip	Quantitative	~ 50/26 **	1.2	Diagnosis	Yes	41
13	16S rRNA	-	Cas9	-	Fluorescent	Quantitative	~ 120	20 CFU/mL##	Diagnosis	No	42
14	IS6110 and IS1081	PCR/ RPA	Cas12a	Two	Fluorescent/strip	Qualitative	~235/ 160 **	0.01 GE/test	Diagnosis	Yes	43

*Turnaround time without nucleic acid extraction step, and it is recalculated according to the original study. **The turnaround time varies depending on the amplification technology and signal output mode.

#The limit of detection (LOD) of the proposed assay is converted to a unified measure (copy/test) based on the original study for comparing between reported methods. ## Raw data reported directly.

$The proposed study mainly focused on tuberculosis (TB) diagnosis, *Mycobacteria* typing, and drug-resistance (DR)-TB screen.

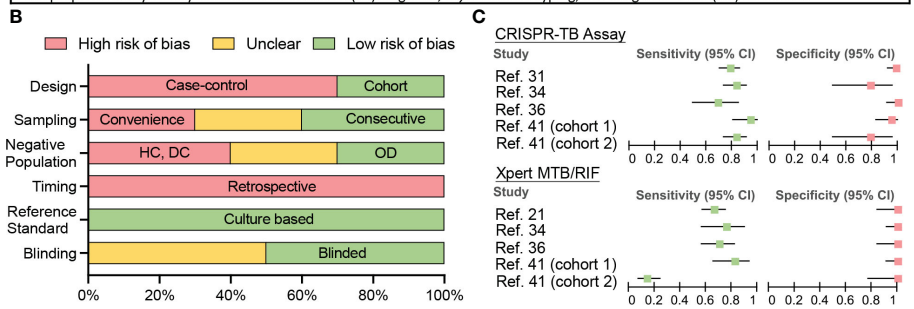

FIGURE 1
Current CRISPR-TB assay parameters and performance. **(A)** Methodological details of 12 studies employing CRISPR-TB assays. **(B)** Summary of QUADAS assessment results for the risk of bias in assessing data quality. Nine studies performed clinical sample evaluations (answers to QUADAS questions are listed in Table S1). The bar length reflects the frequency of an answer for each question. DC, disease contacts; DR, drug-resistant; HC, healthy control; LAMP, loop-mediated isothermal amplification; LOD, the limit of detection; NAA, nucleic acid amplification; OD, other diseases; PCR, polymerase chain reaction; RPA, recombinase polymerase amplification; UR, unreported. **(C)** Forest plot for the sensitivity and specificity of the CRISPR-TB assay and GeneXpert MTB/RIF (Xpert) results when compared with a composite reference standard. Details of the ten clinical specimen or strain validation studies, including control group information and diagnostic performance, are summarized in Table S2.

applications. However, many of these assays also generate fluorescent signals that require additional equipment to read and are thus less suitable for use in remote and resource-limited areas without the development of simple readout devices, although lateral flow strip-based visual readout approaches can present a good alternative for qualitative assays (37, 41, 43).

Proposed assays tend to employ *Mtb*-complex specific multi-copy genes (*IS6110* and IS1081) as diagnostic targets as it provides higher diagnostic sensitivity (31, 33, 34, 36, 37, 41, 43) and several also detects changes in the rifampicin resistance (RR)-determining region (RRDR) of the *rpoB* gene (32, 38) to screen for drug resistance, since this region is altered in 95% of RR-TB cases, and most (>78%) multi-DR TB (MDR-TB) cases (1, 46). However, other *Mtb*-complex specific sequences in single or multi-copy genes (*16s RNA*) can also be used for TB diagnosis, while DR-related mutations in other genes (*rpsl* and *gyrB*) can be employed to predict resistance to other drugs used for TB treatment. It is worth noting that the sequence conservation among *Mtb* complex species (>99%) (47) poses a challenge when attempting to distinguish individual *Mtb* complex species. CRISPR assays can have single base specificity, but many of the current TB assays use IS6110 as a target and this sequence has also been detected in all *Mtb* complex species analyzed by these assays (*M. bovis*, *M. bovis* Bacillus Calmette–Guérin, *M. africanum*, and *M. microti*) (31, 37) Further work is therefore required to identify targets that can distinguish distinct *Mtb* complex species where this information would influence treatment decisions.

2.2 CRISPR-TB assay study quality

Well-designed clinical studies are required to evaluate the diagnostic performance of newly developed assays but have yet to be performed for most CRISPR-TB assays (Figure 1B and Table S1). Only ten studies have analyzed clinical samples, including three studies that used clinically isolated strains instead of patient samples (Figure 1A). All of these seven studies exhibit high bias using a modified Quality Assessment of Diagnostic Accuracy Studies

(QUADAS) evaluation (14) (Table S1) primarily due to their retrospective and case-control designs, lack of consecutive sampling, and the use of controls that can inflate accuracy estimates (Figure 1B). These studies included 1219 individuals, most of whom (74%) were from China, and a substantial fraction (41%) of these individuals lacked reported demographic information and/or clinical characteristics, preventing an accurate assessment of the potential impact of population heterogeneities and comorbidities.

2.3 Diagnostic performance of CRISPR-TB assays

Nine of the ten studies provided at least one microbiological test result from *Mtb* culture and Xpert or had a clear clinical diagnosis to permit accurate assessment of the diagnostic performance of the proposed CRISPR-TB assay, but only four studies (involving five cohorts) were able to provide definitive Xpert results for methodological comparisons (Table S2 and Figure 1C). Unsurprisingly, CRISPR-TB assays tended to have higher diagnostic sensitivity than Xpert, with comparable or slightly decreased specificity, in most of these studies (Figure 1C), although these differences did not achieve significance, likely due to the limited number of individuals in these studies. However, CRISPR-TB assay sensitivity was significantly higher than Xpert (80.5% vs. 57.1%, $p<0.05$) for clinical TB cases with smear-negative sputum results (36). Further, CRISPR-TB assays have significant advantages over conventional tests when employed to analyze specimens that have low *Mtb* concentration (30), and thus be particularly useful in populations where this is a known problem (e.g., young children, patients living with HIV, etc.). For example, conventional TB assays exhibit very poor diagnostic performance (48, 49) in children living with HIV, representing a worst-case scenario for these assays. However, a CRISPR-based blood test for cell-free *Mtb* DNA diagnosed 83.3% of the children diagnosed with TB by microbiological finding or clinical algorithm, while Xpert sputum results identified only 14.5% of these children (Figure 1C) (41).

3 Challenges and outlook for CRISPR-TB assays

CRISPR assays are highly sensitive and specific, programmable, and easy-to-use. These features allow the ultra-sensitive detection of NA targets present at trace levels in complex samples, rapid target switching with different gRNA, and the development of streamlined assay platforms that can be operated in resource-limited settings. However, these properties, which have been extensively employed with assays for other diseases, appear to be underutilized in assays intended for TB diagnosis. As demonstrated in section-two, the methodologies of current CRISPR-TB assays are rudimentary, and high-quality clinical valuation studies are lacking.

3.1 Sample preparation for CRISPR analysis

Most CRISPR-TB assays employ column extraction protocols that involve multiple liquid transfers that confer a high risk for cross-contamination, and simple and efficient NA extraction procedures are not currently employed to avoid this issue. CRISPR assays are highly resistant to inhibitory components, and could, in theory, analyze specimens that have been subjected to chemical reduction or heating steps to inactivate nucleases and release target NAs from pathogens in these samples (31, 50). This would dramatically simplify sample handling and reduce contamination risks and facilitate the development of POC tests, although this approach could also reduce analytical sensitivity due since the approach would not concentrate sample NAs like conventional isolation procedures, and since inhibitory factors present in these lysates could attenuate target amplification in NAA-coupled CRISPR reactions.

Nano-/micro-technology may provide a means to balance assay sensitivity with streamlined sample processing approaches. For example, rapid procedures that enriched NAs using magnetic nanobeads (51) or fibrous materials (52, 53) can efficiently adsorb released SARS-COV-2 RNA for *in situ* target amplification without an elution step. Similarly, a microfluidics device that uses an electric field gradient to rapidly separate free SARS-COV-2 RNA (54) from other factors by isotachophoresis can significantly improve detection efficiency and diagnostic performance. However, while these approaches have been successful in SARS-COV-2 assays using sample lysates, significant optimization may be necessary to employ these methods for TB diagnosis, since *Mtb* lysis and nuclease deactivation steps may require more stringent conditions due to the structure and composition of the *Mtb* cell wall, and greater potential nuclease contributions from *Mtb* and its diagnostic clinical specimens. Further, optimized sample preparation procedures may need to be established for different specimen types (e.g., blood, urine, cerebrospinal fluid, stool, etc.) to permit their use in clinical applications. Incorporating the detection of non-sputum specimens into the scope of CRISPR diagnostics will maximize its ultra-sensitive properties and increase the microbiological confirmation rate of TB, which is a challenge for traditional NAA techniques.

CRISPR assays can also be used to sensitively detect non-NA targets using well-designed approaches where the binding of a functional NA reagent (e.g., aptamer/target NA complex) to a non-NA target releases a target NA sequence recognized by a CRISPR assay (24). CRISPR-TB assays could thus also potentially detect novel non-NA TB biomarkers in noninvasive or minimally invasive samples, such as *Mtb*-derived peptides or LAM in blood (55) or urine (56). Such approaches could provide additional opportunities to diagnose extrapulmonary TB, pediatric TB, and HIV-positive TB cases (57, 58) who are typically diagnosed with reduced sensitivity by standard methods and who are at increased risk for TB-related mortality. However, given the low and highly variable levels of valuable biomarkers in different samples, differentiated and efficient sample pre-treatment protocols may be

required for different types of non-NA markers and different sample types. In addition, it may be critical to construct signal transduction systems with high matrix tolerance and compatibility with non-NA marker types to convert non-NA markers not identified by the CRISPR system into recognizable NA signals.

3.2 CRISPR assay workflow optimizations

Current CRISPR-TB assays typically utilize a separate NAA step to simplify assay development, but this increases the complexity, completion time, and contamination risk of the assay. The NAA and CRISPR reactions can be integrated into a single tube if an external force (e.g., centrifugation) is used to introduce CRISPR reagents after completion of the NAA step to avoid the potential for aerosol contamination during the addition of these reagents (59), although this still requires the use of consecutive NAA and CRISPR reactions that increase the sample-to-answer time of the assay.

Simultaneous NAA and CRISPR reactions can be performed in integrated NNA-CRISPR assays that use isothermal RPA or LAMP reactions for target amplification, which can simplify assay workflows to reduce assay performance times while avoiding the risk of contamination (51, 60, 61). However, such integrated NAA CRISPR reactions can also reduce detection sensitivity, since their buffer conditions may be suboptimal for both reactions and since these reactions are in direct competition (target amplification versus target cleavage), leading to assay designs that favor the NAA reaction to allow target accumulation over CRISPR cleavage and target detection.

It is also possible to eliminate the NAA step to simplify assay workflows and reduce reagent costs and the risk of cross-contamination, but it can significantly reduce assay sensitivity and thus necessitate the use of an ultrasensitive signal readout (62–65) or amplification system (66, 67) to detect weak signals produced in response to low concentration NA targets.

Thus, a CRISPR assay design must consider the workflow and diagnostic performance requirements for its intended application. For example, assays designed to have high diagnostic performance for paucibacillary TB cases (extrapulmonary TB, pediatric TB, and HIV-positive TB) may sacrifice procedure simplicity for sensitivity, while an assay intended as a POC test for TB diagnosis in the general population may prioritize a streamlined workflow over ultrasensitive detection.

3.3 Multiplex assays, target constraints, and quantitative assay readouts

Current CRISPR assays typically detect a single target and are non-quantitative. However, assays that detect a single target may produce false negatives due to strain-specific sequence variations. For example, a test that targets the multi-copy IS6110 insertion element should produce false negative results for *Mtb* strains that lack this insertion element (68, 69). Similarly, single target assays for DR-TB may miss alternate mutations in a gene associated with drug resistance and cannot detect mutations in other genes that confer resistance to other important drugs employed in anti-TB treatment regimens. For example, a test for DRTBRB targeting the RRDR fragment of rpoB to detect major mutations associated with rapamycin and rifabutin resistance could miss MDR-TB cases that lack these mutations (70).

Multiplex CRISPR assays could help address these issues, but are technically challenging to develop as single reaction tests since the trans cleavage activities of the CRISPR/Cas variants used for signal readout in the most popular and sensitive assays lack strong sequence specificity. Single-reaction multiplex CRISPR assays that employ multiple Cas proteins with distinct trans-cleavage substrate preferences have been proposed to address this issue, but no more than four targets can be detected in one reaction due to the limited number of Cas proteins with differential cleavage preferences (22), and even among these proteins there is the potential for significant off-target cleavage and the need to optimize an assay for all four activities.

Microfluidic- or micro-droplet-based approaches may represent a better option for multiplex CRISPR assays as they can perform large numbers of distinct single-target tests in spatially separated regions to avoid target/reporter crosstalk difficulties while simultaneously detecting hundreds or thousands of distinct NA targets (71, 72).

Sequence considerations can also influence which specific target regions can be analyzed in a CRISPR assay, which can present a challenge when an assay must detect a specific sequence associated with a phenotype type of interest (e.g., a SNP associated with resistance to a specific drug). Most CRISPR/Cas systems used for sensitive NA detection require that their target NAs contain a protospacer adjacent motif (PAM) sequence, which is problematic when a sequence of interest does not contain this motif. This issue can be partially addressed by using NAA primers to introduce a PAM sequence into amplicons that contain the sequence of interest (61). However, there are limitations to this approach as this PAM sequence must be introduced in close proximity to the sequence of interest with minimal primer mismatch, and some PAM optimization may be required to obtain specificity for a SNP of interest. An alternate solution is to screen for or bioengineer Cas protein variants that exhibit fewer PAM constraints (73). Cas14 can recognize and cleave single-stranded DNA targets that lack PAM sequences (74), and could serve as a template for the design of new CAS proteins that lack a PAM sequence requirement.

Quantitative CRISPR assays are also necessary to rapidly determine *Mtb* burden and its real-time response to anti-TB therapy as a measure of disease severity and treatment efficacy (41). Standard curves can be used to quantify *Mtb* DNA levels in clinical specimens but can produce highly variable results when analyzing samples that contain only trace amounts of a target sequence (41). CRISPR assays that employ digital droplet technology to achieve absolute quantification can circumvent this problem (23, 75–80), but this approach requires additional equipment and resources. Smartphones have the signal acquisition and data processing properties required for portable quantitative assays suitable for use in resource-limited areas, and their network connectivity also provides a convenient means for data reporting for disease control efforts. Thus, the combination of

CRISPR-based TB assays and smartphone-based readout devices, or other similar portable devices, has the potential to increase the capacity for TB screening and treatment monitoring.

3.4 Clinical validation studies

CRISPR-TB assays have exciting potential to improve TB diagnosis and management, but their translation as clinical applications require their validation in well-designed, adequately powered, and multicenter prospective clinical studies, which have not been conducted for any of the CRISPR-TB assays that have been reported to date. Such studies should ideally include cohorts of extrapulmonary TB, pediatric TB, and HIV-positive TB cases, as these individuals would most benefit from early diagnosis and treatment initiation to reduce their high mortality rates. These studies should also evaluate the relative utility of CRISPR-TB assay results obtained from several types of noninvasive or minimally invasive patient specimens (e.g., urine, stool, fingerstick blood samples) for TB diagnosis in different populations, and for their potential application as CRISPR-TB assays intended for use in resource-limited settings where obtaining sputum or invasive specimens can be difficult or infeasible. Moreover, given the high sensitivity CRISPR, it is recommended that these clinical evaluation studies employ a composite criterion to identify the TB-positive and TB-negative individuals, since the use of a single standard diagnostic method may misdiagnose TB cases, particularly in extrapulmonary, pediatric, or HIV-positive cohorts to skew CRISPR-TB assay sensitivity and specificity estimates.

3.5 Assay accessibility

Future studies should also focus on improving the accessibility of CRISPR-TB assays, as limited clinical laboratory resources or infrastructure may reduce access to or capacity for TB diagnostic tests in areas with high TB incidence and prevalence rates. Such assays should ideally integrate a rapid NA extraction method into the CRISPR-TB assay and employ a rapid and streamlined procedure that does not require significant additional equipment to perform. Ideally, such assays would integrate all their procedures into a single streamlined assay platform (e.g., a microfluidic chip or a test strip) in a direct sample-to-result assay format that would not require technical expertise or any equipment for sample processing or assay readout. Such integrated platforms could potentially be into wearable devices, such as masks (27), for streamlined real-time assessment TB assessment (81). Negative and positive controls should be incorporated into these platforms to permit immediate evaluation for adverse storage and contamination effects and other confounding factors that could decease the accuracy of assay results.

CRISPR-TB assays intended for use in remote and resource-limited areas should also account for the transport and storage conditions these assays will likely face, ideally during their initial development phase, since cold chains are often difficult to maintain in areas with high TB burden. Lyophilized CRISPR reagents can be stored for months at four degrees and weeks at room temperature without significant performance decreases (28, 82). However, assay developers should also determine the stability of a CRISPR-TB assay at the more variable ambient temperatures these assays might be likely to encounter in areas without temperature control. The

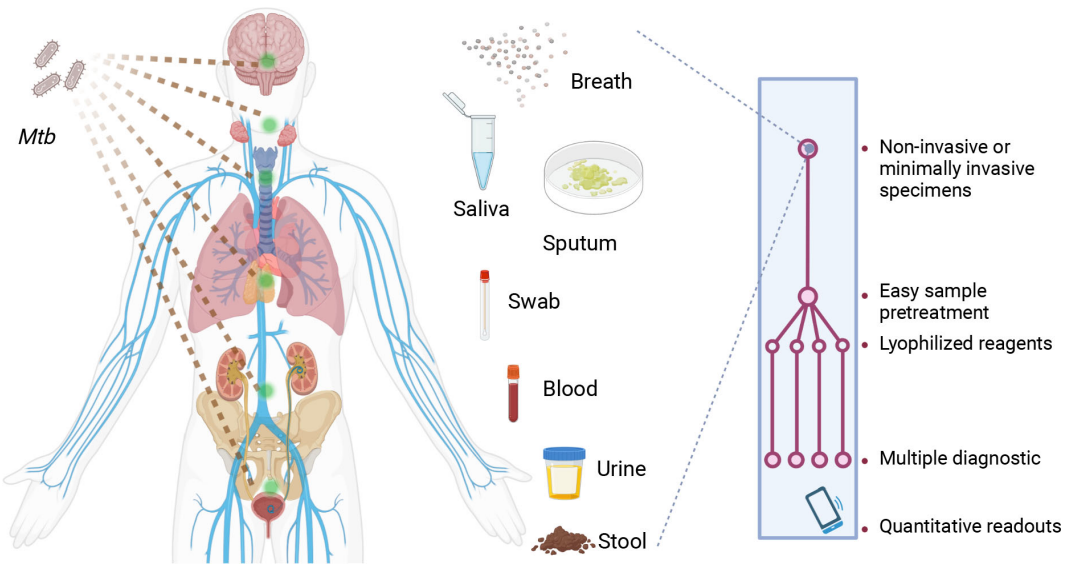

FIGURE 2
Characteristics desired for future CRISPR-TB assays. Future CRISPR-TB assays should ideally analyze noninvasive or minimally invasive diagnostic specimens (e.g., breath aerosol, saliva, sputum, swab, blood, urine and stool samples) and employ an integrated platform with lyophilized reagents to minimize cold chain concerns. These assays should integrate sample treatment and target detection reactions in a streamlined workflow to provide assay results within minutes. The assay readout should also provide quantitative results when read by a smart terminal, and this device should be able to report these results to a central system to facilitate TB control efforts or telemedicine interventions. *Mtb*, *Mycobacterium tuberculosis*.

efforts will also be required to promote the large-scale production of key reagents, such as Cas proteins, to reduce assay development and production costs and to shorten distribution distances, which will require a streamlined licensing procedure for the relevant patents, as has been done for NAA reagents.

4 Perspective on new CRISPR-TB assay development

In summary, CRISPR-TB assays have strong potential to improve the TB diagnosis of TB, but clinical validation studies are required to allow regulatory approval and commercialization for TB diagnosis and treatment evaluation. Substantial refinements are usually also required to translate an initial proof-of-concept CRISPR-TB assay suitable for use in a research laboratory to a clinical application that can be employed at a large-scale in clinical laboratories, clinics, or POC settings. We propose that future CRISPR-TB assays (Figure 2) should ideally employ an integrated platform for sample processing, NA enrichment, and coupled NAA and CRISPR detection that contains lyophilized reagents to minimize assay cold chain concerns. Such platforms should evaluate noninvasive or minimally invasive diagnostic specimens, employ streamlined workflows with rapid sample-to-result times, and employ a readout that can be quantified by a smart terminal that can report results to a central system to aid in TB control efforts or telemedicine interventions. We believe maturing CRISPR-TB assay approaches represent a powerful means of addressing current TB diagnosis and treatment evaluation challenges required to achieve the goals of current TB eradication efforts. Mature CRISPR-TB assays may also prove valuable in non-clinical applications, such as screening for active *Mtb* or *Mtb* complex infections in domestic livestock or wildlife populations (83, 84) as has been done with Xpert. This would be particularly valuable is these analyses could employ blood or fecal specimens to simplify sample collection or population level screening efforts.

Author contributions

ZH and SL conceived the design of this manuscript. ZH and GZ performed the dataset search, article screen, data extraction, and quality appraisal. ZH drafted the manuscript, and GZ, CL, and TH provided critical revision. All authors contributed to the article and approved the submitted version. SL was responsible for the decision to submit the manuscript.

Funding

The work was primarily supported by the Shenzhen Fund for Guangdong Provincial High-level Clinical Key Specialties (No. SZGSP010), the Special Fund for Science and Technology Innovation of Guangdong (No. 2020B1111170014), the Medical Scientific Research Foundation of Guangdong Province (No. A2023170), and Shenzhen Clinicla Research Center for Tuberculosis (202106171415099001).

Conflict of interest

ZH and TH are inventors on a provisional patent application related to this work US Patent US20230087018A1.

The remaining authors declare that the research was conducted in the absence of any commercial or financial relationships that could be construed as a potential conflict of interest.

Publisher's note

Supplementary material

The Supplementary Material for this article can be found online at: https://www.frontiersin.org/articles/10.3389/fimmu.2023.1172035/full#supplementary-material

References

1. WHO. *Global tuberculosis report 2022*. WHO (2022). https://www.who.int/teams/global-tuberculosis-programme/tb-reports/global-tuberculosis-report-2022

2. Chakaya J, Petersen E, Nantanda R, Mungai BN, Migliori GB, Amanullah F, et al. The who global tuberculosis 2021 report - not so good news and turning the tide back to end TB. *Int J Infect Dis* (2022) 124(Suppl 1):S26–S9. doi: 10.1016/j.ijid.2022.03.011

3. Hamada Y, Cirillo DM, Matteelli A, Penn-Nicholson A, Rangaka MX, Ruhwald M. Tests for tuberculosis infection: landscape analysis. *Eur Respir J* (2021) 58 (5):2100167. doi: 10.1183/13993003.00167-2021

4. Fleming KA, Horton S, Wilson ML, Atun R, DeStigter K, Flanigan J, et al. The lancet commission on diagnostics: transforming access to diagnostics. *Lancet* (2021) 398(10315):1997–2050. doi: 10.1016/S0140-6736(21)00673-5

5. Caulfield AJ, Wengenack NL. Diagnosis of active tuberculosis disease: from microscopy to molecular techniques. *J Clin Tuberc Other Mycobact Dis* (2016) 4:33–43. doi: 10.1016/j.jctube.2016.05.005

6. Sester M, Sotgiu G, Lange C, Giehl C, Girardi E, Migliori GB, et al. Interferon-γ release assays for the diagnosis of active tuberculosis: a systematic review and meta-analysis. *Eur Respir J* (2011) 37(1):100–11. doi: 10.1183/09031936.00114810

7. Connell TG, Zar HJ, Nicol MP. Advances in the diagnosis of pulmonary tuberculosis in HIV-infected and HIV-uninfected children. *J Infect Dis* (2011) 204 (suppl_4):S1151–S8. doi: 10.1093/infdis/jir413

8. Gupta RK, Lucas SB, Fielding KL, Lawn SD. Prevalence of tuberculosis in post-mortem studies of HIV-infected adults and children in resource-limited settings: a

systematic review and meta-analysis. *AIDS* (2015) 29(15):1987–2002. doi: 10.1097/QAD.0000000000000802

9. Lee JY. Diagnosis and treatment of extrapulmonary tuberculosis. *Tuberc Respir Dis* (2015) 78(2):47–55. doi: 10.4046/trd.2015.78.2.47

10. Peng YH, Chen CY, Su CH, Muo CH, Chen KF, Liao WC, et al. Increased risk of dementia among patients with pulmonary tuberculosis: a retrospective population-based cohort study. *Am J Alzheimers Dis Other Demen* (2015) 30(6):629–34. doi: 10.1177/1533317515577186

11. Shen CH, Chou CH, Liu FC, Lin TY, Huang WY, Wang YC, et al. Association between tuberculosis and Parkinson disease: a nationwide, population-based cohort study. *Med (Baltimore)* (2016) 95(8):e2883. doi: 10.1097/md.0000000000002883

12. Ahmad M, Ibrahim WH, Sarafandi SA, Shahzada KS, Ahmed S, Haq IU, et al. Diagnostic value of bronchoalveolar lavage in the subset of patients with negative sputum/smear and mycobacterial culture and a suspicion of pulmonary tuberculosis. *Int J Infect Dis* (2019) 82:96–101. doi: 10.1016/j.ijid.2019.03.021

13. MacLean E, Sulis G, Denkinger Claudia M, Johnston James C, Pai M, Ahmad Khan F. Diagnostic accuracy of stool Xpert MTB/RIF for detection of pulmonary tuberculosis in children: a systematic review and meta-analysis. *J Clin Microbiol* (2019) 57(6):10. doi: 10.1128/jcm.02057-18

14. MacLean E, Broger T, Yerlikaya S, Fernandez-Carballo BL, Pai M, Denkinger CM. A systematic review of biomarkers to detect active tuberculosis. *Nat Microbiol* (2019) 4(5):748–58. doi: 10.1038/s41564-019-0380-2

15. Steingart KR, Sohn H, Schiller I, Kloda LA, Boehme CC, Pai M, et al. Xpert® MTB/RIF assay for pulmonary tuberculosis and rifampicin resistance in adults. *Cochrane Db Syst Rev* (2013) 1):CD009593. doi: 10.1002/14651858.CD009593.pub2

16. Ocheretina O, Brandao A, Pang Y, Rodrigues C, Banu S, Ssengooba W, et al. Impact of the bacillary load on the accuracy of rifampicin resistance results by Xpert® MTB/RIF. *Int J Tuberc Lung Dis* (2021) 25(11):881–5. doi: 10.5588/ijtld.21.0564

17. Allahyartorkaman M, Mirsaeidi M, Hamzehloo G, Amini S, Zakiloo M, Nasiri MJ. Low diagnostic accuracy of Xpert MTB/RIF assay for extrapulmonary tuberculosis: a multicenter surveillance. *Sci Rep* (2019) 9(1):18515. doi: 10.1038/s41598-019-55112-y

18. Walzl G, McNerney R, du Plessis N, Bates M, McHugh TD, Chegou NN, et al. Tuberculosis: advances and challenges in development of new diagnostics and biomarkers. *Lancet Infect Dis* (2018) 18(7):e199–210. doi: 10.1016/S1473-3099(18)30111-7

19. Gardiner JL, Karp CL. Transformative tools for tackling tuberculosis. *J Exp Med* (2015) 212(11):1759–69. doi: 10.1084/jem.20151468

20. Fonfara I, Richter H, Bratovič M, Le Rhun A, Charpentier E. The CRISPR-associated DNA-cleaving enzyme Cpf1 also processes precursor CRISPR RNA. *Nature* (2016) 532(7600):517–21. doi: 10.1038/nature17945

21. Gootenberg Jonathan S, Abudayyeh Omar O, Lee Jeong W, Essletzbichler P, Dy Aaron J, Joung J, et al. Nucleic acid detection with CRISPR-Cas13a/C2c2. *Science* (2017) 356(6336):438–42. doi: 10.1126/science.aam9321

22. Gootenberg JS, Abudayyeh OO, Kellner MJ, Joung J, Collins JJ, Zhang F. Multiplexed and portable nucleic acid detection platform with Cas13, Cas12a, and Csm6. *Science* (2018) 360(6387):439–44. doi: 10.1126/science.aaq0179

23. Yue H, Shu B, Tian T, Xiong E, Huang M, Zhu D, et al. Droplet Cas12a assay enables DNA quantification from unamplified samples at the single-molecule level. *Nano Lett* (2021) 21(11):4643–53. doi: 10.1021/acs.nanolett.1c00715

24. Xiong Y, Zhang J, Yang Z, Mou Q, Ma Y, Xiong Y, et al. Functional DNA regulated CRISPR-Cas12a sensors for point-of-care diagnostics of non-nucleic-acid targets. *J Am Chem Soc* (2020) 142(1):207–13. doi: 10.1021/jacs.9b09211

25. Shen J, Zhou X, Shan Y, Yue H, Huang R, Hu J, et al. Sensitive detection of a bacterial pathogen using allosteric probe-initiated catalysis and CRISPR-Cas13a amplification reaction. *Nat Commun* (2020) 11(1):267. doi: 10.1038/s41467-019-14135-9

26. Wang S, Li H, Kou Z, Ren F, Jin Y, Yang L, et al. Highly sensitive and specific detection of hepatitis B virus DNA and drug resistance mutations utilizing the PCR-based CRISPR-Cas13a system. *Clin Microbiol Infect* (2021) 27(3):443–50. doi: 10.1016/j.cmi.2020.04.018

27. Nguyen PQ, Soenksen LR, Donghia NM, Angenent-Mari NM, de Puig H, Huang A, et al. Wearable materials with embedded synthetic biology sensors for biomolecule detection. *Nat Biotechnol* (2021) 39(11):1366–74. doi: 10.1038/s41587-021-00950-3

28. Arizti-Sanz J, Bradley AD, Zhang YB, Boehm CK, Freije CA, Grunberg ME, et al. Simplified Cas13-based assays for the fast identification of SARS-CoV-2 and its variants. *Nat Biomed Eng* (2022) 6(8):932–43. doi: 10.1038/s41551-022-00889-z

29. Chandrasekaran SS, Agrawal S, Fanton A, Jangid AR, Charrez B, Escajeda AM, et al. Rapid detection of SARS-CoV-2 Rna in saliva *Via* Cas13. *Nat Biomed Eng* (2022) 6(8):944–56. doi: 10.1038/s41551-022-00917-y

30. Zhang Y, Qian L, Wei W, Wang Y, Wang B, Lin P, et al. Paired design of dCas9 as a systematic platform for the detection of featured nucleic acid sequences in pathogenic strains. *ACS Synthetic Biol* (2017) 6(2):211–6. doi: 10.1021/acssynbio.6b00215

31. Ai JW, Zhou X, Xu T, Yang M, Chen Y, He GQ, et al. CRISPR-based rapid and ultra-sensitive diagnostic test for mycobacterium tuberculosis. *Emerg Microbes Infect* (2019) 8(1):1361–9. doi: 10.1080/22221751.2019.1664939

32. Xiao GH, He X, Zhang S, Liu YY, Liang ZH, Liu HM, et al. Cas12a/guide RNA-based platform for rapid and accurate identification of major mycobacterium species. *J Clin Microbiol* (2020) 58(2):e01368–19. doi: 10.1128/jcm.01368-19

33. Xu H, Zhang X, Cai Z, Dong X, Chen G, Li Z, et al. An isothermal method for sensitive detection of mycobacterium tuberculosis complex using clustered regularly interspaced short palindromic repeats/Cas12a cis and trans cleavage. *J Mol Diagnost* (2020) 22(8):1020–9. doi: 10.1016/j.jmoldx.2020.04.212

34. Li H, Cui X, Sun L, Deng X, Liu S, Zou X, et al. High concentration of Cas12a effector tolerates more mismatches on ssDNA. *FASEB J* (2021) 35(1):e21153. doi: 10.1096/fj.202001475R

35. Liu P, Wang X, Liang J, Dong Q, Zhang J, Liu D, et al. A recombinase polymerase amplification-coupled Cas12a mutant-based module for efficient detection of streptomycin-resistant mutations in mycobacterium tuberculosis. *Front Microbiol* (2021) 12:796916. doi: 10.3389/fmicb.2021.796916

36. Sam IK, Chen YY, Ma J, Li SY, Ying RY, Li LX, et al. TB-Quick: CRISPR-Cas12b-Assisted rapid and sensitive detection of mycobacterium tuberculosis. *J Infect* (2021) 83(1):54–60. doi: 10.1016/j.jinf.2021.04.032

37. Wang Y, Li JQ, Li SJ, Zhu X, Wang XX, Huang JF, et al. LAMP-CRISPR-Cas12-based diagnostic platform for detection of mycobacterium tuberculosis complex using real-time fluorescence or lateral flow test. *Microchim Acta* (2021) 188(10):347. doi: 10.1007/s00604-021-04985-w

38. Augustin L, Agarwal N. Designing a Cas9/Grna-assisted quantitative real-time PCR (CARP) assay for identification of point mutations leading to rifampicin resistance in the human pathogen mycobacterium tuberculosis. *Gene* (2023) 857:147173. doi: 10.1016/j.gene.2023.147173

39. Bai X, Gao P, Qian K, Yang J, Deng H, Fu T, et al. A highly sensitive and specific detection method for mycobacterium tuberculosis fluoroquinolone resistance mutations utilizing the CRISPR-Cas13a system. *Front Microbiol* (2022) 13:847373. doi: 10.3389/fmicb.2022.847373

40. Huang J, Liang Z, Liu Y, Zhou JD, He FJ. Development of an MSPQC nucleic acid sensor based on CRISPR/ Cas9 for the detection of mycobacterium tuberculosis. *Anal Chem* (2022) 94(32):11409–15. doi: 10.1021/acs.analchem.2c02538

41. Huang Z, LaCourse SM, Kay AW, Stern J, Escudero JN, Youngquist BM, et al. CRISPR detection of circulating cell-free mycobacterium tuberculosis DNA in adults and children, including children with HIV: a molecular diagnostics study. *Lancet Microbe* (2022) 3(7):e482–e92. doi: 10.1016/S2666-5247(22)00087-8

42. Zhou M, Li X, Wen H, Huang B, Ren J, Zhang J. The construction of CRISPR/Cas9-mediated FRET 16S rDNA sensor for detection of mycobacterium tuberculosis. *Analyst* (2023)148:2308-15. doi: 10.1039/D3AN00462G

43. Thakku SG, Lirette J, Murugesan K, Chen J, Theron G, Banaei N, et al. Genome-wide tiled detection of circulating mycobacterium tuberculosis cell-free DNA using Cas13. *Nat Commun* (2023) 14(1):1803. doi: 10.1038/s41467-023-37183-8

44. Chen Janice S, Ma E, Harrington Lucas B, Da Costa M, Tian X, Palefsky Joel M, et al. CRISPR-Cas12a target binding unleashes indiscriminate single-stranded dnase activity. *Science* (2018) 360(6387):436–9. doi: 10.1126/science.aar6245

45. Li SY, Cheng QX, Wang JM, Li XY, Zhang ZL, Gao S, et al. CRISPR-Cas12a-assisted nucleic acid detection. *Cell Discovery* (2018) 4(1):20. doi: 10.1038/s41421-018-0028-z

46. Zaw MT, Emran NA, Lin Z. Mutations inside rifampicin-resistance determining region of rpoB gene associated with rifampicin-resistance in mycobacterium tuberculosis. *J Infect Public Health* (2018) 11(5):605–10. doi: 10.1016/j.jiph.2018.04.005

47. Brosch R, Gordon SV, Pym A, Eiglmeier K, Garnier T, Cole ST. Comparative genomics of the mycobacteria. *Int J Med Microbiol* (2000) 290(2):143–52. doi: 10.1016/S1438-4221(00)80083-1

48. Bell LCK, Noursadeghi M. Pathogenesis of HIV-1 and mycobacterium tuberculosis co-infection. *Nat Rev Microbiol* (2018) 16(2):80–90. doi: 10.1038/nrmicro.2017.128

49. Thomas TA. Tuberculosis in children. *Pediatr Clin North Am* (2017) 64(4):893–909. doi: 10.1016/j.pcl.2017.03.010

50. Myhrvold C, Freije CA, Gootenberg JS, Abudayyeh OO, Metsky HC, Durbin AF, et al. Field-deployable viral diagnostics using CRISPR-Cas13. *Science* (2018) 360(6387):444–8. doi: 10.1126/science.aas8836

51. Joung J, Ladha A, Saito M, Kim N-G, Woolley AE, Segel M, et al. Detection of SARS-CoV-2 with Sherlock one-pot testing. *New Engl J Med* (2020) 383(15):1492–4. doi: 10.1056/NEJMc2026172

52. de Puig H, Lee Rose A, Najjar D, Tan X, Soenksen Luis R, Angenent-Mari Nicolaas M, et al. Minimally instrumented Sherlock (Misherlock) for CRISPR-based point-of-care diagnosis of SARS-CoV-2 and emerging variants. *Sci Adv* (2021) 7(32):eabh2944. doi: 10.1126/sciadv.abh2944

53. Mason MG, Botella JR. Rapid (30-second), equipment-free purification of nucleic acids using easy-to-make dipsticks. *Nat Protoc* (2020) 15(11):3663–77. doi: 10.1038/s41596-020-0392-7

54. Persat A, Marshall LA, Santiago JG. Purification of nucleic acids from whole blood using isotachophoresis. *Anal Chem* (2009) 81(22):9507–11. doi: 10.1021/ac901965v

55. Liu C, Zhao Z, Fan J, Lyon CJ, Wu HJ, Nedelkov D, et al. Quantification of circulating mycobacterium tuberculosis antigen peptides allows rapid diagnosis of

active disease and treatment monitoring. *Proc Natl Acad Sci* (2017) 114(15):3969–74. doi: 10.1073/pnas.1621360114

56. Paris L, Magni R, Zaidi F, Araujo R, Saini N, Harpole M, et al. Urine lipoarabinomannan glycan in HIV-negative patients with pulmonary tuberculosis correlates with disease severity. *Sci Trans Med* (2017) 9(420):eaal2807. doi: 10.1126/scitranslmed.aal2807

57. Yu G, Shen Y, Ye B, Shi Y. Diagnostic accuracy of mycobacterium tuberculosis cell-free DNA for tuberculosis: a systematic review and meta-analysis. *PloS One* (2021) 16(6):e0253658. doi: 10.1371/journal.pone.0253658

58. Liu XH, Xia L, Song B, Wang H, Qian XQ, Wei JH, et al. Stool-based Xpert MTB/RIF ultra assay as a tool for detecting pulmonary tuberculosis in children with abnormal chest imaging: a prospective cohort study. *J Infect* (2021) 82(1):84–9. doi: 10.1016/j.jinf.2020.10.036

59. Wang B, Wang R, Wang D, Wu J, Li J, Wang J, et al. Cas12aVDet: a CRISPR/Cas12a-based platform for rapid and visual nucleic acid detection. *Anal Chem* (2019) 91(19):12156–61. doi: 10.1021/acs.analchem.9b01526

60. Ding X, Yin K, Li Z, Lalla RV, Ballesteros E, Sfeir MM, et al. Ultrasensitive and visual detection of SARS-CoV-2 using all-in-one dual CRISPR-Cas12a assay. *Nat Commun* (2020) 11(1):4711. doi: 10.1038/s41467-020-18575-6

61. Li L, Li S, Wu N, Wu J, Wang G, Zhao G, et al. HOLMESv2: a CRISPR-Cas12b-assisted platform for nucleic acid detection and DNA methylation quantitation. *ACS Synthetic Biol* (2019) 8(10):2228–37. doi: 10.1021/acssynbio.9b00209

62. Yang W, Restrepo-Pérez L, Bengtson M, Heerema SJ, Birnie A, van der Torre J, et al. Detection of CRISPR-dCas9 on DNA with solid-state nanopores. *Nano Lett* (2018) 18(10):6469–74. doi: 10.1021/acs.nanolett.8b02968

63. Weckman NE, Ermann N, Gutierrez R, Chen K, Graham J, Tivony R, et al. Multiplexed DNA identification using site specific dCas9 barcodes and nanopore sensing. *ACS Sens* (2019) 4(8):2065–72. doi: 10.1021/acssensors.9b00686

64. Nouri R, Jiang Y, Lian XL, Guan W. Sequence-specific recognition of HIV-1 DNA with solid-state CRISPR-Cas12a-assisted nanopores (Scan). *ACS Sens* (2020) 5 (5):1273–80. doi: 10.1021/acssensors.0c00497

65. Choi J-H, Lim J, Shin M, Paek S-H, Choi J-W. CRISPR-Cas12a-based nucleic acid amplification-free DNA biosensor *Via* Au nanoparticle-assisted metal-enhanced fluorescence and colorimetric analysis. *Nano Lett* (2021) 21(1):693–9. doi: 10.1021/acs.nanolett.0c04303

66. Shi K, Xie S, Tian R, Wang S, Lu Q, Gao D, et al. A CRISPR-Cas autocatalysis-driven feedback amplification network for supersensitive DNA diagnostics. *Sci Adv* (2021) 7(5):eabc7802. doi: 10.1126/sciadv.abc7802

67. Fozouni P, Son S, Díaz de León Derby M, Knott GJ, Gray CN, D'Ambrosio MV, et al. Amplification-free detection of SARS-CoV-2 with CRISPR-Cas13a and mobile phone microscopy. *Cell* (2021) 184(2):323–33.e9. doi: 10.1016/j.cell.2020.12.001

68. Abraham PR, Chauhan A, Gangane R, Sharma VD, SHIVannavar C. Prevalence of mycobacterium tuberculosis with multiple copies of IS6110 elements in gulbarga, south India. *Int J Mycobacteriol* (2013) 2(4):237–9. doi: 10.1016/j.ijmyco.2013.09.003

69. Narayanan S, Das S, Garg R, Hari L, Rao VB, Frieden TR, et al. Molecular epidemiology of tuberculosis in a rural area of high prevalence in south India: implications for disease control and prevention. *J Clin Microbiol* (2002) 40(12):4785–8. doi: 10.1128/JCM.40.12.4785-4788.2002

70. Xu G, Liu H, Jia X, Wang X, Xu P. Mechanisms and detection methods of mycobacterium tuberculosis rifampicin resistance: the phenomenon of drug resistance is complex. *Tuberculosis* (2021) 128:102083. doi: 10.1016/j.tube.2021.102083

71. Ackerman CM, Myhrvold C, Thakku SG, Freije CA, Metsky HC, Yang DK, et al. Massively multiplexed nucleic acid detection with Cas13. *Nature* (2020) 582 (7811):277–82. doi: 10.1038/s41586-020-2279-8

72. Welch NL, Zhu M, Hua C, Weller J, Mirhashemi ME, Nguyen TG, et al. Multiplexed CRISPR-based microfluidic platform for clinical testing of respiratory viruses and identification of SARS-CoV-2 variants. *Nat Med* (2022) 28(5):1083–94. doi: 10.1038/s41591-022-01734-1

73. Collias D, Beisel CL. CRISPR technologies and the search for the PAM-free nuclease. *Nat Commun* (2021) 12(1):555. doi: 10.1038/s41467-020-20633-y

74. Wei Y, Yang Z, Zong C, Wang B, Ge X, Tan X, et al. Trans single-stranded DNA cleavage *Via* CRISPR/Cas14a1 activated by target RNA without destruction. *Angewandte Chemie Int Edition* (2021) 60(45):24241–7. doi: 10.1002/anie.202110384

75. Park JS, Hsieh K, Chen L, Kaushik A, Trick AY, Wang TH. Digital CRISPR/Cas-assisted assay for rapid and sensitive detection of SARS-CoV-2. *Adv Sci* (2021) 8 (5):2003564. doi: 10.1002/advs.202003564

76. Tian T, Shu B, Jiang Y, Ye M, Liu L, Guo Z, et al. An ultralocalized Cas13a assay enables universal and nucleic acid amplification-free single-molecule RNA diagnostics. *ACS Nano* (2021) 15(1):1167–78. doi: 10.1021/acsnano.0c08165

77. Wu X, Tay JK, Goh CK, Chan C, Lee YH, Springs SL, et al. Digital CRISPR-based method for the rapid detection and absolute quantification of nucleic acids. *Biomaterials* (2021) 274:120876. doi: 10.1016/j.biomaterials.2021.120876

78. Luo X, Xue Y, Ju E, Tao Y, Li M, Zhou L, et al. Digital CRISPR/Cas12b-based platform enabled absolute quantification of viral RNA. *Anal Chimica Acta* (2022) 1192:339336. doi: 10.1016/j.aca.2021.339336

79. Ding X, Yin K, Li Z, Sfeir MM, Liu C. Sensitive quantitative detection of SARS-CoV-2 in clinical samples using digital warm-start CRISPR assay. *Biosens Bioelectron* (2021) 184:113218. doi: 10.1016/j.bios.2021.113218

80. Shinoda H, Taguchi Y, Nakagawa R, Makino A, Okazaki S, Nakano M, et al. Amplification-free RNA detection with CRISPR–Cas13. *Commun Biol* (2021) 4(1):476. doi: 10.1038/s42003-021-02001-8

81. Theron G, Limberis J, Venter R, Smith L, Pietersen E, Esmail A, et al. Bacterial and host determinants of cough aerosol culture positivity in patients with drug-resistant versus drug-susceptible tuberculosis. *Nat Med* (2020) 26(9):1435–43. doi: 10.1038/s41591-020-0940-2

82. Nguyen LT, Rananaware SR, Pizzano BLM, Stone BT, Jain PK. Clinical validation of engineered CRISPR/Cas12a for rapid SARS-CoV-2 detection. *Commun Med* (2022) 2(1):7. doi: 10.1038/s43856-021-00066-4

83. Goosen WJ, Kerr TJ, Kleynhans L, Warren RM, van Helden PD, Persing DH, et al. The Xpert MTB/RIF ultra assay detects mycobacterium tuberculosis complex DNA in white rhinoceros (Ceratotherium simum) and African elephants (Loxodonta africana). *Sci Rep* (2020) 10(1):14482. doi: 10.1038/s41598-020-71568-9

84. Hlokwe TM, Mogano RM. Utility of Xpert® MTB/RIF ultra assay in the rapid diagnosis of bovine tuberculosis in wildlife and livestock animals from south Africa. *Prev Vet Med* (2020) 177:104980. doi: 10.1016/j.prevetmed.2020.104980

frontiers | Frontiers in Immunology

TYPE Review
PUBLISHED 11 August 2023
DOI 10.3389/fimmu.2023.1193058

OPEN ACCESS

EDITED BY
Lanbo Shi,
Rutgers University, Newark, United States

REVIEWED BY
Joanna Kirman,
University of Otago, New Zealand
Mangalakumari Jeyanathan,
McMaster University, Canada

*CORRESPONDENCE
Sung Jae Shin
sjshin@yuhs.ac

RECEIVED 24 March 2023
ACCEPTED 27 July 2023
PUBLISHED 11 August 2023

CITATION
Kim H, Choi H-G and Shin SJ (2023) Bridging the gaps to overcome major hurdles in the development of next-generation tuberculosis vaccines. *Front. Immunol.* 14:1193058. doi: 10.3389/fimmu.2023.1193058

Bridging the gaps to overcome major hurdles in the development of next-generation tuberculosis vaccines

Hongmin Kim[1], Han-Gyu Choi[2] and Sung Jae Shin[1*]

[1]Department of Microbiology, Institute for Immunology and Immunological Diseases, Graduate School of Medical Science, Brain Korea 21 Project, Yonsei University College of Medicine, Seoul, Republic of Korea, [2]Department of Microbiology and Medical Science, College of Medicine, Chungnam National University, Daejeon, Republic of Korea

Although tuberculosis (TB) remains one of the leading causes of death from an infectious disease worldwide, the development of vaccines more effective than bacille Calmette-Guérin (BCG), the only licensed TB vaccine, has progressed slowly even in the context of the tremendous global impact of TB. Most vaccine candidates have been developed to strongly induce interferon-γ (IFN-γ)-producing T-helper type 1 (Th1) cell responses; however, accumulating evidence has suggested that other immune factors are required for optimal protection against *Mycobacterium tuberculosis* (Mtb) infection. In this review, we briefly describe the five hurdles that must be overcome to develop more effective TB vaccines, including those with various purposes and tested in recent promising clinical trials. In addition, we discuss the current knowledge gaps between preclinical experiments and clinical studies regarding peripheral versus tissue-specific immune responses, different underlying conditions of individuals, and newly emerging immune correlates of protection. Moreover, we propose how recently discovered TB risk or susceptibility factors can be better utilized as novel biomarkers for the evaluation of vaccine-induced protection to suggest more practical ways to develop advanced TB vaccines. Vaccines are the most effective tools for reducing mortality and morbidity from infectious diseases, and more advanced technologies and a greater understanding of host-pathogen interactions will provide feasibility and rationale for novel vaccine design and development.

KEYWORDS

***Mycobacterium tuberculosis*, next-generation TB vaccines, immune correlates, immunogenicity, biomarkers**

1 Introduction

Tuberculosis (TB), one of the deadliest infectious diseases, is caused by *Mycobacterium tuberculosis* (Mtb) and was responsible for approximately 1.6 million deaths in 2021 (World Health Organization. Global TB Report 2022). A single licensed TB vaccine called bacille Calmette-Guérin (BCG) has been employed for human use since 1921, and the degree of protection afforded by BCG vaccination varies in different regions of the world (1). Although the protective efficacy of BCG against severe TB forms such as TB meningitis and disseminated extrapulmonary TB before adolescence is well documented, worse protection with highly variable efficacies in individuals of all ages against pulmonary TB continues to be a serious concern (2, 3). Despite the global use of BCG for over 100 years, approximately a quarter of the world's population is considered to have latent Mtb infection. Thus, the development of new TB vaccines that provide greater protection than the BCG vaccine, with the aim of preventing pulmonary TB, is critical for all age groups.

More than 20 TB vaccine candidates with various purposes have entered clinical trials, and 14 candidates are being actively evaluated. However, the unsatisfactory outcomes (for example, the MVA85A and AERAS-422 trials) (4–6) prompt us to try to further understand the complexity of the key protective immune response to Mtb infection and the way to develop vaccines that afford lifelong protection. These trials highlight our current knowledge gaps about protective correlates and controlling factors that can affect vaccine efficacies and outcomes. In this review, we discuss five points that should be considered in the individual stages of vaccine development, from the proposal of novel concepts for next-generation TB vaccines to considerations for practical development.

2 The first hurdle: purpose of vaccines

2.1 Prevention of infection

A vaccine developed for the prevention of infection (POI), given prior to Mtb exposure, should control the incipient infection stage. With much higher rates of infection than evident TB disease in endemic settings, POI trials are shorter and less costly than prevention of disease (POD) trials (7, 8). Therefore, the POI trial can be used as a viable opportunity to understand the mechanisms of vaccine efficacy in humans, providing a platform to select lead candidates for further testing. A major challenge is that there is no available standardized test to measure directly the acquisition, persistence, and clearance of asymptomatic Mtb infection. Currently, assessment of Mtb infection mainly relies on alterations in specific T-cell responses induced after Mtb infection. One of the commercial interferon (IFN)-γ release assay (IGRA), QuantiFERON-TB Gold In-Tube (QFT), measures immunological sensitization to Mtb as a biomarker for Mtb infection. Compared to persistent QFT negatives, recent negative-to-positive QFT tests are associated with higher rates of Mtb infection. Therefore, it may be ideal for conducting clinical trials of prevention of Mtb infection (POI) by novel vaccines using QFT transformation as an efficacy endpoint. A positivity cutoff IFN-γ value (0.35 IU/ml) for QFT conversion is recommended by manufacturers and CDC (9), but the immunological and analytical variability of QFT tests potentially confounds the interpretation of QFT conversion as a clinical trial endpoint (10, 11). Although the tuberculin skin test (TST) can be used as an alternative method for detecting Mtb infection, since specificity is reduced by BCG vaccination or nontuberculous mycobacteria (NTM) infection, novel diagnostic methods for successful clinical results must be developed.

2.2 Prevention of disease

A POD vaccine can be administered either pre- or post-exposure to protect against disease progression after actual Mtb infection. Knight et al. reported epidemiological modeling suggesting that adolescents or young adults are the most effective targets for POD vaccination (12). According to this model, due to children having lower rates of TB notifications, lower proportions of smear-positive pulmonary TB, and making a smaller contribution to TB transmission, a novel TB vaccine targeted at infants shows a reduced immediate impact compared to one targeted at adolescents/adults. Vaccines targeting infants prevent a relatively small number of active cases, resulting in fewer secondary cases being prevented. In contrast, vaccines targeting adolescents/adults directly affect the population with the greatest burden of active TB, such as 10-year-olds vaccinated in schools and those individuals reached in mass campaigns, which leads to a reduction in transmission. Although most vaccine candidates in clinical phases aim to prevent TB disease, POD trials require more time and higher costs than POI trials because of the much lower rate of TB disease than Mtb infection (8). Nevertheless, POD trials can directly reveal Mtb infection because the evaluation is performed by measuring clinical symptoms, chest X-ray, and direct Mtb culture from clinical samples. A recent POD trial with the candidate M72: $AS01_E$ TB vaccine (phase 2b) was conducted in Kenya, South Africa, and Zambia. Efficacy analysis was conducted on a total of 3,283 subjects, and after a period of approximately 2.3 years, the incidence of pulmonary TB was significantly lower in the M72: AS01E group than in the placebo group (13). In this trial, M72: AS01E group showed 54% vaccine efficacy among persons already infected with Mtb, but due to the inclusion of predominantly BCG-vaccinated Mtb-infected adults, it was not possible to determine the extent to which infection-generated or childhood BCG vaccination-elicited responses influenced vaccine efficacy. Similarly, a 3-year extended follow-up study demonstrated 49.7% protection by M72: $AS01_E$ among people already infected with Mtb (14), indicating that vaccine-induced protective immune responses were maintained for at least 3 years. With these promising findings, broader applications to diverse ethnic populations in different geographic settings will be required to conduct reliable clinical trials for POD.

2.3 Prevention of recurrence

Vaccines aimed at the prevention of recurrence (POR) are administered during antibiotic therapy to prevent the recurrence

of TB. TB recurrence generally occurs in approximately 2 to 8% of TB patients even after treatment completion, and the recurrence rate depends on the absence or presence of cavities, bacterial burden, treatment frequency per week, type of antibiotics used and transmission rate. As most cases of recurrent TB disease develop within one year after treatment completion, the targeted populations of POR trials can usually be designated (8), but trial design is complicated due to the long-term treatment period and intervention timing. Multiple promising candidates currently under evaluation for POR include the H56:IC31 and ID93:GLA-SE subunit vaccine candidates, which were noted to prevent reactivation or restrict progression to severe disease in nonhuman primates (NHPs) (15, 16), and the recombinant BCG vaccine candidate VPM1002.

Due to the characteristics of TB, a large number of subjects for trials are needed because approximately 10% of infected individuals are at the onset of the disease. In addition, long-term monitoring is required because the timing of onset is different for each individual. These characteristics make the rapidly increasing economic problem more difficult as the number of clinical trial subjects and the test period increases. Therefore, to overcome these problems, it is important to recruit a reasonably sized experimental group and set endpoints according to the purpose of the experiment, and it is important to discover a correlate of protection (COP) that can predict vaccine efficacy, which will be addressed later in this review.

3 The second hurdle: a gap between experiments and the natural history of TB

Current concepts for the development of TB vaccines depend on experiments emphasizing T-helper type 1 (Th1)-biased immunity, based on early observations (17). For successful vaccine development, an appropriate vaccine model and translation to evaluate vaccine candidates is essential. Therefore, factors such as which animal model to select, which strain of Mtb to use for infection, and which dose to use for challenge are important.

3.1 Mtb infection dose

According to reports, the infection dose that causes TB disease is 1-200 colony-forming units (CFU). TB is transmitted via droplets containing Mtb generated through coughing or sneezing, and the number of droplets generated through a single cough is approximately 1-400 CFU (18, 19). According to another study of TB patients, the average number of aerosolized CFU generated by coughing for 5 minutes was 16 (20). When an individual is infected with Mtb, the actual infection dose may be much lower than the number of bacteria released by coughing because not all aerosols generated by the infected person are inhaled. In addition, it has been reported that symptomatic TB patients release Mtb aerosols not only by cough but also by exhalation, with an aerosol size of 0.5-5 μm, showing that actual infection can be achieved in the context of a sustained low-dose of bacteria (21, 22). However, animal models for vaccine research in the preclinical stage can be established through a single, sufficient infection dose and used to evaluate vaccine efficacy. It is unclear whether the reduction in the bacterial burden by vaccination in the context of single-dose infection is a good predictor of actual clinical vaccine performance. This single-dose challenge could overwhelm or bypass the relevant immunological cascade and mask the full potential of candidate vaccines (23). In a mouse model, ultra-low-dose aerosol infection with 1-3 CFU resulted in characteristics more similar characteristics to human TB, such as highly heterogeneous bacterial burdens and well-circumscribed granulomas, than conventional-dose infection with 50-100 CFU (24). Recently, Dijkman et al. tested the efficacy of pulmonary BCG vaccination in a rhesus macaque model with a 1 CFU Mtb infection every day for 11 days and noted the importance of Th17 cells and IL-10 (25). This study does not represent all situations in which infection occurs, but it does provide a model that accounts for specific persistent and practical infection situations, such as household contacts. These studies suggest that it is necessary to reconsider the infection dose used in preclinical vaccine studies.

3.2 Experimental models

Most individuals who become infected can remain asymptomatic for a long time. Although environmental, cultural, geographical, and contextual characteristics can affect whether infection occurs, TB susceptibility due to host genetic differences has been reported as one of the determinants of TB disease (26). In the case of TB studies, more than 60% of preclinical studies have used mouse models, susceptibility to Mtb differs depending on the mouse strain. The most widely used C57BL/6 mice or BALB/c mice have relatively low susceptibility, whereas DBA/2, CBA/J, I/St, C3H, and A/J strains have relatively high susceptibility (27). In addition, it has been reported that necrotic granulomas found in patients with active TB are not formed in BALB/c or C57BL/6 mice, whereas they are formed in the TB-susceptible mouse strains I/St and C3H (28, 29). Recently, it was confirmed that human-like necrotic granulomas were formed by Mtb infection in a humanized mouse model, and caseous necrotic granulomas showed an immune phenotype and spatial organization similar to those observed in TB patients (30). Arrey et al. presented the utility of this model for the evaluation of a preclinical model of anti-TB drugs in an *in vivo* environment. Zelmer et al. immunized different strains of inbred mice, such as A/J, DBA/2, C57BL/6, and 129S2, displaying different susceptibilities to Mtb with BCG (31). Smith et al. used a "collaborative cross" model system created by crossing inbred and outbred mice to understand the broader host genetic susceptibility spectrum and for use in vaccine efficacy testing (32). These models can confirm the genetic immunological correlation associated with TB vaccine efficacy and can simultaneously be used to identify potential improvements and key defense factors for the development of a robust TB vaccine.

To date, most studies with NHPs have been used to model only acute TB, which is much less prevalent than latent TB in humans

(33). Rhesus macaques develop active TB in approximately 90% of the infected population, whereas cynomolgus macaques develop active TB in only 60% of the infected population. It has also been reported that BCG showed a higher protective efficacy in cynomolgus macaques than in rhesus macaques (34). Rhesus macaques and cynomolgus macaques can develop acute, chronic, or latent TB depending on the route of infection, dose, and Mtb strain used for inoculation.

Vaccine trials employing the NHP model are expensive, but they can serve as a checkpoint for clinical trials, resulting in significant cost savings. Areas-402 induced a strong T-cell response but did not protect rhesus macaques against infection with 200 CFU of Mtb Erdman (35). Conversely, a clinical study of MVA85A without efficacy evaluation was performed with the NHP model, and although it was expensive, the efficacy was not proven in the clinical stage (36, 37). These results suggest that validation of efficacy for TB vaccines via the NHP model to enter the clinical stage may accelerate TB vaccine development.

In an evaluation of vaccine efficacy in animal models, the bacterial burden between vaccinated and non-vaccinated groups is one of the key factors. Previous studies have demonstrated the presence of non-replicating bacterial populations in sputum samples obtained from TB patients (38, 39). These non-replicating subpopulations have been attributed to the existence of persister-like bacilli in a non-replicating state (39). Even in preclinical TB vaccine models, nonculturable or persistent mycobacterial subpopulations may arise due to immunological pressures resulting from the characteristics of the vaccine candidate or vaccine model, which can hinder the accurate evaluation of vaccine efficacy. Resuscitation-promoting factors (Rpfs) are bacterial proteins which are primarily identified by their ability to resuscitate nonreplicating cells *in vitro* and *in vivo* (40, 41). It has been reported that non-replicating bacteria in a patient's sputum can be revived by Rpfs and the culture time can be shortened (42, 43). The application of Rpfs to bacterial culture in conventional media has the potential to reduce errors in vaccine efficacy evaluation that can be caused by nonculturable or persistent subpopulations.

3.3 Translation and interpretation: differential analysis of samples between humans and animals

NHPs show anatomical and physiological similarities with humans as well as a wide range of clinical symptoms of TB, including pulmonary and extrapulmonary signs and symptoms. The NHP model enables the analysis of infected tissue, which is difficult in clinical stages, and at the same time, the disease course can be monitored by measuring parameters on radiographic images and examining body fluid samples, which can also be performed in humans. In addition, the NHP model allows the use of computed tomography and positron emission tomography to observe the progression of Mtb infection to disease in an individual (44). In the clinical phase, blood samples are used to measure immunogenicity. Currently, the Ag-specific T-cell response, multifunctionality of the Ag-specific T-cell response, and Ag-specific IgG antibody titers are commonly evaluated to demonstrate immunogenicity after vaccination (Table 1). However, in the case of vaccine candidates, when the efficacy is evaluated through animal experiments, the analysis is not based on blood but rather on tissues, such as lung, spleen, and lymph nodes. Therefore, it is difficult to apply COPs from tissue-based analysis in preclinical studies to clinical studies. The NHP model enables analysis of indicators applicable to human clinical studies such as blood, urine, and PET-CT results, and analysis of indicators that can be measured only after sacrificing animals, which is possible only in preclinical models. Exploration and verification of significant indicators through this model can lead to an acceleration of vaccine development. Therefore, studies employing the NHP model before the clinical stage can provide meaning beyond simply being the gateway to the clinical stage.

4 The third hurdle: antigen selection

4.1 Universal antigens

Mtb contains approximately 4,000 individual proteins, and most Ags included in current subunit vaccines have been adopted mainly based on their immunodominant properties for T-cell responses in preclinical and clinical settings. Currently, approximately 100 Ags in the preclinical stage (approximately 3% of all Mtb Ags) have been studied (Table 2). Most of the Ags for TB vaccine candidates are abundantly secreted and cell wall-associated proteins, including ESAT6, Ag85B, Ag85A, HSPX, and MPT64. In addition, cell wall-associated or virulence-associated Pro-Glu/Pro-Pro-Glu (PE/PPE) family proteins, a component of M72 subunit and ID93 subunit vaccine candidates, and heparin-binding hemagglutinin also produced promising vaccine-induced protection in mouse models (103, 104). Ags related to latency (DosR, resuscitation-promoting factor) and hypoxia-related proteins are being used for vaccine testing. Furthermore, hypothetical proteins are also used, for example, Rv1767, which is produced by the pathogen during the first week of infection of human cells. Aagaard et al. reported that the dimers EsxD-EsxC, EsxG-EsxH and EsxW-EsxV produced by the ESAT6 secretion system (ESX) were highly immunogenic. Integrating these in a fusion protein form called H65 resulted in a formulation that demonstrated protection efficacy equivalent to that of BCG without interfering with current ESAT6- and CFP10-based diagnostics (105). Liu et al. also purified 1,250 Mtb proteins with an *E. coli* expression system and evaluated cellular and humoral immune responses in human PBMCs and serum, respectively. They eventually identified four Ag candidates, Rv0232, Rv1031, Rv1198, and Rv2016, displaying high immunogenicity (106). Currently, only 11 Ags have been selected as a component, in the form of fusion proteins, in formulations eventually entered into clinical trials (Table 3).

10.3389/fimmu.2023.1193058

TABLE 1 Common and specific immunogenicity assessments of TB vaccines in clinical trials.

Type of vaccine	Name of vaccine	Purpose	Phase	Immunogenicity assessment	Reference
Live attenuated vaccine	MTBVAC	POD	3	■ Frequencies of MTBVAC-specific $CD4^+/CD8^+$ T cells producing one or more cytokines (IFN-γ, TNFα, IL-2, IL-17, or IL-22) ■ IFN-γ response to stimulation with ESAT6 and CFP10 in whole blood ■ IFN-γ ELISpot assay with PBMCs	(45, 46)
	VPM1002	POI, POD, POR	3	■ Concentration of IFN-γ upon PPD stimulation in whole-blood samples determined by ELISA ■ Proportions of distinct subsets of specific $CD4^+/CD8^+$ T cells produced one or more cytokines (IFN-γ, TNF-α, and/or IL-2) simultaneously in whole blood samples in response to PPD stimulation ■ PPD- and Ag85B-specific antibodies (IgG, IgA, and IgM) in serum	(47–49)
	BCG revaccination	POI, POD	3	■ Frequencies of BCG-specific $CD4^+/CD8^+$ T cells expressing at least two of three cytokines (IL-2, IFN-γ, and TNF-α) ■ Change in the concentration of IFN-γ in blood samples ■ $CD4^+$ T-cell subsets expressing IL-17A, IL-17F, or IL-22 (Th17) - either in combination with IFN-γ or IL-10 ■ Frequencies of NKT cells, γδ T cells, and $CD56^{hi/dim}$ NK cells producing IFN-γ	(50–52)
Adjuvanted protein subunit vaccine	$M72/AS01_E$	POD	3	■ The titer of M72-specific IgG antibody in serum ■ Frequencies of M72-specific $CD4^+/CD8^+$ T cells expressing one or more cytokines (IFN-γ and/or IL-2 and/or TNF-α and/or CD40L) simultaneously in PBMCs ■ IFN-γ production by $CD69^+CD56^+$ NK cells after stimulation with M72 peptide pool in PBMCs	(53–56)
	GamTBvac	POD	3	■ Frequencies of vaccine Ag-specific $CD4^+/CD8^+$ T cells expressing IFN-γ, TNF-α, and/or IL-2 in blood samples ■ Change in the concentration of IFN-γ in blood samples ■ The titer of IgG specific to the subunits of GamTBvac (fusion forms, DBD-Ag85A and DBD-ESAT6-CFP10, and subsets Ag85A, ESAT6, CFP10, and DBD)	(57, 58)
	ID93/GLA-SE (QTP-101)	POI, POD	2b	■ Frequencies of cytokine-expressing $CD4^+$ T cells specific to ID93, Rv1813, Rv2608, Rv3619, and Rv3620 ■ IFN-γ and IL-10 cytokine-secreting cells in PBMCs in response to ID93 determined by ELISpot ■ Frequencies of ID93 specific-$CD4^+/CD8^+$ T cells producing one or more cytokines (IFN-γ, TNF, and IL-2) in PBMCs ■ Titer of total IgG specific to ID93 and each fusion-protein antigen component (Rv1813, Rv2608, Rv3619, and Rv3620) ■ Titer of ID93-specific total IgG, IgG1, IgG2, IgG3, and IgG4	(59, 60)
	H56/IC31	POR	2b	■ Frequencies of $CD4^+$ T cells expressing IFN-γ, TNF-α, IL-2 and/or IL-17 after stimulation with H56-fusion protein or peptide pools of Ag85B, ESAT-6 or Rv2660c in whole blood samples ■ Memory phenotypes of H56-specific cytokine-expressing $CD4^+$ T cells ($IFN\text{-}\gamma^+$, $TNF\text{-}\alpha^+$, and/or $IL\text{-}2^+$) ■ Titer of IgG specific to H56 in plasma samples determined by ELISA	(52, 61)
	AEC/BC02	POD	2a	■ Evaluation of IFN-γ and antibody level in blood before and after immunization determined by intracellular cytokine staining ■ Changes in the levels of Ag-specific total IgG antibodies and IgG subclasses (IgG1 and IgG2) ■ Changes in the levels of Ag-specific IFN-γ levels ■ The changes in the proportion of Ag-specific T cells in PBMCs ■ Evaluation of ex vivo intracellular cytokine staining and ELISpot results in blood	(62)

POD, prevention of disease; POI, prevention of infection; POR, prevention of recurrence; ELISpot, enzyme-linked immunospot; PBMCs, peripheral blood mononuclear cells; PPD, purified protein derivative; ELISA, enzyme-linked immunosorbent assay; BCG, bacille Calmette-Guerin, * This paper focuses on subunit vaccines and live attenuated vaccines. Other TB vaccines in clinical studies, such as killed mycobacteria vaccines and viral vectored vaccines, are reviewed in detail in other articles (63, 64).

4.2 Rational antigen selection

The challenge of Ag screening is complicated by the roles of Ags in multiple stages of Mtb infection, particularly chronic and latent infection stages. During Mtb infection in a mouse model, ESAT6 is consistently expressed, but Ag85B is mainly expressed at an early stage when Mtb is actively replicating (116). Mtb infection induced the accumulation of ESAT6-specific $CD4^+$ T cells in the mouse lung parenchyma, but the T cells became functionally exhausted due to chronic stimulation of Ag. Whereas, Ag85B-specific $CD4^+$ T cells maintain memory cell features during infection but contract in numbers by reduced Ag expression during persistent infection (116). These results have important implications for the rational design of TB vaccines tailored to optimize the protection conferred by specific $CD4^+$ T cells that recognize Ag expressed at distinct stages of Mtb infection.

TABLE 2 Mtb antigens identified from preclinical experiments as vaccine components.

Gene accession No.	Antigen name	Rationale	Vaccine type	Route	Booster	Immunological role	Reference
Rv0129c	Ag85C	-	Recombinant bacterial (*L. ivanovii*)	IN	-	IgA secretion; Th1/Th17, TNF-α^+IL-17$^+$ CD8$^+$ T cells	(65)
Rv0159c	PE3	Elicit T-cell responses	Recombinant bacterial (*M. smegmatis*)	IP	-	IL-2/IFN-γ secretion (Th1 response)	(66)
Rv0160c	PE4	-	Recombinant bacterial (*M. smegmatis*)	IP	-	IL-2/TNF-α/IL-6 secretion	(67)
Rv0288	CFP7	Early-stage antigen	Fusion component (protein vaccine)	SC	-	IFN-γ/IL-17 secretion	(68)
Rv0288	CFP7	Early-stage antigen	Fusion component (protein vaccine)	SC	-	IFN-γ/IL-17 secretion	(69)
Rv0572c	DosR	Latency-associated hypothetical protein	Single protein	SC	-	IgG2a/IgG1 ratio, IFN-γ/TNF-α/IL-2 secretion (Th1 response)	(70)
Rv0577	TB27.3	Secreted by actively replicating bacteria	Fusion component (DNA vaccine)	ID	-	IgG2a/IgG1 ratio, IFN-γ/TNF-α secretion (Th1 response), IFN-γ^+ T_{EM} and IL-2$^+$ T_{CM} cells (memory T cells)	(71)
Rv0733	ADK	Screening based on cellular and humoral responses in active TB patients	Single protein	SC	-	IFN-γ^+TNF-α^+IL-2$^+$ CD4$^+$/CD8$^+$ T cell cells	(72)
Rv0915c	PPE14 (Mtb41)	Screening of Mtb expression library with specific T-cell lin	Single antigen (DNA vaccine)	IM	-	IgG2a secretion, IFN-γ secretion (Th1 response)	(73)
Rv0916c	PE7 (Mtb10)	Screening of Mtb expression library with specific T-cell line	Single antigen (DNA vaccine)	IM	-	IgG2a secretion, IFN-γ secretion (Th1 response)	(73)
Rv1009	RpfB	Reactivation	Single antigen (DNA vaccine)	IV	-	IL-2/IFN-γ secretion (Th1 response)	(74)
Rv1009	RpfB	Reactivation	Fusion component (protein vaccine)	SC	-	IgG2a/IgG1 ratio, IFN-γ/TNF-α/IL-2 secretion (Th1 response), IL-2$^+$ multifunctional (TNF-α or IFN-γ) CD4$^+$/CD8$^+$ T cells	(75)
Rv1009	RpfB	Reactivation	Fusion component (protein vaccine)	SC	-	IgG2a/IgG1 ratio, IFN-γ secretion (Th1 response), IFN-γ^+ T_{EM} IL-2$^+$ T_{CM} (memory T cells), multifunctional (IFN-γ/TNF-α/IL-2) CD4$^+$/CD8$^+$ T cells	(76)
Rv1009	RpfB	Reactivation	Single antigen (protein vaccine or DNA vaccine)	SC or IM	-	IFN-γ^+TNF-α^+IL-2$^-$CD107$^+$ CD4$^+$/CD8$^+$ T cells	(77)
Rv1039c	PPE15	Possible secreted antigen	Single antigen (ChAdOx1 viral vector)	IN or ID	- and +	IFN-γ^+/TNF-α^+/IL-17$^+$ CD4$^+$ T cells, CD45$^-$CXCR3^{hi}KLRG^{lo} CD4$^+$/CD8$^+$ T cells	(78)
Rv1174c	TB8.4	Extracellular proteins expressed by replicating bacilli	Fusion component	SC	BCG booster	IFN-γ^+/IL-17$^+$ CD4$^+$ T cells	(69)

(Continued)

TABLE 2 Continued

Gene accession No.	Antigen name	Rationale	Vaccine type	Route	Booster	Immunological role	Reference
			(protein vaccine)				
Rv1174c	TB8.4	Extracellular proteins expressed by replicating bacilli	Fusion component (protein vaccine)	SC	- and +	IFN-γ^+ $CD4^+$ T cells, IgG2a/IgG1 ratio	(79)
Rv1285	CysD	-	Fusion (CysVac2/ $Advax^{CpG}$)	IM or ID	-	Multifunctional (IFN-γ/TNF-α/IL-2) $CD4^+$/$CD8^+$ T cells, local accumulation of neutrophils ($CD45^+CD11b^+Ly6G^+$) and $CD64^+$ macrophages/monocytes ($CD45^+CD64^+CD11b^+Ly6G^-$)	(80)
Rv1419	Unknown	Secreted during proliferation	Single antigen (DNA vaccine-pVAX1 vector)	IM	therapeutic	IFN-γ^+ $CD4^+$ T cells	(81)
Rv1485	hemZ	IFN-γ release in PBMCs from hospitalized TB patients determined using IFN-γ ELISpot assays	Single protein	SC	-	IgG2a/IgG1 ratio, IL-2/TNF-α/IL-6/IFN-γ secretion	(82)
Rv1503c	Conserved protein (glycolipid synthesis)	Regulator PhoPR	Single protein (rBCG, live vaccine)	SC	-	IFN-γ secretion (Th1 response), Multifunctional (IFN-γ/TNF-α/IL-2) $CD4^+$/$CD8^+$ T cells	(83)
Rv1705c	PPE22	IFN-γ release in PBMCs from hospitalized TB patients determined using IFN-γ ELISpot assays	Single protein	SC	-	IgG2a/IgG1 ratio, IL-2/TNF-α/IL-6/IFN-γ secretion	(82)
Rv1733c	DosR	Latency	Single protein or peptide	SC	-	IFN-γ^+ $CD4^+$ T cells	(84)
Rv1738	Unknown	Hypoxic	Fusion component (live vaccine; yeast-based platform)	ID	- or therapeutic	IFN-γ^+IL-17^+ $CD4^+$ T cells	(85)
Rv1767	Hypothetical protein	Might be relevant for intracellular survival	Single protein (rBCG, live vaccine)	ID	-	IFN-γ^+/IL-17^+ $CD4^+$ T cells	(86)
Rv1793	EsxN	Virulence factor	Fusion component (protein vaccine)	SC	-	TNF-α^+/IL-17^+ secretion ratio	(87)
Rv1876	bfrA	Screening from a fraction that strongly induced the activation of immune cells	Single protein	SC	BCG booster	Multifunctional (IFN-γ/TNF-α/IL-2) $CD4^+$ T cells	(88)
Rv1886c*	Ag85B	Extracellular proteins expressed by replicating bacilli	Fusion component (protein vaccine)	SC	-	IFN-γ^+/IL-17^+ $CD4^+$ T cells	(69)

(Continued)

TABLE 2 Continued

Gene accession No.	Antigen name	Rationale	Vaccine type	Route	Booster	Immunological role	Reference
Rv1886c*	Ag85B	Extracellular proteins expressed by replicating bacilli	Fusion (CysVac2/ Advax^{CpG})	IM or ID	-	Multifunctional (IFN-γ/TNF-α/IL-2) CD4$^+$/CD8$^+$ T cells, local accumulation of neutrophils (CD45$^+$CD11b$^+$Ly6G$^+$) and CD64$^+$ macrophages/monocytes (CD45$^+$CD64$^+$CD11b$^+$Ly6G$^-$)	(80)
Rv0228	TB10.4	BCG antigens	Fusion component (protein vaccine)	SC	BCG booster	IFN-γ$^+$ CD4$^+$/CD8$^+$ T cells	(89)
Rv0228	TB10.4	Antimycobacterial immune responses in BCG-immunized humans	Fusion component (viral vector)	IN	BCG-virus vaccine	Multifunctional (IFN-γ/TNF-α, IFN-γ/IL-2) CD44$^+$CD62L$^-$CD4$^+$/CD8$^+$ T cells, IFN-γ$^+$ CD4$^+$ T cells	(90, 91)
Rv2005c	Universal stress protein family protein	Latency	Fusion component (protein vaccine)	SC	Immunotherapy	Muti-functional (IFN-γ/IL-2/TNF-α) CD44$^+$CD4$^+$ T cells, IFN-γ/IL-2/IL-17 secretion	(92)
Rv2031c	HspX	BCG antigens	Fusion component (protein vaccine)	SC	BCG protein	IFN-γ$^+$ CD4$^+$/CD8$^+$ T cells	(89)
Rv2031c	HspX	Immunoadjuvant potential	Fusion component (viral vector)	IN	BCG-virus vaccine	Multifunctional (IFN-γ/TNF-α, IFN-γ/IL-2) CD44$^+$CD62L$^-$CD4$^+$/CD8$^+$ T cells, IFN-γ$^+$ CD4$^+$ T cells	(90, 91)
Rv2031c	HspX	Expressed at the proliferating and dormant stages	Fusion component (protein vaccine)	SC	–	IgG2a/IgG1 ratio, IFN-γ/TNF-α/IL-2 secretion (Th1 response)	(93)
Rv2031c	HspX	Dormancy-related antigen	Fusion component (protein vaccine)	SC	–	IFN-γ$^+$ CD4$^+$ T cells	(94)
Rv2031c	HspX	Dormancy-related antigen	Recombinant bacterial (BCG expressed) fusion protein	Tail	–	IFN-γ$^+$ CD4$^+$ T_{EM} and IL-2$^+$ CD8$^+$ T_{CM} cells	(95)
Rv2031c	HspX	Dormancy-related antigen	Recombinant bacterial (BCG expressed) fusion protein	SC	–	IFN-γ$^+$/IL-17$^+$ CD4$^+$ T cell, IFN-γ$^+$IL2$^+$ CD4$^+$ T cells	(96)
Rv2032	acg	Hypoxic	Recombinant bacterial (*S. cerevisiae* yeast expressed) fusion protein	SC and ID	BCG-yeast	IFN-γ$^+$IL-17$^+$ CD4$^+$ T cells	(85)
Rv2034	ArsR repressor protein	Potential function in Mtb survive in the host	Fusion component +H1 (protein vaccine)	SC		Multifunctional (IFN-γ/TNF-α) CD4$^+$ T cells	(97)
Rv2073c	Probable short chain dehydrogenase	Hypoxic	Fusion component (DNA vaccine)	IM	–	IgG2a/IgG1 ratio, IFN-γ/TNF-α secretion (Th1 response), IFN-γ$^+$ T_{EM} IL-2$^+$ T_{CM} cells (memory T cells)	(71)
Rv2299c	htpG	Screening from a fraction that strongly induced the	Fusion component	SC	+	Multifunctional (IFN-γ/IL-2/TNF-α) CD4$^+$ T cells	(98)

(Continued)

TABLE 2 Continued

Gene accession No.	Antigen name	Rationale	Vaccine type	Route	Booster	Immunological role	Reference
		activation of immune cells	(protein vaccine)				
Rv2608	PPE42	Virulence factor	Fusion component (protein vaccine)		-	TNF-α^+/IL-17^+ secretion ratio	(87)
Rv2628	unknown	Latency	Fusion component (protein vaccine)		-	TNF-α^+/IL-17^+ secretion ratio	(87)
Rv2875	Mpt70	Hypoxic	Fusion component (DNA vaccine)	IM	–	IgG2a/IgG1 ratio, IFN-γ/TNF-α secretion (Th1 response), IFN-γ^+ T_{EM} IL-2^+ T_{CM} cells (memory T cells)	(71)
Rv3019c	esxR	Immunodominant and immunogenic *in vivo*-expressed TB proteins in Mtb-exposed individuals	Fusion component (protein vaccine)	SC	-	Multifunctional (IFN-γ/IL-2/TNF-α) $CD4^+$ T cells, $KLRG^-$ $CD4^+$ T cells	(99)
Rv3020c	esxS	Immunodominant and immunogenic *in vivo*-expressed TB proteins in Mtb-exposed individuals	Fusion component (protein vaccine)	SC	-	Multifunctional (IFN-γ/IL-2/TNF-α) $CD4^+$ T cells, $KLRG^-CD4^+$ T cells	(99)
Rv3044	fecB	Hypoxic	Fusion component (DNA vaccine)	ID	-	IgG2a/IgG1 ratio, IFN-γ/TNF-α secretion (Th1 response), IFN-γ^+ T_{EM} IL-2^+ T_{CM} cells (memory T cells)	(71)
Rv3131	DosR	Hypoxic	Single protein	SC	-	Multifunctional (IFN-γ/IL-2/TNF-α) $CD44^+CD62L^-CD4^+$ T cells, IFN-γ secretion	(100)
Rv3130	tgs1	Hypoxic	Recombinant bacterial (*S. cerevisiae* yeast expressed) fusion protein	SC and ID	BCG-yeast	IFN-γ^+IL-17^+ $CD4^+$ T cells	(85)
Rv3329	Unknown	Immunogenic proteins	Single protein	SC	-	IFN-γ/TNF-α/IL-2/IL-12/IL17 secretion	(101)
Rv3407	vapB47	Latency	Fusion component (protein vaccine)	SC	-	IgG2a/IgG1 ratio, IFN-γ secretion (Th1 response), IFN-γ^+ T_{EM} IL-2^+ T_{CM} cells (memory T cells), Multifunctional (IFN-γ/TNF-α/IL-2) $CD4^+$/$CD8^+$ T cells	(76)
Rv3432c	gadB	Immunogenic proteins	Single protein	SC	-	IFN-γ/TNF-α/IL-2/IL-12/IL17 secretion	(101)
Rv3615c	EspC	Non-BCG antigens	Fusion component (protein vaccine)	SC	BCG booster	IFN-γ^+ $CD4^+$/$CD8^+$ T cells	(89)
Rv3616c	EspA	Non-BCG antigens	Fusion component (protein vaccine)	SC	BCG booster	IFN-γ^+ $CD4^+$/$CD8^+$ T cells	(89)
Rv3803c	MPT51	Immunodominant antigens	Recombinant bacterial (BCG expressed) fusion protein	SC	–	IFN-γ^+/IL-17^+ $CD4^+$ T cells, IFN-γ^+IL2^+ $CD4^+$ T cells	(96)

(Continued)

TABLE 2 Continued

Gene accession No.	Antigen name	Rationale	Vaccine type	Route	Booster	Immunological role	Reference
Rv3804c*	Ag85A	–	Recombinant bacterial (BCG expressed) fusion protein	Tail	–	IFN-γ^+ $CD4^+$ T_{EM} and IL-2^+ $CD8^+$ T_{CM} cells	(95)
Rv3841	bfrB	Hypoxic	Recombinant bacterial (*S. cerevisiae* yeast expressed) fusion protein	SC and ID	BCG-yeast	IFN-γ^+IL-17^+ $CD4^+$ T cells	(85)
Rv3873	PPE68	Immunodominant antigens	Fusion component (protein vaccine)	SC and ID	BCG booster	Multifunctional (IFN-γ/IL-2/TNF-α/IL-17) $CD4^+$ T cells	(102)
Rv3874*	CFP10, esxB	Non-BCG antigens	Fusion component (protein vaccine)	SC	BCG booster	IFN-γ^+ $CD4^+$/$CD8^+$ T cells	(89)
Rv3875*	ESAT6, esxA	Non-BCG antigens	Fusion component (protein vaccine)	SC	BCG booster	IFN-γ^+ $CD4^+$/$CD8^+$ T cells	(89)
Rv3875*	ESAT6, esxA	Virulence factor	Fusion component (protein vaccine)	SC	–	IFN-γ^+ $CD4^+$ T cells	(94)

PBMCs, peripheral blood mononuclear cells; BCG, bacille Calmette–Guérin; rBCG, recombinant BCG; T_{EM} cell, effector memory T cell; T_{CM} cell, central memory T cell, ELISpot, enzyme-linked immunospot; IN, intranasal; IP, intraperitoneal; ID, intradermal; IM, intramuscular; IV, intravenous; SC, subcutaneous; *Antigens in a clinical trial for a TB vaccine.

Although immunodominant Ags are generally accepted to induce superior vaccine efficacy, some studies suggest that Mtb can modulate host immunity through immunodominant Ags. T-cell epitopes among well-known immunodominant Mtb Ags are highly conserved, suggesting the possibility that being recognized by the host through immunodominant Ags may be beneficial for Mtb (117, 118). In addition, T-cell responses to some immunodominant Mtb Ags have been found to be notably greater in active TB patients than in individuals latently infected with Mtb (119, 120), indicating that enhanced T-cell responses may be associated with deteriorated lung inflammation, resulting in subsequent transmission. Therefore, to confirm this possibility, Orr et al. confirmed the efficacy of immune subdominant Ags as a TB vaccine candidate in a mouse model, but little correlation has been found between vaccine efficacy and the immunodominance of Ags during Mtb infection (121).

TABLE 3 Composition and selection of subunit vaccines in the clinical stage.

	Composition	Ag selection	Reference
GamTBvac	■ Ag85A and ESAT6-CFP10 fusion protein/DEAE-dextran-CpG adjuvant	■ Induces strong IFN-γ production and T-cell proliferation (Ag85A) ■ The fusion of Mtb early-secreted Ag (ESAT6, CFP10)	(50, 107, 108)
M72/ $AS01_E$	■ Mtb32A-Mtb39A fusion protein/$AS01_E$ adjuvant	■ Recognized by PBMCs of healthy, disease-free, PPD-positive donors (Mtb32A, Mtb39A) ■ Induces strong T-cell proliferation and IFN-γ production (Mtb32A, Mtb39A)	(53–56, 109, 110)
H56/IC31	■ Ag85B-ESAT6-Rv2660c fusion protein/IC31 adjuvant	■ Early-secreted Ags (Ag85B, ESAT6) ■ Sustained secretion levels in the early and late stages of infection (Rv2660c)	(61, 111, 112)
ID93/ GLA-SE	■ Rv1813-Rv2608-Rv3619-Rv3620 fusion protein/GLA-SE adjuvant	■ A hypothetical protein enriched under hypoxic growth (Rv1813) ■ A probable outer membrane-associated Pro-Pro-Glu (PPE) motif-containing protein (Rv2608) ■ Secreted proteins belonging to the ESAT6 family (Rv3619, Rv3620)	(59, 60, 113)
AEC/BC02	■ ESAT6-CFP10 fusion protein and Ag85B/BC02 adjuvant	■ Strongly recognized by T cells in the early phase of infection (CFP10, ESAT6, Ag85B)	(114, 115)

Furthermore, it is also important to characterize the vaccine potential of Ags likely to be associated with reactivation from latent Mtb infection. A well-characterized bacterial regulon can induce the dormant state of Mtb that is controlled by DosR–DosS, which is induced by immunological pressure of the host such as local hypoxia, nitric oxide, and carbon monoxide (122). These host immune responses can be induced by the vaccine with immunodominant Ag in an active state of Mtb, indicating the potential for immune evasion of Mtb against immune responses produced by vaccines targeting immunodominant Ags in an activated state. Therefore, it is also important to characterize the vaccine potential of Ags likely to be associated with reactivation of latent Mtb infection. Hence, developing novel vaccines that encode genes expressed during the reactivation of a dormant state, such as *rpf*, would be a strategic approach. *In vitro* and *in vivo* transcriptional profiling studies have shown that five *rpf* of Mtb are expressed at varying levels in a growth stage-dependent manner (123, 124). RpfB, one of the five Rpfs produced by Mtb, plays an important role in the resuscitation and growth in a dormant state. In addition, delayed reactivation induced by aminoguanidine in chronic TB was observed in mice infected with a strain lacking *rpfB* (125), and significantly higher T cell responses to recombinant RpfB and RpfE were detected in LTBI than in active TB patients (126), indicating that Rpfs are involved in the reactivation process *in vivo*. Moreover, RpfB has been studied as a promising candidate for DNA vaccines, shown to induce a modest but significant cellular immune response against TB with higher levels of IL-2 and IFN-γ (74). In addition, the RpfB domain can induce a humoral response, and monoclonal antibodies against Rpfs could inhibit TB relapse (127).

4.3 Strategy for fusion proteins

Vaccine strategies using fusion proteins can be designed to include multiple Ags, so they can induce a broader immune response than single Ag vaccines. In addition, this strategy has the advantage of inducing an effective immune response by fusing a protein with low immunogenicity with a protein or peptide with high immunogenicity. The M72 vaccine candidate was formed through a fusion of the Mtb32A and Mtb39A proteins, selected for their ability to provoke T-cell responses in TST-positive healthy adults. On the other hand, multistage subunit vaccines, such as H56 (which contains the latency-associated Ag Rv2660c fused with Ag85B and ESAT6), as well as LT70 and ID93, also incorporate multiple Mtb Ags differentially involved in bacterial growth, virulence, and metabolism (111, 128, 129). A new TB vaccine candidate, H107, that integrates eight individually protective Ags (PPE68, ESAT6, EspI, EspC, EspA, MPT64, MPT70, and MPT83) is highly immunogenic in both mice and humans (102). This fusion protein is composed of 4 ESAT6 molecules in the middle, which led to a significant increase in ESAT-6-specific immunogenicity. H107 with the BCG vaccine could increase Ag coverage to induce robust protective immune responses in a diverse human population by including as many protective/recognizable Ags as possible. While traditional vaccines containing BCG-shared Ags show *in vivo* cross-reactivity to BCG, H107 demonstrates no cross-reactivity and does not impede BCG colonization. Instead, co-administering H107 with BCG results in enhanced adaptive responses against both H107 and BCG (102).

5 The fourth hurdle: immune correlates and protection biomarkers

Unveiling reliable predictive correlates to the immunogenicity and efficacy of TB vaccines allows estimation of vaccine efficacy well in advance of the time required to confirm vaccine efficacy against Mtb infection in the clinical stage. In addition, after the commercialization of a vaccine, successful vaccination can be tracked through reliable COP measurement of vaccinated individuals, and as a result, herd immunity through vaccination can be effectively achieved. Therefore, attempts have been made to identify reliable COPs of TB vaccines, but it is still unclear. Currently, in most vaccine studies in clinical phases, immunogenicity or vaccine-induced protection-related biomarkers are limited to immunological markers, especially IFN-γ-producing T cell responses, polyfunctional T-cell responses, or antibody titers in response to Mtb Ag. Recently, the possibility of developing protective immunity and vaccines for donor unrestricted T cells (DURTs), Th17 cells, antibodies, B cells, and innate immunity beyond Th1 immunity has been reconsidered for TB vaccines (130). Moreover, the association between TB progression and type I IFNs in active TB disease has been reported, but clinical studies on the efficacy and markers of TB vaccines are still lacking. These results raise questions about the sufficiency of T-cell responses induced by vaccination for protection and force us to explore additional biomarkers of vaccine efficacy.

5.1 Correlates of protection in innate immune response to the TB vaccine

Continuous research on innate immune factors related to the efficacy of TB vaccines has been conducted. Strategies that target these innate immune factors have been shown to improve vaccine efficacy. In addition, the characteristics of innate immune factors that correlate with vaccine efficacy show potential as biomarkers of vaccine efficacy (Figure 1).

5.1.1 Monocytes

The monocytes to lymphocytes (ML) ratio in peripheral blood has been reported to be correlated with TB disease risk among HIV-infected patients (131, 132). In addition, it was reported that the ML ratio increased in severe TB patients and more so in males than females even within the TB patient group, showing a correlation with TB progression (133). Interestingly, Zelmer et al. reported that upon inoculating inbred mouse strains of different genetic backgrounds with BCG, the ML ratio correlated with BCG-induced vaccine efficacy against Mtb infection, suggesting that monocytes are deeply involved in the vaccine-induced immune

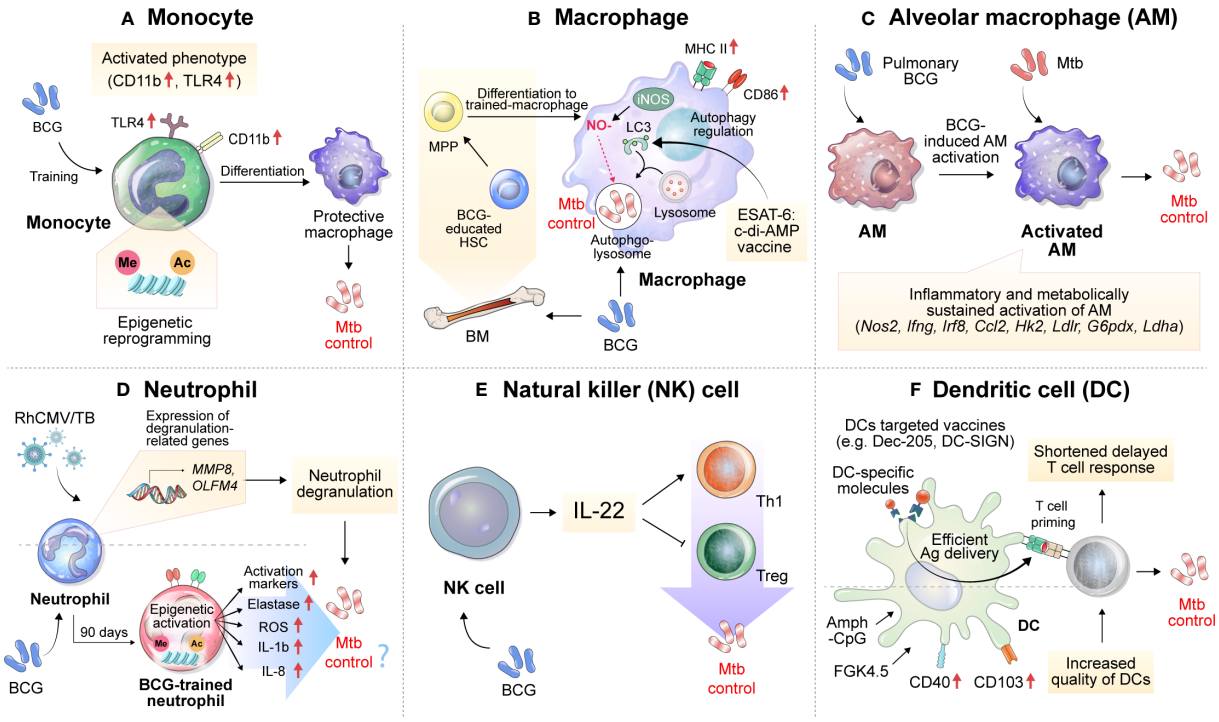

FIGURE 1
Implications of innate immune cells and relevant immune responses for the development of TB vaccines. Immune responses related to TB vaccines are mainly focused on adaptive immunity, especially T cells, but many studies imply the importance of innate immune responses. **(A)** BCG vaccination induces the histone epigenetic reprogramming of monocytes, resulting in an activated phenotype with increased CD11b and TLR4 expression. **(B)** BCG can activate macrophages and educate hematopoietic stem cells (HSCs) to differentiate into more protective macrophages against Mtb infection. Vaccination with ESAT6:c-di-AMP can control Mtb growth by regulating autophagy. **(C)** Alveolar macrophages, which act as first-line defenders against pathogens entering the lungs, are inflammatory and sustainably metabolically activated by BCG mucosal vaccination, which controls the dissemination and growth of Mtb. **(D)** The expression of genes related to neutrophil degranulation such as *MMP8* and *OLFM4* was suggested as a correlate of protection in the RhCMV/TB-vaccinated rhesus macaque model. BCG vaccination in healthy humans induces long-lasting changes in the neutrophil phenotype, characterized by increased expression of activation markers and antimicrobial function, which is associated with genome-wide epigenetic modifications in trimethylation at lysine 4 on histone 3. The enhanced function of human neutrophils persists for at least 3 months after vaccination. **(E)** Depletion of NK cells during BCG vaccination reduces protection against Mtb infection, concomitant with decreased Th1 response and increased Treg levels. The complementation of IL-22 restores the vaccine efficacy of BCG against Mtb infection, which was reduced by NK cell depletion. **(F)** Vaccines targeting DCs by using DC-specific molecules, such as Dec-205 and DC-SIGN can effectively deliver Ags to DCs. An increase in the quality of DCs through treatment with Amph-CpG and FGK4.5 can increase vaccine efficacy via effective T-cell priming. MPP, multipotent progenitor; HSCs, hematopoietic stem cells; NO, nitric oxide; iNOS, inducible nitric oxide synthase; c-di-AMP, c-di-adenosine monophosphate; BM, bone marrow; LC3, microtubule-associated protein 1A/1B-light chain 3; Amph-CpG, amphiphilic form of CpG.

response (31). BCG vaccination induces an increase in inflammatory mediator production by monocytes through histone modifications and specific gene activation (134). After BCG immunization, circulating monocytes in healthy volunteers released two times more cytokines, such as IL-1β and tumor necrosis factor (TNF)-α, upon stimulation with TB nonspecific pathogens. These BCG-trained monocytes had increased expression of CD11b and Toll-like receptor 4 (TLR4), and these immune effects were related to histone epigenetic reprogramming induced by activation of the NOD2 receptor to increase trimethylation of lysine 4 on histone 3 (H3K4m3) (Figure 1A). Interestingly, the effectiveness of trained immunity was maintained for up to one year, and heterogeneous protection by BCG vaccination in terms of neonatal death from other infectious diseases was significantly increased in the infant group aged 1 to 5 years (135). Recently, protection by BCG revaccination has been reported at the clinical stage (50), but the specific protective mechanism has not yet been fully elucidated.

5.1.2 Macrophages

Recently, vaccination with ESAT6:cyclic diadenosine monophosphate (c-di-AMP) was shown to cause significant reductions in the bacterial burdens of the lungs and spleens in a mouse model by regulating autophagy in Mtb-infected macrophages (136). In addition, mouse bone marrow-derived macrophages infected with BCG become epigenetically modified to provide better protection against Mtb infection (137). This macrophage activation phenotype was also reported by Mate et al., and increases in MHC II, CD86, and inducible nitric oxide synthase levels were observed after intranasal (IN)-BCG vaccination but not after subcutaneous (SC) vaccination (Figure 1B).

Alveolar macrophages (AMs) may serve as the first line of defense against respiratory pathogens. However, a mouse model study showed that AM depletion has a protective effect on lung Mtb infection (138). Mtb becomes an exclusive niche for up to 10 days after Mtb infection (139). In addition, Mtb induces a Th1 response by inducing rapid dissemination of bacilli to the lymph nodes in an

IL-1 receptor-dependent manner after AM infection, but poorly transmissible Mtb delays this process, residing inside AMs and developing and promoting the Th17 response (140). These reports suggest that AMs induce a delay in the early immune response during Mtb infection, leading to a delay in protective T-cell immunity.

On the other hand, it has been reported that mucosal vaccination with BCG is effective in inhibiting early dissemination of Mtb by inducing activation while BCG is present in AMs (141). In addition, the formation of trained immunity in mouse AMs through vaccination or infection has been reported (142, 143), and in this context, pulmonary BCG vaccination increases Mtb growth control in AMs early in infection and, through IL-1 signal-dependent Mtb transmission (140), may lead to shortening of the T-cell response delay (Figure 1C). Recently, aerosol vaccination with a human serotype-5 adenovirus (Ad)-vectored TB vaccine (AdHu5Ag85A) was reported in a clinical phase 1b trial. Transcriptomic analysis of AMs isolated from the aerosol AdHu5Ag85A-immunized group in this study showed that aerosol vaccination with AdHu5Ag85A induced persistent transcriptional changes in AMs related to the response to anoxia, inflammatory response to Ag stimulation, tyrosine phosphorylation of signal transducer and activator of transcription proteins, regulation of IL-10 production, response to IL-1 and histone demethylation (144).

5.1.3 Neutrophils

The importance of neutrophil in TB is evidenced by the identification of prominent neutrophil transcription signatures in the blood of TB patients (145). The formation of neutrophil extracellular traps (NETs) induced by type I IFN promotes bacterial growth and disease severity in Mtb-infected mice (146). Given the critical function of neutrophils in TB pathogenesis, it is important to understand their properties in vaccine immune responses.

Monalisa et al. reported that the depletion of neutrophils during vaccination with *Mycobacterium smegmatis* expressing CMX induced a decrease in protection against Mtb infection in a mouse model, with a decrease in Th1 and Th17 responses in lung tissue and spleen, suggesting the function of neutrophils in the formation of T-cell responses (147). Thomas et al. reported the role of neutrophils in the formation of protective immunity by BCG vaccination (148). Seven days after BCG inoculation via the SC route, a slight increase in the frequency of neutrophils was observed in the lung tissue. In addition, the protective immunity induced by BCG was independent of T cells, and it was reported that this effect was maintained until 30 days after vaccination in T cell- or TNF-α-deficient mice. After BCG inoculation, depletion of neutrophils using an anti-Ly6G antibody resulted in protection provided by BCG being reduced by half, and this phenomenon was confirmed regardless of the presence of neutrophils at the time of Mtb infection (148). These results suggest that neutrophils contribute to the generation of protective innate immunity in the early stage of infection rather than direct killing of Mtb. In addition, BCG vaccination of healthy individuals generated phenotypic alterations in neutrophils, with enhanced antimicrobial function as well as upregulation of activation marker expression. The change in human neutrophils lasts for at least three months, along with genome-wide epigenetic remodeling via H3K4m3 modifications (149) (Figure 1D).

Recently, Hansen et al. administered the rhesus cytomegalovirus vectors (RhCMV) encoding Mtb Ag inserts (RhCMV/TB) vaccine to BCG-vaccinated or unvaccinated rhesus macaques (150). Before Mtb-challenge, the transcriptomic analysis of whole blood revealed that the gene expression levels predictive of the RhCMV/TB vaccine effect were predominantly from neutrophils. These genes were linked to innate immunity and pathways related to neutrophil degranulation, which encompassed genes encoding neutrophil granule effector molecules such as MMP8 and CTSG (Figure 1D). However, in the group vaccinated with BCG + RhCMV/TB, a specific set of genes associated with protection, such as *MMP8*, *CTSG*, and *CD52*, showed reduced expression compared to the group vaccinated with RhCMV/TB alone at the early phase of Mtb challenge. These transcriptional profiles correlated with a lower protective ability of BCG + RhCMV/TB than RhCMV/TB vaccine.

5.1.4 Natural killer cells

NK cells accumulate in the lungs during Mtb infection and produce IFN-γ and perforin, but studies on the function of NK cells in vaccine responses are still lacking. BCG-vaccinated mice had an increased number of NK cells in the spleen and peripheral lymph nodes. To determine the function of BCG-induced NK cells, anti-NK1.1 antibodies were administered to BCG-vaccinated mice to deplete NK cells, resulting in decreased protective efficacy of BCG and an increased number of regulatory T cells (Tregs) and a diminished T-cell response (151). The depletion of NK cells resulted in the induction of Tregs and a reduction in T-cell activity after Mtb infection, but supplementation with recombinant IL-22 rescued BCG-induced protection, suggesting the importance of IL-22 in NK cell-mediated protection against BCG vaccination (151) (Figure 1E). On the other hand, Thomas et al. infected mice with H37Rv after depleting NK cells by treatment with an anti-asialo-GM1 antibody during BCG vaccination but found no difference in efficacy after 30 days (148).

5.1.5 Dendritic cells

Delayed T-cell responses are one of the typical characteristics of TB, and to control them, the formation of a protective T-cell response and the accumulation of a considerable number of T cells at the site of inflammation are important. In this process, proper dendritic cell (DC) activation, rapid DC migration, and interaction with T cells are important. According to previous studies with a mouse model, vaccination relieved the delayed T-cell response of the host to some extent, but a delayed $CD4^+$ T-cell response still occurred in the vaccinated host (152, 153), which may be the reason why vaccine-induced TB control is not effective. There have been studies that have focused on the role of DC frequency or activation in the delay of T cell response in vaccination. In a mouse model, vaccination with recombinant BCG-producing FMS-like tyrosine kinase 3 ligand or granulocyte-macrophage colony-

stimulating factor (GM-CSF) increased the frequency of DCs. This increase in DC frequency demonstrated enhanced protection against Mtb infection (154, 155). In addition, in the analysis of the RNA expression profile related to vaccine immunogenicity and efficacy in the PBMCs of recipients of the TB vaccine candidate M72/AS01$_E$, it was confirmed that the increase in the number of activated DCs was induced by vaccination (156). Griffiths et al. reported that after BCG vaccination, an increase in CD103 and CD40 expression on DCs induced through CpG and anti-CD40 antibody (FGK4.5) stimulation increased the number of DCs and strengthened the interaction ability with T cells in the lung, resulting in increased vaccine efficacy against Mtb infection (157) (Figure 1F). These findings indicate that increasing the frequency or quality of DCs can directly affect vaccine efficacy. Moreover, efficient Ag delivery is also directly related to the efficacy of the TB vaccine. Griffiths et al. confirmed that the transfer of DCs loaded with Mtb Ag85B accelerated the delayed T-cell response of mice immunized with BCG or Mtb Ag and increased the vaccine efficacy, showing the importance of DCs in vaccination (157). DC-targeted vaccines through DC-specific molecules such as DEC-205 or DC-SIGN (158, 159) show increased T cell response and vaccine efficacy in mouse model, which emphasis the importance of DCs in TB vaccination (Figure 1F). However, there are still few data on the response of DCs induced by vaccines.

5.2 Correlates of protection in adaptive immune response to the TB vaccine

Protection against Mtb afforded by a TB vaccine in a mouse model appears to correlate with the T_{CM} phenotype, but data are limited. Tissue-resident memory T (T_{RM}) cells, parenchymal-resident noncirculating memory cells that have been studied only relatively recently, reside in tissues for early recognition of infected cells (160). Vaccines that elicit a rapidly accessible T-cell response to the pathogen early in Mtb infection are thought to enable more efficient protection via T_{RM} or T_{EM} cells. Furthermore, the protective role of antibodies in the pathogenesis of TB highlights the need for continuous exploration of the adaptive immune response as a biomarker for vaccine efficacy.

5.2.1 Tissue-resident memory T cells

Since Mtb is transmitted via the aerosol route, generating a pulmonary memory immune response is important for protective immunity, which enables an immediate immune cell response to an infection site. The generation of T_{RM} cells has been shown to correlate with protection against Mtb and is characteristically induced, particularly upon mucosal vaccination (161, 162) (Figure 2A). Mucosal transfer of T_{RM} cells from BCG-vaccinated mice to naïve mice showed that both $CD4^+$ and $CD8^+$ T_{RM} subpopulations can provide partial protection against Mtb infection (163) and can restrict intracellular Mtb survival *in vitro* (164). A recent study using human tissue from surgically resected lungs also demonstrated that the number of IL-17-producing Mtb-specific T_{RM}-like cells in the lungs was inversely correlated with IL-1β levels in the blood, indicating that Mtb-specific T_{RM} cells producing IL-17 may play an important role in controlling Mtb in the human lung (165). These reports suggest that T_{RM} cells are correlated with protection in TB vaccination models, and this cell population could be a target for vaccine strategies for protection against TB. In several disease models, including TB, a strategy called "prime and pull" to recruit memory T cells through booster vaccination to target tissues after prime vaccination has been carried out (166–168). Roces et al. reported a vaccine strategy to boost immunization with H56 protein in the lung mucosa through inhalation after immunization with CAF01:H56, a clinical TB vaccine candidate, by the SC route (169). For the booster vaccination, the poly lactic-co-glycolic acid delivery system, which has been recognized for its safety, was used, and the experiment was designed based on the manufacturing of a powder containing H56. Haddadi et al. parenterally immunized mice using a recombinant replication-deficient chimpanzee Ad-based TB vaccine expressing Ag85A (AdCh68Ag85A) and then immunized the mice with Ag85 complex via the IN route (170). In this study, immunization with Ag85 via the IN route was able to induce an almost 2-log reduction in the bacterial burden in the lung tissue upon Mtb H37Rv infection compared to that in the group that received only parenteral immunization. Importantly, these results demonstrate that the prime and pull strategy for the respiratory mucosa can promote the development of T_{RM} cells as well as the recruitment of Ag-specific T cells into lung tissue. In addition, to effectively pull memory T cells into the respiratory mucosa, it was confirmed that booster vaccination should be given at a time when T cells mainly form a memory type rather than after a short period of time when effector T cells are mainly present after prime vaccination (170).

Direct immunization to the lung, the site of infection, has been reported to be beneficial for the formation of T_{RM} cells. However, Darrah et al. confirmed the level of T_{RM} cells in lung tissue 4 weeks after BCG immunization in an NHP model, BCG delivered by the intravenous (IV) route was able to induce higher levels of T_{RM} cells than BCG injected by the aerosol route (171). Of note, six months after Mtb challenge, nine out of ten macaques with BCG immunization via the IV route produced a significant Ag-specific T-cell response accompanied by highly protective vaccine efficacy compared with those with the intradermal (ID) or aerosol route vaccination; and six of ten macaques administered BCG via the IV route had no detectable levels of infection (171).

The formation of T_{RM} cells was thought to proceed via differentiation from effector T cells *in situ* via transforming growth factor beta (TGF-β) and IL-15 signals when inflammation resolves (172). In addition, at the priming level, mouse Batf3-dependent DCs and human $CD1c^+CD163^+$ DCs producing TGF-β can prime T cells for T_{RM} cell generation in lymphoid tissues (173). These reports may reveal the reason for the finding that systemic immunization via the IV route induces higher T_{RM} cell levels in lung tissue than the aerosol route or direct BCG delivery to the lungs. However, it is a challenge to ensure the safety of the administration method, to analyze the T_{RM} cells and to verify the efficacy in clinical trials.

The generation of inducible bronchus-associated lymphoid tissues (iBALTs), a type of tertiary lymphoid structure (TLS), could be pivotal because increased $CXCR5^+$ $CD4^+$ T cell levels were correlated with a better outcome of TB disease (174, 175)

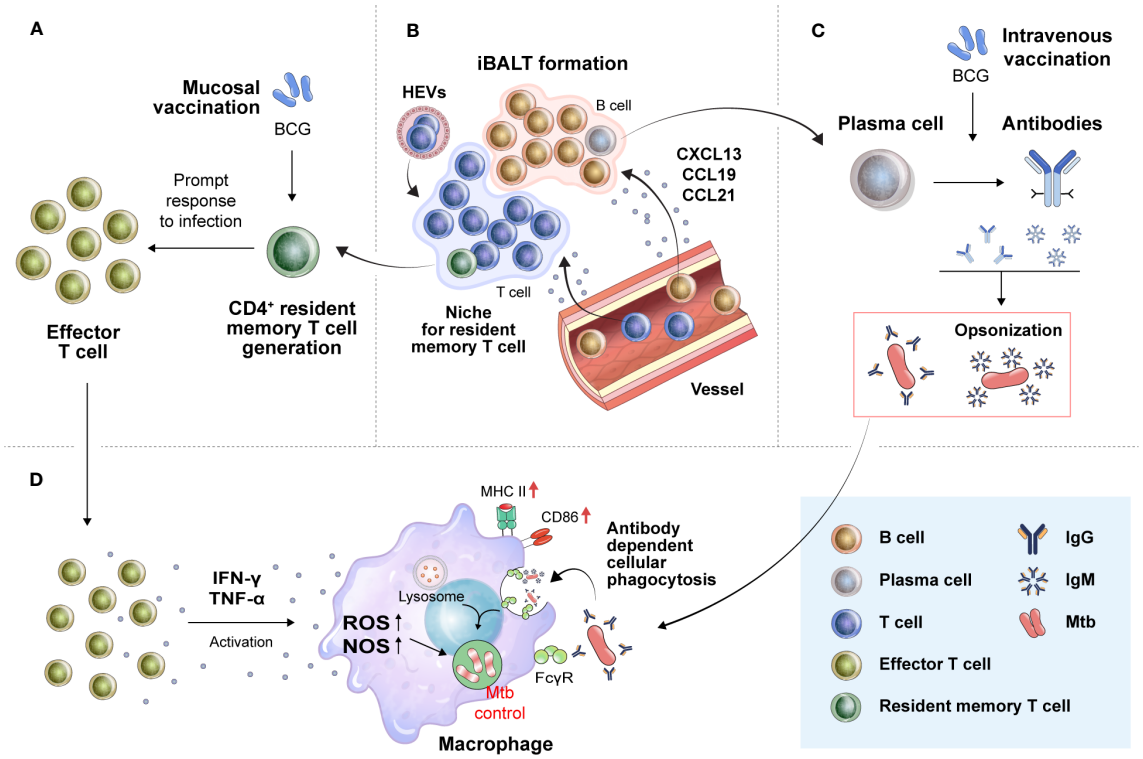

FIGURE 2
Translation of novel immune correlates found in preclinical animal models into humans for the development of more effective TB vaccines. **(A)** Mucosal vaccination can strongly induce T_{RM} cell development. In the early stage of Mtb infection, T_{RM} cells proliferate promptly to effector T cells to combat the bacilli by secreting proinflammatory cytokines. **(B)** T_{RM} cells residing in the lung parenchyma, especially $CD4^+T_{RM}$ cells, are known to be located in tertiary lymphoid structures, such as iBALTs. The formation of iBALTs is regulated by cytokines (IL-17, IL-22, and IL-23) and chemokines (CCL19, CCL21, CXCL12, and CXCL13). Structured iBALT consists of the T-cell zone and B-cell zone. These ectopic lymphoid-like structures provide a place where follicular helper T cells mediate the selection and survival of B cells, resulting in the differentiation of long-lived plasma cells. These processes make it possible to induce *in situ* protective humoral immunity by secreting protective immunoglobulins, such as IgM and IgG. **(C)** These humoral and cellular *in situ* immune responses can create an environment favorable for the host to control Mtb. Immunoglobulins from B cells aggregate Mtb, resulting in the formation of pathogen-antibody complexes. **(D)** The formation of these complexes enhances phagocytic killing activity of macrophages. Proinflammatory cytokines from T cells (IFN-γ and TNF-α) activate macrophages to kill Mtb. T_{RM} cells, tissue-resident memory T cells; iBALTs, inducible bronchus-associated lymphoid tissues; ROS, reactive oxygen species; NOS, nitric oxide synthase; FcgR, Fc gamma receptor.

(Figure 2B). TLSs are formed at sites of infection or chronic inflammation and have also been found in autoimmune disease, allograft rejection, and cancer. Importantly, B cells that respond to tumor-associated TLSs appear to participate in antitumor immunity, as B cells cultured from TLS-containing biopsy samples produced tumor Ag-specific antibodies (176). This ectopic lymphoid structure can also act as a site for B-cell selection and maturation (177) and can provide a niche for memory B cells and T cells (178). In an influenza virus-infected mouse model, $CD8^+$ T_{RM} cells were mainly located in the interstitium extending into the lung parenchyma, whereas $CD4^+$ T_{RM} cells were found in the iBALT niche (179, 180). These reports suggest that iBALT might enable a rapid and effective response to Mtb infection.

5.2.2 Effector memory T cells

Hansen et al. recently tested RhCMV/TB vaccine capable of expressing six or nine Mtb Ags in rhesus macaques (150). Upon infection of the macaques with the Erdman strain almost 1 year after vaccination, it was confirmed that sterile immunity was induced in approximately 40% of the experimental group animals (150). In contrast to previous vaccine strategies aimed at eliciting primarily T_{CM} cell responses, this CMV-based vaccine elicited primarily T_{EM} cell responses. T_{EM} cell population appears to be maintained by continuous restimulation of Mtb-specific T cells by periodic reactivation of the cytomegalovirus, and the authors suggest that protective immunity induced by the RhCMV/TB vaccine can be induced by Mtb-specific T cells from the vaccination. This phenomenon is thought to be due to the high frequency of T_{EM} cells generated by the restimulation of cells (150). However, CMV infection can be fatal in immunocompromised humans (181), and according to a recent study conducted in South Africa, CMV seems to be related to the increase in the incidence of TB in children (182). It is believed that replicating CMV-based vaccines will be needed, but this type of vaccine needs to be proven effective.

5.2.3 IgG/IgM

While the role of humoral immunity in TB has been controversial, several reports have led to a reassessment of the

significance of antibody-mediated immunity in providing protection against Mtb (183–185). Antibodies can play an important role in preventing or eliminating the initial Mtb infection (Figure 2C). Antibodies can bind Mtb and increase macrophage phagocytosis by binding Fc receptors and play an effective role in clearing other intracellular pathogens. Recent studies have shown that antibodies that prevent Mtb infection are present in humans (183, 185). The first suggestion that antibodies may be protective was reported by Teitelbaum et al. (186). Mtb was pretreated with two monoclonal antibodies specific to cell surface Ags and injected through the trachea. Pretreated bacterium-infected mice lived substantially longer than control mice (186). Moreover, Ag85A-specific IgG responses have been associated with reduced TB development (187). Alternative vaccination routes, such as mucosal and IV, result in the production of pulmonary IgA and iBALTs, reducing the bacterial burden (161, 162, 171). Recently, Edward et al. reported that IgM has a negative correlation with Mtb load upon IV-BCG vaccination in macaques (188). They examined antibody responses across several BCG vaccine regimens in NHP models to determine if particular antibody profiles were linked with better Mtb control. Correlation analysis revealed a particularly strong association between plasma and bronchoalveolar lavage IgM responses and reduced Mtb burden upon BCG vaccination. Importantly, elevated Ag-specific IgM titers were observed not only in the lungs but also in the plasma of the IV-vaccinated animals. Furthermore, IgM antibodies enhance the Mtb restriction activity *in vitro*. These reports show the potential of IgG or IgM as a new COP in clinical practice.

These humoral and cellular *in situ* immune responses can be targeted for induction by a TB vaccine. Such a strategy can create a favorable environment for the host to control Mtb. Pathogen-antibody complexes formed by IgM or IgG secreted by B cells can promote the phagocytosis of Mtb by macrophages. A rapid and appropriate T-cell response to infection can induce Mtb control by inducing the activation of macrophages in the early stages of infection (Figure 2D).

5.3 Key compensatory markers

5.3.1 Biomarkers in urine samples

Finding a biomarker for COPs of a TB vaccine in urine offers several advantages over blood with respect to collection and safety. In particular, the development of biomarkers for COPs through urine sampling can be helpful in controlling TB by using vaccines in the least-developed countries, especially in the least-developed countries with a high incidence of TB, because vaccination subjects can continually collect samples themselves after simple education.

The possibility of identifying COPs for TB vaccination via biomarkers in urine is suggested by urine analysis studies on indicators of TB development and treatment. For example, in active TB patients, inflammatory mediators such as IL-8, IL-2, TNF-α, IFN-γ, chemokine ligand (CCL) 5, macrophage inflammatory protein-1 alpha and beta were not detected in the urine, but chemokine (C-X-C motif) ligand (CXCL) 10 was persistently detected (189). Moreover, the level of CXCL10 in urine was decreased in patients treated with TB drugs compared to that in active TB patients (189, 190). However, the CXCL10 level in urine is not a specific biomarker that is increased only by pulmonary TB infection, but it can be used as a limited biomarker because it shows a similar increase in patients with other lung diseases. Lipoarabinomannan (LAM), an Mtb cell wall component detected in urine, was used to establish a urinalysis for diagnosing disseminated TB patients among human immunodeficiency virus (HIV)-infected patients (191, 192). In addition, changes in the levels of 12 metabolites in urine were reported in patients with active TB after anti-TB treatment (193).

Biomarker analysis using urine samples is also being applied in vaccine research. To evaluate the toxicity of two influenza vaccines with different toxicities in a mouse model, hydrogen-1 nuclear magnetic resonance spectroscopy was used to observe changes in urine metabolite levels, and findings were compared with existing toxicity indicators such as weight loss and leukopenia (194). In addition, analysis of changes in urinary cytokine levels, as a predictor of immunogenicity and reactogenicity, induced by the $AS01_E$-adjuvanted hepatitis B vaccine in healthy adults was used to evaluate the effectiveness of the vaccine (NCT01777295). Upon measuring the concentrations of 24 cytokines in the urine of the saline-administered control group and the vaccine group, a transient increase in CCL2 and CXCL10 levels was observed after vaccination (195). These results show the possibility of discovering biomarkers as COPs for TB vaccination through urine analysis.

5.3.2 Type I IFNs

Detrimental roles of type I IFNs in TB pathogenesis have been extensively investigated. However, there have also been reports on the protective role of type I IFNs in relation to TB vaccines. For example, it has been reported that type I IFNs can increase the immunogenicity of the BCG vaccine in mouse models. These reports showed that vaccination with ESX-1-expressing BCG could increase vaccine efficacy against Mtb infection in murine models by increasing ESX-1-dependent type I IFN production (196, 197). In the case of MTBVAC, the double deletion of *phoP* and *fadD26* resulted in a 25- to 45-fold increase in c-di-AMP levels compared to those with Mtb or BCG, which resulted in attenuation of toxicity and high vaccine efficacy in a mouse model through an ESX-1 system-dependent type I IFN response (198, 199). Additionally, vaccination with BCGΔBCG1419c in mouse models had a higher vaccination efficacy than normal BCG vaccination (200). The BCG1419c gene encodes a cyclic diguanosine monophosphate (c-di-GMP) phosphodiesterase that normally functions to hydrolyze c-di-GMP. Vaccination with BCGΔBCG1419c is expected to result in the production of more c-di-GMP, which is thought to have a protective effect by inducing an increase in type I IFN signaling through the TANK-binding kinase 1 and interferon regulatory factor 3 cascade (200, 201). In addition, the administration of IFN-α in combination with BCG vaccination has been shown to increase the efficacy of the TB vaccine in a mouse model (202). These results indicate that type I IFNs may have different functions in TB pathogenesis and vaccine-induced immunity and the positive role of type I IFNs shows their potential as biomarkers for the efficacy of vaccine candidates.

6 The fifth hurdle: further considerations

6.1 Factors affecting vaccine efficacy: preexposure to related and unrelated pathogens

6.1.1 Helminth

Chronic infection with helminths has been well documented in cells secreting IL-10 or TGF-β and induces the induction of Tregs, which downregulate both Th1 and Th2 immune responses and mainly interfere with the function of effector Th1 cells (203). These immunological properties of helminths can affect the efficacy of TB vaccines. BCG immunogenicity was found to be lower in individuals with helminth infection than in those treated with anti-helminthic drugs (204). The reduced responses were associated with decreased purified protein derivative (PPD)-specific IFN-γ and IL-12 production and with an enhanced PPD-specific TGF-β response rather than an increase in the PPD-specific Th2 response itself. Likewise, helminth-infected college students aged 18 to 24 years in Ethiopia who received deworming therapy prior to BCG vaccination displayed relatively more PPD-specific immune responses than untreated control individuals (205). Similarly, maternal infection with helminths during pregnancy negatively influenced the frequency of IFN-γ-producing T cells in the cord blood of neonates (206) as well as the development of Th1 immunity in offspring vaccinated with BCG (207). Recently, Schick et al. reported that *Nippostrongylus brasiliensis* infection-induced production of IL-4 or IL-13 suppressed the H1/CAF01 vaccination-induced Th1/Th17 response in a mouse model (208). These reports show that immunization by vaccination or infection with helminth after vaccination can affect vaccine efficacy. This problem is prominent in most of the world's tropical and subtropical developing countries that have populations that are susceptible to helminth infection.

6.1.2 Nontuberculous mycobacteria

(NTM): NTM have been reported to have cross-reactivity with BCG in humans (209), which is thought to be a factor that may affect the vaccine efficacy of BCG. BCG vaccination has been reported to show some protective effects against NTM infection in humans (210). In a mouse model, exposure to NTM after BCG vaccination also enhances BCG efficacy against Mtb infection (211), suggesting that the impact of NTM infection on BCG efficacy varies depending on factors such as the timing of exposure, route of infection, and viability of NTM. However, prior sensitization to NTM has the potential to stop BCG proliferation, prevent the induction of an effective BCG-directed immune response, and ultimately inhibit the protective effect against Mtb infection (212). Another study reported that oral exposure to *Mycobacterium avium* after BCG vaccination reduced the efficacy of BCG vaccination against Mtb infection in a mouse model (213). Humans are inevitably exposed to NTM via multiple infection sources such as shower water, soil, and pool water. Thus, the effect of NTM exposure and its precise mechanism of action on immunological responses are worth further investigation.

6.2 Vaccine application in the context of underlying diseases

TB is the leading cause of death among people living with HIV, affecting the immune system and eventually waning defense systems against infections, leading to an increase in the risk of TB. It is well-reported that people living with HIV are more than 20 times more susceptible to developing active TB. Therefore, protection against these two diseases is of complementary importance. Because of HIV-related immunosuppression, the TB vaccine may be less immunogenic and less effective in people with HIV infection than in people without HIV infection (214). Because HIV-infected people are a large subpopulation at a high risk of TB infection and disease, it is important to include them in TB vaccine trials. A vaccine that is expected to have a protective effect against HIV is being developed based on a promising vaccine candidate in the TB vaccine clinical stage or BCG vaccine (215).

Diabetes prevalence affects TB incidence and TB mortality, resulting in two to three times the probability of developing TB, two times the risk of death during TB treatment, four times the risk of TB recurrence after completion of treatment, and two times the risk of infection with multidrug-resistant TB (MDR-TB). A cohort study reported that the longer the period of diabetes was, the more associated with TB disease, and TB was more commonly identified in patients with a fasting plasma glucose level over 202 mg/dL (216). In addition, it was confirmed that the higher the glucose concentration in the blood of diabetic patients was, the weaker the adaptive immune response to Mtb (217). Verma et al. established a latent TB infection mouse model and induced diabetes in Mtb-infected mice by administering streptozotocin to investigate the relationship between latent TB and diabetes. These hyperglycemic conditions led to a decrease in MCP-1 and MMP9 levels and increased MMP1 levels in latent TB infection, which may lead to reactivation of latent TB infection by disrupting granulomas (218). Clement et al. reported that metabolic stress caused by hyperglycemia decreases Ag presentation ability and inhibits the proliferation of $CD4^+$ T cells (219). These reports suggest the possibility that diabetes can affect the formation of TB vaccine-induced protective immunity.

6.3 Vaccination for elderly people

In old age, lung structural degeneration as well as changes in immune cell functions make people vulnerable to respiratory diseases, and these age-related immunological changes may also affect vaccine efficacy. The incidence of TB is common in elderly individuals and increases progressively with age, and mortality from TB is also higher in older patients (220). This phenomenon is related to the reactivation of lesions from a dormant state, which is affected by changes in the immune system with aging. In addition, chronic inflammation in aging individuals disrupts T-cell responses, followed by decreased vaccine efficacy. For example, the application of a delayed-type hypersensitivity model of BCG vaccination and TST of aged NHPs showed that the immune

response to antigenic challenges between the tissue site and the periphery is compromised, restricting the optimal immune memory response (221). A follow-up study showed reduced or delayed T-cell recall responses to lung infection sites in aged BCG-vaccinated rhesus macaques (222).

Recently, nonspecific protective efficacy of the BCG vaccine was confirmed against respiratory diseases such as COVID-19 through immunological changes favorable to respiratory infections in elderly people (223, 224). Many findings reveal that this nonspecific protection is generated from innate immune memory via metabolomic and epigenetic reprogramming, also known as trained immunity. Blood samples before and 1 month after BCG vaccination were compared in 82 subjects between the ages of 60 and 80 years (225). It was confirmed that BCG vaccination induced reductions in the levels of pro-inflammatory cytokines (TNF-α, IL-6, IL-1β) and chemokines (CCL2 and CXCL10), acute phase proteins such as C-reactive protein, and matrix metalloproteinases (225, 226). Considering the immune activation by BCG vaccination in elderly people and the positive results of BCG revaccination, BCG revaccination in elderly people may be a beneficial strategy to reduce elderly mortality due to TB.

6.4 Oral vaccination: an alternative route for TB vaccine

TB vaccine candidates currently in the clinical stage are vaccinated through the intramuscular (IM) route or ID route. In addition, studies with noteworthy results in preclinical stages through the aerosol route or the intravenous route have recently been reported. However, studies on oral route vaccination are still limited. In the case of BCG, since the safety of the ID route of BCG for mass vaccination was confirmed by Scandinavian researchers in the 1930s, it has been used until now (227). However, the BCG vaccine was initially developed as an oral vaccine and was used in that form until an incident in Germany in 1930, when the oral BCG vaccine was contaminated with Mtb. In Brazil, oral BCG vaccination was administered to newborns until 1976. Recently, Hoft et al. demonstrated the safety of oral BCG vaccination through a comparative analysis of 68 healthy adults who received BCG via the intradermal (ID) route and the oral route (228). ID-BCG vaccination induced a higher systemic Th1 response than the oral route. In contrast, oral route BCG vaccination produced more elevated Mtb-specific secretory IgA and Mtb-specific bronchoalveolar lavage T cell responses than ID-BCG vaccination (228). A lipid-based formulation has been developed for oral BCG vaccination, and the results of vaccination in BALB/c mice showed increased vaccine efficacy compared to conventional BCG vaccination (229). In addition, to increase the efficacy of oral vaccination of lipid-formulated BCG vaccination, improved vaccine efficacy was confirmed through aerosol infection after oral vaccination with recombinant BCG expressing Ag85B-ESAT6 fusion protein in a guinea pig model (230). The effectiveness of oral vaccination was also confirmed with a subunit vaccine model. Although oral immunization was less effective as a priming vaccination of fusion protein ESAT-6-Ag85B with detoxified monophosphoryl lipid A (MPL), heterogeneous priming and boosting vaccination strategies combined with oral boost induced significant systemic Th1 response, providing protection similar to or exceeding vaccination via the SC route against Mtb infection (231).

Oral vaccination is an appealing route due to the absence of needles, which eliminates the risk of cross-infection, and the ability to administer vaccines without the need for specialized healthcare professionals. Exploring the properties of this unconventional vaccine route presents an additional potential strategy for TB vaccination.

7 Conclusions

Despite recent progress in clinical trials of several vaccine candidates and anti-TB drugs, the World Health Organization (WHO)'s "End TB strategy" milestone of the year 2025 has become challenging due to the coronavirus disease 2019 (COVID-19) pandemic. With the continued high prevalence and the death rate returning to the levels observed 10 years ago, researchers' endeavors to find novel strategies to combat TB have been crippled. Nevertheless, advanced knowledge on new immune factors and consistent efforts to develop vaccine candidates will reveal promising ways to combat TB.

Most vaccine studies have focused on Th1 cells and the effector cytokine IFN-γ as potential indicators of vaccination success and vaccine efficacy. However, as the protective functions of IL-10, which have been considered negative, or novel protective functions of Th17 cells have been revealed through numerous studies, the narrow view of vaccine immunity has been expanded. From this point of view, the understanding of the functions of currently known factors is unlikely to be complete, as the factors can perform different functions in a temporally and spatially diverse immune environment. Novel analyses, such as those based on novel immune indicators, metabolomics and transcriptome analysis, may provide further insight into the complex immune environment and control of TB with vaccines. Furthermore, to progress beyond the existing 'one-size-fits-all' treatment approach, the prescription of a treatment strategy classified according to the patient's condition is being considered (232, 233). These considerations should account for individual characteristics such as underlying disease and epidemiological status. For example, live attenuated vaccines, including the BCG vaccine, can be lethal in HIV-positive patients. In particular, elderly people over the age of 65 years who are very vulnerable to infection can be an important target.

The seriousness of the recent COVID-19 crisis and the quick response of humans to overcome it provide a positive message for overcoming existing diseases such as TB. However, reports of side effects such as myocarditis and severe allergic reactions (234, 235) indicate that immune balance is an important consideration for vaccine development. More than 100 years have passed since Koch first identified Mtb, and many researchers have made efforts, with many advances, to control these vicious bacilli that have killed a tremendous number of people. With numerous vaccine candidates being evaluated in clinical trials, the direction of TB vaccine development seems much more sophisticated than in the past, but achieving the intended goal remains challenging. Although several

candidates showing protective efficacy in animal models eventually failed to exhibit vaccine efficacy in clinical trials, the collection and analysis of data for each candidate, whether successful or not, are obviously valuable to reduce the probability of failure. In addition, the use of BCG or BCG revaccination should be maximized and optimized in combination with other types of vaccine candidates (236). Finally, heterogeneous vaccine strategies with candidates in different phases of clinical trials, such as adjuvanted subunit priming with a vector-based candidate boost, can be another strategy for better inducing pleiotropic protective immunity.

Author contributions

HK and SS elaborated on the subject of the review. HK, H-GC, and SS wrote the manuscript. SS helped write the manuscript, provided helpful ideas and corrected the manuscript. All authors contributed to the article and approved the submitted version.

Funding

This work was supported by a grant (22202MFDS173) from the Ministry of Food and Drug Safety in 2023 and the Korean Health Technology R&D Project through the Korea Health Industry Development Institute (KHIDI), funded by the Ministry of Health and Welfare, Republic of Korea (HV22C0079). The funders had no role in the decision to publish or preparation of the manuscript.

Acknowledgments

The authors thank Medical Illustration & Design (MID), a part of the Medical Research Support Services of Yonsei University College of Medicine, for all artistic support related to this work.

Conflict of interest

The authors declare that the research was conducted in the absence of any commercial or financial relationships that could be construed as a potential conflict of interest.

Publisher's note

References

1. Brazier B, McShane H. Towards new TB vaccines. *Semin Immunopathol* (2020) 42(3):315–31. doi: 10.1007/s00281-020-00794-0

2. Colditz GA, Berkey CS, Mosteller F, Brewer TF, Wilson ME, Burdick E, et al. The efficacy of bacillus Calmette-Guérin vaccination of newborns and infants in the prevention of tuberculosis: meta-analyses of the published literature. *Pediatrics* (1995) 96(1 Pt 1):29–35.

3. Mangtani P, Abubakar I, Ariti C, Beynon R, Pimpin L, Fine PE, et al. Protection by BCG vaccine against tuberculosis: a systematic review of randomized controlled trials. *Clin Infect Dis* (2014) 58(4):470–80. doi: 10.1093/cid/cit790

4. Tameris MD, Hatherill M, Landry BS, Scriba TJ, Snowden MA, Lockhart S, et al. Safety and efficacy of MVA85A, a new tuberculosis vaccine, in infants previously vaccinated with BCG: a randomised, placebo-controlled phase 2b trial. *Lancet* (9871) 2013:1021–8:381. doi: 10.1016/s0140-6736(13)60177-4

5. Ndiaye BP, Thienemann F, Ota M, Landry BS, Camara M, Dièye S, et al. Safety, immunogenicity, and efficacy of the candidate tuberculosis vaccine MVA85A in healthy adults infected with HIV-1: a randomised, placebo-controlled, phase 2 trial. *Lancet Respir Med* (2015) 3(3):190–200. doi: 10.1016/S2213-2600(15)00037-5

6. Hoft DF, Blazevic A, Selimovic A, Turan A, Tennant J, Abate G, et al. Safety and immunogenicity of the recombinant BCG vaccine AERAS-422 in healthy BCG-naïve adults: A randomized, active-controlled, first-in-human phase 1 trial. *EBioMedicine* (2016) 7:278–86. doi: 10.1016/j.ebiom.2016.04.010

7. Garcia-Basteiro AL, White RG, Tait D, Schmidt AC, Rangaka MX, Quaife M, et al. End-point definition and trial design to advance tuberculosis vaccine development. *Eur Respir Rev* (2022) 31(164). doi: 10.1183/16000617.0044-2022

8. Hatherill M, Tait D, McShane H. Clinical testing of tuberculosis vaccine candidates. *Microbiol Spectr* (2016) 4(5). doi: 10.1128/microbiolspec.TBTB2-0015-2016

9. Mazurek GH, Jereb J, Vernon A, LoBue P, Goldberg S, Castro K. Updated guidelines for using Interferon Gamma Release Assays to detect Mycobacterium tuberculosis infection - United States, 2010. *MMWR Recomm Rep* (2010) 59(Rr-5):1–25.

10. Nemes E, Rozot V, Geldenhuys H, Bilek N, Mabwe S, Abrahams D, et al. Optimization and interpretation of serial quantiFERON testing to measure acquisition of *mycobacterium tuberculosis* infection. *Am J Respir Crit Care Med* (2017) 196(5):638–48. doi: 10.1164/rccm.201704-0817OC

11. Tagmouti S, Slater M, Benedetti A, Kik SV, Banaei N, Cattamanchi A, et al. Reproducibility of interferon gamma (IFN-γ) release Assays. A systematic review. *Ann Am Thorac Soc* (2014) 11(8):1267–76. doi: 10.1513/AnnalsATS.201405-188OC

12. Knight GM, Griffiths UK, Sumner T, Laurence YV, Gheorghe A, Vassall A, et al. Impact and cost-effectiveness of new tuberculosis vaccines in low- and middle-income countries. *Proc Natl Acad Sci U S A.* (2014) 111(43):15520–5. doi: 10.1073/pnas.1404386111

13. Van Der Meeren O, Hatherill M, Nduba V, Wilkinson RJ, Muyoyeta M, Van Brakel E, et al. Phase 2b controlled trial of M72/AS01(E) vaccine to prevent tuberculosis. *N Engl J Med* (2018) 379(17):1621–34. doi: 10.1056/NEJMoa1803484

14. Tait DR, Hatherill M, van der Meeren O, Ginsberg AM, Van Brakel E, Salaun B, et al. Final analysis of a trial of M72/AS01(E) vaccine to prevent tuberculosis. *N Engl J Med* (2019) 381(25):2429–39. doi: 10.1056/NEJMoa1909953

15. Coler RN, Bertholet S, Pine SO, Orr MT, Reese V, Windish HP, et al. Therapeutic immunization against *Mycobacterium tuberculosis* is an effective adjunct to antibiotic treatment. *J Infect Dis* (2013) 207(8):1242–52. doi: 10.1093/infdis/jis425

16. Lin PL, Dietrich J, Tan E, Abalos RM, Burgos J, Bigbee C, et al. The multistage vaccine H56 boosts the effects of BCG to protect cynomolgus macaques against active tuberculosis and reactivation of latent *Mycobacterium tuberculosis* infection. *J Clin Invest* (2012) 122(1):303–14. doi: 10.1172/JCI46252

17. Nunes-Alves C, Booty MG, Carpenter SM, Jayaraman P, Rothchild AC, Behar SM. In search of a new paradigm for protective immunity to TB. *Nat Rev Microbiol* (2014) 12(4):289–99. doi: 10.1038/nrmicro3230

18. Balasubramanian V, Wiegeshaus EH, Taylor BT, Smith DW. Pathogenesis of tuberculosis: pathway to apical localization. *Tuber Lung Dis* (1994) 75(3):168–78. doi: 10.1016/0962-8479(94)90002-7

19. Sakamoto K. The pathology of *Mycobacterium tuberculosis* infection. *Vet Pathol* (2012) 49(3):423–39. doi: 10.1177/0300985811429313

20. Fennelly KP, Jones-López EC, Ayakaka I, Kim S, Menyha H, Kirenga B, et al. Variability of infectious aerosols produced during coughing by patients with pulmonary tuberculosis. *Am J Respir Crit Care Med* (2012) 186(5):450–7. doi: 10.1164/rccm.201203-0444OC

21. Dinkele R, Gessner S, McKerry A, Leonard B, Leukes J, Seldon R, et al. Aerosolization of *mycobacterium tuberculosis* by tidal breathing. *Am J Respir Crit Care Med* (2022) 206(2):206–16. doi: 10.1164/rccm.202110-2378OC

22. Scriba TJ, Dinkele R, Warner DF, Mizrahi V. Challenges in TB research. *J Exp Med* (2022) 219(12). doi: 10.1084/jem.20221334

23. Roederer M. Parsimonious determination of the optimal infectious dose of a pathogen for nonhuman primate models. *PloS Pathog* (2015) 11(8):e1005100. doi: 10.1371/journal.ppat.1005100

24. Plumlee CR, Duffy FJ, Gern BH, Delahaye JL, Cohen SB, Stoltzfus CR, et al. Ultra-low dose aerosol infection of mice with *mycobacterium tuberculosis* more closely models human tuberculosis. *Cell Host Microbe* (2021) 29(1):68–82.e5. doi: 10.1016/j.chom.2020.10.003

25. Dijkman K, Sombroek CC, Vervenne RAW, Hofman SO, Boot C, Remarque EJ, et al. Prevention of tuberculosis infection and disease by local BCG in repeatedly exposed rhesus macaques. *Nat Med* (2019) 25(2):255–62. doi: 10.1038/s41591-018-0319-9

26. Cadena AM, Fortune SM, Flynn JL. Heterogeneity in tuberculosis. *Nat Rev Immunol* (2017) 17(11):691–702. doi: 10.1038/nri.2017.69

27. Chackerian AA, Behar SM. Susceptibility to *Mycobacterium tuberculosis*: lessons from inbred strains of mice. *Tuberculosis (Edinb)* (2003) 83(5):279–85. doi: 10.1016/S1472-9792(03)00017-9

28. Kramnik I, Beamer G. Mouse models of human TB pathology: roles in the analysis of necrosis and the development of host-directed therapies. *Semin Immunopathol* (2016) 38(2):221–37. doi: 10.1007/s00281-015-0538-9

29. Kondratieva E, Logunova N, Majorov K, Averbakh M, Apt A. Host genetics in granuloma formation: human-like lung pathology in mice with reciprocal genetic susceptibility to M. tuberculosis and *M. avium*. *PloS One* (2010) 5(5):e10515. doi: 10.1371/journal.pone.0010515

30. Arrey F, Löwe D, Kuhlmann S, Kaiser P, Moura-Alves P, Krishnamoorthy G, et al. Humanized mouse model mimicking pathology of human tuberculosis for *in vivo* evaluation of drug regimens. *Front Immunol* (2019) 10:89. doi: 10.3389/fimmu.2019.00089

31. Zelmer A, Stockdale L, Prabowo SA, Cia F, Spink N, Gibb M, et al. High monocyte to lymphocyte ratio is associated with impaired protection after subcutaneous administration of BCG in a mouse model of tuberculosis. *F1000Res* (2018) 7:296. doi: 10.12688/f1000research.14239.2

32. Smith CM, Proulx MK, Olive AJ, Laddy D, Mishra BB, Moss C, et al. Tuberculosis susceptibility and vaccine protection are independently controlled by host genotype. *mBio* (2016) 7(5). doi: 10.1128/mBio.01516-16

33. Peña JC, Ho WZ. Monkey models of tuberculosis: lessons learned. *Infect Immun* (2015) 83(3):852–62. doi: 10.1128/IAI.02850-14

34. Langermans JA, Andersen P, van Soolingen D, Vervenne RA, Frost PA, van der Laan T, et al. Divergent effect of bacillus Calmette-Guérin (BCG) vaccination on *Mycobacterium tuberculosis* infection in highly related macaque species: implications for primate models in tuberculosis vaccine research. *Proc Natl Acad Sci U S A*. (2001) 98 (20):11497–502. doi: 10.1073/pnas.201404898

35. Darrah PA, Bolton DL, Lackner AA, Kaushal D, Aye PP, Mehra S, et al. Aerosol vaccination with AERAS-402 elicits robust cellular immune responses in the lungs of rhesus macaques but fails to protect against high-dose *Mycobacterium tuberculosis* challenge. *J Immunol* (2014) 193(4):1799–811. doi: 10.4049/jimmunol.1400676

36. Sharpe SA, McShane H, Dennis MJ, Basaraba RJ, Gleeson F, Hall G, et al. Establishment of an aerosol challenge model of tuberculosis in rhesus macaques and an evaluation of endpoints for vaccine testing. *Clin Vaccine Immunol* (2010) 17(8):1170–82. doi: 10.1128/CVI.00079-10

37. Verreck FA, Vervenne RA, Kondova I, van Kralingen KW, Remarque EJ, Braskamp G, et al. MVA.85A boosting of BCG and an attenuated, phoP deficient *M. tuberculosis* vaccine both show protective efficacy against tuberculosis in rhesus macaques. *PloS One* (2009) 4(4):e5264. doi: 10.1371/journal.pone.0005264

38. Daniel J, Deb C, Dubey VS, Sirakova TD, Abomoelak B, Morbidoni HR, et al. Induction of a novel class of diacylglycerol acyltransferases and triacylglycerol accumulation in *Mycobacterium tuberculosis* as it goes into a dormancy-like state in culture. *J Bacteriol* (2004) 186(15):5017–30. doi: 10.1128/JB.186.15.5017-5030.2004

39. Garton NJ, Waddell SJ, Sherratt AL, Lee SM, Smith RJ, Senner C, et al. Cytological and transcript analyses reveal fat and lazy persister-like bacilli in tuberculous sputum. *PloS Med* (2008) 5(4):e75. doi: 10.1371/journal.pmed.0050075

40. Rosser A, Stover C, Pareek M, Mukamolova GV. Resuscitation-promoting factors are important determinants of the pathophysiology in *Mycobacterium tuberculosis* infection. *Crit Rev Microbiol* (2017) 43(5):621–30. doi: 10.1080/1040841X.2017.1283485

41. Downing KJ, Mischenko VV, Shleeva MO, Young DI, Young M, Kaprelyants AS, et al. Mutants of *Mycobacterium tuberculosis* lacking three of the five rpf-like genes are defective for growth *in vivo* and for resuscitation *in vitro*. *Infect Immun* (2005) 73 (5):3038–43. doi: 10.1128/IAI.73.5.3038-3043.2005

42. Mukamolova GV, Turapov O, Malkin J, Woltmann G, Barer MR. Resuscitation-promoting factors reveal an occult population of tubercle Bacilli in Sputum. *Am J Respir Crit Care Med* (2010) 181(2):174–80. doi: 10.1164/rccm.200905-0661OC

43. Huang W, Qi Y, Diao Y, Yang F, Zha X, Ren C, et al. Use of resuscitation-promoting factor proteins improves the sensitivity of culture-based tuberculosis testing in special samples. *Am J Respir Crit Care Med* (2014) 189(5):612–4. doi: 10.1164/rccm.201310-1899LE

44. White AG, Maiello P, Coleman MT, Tomko JA, Frye LJ, Scanga CA, et al. Analysis of 18FDG PET/CT imaging as a tool for studying *mycobacterium tuberculosis* infection and treatment in non-human primates. *J Vis Exp* (2017) 127. doi: 10.3791/56375

45. Tameris M, Mearns H, Penn-Nicholson A, Gregg Y, Bilek N, Mabwe S, et al. Live-attenuated *Mycobacterium tuberculosis* vaccine MTBVAC versus BCG in adults and neonates: a randomised controlled, double-blind dose-escalation trial. *Lancet Respir Med* (2019) 7(9):757–70. doi: 10.1016/S2213-2600(19)30251-6

46. Spertini F, Audran R, Chakour R, Karoui O, Steiner-Monard V, Thierry AC, et al. Safety of human immunisation with a live-attenuated *Mycobacterium tuberculosis* vaccine: a randomised, double-blind, controlled phase I trial. *Lancet Respir Med* (2015) 3(12):953–62. doi: 10.1016/S2213-2600(15)00435-X

47. Grode L, Ganoza CA, Brohm C, Weiner J3rd, Eisele B, Kaufmann SH. Safety and immunogenicity of the recombinant BCG vaccine VPM1002 in a phase 1 open-label randomized clinical trial. *Vaccine* (2013) 31(9):1340–8. doi: 10.1016/j.vaccine.2012.12.053

48. Loxton AG, Knaul JK, Grode L, Gutschmidt A, Meller C, Eisele B, et al. Safety and immunogenicity of the recombinant *mycobacterium bovis* BCG vaccine VPM1002 in HIV-unexposed newborn infants in South Africa. *Clin Vaccine Immunol* (2017) 24 (2). doi: 10.1128/CVI.00439-16

49. Cotton MF, Madhi SA, Luabeya AK, Tameris M, Hesseling AC, Shenje J, et al. Safety and immunogenicity of VPM1002 versus BCG in South African newborn babies: a randomised, phase 2 non-inferiority double-blind controlled trial. *Lancet Infect Dis* (2022) 22(10):1472–83. doi: 10.1016/S1473-3099(22)00222-5

50. Nemes E, Geldenhuys H, Rozot V, Rutkowski KT, Ratangee F, Bilek N, et al. Prevention of M. tuberculosis infection with H4:IC31 vaccine or BCG revaccination. *N Engl J Med* (2018) 379(2):138–49. doi: 10.1056/NEJMoa1714021

51. Rakshit S, Ahmed A, Adiga V, Sundararaj BK, Sahoo PN, Kenneth J, et al. BCG revaccination boosts adaptive polyfunctional Th1/Th17 and innate effectors in IGRA+ and IGRA- Indian adults. *JCI Insight* (2019) 4(24). doi: 10.1172/jci.insight.130540

52. Bekker LG, Dintwe O, Fiore-Gartland A, Middelkoop K, Hutter J, Williams A, et al. A phase 1b randomized study of the safety and immunological responses to vaccination with H4:IC31, H56:IC31, and BCG revaccination in *Mycobacterium tuberculosis*-uninfected adolescents in Cape Town, South Africa. *EClinicalMedicine* (2020) 21:100313. doi: 10.1016/j.eclinm.2020.100313

53. Montoya J, Solon JA, Cunanan SR, Acosta L, Bollaerts A, Moris P, et al. A randomized, controlled dose-finding Phase II study of the M72/AS01 candidate tuberculosis vaccine in healthy PPD-positive adults. *J Clin Immunol* (2013) 33 (8):1360–75. doi: 10.1007/s10875-013-9949-3

54. Penn-Nicholson A, Geldenhuys H, Burny W, van der Most R, Day CL, Jongert E, et al. Safety and immunogenicity of candidate vaccine M72/AS01E in adolescents in a TB endemic setting. *Vaccine* (2015) 33(32):4025–34. doi: 10.1016/j.vaccine.2015.05.088

55. Gillard P, Yang PC, Danilovits M, Su WJ, Cheng SL, Pehme L, et al. Safety and immunogenicity of the M72/AS01E candidate tuberculosis vaccine in adults with tuberculosis: A phase II randomised study. *Tuberculosis (Edinb)* (2016) 100:118–27. doi: 10.1016/j.tube.2016.07.005

56. Kumarasamy N, Poongulali S, Beulah FE, Akite EJ, Ayuk LN, Bollaerts A, et al. Long-term safety and immunogenicity of the M72/AS01E candidate tuberculosis vaccine in HIV-positive and -negative Indian adults: Results from a phase II randomized controlled trial. *Med (Baltimore)* (2018) 97(45):e13120. doi: 10.1097/MD.0000000000013120

57. Tkachuk AP, Bykonia EN, Popova LI, Kleymenov DA, Semashko MA, Chulanov VP, et al. Safety and immunogenicity of the gamTBvac, the recombinant subunit tuberculosis vaccine candidate: A phase II, multi-center, double-blind, randomized, placebo-controlled study. *Vaccines (Basel)* (2020) 8(4). doi: 10.3390/vaccines8040652

58. Vasina DV, Kleymenov DA, Manuylov VA, Mazunina EP, Koptev EY, Tukhovskaya EA, et al. First-in-human trials of gamTBvac, a recombinant subunit tuberculosis vaccine candidate: safety and immunogenicity assessment. *Vaccines (Basel)* (2019) 7(4). doi: 10.3390/vaccines7040166

59. Penn-Nicholson A, Tameris M, Smit E, Day TA, Musvosvi M, Jayashankar L, et al. Safety and immunogenicity of the novel tuberculosis vaccine ID93 + GLA-SE in BCG-vaccinated healthy adults in South Africa: a randomised, double-blind, placebo-controlled phase 1 trial. *Lancet Respir Med* (2018) 6(4):287–98. doi: 10.1016/S2213-2600(18)30077-8

60. Day TA, Penn-Nicholson A, Luabeya AKK, Fiore-Gartland A, Du Plessis N, Loxton AG, et al. Safety and immunogenicity of the adjunct therapeutic vaccine ID93 + GLA-SE in adults who have completed treatment for tuberculosis: a randomised, double-blind, placebo-controlled, phase 2a trial. *Lancet Respir Med* (2021) 9(4):373–86. doi: 10.1016/S2213-2600(20)30319-2

61. Luabeya AK, Kagina BM, Tameris MD, Geldenhuys H, Hoff ST, Shi Z, et al. First-in-human trial of the post-exposure tuberculosis vaccine H56:IC31 in *Mycobacterium tuberculosis* infected and non-infected healthy adults. *Vaccine* (2015) 33(33):4130–40. doi: 10.1016/j.vaccine.2015.06.051

62. Lu JB, Chen BW, Wang GZ, Fu LL, Shen XB, Su C, et al. Recombinant tuberculosis vaccine AEC/BC02 induces antigen-specific cellular responses in mice and protects Guinea pigs in a model of latent infection. *J Microbiol Immunol Infect* (2015) 48(6):597–603. doi: 10.1016/j.jmii.2014.03.005

63. Méndez-Samperio P. Development of tuberculosis vaccines in clinical trials: Current status. *Scand J Immunol* (2018) 88(4):e12710. doi: 10.1111/sji.12710

64. Hu Z, Lu SH, Lowrie DB, Fan XY. Research advances for virus-vectored tuberculosis vaccines and latest findings on tuberculosis vaccine development. *Front Immunol* (2022) 13:895020. doi: 10.3389/fimmu.2022.895020

65. Jiang MJ, Liu SJ, Su L, Zhang X, Li YY, Tang T, et al. Intranasal vaccination with Listeria ivanovii as vector of *Mycobacterium tuberculosis* antigens promotes specific lung-localized cellular and humoral immune responses. *Sci Rep* (2020) 10(1):302. doi: 10.1038/s41598-019-57245-6

66. Singh SK, Kumari R, Singh DK, Tiwari S, Singh PK, Sharma S, et al. Putative roles of a proline-glutamic acid-rich protein (PE3) in intracellular survival and as a candidate for subunit vaccine against Mycobacterium tuberculosis. *Med Microbiol Immunol* (2013) 202(5):365–77. doi: 10.1007/s00430-013-0299-9

67. Singh SK, Tripathi DK, Singh PK, Sharma S, Srivastava KK. Protective and survival efficacies of Rv0160c protein in murine model of Mycobacterium tuberculosis. *Appl Microbiol Biotechnol* (2013) 97(13):5825–37. doi: 10.1007/s00253-012-4493-2

68. Niu H, Hu L, Li Q, Da Z, Wang B, Tang K, et al. Construction and evaluation of a multistage *Mycobacterium tuberculosis* subunit vaccine candidate Mtb10.4-HspX. *Vaccine* (2011) 29(51):9451–8. doi: 10.1016/j.vaccine.2011.10.032

69. Xin Q, Niu H, Li Z, Zhang G, Hu L, Wang B, et al. Subunit vaccine consisting of multi-stage antigens has high protective efficacy against *Mycobacterium tuberculosis* infection in mice. *PloS One* (2013) 8(8):e72745. doi: 10.1371/journal.pone.0072745

70. Mao L, Xu L, Wang X, Xing Y, Wang J, Zhang Y, et al. Enhanced immunogenicity of the tuberculosis subunit Rv0572c vaccine delivered in DMT liposome adjuvant as a BCG-booster. *Tuberculosis (Edinb)* (2022) 134:102186. doi: 10.1016/j.tube.2022.102186

71. Tian M, Zhou Z, Tan S, Fan X, Li L, Ullah N. Formulation in DDA-MPLA-TDB Liposome Enhances the Immunogenicity and Protective Efficacy of a DNA Vaccine against *Mycobacterium tuberculosis* Infection. *Front Immunol* (2018) 9:310. doi: 10.3389/fimmu.2018.00310

72. Xiao Y, Sha W, Tian Z, Chen Y, Ji P, Sun Q, et al. Adenylate kinase: a novel antigen for immunodiagnosis and subunit vaccine against tuberculosis. *J Mol Med (Berl)* (2016) 94(7):823–34. doi: 10.1007/s00109-016-1392-5

73. Skeiky YA, Ovendale PJ, Jen S, Alderson MR, Dillon DC, Smith S, et al. T cell expression cloning of a *Mycobacterium tuberculosis* gene encoding a protective antigen associated with the early control of infection. *J Immunol* (2000) 165(12):7140–9. doi: 10.4049/jimmunol.165.12.7140

74. ROmano M, Aryan E, Korf H, Bruffaerts N, Franken CL, Ottenhoff TH, et al. Potential of *Mycobacterium tuberculosis* resuscitation-promoting factors as antigens in novel tuberculosis sub-unit vaccines. *Microbes Infect* (2012) 14(1):86–95. doi: 10.1016/j.micinf.2011.08.011

75. Yu Q, Wang X, Fan X. A new adjuvant MTOM mediates *mycobacterium tuberculosis* subunit vaccine to enhance th1-type T cell immune responses and IL-2(+) T cells. *Front Immunol* (2017) 8:585. doi: 10.3389/fimmu.2017.00585

76. Ma J, Tian M, Fan X, Yu Q, Jing Y, Wang W, et al. *Mycobacterium tuberculosis* multistage antigens confer comprehensive protection against pre- and post-exposure infections by driving Th1-type T cell immunity. *Oncotarget* (2016) 7(39):63804–15. doi: 10.18632/oncotarget.11542

77. Lee J, Kim J, Lee J, Shin SJ, Shin EC. DNA immunization of *Mycobacterium tuberculosis* resuscitation-promoting factor B elicits polyfunctional CD8(+) T cell responses. *Clin Exp Vaccine Res* (2014) 3(2):235–43. doi: 10.7774/cevr.2014.3.2.235

78. Stylianou E, Harrington-Kandt R, Beglov J, Bull N, Pinpathomrat N, Swarbrick GM, et al. Identification and evaluation of novel protective antigens for the development of a candidate tuberculosis subunit vaccine. *Infect Immun* (2018) 86(7). doi: 10.1128/IAI.00014-18

79. Li Q, Yu H, Zhang Y, Wang B, Jiang W, Da Z, et al. Immunogenicity and protective efficacy of a fusion protein vaccine consisting of antigen Ag85B and HspX against *Mycobacterium tuberculosis* infection in mice. *Scand J Immunol* (2011) 73 (6):568–76. doi: 10.1111/j.1365-3083.2011.02531.x

80. Counoupas C, Pinto R, Nagalingam G, Britton WJ, Petrovsky N, Triccas JA. Delta inulin-based adjuvants promote the generation of polyfunctional CD4(+) T cell responses and protection against *Mycobacterium tuberculosis* infection. *Sci Rep* (2017) 7(1):8582. doi: 10.1038/s41598-017-09119-y

81. Liang Y, Zhang X, Xiao L, Bai X, Wang X, Yang Y, et al. Immunogenicity and therapeutic effects of pVAX1- rv1419 DNA from *Mycobacterium tuberculosis*. *Curr Gene Ther* (2016) 16(4):249–255. doi: 10.2174/1566523216666161102170123

82. Wang Y, Li Z, Wu S, Fleming J, Li C, Zhu G, et al. Systematic evaluation of *mycobacterium tuberculosis* proteins for antigenic properties identifies rv1485 and rv1705c as potential protective subunit vaccine candidates. *Infect Immun* (2021) 89(3). doi: 10.1128/IAI.00585-20

83. Levillain F, Kim H, Woong Kwon K, Clark S, Cia F, Malaga W, et al. Preclinical assessment of a new live attenuated *Mycobacterium tuberculosis* Beijing-based vaccine for tuberculosis. *Vaccine* (2020) 38(6):1416–23. doi: 10.1016/j.vaccine.2019.11.085

84. Coppola M, van den Eeden SJ, Wilson L, Franken KL, Ottenhoff TH, Geluk A. Synthetic Long Peptide Derived from *Mycobacterium tuberculosis* Latency Antigen Rv1733c Protects against Tuberculosis. *Clin Vaccine Immunol* (2015) 22(9):1060–9. doi: 10.1128/CVI.00271-15

85. King TH, Shanley CA, Guo Z, Bellgrau D, Rodell T, Furney S, et al. GI-19007, a Novel Saccharomyces cerevisiae-Based Therapeutic Vaccine against Tuberculosis. *Clin Vaccine Immunol* (2017) 24(12). doi: 10.1128/CVI.00245-17

86. Speranza V, Colone A, Cicconi R, Palmieri G, Giovannini D, Grassi M, et al. Recombinant BCG-Rv1767 amount determines, *in vivo*, antigen-specific T cells location, frequency, and protective outcome. *Microb Pathog* (2010) 48(5):150–9. doi: 10.1016/j.micpath.2010.02.003

87. Sulman S, Savidge BO, Alqaseer K, Das MK, Nezam Abadi N, Pearl JE, et al. Balance between Protection and Pathogenic Response to Aerosol Challenge with *Mycobacterium tuberculosis* (Mtb) in Mice Vaccinated with TriFu64, a Fusion Consisting of Three Mtb Antigens. *Vaccines (Basel)* (2021) 9(5). doi: 10.3390/vaccines9050519

88. Choi S, Choi HG, Back YW, Park HS, Lee KI, Gurmessa SK, et al. A dendritic cell-activating rv1876 protein elicits *mycobacterium bovis* BCG-prime effect via th1-immune response. *Biomolecules* (2021) 11(9). doi: 10.3390/biom11091306

89. Lv W, He P, Ma Y, Tan D, Li F, Xie T, et al. Optimizing the boosting schedule of subunit vaccines consisting of BCG and "Non-BCG" Antigens to induce long-term immune memory. *Front Immunol* (2022) 13:862726. doi: 10.3389/fimmu.2022.862726

90. Vasilyev K, Shurygina AP, Zabolotnykh N, Sergeeva M, ROmanovskaya-ROmanko E, Pulkina A, et al. Enhancement of the Local CD8(+) T-Cellular Immune Response to Mycobacterium tuberculosis in BCG-Primed Mice after Intranasal Administration of Influenza Vector Vaccine Carrying TB10.4 and HspX Antigens. *Vaccines (Basel)* (2021) 9(11). doi: 10.3390/vaccines9111273

91. Sergeeva M, ROmanovskaya-ROmanko E, Zabolotnyh N, Pulkina A, Vasilyev K, Shurigina AP, et al. Mucosal Influenza Vector Vaccine Carrying TB10.4 and HspX Antigens Provides Protection against Mycobacterium tuberculosis in Mice and Guinea Pigs. *Vaccines (Basel)* (2021) 9(4). doi: 10.3390/vaccines9040394

92. Back YW, Shin KW, Choi S, Park HS, Lee KI, Choi HG, et al. *Mycobacterium tuberculosis* rv2005c induces dendritic cell maturation and th1 responses and exhibits immunotherapeutic activity by fusion with the rv2882c protein. *Vaccines (Basel)* (2020) 8(3). doi: 10.3390/vaccines8030370

93. Liu W, Li J, Niu H, Lin X, Li R, Wang Y, et al. Immunogenicity and protective efficacy of multistage vaccine candidates (Mtb8.4-HspX and HspX-Mtb8.4) against *Mycobacterium tuberculosis* infection in mice. *Int Immunopharmacol* (2017) 53:83–9. doi: 10.1016/j.intimp.2017.10.015

94. Niu H, Peng J, Bai C, Liu X, Hu L, Luo Y, et al. Multi-Stage Tuberculosis Subunit Vaccine Candidate LT69 Provides High Protection against *Mycobacterium tuberculosis* Infection in Mice. *PloS One* (2015) 10(6):e0130641. doi: 10.1371/journal.pone.0130641

95. Liang J, Teng X, Yuan X, Zhang Y, Shi C, Yue T, et al. Enhanced and durable protective immune responses induced by a cocktail of recombinant BCG strains expressing antigens of multistage of Mycobacterium tuberculosis. *Mol Immunol* (2015) 66(2):392–401. doi: 10.1016/j.molimm.2015.04.017

96. da Costa AC, Costa-Júnior Ade O, de Oliveira FM, Nogueira SV, Rosa JD, Resende DP, et al. A new recombinant BCG vaccine induces specific Th17 and Th1 effector cells with higher protective efficacy against tuberculosis. *PloS One* (2014) 9(11): e112848. doi: 10.1371/journal.pone.0112848

97. Commandeur S, van den Eeden SJ, Dijkman K, Clark SO, van Meijgaarden KE, Wilson L, et al. The *in vivo* expressed *Mycobacterium tuberculosis* (IVE-TB) antigen Rv2034 induces $CD4^+$ T-cells that protect against pulmonary infection in HLA-DR transgenic mice and Guinea pigs. *Vaccine* (2014) 32(29):3580–8. doi: 10.1016/j.vaccine.2014.05.005

98. Choi HG, Choi S, Back YW, Paik S, Park HS, Kim WS, et al. Rv2299c, a novel dendritic cell-activating antigen of *Mycobacterium tuberculosis*, fused-ESAT-6 subunit vaccine confers improved and durable protection against the hypervirulent strain HN878 in mice. *Oncotarget* (2017) 8(12):19947–67. doi: 10.18632/oncotarget.15256

99. Clemmensen HS, Knudsen NPH, Billeskov R, Rosenkrands I, Jungersen G, Aagaard C, et al. Rescuing ESAT-6 specific CD4 T cells from terminal differentiation is critical for long-term control of murine mtb infection. *Front Immunol* (2020) 11:585359. doi: 10.3389/fimmu.2020.585359

100. Kwon KW, Kim WS, Kim H, Han SJ, Hahn MY, Lee JS, et al. Novel vaccine potential of Rv3131, a DosR regulon-encoded putative nitroreductase, against hyper-virulent *Mycobacterium tuberculosis* strain K. *Sci Rep* (2017) 7:44151. doi: 10.1038/srep44151

101. Jones GJ, Khatri BL, Garcia-Pelayo MC, Kaveh DA, Bachy VS, Hogarth PJ, et al. Development of an unbiased antigen-mining approach to identify novel vaccine antigens and diagnostic reagents for bovine tuberculosis. *Clin Vaccine Immunol* (2013) 20(11):1675–82. doi: 10.1128/CVI.00416-13

102. Woodworth JS, Clemmensen HS, Battey H, Dijkman K, Lindenstrøm T, Laureano RS, et al. A *Mycobacterium tuberculosis*-specific subunit vaccine that provides synergistic immunity upon co-administration with Bacillus Calmette-Guérin. *Nat Commun* (2021) 12(1):6658. doi: 10.1038/s41467-021-26934-0

103. Leroux-Roels I, Forgus S, De Boever F, Clement F, Demoitié MA, Mettens P, et al. Improved $CD4^+$ T cell responses to *Mycobacterium tuberculosis* in PPD-negative adults by M72/AS01 as compared to the M72/AS02 and Mtb72F/AS02 tuberculosis candidate vaccine formulations: a randomized trial. *Vaccine* (2013) 31(17):2196–206. doi: 10.1016/j.vaccine.2012.05.035

104. Pethe K, Alonso S, Biet F, Delogu G, Brennan MJ, Locht C, et al. The heparin-binding haemagglutinin of M. tuberculosis is required for extrapulmonary dissemination. *Nature* (2001) 412(6843):190–4. doi: 10.1038/35084083

105. Knudsen NP, Nørskov-Lauritsen S, Dolganov GM, Schoolnik GK, Lindenstrøm T, Andersen P, et al. Tuberculosis vaccine with high predicted population coverage and compatibility with modern diagnostics. *Proc Natl Acad Sci U S A.* (2014) 111(3):1096–101. doi: 10.1073/pnas.1314973111

106. Liu L, Zhang WJ, Zheng J, Fu H, Chen Q, Zhang Z, et al. Exploration of novel cellular and serological antigen biomarkers in the ORFeome of Mycobacterium tuberculosis. *Mol Cell Proteomics* (2014) 13(3):897–906. doi: 10.1074/mcp.M113.032623

107. Brennan MJ, Clagett B, Fitzgerald H, Chen V, Williams A, Izzo AA, et al. Preclinical evidence for implementing a prime-boost vaccine strategy for tuberculosis. *Vaccine* (2012) 30(18):2811–23. doi: 10.1016/j.vaccine.2012.02.036

108. Brennan MJ, Thole J. Tuberculosis vaccines: a strategic blueprint for the next decade. *Tuberculosis (Edinb)* (2012) 92 Suppl 1:S6–13. doi: 10.1016/S1472-9792(12)70005-7

109. Coler RN, Skeiky YA, Vedvick T, Bement T, Ovendale P, Campos-Neto A, et al. Molecular cloning and immunologic reactivity of a novel low molecular mass antigen of Mycobacterium tuberculosis. *J Immunol* (1998) 161(5):2356–64. doi: 10.4049/jimmunol.161.5.2356

110. Skeiky YA, Lodes MJ, Guderian JA, Mohamath R, Bement T, Alderson MR, et al. Cloning, expression, and immunological evaluation of two putative secreted serine protease antigens of Mycobacterium tuberculosis. *Infect Immun* (1999) 67(8):3998–4007. doi: 10.1128/IAI.67.8.3998-4007.1999

111. Aagaard C, Hoang T, Dietrich J, Cardona PJ, Izzo A, Dolganov G, et al. A multistage tuberculosis vaccine that confers efficient protection before and after exposure. *Nat Med* (2011) 17(2):189–94. doi: 10.1038/nm.2285

112. Jenum S, Tonby K, Rueegg CS, Rühwald M, Kristiansen MP, Bang P, et al. A Phase I/II randomized trial of H56:IC31 vaccination and adjunctive cyclooxygenase-2-inhibitor treatment in tuberculosis patients. *Nat Commun* (2021) 12(1):6774. doi: 10.1038/s41467-021-27029-6

113. Coler RN, Day TA, Ellis R, Piazza FM, Beckmann AM, Vergara J, et al. The TLR-4 agonist adjuvant, GLA-SE, improves magnitude and quality of immune responses elicited by the ID93 tuberculosis vaccine: first-in-human trial. *NPJ Vaccines* (2018) 3:34. doi: 10.1038/s41541-018-0057-5

114. Liu W, Xu Y, Yan J, Shen H, Yang E, Wang H. Ag85B synergizes with ESAT-6 to induce efficient and long-term immunity of C57BL/6 mice primed with recombinant Bacille Calmette-Guerin. *Exp Ther Med* (2017) 13(1):208–14. doi: 10.3892/etm.2016.3944

115. Farsiani H, Mosavat A, Soleimanpour S, Sadeghian H, Akbari Eydgahi MR, Ghazvini K, et al. Fc-based delivery system enhances immunogenicity of a tuberculosis subunit vaccine candidate consisting of the ESAT-6:CFP-10 complex. *Mol Biosyst* (2016) 12(7):2189–201. doi: 10.1039/C6MB00174B

116. Moguche AO, Musvosvi M, Penn-Nicholson A, Plumlee CR, Mearns H, Geldenhuys H, et al. Antigen availability shapes T cell differentiation and function during tuberculosis. *Cell Host Microbe* (2017) 21(6):695–706.e5. doi: 10.1016/j.chom.2017.05.012

117. Comas I, Chakravartti J, Small PM, Galagan J, Niemann S, Kremer K, et al. Human T cell epitopes of *Mycobacterium tuberculosis* are evolutionarily hyperconserved. *Nat Genet* (2010) 42(6):498–503. doi: 10.1038/ng.590

118. Copin R, Coscollá M, Seiffert SN, Bothamley G, Sutherland J, Mbayo G, et al. Sequence diversity in the pe_pgrs genes of *Mycobacterium tuberculosis* is independent of human T cell recognition. *mBio* (2014) 5(1):e00960–13. doi: 10.1128/mBio.00960-13

119. Sutherland JS, Adetifa IM, Hill PC, Adegbola RA, Ota MO. Pattern and diversity of cytokine production differentiates between *Mycobacterium tuberculosis* infection and disease. *Eur J Immunol* (2009) 39(3):723–9. doi: 10.1002/eji.200838693

120. Caccamo N, Guggino G, Joosten SA, Gelsomino G, Di Carlo P, Titone L, et al. Multifunctional CD4(+) T cells correlate with active *Mycobacterium tuberculosis* infection. *Eur J Immunol* (2010) 40(8):2211–20. doi: 10.1002/eji.201040455

121. Orr MT, Ireton GC, Beebe EA, Huang PW, Reese VA, Argilla D, et al. Immune subdominant antigens as vaccine candidates against Mycobacterium tuberculosis. *J Immunol* (2014) 193(6):2911–8. doi: 10.4049/jimmunol.1401103

122. Kundu M, Basu J. Applications of transcriptomics and proteomics for understanding dormancy and resuscitation in mycobacterium tuberculosis. *Front Microbiol* (2021) 12:642487. doi: 10.3389/fmicb.2021.642487

123. Tufariello JM, Jacobs WRJr., Chan J. Individual *Mycobacterium tuberculosis* resuscitation-promoting factor homologues are dispensable for growth *in vitro* and *in vivo*. *Infect Immun* (2004) 72(1):515–26. doi: 10.1128/IAI.72.1.515-526.2004

124. Gupta RK, Srivastava BS, Srivastava R. Comparative expression analysis of rpf-like genes of *Mycobacterium tuberculosis* H37Rv under different physiological stress and growth conditions. *Microbiol (Reading)* (2010) 156(Pt 9):2714–22. doi: 10.1099/mic.0.037622-0

125. Tufariello JM, Mi K, Xu J, Manabe YC, Kesavan AK, Drumm J, et al. Deletion of the *Mycobacterium tuberculosis* resuscitation-promoting factor Rv1009 gene results in delayed reactivation from chronic tuberculosis. *Infect Immun* (2006) 74(5):2985–95. doi: 10.1128/IAI.74.5.2985-2995.2006

126. Schuck SD, Mueller H, Kunitz F, Neher A, Hoffmann H, Franken KL, et al. Identification of T-cell antigens specific for latent *mycobacterium tuberculosis* infection. *PloS One* (2009) 4(5):e5590. doi: 10.1371/journal.pone.0005590

127. Fan A, Jian W, Shi C, Ma Y, Wang L, Peng D, et al. Production and characterization of monoclonal antibody against *Mycobacterium tuberculosis* RpfB domain. *Hybridoma (Larchmt)* (2010) 29(4):327–32. doi: 10.1089/hyb.2010.0007

128. Bertholet S, Ireton GC, Ordway DJ, Windish HP, Pine SO, Kahn M, et al. A defined tuberculosis vaccine candidate boosts BCG and protects against multidrug-resistant Mycobacterium tuberculosis. *Sci Transl Med* (2010) 2(53):53ra74. doi: 10.1126/scitranslmed.3001094

129. Liu X, Peng J, Hu L, Luo Y, Niu H, Bai C, et al. A multistage *mycobacterium tuberculosis* subunit vaccine LT70 including latency antigen Rv2626c induces long-term protection against tuberculosis. *Hum Vaccin Immunother* (2016) 12(7):1670–7. doi: 10.1080/21645515.2016.1141159

130. Dijkman K, Coler RN, Joosten SA. Editorial: Beyond Th1: Novel concepts in tuberculosis vaccine immunology. *Front Immunol* (2022) 13:1059011. doi: 10.3389/fimmu.2022.1059011

131. Naranbhai V, Hill AV, Abdool Karim SS, Naidoo K, Abdool Karim Q, Warimwe GM, et al. Ratio of monocytes to lymphocytes in peripheral blood identifies adults at risk of incident tuberculosis among HIV-infected adults initiating antiretroviral therapy. *J Infect Dis* (2014) 209(4):500–9. doi: 10.1093/infdis/jit494

132. Naranbhai V, Moodley D, Chipato T, Stranix-Chibanda L, Nakabaiito C, Kamateeka M, et al. The association between the ratio of monocytes: lymphocytes and risk of tuberculosis among HIV-infected postpartum women. *J Acquir Immune Defic Syndr* (2014) 67(5):573–5. doi: 10.1097/QAI.0000000000000353

133. Buttle TS, Hummerstone CY, Billahalli T, Ward RJB, Barnes KE, Marshall NJ, et al. The monocyte-to-lymphocyte ratio: Sex-specific differences in the tuberculosis disease spectrum, diagnostic indices and defining normal ranges. *PloS One* (2021) 16(8):e0247745. doi: 10.1371/journal.pone.0247745

134. Kleinnijenhuis J, Quintin J, Preijers F, Joosten LA, Ifrim DC, Saeed S, et al. Bacille Calmette-Guerin induces NOD2-dependent nonspecific protection from reinfection via epigenetic reprogramming of monocytes. *Proc Natl Acad Sci U S A.* (2012) 109(43):17537–42. doi: 10.1073/pnas.1202870109

135. Nankabirwa V, Tumwine JK, Mugaba PM, Tylleskär T, Sommerfelt H. Child survival and BCG vaccination: a community based prospective cohort study in Uganda. *BMC Public Health* (2015) 15:175. doi: 10.1186/s12889-015-1497-8

136. Ning H, Zhang W, Kang J, Ding T, Liang X, Lu Y, et al. Subunit vaccine ESAT-6:c-di-AMP delivered by intranasal route elicits immune responses and protects against *mycobacterium tuberculosis* infection. *Front Cell Infect Microbiol* (2021) 11:647220. doi: 10.3389/fcimb.2021.647220

137. Kaufmann E, Sanz J, Dunn JL, Khan N, Mendonça LE, Pacis A, et al. BCG educates hematopoietic stem cells to generate protective innate immunity against tuberculosis. *Cell* (2018) 172(1-2):176–90.e19. doi: 10.1016/j.cell.2017.12.031

138. Leemans JC, Juffermans NP, Florquin S, van Rooijen N, Vervoordeldonk MJ, Verbon A, et al. Depletion of alveolar macrophages exerts protective effects in pulmonary tuberculosis in mice. *J Immunol* (2001) 166(7):4604–11. doi: 10.4049/jimmunol.166.7.4604

139. Rothchild AC, Olson GS, Nemeth J, Amon LM, Mai D, Gold ES, et al. Alveolar macrophages generate a noncanonical NRF2-driven transcriptional response to Mycobacterium tuberculosis *in vivo*. *Sci Immunol* (2019) 4(37). doi: 10.1126/sciimmunol.aaw6693

140. Lovey A, Verma S, Kaipilyawar V, Ribeiro-Rodrigues R, Husain S, Palaci M, et al. Early alveolar macrophage response and IL-1R-dependent T cell priming determine transmissibility of *Mycobacterium tuberculosis* strains. *Nat Commun* (2022) 13(1):884. doi: 10.1038/s41467-022-28506-2

141. Mata E, Tarancon R, Guerrero C, Moreo E, Moreau F, Uranga S, et al. Pulmonary BCG induces lung-resident macrophage activation and confers long-term protection against tuberculosis. *Sci Immunol* (2021) 6(63):eabc2934. doi: 10.1126/sciimmunol.abc2934

142. Gu H, Zeng X, Peng L, Xiang C, Zhou Y, Zhang X, et al. Vaccination induces rapid protection against bacterial pneumonia via training alveolar macrophage in mice. *Elife* (2021) 10. doi: 10.7554/eLife.69951

143. Yao Y, Jeyanathan M, Haddadi S, Barra NG, Vaseghi-Shanjani M, Damjanovic D, et al. Induction of autonomous memory alveolar macrophages requires T cell help and is critical to trained immunity. *Cell* (2018) 175(6):1634–50.e17. doi: 10.1016/j.cell.2018.09.042

144. Jeyanathan M, Fritz DK, Afkhami S, Aguirre E, Howie KJ, Zganiacz A, et al. Aerosol delivery, but not intramuscular injection, of adenovirus-vectored tuberculosis vaccine induces respiratory-mucosal immunity in humans. *JCI Insight* (2022) 7(3). doi: 10.1172/jci.insight.155655

145. Berry MP, Graham CM, McNab FW, Xu Z, Bloch SA, Oni T, et al. An interferon-inducible neutrophil-driven blood transcriptional signature in human tuberculosis. *Nature* (2010) 466(7309):973–7. doi: 10.1038/nature09247

146. Moreira-Teixeira L, Stimpson PJ, Stavropoulos E, Hadebe S, Chakravarty P, Ioannou M, et al. Type I IFN exacerbates disease in tuberculosis-susceptible mice by inducing neutrophil-mediated lung inflammation and NETosis. *Nat Commun* (2020) 11(1):5566. doi: 10.1038/s41467-020-19412-6

147. Trentini MM, de Oliveira FM, Kipnis A, Junqueira-Kipnis AP. The Role of Neutrophils in the Induction of Specific Th1 and Th17 during Vaccination against Tuberculosis. *Front Microbiol* (2016) 7:898. doi: 10.3389/fmicb.2016.00898

148. Bickett TE, McLean J, Creissen E, Izzo L, Hagan C, Izzo AJ, et al. Characterizing the BCG induced macrophage and neutrophil mechanisms for defense against mycobacterium tuberculosis. *Front Immunol* (2020) 11:1202. doi: 10.3389/fimmu.2020.01202

149. Moorlag S, Rodriguez-Rosales YA, Gillard J, Fanucchi S, Theunissen K, Novakovic B, et al. BCG vaccination induces long-term functional reprogramming of human neutrophils. *Cell Rep* (2020) 33(7):108387. doi: 10.1016/j.celrep.2020.108387

150. Hansen SG, Zak DE, Xu G, Ford JC, Marshall EE, Malouli D, et al. Prevention of tuberculosis in rhesus macaques by a cytomegalovirus-based vaccine. *Nat Med* (2018) 24(2):130–43. doi: 10.1038/nm.4473

151. Dhiman R, Periasamy S, Barnes PF, Jaiswal AG, Paidipally P, Barnes AB, et al. NK1.1$^+$ cells and IL-22 regulate vaccine-induced protective immunity against challenge with *Mycobacterium tuberculosis*. *J Immunol* (2012) 189(2):897–905. doi: 10.4049/jimmunol.1102833

152. Khader SA, Bell GK, Pearl JE, Fountain JJ, Rangel-Moreno J, Cilley GE, et al. IL-23 and IL-17 in the establishment of protective pulmonary CD4$^+$ T cell responses after vaccination and during *Mycobacterium tuberculosis* challenge. *Nat Immunol* (2007) 8(4):369–77. doi: 10.1038/ni1449

153. Monin L, Griffiths KL, Slight S, Lin Y, Rangel-Moreno J, Khader SA. Immune requirements for protective Th17 recall responses to *Mycobacterium tuberculosis* challenge. *Mucosal Immunol* (2015) 8(5):1099–109. doi: 10.1038/mi.2014.136

154. Nambiar JK, Ryan AA, Kong CU, Britton WJ, Triccas JA. Modulation of pulmonary DC function by vaccine-encoded GM-CSF enhances protective immunity against *Mycobacterium tuberculosis* infection. *Eur J Immunol* (2010) 40(1):153–61. doi: 10.1002/eji.200939665

155. Triccas JA, Shklovskaya E, Spratt J, Ryan AA, Palendira U, Fazekas de St Groth B, et al. Effects of DNA- and *Mycobacterium bovis* BCG-based delivery of the Flt3 ligand on protective immunity to Mycobacterium tuberculosis. *Infect Immun* (2007) 75 (11):5368–75. doi: 10.1128/IAI.00322-07

156. van den Berg RA, De Mot L, Leroux-Roels G, Bechtold V, Clement F, Coccia M, et al. Adjuvant-associated peripheral blood mRNA profiles and kinetics induced by the adjuvanted recombinant protein candidate tuberculosis vaccine M72/AS01 in bacillus calmette-guérin-vaccinated adults. *Front Immunol* (2018) 9:564. doi: 10.3389/fimmu.2018.00564

157. Griffiths KL, Ahmed M, Das S, Gopal R, Horne W, Connell TD, et al. Targeting dendritic cells to accelerate T-cell activation overcomes a bottleneck in tuberculosis vaccine efficacy. *Nat Commun* (2016) 7:13894. doi: 10.1038/ncomms13894

158. Silva-Sánchez A, Meza-Pérez S, Flores-Langarica A, Donis-Maturano L, Estrada-García I, Calderón-Amador J, et al. ESAT-6 Targeting to DEC205$^+$ Antigen Presenting Cells Induces Specific-T Cell Responses against ESAT-6 and Reduces Pulmonary Infection with Virulent Mycobacterium tuberculosis. *PloS One* (2015) 10 (4):e0124828. doi: 10.1371/journal.pone.0124828

159. Velasquez LN, Stüve P, Gentilini MV, Swallow M, Bartel J, Lycke NY, et al. Targeting *Mycobacterium tuberculosis* Antigens to Dendritic Cells via the DC-Specific-ICAM3-Grabbing-Nonintegrin Receptor Induces Strong T-Helper 1 Immune Responses. *Front Immunol* (2018) 9:471. doi: 10.3389/fimmu.2018.00471

160. Schenkel JM, Fraser KA, Vezys V, Masopust D. Sensing and alarm function of resident memory CD8$^+$ T cells. *Nat Immunol* (2013) 14(5):509–13. doi: 10.1038/ni.2568

161. Christensen D, Mortensen R, Rosenkrands I, Dietrich J, Andersen P. Vaccine-induced Th17 cells are established as resident memory cells in the lung and promote local IgA responses. *Mucosal Immunol* (2017) 10(1):260–70. doi: 10.1038/mi.2016.28

162. Counoupas C, Ferrell KC, Ashhurst A, Bhattacharyya ND, Nagalingam G, Stewart EL, et al. Mucosal delivery of a multistage subunit vaccine promotes development of lung-resident memory T cells and affords interleukin-17-dependent protection against pulmonary tuberculosis. *NPJ Vaccines* (2020) 5(1):105. doi: 10.1038/s41541-020-00255-7

163. Perdomo C, Zedler U, Kühl AA, Lozza L, Saikali P, Sander LE, et al. Mucosal BCG vaccination induces protective lung-resident memory T cell populations against tuberculosis. *mBio* (2016) 7(6). doi: 10.1128/mBio.01686-16

164. Yang Q, Zhang M, Chen Q, Chen W, Wei C, Qiao K, et al. Cutting edge: characterization of human tissue-resident memory T cells at different infection sites in patients with tuberculosis. *J Immunol* (2020) 204(9):2331–6. doi: 10.4049/jimmunol.1901326

165. Ogongo P, Tezera LB, Ardain A, Nhamoyebonde S, Ramsuran D, Singh A, et al. Tissue-resident-like CD4$^+$ T cells secreting IL-17 control Mycobacterium tuberculosis in the human lung. *J Clin Invest* (2021) 131(10). doi: 10.1172/JCI142014

166. He Q, Jiang L, Cao K, Zhang L, Xie X, Zhang S, et al. A systemic prime-intrarectal pull strategy raises rectum-resident CD8$^+$ T cells for effective protection in a murine model of LM-OVA infection. *Front Immunol* (2020) 11:571248. doi: 10.3389/fimmu.2020.571248

167. Çuburu N, Kim R, Guittard GC, Thompson CD, Day PM, Hamm DE, et al. A prime-pull-amplify vaccination strategy to maximize induction of circulating and genital-resident intraepithelial CD8(+) memory T cells. *J Immunol* (2019) 202 (4):1250–64. doi: 10.4049/jimmunol.1800219

168. Bernstein DI, Cardin RD, Bravo FJ, Awasthi S, Lu P, Pullum DA, et al. Successful application of prime and pull strategy for a therapeutic HSV vaccine. *NPJ Vaccines* (2019) 4:33. doi: 10.1038/s41541-019-0129-1

169. Roces CB, Hussain MT, Schmidt ST, Christensen D, Perrie Y. Investigating prime-pull vaccination through a combination of parenteral vaccination and intranasal boosting. *Vaccines (Basel)* (2019) 8(1). doi: 10.3390/vaccines8010010

170. Haddadi S, Vaseghi-Shanjani M, Yao Y, Afkhami S, D'Agostino MR, Zganiacz A, et al. Mucosal-pull induction of lung-resident memory CD8 T cells in parenteral TB vaccine-primed hosts requires cognate antigens and CD4 T cells. *Front Immunol* (2019) 10:2075. doi: 10.3389/fimmu.2019.02075

171. Darrah PA, Zeppa JJ, Maiello P, Hackney JA, Wadsworth MH2nd, Hughes TK, et al. Prevention of tuberculosis in macaques after intravenous BCG immunization. *Nature* (2020) 577(7788):95–102. doi: 10.1038/s41586-019-1817-8

172. Hirai T, Yang Y, Zenke Y, Li H, Chaudhri VK, de la Cruz Diaz JS, et al. Competition for active TGFβ Cytokine allows for selective retention of antigen-specific tissue- resident memory T cells in the epidermal niche. *Immunity* (2021) 54(1):84–98.e5. doi: 10.1016/j.immuni.2020.10.022

173. Bourdely P, Anselmi G, Vaivode K, Ramos RN, Missolo-Koussou Y, Hidalgo S, et al. Transcriptional and functional analysis of CD1c(+) human dendritic cells identifies a CD163(+) subset priming CD8(+)CD103(+) T cells. *Immunity* (2020) 53 (2):335–52.e8. doi: 10.1016/j.immuni.2020.06.002

174. Khader SA, Guglani L, Rangel-Moreno J, Gopal R, Junecko BA, Fountain JJ, et al. IL-23 is required for long-term control of *Mycobacterium tuberculosis* and B cell follicle formation in the infected lung. *J Immunol* (2011) 187(10):5402–7. doi: 10.4049/jimmunol.1101377

175. Slight SR, Rangel-Moreno J, Gopal R, Lin Y, Fallert Junecko BA, Mehra S, et al. CXCR5$^+$ T helper cells mediate protective immunity against tuberculosis. *J Clin Invest* (2013) 123(2):712–26. doi: 10.1172/JCI65728

176. Germain C, Gnjatic S, Tamzalit F, Knockaert S, Remark R, Goc J, et al. Presence of B cells in tertiary lymphoid structures is associated with a protective immunity in patients with lung cancer. *Am J Respir Crit Care Med* (2014) 189(7):832–44. doi: 10.1164/rccm.201309-1611OC

177. Tan HX, Esterbauer R, Vanderven HA, Juno JA, Kent SJ, Wheatley AK. Inducible bronchus-associated lymphoid tissues (iBALT) serve as sites of B cell selection and maturation following influenza infection in mice. *Front Immunol* (2019) 10:611. doi: 10.3389/fimmu.2019.00611

178. Moyron-Quiroz JE, Rangel-Moreno J, Hartson L, Kusser K, Tighe MP, Klonowski KD, et al. Persistence and responsiveness of immunologic memory in the absence of secondary lymphoid organs. *Immunity* (2006) 25(4):643–54. doi: 10.1016/j.immuni.2006.08.022

179. Takamura S, Yagi H, Hakata Y, Motozono C, McMaster SR, Masumoto T, et al. Specific niches for lung-resident memory CD8$^+$ T cells at the site of tissue regeneration enable CD69-independent maintenance. *J Exp Med* (2016) 213(13):3057–73. doi: 10.1084/jem.20160938

180. Takamura S. Niches for the long-term maintenance of tissue-resident memory T cells. *Front Immunol* (2018) 9:1214. doi: 10.3389/fimmu.2018.01214

181. Gompels UA, Larke N, Sanz-Ramos M, Bates M, Musonda K, Manno D, et al. Human cytomegalovirus infant infection adversely affects growth and development in maternally HIV-exposed and unexposed infants in Zambia. *Clin Infect Dis* (2012) 54 (3):434–42. doi: 10.1093/cid/cir837

182. Martinez L, Nicol MP, Wedderburn CJ, Stadler A, Botha M, Workman L, et al. Cytomegalovirus acquisition in infancy and the risk of tuberculosis disease in childhood: a longitudinal birth cohort study in Cape Town, South Africa. *Lancet Glob Health* (2021) 9(12):e1740–e9. doi: 10.1016/S2214-109X(21)00407-1

183. Li H, Wang XX, Wang B, Fu L, Liu G, Lu Y, et al. Latently and uninfected healthcare workers exposed to TB make protective antibodies against Mycobacterium tuberculosis. *Proc Natl Acad Sci U.S.A.* (2017) 114(19):5023–8. doi: 10.1073/pnas.1611776114

184. Zimmermann N, Thormann V, Hu B, Köhler AB, Imai-Matsushima A, Locht C, et al. Human isotype-dependent inhibitory antibody responses against Mycobacterium tuberculosis. *EMBO Mol Med* (2016) 8(11):1325–39. doi: 10.15252/emmm.201606330

185. Lu LL, Chung AW, Rosebrock TR, Ghebremichael M, Yu WH, Grace PS, et al. A functional role for antibodies in tuberculosis. *Cell* (2016) 167(2):433–43.e14. doi: 10.1016/j.cell.2016.08.072

186. Teitelbaum R, Glatman-Freedman A, Chen B, Robbins JB, Unanue E, Casadevall A, et al. A mAb recognizing a surface antigen of *Mycobacterium tuberculosis* enhances host survival. *Proc Natl Acad Sci U S A.* (1998) 95(26):15688–93. doi: 10.1073/pnas.95.26.15688

187. Fletcher HA, Snowden MA, Landry B, Rida W, Satti I, Harris SA, et al. T-cell activation is an immune correlate of risk in BCG vaccinated infants. *Nat Commun* (2016) 7:11290. doi: 10.1038/ncomms11290

188. Irvine EB, O'Neil A, Darrah PA, Shin S, Choudhary A, Li W, et al. Robust IgM responses following intravenous vaccination with Bacille Calmette-Guérin associate with prevention of *Mycobacterium tuberculosis* infection in macaques. *Nat Immunol* (2021) 22(12):1515–23. doi: 10.1038/s41590-021-01066-1

189. Cannas A, Calvo L, Chiacchio T, Cuzzi G, Vanini V, Lauria FN, et al. IP-10 detection in urine is associated with lung diseases. *BMC Infect Dis* (2010) 10:333. doi: 10.1186/1471-2334-10-333

190. Kim SY, Kim J, Kim DR, Kang YA, Bong S, Lee J, et al. Urine IP-10 as a biomarker of therapeutic response in patients with active pulmonary tuberculosis. *BMC Infect Dis* (2018) 18(1):240. doi: 10.1186/s12879-018-3144-3

191. Kerkhoff AD, Barr DA, Schutz C, Burton R, Nicol MP, Lawn SD, et al. Disseminated tuberculosis among hospitalised HIV patients in South Africa: a common condition that can be rapidly diagnosed using urine-based assays. *Sci Rep* (2017) 7(1):10931. doi: 10.1038/s41598-017-09895-7

192. Lawn SD, Kerkhoff AD, Burton R, Schutz C, Boulle A, Vogt M, et al. Diagnostic accuracy, incremental yield and prognostic value of Determine TB-LAM for routine diagnostic testing for tuberculosis in HIV-infected patients requiring acute hospital

admission in South Africa: a prospective cohort. *BMC Med* (2017) 15(1):67. doi: 10.1186/s12916-017-0822-8

193. Fitzgerald BL, Islam MN, Graham B, Mahapatra S, Webb K, Boom WH, et al. Elucidation of a human urine metabolite as a seryl-leucine glycopeptide and as a biomarker of effective anti-tuberculosis therapy. *ACS Infect Dis* (2019) 5(3):353–64. doi: 10.1021/acsinfecdis.8b00241

194. Sasaki E, Kusunoki H, Momose H, Furuhata K, Hosoda K, Wakamatsu K, et al. Changes of urine metabolite profiles are induced by inactivated influenza vaccine inoculations in mice. *Sci Rep* (2019) 9(1):16249. doi: 10.1038/s41598-019-52686-5

195. Burny W, Hervé C, Caubet M, Yarzabal JP, Didierlaurent AM. Utility of urinary cytokine levels as predictors of the immunogenicity and reactogenicity of AS01-adjuvanted hepatitis B vaccine in healthy adults. *Vaccine* (2022) 40(19):2714–22. doi: 10.1016/j.vaccine.2022.03.050

196. Gröschel MI, Sayes F, Shin SJ, Frigui W, Pawlik A, Orgeur M, et al. Recombinant BCG expressing ESX-1 of *mycobacterium marinum* combines low virulence with cytosolic immune signaling and improved TB protection. *Cell Rep* (2017) 18(11):2752–65. doi: 10.1016/j.celrep.2017.02.057

197. Bottai D, Frigui W, Clark S, Rayner E, Zelmer A, Andreu N, et al. Increased protective efficacy of recombinant BCG strains expressing virulence-neutral proteins of the ESX-1 secretion system. *Vaccine* (2015) 33(23):2710–8. doi: 10.1016/j.vaccine.2015.03.083

198. Pérez I, Campos-Pardos E, Díaz C, Uranga S, Sayes F, Vicente F, et al. The *Mycobacterium tuberculosis* PhoPR virulence system regulates expression of the universal second messenger c-di-AMP and impacts vaccine safety and efficacy. *Mol Ther Nucleic Acids* (2022) 27:1235–48. doi: 10.1016/j.omtn.2022.02.011

199. El Zowalaty ME, Ashour HM. Paving the way to a new class of efficient and safe tuberculosis vaccines: The role of c-di-AMP in *Mycobacterium tuberculosis* immunity and virulence. *Mol Ther Nucleic Acids* (2022) 30:13–4. doi: 10.1016/j.omtn.2022.08.034

200. Aceves-Sánchez MJ, Flores-Valdez MA, Pedroza-Roldán C, Creissen E, Izzo L, Silva-Angulo F, et al. Vaccination with BCGΔBCG1419c protects against pulmonary and extrapulmonary TB and is safer than BCG. *Sci Rep* (2021) 11(1):12417. doi: 10.1038/s41598-021-91993-8

201. Velázquez-Fernández JB, Ferreira-Souza GHM, Rodríguez-Campos J, Aceves-Sánchez MJ, Bravo-Madrigal J, Vallejo-Cardona AA, et al. Proteomic characterization of a second-generation version of the BCGΔBCG1419c vaccine candidate by means of electrospray-ionization quadrupole time-of-flight mass spectrometry. *Pathog Dis* (2021) 79(1). doi: 10.1093/femspd/ftaa070

202. Rivas-Santiago CE, Guerrero GG. IFN-α Boosting of *Mycobacterium bovis* Bacillus Calmette Güerin-Vaccine Promoted Th1 Type Cellular Response and Protection against M. tuberculosis Infection. *BioMed Res Int* (2017) 2017:8796760. doi: 10.1155/2017/8796760

203. Babu S, Blauvelt CP, Kumaraswami V, Nutman TB. Regulatory networks induced by live parasites impair both Th1 and Th2 pathways in patent lymphatic filariasis: implications for parasite persistence. *J Immunol* (2006) 176(5):3248–56. doi: 10.4049/jimmunol.176.5.3248

204. Elias D, Britton S, Aseffa A, Engers H, Akuffo H. Poor immunogenicity of BCG in helminth infected population is associated with increased *in vitro* TGF-beta production. *Vaccine* (2008) 26(31):3897–902. doi: 10.1016/j.vaccine.2008.04.083

205. Elias D, Wolday D, Akuffo H, Petros B, Bronner U, Britton S. Effect of deworming on human T cell responses to mycobacterial antigens in helminth-exposed individuals before and after bacille Calmette-Guérin (BCG) vaccination. *Clin Exp Immunol* (2001) 123(2):219–25. doi: 10.1046/j.1365-2249.2001.01446.x

206. Gebreegziabiher D, Desta K, Desalegn G, Howe R, Abebe M. The effect of maternal helminth infection on maternal and neonatal immune function and immunity to tuberculosis. *PloS One* (2014) 9(4):e93429. doi: 10.1371/journal.pone.0093429

207. Malhotra I, Mungai P, Wamachi A, Kioko J, Ouma JH, Kazura JW, et al. Helminth- and Bacillus Calmette-Guérin-induced immunity in children sensitized in *utero* to filariasis and schistosomiasis. *J Immunol* (1999) 162(11):6843–8. doi: 10.4049/jimmunol.162.11.6843

208. Schick J, Altunay M, Lacorcia M, Marschner N, Westermann S, Schluckebier J, et al. IL-4 and helminth infection downregulate MINCLE-dependent macrophage response to mycobacteria and Th17 adjuvanticity. *Elife* (2023) 12. doi: 10.7554/eLife.72923

209. Abate G, Hamzabegovic F, Eickhoff CS, Hoft DF. BCG Vaccination Induces M. avium and *M. abscessus* Cross-Protective Immunity. *Front Immunol* (2019) 10:234. doi: 10.3389/fimmu.2019.00234

210. Zimmermann P, Finn A, Curtis N. Does BCG vaccination protect against nontuberculous mycobacterial infection? A systematic review and meta-analysis. *J Infect Dis* (2018) 218(5):679–87. doi: 10.1093/infdis/jiy207

211. Poyntz HC, Stylianou E, Griffiths KL, Marsay L, Checkley AM, McShane H. Non-tuberculous mycobacteria have diverse effects on BCG efficacy against Mycobacterium tuberculosis. *Tuberculosis (Edinb)* (2014) 94(3):226–37. doi: 10.1016/j.tube.2013.12.006

212. Brandt L, Feino Cunha J, Weinreich Olsen A, Chilima B, Hirsch P, Appelberg R, et al. Failure of the *Mycobacterium bovis* BCG vaccine: some species of environmental mycobacteria block multiplication of BCG and induction of protective immunity to tuberculosis. *Infect Immun* (2002) 70(2):672–8. doi: 10.1128/IAI.70.2.672-678.2002

213. Flaherty DK, Vesosky B, Beamer GL, Stromberg P, Turner J. Exposure to Mycobacterium avium can modulate established immunity against *Mycobacterium tuberculosis* infection generated by *Mycobacterium bovis* BCG vaccination. *J Leukoc Biol* (2006) 80(6):1262–71. doi: 10.1189/jlb.0606407

214. Scriba TJ, Tameris M, Smit E, van der Merwe L, Hughes EJ, Kadira B, et al. A phase IIa trial of the new tuberculosis vaccine, MVA85A, in HIV- and/or *Mycobacterium tuberculosis*-infected adults. *Am J Respir Crit Care Med* (2012) 185 (7):769–78. doi: 10.1164/rccm.201108-1548OC

215. Sharan R, Kaushal D. Vaccine strategies for the Mtb/HIV copandemic. *NPJ Vaccines* (2020) 5:95. doi: 10.1038/s41541-020-00245-9

216. Yoo JE, Kim D, Han K, Rhee SY, Shin DW, Lee H. Diabetes status and association with risk of tuberculosis among Korean adults. *JAMA Netw Open* (2021) 4 (9):e2126099. doi: 10.1001/jamanetworkopen.2021.26099

217. Ajie M, van Heck JIP, Janssen AWM, Meijer RI, Tack CJ, Stienstra R. Disease duration and chronic complications associate with immune activation in individuals with longstanding type 1 diabetes. *J Clin Endocrinol Metab* (2023) 108(8):1909–1920. doi: 10.1210/clinem/dgad087

218. Verma A, Kaur M, Luthra P, Singh L, Aggarwal D, Verma I, et al. Immunological aspects of host-pathogen crosstalk in the co-pathogenesis of diabetes and latent tuberculosis. *Front Cell Infect Microbiol* (2022) 12:957512. doi: 10.3389/fcimb.2022.957512

219. Clement CC, Nanaware PP, Yamazaki T, Negroni MP, Ramesh K, Morozova K, et al. Pleiotropic consequences of metabolic stress for the major histocompatibility complex class II molecule antigen processing and presentation machinery. *Immunity* (2021) 54(4):721–36.e10. doi: 10.1016/j.immuni.2021.02.019

220. Chambers ES, Akbar AN. Can blocking inflammation enhance immunity during aging? *J Allergy Clin Immunol* (2020) 145(5):1323–31. doi: 10.1016/j.jaci.2020.03.016

221. Scordo JM, Piergallini TJ, Reuter N, Headley CA, Hodara VL, Gonzalez O, et al. Local immune responses to tuberculin skin challenge in *Mycobacterium bovis* BCG-vaccinated baboons: a pilot study of younger and older animals. *Immun Ageing* (2021) 18(1):16. doi: 10.1186/s12979-021-00229-w

222. Scordo JM, Piergallini TJ, Olmo-Fontánez AM, Thomas A, Raué HP, Slifka M, et al. Recall responses in the lung environment are impacted by age in a pilot study of *Mycobacterium bovis*-BCG vaccinated rhesus macaques. *Exp Gerontol* (2022) 167:111904. doi: 10.1016/j.exger.2022.111904

223. Giamarellos-Bourboulis EJ, Tsilika M, Moorlag S, Antonakos N, Kotsaki A, Domínguez-Andrés J, et al. Activate: randomized clinical trial of BCG vaccination against infection in the elderly. *Cell* (2020) 183(2):315–23.e9. doi: 10.1016/j.cell.2020.08.051

224. Tsilika M, Taks E, Dolianitis K, Kotsaki A, Leventogiannis K, Damoulari C, et al. ACTIVATE-2: A double-blind randomized trial of BCG vaccination against COVID-19 in individuals at risk. *Front Immunol* (2022) 13:873067. doi: 10.3389/fimmu.2022.873067

225. Schultze JL, Aschenbrenner AC. COVID-19 and the human innate immune system. *Cell* (2021) 184(7):1671–92. doi: 10.1016/j.cell.2021.02.029

226. Pavan Kumar N, Padmapriyadarsini C, Rajamanickam A, Marinaik SB, Nancy A, Padmanaban S, et al. Effect of BCG vaccination on proinflammatory responses in elderly individuals. *Sci Adv* (2021) 7(32). doi: 10.1126/sciadv.abg7181

227. Monteiro-Maia R, Pinho RT. Oral bacillus Calmette-Guérin vaccine against tuberculosis: why not? *Mem Inst Oswaldo Cruz* (2014) 109(6):838–45. doi: 10.1590/0074-0276140091

228. Hoft DF, Xia M, Zhang GL, Blazevic A, Tennant J, Kaplan C, et al. PO and ID BCG vaccination in humans induce distinct mucosal and systemic immune responses and CD4(+) T cell transcriptomal molecular signatures. *Mucosal Immunol* (2018) 11 (2):486–95. doi: 10.1038/mi.2017.67

229. Aldwell FE, Tucker IG, de Lisle GW, Buddle BM. Oral delivery of *Mycobacterium bovis* BCG in a lipid formulation induces resistance to pulmonary tuberculosis in mice. *Infect Immun* (2003) 71(1):101–8. doi: 10.1128/IAI.71.1.101-108.2003

230. Clark SO, Kelly DL, Badell E, Castello-Branco LR, Aldwell F, Winter N, et al. Oral delivery of BCG Moreau Rio de Janeiro gives equivalent protection against tuberculosis but with reduced pathology compared to parenteral BCG Danish vaccination. *Vaccine* (2010) 28(43):7109–16. doi: 10.1016/j.vaccine.2010.07.087

231. Doherty TM, Olsen AW, van Pinxteren L, Andersen P. Oral vaccination with subunit vaccines protects animals against aerosol infection with Mycobacterium tuberculosis. *Infect Immun* (2002) 70(6):3111–21. doi: 10.1128/IAI.70.6.3111-3121.2002

232. Imperial MZ, Nahid P, Phillips PPJ, Davies GR, Fielding K, Hanna D, et al. A patient-level pooled analysis of treatment-shortening regimens for drug-susceptible pulmonary tuberculosis. *Nat Med* (2018) 24(11):1708–15. doi: 10.1038/s41591-018-0224-2

233. Dartois VA, Rubin EJ. Anti-tuberculosis treatment strategies and drug development: challenges and priorities. *Nat Rev Microbiol* (2022) 20(11):685–701. doi: 10.1038/s41579-022-00731-y

234. Pillay J, Gaudet L, Wingert A, Bialy L, Mackie AS, Paterson DI, et al. Incidence, risk factors, natural history, and hypothesised mechanisms of myocarditis and pericarditis following covid-19 vaccination: living evidence syntheses and review. *Bmj* (2022) 378:e069445. doi: 10.1136/bmj-2021-069445

235. Chu DK, Abrams EM, Golden DBK, Blumenthal KG, Wolfson AR, Stone CAJr., et al. Risk of second allergic reaction to SARS-coV-2 vaccines: A systematic review and meta-analysis. *JAMA Intern Med* (2022) 182(4):376–85. doi: 10.1001/jamainternmed.2021.8515

236. Tagliabue A, Boraschi D, Leite LCC, Kaufmann SHE. 100 years of BCG immunization: past, present, and future. *Vaccines (Basel)* (2022) 10(10). doi: 10.3390/vaccines10101743

frontiers | Frontiers in Immunology

TYPE Review
PUBLISHED 15 August 2023
DOI 10.3389/fimmu.2023.1238586

OPEN ACCESS

EDITED BY
Subash Babu,
International Centers for Excellence in Research (ICER), India

REVIEWED BY
Joanna Kirman,
University of Otago, New Zealand
Andre Bafica,
Federal University of Santa Catarina, Brazil

*CORRESPONDENCE
Xiao-yong Fan
xyfan008@fudan.edu.cn
Zhi-dong Hu
huzhidong@fudan.edu.cn

RECEIVED 12 June 2023
ACCEPTED 25 July 2023
PUBLISHED 15 August 2023

CITATION
Zhang Y, Xu J-c, Hu Z-d and Fan X-y (2023) Advances in protein subunit vaccines against tuberculosis. *Front. Immunol.* 14:1238586. doi: 10.3389/fimmu.2023.1238586

Advances in protein subunit vaccines against tuberculosis

Ying Zhang[1], Jin-chuan Xu[1], Zhi-dong Hu[1,2]* and Xiao-yong Fan[1,2]*

[1]Shanghai Public Health Clinical Center, Shanghai Institute of Infectious Disease and Biosecurity, Fudan University, Shanghai, China, [2]TB Center, Shanghai Emerging and Re-emerging Infectious Disease Institute, Fudan University, Shanghai, China

Tuberculosis (TB), also known as the "White Plague", is caused by *Mycobacterium tuberculosis* (*Mtb*). Before the COVID-19 epidemic, TB had the highest mortality rate of any single infectious disease. Vaccination is considered one of the most effective strategies for controlling TB. Despite the limitations of the Bacille Calmette-Guérin (BCG) vaccine in terms of protection against TB among adults, it is currently the only licensed TB vaccine. Recently, with the evolution of bioinformatics and structural biology techniques to screen and optimize protective antigens of *Mtb*, the tremendous potential of protein subunit vaccines is being exploited. Multistage subunit vaccines obtained by fusing immunodominant antigens from different stages of TB infection are being used both to prevent and to treat TB. Additionally, the development of novel adjuvants is compensating for weaknesses of immunogenicity, which is conducive to the flourishing of subunit vaccines. With advances in the development of animal models, preclinical vaccine protection assessments are becoming increasingly accurate. This review summarizes progress in the research of protein subunit TB vaccines during the past decades to facilitate the further optimization of protein subunit vaccines that may eradicate TB.

KEYWORDS

tuberculosis, protein subunit vaccines, antigen epitopes, adjuvants, clinical trials, animal models

1 Introduction

Tuberculosis (TB), caused by *Mycobacterium tuberculosis* (*Mtb*), has afflicted humans for thousands of years. *Mtb* is highly contagious and colonizes the respiratory tract through airborne droplets (1). TB remains a serious threat to public health, with 10.6 million new cases and 1.6 million deaths reported worldwide in 2021 (2). In addition, enormous challenges for TB prevention and treatment are posed by the emergence of multidrug-resistant TB (MDR-TB) (3), the lack of effective methods for the differential diagnosis of latent TB infection (LTBI) (4), immune disorder caused by co-infection with HIV (5).

The development of the Bacille Calmette- Guérin (BCG) vaccine was a major milestone in the history of global TB control. Even though it has been more than 100 years since BCG

was developed, BCG is still the only licensed TB vaccine worldwide. However, its protective efficiency is still controversial due to its limited immune protection in adults (6). Therefore, a more effective TB vaccine that protects against different stages of the disease's development is urgently needed.

The main TB vaccine candidates include live attenuated vaccines, inactivated vaccines, recombinant viral vector vaccines, and protein subunit vaccines. Since both whole-cell-based and virus-based vaccines pose potential risks to human health, protein-subunit vaccines consisting of protective antigens may be safer and more attractive (7). However, the biggest concern with protein subunit vaccines is inadequate immunogenicity, therefore, optimizing the vaccine composition to trigger a potent and long-lasting immune response is crucial. Novel vaccine adjuvants are powerful tools that may overcome the immunogenicity limitations of protein subunit vaccines.

In this review, we focus on the advances in antigen optimization, adjuvant selection, clinical trials, animal models, and vaccination strategies of protein subunit vaccines, which may foretell the future of TB vaccine research and development.

2 Protein epitope optimization strategy

The complex genetic composition, multiple immune evasion strategies, and the lack of rigorous immune markers make the identification of key protective epitopes against *Mtb* a major challenge. Several methods have been used to predict the optimal epitopes for vaccine design.

Although $CD4^+$ T cells are necessary to protect against TB, they may not be sufficient to obtain a completely protective immune response (8). Many researchers have focused on identifying antigens that stimulate the $CD8^+$ T-cell-mediated responses that also play a protective role against TB and latent TB infection (LTBI) (9). Additionally, a growing number of studies have shown that antibodies produced by B cells contribute to the fight against TB (10). Therefore, vaccines that induce combined $CD4^+$, $CD8^+$ T-, and B-cell immune responses may be the most effective. Bioinformatics tools enable the rapid analysis of the entire genome and proteome of pathogens to predict potentially protective T- or B-cell epitopes and the character of their specific binding to major histocompatibility complex (MHC) molecules (11).

The structure of an antigen determines the specificity, affinity, and accessibility of the binding sites to MHC or antibody, which affects the potency of the immune response (12). Therefore, antigen geometry can be another critical factor in vaccine design (13). "Reverse vaccinology" was proposed 20 years ago, based on the availability of genome sequence information to design vaccines. With the development and application of immunology, proteomics, systems biology, and structural biology, we have entered the era of "Reverse vaccinology 2.0", in which the structural features of antigens and antibodies are used to guide the design of recombinant vaccine antigens. Developments in X-ray crystallography, electron microscopy, and computational biology have all contributed (14). Currently, AlphaFold2 is the most advanced protein 3D structure prediction tool (15). By predicting and analyzing the higher configuration of the 3D antigen structure, the linear epitopes for T-cell receptors and the conformational epitopes for B-cell receptors can be comprehensively optimized to improve vaccine protective efficiency (16).

Combining bioinformatics, structural information, and the AlphaFold2 prediction model to obtain the structural basis underlying protective immune responses to key epitopes is now a popular design strategy to get efficient, long-term, and broad-spectrum responses with multi-epitope TB protein subunit vaccine candidates (14–17).

3 Protective antigens of *Mtb*

The composition of *Mtb* is complex, and many components exhibit immunogenicity. According to different characteristics and associated growth states, *Mtb* antigens are mainly divided into the following types:

3.1 Antigens on the cell wall and capsule

The cell wall and capsule of *Mtb* contain a large number of glycolipids, lipoproteins, and glycoproteins such as cord factor, phthiocerol dimycocerosates, phosphatidylethanolamine, diacyl trehaloses, lipoarabinomannan, phosphatidyl-myoinositol mannosides, and heparin-binding adhesin, etc. (18, 19) They can activate immune responses and serve as candidate antigens or adjuvants for TB vaccines.

3.2 Secretory antigens

Mtb can secrete numerous proteins, some of which can inhibit or induce the host immune response by promoting immune escape or activating immune signaling pathways, respectively. Most of the candidate proteins for existing TB vaccines are based on those found as secreted antigens during logarithmic growth of *Mtb*, such as Ag85A/B, ESAT-6, CFP10, TB10.4, MPT64, and PPE18 (20). The secretory antigens are ideal candidate antigens for the recombinant protein subunit vaccine because of their strong immunogenicity and ease of heterologous expression and amplification.

3.3 Dormancy phase antigens

The antigens modulated under the DosR regulon are the main proteins involved in the dormant survival process of *Mtb*. A total of 48 structural proteins are known to be involved in aerobic respiration and carbon monoxide inhibition; representative genes include *HspX*, *Rv2623*, *Rv2660c*, etc. (21) Members of the durable hypoxia response (EHR) regulon are structural genes induced after exposure to hypoxia. EHR proteins are presumed to be involved in the adaptation and survival of bacteria during a long-term

bacteriostatic process (22). Members of the DosR and EHR regulons are considered promising antigens to be incorporated into protein subunit vaccines for treating LTBI (23).

3.4 Resuscitation phase antigens

Resuscitation promotion factors (Rpfs) are involved in the resuscitation and reactivation of dormant *Mtb* infection and induce specific humoral and cellular immune responses in individuals with LTBI (24). There are 5 Rpf-like proteins (RpfA, RpfB, RpfC, RpfD, and RpfE) with partially overlapping functions in *Mtb*. Rpfs, especially RpfB, can trigger a memory T-cell response and has been hypothesized to be an essential antigenic target controlling bacterial activation. Rpfs can be used as candidate antigens for protein subunit vaccines against LTBI infection (25).

3.5 BCG regions of difference (RD) antigens

BCG strains have structures similar to *Mtb*, but 16 genomic region of difference (RD) antigens are deficient in BCG compared to *Mtb* (26). The RD1 gene products contain a variety of potential virulence factors, such as ESAT-6 and CFP10 (26). They play multiple roles in *Mtb* progression and pathogenicity, and are considered suitable candidates for use in treatment and diagnosis (27). The poor protective effect of BCG may be related to the loss of a large number of genes encoding protective antigens. Therefore, RD antigens should be emphasized in constructing recombinant protein subunit vaccines.

4 Adjuvants

With the limitations in immunogenicity and bioavailability, excellent adjuvants are critical for protein subunit vaccines. Alum has been the only licensed adjuvant in human vaccines for several decades. However, it has been considered unsuitable for vaccines against intracellular pathogens such as *Mtb* due to its insufficient ability to induce Th1 cellular immunity and $CD8^+$ cytotoxic responses. TB-specific adjuvants that induce a strong immune response in the lungs but minimize the corresponding tissue damage are ideal. In order to meet the needs of TB vaccine development, a workshop entitled "Vaccine Adjuvants for Advancing the treatment of Mycobacterium tuberculosis" was held in July 2020, and factors correlates of protective immunity, targeting specific immune cells, immune evasion mechanisms, and animal models were identified as four research areas critical to the development of optimal TB vaccine adjuvants (28). In recent years, a variety of novel adjuvants have been developed, and most available protein subunit vaccine adjuvants are based on Toll-like receptor (TLR) agonists and use liposomes and emulsions as delivery vehicles as shown in Table 1. In addition, nanoparticle-based adjuvants have received extensive attention in recent years, and various novel nanoadjuvants have been used in some of these vaccines.

4.1 CAF01

CAF01 comprises cationic surfactant lipid-based liposomes dimethyldioctadecylammonium (DDA) and glycolipid immunomodulator trehalose-6,6-dibehenate (TDB). DDA is a potent adjuvant capable of eliciting cellular and humoral immune responses (46). TDB is a synthetic analog of mycobacterial cord factor that is located in the cell wall of mycobacteria and has intrinsic immunostimulatory properties that activate Mincle (47). TDB incorporated with DDA creates a stable liposome by forming hydrogen bonds between the liposome membrane and the surrounding water. CAF01 has been shown to generate a Th1/Th17 polarization response via Mincle-dependent IL-1 production and subsequent MyD88 signaling (48).

4.2 AS01 and DMT

AS01 is a liposome-based adjuvant that consists of the 3-O-desacyl-4′-monophosphoryl lipid A (MPL) and the saponin QS-21 (*Quillaja saponaria* extract), co-prepared in the presence of cholesterol (73). MPL acts as a TLR4 agonist, stimulates NF-κB transcriptional activity, and induces a Th1 response. QS-21 can enhance the antigen presentation ability of antigen-presenting cells (APCs) and activate/differentiate T cells towards Th1 immune responses. DMT is a combination of the MPL, DDA, and TDB that provides more potent and longer-lasting protective efficacy, including antigen-specific $CD4^+$ Th1 response, IFN-γ^+ $CD8^+$ CTL response, and limited humoral response (42).

4.3 GLA-SE

GLA-SE is a mixture of the TLR4 agonist glucopyranosyl lipid A (GLA) and squalene emulsion (SE) (56). GLA is a synthetic lipopolysaccharide (LPS) derivative that maintains vigorous immunostimulatory activity and has low toxicity (57). SE is able to increase the secretion of proinflammatory cytokines such as IL-6, IL-12, and TNF (58). Both GLA and SE alone can promote IgG2 response, while the combination of GLA-SE can induce considerable Th1 response (56).

4.4 IC31

IC31 comprises the synthetic, positively charged antimicrobial peptide KLKL5KLK and oligodeoxynucleotide 1a (ODN1a) (64). ODN1a is an immune stimulatory molecule that promotes Th1-biased immune responses through the TLR9/MyD88 pathway. KLK can act as an immune stimulator that aids transfer into cells in the absence of cell membrane permeability, allowing more efficient functioning of intracellular TLRs (65). KLK induces a Th2 immune response when used alone and a stronger Th1 and Th2 immunity when combined with ODNla (66, 67).

TABLE 1 Protein subunit vaccine candidates undergoing pre-clinical and clinical trials.

Vaccine Candidates	Antigens	Adjuvants	Adjuvant components	Adjuvant targets	Immune responses	Immunization strategies	Trial phases	References
CysVac2/ Advax	CysD, Ag85B	Advax	Delta isoform of inulin formed cationic particles (1-2 µm)	–	IL-17-secreting lung-resident $CD4^+$ memory T cells (IFN-γ, TNF-α, IL-2, IL-17)	Prevention, and therapeutic	Pre-clinical	(29–35)
LT70	ESAT-6, Ag85B, peptide 190–198 of MPT64, Mtb8.4, Rv2626c	DDA/PolyI:C	DDA and PolyI:C	TLR-3	$CD4^+$ T cells (IFN-γ, IL-2) and antigen-specific IgG1 and IgG2c	BCG booster Therapeutic	Pre-clinical	(36–41)
CFMO-DMT	Rv2875, Rv3044, Rv2073c, Rv0577	DMT	DDA, MPL and TDB	TLR-4	$CD4^+$ T cells (IFN-γ, IL-2, TNF-α, IL-17A) and IFN-γ^+ $CD8^+$ T cells	Prevention, therapeutic, and prevent recurrence	Pre-clinical	(42–45)
H64/H74: CAF01	H64 (EsxA, EspD, EspC, EspE, EspR, PE35); H74 (EspB, EsxA, EspD, EspC, EspA, EspR)	CAF01	DDA and TDB	Mincle	$CD4^+$ T cells (TNF-α, IL-2)	BCG booster	Pre-clinical	(46–49)
H107	PPE68, ESAT-6, EspI, EspC, EspA, MPT64, MPT70, MPT83	–	–	–	Less-differentiated CD4 Th1 cells and increased Th17 responses	BCG booster	Pre-clinical	(50)
AEC/BC02	Ag85B, ESAT-6-CFP10	BC02	CpG DNA fragment and aluminum salt	TLR-9	$CD4^+$ T cells (IFN-γ, IL-2) and antigen-specific IgG, IgG1, and IgG2a	Prevention, and therapeutic	Phase I	(51–55)
ID93+GLA-SE	Rv2608, Rv3619, Rv3620, Rv1813	GLA-SE	GLA in a stable oil-in-water SE	TLR-4	$CD4^+$ T cells (IFN-γ, TNF-α, IL-2) and antigen-specific IgG1 and IgG3	BCG booster, therapeutic, and prevent recurrence	Phase IIa	(56–63)
H56:IC31	Ag85B, ESAT6, Rv2660c	IC31	Antimicrobial peptide KLKL5KLK and ODN1a	TLR-9	$CD4^+$ T cells (IFN-γ, TNF-α, IL-2) and antigen-specific IgG	BCG booster, therapeutic, and prevent recurrence	Phase IIb	(64–72)
M72/$AS01_E$	Mtb 32A, Mtb 39A	AS01E	MPL and the saponin component QS21 co-prepared in cholesterol	TLR-4	$CD4^+$ T cells (IFN-γ, IL-2, TNF-α, IL-17), $CD8^+$ T cells (IFN-γ or TNF-α), NK cell IFN-γ, and antigen-specific IgG	BCG booster, and therapeutic	Phase IIb	(73–82)
Gam TBvac	ESAT-6, CFP10, Ag85A	Dextran/ CpG	DEAE-dextran polymer associating with BCG-derived unmethylated CpG oligodeoxynucleotide	TLR-9	$CD4^+$ T cells (IFN-γ, IL-2, TNF-α), $CD8^+$ T cell IFN-γ, and antigen-specific IgG	BCG booster	Phase IIb	(29, 83–87)

DDA, dimethyldioctadecylammonium; PolyI:C, polyinosinic-polycytidylic acid; MPL, ligand3-O-desacyl-4′-monophosphoryl lipid A; TDB, trehalose-6,6-dibehenate; CpG, cellular guanine phosphate; GLA, Glucopyranosyl Lipid A; SE, squalene emulsion; ODN1a, oligodeoxynucleotide (ODN) 1a; DEAE, Polycationic diethylaminoethyl.

4.5 Dextran/CpG

Dextran/CpG is a novel adjuvant developed with diethyl aminoethyl (DEAE)-dextran and CpG ODN (83). CpG is a TLR9 agonist with the ability to promote Th1 immune responses (secretion of IFN-γ, TNF-α, and IL-12 cytokines), opsonizing antibodies (IgG2a), and potent $CD8^+$ T cell responses (84). Dextran interacts with DC-SIGN family receptors, mannose receptors, and langerin, all triggering innate immunity that promotes inflammation. Furthermore, Dextran/CpG adjuvant

enhances activation of lymph node-resident APCs, thus enhancing T-cell priming (29, 83).

4.6 Advax

Advax is a novel cationic adjuvant based on the Delta inulin isoform and has a diameter of about 1-2 μm (30). Advax-based adjuvants have been shown to promote protective immunity against several pathogens in various animal species (31, 32). The potent chemotactic effect induced by Advax enables leukocyte recruitment to the site of inoculation and elicits a broad range of immune responses, including humoral response, Th1, Th2, and Th17 T-cell responses (31).

4.7 BC02

BC02 consists of BCG-derived unmethylated CpG DNA fragments and aluminum salts ($Al(OH)_3$) (51). CpG tends to induce Th1-type immune responses, while alum skews the response to promote the Th2 response to secrete IL-4 and IL-5 cytokines and produce IgG1 and IgE-type antibodies (52). BC02 induces robust Th1 and Th2 responses with acceptable safety (51).

4.8 DDA/poly(I:C)

DDA/poly(I:C) is composed of cationic liposome vector DDA and polyriboinosinic acid–polyribocytidylic acid, poly(I:C). Poly(I:C) mimics viral dsRNA and is a promising immune stimulator candidate for vaccines against intracellular pathogens. Poly(I:C) signaling primarily depends on TLR3 and melanoma differentiation-associated gene-5 (MDA-5) (36). Moreover, poly(I:C) induces strong Th1-skewed immune responses, with enhanced IFN-γ, IL-6, IL-12p70 as well as high antigen-specific IgG antibody (37, 38).

4.9 Nanoadjuvants

With the development of nanotechnology and the increasing understanding of immune responses to metals, different types of inorganic nanoadjuvants have been developed, including manganese (88), iron (89), silicon (90), magnesium (91), and gold-based adjuvants (92), etc. The commonly used polymers are poly-lactic-co-glycolic acid (PLGA), which can be constructed into nano- or larger particles to improve immune response efficiency (93). Compared with the traditional adjuvants, the novel inorganic nanoadjuvants can better activate both humoral and cellular immunity, induce a more balanced Th1/Th2 immune response and improve the safety and effectiveness of vaccines (94). Inorganic nanoadjuvants have been used in vaccines for various diseases, such as coronavirus (95), cancer (91, 96), and pertussis (97). Nanoadjuvants for TB vaccines are also being developed to enhance the immune response and extend the duration of protection (98, 99).

5 Pre-clinical and clinical trials

Pre-clinical and clinical trials are always needed to evaluate the safety and efficacy of novel vaccine candidates. We summarize the significant progression of protein subunit vaccines in recent trials.

5.1 Pre-clinical phases

5.1.1 CysVac2/Advax

CysD is an important protein in the sulfur assimilation pathway of *Mtb* that is up-regulated during LTBI (33). CysVac2, which consists of CysD and the acute phase antigen Ag85B, is an effective prophylactic and therapeutic vaccine, particularly effective in controlling an advanced infection (34). Notably, administration of CysVac2 to mice previously infected with TB significantly reduced bacterial load and immunopathological damage in the lungs compared to mice vaccinated with BCG (33). CysVac2 with Advax elicited multifunctional $CD4^+$ T cells with enhanced secretion of IFN-γ, TNF, and IL-2. Moreover, CysVac2/Advax induced the accumulation of lung-resident memory T cells expressing IL-17 and RORγT before and after the *Mtb* aerosol challenge (35). Thus, CysVac2/Advax was shown to be a suitable vaccine candidate for the control of TB pulmonary infection.

5.1.2 LT70

LT70 is a multistage protein subunit vaccine composed of antigens prominent at different metabolic stages of the *Mtb* life cycle, including ESAT-6, Ag85B, peptide 190-198 of MPT64, proliferative phase antigen Mtb8.4 and latency-associated antigen Rv2626c, with DDA/Poly(I:C) as an adjuvant (39). In a murine model, LT70 induced robust antigen-specific humoral (secretion of IgG1 and IgG2c antibodies) and Th1 cell immunity response (IFN-γ, IL-2) with immune protection against *Mtb* infection superior to that provided by BCG. When used as a booster vaccine, it enhanced the protective effect of BCG by reducing the bacterial load in the lungs of mice (39). Another study showed that LT70 had a significant therapeutic effect on LTBI in mice (40). In addition, prolonged LT70 inoculation intervals (0-4-12w) produced stronger protective effects and tended to induce long-term central memory T cells (T_{CM}, stronger IL-2 secretion capacity) rather than effector memory T cells (T_{EM}, stronger IFN-γ secretion capacity) (41).

5.1.3 CFMO-DMT

CMFO is a multistage subunit vaccine (containing Rv2875, Rv3044, Rv2073c, and Rv0577) administered subcutaneously adjuvanted with DMT (43, 44). CMFO-DMT could induce the immune response of IFN-γ^+ or IL-2^+ $CD4^+$ T cells and IFN-γ^+ $CD8^+$ T_{EM} cells in spleen more effectively than BCG (43–45). CMFO-DMT prevented *Mtb* reactivation by eliminating the bacterial load from the lung and spleen in LTBI mice (43),

suggesting CMFO-DMT is a promising adult TB vaccine candidate for preventive and therapeutic purposes.

5.1.4 H64/H74/H107

H64 (EsxA, EspD, EspC, EspE, EspR, and PE35), H74 (EspB, EsxA, EspD, EspC, EspA, and EspR), and H107 (PPE68, ESAT-6, EspI, EspC, EspA, MPT64, MPT70, and MPT83) are protein subunit vaccines composed of *Mtb*–specific antigens (49, 50). H64, and H74 showed comparable protection to H65 (consisting of antigens also present in BCG) in mice and guinea pigs. However, when used as a BCG booster vaccine, H65-induced highly differentiated $CD4^+$ T cells that did not contribute to the protective effect of BCG, while H64 and H74 induced less differentiated and versatile $CD4^+$ T cells (secreting TNF-α alone or TNF-α and IL-2 in combination) with a protective effect against *Mtb* pulmonary infection (49). H107 vaccination also significantly increased the clonal diversity of the BCG-induced $CD4^+$ T cell repertoire, including Th17-responsive and poorly differentiated memory $CD4^+$ Th1 cells (50). Therefore, protein subunit vaccines containing *Mtb*-specific antigens may have more potential to serve as booster vaccines in BCG-primed populations.

5.2 Phase I clinical trials

5.2.1 AEC/BC02

AEC/BC02 is a vaccine candidate for LTBI consisting of Ag85B and the fusion protein ESAT-6-CFP10 with adjuvant BC02 (53). Preclinical studies have shown that AEC/BC02 can induce long-term antigen-specific cellular immune responses in mice. In addition, AEC/BC02 reduced the risk of the Koch phenomenon in a guinea pig LTBI model (51, 54). In a murine LTBI model, after AEC/BC02 therapy, the bacterial load in the spleen and lung was significantly reduced. Furthermore, AEC/BC02 induced a significant Th1 response with antigen-specific release of IFN-γ, IL-2, and IgG (IgG1, and IgG2) (55). A phase Ib clinical trial evaluating the safety and immunogenicity of AEC/BC02 in healthy adults has been completed (NCT04239313), and volunteers are currently being recruited for phase II trials.

5.3 Phase II clinical trials

5.3.1 ID93+GLA-SE

ID93+GLA-SE comprises four *Mtb* antigens (Rv2608, Rv3619, Rv3620, and Rv1813) with GLA-SE as an adjuvant (59). In mice and guinea pigs, ID93+GLA-SE protected against *Mtb* virulent strain H37Rv and multidrug-resistant strain TN5904 (60). ID93+GLA-SE combined with the first-line anti-TB drugs rifampicin and isoniazid showed therapeutic efficacy in *Mtb*-infected mice and nonhuman primate (NHP) models (61). ID93+GLA-SE was found to provide long-lasting protection by inducing antigen-specific IgG1 and IgG3 and multifunctional $CD4^+$ T cell responses with enhanced IFN-γ, TNF, and IL-2 secretion in a phase I trial (59, 62). A phase IIa trial showed that ID93+GLA-SE enhanced therapeutic efficacy and reduced disease recurrence by inducing robust cellular and humoral immune responses (63). Phase IIb trials that are aimed at preventing TB recurrence are currently in preparation.

5.3.2 H56:IC31

H56:IC31 is formed by Ag85B, ESAT-6, and Rv2660c protein fusion with adjuvant IC31. Due to the presence of the latency-associated protein Rv2660c, a protective effect of H56 in the murine LTBI model was expected and this was observed (68). In NHP aerosol challenge models, H56:1C31 limited the development of advanced infection and LTBI (69). In a phase I trial, the vaccine induced antigen-specific IgG and $CD4^+$ T cell responses (IFN-γ, TNF-α, IL-2) (70). In a phase I/IIa clinical trial, variations in the dose and time of H56:IC31 inoculation were studied. Two to three vaccination doses were optimal with acceptable safety and tolerability (71). Phase IIb trials of H56:IC31 to reduce TB recurrence in HIV-negative patients receiving anti-TB chemotherapy are ongoing (NCT03512249) (72).

5.3.3 M72/AS01$_E$

M72/AS01$_E$ is composed of two immunogenic *Mtb* fusion proteins (Mtb32A and Mtb39A) with AS01$_E$ as an adjuvant. M72/AS01$_E$ protected against *Mtb* invasion after aerosol infection when administered intramuscularly to C57BL/6 mice and guinea pigs (74). When used as a BCG booster vaccine, M72/AS01$_E$ provided long-term protection and improved guinea pig and NHP survival post *Mtb* infection (75, 76). The vaccine was protective against TB in adults in a phase II trial, but the trial was suspended because local reactions were observed in some vaccinated individuals (77). The safety and immunogenicity of M72/AS01$_E$ were evaluated in HIV-negative adolescents in TB-endemic areas. The results showed that M72/AS01$_E$ was safe and could induce M72/AS01$_E$ -specific IgG antibody, $CD4^+$ (IFN-γ, TNF-α, IL-2 and/or IL-17), $CD8^+$ (IFN-γ, TNF-α) T-cells and antigen-dependent NK cell IFN-γ production (78). Another phase II trial, in India, showed elevated cellular and humoral responses by M72/AS01$_E$ in both HIV-negative and HIV-positive individuals that persisted for 3 years with no safety concerns (79). Subsequently, a Phase II clinical trial showed that M72/AS01$_E$ provided 54% protection against progression to active pulmonary TB in LTBI adults, without significant adverse effects (80). In a randomized placebo-controlled phase IIb study, M72/AS01$_E$ protected adults against active TB by 49.7% for at least 3 years without serious safety concerns (81). However, it is doubtful that the excellent protection of M72/AS01$_E$ is mainly based on data from a single population, and large-scale long-term trials in a wider population are needed (82).

5.3.4 GamTBvac

The GamTBvac vaccine combines TB antigens ESAT-6, CFP10, and Ag85A with a novel adjuvant, dextran/CpG. GamTBvac showed significant immunogenicity and protection in *Mtb*-infected mice and guinea pigs when used as a BCG booster vaccine (85). GamTBvac was found to be immunogenic and safe

in a phase I trial in BCG-vaccinated, uninfected healthy people (86). A completed phase IIa trial showed that GamTBvac was safe and had considerable immunogenicity in inducing $CD4^+$ T cells expressing Th1 cytokines (IFN-γ, IL-2, and TNF-α), $CD8^+$ T cells secreting IFN-γ, and IgG responses (87). Phase III trials to evaluate the vaccine's protective efficacy against TB in large populations are currently enrolling volunteers (NCT04975737).

6 Animal models

Evaluating vaccine safety and protection in animal models is obligatory before a vaccine enters clinical trials. The development of animal models of TB has advanced the understanding of host responses to *Mtb* infection and accelerated the development of TB vaccines. Currently, many animal models are used for TB vaccine evaluation (Figure 1).

6.1 Mice

Mice provide the most widely used models due to the advantages of relatively low price, short experiment cycle, mature immunological evaluation indicators, abundant commercial reagents and genetically modified inbred strains (100). The mouse strains most commonly used in evaluating the immune efficacy of TB vaccines are BALB/c and C57BL/6, which are sensitive to TB vaccines immunization routes (101). However, the immune response induced by TB vaccine was different in BALB/c and C57BL/6 mice. M Carmen Garcia-Pelayo et al. found that although BCG present equally protective in BALB/c and C57BL/6 mice, it was display more enhanced Th1 and Th17 response in BALB/c mice than C57BL/6 mice (102). In another study, ChAdOx1.PPE15 as a booster vaccine for BCG improved the efficacy of BCG in C57BL/6 mice, but not in BALB/c mice (103). The susceptibility to TB and the protective responses to the vaccines vary according to the route of infection and immunization. Subcutaneous immunization is the most classic immunization method for TB vaccine, but mucosal immunization has received extensive attention in the pathogenic bacteria infected by mucosal route. A multivalent chimpanzee adenovirus vectored vaccine developed by Sam Afkhami et al. showed strong protection against both replicating and dormant *Mtb* through mucosal immunization (104). Previous research by Claudio Counoupas et al. have shown that intratracheal instillation of CysVac2/Advax protected mice more effectively than the intramuscular vaccine (35).

However, despite a high genetic similarity between mice and humans, significant differences in clinical immune responses between mice and humans have stalled clinical trials of many novel vaccines that had previously shown considerable efficacy in murine models. To overcome this problem, humanized mouse models have been extensively studied in recent years. Humanized mice have a reshaped immune system, making the immune responses more like those of humans. They have been widely used in studies of epitopes and epitope-based TB protein subunit vaccine development (105). Although the use of humanized murine models has enabled many advances in TB vaccine research, deficiencies in the models such as the inability to establish LTBI and granulomas (100), abnormal T-cell responses, and the inability to control bacterial load have limited their use.

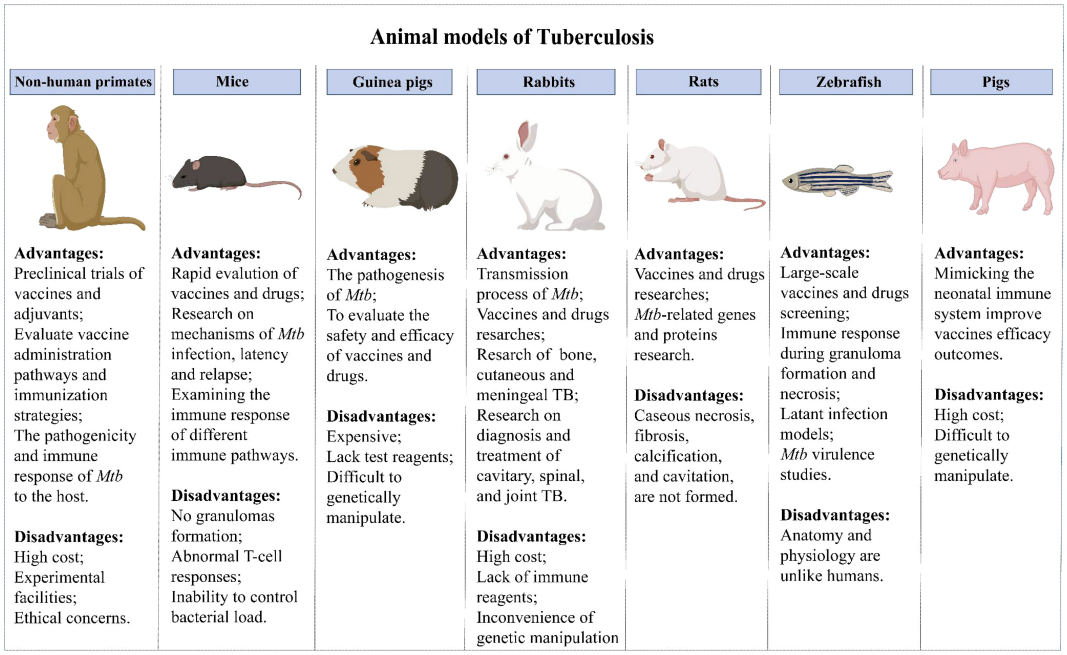

FIGURE 1
Animal models of Tuberculosis.

6.2 NHPs

NHPs can better represent the human immune responses for assessment of the safety and efficacy of TB vaccines and adjuvants due to the close genetic and pathophysiological similarities between NHPs and humans. Rhesus macaques (RM) and cynomolgus macaques (CM) are the most commonly used primate models for TB vaccine research. It is well known that there are differences between macaque species in their ability to control disease progression, with RM showing higher rates of progression and higher levels of bacterial burden compared to CM (106). RM are often used in vaccine evaluation studies because the results of infection are more uniform than CM, while RM are often used in drug evaluation studies because they are better able to control the disease (107). NHPs provide essential insights into host-pathogen interactions during TB infection by simulating the pathogenesis of TB in humans, including the occurrence of LTBI and granuloma formation (108). NHPs can be used to evaluate the immune effect of different vaccine administration pathways and immunization strategies (75, 109).

The use of the NHP models has brought some breakthroughs in TB vaccine development in recent years. First of all, the preclinical evaluation of novel vaccines by the NHP model has facilitated the transformation of vaccines to prevent and therapy *Mtb* infection (110–112). The ultra-low dose aerosol-infected NHP model better simulates the course of human infection with TB and can accurately evaluate the vaccine immune efficacy (113). Moreover, using NHP makes it possible to study the interactions of cells within lung granulomas, which cannot be done in human samples. Laura Hunter et al. used infection in RM and CM models to determine the basic composition of granulomas induced after infection with the *Mtb* Erdman strain, as well as the spatial distribution of immune cells in granulomas in RM and CM and changes over time (114). This informs research into TB vaccines and treatments, and may provide novel immunotherapy strategies against TB. Furthermore, the development of body scanning technology, particularly the combination of PET and CT scans, has made it possible to quantitatively evaluate the protective efficacy of TB vaccines in NHP models (115–117). This strategy allows vaccine evaluation in less time and at a lower cost. However, the high cost of the animals and experimental facilities, as well as the limited quantity available, have hindered their widespread application.

6.3 Guinea pigs

Guinea pigs are also a commonly used animal model in the study of TB. Guinea pigs are more susceptible to *Mtb* than mice and can form classical granulomas similar to humans (118). Therefore, they are suited to studies of the pathogenesis of TB and the assessment of vaccines and drugs (119). Guinea pigs have also been used to study the response of Ag-specific T cells to mycobacterium lipids and lipopeptide-rich Ag preparations (120). Diabetes can fuel TB epidemics, and T2D co-infection with TB has been modeled in guinea pigs in recent years and used to test novel therapy approaches (121–123). However, guinea pigs are more expensive, lack test reagents, and are more difficult to genetically manipulate than mice. Adjuvant subunit vaccines tend to be less protective in guinea pigs than in mice, resulting in few successful trials of adjuvants in guinea pig models (60, 124). The cause of the limited protective immunity provided by adjuvants in guinea pig models awaits clarification, and more tools and reagents are needed for guinea pig models.

6.4 Pigs

The immunity to *Mtb* infection in neonates is markedly distinct from that in adults. Innate and adaptive immune responses in infants cannot be inferred from adult human or animal models (125). Due to their high similarity to humans in terms of anatomy, genetics, and immune response, pigs are widely used in numerous studies (126, 127). The isolated and sterile state of the porcine fetus during pregnancy is conducive to the study of the interaction between the immature immune system and microorganisms and to determine the changes in the immune structure and function during fetus development (128). Surprisingly, pigs can undergo pathological changes to *Mtb* infection including caseous necrosis, liquefaction, and cavitation and mimic the immune response of vaccination BCG in humans (129). Mimicking the human neonatal immune system in pigs could improve our understanding of the infant immune response to TB. More neonatal and early-life animal models are needed to advance the development of anti-TB vaccines and drugs for neonates.

6.5 Other animal models

Other animal models, such as rabbits, rats, and zebrafish, have also been used in *Mtb* vaccine evaluation. Depending on the characteristics of each model, they have been used in different ways. Rabbits are usually infected with *Mtb* by aerosol route (130), and susceptibility to *Mtb* varies among different populations (131). Most rabbits available today are highly resistant to infection with *Mtb* (As Lurie's - susceptible breed have become extinct), but highly susceptible to infection with the closely related *Mycobacterium bovis*. They can form granulomas, liquefaction, and cavities similar to the events found in humans, making them suitable for the study of processes leading to transmission of *Mtb* as well as for vaccine and drug research. In addition, the rabbit model has been used in studies of cavitary, spinal, joint, cutaneous, and meningeal TB (132, 133). However, due to the high cost, lack of immune reagents, and the inconvenience of genetic manipulation, the utility of the rabbit model is limited.

The types of rats commonly used in TB studies are American cotton rats, Wistar rats and diabetic rat strains. Several studies have found that rats exhibit delayed hypersensitivity to *Mtb* infection (134). *Mtb* infected rats can form well-organized granulomas, including epithelioid cells, multinucleated giant cells and foam macrophages, etc., which provide a common research object for the study of host control of *Mtb* and the establishment of latent infection (135). Rats are suitable for TB-related gene and protein

research and have the advantages of low cost and simple blood collection, befitting vaccine and drug research (135). Yet, pathological changes in human lungs, such as caseous necrosis, fibrosis, calcification, and cavitation, are not formed in rats.

Recently, zebrafish have attracted increased attention as an animal model for TB. Zebrafish infected with *M. marinum* can form a typical granulomatous structure, which provides an excellent model for scientists to further study the mechanism of granulomatous formation (136, 137). Moreover, zebrafish have the advantages of visual monitoring, convenient genetic manipulation, fast reproduction, and low cost, they are now widely used for bacterial virulence studies and large-scale vaccine and drug screening. The immune responses during granuloma formation and necrosis can be well monitored, making zebrafish one of the best choices for studying latent TB infection (138, 139). Nevertheless, anatomical and physiological differences between zebrafish and humans impede the application of zebrafish models for vaccine development.

6.6 Ultra-low dose infection models

TB is characteristically caused by respiratory infection when the smallest aerosol droplets containing only 1 or 2 colonies reach the alveolar spaces (1). Hence, the high-dose challenge that has been typically used in animal models might have contributed to discrepant results between pre-clinical and clinical trials. To better simulate the natural human infection process, ultra-low dose infection models have been developed. Infection of conventional mice with 1-3 CFU *Mtb* produced granulomas with well-defined boundaries similar to human granulomas (140). In addition, the ultra-low dose aerosol-infected NHP model more closely mimicked the process of human natural TB infection. It is being used as a precise and sensitive system to assess the effectiveness of TB vaccines (113).

7 Vaccination strategies of protein subunit vaccines

Vaccination strategies are critical to the effectiveness of protein subunit vaccines (Figure 2). *Mtb* metabolism is profoundly influenced by the different pathophysiological states in different stages of infection. Although current TB vaccines mainly consist of early secreted antigens of *Mtb* and are used for prevention of infection, they are less than ideal in controlling LTBI and active TB. Protein subunit vaccines currently in clinical trials have jumped out of this framework, with M72/AS01E prevents latent infected people exposed to *Mtb* from developing active pulmonary TB disease, and ID93 +GLA-SE and H56:IC31 showing promise in the treatment of people with active TB infection. Even more promising is the fact that several multistage protein subunit vaccines comprised of *Mtb* antigens expressed in early growth, dormancy, and resuscitation phases for both prevention and treatment of TB infection have entered pre-clinical (CysVac2, LT70, and CMFO) and clinical trials (H56 and ID93) (35, 39, 43, 63, 71).

Protein subunit vaccines are often used as booster vaccines after BCG priming, and when the antigen in the booster vaccine is shared with BCG, its boosting effect is impaired. BCG vaccination induces highly differentiated $CD4^+$ Th1 cells, and the functional plasticity of these cells is limited. Moreover, BCG-generated immunity impedes the subsequent induction of additional protective T cells with memory and lung homing potential by the booster vaccine (141). Therefore, the development of protein subunit vaccine candidates based on *Mtb*-specific antigens (such as H64, H74, and H107) may circumvent this dilemma (49, 50).

Preclinical and clinical trials have shown that some protein subunit vaccines (H56, LT70, CFMO) can elicit more robust protection than BCG when used alone, suggesting that such a vaccine could use as an alternative to BCG (39, 43, 68). However,

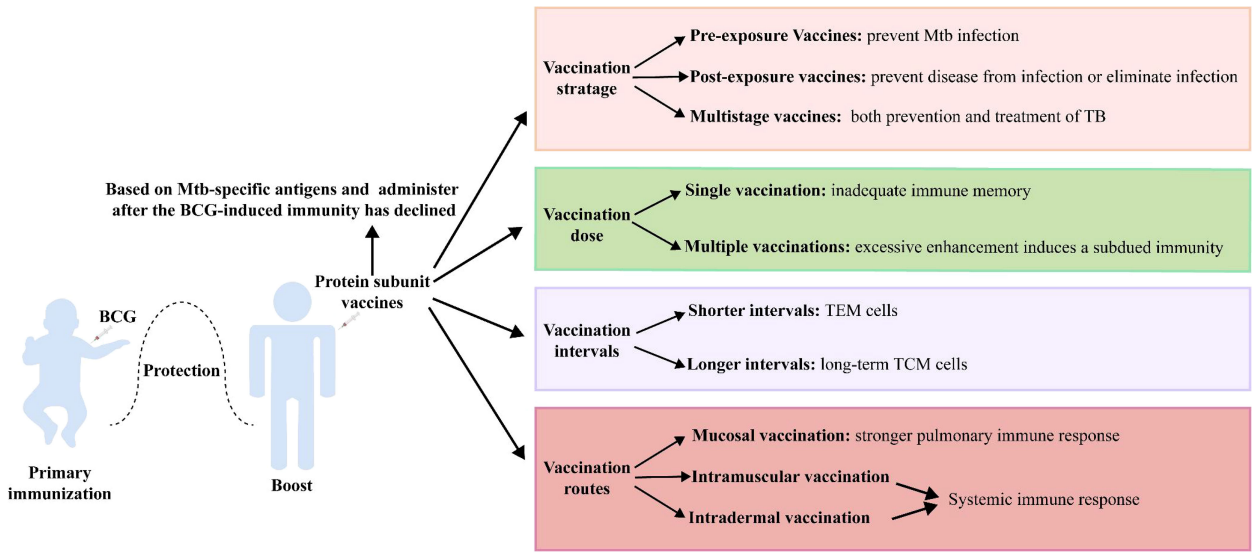

FIGURE 2
Vaccination strategies of protein subunit vaccines.

BCG has definite efficacy against childhood TB and is almost universally given to infants as soon as they are born, so that replacement with an alternative vaccine presents ethical and practical challenges. Consequently, a protein subunit vaccine is more likely to use initially as a booster vaccine. Tests have shown that the protective effect of a BCG-booster vaccine is more pronounced when the immune response to BCG is attenuated (49, 142). One explanation for this could be that reduced levels of BCG-induced immunity open the opportunity for protein subunit vaccines to initiate less differentiated T-cell responses. Therefore, it seems more reasonable to administer the protein subunit vaccine after the BCG-induced immunity has declined (49).

The dose and time of boosting with a protein subunit vaccine are also pivotal factors affecting the effect. Multiple vaccinations are usually required to obtain a substantial immune memory with protein subunit vaccines. However, excessive enhancement induces the production of Tregs, leading to a subdued protective effect of the vaccine (143). Moreover, the interval between vaccinations may impact the type of immunological memory. The strategy with protein subunit vaccines is usually a 2- or 3-week booster regimen, which elicits more T_{EM} cells. A booster regimen with longer intervals of 4 weeks appeared to favor the generation of long-term T_{CM} cells (41).

Finally, different vaccination routes exert a significant influence on efficacy. *Mtb* is transmitted through the respiratory tract, and the protective effect of specific B-cell and strong central memory $CD4^+$ and $CD8^+$ T-cell responses activated by respiratory mucosal vaccination against *Mtb* infection should be an important consideration (144, 145). Zhang Y et al. found that Ag85A-Mtb32 in adenoviral vectored TB vaccine was more likely to induce systemic immune response through subcutaneous and muscular inoculation, while oral and nasal mucosal immune pathways induced stronger pulmonary immune response (105). Moreover, trained immunity was more strongly induced by submucosal BCG or MTBVAC vaccination than by standard intradermal vaccination (146). A variety of immunostimulatory adjuvants (e.g., bacterial toxins, TLR ligands, and cytokines) and nanoparticle adjuvants (e.g., virus-like particles, liposomes, and protoplasts) have been used in mucosal vaccines to enhance the immune responses (147).

8 Conclusion

Vaccines are powerful weapons for people to prevent and treatment many diseases. The sudden outbreak of the COVID-19 has pushed the development of vaccinology to a climax, and also provided valuable guidance for the development of TB vaccines. The BCG vaccine is undoubtedly one of the most potent weapons that humankind has acquired in the struggle against TB, but its limited protective effect is not sufficient to win the war. Based on the existing WHO-recommended immunization strategy for TB vaccines, protein subunit TB vaccines for specific populations (BCG-immunized, LTBI, and HIV-infected, etc.) have great potential for development and utilization. By far, multiple protein subunit TB vaccines have entered clinical or preclinical trials and have broken the barrier that BCG can only be used for pre-infection prevention. And even some vaccines have shown surprising protection in post-exposure prophylaxis in people with LTBI and in the treatment of people with active TB infection. Rapidly evolved bioinformatics and structural informatics technologies represent a large reservoir to filter out plentiful numbers of *Mtb*-protective antigens. Training immunity has been proposed in recent years and has received extensive attention in the field of TB. Trained immune cells are able to produce a rapid and effective protective response against *Mtb* attacks. Therefore, the activation of trained immunity should be considered in the development of vaccines and adjuvants. With the participation of various novel adjuvants, as well as the continuous optimization of animal models and vaccination strategies, effective protein subunit vaccines can be expected in the future to help achieve the grand goal of TB eradication.

Author contributions

XF, and ZH contributed to the conception and revised of this manuscript. ZY and JX drafted and revised the manuscript. All authors contributed to the article and approved the submitted version.

Funding

The work was supported by the grants from National Key Research and Development Program of China (2022YFC2302900, 2021YFC2301503), National Natural and Science Foundation of China (82171815, 82171739), Shanghai Hygiene and Health Outstanding Leader Project (2022XD060), Shanghai Science and Technology Commission (20Y11903400).

Acknowledgments

We thank Dr. Douglas B. Lowrie for his critical comments and suggestions to improve the manuscript.

Conflict of interest

The authors declare that the research was conducted in the absence of any commercial or financial relationships that could be construed as a potential conflict of interest.

Publisher's note

References

1. Donald PR, Diacon AH, Lange C, Demers AM, von Groote-Bidlingmaier F, Nardell E. Droplets, dust and guinea pigs: an historical review of tuberculosis transmission research, 1878-1940. *Int J Tuberc Lung Dis* (2018) 22(9):972–82. doi: 10.5588/ijtld.18.0173

2. WHO. *Global Tuberculosis Report 2022*. Geneva: World Health Organization (2022). Licence: CC BY-NC-SA 3.0 IGO.

3. Allue-Guardia A, Garcia JI, Torrelles JB. Evolution of drug-resistant mycobacterium tuberculosis strains and their adaptation to the human lung environment. *Front Microbiol* (2021) 12:612675. doi: 10.3389/fmicb.2021.612675

4. Gong W, Wu X. Differential diagnosis of latent tuberculosis infection and active tuberculosis: A key to a successful tuberculosis control strategy. *Front Microbiol* (2021) 12:745592. doi: 10.3389/fmicb.2021.745592

5. Bell LCK, Noursadeghi M. Pathogenesis of hiv-1 and mycobacterium tuberculosis co-infection. *Nat Rev Microbiol* (2018) 16(2):80–90. doi: 10.1038/nrmicro.2017.128

6. Lange C, Aaby P, Behr MA, Donald PR, Kaufmann SHE, Netea MG, et al. 100 years of mycobacterium bovis bacille calmette-guerin. *Lancet Infect Dis* (2022) 22(1): e2–e12. doi: 10.1016/S1473-3099(21)00403-5

7. Khademi F, Derakhshan M, Yousefi-Avarvand A, Tafaghodi M, Soleimanpour S. Multi-stage subunit vaccines against mycobacterium tuberculosis: an alternative to the bcg vaccine or a bcg-prime boost? *Expert Rev Vaccines* (2018) 17(1):31–44. doi: 10.1080/14760584.2018.1406309

8. Schrager LK, Vekemens J, Drager N, Lewinsohn DM, Olesen OF. The status of tuberculosis vaccine development. *Lancet Infect Dis* (2020) 20(3):e28–37. doi: 10.1016/s1473-3099(19)30625-5

9. Lewinsohn DA, Swarbrick GM, Park B, Cansler ME, Null MD, Toren KG, et al. Comprehensive definition of human immunodominant cd8 antigens in tuberculosis. *NPJ Vaccines* (2017) 2:8. doi: 10.1038/s41541-017-0008-6

10. Irvine EB, O'Neil A, Darrah PA, Shin S, Choudhary A, Li W, et al. Robust igm responses following intravenous vaccination with bacille calmette-guerin associate with prevention of mycobacterium tuberculosis infection in macaques. *Nat Immunol* (2021) 22(12):1515–23. doi: 10.1038/s41590-021-01066-1

11. Gong W, Pan C, Cheng P, Wang J, Zhao G, Wu X. Peptide-based vaccines for tuberculosis. *Front Immunol* (2022) 13:830497. doi: 10.3389/fimmu.2022.830497

12. Williams WV, Weiner DB, Kieber-Emmons T, Greene MI. Antibody geometry and form: three-dimensional relationships between anti-idiotypic antibodies and external antigens. *Trends Biotechnol* (1990) 8(9):256–63. doi: 10.1016/0167-7799(90)90188-4

13. Hoyos D, Greenbaum BD. Perfecting antigen prediction. *J Exp Med* (2022) 219 (9):e20220846. doi: 10.1084/jem.20220846

14. Rappuoli R, Bottomley MJ, D'Oro U, Finco O, De Gregorio E. Reverse vaccinology 2.0: human immunology instructs vaccine antigen design. *J Exp Med* (2016) 213(4):469–81. doi: 10.1084/jem.20151960

15. Jumper J, Evans R, Pritzel A, Green T, Figurnov M, Ronneberger O, et al. Highly accurate protein structure prediction with alphafold. *Nature* (2021) 596(7873):583–9. doi: 10.1038/s41586-021-03819-2

16. Zeng D, Xin J, Yang K, Guo S, Wang Q, Gao Y, et al. A hemagglutinin stem vaccine designed rationally by alphafold2 confers broad protection against influenza B infection. *Viruses* (2022) 14(6):1305. doi: 10.3390/v14061305

17. Monterrubio-Lopez GP, Gonzalez YMJA, Ribas-Aparicio RM. Identification of novel potential vaccine candidates against tuberculosis based on reverse vaccinology. *BioMed Res Int* (2015) 2015:483150. doi: 10.1155/2015/483150

18. Correia-Neves M, Sundling C, Cooper A, Kallenius G. LipoarabinOmannan in active and passive protection against tuberculosis. *Front Immunol* (2019) 10:1968. doi: 10.3389/fimmu.2019.01968

19. Wolfe LM, Mahaffey SB, Kruh NA, Dobos KM. Proteomic definition of the cell wall of mycobacterium tuberculosis. *J Proteome Res* (2010) 9(11):5816–26. doi: 10.1021/pr1005873

20. Pal R, Bisht MK, Mukhopadhyay S. Secretory proteins of mycobacterium tuberculosis and their roles in modulation of host immune responses: focus on therapeutic targets. *FEBS J* (2022) 289(14):4146–71. doi: 10.1111/febs.16369

21. Boon C, Dick T. How mycobacterium tuberculosis goes to sleep: the dormancy survival regulator dosr a decade later. *Future Microbiol* (2012) 7(4):513–8. doi: 10.2217/fmb.12.14

22. Rustad TR, Harrell MI, Liao R, Sherman DR. The enduring hypoxic response of mycobacterium tuberculosis. *PloS One* (2008) 3(1):e1502. doi: 10.1371/journal.pone.0001502

23. Murphy DJ, Brown JR. Novel drug target strategies against mycobacterium tuberculosis. *Curr Opin Microbiol* (2008) 11(5):422–7. doi: 10.1016/j.mib.2008.08.001

24. Serra-Vidal MM, Latorre I, Franken KL, Diaz J, de Souza-Galvao ML, Casas I, et al. Immunogenicity of 60 novel latency-related antigens of mycobacterium tuberculosis. *Front Microbiol* (2014) 5:517. doi: 10.3389/fmicb.2014.00517

25. ROmano M, Aryan E, Korf H, Bruffaerts N, Franken CL, Ottenhoff TH, et al. Potential of mycobacterium tuberculosis resuscitation-promoting factors as antigens in novel tuberculosis sub-unit vaccines. *Microbes Infect* (2012) 14(1):86–95. doi: 10.1016/j.micinf.2011.08.011

26. Lewis KN, Liao R, Guinn KM, Hickey MJ, Smith S, Behr MA, et al. Deletion of rd1 from mycobacterium tuberculosis mimics bacille calmette-guerin attenuation. *J Infect Dis* (2003) 187(1):117–23. doi: 10.1086/345862

27. Daugelat S, Kowall J, Mattow J, Bumann D, Winter R, Hurwitz R, et al. The rd1 proteins of mycobacterium tuberculosis: expression in mycobacterium smegmatis and biochemical characterization. *Microbes Infect* (2003) 5(12):1082–95. doi: 10.1016/s1286-4579(03)00205-3

28. Enriquez AB, Izzo A, Miller SM, Stewart EL, Mahon RN, Frank DJ, et al. Advancing adjuvants for mycobacterium tuberculosis therapeutics. *Front Immunol* (2021) 12:740117. doi: 10.3389/fimmu.2021.740117

29. Xu X, Jin Z, Liu Y, Gong H, Sun Q, Zhang W, et al. Carbohydrate-based adjuvants activate tumor-specific th1 and cd8(+) T-cell responses and reduce the immunosuppressive activity of mdscs. *Cancer Lett* (2019) 440-441:94–105. doi: 10.1016/j.canlet.2018.10.013

30. Quan DH, Counoupas C, Nagalingam G, Pinto R, Petrovsky N, Britton WJ, et al. Advax adjuvant formulations promote protective immunity against aerosol mycobacterium tuberculosis in the absence of deleterious inflammation and reactogenicity. *Vaccine* (2021) 39(14):1990–6. doi: 10.1016/j.vaccine.2021.02.041

31. Hayashi M, Aoshi T, Haseda Y, Kobiyama K, Wijaya E, Nakatsu N, et al. Advax, a delta inulin microparticle, potentiates in-built adjuvant property of co-administered vaccines. *EBioMedicine* (2017) 15:127–36. doi: 10.1016/j.ebiom.2016.11.015

32. Tomar J, Patil HP, Bracho G, Tonnis WF, Frijlink HW, Petrovsky N, et al. Advax augments B and T cell responses upon influenza vaccination via the respiratory tract and enables complete protection of mice against lethal influenza virus challenge. *J Control Release* (2018) 288:199–211. doi: 10.1016/j.jconrel.2018.09.006

33. Counoupas C, Pinto R, Nagalingam G, Hill-Cawthorne GA, Feng CG, Britton WJ, et al. Mycobacterium tuberculosis components expressed during chronic infection of the lung contribute to long-term control of pulmonary tuberculosis in mice. *NPJ Vaccines* (2016) 1:16012. doi: 10.1038/npjvaccines.2016.12

34. Counoupas C, Pinto R, Nagalingam G, Britton WJ, Petrovsky N, Triccas JA. Delta inulin-based adjuvants promote the generation of polyfunctional cd4(+) T cell responses and protection against mycobacterium tuberculosis infection. *Sci Rep* (2017) 7(1):8582. doi: 10.1038/s41598-017-09119-y

35. Counoupas C, Ferrell KC, Ashhurst A, Bhattacharyya ND, Nagalingam G, Stewart EL, et al. Mucosal delivery of a multistage subunit vaccine promotes development of lung-resident memory T cells and affords interleukin-17-dependent protection against pulmonary tuberculosis. *NPJ Vaccines* (2020) 5(1):105. doi: 10.1038/s41541-020-00255-7

36. Hafner AM, Corthésy B. Merkle HP. Particulate formulations for the delivery of poly(I:C) as vaccine adjuvant. *Adv Drug Delivery Rev* (2013) 65(10):1386–99. doi: 10.1016/j.addr.2013.05.013

37. Tewari K, Flynn BJ, Boscardin SB, Kastenmueller K, Salazar AM, Anderson CA, et al. Poly(I:C) is an effective adjuvant for antibody and multi-functional cd4+ T cell responses to plasmodium falciparum circumsporozoite protein (Csp) and Adec-csp in non human primates. *Vaccine* (2010) 28(45):7256–66. doi: 10.1016/j.vaccine.2010.08.098

38. Stahl-Hennig C, Eisenblätter M, Jasny E, Rzehak T, Tenner-Racz K, Trumpfheller C, et al. Synthetic double-stranded rnas are adjuvants for the induction of T helper 1 and humoral immune responses to human papillomavirus in rhesus macaques. *PloS Pathog* (2009) 5(4):e1000373. doi: 10.1371/journal.ppat.1000373

39. Liu X, Peng J, Hu L, Luo Y, Niu H, Bai C, et al. A multistage mycobacterium tuberculosis subunit vaccine lt70 including latency antigen rv2626c induces long-term protection against tuberculosis. *Hum Vaccin Immunother* (2016) 12(7):1670–7. doi: 10.1080/21645515.2016.1141159

40. Li F, Kang H, Li J, Zhang D, Zhang Y, Dannenberg AMJr., et al. Subunit vaccines consisting of antigens from dormant and replicating bacteria show promising therapeutic effect against mycobacterium bovis bcg latent infection. *Scand J Immunol* (2017) 85(6):425–32. doi: 10.1111/sji.12556

41. Bai C, He J, Niu H, Hu L, Luo Y, Liu X, et al. Prolonged intervals during mycobacterium tuberculosis subunit vaccine boosting contributes to eliciting immunity mediated by central memory-like T cells. *Tuberculosis (Edinb)* (2018) 110:104–11. doi: 10.1016/j.tube.2018.04.006

42. Tian M, Zhou Z, Tan S, Fan X, Li L, Ullah N. Formulation in dda-mpla-tdb liposome enhances the immunogenicity and protective efficacy of a DNA vaccine against mycobacterium tuberculosis infection. *Front Immunol* (2018) 9:310. doi: 10.3389/fimmu.2018.00310

43. Ma J, Teng X, Wang X, Fan X, Wu Y, Tian M, et al. A multistage subunit vaccine effectively protects mice against primary progressive tuberculosis, latency and reactivation. *EBioMedicine* (2017) 22:143–54. doi: 10.1016/j.ebiom.2017.07.005

44. Ullah N, Hao L, Wu Y, Zhang Y, Lei Q, Banga Ndzouboukou JL, et al. Differential immunogenicity and protective efficacy elicited by mto- and dmt-adjuvanted cmfo subunit vaccines against mycobacterium tuberculosis infection. *J Immunol Res* (2020) 2020:2083793. doi: 10.1155/2020/2083793

45. Hao L, Wu Y, Zhang Y, Zhou Z, Lei Q, Ullah N, et al. Combinational prr agonists in liposomal adjuvant enhances immunogenicity and protective efficacy in a tuberculosis subunit vaccine. *Front Immunol* (2020) 11:575504. doi: 10.3389/fimmu.2020.575504

46. Hilgers LA, Snippe H. Dda as an immunological adjuvant. *Res Immunol* (1992) 143(5):494–503. doi: 10.1016/0923-2494(92)80060-x. discussion 74-6.

47. Ishikawa E, Ishikawa T, Morita YS, Toyonaga K, Yamada H, Takeuchi O, et al. Direct recognition of the mycobacterial glycolipid, trehalose dimycolate, by C-type lectin mincle. *J Exp Med* (2009) 206(13):2879–88. doi: 10.1084/jem.20091750

48. van Dissel JT, Joosten SA, Hoff ST, Soonawala D, Prins C, Hokey DA, et al. A novel liposomal adjuvant system, caf01, promotes long-lived mycobacterium tuberculosis-specific T-cell responses in human. *Vaccine* (2014) 32(52):7098–107. doi: 10.1016/j.vaccine.2014.10.036

49. Aagaard C, Knudsen NPH, Sohn I, Izzo AA, Kim H, Kristiansen EH, et al. Immunization with mycobacterium tuberculosis-specific antigens bypasses T cell differentiation from prior bacillus calmette-guérin vaccination and improves protection in mice. *J Immunol* (2020) 205(8):2146–55. doi: 10.4049/jimmunol.2000563

50. Woodworth JS, Clemmensen HS, Battey H, Dijkman K, Lindenstrøm T, Laureano RS, et al. A mycobacterium tuberculosis-specific subunit vaccine that provides synergistic immunity upon co-administration with bacillus calmette-guérin. *Nat Commun* (2021) 12(1):6658. doi: 10.1038/s41467-021-26934-0

51. Lu JB, Chen BW, Wang GZ, Fu LL, Shen XB, Su C, et al. Recombinant tuberculosis vaccine aec/bc02 induces antigen-specific cellular responses in mice and protects Guinea pigs in a model of latent infection. *J Microbiol Immunol Infect* (2015) 48(6):597–603. doi: 10.1016/j.jmii.2014.03.005

52. Bomford R. Will adjuvants be needed for vaccines of the future? *Dev Biol Stand* (1998) 92:13–7. doi: 10.1038/s41423-021-00669-w

53. Chen L, Xu M, Wang ZY, Chen BW, Du WX, Su C, et al. The development and preliminary evaluation of a new mycobacterium tuberculosis vaccine comprising ag85b, hspx and cfp-10:Esat-6 fusion protein with cpg DNA and aluminum hydroxide adjuvants. *FEMS Immunol Med Microbiol* (2010) 59(1):42–52. doi: 10.1111/j.1574-695X.2010.00660.x

54. Lu JB, Cheng BW, Deng HQ, Su C, Shen XB, Du WX, et al. Analysis of koch phenomenon of mycobacterium tuberculosis-infected Guinea pigs vaccinated with recombinant tuberculosis vaccine aec/bc02. *Zhonghua Jie He He Hu Xi Za Zhi* (2016) 39(7):524–8. doi: 10.3760/cma.j.issn.1001-0939.2016.07.007

55. Lu J, Guo X, Wang C, Du W, Shen X, Su C, et al. Therapeutic effect of subunit vaccine aec/bc02 on mycobacterium tuberculosis post-chemotherapy relapse using a latent infection murine model. *Vaccines (Basel)* (2022) 10(5):825. doi: 10.3390/vaccines10050825

56. Dubois Cauwelaert N, Desbien AL, Hudson TE, Pine SO, Reed SG, Coler RN, et al. The tlr4 agonist vaccine adjuvant, gla-se, requires canonical and atypical mechanisms of action for th1 induction. *PloS One* (2016) 11(1):e0146372. doi: 10.1371/journal.pone.0146372

57. Coler RN, Bertholet S, Moutaftsi M, Guderian JA, Windish HP, Baldwin SL, et al. Development and characterization of synthetic glucopyranosyl lipid adjuvant system as a vaccine adjuvant. *PloS One* (2011) 6(1):e16333. doi: 10.1371/journal.pone.0016333

58. Kim EH, Woodruff MC, Grigoryan L, Maier B, Lee SH, Mandal P, et al. Squalene Emulsion-Based Vaccine Adjuvants Stimulate Cd8 T Cell, but Not Antibody Responses, through a Ripk3-Dependent Pathway. *Elife* (2020) 9:e52687. doi: 10.7554/eLife.52687

59. Penn-Nicholson A, Tameris M, Smit E, Day TA, Musvosvi M, Jayashankar L, et al. Safety and immunogenicity of the novel tuberculosis vaccine id93 + Gla-se in bcg-vaccinated healthy adults in South Africa: A randomised, double-blind, placebo-controlled phase 1 trial. *Lancet Respir Med* (2018) 6(4):287–98. doi: 10.1016/s2213-2600(18)30077-8

60. Baldwin SL, Bertholet S, Reese VA, Ching LK, Reed SG, Coler RN. The importance of adjuvant formulation in the development of a tuberculosis vaccine. *J Immunol* (2012) 188(5):2189–97. doi: 10.4049/jimmunol.1102696

61. Coler RN, Bertholet S, Pine SO, Orr MT, Reese V, Windish HP, et al. Therapeutic immunization against mycobacterium tuberculosis is an effective adjunct to antibiotic treatment. *J Infect Dis* (2013) 207(8):1242–52. doi: 10.1093/infdis/jis425

62. Coler RN, Day TA, Ellis R, Piazza FM, Beckmann AM, Vergara J, et al. The tlr-4 agonist adjuvant, gla-se, improves magnitude and quality of immune responses elicited by the id93 tuberculosis vaccine: first-in-human trial. *NPJ Vaccines* (2018) 3:34. doi: 10.1038/s41541-018-0057-5

63. Day TA, Penn-Nicholson A, Luabeya AKK, Fiore-Gartland A, Du Plessis N, Loxton AG, et al. Safety and immunogenicity of the adjunct therapeutic vaccine id93 + Gla-se in adults who have completed treatment for tuberculosis: A randomised, double-blind, placebo-controlled, phase 2a trial. *Lancet Respir Med* (2021) 9(4):373–86. doi: 10.1016/s2213-2600(20)30319-2

64. Khademi F, Taheri RA, Momtazi-Borojeni AA, Farnoosh G, Johnston TP, Sahebkar A. Potential of cationic liposomes as adjuvants/delivery systems for tuberculosis subunit vaccines. *Rev Physiol Biochem Pharmacol* (2018) 175:47–69. doi: 10.1007/112_2018_9

65. Fritz JH, Brunner S, Birnstiel ML, Buschle M, Gabain A, Mattner F, et al. The artificial antimicrobial peptide klkllllllklk induces predominantly a th2-type immune response to co-injected antigens. *Vaccine* (2004) 22(25-26):3274–84. doi: 10.1016/j.vaccine.2004.03.007

66. Aichinger MC, Ginzler M, Weghuber J, Zimmermann L, Riedl K, Schütz G, et al. Adjuvating the adjuvant: facilitated delivery of an immunomodulatory oligonucleotide to tlr9 by a cationic antimicrobial peptide in dendritic cells. *Vaccine* (2011) 29(3):426–36. doi: 10.1016/j.vaccine.2010.11.003

67. Schellack C, Prinz K, Egyed A, Fritz JH, Wittmann B, Ginzler M, et al. Ic31, a novel adjuvant signaling via tlr9, induces potent cellular and humoral immune responses. *Vaccine* (2006) 24(26):5461–72. doi: 10.1016/j.vaccine.2006.03.071

68. Aagaard C, Hoang T, Dietrich J, Cardona PJ, Izzo A, Dolganov G, et al. A Multistage Tuberculosis Vaccine That Confers Efficient Protection before and after Exposure. *Nat Med* (2011) 17(2):189–94. doi: 10.1038/nm.2285

69. Lin PL, Dietrich J, Tan E, Abalos RM, Burgos J, Bigbee C, et al. The multistage vaccine H56 boosts the effects of bcg to protect cynomolgus macaques against active tuberculosis and reactivation of latent mycobacterium tuberculosis infection. *J Clin Invest* (2012) 122(1):303–14. doi: 10.1172/jci46252

70. Luabeya AK, Kagina BM, Tameris MD, Geldenhuys H, Hoff ST, Shi Z, et al. First-in-human trial of the post-exposure tuberculosis vaccine H56:Ic31 in mycobacterium tuberculosis infected and non-infected healthy adults. *Vaccine* (2015) 33(33):4130–40. doi: 10.1016/j.vaccine.2015.06.051

71. Suliman S, Luabeya AKK, Geldenhuys H, Tameris M, Hoff ST, Shi Z, et al. Dose optimization of H56:Ic31 vaccine for tuberculosis-endemic populations. A double-blind, placebo-controlled, dose-selection trial. *Am J Respir Crit Care Med* (2019) 199 (2):220–31. doi: 10.1164/rccm.201802-0366OC

72. Li J, Zhao A, Tang J, Wang G, Shi Y, Zhan L, et al. Tuberculosis vaccine development: from classic to clinical candidates. *Eur J Clin Microbiol Infect Dis* (2020) 39(8):1405–25. doi: 10.1007/s10096-020-03843-6

73. Didierlaurent AM, Laupèze B, Di Pasquale A, Hergli N, Collignon C, Garçon N. Adjuvant system as01: helping to overcome the challenges of modern vaccines. *Expert Rev Vaccines* (2017) 16(1):55–63. doi: 10.1080/14760584.2016.1213632

74. Skeiky YA, Alderson MR, Ovendale PJ, Guderian JA, Brandt L, Dillon DC, et al. Differential immune responses and protective efficacy induced by components of a tuberculosis polyprotein vaccine, mtb72f, delivered as naked DNA or recombinant protein. *J Immunol* (2004) 172(12):7618–28. doi: 10.4049/jimmunol.172.12.7618

75. Reed SG, Coler RN, Dalemans W, Tan EV, DeLa Cruz EC, Basaraba RJ, et al. Defined tuberculosis vaccine, mtb72f/as02a, evidence of protection in cynomolgus monkeys. *Proc Natl Acad Sci U.S.A.* (2009) 106(7):2301–6. doi: 10.1073/pnas.0712077106

76. Brandt L, Skeiky YA, Alderson MR, Lobet Y, Dalemans W, Turner OC, et al. The protective effect of the mycobacterium bovis bcg vaccine is increased by coadministration with the mycobacterium tuberculosis 72-kilodalton fusion polyprotein mtb72f in M. Tuberculosis-infected Guinea pigs. *Infect Immun* (2004) 72(11):6622–32. doi: 10.1128/iai.72.11.6622-6632.2004

77. Gillard P, Yang PC, Danilovits M, Su WJ, Cheng SL, Pehme L, et al. Safety and immunogenicity of the M72/as01e candidate tuberculosis vaccine in adults with tuberculosis: A phase ii randomised study. *Tuberculosis (Edinb)* (2016) 100:118–27. doi: 10.1016/j.tube.2016.07.005

78. Penn-Nicholson A, Geldenhuys H, Burny W, van der Most R, Day CL, Jongert E, et al. Safety and immunogenicity of candidate vaccine M72/as01e in adolescents in a tb endemic setting. *Vaccine* (2015) 33(32):4025–34. doi: 10.1016/j.vaccine.2015.05.088

79. Kumarasamy N, Poongulali S, Beulah FE, Akite EJ, Ayuk LN, Bollaerts A, et al. Long-term safety and immunogenicity of the M72/as01e candidate tuberculosis vaccine in hiv-positive and -negative Indian adults: results from a phase ii randomized controlled trial. *Med (Baltimore)* (2018) 97(45):e13120. doi: 10.1097/md.0000000000013120

80. Van Der Meeren O, Hatherill M, Nduba V, Wilkinson RJ, Muyoyeta M, Van Brakel E, et al. Phase 2b controlled trial of M72/as01(E) vaccine to prevent tuberculosis. *N Engl J Med* (2018) 379(17):1621–34. doi: 10.1056/NEJMoa1803484

81. Tait DR, Hatherill M, van der Meeren O, Ginsberg AM, Van Brakel E, Salaun B, et al. Final analysis of a trial of M72/as01(E) vaccine to prevent tuberculosis. *N Engl J Med* (2019) 381(25):2429–39. doi: 10.1056/NEJMoa1909953

82. Ottenhoff THM. A trial of M72/as01e vaccine to prevent tuberculosis. *N Engl J Med* (2020) 382(16):1576–7. doi: 10.1056/NEJMc2001364

83. Zhang W, An M, Xi J, Liu H. Targeting cpg adjuvant to lymph node via dextran conjugate enhances antitumor immunotherapy. *Bioconjug Chem* (2017) 28(7):1993–2000. doi: 10.1021/acs.bioconjchem.7b00313

84. Brazolot Millan CL, Weeratna R, Krieg AM, Siegrist CA, Davis HL. Cpg DNA can induce strong th1 humoral and cell-mediated immune responses against hepatitis B surface antigen in young mice. *Proc Natl Acad Sci U.S.A.* (1998) 95(26):15553–8. doi: 10.1073/pnas.95.26.15553

85. Tkachuk AP, Gushchin VA, Potapov VD, Demidenko AV, Lunin VG, Gintsburg AL. Multi-subunit bcg booster vaccine gamtbvac: assessment of immunogenicity and protective efficacy in murine and Guinea pig tb models. *PloS One* (2017) 12(4):e0176784. doi: 10.1371/journal.pone.0176784

86. Vasina DV, Kleymenov DA, Manuylov VA, Mazunina EP, Koptev EY, Tukhovskaya EA, et al. First-in-human trials of gamtbvac, a recombinant subunit tuberculosis vaccine candidate: safety and immunogenicity assessment. *Vaccines (Basel)* (2019) 7(4):166. doi: 10.3390/vaccines7040166

87. Tkachuk AP, Bykonia EN, Popova LI, Kleymenov DA, Semashko MA, Chulanov VP, et al. Safety and immunogenicity of the gamtbvac, the recombinant subunit tuberculosis vaccine candidate: A phase ii, multi-center, double-blind, randomized, placebo-controlled study. *Vaccines* (2020) 8(4):652. doi: 10.3390/vaccines8040652

88. Zhang R, Wang C, Guan Y, Wei X, Sha M, Yi M, et al. Manganese salts function as potent adjuvants. *Cell Mol Immunol* (2021) 18(5):1222–34. doi: 10.1038/s41423-021-00669-w

89. Zhao Y, Zhao X, Cheng Y, Guo X, Yuan W. Iron oxide nanoparticles-based vaccine delivery for cancer treatment. *Mol Pharm* (2018) 15(5):1791–9. doi: 10.1021/acs.molpharmaceut.7b01103

90. Kim J, Li WA, Choi Y, Lewin SA, Verbeke CS, Dranoff G, et al. Injectable, spontaneously assembling, inorganic scaffolds modulate immune cells *in vivo* and increase vaccine efficacy. *Nat Biotechnol* (2015) 33(1):64–72. doi: 10.1038/nbt.3071

91. Dai H, Huang Y, Guo J, Li L, Ke Y, Cen L, et al. Engineering a hemomap nanovaccine for inducing immune responses against melanoma. *ACS Appl Mater Interfaces* (2022) 14(47):52634–42. doi: 10.1021/acsami.2c14379

92. Zhou Q, Zhang Y, Du J, Li Y, Zhou Y, Fu Q, et al. Different-sized gold nanoparticle activator/antigen increases dendritic cells accumulation in liver-draining lymph nodes and cd8+ T cell responses. *ACS Nano* (2016) 10(2):2678–92. doi: 10.1021/acsnano.5b07716

93. Danhier F, Ansorena E, Silva JM, Coco R, Le Breton A, Préat V. Plga-based nanoparticles: an overview of biomedical applications. *J Control Release* (2012) 161 (2):505–22. doi: 10.1016/j.jconrel.2012.01.043

94. Li X, Wang X, Ito A. Tailoring inorganic nanoadjuvants towards next-generation vaccines. *Chem Soc Rev* (2018) 47(13):4954–80. doi: 10.1039/c8cs00028j

95. Rodrigues KA, Rodriguez-Aponte SA, Dalvie NC, Lee JH, Abraham W, Carnathan DG, et al. Phosphate-mediated coanchoring of rbd immunogens and molecular adjuvants to alum potentiates humoral immunity against Sars-Cov-2. *Sci Adv* (2021) 7(50):eabj6538. doi: 10.1126/sciadv.abj6538

96. Chen A, Wu L, Luo Y, Lu S, Wang Y, Zhou Z, et al. Deep tumor penetrating gold nano-adjuvant for nir-ii-triggered in situ tumor vaccination. *Small* (2022) 18(20): e2200993. doi: 10.1002/smll.202200993

97. Li D, Xu M, Li G, Zheng Y, Zhang Y, Xia D, et al. Mg/al-ldh as a nano-adjuvant for pertussis vaccine: A evaluation compared with aluminum hydroxide adjuvant. *Nanotechnology* (2022) 33(23):10. doi: 10.1088/1361-6528/ac56f3

98. Yousefi Avarvand A, Meshkat Z, Khademi F, Tafaghodi M. Immunogenicity of hspx/esxs fusion protein of mycobacterium tuberculosis along with iscomatrix and pluscom nano-adjuvants after subcutaneous administration in animal model. *Microb Pathog* (2021) 154:104842. doi: 10.1016/j.micpath.2021.104842

99. Qian K, Shan L, Shang S, Li T, Wang S, Wei M, et al. Manganese enhances macrophage defense against mycobacterium tuberculosis via the sting-tnf signaling pathway. *Int Immunopharmacol* (2022) 113(Pt B):109471. doi: 10.1016/j.intimp.2022.109471

100. Gong W, Liang Y, Wu X. Animal models of tuberculosis vaccine research: an important component in the fight against tuberculosis. *BioMed Res Int* (2020) 2020:4263079. doi: 10.1155/2020/4263079

101. Mata E, Tarancon R, Guerrero C, Moreo E, Moreau F, Uranga S, et al. Pulmonary bcg induces lung-resident macrophage activation and confers long-term protection against tuberculosis. *Sci Immunol* (2021) 6(63):eabc2934. doi: 10.1126/sciimmunol.abc2934

102. Garcia-Pelayo MC, Bachy VS, Kaveh DA, Hogarth PJ. Balb/C mice display more enhanced bcg vaccine induced th1 and th17 response than C57bl/6 mice but have equivalent protection. *Tuberculosis (Edinb)* (2015) 95(1):48–53. doi: 10.1016/j.tube.2014.10.012

103. Stylianou E, Harrington-Kandt R, Beglov J, Bull N, Pinpathomrat N, Swarbrick GM, et al. Identification and evaluation of novel protective antigens for the development of a candidate tuberculosis subunit vaccine. *Infect Immun* (2018) 86(7): e00014–18. doi: 10.1128/iai.00014-18

104. Afkhami S, D'Agostino MR, Vaseghi-Shanjani M, Lepard M, Yang JX, Lai R, et al. Intranasal multivalent adenoviral-vectored vaccine protects against replicating and dormant M.Tb in conventional and humanized mice. *NPJ Vaccines* (2023) 8(1):25. doi: 10.1038/s41541-023-00623-z

105. Gong W, Liang Y, Mi J, Jia Z, Xue Y, Wang J, et al. Peptides-based vaccine mp3rt induced protective immunity against mycobacterium tuberculosis infection in a humanized mouse model. *Front Immunol* (2021) 12:666290. doi: 10.3389/fimmu.2021.666290

106. Maiello P, DiFazio RM, Cadena AM, Rodgers MA, Lin PL, Scanga CA, et al. Rhesus macaques are more susceptible to progressive tuberculosis than cynomolgus macaques: A quantitative comparison. *Infect Immun* (2018) 86(2):e00505–17. doi: 10.1128/iai.00505-17

107. Peña JC, Ho WZ. Non-human primate models of tuberculosis. *Microbiol Spectr* (2016) 4(4):10. doi: 10.1128/microbiolspec.TBTB2-0007-2016

108. Luciw PA, Oslund KL, Yang XW, Adamson L, Ravindran R, Canfield DR, et al. Stereological analysis of bacterial load and lung lesions in nonhuman primates (Rhesus macaques) experimentally infected with mycobacterium tuberculosis. *Am J Physiol Lung Cell Mol Physiol* (2011) 301(5):L731–8. doi: 10.1152/ajplung.00120.2011

109. Darrah PA, Zeppa JJ, Maiello P, Hackney JA, Wadsworth MH2nd, Hughes TK, et al. Prevention of tuberculosis in macaques after intravenous bcg immunization. *Nature* (2020) 577(7788):95–102. doi: 10.1038/s41586-019-1817-8

110. Rivera-Hernandez T, Carnathan DG, Moyle PM, Toth I, West NP, Young PR, et al. The contribution of non-human primate models to the development of human vaccines. *Discovery Med* (2014) 18(101):313–22.

111. Verreck FA, Vervenne RA, Kondova I, van Kralingen KW, Remarque EJ, Braskamp G, et al. Mva.85a boosting of bcg and an attenuated, phop deficient M. Tuberculosis vaccine both show protective efficacy against tuberculosis in rhesus macaques. *PloS One* (2009) 4(4):e5264. doi: 10.1371/journal.pone.0005264

112. Rahman S, Magalhaes I, Rahman J, Ahmed RK, Sizemore DR, Scanga CA, et al. Prime-boost vaccination with rbcg/rad35 enhances cd8$^+$ Cytolytic T-cell responses in lesions from mycobacterium tuberculosis-infected primates. *Mol Med* (2012) 18 (1):647–58. doi: 10.2119/molmed.2011.00222

113. White AD, Sarfas C, Sibley LS, Gullick J, Clark S, Rayner E, et al. Protective efficacy of inhaled bcg vaccination against ultra-low dose aerosol M. Tuberculosis challenge in rhesus macaques. *Pharmaceutics* (2020) 12(5):394. doi: 10.3390/pharmaceutics12050394

114. Hunter L, Hingley-Wilson S, Stewart GR, Sharpe SA, Salguero FJ. Dynamics of macrophage, T and B cell infiltration within pulmonary granulomas induced by mycobacterium tuberculosis in two non-human primate models of aerosol infection. *Front Immunol* (2021) 12:776913. doi: 10.3389/fimmu.2021.776913

115. Coleman MT, Maiello P, Tomko J, Frye LJ, Fillmore D, Janssen C, et al. Early changes by (18)Fluorodeoxyglucose positron emission tomography coregistered with computed tomography predict outcome after mycobacterium tuberculosis infection in cynomolgus macaques. *Infect Immun* (2014) 82(6):2400–4. doi: 10.1128/iai.01599-13

116. Laddy DJ, Bonavia A, Hanekom WA, Kaushal D, Williams A, Roederer M, et al. Toward tuberculosis vaccine development: recommendations for nonhuman primate study design. *Infect Immun* (2018) 86(2):e00776–17. doi: 10.1128/iai.00776-17

117. White AG, Maiello P, Coleman MT, Tomko JA, Frye LJ, Scanga CA, et al. Analysis of 18fdg pet/ct imaging as a tool for studying mycobacterium tuberculosis infection and treatment in non-human primates. *J Vis Exp* (2017) (127):56375. doi: 10.3791/56375

118. Dubos RJ. The tubercle bacillus and tuberculosis. *Am Sci* (1949) 37(3):353–70.

119. Clark S, Hall Y, Williams A. Animal models of tuberculosis: Guinea pigs. *Cold Spring Harb Perspect Med* (2014) 5(5):a018572. doi: 10.1101/cshperspect.a018572

120. Kaufmann E, Spohr C, Battenfeld S, De Paepe D, Holzhauser T, Balks E, et al. Bcg vaccination induces robust cd4+ T cell responses to mycobacterium tuberculosis complex-specific lipopeptides in Guinea pigs. *J Immunol* (2016) 196(6):2723–32. doi: 10.4049/jimmunol.1502307

121. Podell BK, Ackart DF, Obregon-Henao A, Eck SP, Henao-Tamayo M, Richardson M, et al. Increased severity of tuberculosis in Guinea pigs with type 2 diabetes: A model of diabetes-tuberculosis comorbidity. *Am J Pathol* (2014) 184 (4):1104–18. doi: 10.1016/j.ajpath.2013.12.015

122. Podell BK, Ackart DF, Richardson MA, DiLisio JE, Pulford B, Basaraba RJ. A model of type 2 diabetes in the Guinea pig using sequential diet-induced glucose intolerance and streptozotocin treatment. *Dis Model Mech* (2017) 10(2):151–62. doi: 10.1242/dmm.025593

123. Dooley KE, Chaisson RE. Tuberculosis and diabetes mellitus: convergence of two epidemics. *Lancet Infect Dis* (2009) 9(12):737–46. doi: 10.1016/s1473-3099(09)70282-8

124. Vipond J, Clark SO, Hatch GJ, Vipond R, Marie Agger E, Tree JA, et al. Re-formulation of selected DNA vaccine candidates and their evaluation as protein vaccines using a Guinea pig aerosol infection model of tuberculosis. *Tuberculosis (Edinb)* (2006) 86(3-4):218–24. doi: 10.1016/j.tube.2006.01.014

125. Saso A, Kampmann B. Vaccine responses in newborns. *Semin Immunopathol* (2017) 39(6):627–42. doi: 10.1007/s00281-017-0654-9

126. Sinkora M, Butler JE. The ontogeny of the porcine immune system. *Dev Comp Immunol* (2009) 33(3):273–83. doi: 10.1016/j.dci.2008.07.011

127. Rubic-Schneider T, Christen B, Brees D, Kammüller M. Minipigs in translational immunosafety sciences: A perspective. *Toxicol Pathol* (2016) 44(3):315–24. doi: 10.1177/0192623315621628

128. Tlaskalova-Hogenova H, Mandel L, Trebichavsky I, Kovaru F, Barot R, Sterzl J. Development of immune responses in early pig ontogeny. *Vet Immunol Immunopathol* (1994) 43(1-3):135–42. doi: 10.1016/0165-2427(94)90129-5

129. Ramos L, Obregon-Henao A, Henao-Tamayo M, Bowen R, Izzo A, Lunney JK, et al. Minipigs as a neonatal animal model for tuberculosis vaccine efficacy testing. *Vet Immunol Immunopathol* (2019) 215:109884. doi: 10.1016/j.vetimm.2019.109884

130. Manabe YC, Kesavan AK, Lopez-Molina J, Hatem CL, Brooks M, Fujiwara R, et al. The aerosol rabbit model of tb latency, reactivation and immune reconstitution inflammatory syndrome. *Tuberculosis (Edinb)* (2008) 88(3):187–96. doi: 10.1016/j.tube.2007.10.006

131. Lurie MB, Zappasodi P, Tickner C. On the nature of genetic resistance to tuberculosis in the light of the host-parasite relationships in natively resistant and susceptible rabbits. *Am Rev Tuberc* (1955) 72(3):297–329. doi: 10.1164/artpd.1955.72.3.297

132. Tsenova L, Ellison E, Harbacheuski R, Moreira AL, Kurepina N, Reed MB, et al. Virulence of selected mycobacterium tuberculosis clinical isolates in the rabbit model of meningitis is dependent on phenolic glycolipid produced by the bacilli. *J Infect Dis* (2005) 192(1):98–106. doi: 10.1086/430614

133. Sun H, Ma X, Zhang G, Luo Y, Tang K, Lin X, et al. Effects of immunomodulators on liquefaction and ulceration in the rabbit skin model of tuberculosis. *Tuberculosis (Edinb)* (2012) 92(4):345–50. doi: 10.1016/j.tube.2012.03.005

134. Gray DF. The relative natural resistance of rats and mice to experimental pulmonary tuberculosis. *J Hyg (Lond)* (1961) 59(4):471–7. doi: 10.1017/s0022172400039164

135. Singhal A, Aliouat el M, Hervé M, Mathys V, Kiass M, Creusy C, et al. Experimental tuberculosis in the wistar rat: A model for protective immunity and control of infection. *PloS One* (2011) 6(4):e18632. doi: 10.1371/journal.pone.0018632

136. Ramakrishnan L. The zebrafish guide to tuberculosis immunity and treatment. *Cold Spring Harb Symp Quant Biol* (2013) 78:179–92. doi: 10.1101/sqb.2013.78.023283

137. Volkman HE, Pozos TC, Zheng J, Davis JM, Rawls JF, Ramakrishnan L. Tuberculous granuloma induction via interaction of a bacterial secreted protein with host epithelium. *Science* (2010) 327(5964):466–9. doi: 10.1126/science.1179663

138. Bouz G, Al Hasawi N. The zebrafish model of tuberculosis - no lungs needed. *Crit Rev Microbiol* (2018) 44(6):779–92. doi: 10.1080/1040841x.2018.1523132

139. van Leeuwen LM, van der Sar AM, Bitter W. Animal models of tuberculosis: zebrafish. *Cold Spring Harb Perspect Med* (2014) 5(3):a018580. doi: 10.1101/cshperspect.a018580

140. Plumlee CR, Duffy FJ, Gern BH, Delahaye JL, Cohen SB, Stoltzfus CR, et al. Ultra-low dose aerosol infection of mice with mycobacterium tuberculosis more closely models human tuberculosis. *Cell Host Microbe* (2021) 29(1):68–82.e5. doi: 10.1016/j.chom.2020.10.003

141. Zhu J, Paul WE. Heterogeneity and plasticity of T helper cells. *Cell Res* (2010) 20(1):4–12. doi: 10.1038/cr.2009.138

142. ROmano M, D'Souza S, Adnet PY, Laali R, Jurion F, Palfliet K, et al. Priming but Not Boosting with Plasmid DNA Encoding Mycolyl-Transferase Ag85a from Mycobacterium Tuberculosis Increases the Survival Time of Mycobacterium Bovis Bcg Vaccinated Mice against Low Dose Intravenous Challenge with M. Tuberculosis H37rv. *Vaccine* (2006) 24(16):3353–64. doi: 10.1016/j.vaccine.2005.12.066

143. Luo Y, Jiang W, Da Z, Wang B, Hu L, Zhang Y, et al. Subunit vaccine candidate amm down-regulated the regulatory T cells and enhanced the protective immunity of bcg on a suitable schedule. *Scand J Immunol* (2012) 75(3):293–300. doi: 10.1111/j.1365-3083.2011.02666.x

144. Chai Q, Lu Z, Liu CH. Host defense mechanisms against mycobacterium tuberculosis. *Cell Mol Life Sci* (2020) 77(10):1859–78. doi: 10.1007/s00018-019-03353-5

145. Khan A, Sayedahmed EE, Singh VK, Mishra A, Dorta-Estremera S, Nookala S, et al. A recombinant bovine adenoviral mucosal vaccine expressing mycobacterial antigen-85b generates robust protection against tuberculosis in mice. *Cell Rep Med* (2021) 2(8):100372. doi: 10.1016/j.xcrm.2021.100372

146. Vierboom MPM, Dijkman K, Sombroek CC, Hofman SO, Boot C, Vervenne RAW, et al. Stronger induction of trained immunity by mucosal bcg or mtbvac vaccination compared to standard intradermal vaccination. *Cell Rep Med* (2021) 2(1):100185. doi: 10.1016/j.xcrm.2020.100185

147. Li M, Wang Y, Sun Y, Cui H, Zhu SJ, Qiu HJ. Mucosal vaccines: strategies and challenges. *Immunol Lett* (2020) 217:116–25. doi: 10.1016/j.imlet.2019.10.013

frontiers | Frontiers in Immunology

TYPE Brief Research Report
PUBLISHED 01 September 2023
DOI 10.3389/fimmu.2023.1216262

Check for updates

OPEN ACCESS

EDITED BY
Zhidong Hu,
Fudan University, China

REVIEWED BY
Victor Lorente-Leal,
Complutense University of Madrid (UCM), Spain
Eduard A. Shuralev,
Kazan Federal University, Russia
Brianna R. Beechler,
Oregon State University, United States

*CORRESPONDENCE
Tanya J. Kerr
tjkerr@sun.ac.za

†These authors have contributed equally to this work

RECEIVED 03 May 2023
ACCEPTED 14 June 2023
PUBLISHED 01 September 2023

CITATION
Gumbo R, Goosen WJ, Buss PE, de Klerk-Lorist L-M, Lyashchenko K, Warren RM, van Helden PD, Miller MA and Kerr TJ (2023) "Spotting" *Mycobacterium bovis* infection in leopards (*Panthera pardus*) – novel application of diagnostic tools. *Front. Immunol.* 14:1216262. doi: 10.3389/fimmu.2023.1216262

"Spotting" *Mycobacterium bovis* infection in leopards (*Panthera pardus*) – novel application of diagnostic tools

Rachiel Gumbo[1], Wynand J. Goosen[1], Peter E. Buss[2], Lin-Mari de Klerk-Lorist[3], Konstantin Lyashchenko[4], Robin M. Warren[1], Paul D. van Helden[1], Michele A. Miller[1†] and Tanya J. Kerr[1*†]

[1]DSI-NRF Centre of Excellence for Biomedical Tuberculosis Research, SAMRC Centre for Tuberculosis Research, Division of Molecular Biology and Human Genetics, Faculty of Medicine and Health Sciences, Stellenbosch University, Cape Town, South Africa, [2]South African National Parks, Veterinary Wildlife Services, Kruger National Park, Skukuza, South Africa, [3]Skukuza State Veterinary Office, Department of Agriculture, Land Reform and Rural Development, Skukuza, South Africa, [4]Chembio Diagnostic Systems, Inc., Medford, New York, NY, United States

Background: *Mycobacterium bovis* (*M. bovis*) is the causative agent of animal tuberculosis (TB) which poses a threat to many of South Africa's most iconic wildlife species, including leopards (*Panthera pardus*). Due to limited tests for wildlife, the development of accurate ante-mortem tests for TB diagnosis in African big cat populations is urgently required. The aim of this study was to evaluate currently available immunological assays for their ability to detect *M. bovis* infection in leopards.

Methods: Leopard whole blood (n=19) was stimulated using the QuantiFERON Gold Plus In-Tube System (QFT) to evaluate cytokine gene expression and protein production, along with serological assays. The GeneXpert® MTB/RIF Ultra (GXU®) qPCR assay, mycobacterial culture, and speciation by genomic regions of difference PCR, was used to confirm *M. bovis* infection in leopards.

Results: *Mycobacterium bovis* infection was confirmed in six leopards and individuals that were tuberculin skin test (TST) negative were used for comparison. The GXU® assay was positive using all available tissue homogenates (n=5) from *M. bovis* culture positive animals. *Mycobacterium bovis* culture-confirmed leopards had greater antigen-specific responses, in the QFT interferon gamma release assay, *CXCL9* and *CXCL10* gene expression assays, compared to TST-negative individuals. One *M. bovis* culture-confirmed leopard had detectable antibodies using the DPP® Vet TB assay.

Conclusion: Preliminary results demonstrated that immunoassays and TST may be potential tools to identify *M. bovis*-infected leopards. The GXU® assay provided rapid direct detection of infected leopards. Further studies should aim to improve TB diagnosis in wild felids, which will facilitate disease surveillance and screening.

KEYWORDS

DPP® Vet TB assay, gene expression assay, GeneXpert® MTB/RIF Ultra qPCR assay, interferon-gamma release assay, leopard, *Mycobacterium bovis*, *Panthera pardus*, tuberculin skin test

1 Introduction

Leopards (*Panthera pardus*) occupy diverse habitats across Africa and Asia, but are listed as vulnerable, with some populations decreasing (1). These iconic species play a role in terrestrial ecosystem functions, biodiversity maintenance, ecotourism industries, and cultural rituals in some South African societies (2, 3). However, apex predators including leopards are threatened by ecological disturbances, climate change, and infectious diseases (4, 5). Infections in wild felids include multi-host pathogens such as *Mycobacterium bovis* (*M. bovis*), a member of the *Mycobacterium tuberculosis* complex (MTBC), which is acquired by ingesting infected prey (4). This results in animal tuberculosis (TB), a chronic progressive disease in domestic animals and wildlife, as well as zoonotic TB in humans (6, 7).

Conservation programs often require translocation of individuals to maintain genetic diversity or reintroduce animals into past or new regions (8). However, the presence of infectious disease could threaten the success of these programs (9). Since movement of infected felids carries a potential risk of introducing *M. bovis* into naive populations, it is crucial to develop accurate ante-mortem tests to diagnose *M. bovis* infection prior to translocation as well as perform surveillance. However, ante-mortem TB diagnosis and management have been hampered by the lack of reliable validated tests for many wildlife species (10, 11).

Currently, the tuberculin skin test (TST) is the most widely used ante-mortem test for diagnosing *M. bovis* infection in large wild felids (11). However, performing two immobilizations 72 hours apart is considered impractical in free-ranging wildlife. Therefore, there is an urgent need for the development of single-capture TB diagnostic assays. Although serological tests have been evaluated for TB detection in African lions (*Panthera leo*), results suggested insufficient sensitivity of the assay during early infection (12). However, assays based on *in vitro* cell-mediated immune (CMI) responses appear to be more sensitive for identifying infected individuals (11). Stimulation with specific mycobacterial peptides, such as the early secretory antigenic target 6 kDa (ESAT-6) and culture filtrate protein 10 kDa (CFP-10) in the QuantiFERON®-TB Gold Plus (QFT) tubes (Qiagen, Hilden, 40724, Germany), has been used to elicit cytokine/chemokine responses, measured by gene expression or enzyme-linked immunosorbent assays (ELISAs). This approach has been explored in a variety of wild carnivore species including cheetahs (*Acinonyx jubatus*), spotted hyenas (*Crocuta crocuta*), African wild dogs (*Lycaon pictus*), and African lions (13–16). Previous studies have shown the upregulation of the C-X-C motif ligand 9 (*CXCL9*) gene to be a sensitive diagnostic biomarker for *M. bovis* infection in African lions and a single cheetah (16, 17). Cytokine release assays (CRA) have also shown diagnostic potential in cheetahs and African lions (13, 18). Therefore, the aim of this study was to evaluate immunological assays, previously validated in African lions and cheetahs, to identify potential TB diagnostic tests for leopards. The development of a blood-based test would facilitate screening of individuals and disease surveillance of leopard populations.

2 Materials and methods

Between 2011 and 2022, blood (n = 19) and post-mortem tissue (n = 6) samples were opportunistically collected for purposes unrelated to this study from free-ranging leopards in the Greater Kruger National Park (GKNP), South Africa, which is considered endemic for *M. bovis* (6). Blood samples were collected during the first immobilization for those animals that were immobilized twice to perform the TST. The sex and age category (adult > 4 years; sub-adult 2-4 years; juvenile <2 years) were recorded at the time of sample collection. Wildlife veterinarians performed examinations and leopards in good body condition, without visual evidence of illness or injury were released after immobilization. Leopards that were in poor body condition, with significant wounds, injuries, or other clinical abnormalities (ex. impaled with porcupine quills) and assessed to have a poor long-term prognosis were euthanized. Post-mortem examinations were performed, and tissues were collected for *M. bovis* detection. Testing for other infections or diseases was not performed. Since samples were acquired opportunistically, not all samples were available from every individual. South African Veterinary Council (SAVC)-registered wildlife veterinarians were responsible for all animal-related procedures. The study protocol was approved by the Stellenbosch University Animal Care and Use Research Ethics Committee (SU-ACU-2020-14571) and the Stellenbosch University Biological and Environmental Safety Research Ethics Committee (SU-BEE-2021-22561). Section 20 approval was granted by the South African Department of Agriculture, Land Reform and Rural Development (DALRRD 12/11/1/7/2A-1143NC).

Post-mortem samples, including lymph nodes (head, thoracic, abdominal, peripheral) and lungs, were collected from six leopards and processed for mycobacterial culture as previously described (19). Bacterial isolates were genetically speciated by genomic regions of difference PCR (20). As a rapid ancillary method to mycobacterial culture, the GeneXpert® MTB/RIF Ultra (GXU®) qPCR assay (Cepheid Inc., Sunnyvale, CA 94089, USA) was used to confirm the presence of MTBC DNA directly in tissue homogenates as previously described (19). A positive MTBC result was defined as all readouts except "MTBC not detected" (21).

Once immobilized, the single intradermal cervical test (SICT) and single intradermal comparative cervical test (SICCT) were performed by veterinarians in accordance with the procedures described for lions (22). Individuals were immobilized 72 hours later, and skin thickness (ST) measured at the bovine and avian purified protein derivative (PPD) injection sites and observed for oedema, redness, and necrosis. Results were calculated and categorized as previously described in lions (23). In this study, the single intradermal comparative cervical test (SICCT) results were used to classify animals as TST positive or negative; an animal was considered SICCT positive if an increase in skin thickness at the bovine PPD site was ≥ 2 mm and the bovine PPD response was greater than the avian PPD response (23).

Whole blood (lithium heparin and serum) was collected in BD Vacutainer® blood collection tubes (Becton, Dickinson and

Company, Sparks, MD 21152, USA) prior to performing the TST. Blood was transported in a Styrofoam box to the laboratory at room temperature and processed less than two hours after collection. Blood was processed for serum and stimulated using QFT, as previously described (13, 16). Pokeweed mitogen (PWM; 10 µg/ml final concentration in phosphate buffered saline (PBS); Sigma-Aldrich, St. Louis, MO 63118, USA) was added to the QFT mitogen tube to ensure adequate stimulation. After 24 hours of incubation at 37°C for 24 hours, plasma supernatant was collected and stored at -80°C for CRAs, while the remaining cell pellet was stabilized in 1.3 ml of RNALater® (Ambion, Austin, TX, 78744, USA) and stored at -80°C for cytokine gene expression assays (GEA).

Following the manufacturer's instructions, sera were screened using the Chembio DPP® Vet TB for Elephants rapid serological assay (Chembio Diagnostic Systems, Inc., Medford, NY 11763, USA), as previously described for lions (12). This assay detects the presence of antibodies to mycobacterial antigens MPB83 (test line 1) and ESAT-6/CFP-10 (test line 2), using a species non-specific detection system. Quantitative results were obtained using a DPP® optical reader (Chembio) to measure reflectance in relative light units (RLU), with a RLU ≥ 5 (manufacturer's recommended visual cut-off value) considered antibody positive (12).

The concentration (ng/µl) and purity (A260/A280 and A260/A230 ratios) of extracted RNA from the QFT cell pellets were measured in single replicates per sample using a Nanodrop 1000 spectrophotometer (ThermoFisher Scientific, Wilmington, NC 28401, USA), reversed transcribed to cDNA, and was used to evaluate the performance of the cytokine GEAs, as previously described for use in African lions (16). To evaluate real-time quantitative polymerase chain reaction (qPCR) primer compatibility between lions and leopards, partial messenger RNA (mRNA) transcripts for the target genes *CXCL9*, C-X-C motif chemokine ligand 10 (*CXCL10)*, and interferon-gamma (*IFN-γ*), and reference genes including tyrosine 3-monooxygenase/tryptophan 5-monooxygenase activation protein zeta polypeptide (*YWHAZ*), TATA box-binding protein (*TBP*), β-2-microglobulin (*B2M*), and glyceraldehyde-3-phosphate dehydrogenase (*GAPDH*), were amplified and sequenced using lion PCR primers (sequencing primers), as previously described (16). The newly generated leopard sequences were authenticated (24) and deposited into the NCBI GenBank® genetic sequence database (http://www.ncbi.nlm.nih.gov/genbank/) (25) under the accession numbers OP894012 – OP894028. The gene sequences of lions and leopards were aligned (26) to evaluate sequence identity between species as well as to evaluate compatibility of qPCR primers for downstream analysis.

Real-time qPCR amplification efficiencies for both target and reference genes were determined using a five-fold serial dilution over a 625-fold range using pooled cDNA from five randomly selected leopards. Inefficient genes (90% > efficiency > 110%) were excluded from further analysis. To validate the use of the relative quantification method described (27), the amplification efficiencies of the most stable reference gene real-time qPCRs were compared to those of the target genes to evaluate compatibility (28, 29), as described in African lions (16). Relative abundances of *CXCL9* and *CXCL10* mRNA and changes in regulation were determined as previously described (27, 30). The infection status of leopards based on *CXCL9* GEA results was determined using the previously calculated African lion cut-off value (5-fold change) (16).

The R&D Systems Feline DuoSet® ELISA development kits (R&D Systems, Inc., Minneapolis, MN 55413, USA) for TNF-α (catalogue no. DY2586) and IL-1β (catalogue no. DY1796), and the Mabtech Cat IFN-γ ELISA^{Basic} kit (catalogue no. 3122-1H-20; Mabtech AB, Nacka Strand, SE-131 28, Sweden) were evaluated to determine if native leopard cytokines could be detected in stimulated whole blood plasma as previously shown in cheetah (13) and lions (18). A four-parameter logistic (4PL) regression analysis was performed using GraphPad Prism 7 for Windows (version 7.04, GraphPad Software, Inc., San Diego, CA 92108, USA; www.graphpad.com). The differences between unstimulated and mitogen responses for the three cytokine release assays were evaluated using a one-tailed paired Student t-test. The infection status of leopards based on QFT Mabtech Cat IGRA results was determined using the previously calculated African lion cut-off value (33 pg/ml) (18).

Proportions of GEA and IGRA test positive leopards in *M. bovis* culture positive and TST-negative cohorts were compared using the Fishers' exact test. Blood-based assay results were also evaluated in parallel. Parallel test interpretation was performed by categorizing an individual leopard as positive if either test result was positive, based on previously described African lion cut-off values. A p-value < 0.05 was considered statistically significant. All statistical tests were performed using GraphPad Prism 7 for Windows (version 7.04, Graphpad Software, Inc.).

3 Results

In this study, a total of 19 leopards, 12 males and 7 females, including 16 adults, 1 sub-adult and 2 juveniles, were tested using different ante-mortem (TST, DPP®, GEA, and IGRA) and post-mortem (mycobacterial culture and GXU®) techniques. Results are summarized in Table 1. *Mycobacterium bovis* infection was confirmed in six leopards by mycobacterial culture of post-mortem tissues and speciation by RD PCR. Using tissue homogenates, available for five leopards, the GXU® was successful in detecting MTBC DNA in all five *M. bovis* culture-confirmed leopards, providing same day results (Table 1).

Eight leopards were tested using the TST, including three *M. bovis* culture-confirmed individuals. Skin fold thickness measurements at the avian and bovine PPD injection sites are shown in Supplementary Table S1. The three culture positive leopards were SICCT positive, and the remaining animals were SICCT negative, even though measurement values for KNP-11/121 and KNP-11/236 were unavailable (Table 1). None of the TST negative (presumed *M. bovis*-uninfected) leopards were euthanized and therefore, there were no post-mortem tissues available for mycobacterial culture confirmation.

Sixteen leopards were screened for antibodies to mycobacterial antigens using the DPP® Vet TB assay. Of the six culture-confirmed *M. bovis*-infected individuals, leopard KNP-19/260 was the only individual with detectable antibodies to mycobacterial antigen MPB83, and none to antigen ESAT6/CFP10 (Table 1,

TABLE 1 Summary of demographic information, *Mycobacterium bovis* infection status, and test results of 19 free-ranging leopards (*Panthera pardus*) sampled in Greater Kruger National Park, South Africa and tested using different ante-mortem (TST, DPP®, GEA, and IGRA) and post-mortem (mycobacterial culture and GXU®) techniques.

Leopard Identification Number	Age	Sex	Sample Year	TST	TB lesions present	Mycobacterial Culture and Speciation	GXU®	DPP®	QFT *CXCL9* GEA	QFT *CXCL10* GEA	QFT Mabtech Cat IGRA
KNP-19/260	Adult	Female	2019	pos	yes	*M. bovis*	MTBC detected - low	pos	pos	unknown	neg
KNP-19/07/01	Adult	Male	2019	pos	yes	*M. bovis*	MTBC detected - high	neg	neg	unknown	pos
KNP-19/279	Adult	Male	2019	pos	yes	*M. bovis*	MTBC detected - low	neg	pos	unknown	pos
KNP-18/660	Juvenile	Female	2018	n/d	no	*M. bovis*	n/d	neg	pos	unknown	pos
KNP-22/728	Adult	Male	2022	n/d	yes	*M. bovis*	MTBC detected - medium	neg	pos	unknown	neg
KNP-22/853	Adult	Male	2022	n/d	yes	*M. bovis*	MTBC detected - low	neg	neg	unknown	neg
KNP-11/121	Adult	Male	2011	neg	n/a	n/d	n/d	n/d	n/d	unknown	invalid
KNP-11/236	Adult	Male	2011	neg	n/a	n/d	n/d	n/d	n/d	unknown	neg
KNP-16/155	Adult	Female	2016	neg	n/a	n/d	n/d	neg	neg	unknown	invalid
KNP-18/426	Juvenile	Female	2018	neg	n/a	n/d	n/d	neg	neg	unknown	neg
KNP-20/58	Adult	Female	2020	neg	n/a	n/d	n/d	neg	neg	unknown	neg
KNP-14/228	Adult	Male	2014	n/d	n/a	n/d	n/d	n/d	pos	unknown	neg
KNP-17/682	Adult	Female	2017	n/d	n/a	n/d	n/d	neg	n/d	unknown	n/d
KNP-17/752	Adult	Male	2017	n/d	n/a	n/d	n/d	neg	pos	unknown	pos
KNP-18/35	Adult	Male	2018	n/d	n/a	n/d	n/d	neg	neg	unknown	neg
KNP-18/234	Adult	Female	2018	n/d	n/a	n/d	n/d	neg	neg	unknown	neg
KNP-18/526	Adult	Male	2018	n/d	n/a	n/d	n/d	neg	neg	unknown	neg
KNP-18/425	Sub-adult	Male	2018	n/d	n/a	n/d	n/d	neg	pos	unknown	pos
KNP-22/576	Adult	Male	2022	n/d	n/a	n/d	n/d	neg	n/d	unknown	pos

Age, Adult > 4 years; sub-adult 2-4 years; juvenile < 2 years; TST, tuberculin skin test; GXU®, GeneXpert® MTB/RIF Ultra; MTBC, Mycobacterium tuberculosis complex; DPP®, Dual path platform® Vet TB assay; QFT, QuantiFERON®-TB Gold Plus; GEA, gene expression assay; CXCL9, C-X-C motif ligand 9; CXCL10, C-X-C motif chemokine ligand 10; IGRA, interferon gamma release assay; M. bovis, Mycobacterium bovis; pos, positive; neg, negative; n/d, not done; n/a, not applicable; unknown, In the absence of an existing CXCL10 cut-off value, the GEA test results for CXCL10 were unknown.

Supplementary Table S2). Five culture positive leopards had post-mortem lesions consistent with TB; only KNP-18/660, a juvenile leopard with confirmed *M. bovis* infection did not have gross TB lesions present. The remaining 10 leopards (3 TST-negative, 7 with unknown status) were seronegative.

Stimulated whole blood cell pellets were available from 15 leopards. Three mitogen-stimulated leopard samples were selected for initial PCRs using previously described lion primers (16). Partial mRNA transcripts for reference (*YWHAZ*, *TBP* and *GAPDH*), and target (*CXCL9*, *CXCL10*, and *IFN-γ*) genes were amplified, although the reference gene *B2M* PCR, failed to produce amplicons. Sequence alignments for the target and reference genes showed >95% sequence identity when lion and leopard sequences were compared. In addition, lion qPCR primers (16) showed 100% sequence identity to the leopard primer region, and successfully amplified these genes in leopard samples. Amplification efficiencies of all genes were 90-110% (Supplementary Table S3), except *IFN-γ* and *TBP*. Reference gene *YWHAZ* was confirmed to be the most stably expressed gene and was compatible with *CXCL9* and *CXCL10*.

The abundances of target genes *CXCL9* and *CXCL10* relative to the optimal reference gene are shown as fold change values in Supplementary Table S4. Poor mitogen responses (fold change <5) were observed in 8 of the 15 leopards. Using the African lion cut-off

value (fold change ≥5), the *CXCL9* GEA correctly identified 4/6 *M. bovis* culture-confirmed leopards (Figure 1). Similar results were observed for the *CXCL10* GEA with higher upregulation observed for the same four leopards (Supplementary Table S4). Although KNP-22/853 was negative in the *CXCL9* GEA (4.42-fold change), upregulation of antigen-specific *CXCL10* (53.2-fold change) was observed. Leopards with TST-negative results had low level expression of both *CXCL9* and *CXCL10* (Supplementary Table S4). Of the six leopards with unknown infection status, three had positive *CXCL9* results along with *CXCL10* upregulation (Supplementary Table S4). When *CXCL9* GEA results for leopards that were *M. bovis* culture positive (n = 6) were compared to TST-negative animals (n = 3), no significant association was observed (p = 0.12).

All three feline cytokine ELISAs (TNF-α, IL-1β, and IFN-γ) were able to detect cytokine production in QFT mitogen stimulated leopard samples (Supplementary Table S5). Significant differences in cytokine concentrations were observed between QFT mitogen stimulated and QFT nil samples, using R&D Feline IL-1β (p = 0.009), R&D Feline TNF-α (p = 0.046) and Mabtech cat IFN-γ (p = 0.046, Supplementary Table S5) ELISAs. The coefficients of variation (CV) for the TNF-α and IFN-γ release assays were below 30% while the IL-1β assay had an increased CV (173.3%) because of the background signal observed at the 1:2 sample dilution (Supplementary Table S5).

A subset of samples from *M. bovis* culture positive (n=3) and TST-negative leopards (n=1) produced valid mitogen responses in all three cytokine release assays using a 1:4 dilution of leopard plasma (Supplementary Table S6). The R&D Feline IL-1β and Mabtech Cat IFN-γ ELISAs detected an antigen-specific response in 2/3 *M. bovis* culture positive leopards, while the R&D Feline TNF-α ELISA showed an antigen-specific response in only 1/3 *M. bovis* culture positive leopards (Supplementary Table S6). Since the QFT Mabtech Cat IGRA has been validated for lions, it was selected for further evaluation.

Using the African lion cut-off value (33pg/ml), the QFT Mabtech Cat IGRA correctly identified 3/6 *M. bovis* culture-confirmed leopards (Figure 2). Of the three TST-negative individuals with valid IGRA results, all three had little to no antigen-specific IFN-γ (Figure 2, Supplementary Table S7). However, there was no significant association observed between *M. bovis* infection status and QFT Mabtech Cat IGRA results (p = 0.24). Three out of seven leopards, with unknown infection status, were identified as IGRA positive (Supplementary Table S7). Two of the IGRA positive leopards also had GEA results, which were positive in the *CXCL9* GEA and showed upregulation of *CXCL10* (30 and 26.97-fold change; Supplementary Table S4).

No single blood-based test nor parallel interpretation of combined tests was able to correctly identify all six culture positive leopards. However, when the a) *CXCL9* GEA and IGRA, and b) DPP®, IGRA, and *CXCL9* GEA were evaluated in parallel, 5/6 culture positive individuals were correctly identified (Figure 3).

4 Discussion

This study demonstrated that existing assays, previously evaluated for TB diagnosis in African lions (12, 16, 18, 31) and

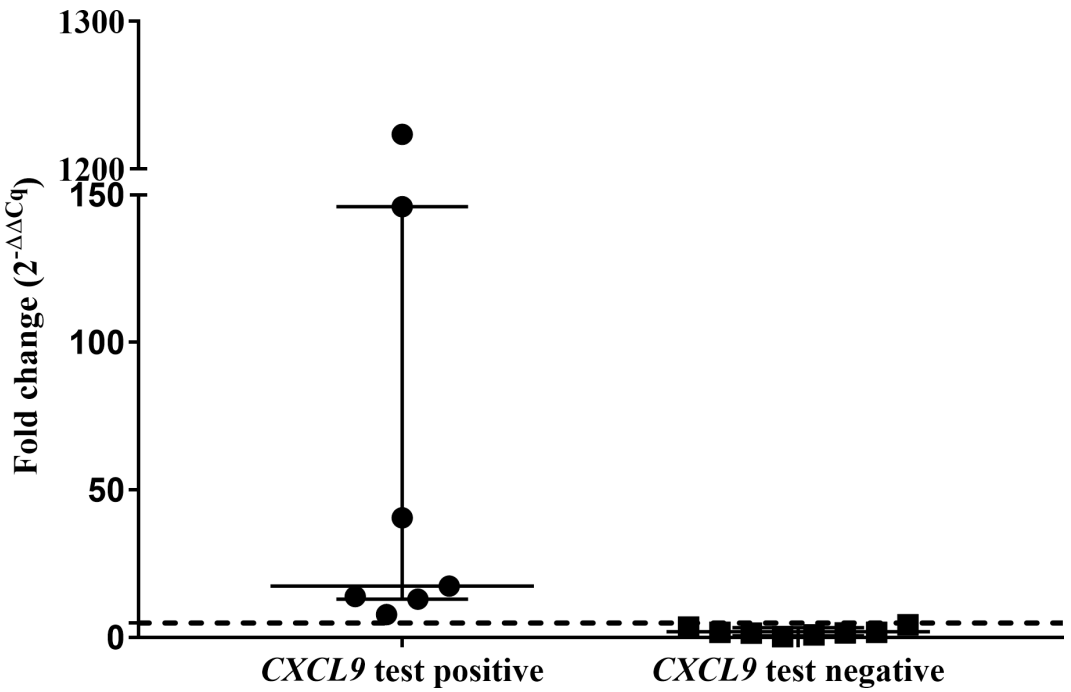

FIGURE 1
Antigen-specific *CXCL9* mRNA fold change ($2^{-\Delta\Delta Cq}$) of test positive (n=7) and test negative leopards (n=8) using the QFT *CXCL9* GEA. Medians and inter-quartile ranges are indicated by horizontal bars. The lion assay cut-off value (5-fold change) is shown as a dotted line on the y-axis (16). There was a statistically significant difference between the test results (p = 0.0002).

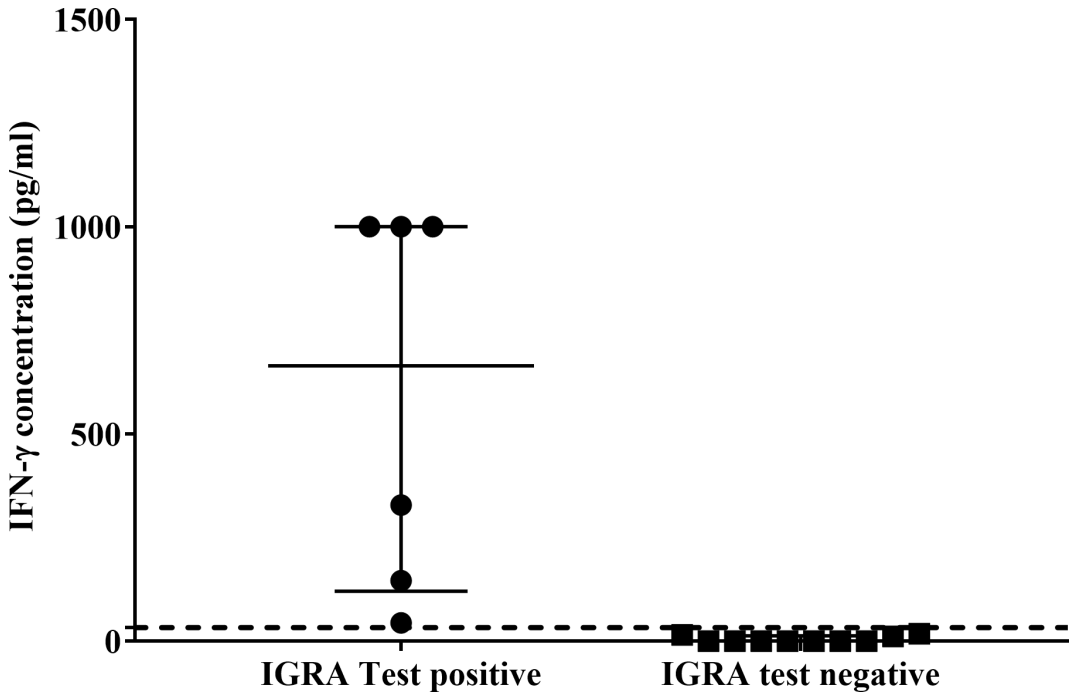

FIGURE 2
Antigen-specific interferon-gamma (IFN-γ) concentrations (pg/ml) of QFT Mabtech Cat IGRA positive (n=6) and negative (n=10) leopards. Medians and inter-quartile ranges are indicated by horizontal bars. The lion assay cut-off value (33 pg/ml) is shown as a dotted line on the y-axis (18). There was a statistically significant difference between the test results (p = 0.0001). High IFN-γ concentrations above the recombinant IFN-γ standard range (7.81 – 1000 pg/ml) for the assay were assigned the highest known standard concentration.

cheetahs (13), showed potential for detecting *M. bovis*-infected leopards. The GXU® was able to detect MTBC DNA in all five culture positive leopards that were tested, providing rapid results in a significantly shorter time than mycobacterial culture. In addition, all *M. bovis* culture-confirmed leopards had positive results in the SICCT, supporting the use of the TST in leopards. Using blood-based assays, the QFT *CXCL9* GEA correctly identified 4/6 *M. bovis* culture-confirmed leopards using the African lion cut-off value. All except one *M. bovis* culture positive leopard also showed upregulation of antigen-specific *CXCL10* gene expression, although an assay cut-off value was unavailable. There was no antigen-specific cytokine upregulation observed in TST-negative leopards, suggesting that both GEAs were able to detect immune sensitization to *M. bovis*. In addition, the QFT domestic cat IGRA correctly identified 3/6 *M. bovis* culture-confirmed leopards using the African lion cut-off value, although only one infected leopard had detectable anti-mycobacterial antibodies. Parallel interpretation, using the QFT *CXCL9* GEA and IGRA, provided the most sensitive approach by identifying 5/6 *M. bovis* culture-confirmed leopards. Overall, findings in this pilot study support further investigations to determine leopard specific cut-off values and test performance of these assays in this species.

The GXU® was 100% sensitive, providing a rapid ancillary diagnostic test for the detection of MTBC DNA (targeting IS*6110* and IS*1081*) from tissue homogenates, although it is unknown whether it will be sensitive when applied to respiratory samples, for antemortem diagnosis of leopards (21), or in leopards without TB-compatible lesions. Since vigorous decontamination of samples prior to mycobacterial culture can cause false negative results, GXU® may enhance detection of MTBC in paucibacillary or non-viable MTBC samples, providing a valuable screening tool (32). However, the GXU® cannot differentiate viable from non-viable mycobacteria nor distinguish between members of MTBC, which is important when investigating transmission.

The TST is the primary diagnostic tool used for the identification of *M. bovis*-infected domestic and wild animals (33). Although the TST has not been validated in most wild felid species, the findings in this study support its use in leopards. To account for possible cross-reactions with environmental mycobacteria, the SICCT was used since it takes into account responses to *M. avium* antigens (22, 23). Although studies in other species have reported that the SICCT has reduced sensitivity (34), all *M. bovis* culture-confirmed leopards (n=3) tested with SICCT in this study were positive. Interestingly, the TST in carnivores uses an increased volume of PPDs (0.2 ml), which is based on previous studies to optimize detection of a delayed-type hypersensitivity response (22). One of the limitations of the TST is the bias introduced through interpretation by different operators. Since TST is not validated in most wild species, the risk of misinterpretation remains.

Blood-based assays are logistically easier, and potentially less subjective to use in wildlife than the TST. Although assays to detect antimicrobial antibodies have been evaluated in wild carnivores, they appear to have suboptimal sensitivity unless disease is present (12, 13, 15). Therefore, it was expected that leopards with advanced disease might have detectable humoral response. One leopard

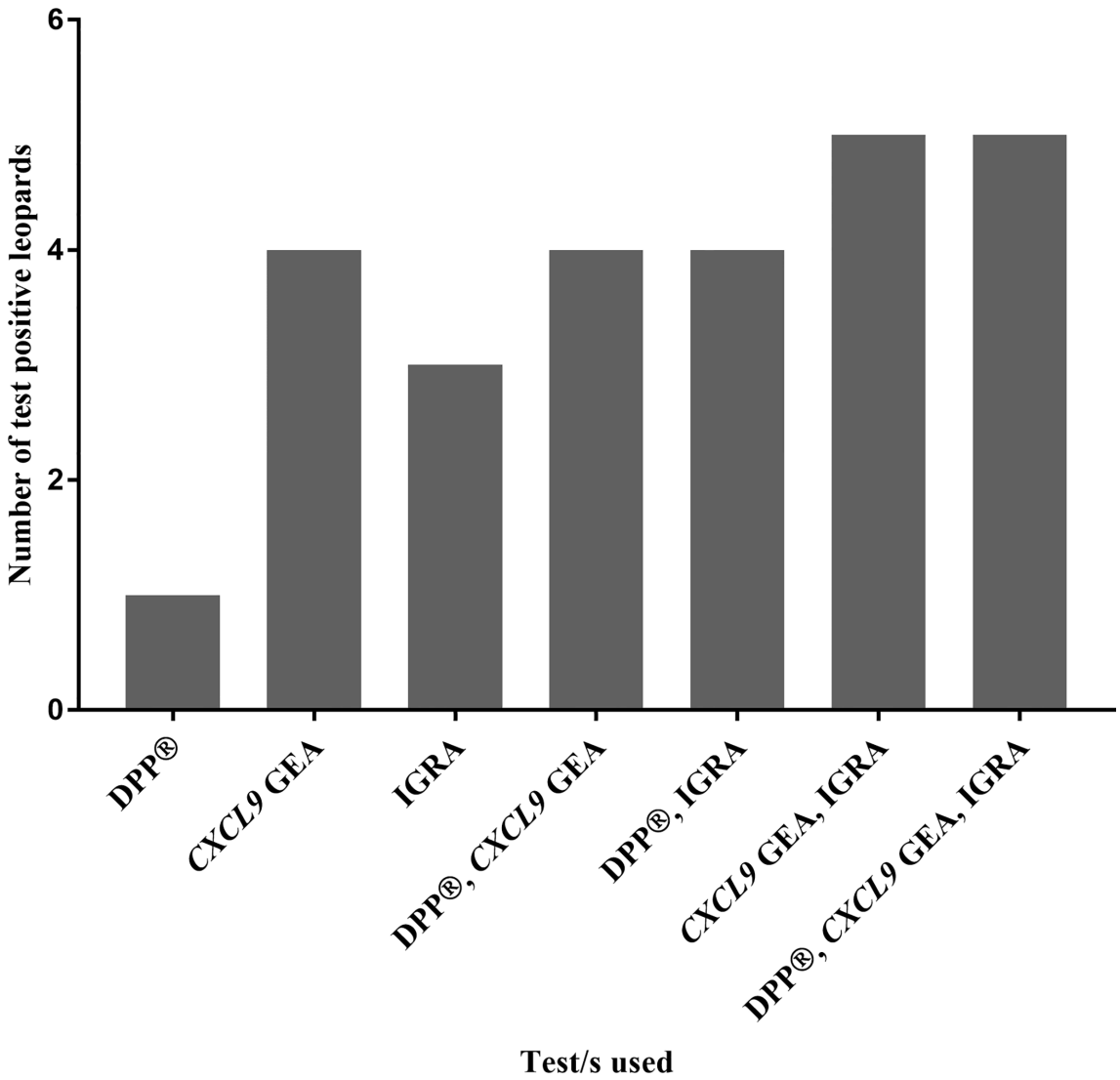

FIGURE 3
Numbers of test positive leopards, out of a cohort of *Mycobacterium bovis*-infected leopards (n = 6) confirmed by culture, are shown based on blood-based assay results (Dual Path Platform (DPP®) Vet TB Assay, QFT *CXCL9* gene expression assay, and QFT Mabtech Cat interferon gamma release assay) individually and in combination.

(KNP-19/260), that showed extensive pulmonary pathological changes associated with TB, was positive for antibodies to mycobacterial antigen MPB83 using the DPP® assay. However, the negative DPP® results in the other *M. bovis* culture-confirmed leopards with disease could have been due to anergy associated with advanced disease or a humoral response to other mycobacterial antigens not included in the DPP® assay. Typically, the humoral immune response in TB develops later in the course of infection and may take months to reach detectable levels (31, 35). Although the DPP® assay does not appear to be sensitive for screening leopards, serological tests are useful since serum is easily obtained, tests are suitable for field use, results are rapid, and tests can be done with retrospective serum samples. Therefore, the DPP® assay may be useful for screening selected leopards when disease is suspected.

Cell-mediated immune responses to TB are considered to be an early and more sensitive method to detect infection (36). Cytokine TB biomarker discovery has led to the development of antigen-specific GEAs in a number of species (11). Due to the taxonomic relatedness between lions and leopards, it was not surprising that the cytokine/chemokine primers for lions resulted in amplification of leopard target and reference genes (16, 37). Analyses showed the leopard sequences were a perfect match to those of the lion and supported further evaluation of lion *CXCL9* and *CXL10* GEAs in leopards. Results in leopards that exhibited poor mitogen and antigen-specific responses were considered invalid. However, some leopards had significant upregulation of antigen-specific cytokine genes expression, despite poor mitogen response. These results suggested that these individuals likely had *M. bovis* immune sensitization. Possible explanations for poor mitogen responses observed in leopards could be due to selection of mitogens (i.e., PHA and PWM not being optimal mitogens), sampling handling that affected viability, immunocompromise due to advanced

disease, or suboptimal incubation time for blood stimulation (38–40). Therefore, further investigation of mitogen responses is required in leopards.

Both GEAs demonstrated the ability to detect antigen-specific upregulation of *CXCL9* and *CXCL10* in *M. bovis* culture-confirmed infected leopards. The upregulation of *CXCL9* has been reported as a sensitive diagnostic biomarker for *M. bovis* infection in African lions (16). However, in this study, both *CXCL9* and *CXCL10* showed an upregulation in some *M. bovis* culture-confirmed individuals, suggesting that these may be potential biomarkers for leopards. Additional studies should focus on optimizing these assays and determining leopard specific cut-off values, using a larger cohort with known infection status.

Although the cytokine GEAs showed promise, CRAs, especially IGRA, are more commonly used for screening humans and animals for TB (11, 36, 41). Even though all screened feline cytokine ELISA kits (TNF-α, IL-1β, and IFN-γ) were able to detect the cytokine of interest, the Mabtech Cat IFN-γ ELISA appeared to be the best for differentiating between *M. bovis* culture positive and TST-negative leopards. Due to the high homology (97-100%) between IFN-γ sequences from cheetahs, lions, and domestic cats (42), it was not surprising that the anti-cat IFN-γ antibodies were able to cross-react with native leopard, as well as cheetah and lion, IFN-γ in previous studies (13, 18).

The QFT Mabtech Cat IGRA correctly identified half of the *M. bovis* culture-confirmed leopards, using the African lion IGRA cut-off value, which suggests further investigations should determine if a leopard specific IGRA cut-off value would improve performance. It is also possible that lack of response was due to anergy, associated with advanced TB-related disease in two of the leopards (KNP-19/260 and KNP-22/853). However, these individuals exhibited valid mitogen responses. Therefore, it is crucial that immunoassay results are interpreted in conjunction with the history and clinical evaluation of leopards to avoid misclassification.

Even though both the QFT Mabtech Cat IGRA and *CXCL9* GEA correctly identified a proportion of TST-negative leopards (n=3; two had invalid IGRA responses) as negative (estimated 100% specificity), the calculated sensitivities of these assays were 50% and 67%, respectively. However, when these tests were interpreted in parallel, five of six *M. bovis* culture-confirmed leopards were correctly diagnosed.

Although the QFT Mabtech Cat IGRA, *CXCL9* and *CXCL10* GEAs demonstrated potential to identify *M. bovis* culture positive leopards and could be performed with a single blood sample, there were limitations to this study. While proportions of test positive individuals of *M. bovis* culture-confirmed and TST-negative leopards showed a trend, this requires further investigation to determine significance. In addition, there were no culture negative individuals to confirm absence of infection, some of the *M. bovis* culture-confirmed leopards had advanced disease (which could result in immunocompromise), and not every sample type was available for comparison in every individual. This preliminary study indicates that immunoassays may be useful for TB detection in leopards, but species-specific assay cut-off values should be determined in a larger study cohort of TB-endemic and TB-free leopard population to confirm the utility of this approach.

5 Conclusion

This pilot study suggested that blood-based assays used in parallel (QFT IGRA, QFT *CXCL9* GEA) show promise for detecting *M. bovis* culture positive leopards. However, future studies should validate use of the TST in leopards and the blood-based assays to improve performance and provide a single capture testing method. The incorporation of these diagnostic tools into routine screening of leopards and other wild felids for health assessment or as translocation candidates could improve TB detection and prevent spread of infection.

Data availability statement

The datasets presented in this study can be found in online repositories. The names of the repository/repositories and accession number(s) can be found in the article/Supplementary Material.

Ethics statement

The animal study was reviewed and approved by Stellenbosch University Animal Care and Use Research Ethics Committee.

Author contributions

The work presented here was carried out in collaboration between all authors. RG, MM, and TK developed and designed the study. RG conducted experiments and analyzed the data. PB and L-MdK-L was involved with sample collection and clinical data. Original manuscript draft was prepared by RG and WG contributed to data analysis. MM, RW, PvH, and KL provided funding and feedback for the study. All authors contributed to the article and approved the submitted version.

Funding

This research was funded by the South African Medical Research Council (SAMRC) Centre for Tuberculosis Research, National Research Foundation (NRF) South African Research Chair Initiative (SARChI grant 86949), American Association of Zoo Veterinarians (AAZV) Wild Animal Health Fund (WAHF) (AAZV WAHF Grant 2020 #4) and The Harry Crossley Foundation. Funding to RG was provided through a Stellenbosch University (SU) Postgraduate Scholarship (2021) and German Academic Exchange Service (DAAD) In-Region Scholarship SUN MBHG South Africa (2022-2023). Funding to TK was provided through DSI-NRF PDP Fellowship within the SAMRC Centre for Tuberculosis Research.

Acknowledgments

The authors wish to acknowledge Guy Hausler, Tebogo Manamela, Leana Freese, and Dr. Lufuno Netshitavhadulu from

the South African National Parks (SANParks) Veterinary Wildlife Services, Kruger National Park (KNP), Skukuza, South Africa and Dr. Louis van Schalkwyk from Skukuza State Veterinary Office, Department of Agriculture, Land Reform and Rural Development, Skukuza, South Africa.

Conflict of interest

The authors declare that the research was conducted in the absence of any commercial or financial relationships that could be construed as a potential conflict of interest.

Dr. KL is affiliated with Chembio Diagnostic Systems, Inc., the manufacturer of the DPP® Vet TB for Elephants serological assay.

Publisher's note

Supplementary material

The Supplementary Material for this article can be found online at: https://www.frontiersin.org/articles/10.3389/fimmu.2023.1216262/full#supplementary-material

References

1. Stein AB, Athreya V, Gerngross P, Balme G, Henschel P, Karanth U, et al. *Panthera pardus* (amended version of 2019 assessment). *IUCN Red List Threat Species* (2020), T15954A163991139. doi: 10.2305/IUCN.UK.2020-1.RLTS.T15954A163991139.en

2. Stier AC, Samhouri JF, Novak M, Marshall KN, Ward EJ, Holt RD, et al. Ecosystem context and historical contingency in apex predator recoveries. *Sci Adv* (2016) 2(5):e1501769. doi: 10.1126/sciadv.1501769

3. Naude VN, Balme GA, Rogan MS, Needham MD, Whittington-Jones G, Dickerson T, et al. Longitudinal assessment of illegal leopard skin use in ceremonial regalia and acceptance of faux alternatives among followers of the shembe church, south Africa. *Conserv Sci Pract* (2020) 2:e289. doi: 10.1111/csp2.289

4. Munson L, Terio KA, Ryser-Degiorgis M-P, Lane EP, Courchamp F. Wild felid diseases: conservation implications and management strategies. In: Macdonald D, Loveridge A, editors. *Biology and conservation of wild felids*. New York USA: Oxford University Press (2010). p. 237–59.

5. Cheng BS, Komoroske LM, Grosholz ED. Trophic sensitivity of invasive predator and native prey interactions: integrating environmental context and climate change. *Funct Ecol* (2017) 31(3):642–52. doi: 10.1111/1365-2435.12759

6. Michel AL, Bengis RG, Keet DF, Hofmeyr M, de KLM, PC C, et al. Wildlife tuberculosis in south African conservation areas: implications and challenges. *Vet Microbiol* (2006) 112(2–4):91–100. doi: 10.1016/j.vetmic.2005.11.035

7. Doran P, Carson J, Costello E, More S. An outbreak of tuberculosis affecting cattle and people on an Irish dairy farm, following the consumption of raw milk. *Ir Vet J* (2009) 62(6):390–7. doi: 10.1186/2046-0481-62-6-390

8. Buk KG, van der Merwe VC, Marnewick K, Funston PJ. Conservation of severely fragmented populations: lessons from the transformation of uncoordinated reintroductions of cheetahs (*Acinonyx jubatus*) into a managed metapopulation with self-sustained growth. *Biodivers Conserv* (2018) 27(13):3393–423. doi: 10.1007/s10531-018-1606-y

9. Kock RA, Woodford MH, Rossiter PB. Disease risks associated with the translocation of wildlife. *Rev Sci Tech* (2010) 29(2):329–50. doi: 10.20506/rst.29.2.1980

10. Maas M, Michel AL, Rutten VPMG. Facts and dilemmas in diagnosis of tuberculosis in wildlife. *Comp Immunol Microbiol Infect Dis* (2013) 36(3):269–85. doi: 10.1016/j.cimid.2012.10.010

11. Bernitz N, Kerr TJ, Goosen WJ, Chileshe J, Higgitt RL, Roos EO, et al. Review of diagnostic tests for detection of *Mycobacterium bovis* infection in south African wildlife. *Front Vet Sci* (2021) 8:588697. doi: 10.3389/fvets.2021.588697

12. Miller M, Joubert J, Mathebula N, De Klerk-Lorist L-M, Lyashchenko KP, Bengis R, et al. Detection of antibodies to tuberculosis antigens in free-ranging lions (*Panthera leo*) infected with *Mycobacterium bovis* in Kruger national park, south Africa. *J Zoo Wildl Med* (2012) 43(2):317–23. doi: 10.1638/2011-0171.1

13. Gumbo R, Crockett E, Goosen WJ, Warren RM, van Helden PD, Miller MA, et al. Cytokine-release assay for the detection of *Mycobacterium bovis* infection in cheetah (*Acinonyx jubatus*). *J Zoo Wildl Med* (2021) 52(4):1113–22. doi: 10.1638/2021-0063

14. Higgitt RL, Buss PE, van Helden PD, Miller MA, Parsons SD. Development of gene expression assays measuring immune responses in the spotted hyena (*Crocuta crocuta*). *Afr Zool* (2017) 52(2):99–104. doi: 10.1080/15627020.2017.1309300

15. Higgitt RL, Schalkwyk OLv, DeKlerk-Lorist L-M, Buss PE, Caldwell P, Rossouw L, et al. An interferon gamma release assay for the detection of immune sensitization to *Mycobacterium bovis* in African wild dogs (*Lycaon pictus*). *J Wildl Dis* (2019) 55 (3):529–36. doi: 10.7589/2018-03-089

16. Olivier TT, Viljoen IM, Hofmeyr J, Hausler GA, Goosen WJ, Tordiffe ASW, et al. Development of a gene expression assay for the diagnosis of *Mycobacterium bovis* infection in African lions (*Panthera leo*). *Transbound Emerg Dis* (2015) 64(3):774–81. doi: 10.1111/tbed.12436

17. Kerr TJ, Gumbo R, Goosen WJ, Rogers P, Last RD, Miller MA. Novel techniques for detection of *Mycobacterium bovis* infection in a cheetah. *Emerg Infect Dis* (2020) 26 (3):630–1. doi: 10.3201/eid2603.191542

18. Gumbo R, Sylvester TT, Goosen WJ, Buss PE, de Klerk-Lorist L-M, van Schalkwyk OL, et al. Adaptation and diagnostic potential of a commercial cat interferon gamma release assay for the detection of *Mycobacterium bovis* infection in African lions (*Panthera leo*). *Pathogens* (2022) 11:765. doi: 10.3390/pathogens11070765

19. Kerr TJ, Goosen WJ, Gumbo R, Klerk-Lorist L, Pretorius O, Buss PE, et al. Diagnosis of *Mycobacterium bovis* infection in free-ranging common hippopotamus (*Hippopotamus amphibius*). *Transbound Emerg Dis* (2022) 69(2):378–84. doi: 10.1111/tbed.13989

20. Warren RM, Gey van Pittius NC, Barnard M, Hesseling A, Engelke E, de Kock M, et al. Differentiation of *Mycobacterium tuberculosis* complex by PCR amplification of genomic regions of difference. *Int J Tuberc Lung Dis* (2006) 10(7):818–22.

21. Chakravorty S, Simmons AM, Rowneki M, Parmar H, Cao Y, Ryan J, et al. The new xpert MTB/RIF ultra: improving detection of *Mycobacterium tuberculosis* and resistance to rifampin in an assay suitable for point-of-care testing. *MBio* (2017) 8(4): e00812–17. doi: 10.1128/mBio.00812-17

22. Keet DF, Michel AL, Bengis RG, Becker P, van Dyk DS, van Vuuren M, et al. Intradermal tuberculin testing of wild African lions (*Panthera leo*) naturally exposed to infection with *Mycobacterium bovis*. *Vet Microbiol* (2010) 144:384–91. doi: 10.1016/j.vetmic.2010.01.028

23. Viljoen IM, Sylvester TT, Parsons SDC, Millar RP, Helden PDv, Miller MA. Performance of the tuberculin skin test in *Mycobacterium bovis*–exposed and –unexposed African lions (*Panthera leo*). *J Wildl Dis* (2019) 55(3):537–43. doi: 10.7589/2018-06-163

24. Altschul SF, Gish W, Miller W, Myers EW, Lipman DJ. Basic local alignment search tool. *J Mol Biol* (1990) 215(3):403–10. doi: 10.1016/S0022-2836(05)80360-2

25. Benson DA, Cavanaugh M, Clark K, Karsch-Mizrachi I, Lipman DJ, Ostell J, et al. GenBank. *Nucleic Acids Res* (2013) 41:D36–42. doi: 10.1093/nar/gks1195

26. Sievers F, Wilm A, Dineen D, Gibson TJ, Karplus K, Li W, et al. Fast, scalable generation of high-quality protein multiple sequence alignments using clustal omega. *Mol Syst Biol* (2011) 7(1):539. doi: 10.1038/msb.2011.75

27. Livak KJ, Schmittgen TD. Analysis of relative gene expression data using real-time quantitative PCR and the $2^{-\Delta\Delta CT}$ method. *Methods* (2001) 25(4):402–8. doi: 10.1006/meth.2001.1262

28. Andersen CL, Jensen JL, Ørntoft TF. Normalization of real-time quantitative reverse transcription-PCR data: a model-based variance estimation approach to identify genes suited for normalization, applied to bladder and colon cancer data sets. *Cancer Res* (2004) 64(15):5245–50. doi: 10.1158/0008-5472.CAN-04-0496

29. Vandesompele J, De Preter K, Pattyn F, Poppe B, Van Roy N, De Paepe A, et al. Accurate normalization of real-time quantitative RT-PCR data by geometric averaging of multiple internal control genes. *Genome Biol* (2002) 3(7):research0034. doi: 10.1186/gb-2002-3-7-research0034

30. Radonić A, Thulke S, Mackay IM, Landt O, Siegert W, Nitsche A. Guideline to reference gene selection for quantitative real-time PCR. *Biochem Biophys Res Commun* (2004) 313(4):856–62. doi: 10.1016/j.bbrc.2003.11.177

31. Miller MA, Buss P, Sylvester TT, Lyashchenko KP, DeKlerk-Lorist L-M, Bengis R, et al. *Mycobacterium bovis* in free-ranging lions (*Panthera leo*) [[/amp]]mdash; evaluation of serological and tuberculin skin tests for detection of infection and disease. *J Zoo Wildl Med* (2019) 50(1):7–15. doi: 10.1638/2017-0187

32. Goosen WJ, Kerr TJ, Kleynhans L, Warren RM, van Helden PD, Persing DH, et al. The xpert MTB/RIF ultra assay detects *Mycobacterium tuberculosis* complex DNA in white rhinoceros (*Ceratotherium simum*) and African elephants (*Loxodonta africana*). *Sci Rep* (2020) 10(1):14482. doi: 10.1038/s41598-020-71568-9

33. Byrne AW, Barrett D, Breslin P, Ryan E. Can more information be extracted from bovine TB skin test outcomes to inform animal risk management? a retrospective observational animal-level study. *Prev Vet Med* (2022) 208:105761. doi: 10.1016/j.prevetmed.2022.105761

34. Smith K, Bernitz N, Cooper D, Kerr TJ, de Waal CR, Clarke C, et al. Optimisation of the tuberculin skin test for detection of *Mycobacterium bovis* in African buffaloes (*Syncerus caffer*). *Prev Vet Med* (2021) 188:105254. doi: 10.1016/j.prevetmed.2020.105254

35. Welsh MD, Cunningham RT, Corbett DM, Girvin RM, McNair J, Skuce RA, et al. Influence of pathological progression on the balance between cellular and humoral immune responses in bovine tuberculosis. *Immunology* (2005) 114(1):101–11. doi: 10.1111/j.1365-2567.2004.02003.x

36. de la Rua-Domenech R, Goodchild AT, Vordermeier HM, Hewinson RG, Christiansen KH, Clifton-Hadley RS. Ante mortem diagnosis of tuberculosis in cattle: a review of the tuberculin tests, gamma-interferon assay and other ancillary diagnostic techniques. *Res Vet Sci* (2006) 81(2):190–210. doi: 10.1016/j.rvsc.2005.11.005

37. Johnson WE, Eizirik E, Pecon-Slattery J, Murphy WJ, Antunes A, Teeling E, et al. The late Miocene radiation of modern felidae: a genetic assessment. *Science* (2006) 311(5757):73–7. doi: 10.1126/science.1122277

38. Vance CK, Kennedy-Stoskopf S, Obringer AR, Roth TL. Comparative studies of mitogen- and antigen-induced lymphocyte proliferation in four captive rhinoceros species. *J Zoo Wildl Med* (2004) 35(4):435–46. doi: 10.1638/04-014

39. de Waal CR, Kleynhans L, Parsons SDC, Goosen WJ, Hausler G, Buss PE, et al. Development of a cytokine gene expression assay for the relative quantification of the African elephant (*Loxodonta africana*) cell-mediated immune responses. *Cytokine* (2021) 141:155453. doi: 10.1016/j.cyto.2021.155453

40. Dwyer R, Witte C, Buss P, Manamela T, Freese L, Hausler G, et al. Reduced capability of refrigerated white rhinoceros whole blood to produce interferon-gamma upon mitogen stimulation. *Vet Immunol Immunopathol* (2022) 252:110485. doi: 10.1016/j.vetimm.2022.110485

41. Sharma SK, Vashishtha R, Chauhan LS, Sreenivas V, Seth D. Comparison of TST and IGRA in diagnosis of latent tuberculosis infection in a high TB-burden setting. *PLoS One* (2017) 12(1):e0169539. doi: 10.1371/journal.pone.0169539

42. Maas M, Van Rhijn I, Allsopp MTEP, Rutten VPMG. Lion (*Panthera leo*) and cheetah (*Acinonyx jubatus*) IFN-γ sequences. *Vet Immunol Immunopathol* (2010) 134 (3–4):296–8. doi: 10.1016/j.vetimm.2009.10.001

frontiers | Frontiers in Immunology

TYPE Original Research
PUBLISHED 15 September 2023
DOI 10.3389/fimmu.2023.1238132

OPEN ACCESS

EDITED BY
Zhidong Hu,
Fudan University, China

REVIEWED BY
Pooja Singh,
University of Alabama at Birmingham, United States
Krishnaveni Mohareer,
University of Hyderabad, India

*CORRESPONDENCE
Bożena Dziadek
bozena.dziadek@biol.uni.lodz.pl
Jarosław Dziadek
jdziadek@cbm.pan.pl

†These authors have contributed equally to this work and share first authorship

RECEIVED 10 June 2023
ACCEPTED 28 August 2023
PUBLISHED 15 September 2023

CITATION
Kawka M, Płocińska R, Płociński P, Pawełczyk J, Słomka M, Gatkowska J, Dzitko K, Dziadek B and Dziadek J (2023) The functional response of human monocyte-derived macrophages to serum amyloid A and *Mycobacterium tuberculosis* infection.
Front. Immunol. 14:1238132.
doi: 10.3389/fimmu.2023.1238132

The functional response of human monocyte-derived macrophages to serum amyloid A and *Mycobacterium tuberculosis* infection

Malwina Kawka[1†], Renata Płocińska[2†], Przemysław Płociński[2], Jakub Pawełczyk[2], Marcin Słomka[3], Justyna Gatkowska[1], Katarzyna Dzitko[1], Bożena Dziadek[1*] and Jarosław Dziadek[2*]

[1]Department of Molecular Microbiology, Faculty of Biology and Environmental Protection, University of Lodz, Lodz, Poland, [2]Institute of Medical Biology, Polish Academy of Sciences, Lodz, Poland, [3]Biobank Lab, Department of Oncobiology and Epigenetics, Faculty of Biology and Environmental Protection, University of Lodz, Lodz, Poland

Introduction: In the course of tuberculosis (TB), the level of major acute phase protein, namely serum amyloid A (hSAA-1), increases up to a hundredfold in the pleural fluids of infected individuals. Tubercle bacilli infecting the human host can be opsonized by hSAA-1, which affects bacterial entry into human macrophages and their intracellular multiplication.

Methods: We applied global RNA sequencing to evaluate the functional response of human monocyte-derived macrophages (MDMs), isolated from healthy blood donors, under elevated hSAA-1 conditions and during infection with nonopsonized and hSAA-1-opsonized *Mycobacterium tuberculosis* (*Mtb*). In the same infection model, we also examined the functional response of mycobacteria to the intracellular environment of macrophages in the presence and absence of hSAA-1. The RNASeq analysis was validated using qPCR. The functional response of MDMs to hSAA-1 and/or tubercle bacilli was also evaluated for selected cytokines at the protein level by applying the Milliplex system.

Findings: Transcriptomes of MDMs cultured in the presence of hSAA-1 or infected with *Mtb* showed a high degree of similarity for both upregulated and downregulated genes involved mainly in processes related to cell division and immune response, respectively. Among the most induced genes, across both hSAA-1 and *Mtb* infection conditions, CXCL8, CCL15, CCL5, IL-1β, and receptors for IL-7 and IL-2 were identified. We also observed the same pattern of upregulated pro-inflammatory cytokines (TNFα, IL-6, IL-12, IL-18, IL-23, and IL-1) and downregulated anti-inflammatory cytokines (IL-10, TGFβ, and antimicrobial peptide cathelicidin) in the hSAA-1 treated-MDMs or the phagocytes infected with tubercle bacilli. At this early stage of infection, *Mtb* genes affected by the inside microenvironment of MDMs are strictly involved in iron scavenging, adaptation to hypoxia, low pH, and increasing levels of CO_2. The genes for the synthesis and transport of virulence lipids, but not cholesterol/fatty acid degradation, were also upregulated.

Conclusion: Elevated serum hSAA-1 levels in tuberculosis enhance the response of host phagocytes to infection, including macrophages that have not yet been in contact with mycobacteria. SAA induces antigen processing and presentation processes by professional phagocytes reversing the inhibition caused by *Mtb* infection.

KEYWORDS

tuberculosis, human serum amyloid A, monocyte-derived macrophages, immunological response, host-pathogen transcriptomics

1 Introduction

Mycobacterium tuberculosis (*Mtb*) is a causative agent of tuberculosis (TB), an infectious disease that affects millions of people worldwide. TB remains a major global health problem, with an estimated 10.6 million cases globally and 1.6 million deaths worldwide in 2021, according to the World Health Organization (WHO) Global Tuberculosis Report 2022 (1). *Mtb* is a slow-growing bacterium with a complex cell wall that makes it resistant to many antibiotics and allows it to evade the host's immune system (2). The transmission of TB occurs through inhalation of respiratory droplets containing bacteria, which are excreted from an infected person during coughing, sneezing or talking. The bacteria can then infect the lungs and other parts of the body of a newly infected individual, leading to the development of TB (2, 3). The pathogenesis of TB is complex and involves a network of interactions between the bacterium and the host's immune response. Several factors contribute to the development of active TB, including host genetics, environmental factors, and the virulence of the infecting strain. The disease can cause distress to multiple organs, but primarily affects the lungs, leading to symptoms such as cough, fever, and weight loss (4, 5). The immune response to *Mtb* involves a complex interplay between the innate and adaptive immune systems, which work together to control the infection. The initial immune response to *Mtb* is mediated by innate immune cells, including macrophages and dendritic cells, capable of engulfing and phagocytosing the bacteria. Once inside the phagosome, *Mtb* evades eradication by manipulating the host immune response, preventing acidification of the phagosome and avoiding exposure to lysosomal enzymes. To counteract these strategies, innate immune cells secrete cytokines and chemokines that recruit other immune cells to the site of infection, including neutrophils, natural killer cells, and T cells. This results in the formation of granulomas, which are dense, granule-like aggregates of immune cells that surround the infected macrophages and sequester the bacteria. In granulomas *Mtb* can enter a dormant state where it can persist for years without causing disease. Reactivation of the bacterial infection can occur if the immune system becomes compromised, as in the case of HIV coinfection or immunosuppressive therapy, leading to the development of TB (6, 7). The adaptive immune response to *Mtb* is primarily mediated by $CD4^+$ T-cells, which recognize tubercle bacilli antigens presented by antigen-presenting cells (APCs) e.g. Ag85B (8), a wide range of peptides from proteins of secretion systems ESX-1, ESX-3, ESX-5 and also membrane-bound protease FtsH and putative conserved ATPase (9, 10). As for the group of *Mtb* non-protein components presented by APC, it has been shown to belong to it monoglycosolated mycolic acids, phospatydilinositols (e.g. LAM, PIM2, and PIM6), and diacylated sulfoglycolipids (11). Once activated, $CD4^+$ T-cells differentiate into T helper 1 (Th1) cells, which secrete cytokines such as interferon-gamma (IFN-γ) and tumor necrosis factor-alpha (TNF-α) that activate macrophages and enhance their bactericidal activity (12, 13). In addition to Th1 cells, other $CD4^+$ T cell subsets, such as Th17 and regulatory T-cells, also play a role in the immune response to *Mtb*. Th17 cells secrete cytokines including IL-17 that recruit neutrophils and enhance their ability to kill *Mtb*, while regulatory T cells help to dampen the inflammatory response and prevent tissue damage. However, the precise role of Th17 cells during *Mtb* infection is not fully clear due to their potential contribution to tuberculosis pathology and progression (14, 15).

Serum amyloid A (SAA), together with C-reactive protein, is classified as a positive, major acute-phase protein that is produced mainly by liver hepatocytes, and is present in low concentrations (1-2 μg/mL) in the blood of healthy individuals. However, during inflammation or infection, the concentration of SAA can increase dramatically within the first 4 hours, reaching values up to 1000-fold higher than baseline levels. Among the four isoforms of human SAA, namely SAA1, SAA2, SAA3 and SAA4, only two of them, SAA1 and SAA2, are considered acute phase proteins (A-SAA) (16). During the inflammatory response, mediators of A-SAA synthesis are endogenous and exogenous factors including IL-6, IL-1, TNF-α, bacterial endotoxin, and glucocorticoids (17–19). The high evolutionary conserved nature among vertebrates, low physiological serum concentration, and lack of documented deficiencies related to A-SAA indicate a significant biological role of this acute-phase protein. A-SAA is characterized by pleiotropic functional activity necessary to maintain homeostasis, which is associated not only with its high immunomodulatory potential but also with the involvement of A-SAA in tissue repair processes. Engagement of A-SAA in tissue regeneration and repair relay on its role in the mobilization of cholesterol, and functioning as an

angiogenic and retinol-binding protein (16, 20). The immunomodulatory functions of A-SAA depend on its proinflammatory and anti-inflammatory properties related to, inter alia, stimulation of the synthesis of many cytokines (e.g., TNF-α, IL-1β, IL-6, IL-23, GM-CSF, IL-10) and chemokines (e.g., CXCL8, CCL2), and an ability to activate the NLRP3 inflammasome of macrophages (17, 21). As a part of the innate immune system A-SAA plays an important role in the response to various infectious agents. The ability of A-SAA to opsonize pathogenic microorganisms allows the classification of this protein as one of the circulating pattern recognition receptors (PRRs) recognizing pathogen-associated molecular patterns (PAMPs). The specific binding interactions with A-SAA were described for gram-negative bacteria, including *Escherichia coli*, *Salmonella enterica*, *Shigella flexneri*, *Pseudomonas aeruginosa*, *Vibrio cholerae*, *Klebsiella pneumoniae* and *Serratia marcescens*. Furthermore, bacterial proteins, namely OmpA (*E. coli*) and its homolog OprF (*P. aeruginosa*) were identified as A-SAA ligands (22). Further study revealed that opsonization of gram-negative bacteria with A-SAA at physiological concentrations of this protein promotes their phagocytosis by neutrophils and macrophages and stimulates inflammatory mechanisms of professional phagocytes relying on increased synthesis of IL-10 and TNF-α (23).

More recently we described the specific interaction of human A-SAA (SAA1) with *Mtb* and identified 5 mycobacterial membrane proteins, namely AtpA (Rv1308), ABC (Rv2477c), EspB (Rv3881c), TB18.6 (Rv2140c) and ThiC (Rv0423c) as the pathogen effectors responsible for this interaction. The opsonization of tubercle bacilli with SAA1 favored bacterial entry into human monocyte-derived macrophages (MDMs), accompanied by a substantial increase in the load of intracellularly multiplying and surviving bacteria (24).

Here, using global transcriptomics analyses, we evaluated the functional response of human MDMs, isolated from the blood of healthy donors under elevated SAA-1 conditions and during infection with nonopsonized and SAA1-opsonized tubercle bacilli. Furthermore, we examined the functional response of mycobacteria to the intracellular environment of MDMs in the presence and absence of SAA1.

2 Materials and methods

2.1 Preparation of human MDMs and infection with *Mtb* and stimulation with human SAA1

Human monocytes were isolated from commercially available (Regional Blood Donation Station, Lodz, Poland) and freshly prepared buffy coats from anonymous healthy human blood donors (24, 25). Briefly, differentiation of MDMs was performed within 6 days of culturing 2.5×10^6 blood monocytes in 2.5 mL of IMDM medium (Cytogen GmbH, Greven, Germany) containing 10 ng/mL macrophage colony-stimulating factor (M-CSF), (Thermo Fisher Scientific, Waltham, MA, USA) in 6-well tissue plates (Corning Incorporated, Corning, NY, USA) at 37°C in a humidified atmosphere of 10% CO_2/90% air. Next, the cells were thoroughly washed three times to remove any nonadherent cells and antibacterial antibiotics and left to rest overnight.

We sought to determine the functional responses of MDMs to serum amyloid A and SAA-opsonized and nonopsonized *Mtb* at the transcriptome and cytokine levels as well as the transcriptional response of intracellularly located nonopsonized and opsonized tubercle bacilli. Live *Mtb* cells were subjected to initial interactions with human SAA1 (ProSpec-Tany TechnoGene Ltd., Ness-Ziona, Israel) at a final concentration of 15 μg/mL in IMDM containing 0.1% BSA (Sigma, St. Louis, MO, United States) and 3 mM $CaCl_2$ (Sigma Aldrich) for 90 min at 37°C (warm water bath) with gentle shaking every 30 min. The MDMs were infected with tubercle bacilli, as described by Kawka et al. (24), or were stimulated with human SAA1. Briefly, prior to infection, the culture medium was replaced with 2 mL human serum-free medium supplemented with 0.2% BSA, employing three washes to remove the excess SAA1 present in human serum (SAA1 concentrations in human sera were assessed by an SAA human ELISA Kit, Hycult®Biotech, Wayne, USA). Then the separate MDM cultures were infected with nonopsonized and SAA1-opsonized *Mtb* at an MOI of 1:20 or were treated with human SAA1 at a final concentration of 15 μg/mL. After 2 h of incubation of *Mtb*-infected MDMs, at 37°C in a humidified atmosphere of 10% CO_2/90% air, the extracellularly located tubercle bacilli were removed by extensive washing using IMDM medium. After 24 h of incubation supernatants were collected from the experimental and control cultures to determine the concentrations of selected cytokines. MDMs incubated with the medium alone and intracellularly located nonopsonized *Mtb* served as controls. To analyze the transcriptional response of MDMs and the pathogen, human cells were lysed with 2 mL of cold RLT Buffer (QIAGEN, Hilden, Germany) on ice for 5 min to isolate bacterial and human RNA.

Macrophages from four independent healthy blood donors were used to perform the experiments.

2.2 RNA extraction and RNA-Seq library construction

Following the infection cycle, macrophages were lysed in RNA later reagent (Invitrogen™, Walthman, MA, USA) following the manufacturer's protocol and were then centrifuged at 8,000 rpm for 15 minutes at 4°C to collect cell debris and mycobacteria. The supernatant was mixed with 3 volumes of TRIzol LS Reagent (Thermo Fisher Scientific, Waltham, MA, USA) and macrophage RNA was isolated using the Direct-zol™ RNA MiniPrep Plus reagent kit (Zymo Research, Irvine, CA, USA) according to the manufacturer's instructions. First, TRIzol cell lysate was mixed with an equal volume of 95% ethanol, transferred onto a Zymo-Spin IIC column and centrifuged. The column was washed with Direct-zol RNA PreWash, followed by RNA Wash Buffer and RNA was eluted with DNase/RNase Free Water. Total RNA from bacterial strains was isolated using TRIzol LS reagent as described previously (24, 26). Briefly, cells were disrupted twice using the MP disruptor system with the Quick prep adapter (MP Biomedicals, Irvine, CA, USA) and 0.1 mm silica spheres. DNA contamination of the RNA

samples was removed using a TURBO DNA-*free*™ Kit (Thermo Fisher Scientific, Waltham, MA, USA) according to the manufacturer's protocol. The integrity and quantity of RNA were examined using an Agilent 2100 BioAnalyzer fitted with an Agilent RNA 6000 Nano Kit, following the manufacturer's instructions (Agilent Technologies, Santa Clara, CA, USA).

The total RNA sequencing libraries were prepared as described previously in Plocinski et al., 2019 with minor modifications. Briefly, 2 µg of AMPure XP (Becton Dickinson, Burlington, NC, USA) bead-purified RNA was treated with a Ribo-off rRNA Depletion Kit (Human/Mouse/Rat, Vazyme, Nanjing, Jiangsu, China) to deplete rRNA (including cytoplasmic 28S, 18S, 5S rRNA, and mitochondrial 12S, 5.8S rRNA) from human total RNA (Illumina, San Diego, CA, USA) following the protocol accompanying the kit. The Ribo-Zero rRNA Removal Kit (Illumina, San Diego, CA, USA) was applied in the case of bacterial RNA. The sequencing libraries were prepared following the manufacturer's instructions for the KAPA Stranded RNA-Seq Kit, (KAPA Biosystems, Roche, Basel, Switzerland). The quantity and quality of libraries were inspected on an Agilent 2100 BioAnalyzer fitted with a DNA 1000 chip. The obtained cDNA libraries were sequenced using a NextSeq 500 System (Illumina and a NextSeq 500/550 Mid Output v2 Sequencing Kit (150 cycles), (Illumina, San Diego, CA, USA), thus guaranteeing 3 to 10 million paired-end reads per sample in the case of bacterial libraries and 10 to 25 million paired-end reads in the case of human origin libraries. RNA isolation, library generation, and RNA sequencing were performed in three independent replicates.

2.3 RNA-seq data analysis

For RNA-Seq data analyses, raw sequencing data were processed with Cutadapt v. 2.8. to remove sequencing adapters (27). Quality trimming with Sickle v.1.33 was then applied, allowing 30% quality and a minimal read length of 20 bp. Reads meeting the required criteria were next aligned to appropriate genomes using the Bowtie2 short read aligner (28) in the case of bacterial RNA or with the help of STAR RNA-seq aligner v.2.7 (29). The genome reference for *M. tuberculosis* H37Rv (https://mycobrowser.epfl.ch/releases, accessed on 12th April 2023; NC_000962.3, v.4) was obtained from the mycobrowser database and the human genome GRCh38 was retrieved from the gencode database (https://www.gencodegenes.org/human/, downloaded on 1st Dec 2018). Aligned data format transformations, sorting and indexing were performed with SAMtools v.1.9 (30) and BEDTools v. 2.27 (31) software suite to generate bedgraphs, whenever needed. While human reads were counted into transcript features within the STAR script, HTSeq v.0.13 was applied for bacterial reads counting (32). Sequencing results were visualized using Integrative Genomics Viewer (IGV) (33). Transcriptional changes were estimated with the online Degust RNA-Seq analysis platform with default parameters (http://degust.erc.monash.edu/, originally designed by D.R. Powell (34) or alternatively with help of the iDEP 96 online platform (http://bioinformatics.sdstate.edu/idep96/, accessed on 12th April 2023 (35). Genes (bacteria) or transcripts (human) with a log2 fold change greater than an absolute value of 1.585 (changing three times or more) and a false discovery rate (FDR) of <0.05 were considered differentially expressed in the current study.

2.4 Real-time PCR analysis

The qRTPCR technique was applied as a validation experiment of RNA-Seq data. Reverse transcription was performed using SuperScript III First-Strand Synthesis Super Mix (MP Biomedicals, Irvine, CA, USA) and random hexamers. The expression profile of the studied genes (CXCL8, CCL19, CSF2) was analyzed by qRTPCR using TaqMan chemistry and TaqMan™ Universal PCR Master Mix (Thermo Fisher Scientific, Waltham, MA, USA). The total reaction of 20 µl containing 1X TaqMan™ Universal PCR Master Mix, 1X TaqMan Gene Expression Assay (FAM) and 10 ng of cDNA was activated at 50°C for 2 minutes in order UNG incubation, followed by DNA Polymerase activation at 95 for 10 minutes. Next, 40 cycles of denaturation at 95°C for 15 seconds were followed by annealing/extention at 60°C for 1 minute. qRTPCR assays were run in triplicates on a QuantStudio™ 5 instrument (Applied Biosystems, Carlsbad, California, USA) in 96-well plates. Individual TaqMan Gene Assays with verified amplification efficiencies were purchased from Thermo Fisher Scientific and their corresponding product numbers are listed in Table S1. The number of tested transcripts was normalized to the glyceraldehyde-3-phosphate dehydrogenase (GAPDH) housekeeping gene and relative fold changes in gene expression in comparison to the control strain were calculated using the delta method ($2^{-\Delta\Delta CT}$).

2.5 Milliplex assay

The concentrations of cytokines, namely G-CSF (CSF3), GM-CSF (CSF2), IL-1α, IL-1β, IL-6, IL-8 (CXCL8), IL-12p40, IL-15, IL-27, TNF-α, CXCL10, CCL2, CCL7, CCL3, CCL4, and CCL5, were determined by applying a commercially available kit for the Milliplex® Multiplex assay and Luminex® Instrument (MERK KGaA, Darmstad, Germany) according to the manufacturer's recommendations. Milliplex® multiplex assays use the proprietary Luminex® xMAP® bead-based multiplex assay platform. Each magnetic MagPlex® microsphere bead is fluorescently coded with one of 500 specific ratios of two fluorophores (each spectrally distinct set is known as a bead region, fluorescent at λex 635 nm). Additionally, analyte-specific capture antibodies are bound to beads of a specific region, and the beads-bound analyte is detected with biotinylated secondary antibodies. The Luminex® instrument detects individual beads by region plus the streptavidin-conjugated R-Phycoerythrin (SAPE) signal, λex 525 nm, indicating the analyte is present. In short, wells of 96-well titration plates were washed with Wash Buffer at room temperature for 10 min with constant shaking using a plate shaker. Then 25 µL of standard or assay buffer or matrix solution or samples of collected culture media were added to appropriate

standard and control wells, background and sample wells, background, standard and control wells, and sample wells, respectively. Furthermore, the 25 µL of premixed beads were introduced to each well and all samples were incubated overnight (16-18 h) at 2-8 °C. On the next day, all wells were washed three times with 200 µL Wash Buffer and the immunoreaction was revealed using 25 µL Detection Antibodies and 25 µL Streptavidin-Phycoerythrin solution per well. After 30 min of incubation, all wells were again washed three times, and finally, 150 µL of Drive Fluid was added to each well and the plate was incubated for 5 min with constant shaking. To determine fluorescence values for standard, experimental, control, and background samples Luminex® equipment was employed. The results were analyzed, and median fluorescent intensity parameters were calculated using dedicated Milliplex assay Belysa™ software (MERK KGaA, Darmstad, Germany).

The assay was performed for three independent healthy blood donors and the samples of collected culture supernatants were run in triplicate.

3 Results

We have recently reported that *M. tuberculosis* specifically binds hSAA-1 and the opsonization with 5-fold higher, than the physiological concentration of this acute phase protein favoring bacterial entry into human macrophages and increasing the load of intracellularly multiplying and surviving bacteria (24). On the other hand, an early study by Samaha et al. (36) documented elevated levels of hSAA in both the sera and pleural fluids of tuberculosis patients (93 µg/mL), compared to the physiological concentration of this acute protein (1-2 µg/mL). Here, we asked whether the opsonization of tubercle bacilli with hSAA-1 affects the functional response of professional phagocytes to mycobacterial infection. To answer this question, we applied global RNASeq analysis of total RNAs isolated from human macrophages, prepared from buffy coats of healthy blood donors, to compare the transcription profiles of control MDMs with transcriptomes of MDMs infected with tubercle bacilli, MDMs treated with 5-fold higher than physiological concentration of hSAA-1 (15 µg/mL), and MDMs infected with *Mtb* opsonized with hSAA-1 at concentration of 15 µg/ml. Additionally, we evaluated the transcriptional response of nonopsonized and SAA-1 opsonized tubercle bacilli to the intracellular environment of human macrophages.

MDMs isolated from four healthy blood donors treated or not with hSAA-1 and MDMs infected with opsonized or nonopsonized tubercle bacilli were subjected to total RNA isolation and preparation of RNA libraries for sequencing. Satisfactory quality of RNA (RIN≥7), allowing for sequencing library preparation was obtained from MDMs of three blood donors (three repeats for each blood donor) in the case of control macrophages and macrophages treated with hSAA-1 and from four donors for MDMs infected with opsonized and nonopsonized mycobacteria. As expected, the principal component analysis (PCA) showed that the samples of the repeats of uninfected MDMs, as well as MDMs infected with tubercle bacilli, clustered separately of individual donors (Figure S1). By identifying the differentially expressed genes (DEGs) in uninfected MDMs of individual patients we found that approximately 500 to 2,000 genes were differentially expressed (minimum fold change 4, FDR cutoff 0.1) between donors (Table S2). The comparisons of DEGs in infected MDMs of individual patients, showing the different donors' responses to the infection, allowed us to find approximately 300 to 1,200 differentially expressed genes (min fold change 4, FDR cutoff 0.1) between donors. Then, based on all obtained sequences (RNASeq), comparative analyses were carried out to identify the functional response of MDMs to the presence of hSAA-1 and infection with hSAA-1-opsonized and nonopsonized *M. tuberculosis*. Principal component analysis (PCA) of all samples showed that the samples from uninfected macrophages clustered separately from the infected cells and the samples collected from the cells treated with hSAA-1 (Figure S2). The differential analysis of gene expression comparing all individual samples to untreated MDMs identified 1392 downregulated and 429 upregulated genes in MDMs infected with opsonized or nonopsonized *Mtb* or treated with hSAA-1 (Figure S3).

Treatment of MDMs with 5-fold higher than physiological concentrations of hSAA-1, namely 15 µg/mL, for 24 h resulted in alteration of the expression of 684 genes (Log2FC =|1.583|; fold change = |3|; FDR > 0.05). Of these 684 genes, 315 genes were downregulated, and 369 were overexpressed. Furthermore, the infection of MDMs with *Mtb* (MOI 10:1) significantly affected the expression of 633 genes, applying the same criteria of analysis, including 408 downregulated and 225 upregulated genes. Both, treatment with hSAA-1 and infection with *Mtb* led to inhibition of gene expression associated with cell division, cell cycle, nucleosome assembly and organization, and chromosome segregation. On the other hand, the most upregulated genes were classified in the immune response, cytokine-mediated signaling pathway, and response to external biotic stimulus (Figure 1). Among the up- and downregulated genes 157 and 191 genes, respectively, were affected by each stimulus.

The RNASeq analyses of MDMs were validated using quantitative RTPCR based on CCL19, highly induced in the presence of hSAA-1, CSF-2, induced after infection with tubercle bacilli, and CXCL8, induced in the presence of either stimuli. The qRTPCR was normalized based on GAPDH housekeeping gene expression (Figure 2).

3.1 The functional response of human macrophages to the infection with tubercle bacilli

Within the 364 MDM genes upregulated after infection with *Mtb* 223 were annotated as immune-related. The top ten most induced *Mtb*-infected MDM genes contained chemokines and cytokines, namely CXCL8, CCL15, CCL5, IL-1β, and receptor for IL-7 (Table S3). As expected the genes encoding other proinflammatory cytokines such as TNFα, IL-6, IL-12, IL-18 and IL-23 were upregulated in MDMs infected with tubercle bacilli, however, the anti-inflammatory cytokines, IL-10 and TGF-β, as

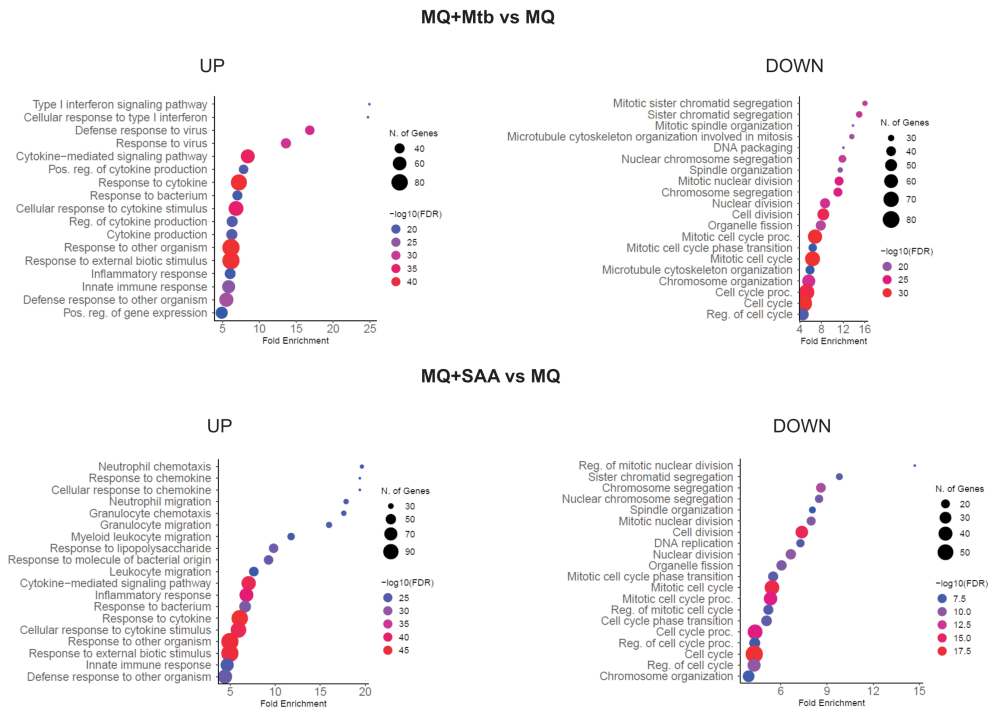

FIGURE 1
GO biological process enrichment analysis and dotplot charts. MQ represents control macrophages, MQ+Mtb, macrophages infected with *Mtb*; MQ +SAA, macrophages treated with SAA. The diagram was generated by ShinyGO 0.77.

well as the antimicrobial peptide cathelicidin were downregulated. As mentioned above, infection with *Mtb* also induced a large number of genes encoding chemokines of the CC and CXC subfamilies, especially chemokines interacting with the receptors CCR5 (CCL3, CCL4, CCL5, CCL8), CXCR1 (CXCL1, CXCL5, CXCL6, CXCL8), CXCR2 (CXCL2, CXCL3, CXCL7), and CXCR3 (CXCL9, CXCL10, CXCL11); however, the receptors CXCR1 and CXCR2 per se were downregulated. The other upregulated cytokines included IL-7, IL-15, CSF2 and their receptors, and CSF3. The upregulated cytokines of the TNF family were TNF, TRAIL, and BAFF, and those of the TGF-β family were INHBA and BMP6. In addition to the abovementioned anti-inflammatory cytokines we also observed the reduced expression of other chemokines and cytokines such as CCL28, CXCL12, and IL-16 (Figure S4). Despite the strong overproduction of many chemokines, the chemokine receptors and genes of the chemokine signaling pathway were usually unaffected or downregulated in *Mtb* infected MDMs. The most important exception to this negative regulation is that the Jak-STAT signaling pathway was significantly induced in the infected MDMs.

The early response to *Mtb* infection is the internalization and intracellular killing of bacilli by alveolar macrophages. Two genes

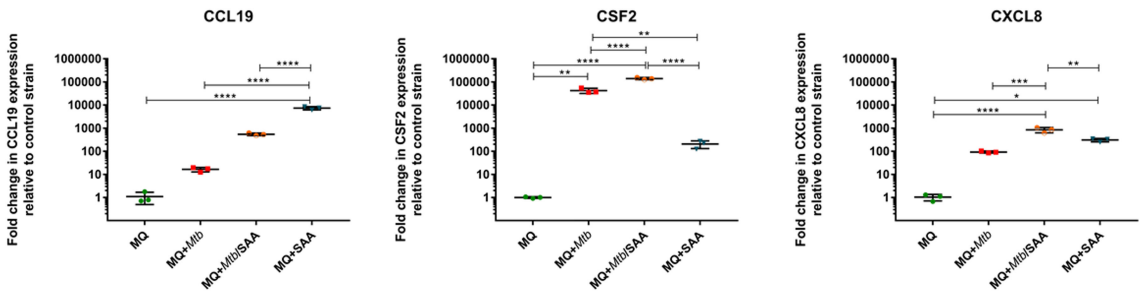

FIGURE 2
RTPCR (TaqMan) analysis of transcripts for CCL19, CSF2, and CXCL8 genes of MDMs. MQ represents control macrophages, MQ+*Mtb*, macrophages infected with *Mtb*; MQ+*Mtb*/SAA, macrophages infected with *Mtb* opsonized with SAA; MQ+SAA, macrophages treated with SAA. The number of tested transcripts was normalized to the glyceraldehyde-3-phosphate dehydrogenase (GAPDH) housekeeping gene and relative fold changes in gene expression in comparison to the control strain were calculated using the delta method (2-ΔΔCT). The data distribution was evaluated by the Shapiro-Wilk normality test. Statistical analysis was performed by one-way ANOVA with a *post-hoc* Tukey test. *represents $p<0.05$, **$p<0.0021$, ***$p<0.0002$, ****$p<0.0001$.

encoding proteins involved in the phagosome formation process, namely coronin and F-actin, were downregulated in infected MDMs. In the early phagosome, weaker expression was observed for vATPase engaged in the phagosome acidification process. Genes encoding major proteins of mature phagosomes, such as Rab7, dynein, and TUBB were also silenced in the infected MDMs. Furthermore, the mature phagosomes are fused to lysosomes and reactive oxygen species are produced to kill intracellularly deposited bacilli. A few genes involved in this process are downregulated in the infected MDMs including major lysosomal membrane protein LAMP, Sec61, lysosomal acid hydrolase MPO and two genes of NADPH oxidase complex p22phox and p40phox. On the other hand, the TAP and p47phox genes are overexpressed. The processed bacterial antigens can be presented by MDMs on the major histocompatibility complex (MHC) molecules class I and class II, to the cells of adaptive immune response. Antigen processing and presentation by MDMs infected with tubercle bacilli can be affected due to the downregulation of MHC class II expression. The phagocytosis process can be facilitated by a number of receptors present on the surface of macrophages. The complement receptor CR1, opsonin iC3b, integrins αVβ3 and α5β1, and scavenger receptor LOX-1 are overexpressed in MDMs infected with *Mtb*. On the other hand, Fc receptor FcyR, Toll-like receptors TLR4, TLR5, and CD14, C-lectin receptors MR and DC-SIGN, scavenger receptors SRA1, MARCO, SRB1, CD36, and collectins are attenuated in infected MDMs. The major phagosome and phagolysosome genes expressed in MDMs and MDMs infected with *M. tuberculosis* are depicted in Figure 3.

3.2 The functional response of human macrophages in the presence of elevated level of hSAA-1

A total of 269 out of 467 MDM genes upregulated in the presence of an elevated concentration (15 μg/mL) of hSAA-1 were classified as immune-related. The top ten most induced hSAA-1 treated MDM genes contained the same chemokines and cytokines as those induced by *Mtb* infection, such as CXCL8, CCL15, CCL5, IL-1β, and receptors for IL-7 and IL-2 (Table S3). We also observed the same pattern of upregulated proinflammatory cytokines (TNFα, IL-6, IL-12, IL-18, and IL-23) and downregulated anti-inflammatory cytokines (IL-10, TGFβ, and antimicrobial peptide cathelicidin) in MDMs treated with hSAA-1 or infected with tubercle bacilli. In the presence of hSAA-1 MDMs induced very similar, but not identical, patterns of genes encoding chemokines of

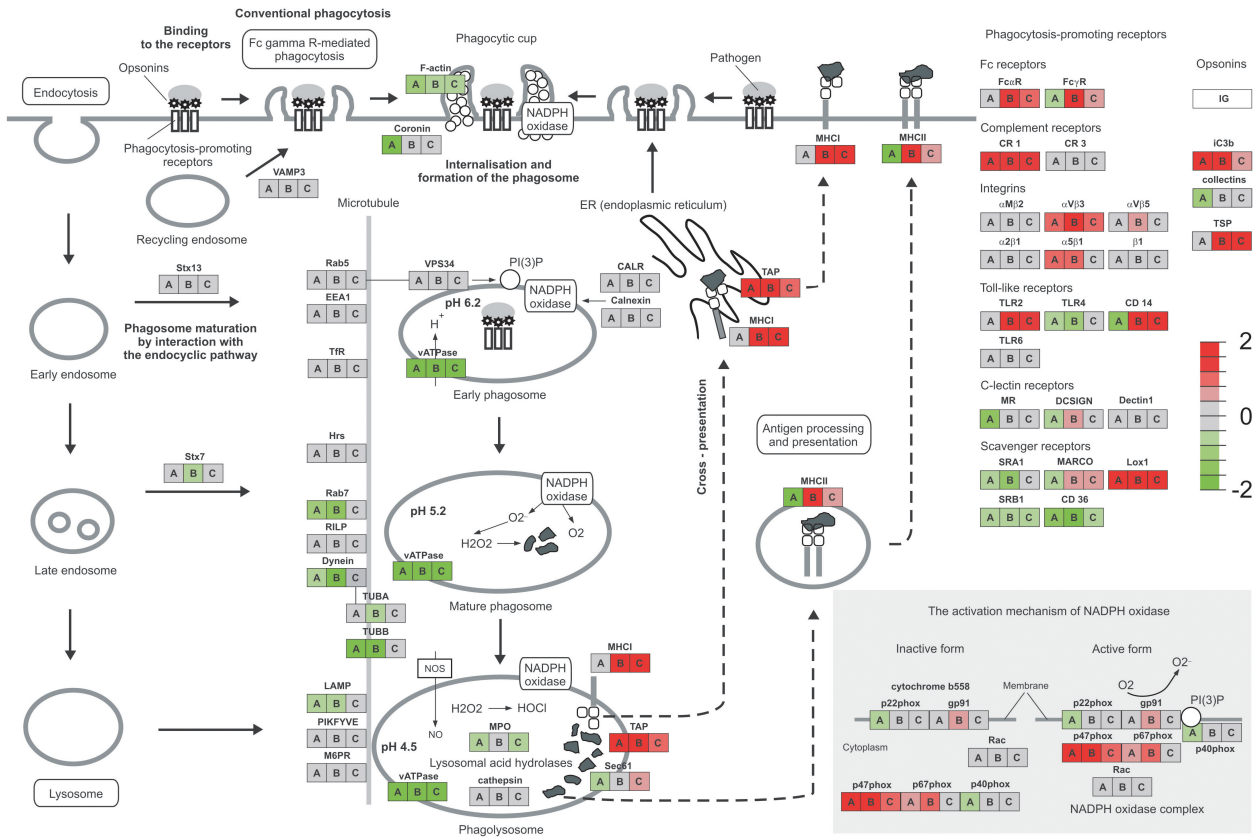

FIGURE 3
Phagosome and phagocytosis promoting receptors of MDMs. The expression level of genes compared to the control is presented as a heatmap. MDMs infected with *Mtb* are represented by A, hSAA-1 treated MDMs by B, MDMs infected with hSAA-1 opsonized *Mtb* compared to MDMs infected with nonopsonized *Mtb* by C. The analysis was completed based on total RNA sequencing isolated from MDMs of three blood donors (control MDMs and hSAA-1 treated MDMs) or four blood donors (MDMs infected with hSAA-1 opsonized or nonopsonized *Mtb*) in three biological repeats each, completed separately for each comparison using the iDEP.96 platform and presented at each gene as A, B, and C.

the CC and CXC subfamilies. Additionally, apart from chemokines interacting with the receptors CCR5 (CCL3, CCL4, CCL5, CCL8), CXCR1 (CXCL1, CXCL5, CXCL6, CXCL8), CXCR2 (CXCL2, CXCL3, CXCL7), and CXCR3 (CXCL9, CXCL10, CXCL11) which were induced by both stimuli, hSAA-1 also induced the chemokine ligand of the CXCR5 receptor, namely CXCL13. The receptors CXCR1 and CXCR2 were downregulated, and the receptor CXCR5 was upregulated. The other cytokines upregulated in the presence of hSAA-1 included IL-7, IL-15, CSF2 and their receptors, and CSF3. The upregulated cytokines in the TNF family were TNF, VEGI, and CD70, and those in the TGF-β family were INHBA and BMP6. The downregulated cytokine pattern in hSAA-1 treated or *Mtb* infected MDMs was also very similar with a few additional cytokines downregulated in the presence of hSAA-1 (e.g., LEP, IFNA, OX-40 L, BMP2) (Figure S5). MDMs treated with hSAA-1 presented strong overproduction of many chemokines and only a few upregulated chemokine receptors such as CXCR5 and CCR7. In the downstream chemokine signaling pathway, hSAA-1 induced Jak-STAT, IκB, and NFκB genes. The main difference between hSAA-1 treatment and *Mtb* infection of MDMs in the internalization and phagosome formation process is downregulation of coronin observed only after *Mtb* infection. The acidification of phagosomes is affected by vATPase downregulation in the presence of both stimuli. In contrast to infection with *Mtb* in which MHC class II was downregulated, MHC class I and II were significantly overexpressed in the presence of hSAA-1, indicating the role of this stimulus in the induction of antigen processing and presentation. The other significant difference between both stimuli was the MDM downregulation of lysosomal acid hydrolases and genes encoding some subunits of the NADPH oxidase complex, exclusively after infection of MDMs with *Mtb*. Additionally, except for p47phox and p67phox, treatment with hSAA-1 also induced the expression of gp91, the other component of NADPH oxidase. Different transcriptional responses to tubercle bacilli infection and treatment with hSAA-1 were also observed for genes encoding phagocytosis promoting receptors. hSAA-1 induced the expression of Fc receptors (FcαR, FcyR), which were unaffected (FcαR) or downregulated (FcyR) after *Mtb* infection. The complement receptor CR1, opsonin iC3b, integrins αVβ3 and α5β1, and scavenger receptor LOX-1 were overexpressed in MDMs treated with hSAA-1 or infected with *Mtb*. However, exclusively MDMs treated with hSAA-1 also induced genes coding for thrombospondin (TSP), Toll-like receptor TLR2, CD14 (downregulated in infected MDMs), C-lectin receptor DC-SIGN and scavenger receptor MARCO (Figure 3).

3.3 hSAA-1 enhances the functional response of MDMs to *M. tuberculosis* infection

Since hSAA-1 opsonizes tubercle bacilli, we asked whether such opsonization modulates the functional response of MDMs to the infection with *Mtb*. The *in vitro* opsonized bacilli were used for infection of MDMs, and then 24 h postinfection total RNA was isolated and sequenced. Comparing RNASeq analysis for MDMs infected with nonopsonized and hSAA-1-opsonized *Mtb*, 96 genes with significantly affected expression (FDR=0.05, fold change=3, Log2FC=1.583) were detected, including 90 overexpressed genes. The top ten most induced genes of MDMs infected with opsonized bacilli, compared to MDMs infected with nonopsonized bacilli, contained interleukins IL-12β, IL-1β and CCL1 chemokine, and receptor for IL-2 (Table S3). Most chemokines of the CC and CXC subfamilies overexpressed in MDMs treated with hSAA-1 or in MDMs infected with tubercle bacilli presented synergistic effects in MDMs infected with opsonized bacilli resulting in elevated levels of transcripts (e.g., CCL3, CCL4, CXCL1); however, CCL19 and CCL7 presented elevated levels of transcripts exclusively in the presence of hSAA-1 (Figure 4, Figure S6).

On the other hand, CXCL11 was downregulated in the presence of opsonized bacilli compared to MDMs infected with nonopsonized *Mtb*. The downregulation dependent on hSAA-1 opsonization of tubercle bacilli was also determined for genes encoding the IL-9 receptor, OX40 ligand (OX40L) of the TNF family and growth differentiation factor GDF9. The hSAA-1 dependent upregulation was identified for a few genes encoding cytokines (IL-10, lymphotoxin β - LTβ) and cytokine receptors (IL-12R, IL-17R, IL-10R, activin A receptor like-protein 1 -ACVRL1), (Figure S6). The opsonization of tubercle bacilli with hSAA-1 also affects the expression of a few genes encoding proteins involved in phagosome formation, maturation and fusion to lysosomes. If MDMs are infected with hSAA-1-opsonized bacilli, the F-actin, vATPase and myeloperoxidase (MPO) genes are attenuated compared to infection with nonopsonized bacilli; however, genes encoding transporters associated with antigen processing (TAP) and MHC class I and II molecules are significantly upregulated. The opsonized bacilli also upregulate a component of the NADPH oxidase complex, namely p47phox. Within the phagocytosis-promoting receptors, the opsonization of *Mtb* with hSAA-1, led to the upregulation of Fc receptors (FcαR, FcyR), complement receptor CR1, integrin αVβ3, Toll-like receptor TLR2, CD14, scavenger receptor LOX-1, TSP and opsonin iC3b. On the other hand, hSAA-1 inhibits the expression of scavenger receptors SRB1 and CD36 (Figure 3).

3.4 The response of human professional phagocytes to hSAA-1 and *M. tuberculosis* infection is detectable at the protein level

The functional response of MDMs to hSAA-1 and/or tubercle bacilli was verified for selected cytokines at the protein level by applying the Milliplex system. The concentrations of protein were determined in the culture medium of MDMs, MDMs treated with 5-fold higher than physiological concentration of hSAA-1 (15 μg/mL), MDMs infected with tubercle bacilli, and MDMs infected with *Mtb* opsonized with hSAA-1. Based on the RNASeq results, sixteen cytokines were selected for the analysis and included cytokines induced in the presence of either stimulus (TNF-α, CCL5, CXCL8, CCL4, IL-15, IL-1β, IL-6, CCL3, CSF3), induced exclusively by hSAA-1 (CCL3, IL-12β, CCL2), induced exclusively by infection with *M. tuberculosis* (CSF2, IL-27, CXCL10), and induced only in the presence of both stimuli (CCL7), (Table S3). Cytokines were identified in the culture medium of control MDMs at various

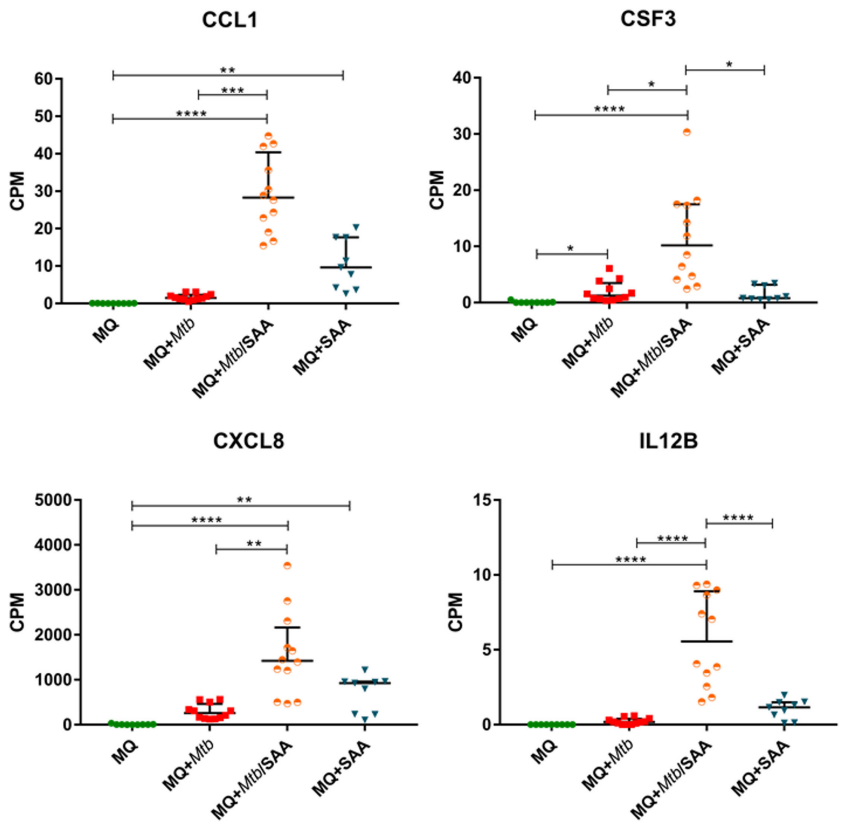

FIGURE 4
MDM gene expression of selected cytokines. CPM (counts per million) analysis of transcripts for selected cytokines in control MDMs (MQ), MDMs infected with nonopsonized *Mtb* (MQ+Mtb), hSAA-1 opsonized *Mtb* (MQ+Mtb/SAA), and MDMs treated with hSAA-1 (MQ+SAA). The assay was performed for three (MQ, MQ+SAA) or four (MQ+Mtb, MQ+Mtb/SAA) independent healthy blood donors in three biological repeats each. Statistical analysis was performed by nonparametric data distribution, which was evaluated by the Shapiro-Wilk normality test. Furthermore, statistical analysis was performed by Kruskal-Wallis one-way ANOVA with *post-hoc* Dunn's test or one-way ANOVA with *post-hoc* Tukey's test (IL12B). *represents $p<0.05$, **$p<0.0021$, ***$p<0.0002$, ****$p<0.0001$.

concentrations. The most abundant cytokines detected at concentrations over 1000 pg/mL in the culture medium of control MDMs were CCL2 and CXCL8. On the other hand, the concentrations of CCL5, CSF2, CXCL10 and IL-12β were below 1 pg/mL. The other cytokines produced by control MDMs were at concentrations >1<10 pg/mL (IL-15, IL-1β, CSF3), >10<100 pg/mL (CCL4, IL-27, IL-6, CCL3), and >100<1000 pg/mL (CCL7). The treatment of MDMs with hSAA-1 increased the concentrations of cytokines over 9.5 ng/mL (IL-6, CXCL8, CCL2, CCL3, CCL5, TNF-α), 1 ng/mL (CSF3, CSF2, IL-12B, CXCL10, CCL7, CCL4), 100 pg/mL (IL-27), 10 pg/mL (IL-15) and >1<10 pg/mL (IL-1α, IL-1β). The lowest 4-fold increase in the cytokine concentration after treatment with hSAA-1 was noted for interleukin IL-27, and the most abundant increase in the concentrations was observed for CCL5, CSF2, IL-12β, and CXCL10. Infection of MDMs with tubercle bacilli led to an increase in the concentration of most tested cytokines except CCL2 and IL-27. The highest concentrations, over 9.5 ng/mL were detected for CXCL8 and CCL3. The culture medium of MDMs infected with *Mtb* also contained over 1 ng/mL of CSF3, CCL2 (decrease in concentrations compared to control MDMs), CCL7, CCL4 and TNF-α. The cytokines IL-6, IL-27, and CCL5 were detected at concentrations over 100 pg/mL, CSF2, IL-1α, IL-1β, IL-12β and CXCL10 at concentrations above 10 pg/mL, and IL-15 at concentrations below 10 pg/mL. The most significant, at least 100-fold, increase in the concentrations was detected for CSF2, CSF3, IL-1α, CCL3, CCL4, CCL5 and TNF-α. The infection of MDMs with *Mtb* opsonized with hSAA-1, compared to the infection with nonopsonized bacilli, led to at least a 2-fold increase in the concentrations of CSF2, CSF3, IL-1α, IL-1β, IL-6, IL-12, CCL15, and TNF-α with the most potent 10-fold increase observed for CCL5. The concentrations of other tested cytokines (CXCL8, IL-15, IL-27, CXCL10, CCL2, CCL7, CCL3, CCL4) were at similar levels in the media of MDMs infected with opsonized and nonopsonized bacilli (Figure 5, Figure S7).

3.5 The functional response of tubercle bacilli to the intracellular environment of human macrophages

Human monocyte-derived macrophages obtained from buffy coats of four healthy blood donors were infected with *Mtb* opsonized or nonopsonized with hSAA-1. The bacilli were

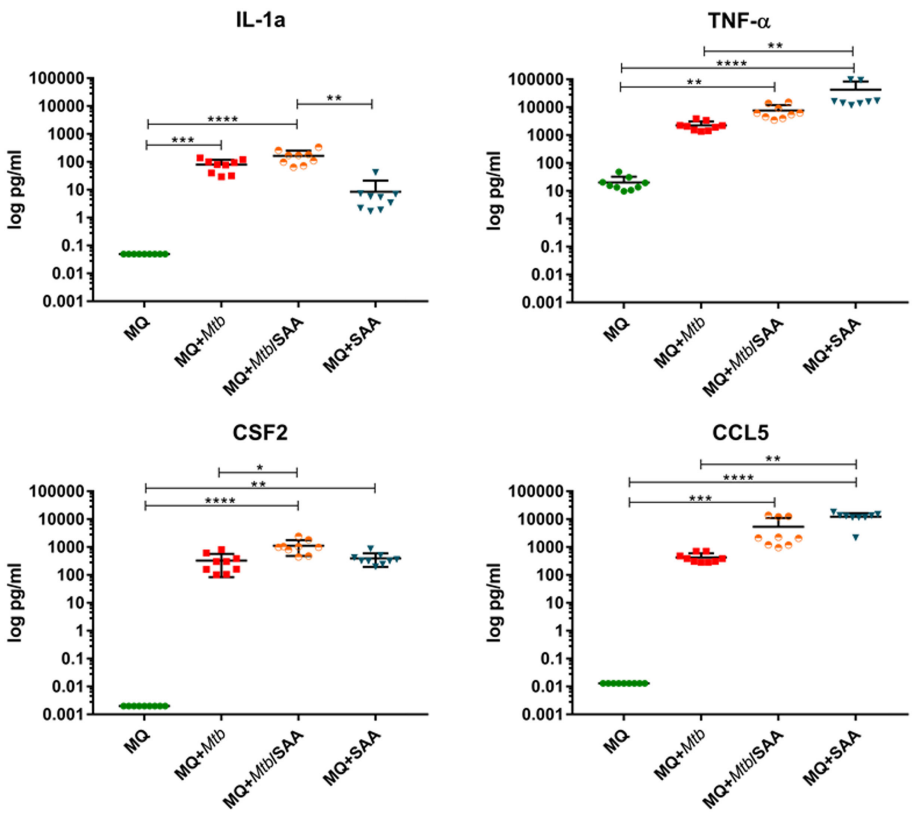

FIGURE 5
The concentrations of selected cytokines were determined using the Milliplex system. The protein level was assessed in the cell supernatant of control MDMs (MQ), MDMs infected with nonopsonized *Mtb* (MQ+*Mtb*), hSAA-1 opsonized *Mtb* (MQ+*Mtb*/SAA), and MDMs treated with hSAA-1 (MQ +SAA). The assay was performed for three independent healthy blood donors and the samples of collected culture supernatants were run in triplicate. The data distribution was evaluated by the Shapiro-Wilk normality test. Furthermore, statistical analysis was performed by Kruskal-Wallis one-way ANOVA with *post-hoc* Dunn's test. *represents p<0.05, **p<0.0021, ***p<0.0002, ****p<0.0001.

released from phagocytes 24 h postinfection and used for RNA isolation and sequencing. The control bacilli were incubated in the same media without MDMs for the same time. The bioinformatic analysis of RNASeq data shows the global response of bacilli to the intracellular environment of macrophages and the potential modulation of this response by hSAA-1. Based on our selection criteria for differentially expressed genes (Log2FC = |1.583|; fold change = |3|; false discovery rate (FDR) of <0.05), global transcriptional analysis of tubercle bacilli released from macrophages identified 302 genes presenting significantly changed expression levels. Of these 139 genes were upregulated, while 163 were downregulated. Among the most enriched GO pathways in DEGs of tubercle bacilli residing in human macrophages the cellular response to iron starvation, metal ion homeostasis, response to hypoxia and response to other organisms or abiotic stimuli were identified (Figure 6).

A massive increase in expression of the whole IdeR-regulated machinery of siderophore-based iron acquisition (MbtA-G, IrtAB, MmpL4/S4, HisE, PPE37, Rv3403c, Rv3839) (37) and critical for survival under host-mediated stress regulators of siderophore synthesis (HubB) (38) confirms that tubercle bacilli extensively prevent iron sequestration inside macrophages. The intracellular environment of MDMs increases the expression of a whole set of virulence regulators (EspR, Lsr2, WhiB1, WhiB2) and proteins that directly coordinate the inhibition of phagosomal maturation (SapM, EsxH, AprB), phagosomal rupture, biofilm formation, pH sensing, escape from the phagolysosome or modulate the T-cell response and secretion of immunomodulatory PE/PPE proteins (39–41). Moreover, a significant change in the expression of secretion systems such as SEC, TAT, ESX-1, and ESX-3 involved in host-pathogen encounters, promoting growth in macrophages and inhibiting the host immune response was also identified (42, 43). Overall, many identified DEGs represent regulons of two-component signal transduction systems that are strictly involved in response to hypoxia, NO level, low pH, and adaptation to the increasing level of CO_2 (PhoPR, DevR-DevS, TrcRS, KdpDE) including the significant overrepresentation of PhoPR-regulated genes, within upregulated CDSs and an almost complete set of DevR-DevS system genes, within downregulated CDSs. PhoPR regulates approximately 80 to 150 genes essential for virulence and complex lipid biosynthesis (40). Indeed, a closer look at the lipid metabolism pathways upregulated upon infection reveals significant induction of almost a complete array of genes encoding the synthesis and transport of sulfolipids, acylated trehaloses, or phenolic glycolipids – lipids playing crucial roles in mycobacterial virulence (44) (Figure 7).

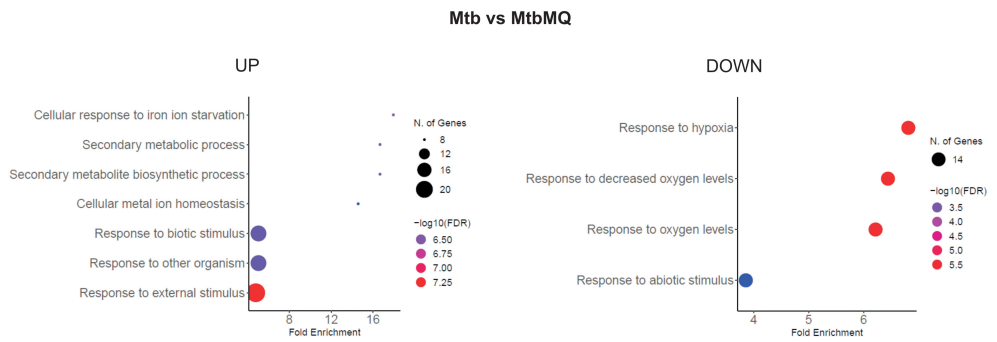

FIGURE 6
GO biological process enrichment analysis of *Mtb* intracellular environment-induced changes. Mtb represents control bacilli, MtbMQ represents *Mtb* isolated from MDMs. The diagram was generated by ShinyGO 0.77.

Along with increased virulence lipid synthesis, the data also suggests induction of the cell wall mycolic acid remodeling program and modification in arabinogalactan mycolylation or lipid glycosylation patterns. Conversely, we observed extremely strong downregulation of the DevR-DevS-regulated triacylglycerol synthesis gene – *tgs-1* and the absence of any transcriptional response within lipid catabolism or pathways ameliorating lipid degradation metabolites such as the methylmalonyl pathway or methylcitrate cycle, with the exception of increased isocitrate lyase - *icl*1 gene expression also involved in TCA and the glyoxylate cycle. To analyze

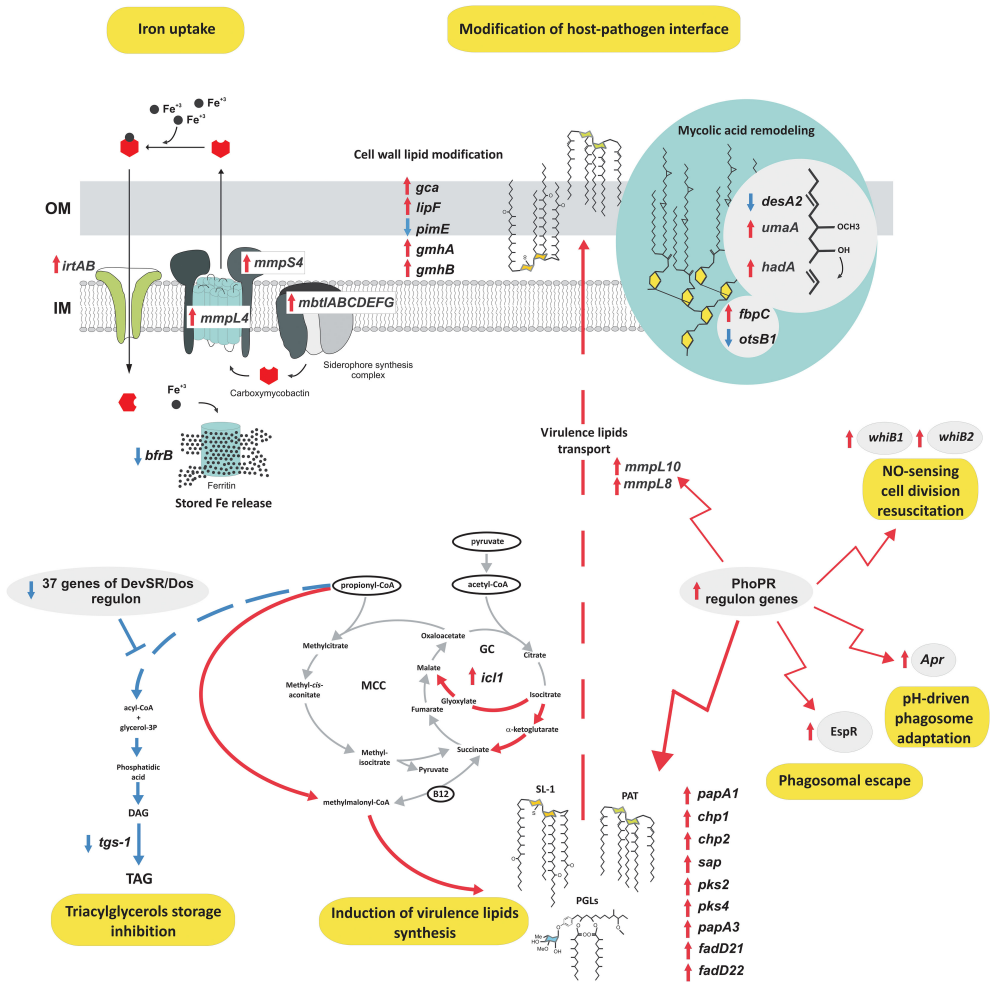

FIGURE 7
The functional response of tubercle bacilli to the intracellular environment of MDMs. Red arrows, upregulation; blue arrows, downregulation; IM, inner membrane; OM, outer membrane; SL, sulfolipids; PAT, polyacylated trehalose; PGL, phenolic glycolipids.

the specific effect of hSAA-1 opsonization on the transcriptional profile of tubercle bacilli infecting human macrophages we compared the transcriptional response of opsonized and nonopsonized *Mtb* to the intraphagosomal environment. The previously identified *in vitro* response of *Mtb* to SAA was not considered in this analysis (24). Principal component analysis (PCA) demonstrated that transcriptomic responses of the opsonized and nonopsonized bacteria are clustered (Figure S8). Indeed, their response to the intraphagosomal environment was almost identical in most aspects mentioned above, however, a detailed comparison of DEGs between these two datasets allowed the identification of 11 genes whose infection-induced expression change was found to be specific only for the bacilli opsonized with hSAA-1 (Table S4). Conversely, 28 genes differentially expressed in nonopsonized bacilli infecting MDMs displayed unchanged expression in *Mtb* opsonized with hSAA-1 (Table S4). Most of the 39 mentioned genes represent membrane/transmembrane or cell wall-associated/secreted proteins, transcriptional regulatory proteins, elements of efflux systems, or toxin-antitoxin components. The common feature is their presumed exposition in the host-pathogen interface, reported antigenicity, involvement in virulence, stress adaptation, or metal ion/drug efflux.

4 Discussion

Alveolar macrophages (AMs) and interstitial macrophages (IMs) are two major macrophage subsets in the lungs. AMs located in the alveolar space of the lung present higher engulfment capacity against antigens and pathogens and constitute the first line of defense. AMs play a central role in homeostasis, tissue remodeling and during pathogen infection and inflammation, and produce various cytokines such as TGF-β, IL-6, and type I interferons (45). IMs form a heterogeneous population in the parenchyma, between the microvascular endothelium and alveolar epithelium, engulf bacteria and secrete IL-1, IL-6, IL-10, and TNF-α (46). The capacity of macrophages is modulated by a number of factors including SAA1, which is highly upregulated in response to inflammation, as well as, during tuberculosis. MDMs, which we used in our study, are considered the current best alternative experimental model to alveolar macrophages containing two different cell types, namely tissue-resident alveolar macrophages (TR-AMs) and monocyte-derived alveolar macrophages (MdAMs). Although TrAMs and MdAMs possess different origins and some transcriptional characteristics, both subsets of these cells are important in pathogen clearance, initiation and resolution of inflammation, and lung tissue recovery. Additionally, MdAMs, originating from blood monocytes recruited to the lungs by cytokines and chemokines produced by TrAMs and other cells, could also participate in the restoration of a depleted pool of TrAMs (4, 47). However, despite the cooperation of TrAMs and MdAMs during *Mtb* infection, these two populations of lung macrophages possess different phenotypes. While MdAMs are polarized to the M1 type of macrophages, TrAMs cells exhibit characteristics of both classically and alternatively activated M1 and M2 macrophages, respectively (48). Despite the high level of expression of mannose receptors, type A scavenger receptors, TLR9 receptor, and high phagocytic activity, the suppressor properties of these cells are indicated, due to the low activity of the TLR2 receptor, CD80 and CD86 costimulatory molecules, and weak bactericidal activity, and limited synthesis of reactive oxygen compounds compared to peripheral blood monocytes and neutrophils (45, 49–52). In addition, the reduced ability of TrAMs to present antigens, as well as their inhibitory effect on the activity of dendritic cells and lymphocyte activation, are also emphasized (53–56). Considering the above-mentioned differences between MdAMs and TrAMs, it can be cautiously noted that the response of these two types of macrophages to hSAA-1 stimulation and infection by non-opsonized and hSAA-1-opsonized tubercle bacilli may differ, however, a reliable response requires further research.

Here, we analyzed the functional response of MDMs to a 5-fold higher than physiological concentration of hSAA-1 (15 μg/mL) in comparison to the response of MDMs to *Mtb* infection. We found that at the cytokine gene expression level the phagocyte response to both stimuli was very similar, with abundant expression of genes coding for pro-inflammatory cytokines, as well as chemokines CXCL8, CCL15, CCL5, and downregulation of anti-inflammatory cytokines. The only cytokines induced by hSAA-1 but not by tubercle bacilli were chemokines CCL19 and CXCL13. On the other hand, the TNF-family cytokine TRAIL (TNF-related apoptosis-inducing ligand) was upregulated after infection but not after hSAA-1 treatment. CCL19 was described as a strong chemotactic factor for B cells and various subpopulations of T lymphocytes (57), and CXCL13 is selectively chemotactic for B cells and elicits its effects by interacting with chemokine receptor CXCR5 (58), which was also upregulated as a result of hSAA-1 stimulation. TRAIL is a protein that functions as a ligand that induces caspase-8-dependent apoptosis. In cells expressing DcR2 (Decoy receptor 2), TRAIL binding activates NFκB, leading to transcription of genes known to antagonize the death signaling pathway and/or to promote inflammation (59).

The analysis of the functional response of MDMs to the hSAA-1 opsonized bacilli has shown that the response to both stimuli is not only very similar but also has a synergistic effect for many genes encoding cytokines (Table S5). However, in some cases, the opsonization of *Mtb* with the human acute phase protein had the opposite effect compared to that induced by each stimulus individually. MDMs infected with the opsonized tubercle bacilli, compared to MDMs infected with the nonopsonized pathogen, downregulated CXCL11 and upregulated IL-10 genes which were upregulated and downregulated in the phagocytes treated by hSAA-1 and infected with nonopsonized *Mtb*, respectively. CXCL11 is chemokine strongly induced by IFN-γ and IFN-β, chemotactic for activated T cells (60). IL-10, known as human cytokine synthesis inhibitory factor (CSIF), is an anti-inflammatory cytokine with multiple, pleiotropic effects related to immunoregulation and inflammation. It downregulates the expression of Th1 cytokines, MHC class II antigens, and costimulatory molecules on macrophages. It also enhances B-cell survival, proliferation, and antibody production. IL-10 can block NF-κB activity and is involved in the regulation of the JAK-STAT signaling pathway induced in both MDMs treated with hSAA-1 and infected with *Mtb*. IL-10 induces STAT3 signaling via phosphorylation of the cytoplasmic tail of the IL-10 receptor (61). A similar response to

infection with virulent *M. tuberculosis* H37Rv, compared to avirulent *M. tuberculosis* H37Ra and *M. bovis* BCG, was reported for the THP-1 human macrophage cell line. Authors observed significant increase in the expression of IL-1β, TNF-α, CCL3, CCL4, CSF2 and downregulation of IL-10 and CCL2. An increased gene expression profile was also observed for chemokines such as CXCL1, CXCL2, CXCL3, CXCL8, CCL3, and CXCL4 engaged in the recruitment of polymorphonuclear cells, such as neutrophils. Of the listed cytokines, in our MDM model, we observed a different response only for the chemokines CCL2 presenting a chemotactic activity for monocytes and basophils, and CXCL4 a strong chemoattractant for neutrophils, fibroblasts, and monocytes, both showing increased expression in the presence of the nonopsonized and, in particular, opsonized mycobacteria. The infection of THP-1 with virulent bacilli selectively induced IL-23 rather than IL-12 and the enhanced expression of IL-17RB and IL-17RE receptors indicating the Th17-dominated inflammatory T-cell response (62). However, infected MDMs induced the expression of both IL-23 and IL-12 and significantly downregulated the expression of IL-17 receptors. Neither infection with *Mtb* nor treatment with hSAA-1 induced the expression of Th2 cytokines in MDMs, namely IL-4 and IL-13, which polarize macrophages to an M2 activation status (63–65). At least at the time of analysis, 24 h postinfection, MDMs presented proinflammatory M1 polarization.

The response of MDMs to hSAA-1 and *Mtb* infection revealed more differences in the gene expression encoding players in phagosome formation, maturation, and phagolysosome fusion. Although both factors inhibit phagosome acidification through downregulation of vacuolar ATPase (vATPase) (66), genes encoding coronin, lysosomal acid hydrolases, Sec61 translocating antigens from the endosomal compartments to the cytosol (67) and some components of the NADPH oxidase complex were downregulated exclusively in *Mtb* infected MDMs. On the other hand, both stimuli enhanced the expression of TAP, which is involved in antigen processing and translocation; however, hSAA-1 exclusively affects antigen processing and presentation by overexpression of MHC class I and II molecules, with the latter being downregulated in *Mtb* infected MDMs. Manipulation and inhibition of antigen processing and presentation are considered highly evolved evasion strategies of *Mtb* resulting in its intracellular persistence in the hostile microenvironment of macrophages and in an altered specific T-cell adaptive immune response. One of these pathways disrupted by tubercle bacilli is antigen processing and presentation served by MHC II molecules. After infection, *Mtb* can affect the expression of MHC class II in macrophages by blocking the fusion of phagosomes with lysosomes and phagosome acidification (11, 68). Inhibition of phagolysosome fusion could potentially be a result of the functional activity of *Mtb* proteins (e.g. kinase G) and is indicated as an important mechanism allowing tubercle bacilli to avoid the activity of lysosomal hydrolases (69), which are also downregulated by the pathogen. Consequently, the lack of development of the phagolysosome compartment disrupts intracellular processing of the bacterial antigens and loading of the peptides onto MHC class II molecules. The diminished phagosome acidification level could also be related to the downregulation of vacuolar proton-ATPase expression observed in our study. The studies performed in other laboratories revealed selective inhibition of incorporation or retention of intact vATPase by the mycobacterial phagosome, which could result in the arrest of the phagosome acidification and bacterial antigen processing and presentation to the $CD4^+$ T lymphocytes responsible for the development of an effective adaptive immune response (70). Surprisingly, the expression of the gene encoding vATPase was also downregulated by SAA1; however, it did not lead to the downregulation of the expression of MHC class II, which was overexpressed in SAA1-stimulated macrophages. In addition to manipulating MHC II-dependent antigen processing and presentation, *Mtb* can also affect the MHC class I pathway due to the noted downregulation of Sec61 translocation and upregulation of TAP transporters, which are engaged in the translocation of proteins to the cytosol (71) and phagosomal processing of tubercle bacilli antigens and their loading onto MHC I molecules (72, 73).

Significant differences are also observed in gene expression for phagocytosis promoting receptors in MDMs treated with hSAA-1 or infected with tubercle bacilli. Fc receptors (FcαR, FcγR), Toll-like receptor TLR2 and cell surface receptor and differentiation marker CD14 were exclusively overproduced in the presence of hSAA-1 and downregulated (FcγR, TLR2, TLR4, CD14) during infection. The C-lectin receptor DCSIGN, scavenger receptor MARCO and collectins were downregulated during infection but not in MDMs stimulated with hSAA-1. On the other hand, both stimuli induced complement opsonin iC3b, complement receptor CR1, and scavenger receptor LOX-1, and suppressed TLR4. The immune response to tubercle bacilli is initiated by PRRs including Toll-like receptors, nucleotide-binding domain and leucine-rich repeat-containing receptors (NLRs), C-type lectin receptors (CLRs) and cyclic GMP-AMP synthase (cGAS) (74),. The mouse model revealed that TLR2 recognizes bacterial lipoproteins and lipoglycans, and TLR9 recognizes unmethylated CpG DNA as the most important in the control of *Mtb* infection (75–78). We found that genes encoding TLR2 and CD14 are highly induced in human macrophages treated with hSAA-1 alone or infected with hSAA-1-opsonized tubercle bacilli but are not affected (TLR2) or suppressed (CD14) in macrophages infected with nonopsonized *Mtb*. In contrast, increased CD14 expression was observed in THP-1 cells infected with virulent and avirulent tubercle bacilli (62). As reported, CD14 constitutively interacts with the MyD88-dependent TLR7 and TLR9 pathways and is required for TLR7- and TLR9-dependent induction of proinflammatory cytokines *in vitro* and for TLR9-dependent innate immune responses in mice (79). The cell wall components of tubercle bacilli, such as glycolipids and lipoarabinomannan can be recognized by CLRs including DC-SIGN, mannose receptor (MR) or Dectin-1 (80–83). DCSIGN and MR were downregulated in MDMs infected with *Mtb* and not affected (MR, Dectin-1) or slightly induced (DCSIGN) in hSAA-1-treated human macrophages. Among the scavenger receptors, LOX-1 was highly induced in MDMs both during mycobacterial infection and hSAA-1 stimulation. hSAA-1 also induced expression of the MARCO receptor, which was downregulated during infection, similar to the SRA1, SRB1, and CD36 receptors. LOX-1 is involved in the accumulation of oxidized low-density lipoprotein

particles (OxLDL) within vascular cells. LOX-1 mediates OxLDL endocytosis via a clathrin-independent internalization pathway. Transgenic animal model studies have shown that LOX-1 plays a significant role in atherosclerotic plaque initiation and progression. LOX-1 endocytosis is also potentially important in immune surveillance as it has been shown to regulate antigen presentation by MHC class I and II molecules (84). Elevated surface expression of the type 1 scavenger receptors CD36 and LOX-1 was also reported for guinea pig macrophages infected with *Mtb*, which facilitated the uptake of oxidized host macromolecules including OxLDL (85).

We also analyzed the functional response of MDMs to hSAA-1 and *Mtb* infection at the protein level. Most of the selected cytokines were upregulated in MDMs treated with hSAA-1, except IL-27 and CCL7. The genes encoding these cytokines were also classified as uninduced in RNASeq analysis. On the other hand, CXCL10 and CSF2 were also uninduced at the RNA level but overproduced at the protein level. The discrepancy can result due to the cut off value (fold change=3) used in RNASeq analysis, since genes for CXCL10 and CSF2 were upregulated, however, to a lower extent (fold change 1.2 and 1.6, respectively). Infection of MDMs with non-opsonized bacilli induced, at least 10-fold, the synthesis of most tested cytokines except IL-15, IL-27, CCL2 and CCL7. Chemokines CCL2 and CCL7 were also uninduced at the RNA level; however, IL-15 and IL-27 genes were significantly upregulated in RNASeq. The IL-27 concentration was quite high in control, uninfected MDMs (>70 pg/mL) and increased after infection by approximately 50% (106.5 pg/mL). The amount of IL-15 also increased by approximately 50% after infection with *Mtb*, which is significantly less than the mRNA level, suggesting posttranscriptional control. We did not observe much difference in the tested cytokines in MDMs infected with the opsonized and nonopsonized bacilli. The only cytokine with a concentration that increased more than 10-fold (from 206 to 2705 pg/mL) when the opsonized bacilli were used, was the chemokine CCL5; however, the concentrations of other cytokines (CSF3, CSF2, IL-1α, IL-1β, IL-6, IL-12, TNF-α) increased to a lesser extent. CCL5 was also upregulated at the mRNA level in MDMs after infection with opsonized bacilli, even though memory $CD8^+$ T-cells have a large amount of preformed CCL5 mRNA in the cytoplasm and chemokine secretion was reported to be dependent only on translation (86). CCL5 is characterized by proinflammatory activity and chemotactic activity for T cells, eosinophils, basophils, monocytes, natural killer (NK) cells, dendritic cells, and mastocytes (87).

During infection, *Mtb* must adapt to changing conditions. A global adaptive response resulting from changes in available carbon sources, pH, oxygen access, is essential in macrophages, granulomas and during the reactivation process. Transcriptomic profiles of *Mtb* reactivating from hypoxia-induced non-replicating persistence revealed a global gene expression reprogramming with number of up-regulated transcription regulons and metabolic pathways, including those involved in metal transport and remobilization, second messenger-mediated responses, DNA repair and recombination, and synthesis of major cell wall components (88). During infection, *Mtb* must adapt to changing conditions. A global adaptive response resulting from changes in available carbon sources, pH, oxygen access, is essential in macrophages, granulomas and during the reactivation process. Transcriptomic profiles of *Mtb* reactivating from hypoxia-induced non-replicating persistence revealed a global gene expression reprogramming with number of up-regulated transcription regulons and metabolic pathways, including those involved in metal transport and remobilization, second messenger-mediated responses, DNA repair and recombination, and synthesis of major cell wall components of *Mtb* located inside macrophages for 24 h. The analysis of DEGs representing enriched metabolic clusters in bacilli isolated from MDMs clearly demonstrates that at the early stage of infection, *Mtb* activates at least two main virulence strategies: immune modulation, and phagosomal survival and rupture. It is, in turn, accompanied by unchanged or downregulated expression within pathways specific for prolonged infection, granuloma formation, and dormancy (e.g. DevR-DevS regulon). The *Mtb* genes affected by the intracellular environment of MDMs are strictly involved in response to hypoxia, NO level, low pH, adaptation to the increasing level of CO_2, synthesis of virulence effectors (e.g. PhoPR regulon), and secretion systems such as SEC, TAT, ESX-1, and ESX-3. At this early stage of infection, the results also showed high upregulation of genes for the synthesis and transport of surface-exposed lipids such as sulfolipids, acylated trehaloses, or phenolic glycolipids that constitute the hydrophobic barrier around the bacterium and are also known as modulators of host cell function, acting as highly potent virulence modulators (89). Interestingly, 24 h postinfection, those events are apparently not accompanied by the increased utilization of lipids as the energy source or energy reserve. Neither the cholesterol/fatty acid degradation pathway nor the methylcitrate cycle ameliorating the degradation of lipid metabolites, namely propionyl-CoA, was induced. Moreover, we observed extremely strong downregulation of the DevR-DevS-regulated *tgs-1* gene encoding an enzyme that synthesizes triacylglycerol, a major energy reserve for resuscitation from dormancy (44). This suggests a clear orientation of *Mtb* lipid metabolism during early infection of MDMs toward modification of the lipid host-pathogen interface to modulate the host response and promote survival within the phagosome. In previously published analyses of the *Mtb* transcriptional response to the macrophage environment, the authors suggest rapid remodeling of metabolism to consume lipids, especially cholesterol, and activation of the metylcitrate cycle ameliorating lipid catabolism end-products (90–93). However, our data show that the early stage of infection is not accompanied by any dramatic changes in central carbon and energy metabolism and shows no transcriptomic signs of lipid consumption/storage or nutrient starvation suggesting that macrophages are still abundant in diverse, readily available carbon sources. We also did not find transcriptional signs of bypassing the citric acid cycle oxidative pathway or upregulation of the methylcitrate cycle which together with the increase in isocitrate lyase gene – *icl1* expression and very strict repression of the DevR-DevS regulon suggest that 24 hours postinfection bacteria are still actively dividing and intensively metabolizing in an oxygen-dependent manner, despite activation of some mechanisms sensing increasing CO_2 levels. The shape of the delineated transcriptome does not resemble the typical changes observed for conditions mimicking persistent macrophage stress (94) such as exposure to nutrient starvation or non-dividing

stationary phase, with only mild signs of preparation to withstand low pH and upcoming oxygen depletion. Overall, contrary to previous analyses, our data show that although capable of cometabolizing multiple carbon sources, *M. tuberculosis* at the early stage of infection gives priority to nutrients whose utilization is not as energy-consuming as lipids. Most transcriptomic changes at this stage are oriented into cell surface armor synthesis/remodeling, preventing recognition or intraphagosomal killing.

We have previously shown that *in vitro* opsonization of tubercle bacilli with hSAA-1 affects a moderate set of *Mtb* genes (24). Here, we observed that hSAA-1 opsonization modulates the functional response of *Mtb* to the intracellular environment of macrophages. Among the genes affected by hSAA-1 opsonization during infection, three genes (*rv1195*, *rv2856b*, *rv3093c*) were upregulated exclusively in *Mtb* opsonized with hSAA-1. PE13 encoded by *rv1195* enhances the survival of bacilli under stress conditions such as the presence of H_2O_2, SDS, or low pH, and is actively engaged in the interaction between pathogen and host, signaling through the p38-ERK-NF-κB axis, and apoptosis (95). *Rv2856b*/NicT belongs to the family of *Mtb* metal transporters and behaves as a drug efflux pump facilitating cross-resistance to several antibiotics including isoniazid (96) and *Rv3093c* is a SigM-regulated oxidoreductase of unknown function. Among the eight genes (*Rv1405c*, *Rv2661c*, *Rv1684*, *Rv1137c*, *Rv0974c*, *Rv0744ac*, *Rv1815*, *Rv0157a*) exclusively downregulated in hSAA-1 opsonized mycobacteria infecting macrophages, *Rv1405c* encodes a virulence-associated methyltransferase involved in the adaptation of *Mtb* to acid stress (97). *Rv2661c* is involved in phenotypic drug tolerance and associated with *in vivo* infection (98). Among other genes of known function, *Rv1684* is an NO-specific response gene (99). *Rv1137c* may be involved in the posttranslational modification of prenylated proteins (100), *Rv0974c* encodes acyl-CoA carboxylase AccD2, which is probably involved in amino acid biosynthesis (101) and *Rv0744Ac* is a possible transcriptional regulatory protein. Our study also identified 28 genes whose differential expression in response to the intraphagosomal environment was abolished in hSAA-1 opsonized *Mtb* infecting MDMs under the same conditions. Additionally, in this case, most genes represent membrane or secreted antigenic proteins, immunomodulators, and the elements of toxin-antitoxin systems. Interestingly, we found that hSAA-1 opsonization prevents the upregulation of the virulence-related *rv2352c* gene during infection. *Rv2352c* encodes the PPE38 protein that, if overexpressed, inhibits macrophage MHC-I expression and the CD8+ T-cell response (102). This may explain why opsonized but not nonopsonized *Mtb* induces the expression of MHC-I.

Considering our research and literature data, it can be assumed that the observed, elevated SAA-1 level in tuberculosis patients modulates both, the host immune response and the functional response of mycobacteria during infection. The response of macrophages treated with SAA-1 to *Mtb* infection seems to be much stronger and enhanced by the induction of both, innate (MHC-I engagement of natural killer cells) and adaptive (MHC-I through peptides presented to cytotoxic T cells and MHC-II dedicated to adaptive immunity) immune responses (103–105). On the other hand, the opsonization of tubercle bacilli by SAA-1 may facilitate the adaptation of mycobacteria to stress conditions during infection.

Data availability statement

The original contributions presented in the study are publicly available. This data can be found here: https://www.ncbi.nlm.nih.gov/bioproject/PRJNA1001595.

Ethics statement

Ethical approval was not required for the studies on humans in accordance with the local legislation and institutional requirements because only commercially available established cell lines were used.

Author contributions

The concept of the study was designed by BD and JD. Experimental design was performed by MK, RP, BD, and PP. Experiments were performed by MK, RP, PP, BD, JG, KD, and MS. BD, JP, and JD wrote the manuscript. The manuscript was reviewed by all coauthors. All authors contributed to the article and approved the submitted version.

Funding

This study was funded by National Science Centre (Poland) grant: UMO 2016/23/B/NZ7/01204.

Conflict of interest

The authors declare that the research was conducted in the absence of any commercial or financial relationships that could be construed as a potential conflict of interest.

Publisher's note

Supplementary material

The Supplementary Material for this article can be found online at: https://www.frontiersin.org/articles/10.3389/fimmu.2023.1238132/full#supplementary-material

References

1. World Health Organization. *Global tuberculosis report 2022* (2022). Available at: https://www.who.int/teams/global-tuberculosis-programme/tb-reports/global-tuberculosis-report-2022.

2. Gengenbacher M, Kaufmann SH. Mycobacterium tuberculosis: success through dormancy. *FEMS Microbiol Rev* (2012) 36(3):514–32. doi: 10.1111/j.1574-6976.2012.00331.x

3. World Health Organization. *Tuberculosis* (2023). Available at: https://www.who.int/news-room/fact-sheets/detail/tuberculosis.

4. Simper JD, Perez E, Schlesinger LS, Azad AK. Resistance and Susceptibility Immune Factors at Play during Mycobacterium tuberculosis Infection of Macrophages. *Pathogens* (2022) 11(10):1153. doi: 10.3390/pathogens11101153

5. Moule MG, Cirillo JD. Mycobacterium tuberculosis dissemination plays a critical role in pathogenesis. *Front Cell Infect Microbiol* (2020) 10:65. doi: 10.3389/fcimb.2020.00065

6. Orme IM. A new unifying theory of the pathogenesis of tuberculosis. *Tuberculosis (Edinb)* (2014) 94(1):8–14. doi: 10.1016/j.tube.2013.07.004

7. Boom WH, Schaible UE, Achkar JM. The knowns and unknowns of latent Mycobacterium tuberculosis infection. *J Clin Invest* (2021) 131(3):e136222. doi: 10.1172/JCI136222

8. Singh CR, Moulton RA, Armitige LY, Bidani A, Snuggs M, Dhandayuthapani S, et al. Processing and presentation of a mycobacterial antigen 85B epitope by murine macrophages is dependent on the phagosomal acquisition of vacuolar proton ATPase and in *situ* activation of cathepsin D. *J Immunol* (2006) 177(5):3250–9. doi: 10.4049/jimmunol.177.5.3250

9. McMurtrey C, Harriff MJ, Swarbrick GM, Duncan A, Cansler M, Null M, et al. T cell recognition of Mycobacterium tuberculosis peptides presented by HLA-E derived from infected human cells. *PloS One* (2017) 12(11):e0188288. doi: 10.1371/journal.pone.0188288

10. Leddy O, White FM, Bryson BD. Immunopeptidomics reveals determinants of Mycobacterium tuberculosis antigen presentation on MHC class I. *Elife* (2023) 12: e84070. doi: 10.7554/eLife.84070

11. Baena A, Porcelli SA. Evasion and subversion of antigen presentation by Mycobacterium tuberculosis. *Tissue Antigens* (2009) 74(3):189–204. doi: 10.1111/j.1399-0039.2009.01301.x

12. Cooper AM. Cell-mediated immune responses in tuberculosis. *Annu Rev Immunol* (2009) 27:393–422. doi: 10.1146/annurev.immunol.021908.132703

13. Flynn JL, Chan J. Immunology of tuberculosis. *Annu Rev Immunol* (2001) 19:93–129. doi: 10.1146/annurev.immunol.19.1.93

14. Lyadova IV, Panteleev AV. Th1 and th17 cells in tuberculosis: protection, pathology, and biomarkers. *Mediators Inflamm* (2015) 2015:854507. doi: 10.1155/2015/854507

15. Cardona P, Cardona PJ. Regulatory T cells in mycobacterium tuberculosis infection. *Front Immunol* (2019) 10:2139. doi: 10.3389/fimmu.2019.02139

16. De Buck M, Gouwy M, Wang JM, Van Snick J, Opdenakker G, Struyf S, et al. (SAA) variants and their concentration-dependent functions during host insults. *Curr Med Chem* (2016) 23(17):1725–55. doi: 10.2174/0929867323666160418114600

17. Eklund KK, Niemi K, Kovanen PT. Immune functions of serum amyloid A. *Crit Rev Immunol* (2012) 32(4):335–48. doi: 10.1615/CritRevImmunol.v32.i4.40

18. Ganapathi MK, Rzewnicki D, Samols D, Jiang SL, Kushner I. Effect of combinations of cytokines and hormones on synthesis of serum amyloid A and C-reactive protein in Hep 3B cells. *J Immunol* (1991) 147(4):1261–5. doi: 10.4049/jimmunol.147.4.1261

19. Migita K, Abiru S, Nakamura M, Komori A, Yoshida Y, Yokoyama T, et al. Lipopolysaccharide signaling induces serum amyloid A (SAA) synthesis in human hepatocytes *in vitro*. *FEBS Lett* (2004) 569(1-3):235–9. doi: 10.1016/j.febslet.2004.05.072

20. Urieli-Shoval S, Linke RP, Matzner Y. Expression and function of serum amyloid A, a major acute-phase protein, in normal and disease states. *Curr Opin Hematol* (2000) 7(1):64–9. doi: 10.1097/00062752-200001000-00012

21. Ye RD, Sun L. Emerging functions of serum amyloid A in inflammation. *J Leukoc Biol* (2015) 98(6):923–9. doi: 10.1189/jlb.3VMR0315-080R

22. Hari-Dass R, Shah C, Meyer DJ, Raynes JG. Serum amyloid A protein binds to outer membrane protein A of gram-negative bacteria. *J Biol Chem* (2005) 280 (19):18562–7. doi: 10.1074/jbc.M500490200

23. Shah C, Hari-Dass R, Raynes JG. Serum amyloid A is an innate immune opsonin for Gram-negative bacteria. *Blood* (2006) 108(5):1751–7. doi: 10.1182/blood-2005-11-011932

24. Kawka M, Brzostek A, Dzitko K, Kryczka J, Bednarek R, Plocinska R, et al. Mycobacterium tuberculosis binds human serum amyloid A, and the interaction modulates the colonization of human macrophages and the transcriptional response of the pathogen. *Cells* (2021) 10(5):1264. doi: 10.3390/cells10051264

25. Korycka-Machala M, Viljoen A, Pawelczyk J, Borowka P, Dziadek B, Gobis K, et al. 1H-benzo[d]Imidazole derivatives affect mmpL3 in mycobacterium tuberculosis. *Antimicrob Agents Chemother* (2019) 63(10):e00441-19.

26. Pawelczyk J, Brzostek A, Kremer L, Dziadek B, Rumijowska-Galewicz A, Fiolka M, et al. AccD6, a key carboxyltransferase essential for mycolic acid synthesis in Mycobacterium tuberculosis, is dispensable in a nonpathogenic strain. *J Bacteriol* (2011) 193(24):6960–72. doi: 10.1128/JB.05638-11

27. Martin M. Cutadapt removes adapter sequences from high-throughput sequencing reads. *EMBnet J* (2011) 17:10–2. doi: 10.14806/ej.17.1.200

28. Langmead B, Salzberg SL. Fast gapped-read alignment with Bowtie 2. *Nat Methods* (2012) 9(4):357–9. doi: 10.1038/nmeth.1923

29. Dobin A, Davis CA, Schlesinger F, Drenkow J, Zaleski C, Jha S, et al. STAR: ultrafast universal RNA-seq aligner. *Bioinformatics* (2013) 29(1):15–21. doi: 10.1093/bioinformatics/bts635

30. Li H, Handsaker B, Wysoker A, Fennell T, Ruan J, Homer N, et al. The sequence alignment/map format and SAMtools. *Bioinformatics* (2009) 25(16):2078–9. doi: 10.1093/bioinformatics/btp352

31. Quinlan AR, Hall IM. BEDTools: a flexible suite of utilities for comparing genomic features. *Bioinformatics* (2010) 26(6):841–2. doi: 10.1093/bioinformatics/btq033

32. Anders S, Pyl PT, Huber W. HTSeq–a Python framework to work with high-throughput sequencing data. *Bioinformatics* (2015) 31(2):166–9. doi: 10.1093/bioinformatics/btu638

33. Robinson JT, Thorvaldsdottir H, Winckler W, Guttman M, Lander ES, Getz G, et al. Integrative genomics viewer. *Nat Biotechnol* (2011) 29(1):24–6. doi: 10.1038/nbt.1754

34. Powell DR. *Degust: interactive RNA-seq analysis*. Available at http://degust.erc.monash.edu

35. Ge SX, Son EW, Yao R. iDEP: an integrated web application for differential expression and pathway analysis of RNA-Seq data. *BMC Bioinf* (2018) 19(1):534. doi: 10.1186/s12859-018-2486-6

36. Samaha HMS, Elsaid AR, Elzehery R, Elhelaly R. C-reactive protein and serum amyloid A levels in discriminating Malignant from non-Malignant pleural effusion. *Egypt J Chest Dis Tuberc* (2015) 64(4):887–92. doi: 10.1016/j.ejcdt.2015.04.004

37. Marcela Rodriguez G, Neyrolles O. Metallobiology of tuberculosis. *Microbiol Spectr* (2014) 2(3):10.1128/microbiolspec. doi: 10.1128/microbiolspec.MGM2-0012-2013

38. Singh N, Sharma N, Singh P, Pandey M, Ilyas M, Sisodiya L, et al. HupB, a nucleoid-associated protein, is critical for survival of Mycobacterium tuberculosis under host-mediated stresses and for enhanced tolerance to key first-line antibiotics. *Front Microbiol* (2022) 13:937970. doi: 10.3389/fmicb.2022.937970

39. Kolodziej M, Trojanowski D, Bury K, Holowka J, Matysik W, Kakolewska H, et al. Lsr2, a nucleoid-associated protein influencing mycobacterial cell cycle. *Sci Rep* (2021) 11(1):2910. doi: 10.1038/s41598-021-82295-0

40. Zondervan NA, van Dam JCJ, Schaap PJ, Martins Dos Santos VAP, Suarez-Diez M. Regulation of three virulence strategies of mycobacterium tuberculosis: A success story. *Int J Mol Sci* (2018) 19(2). doi: 10.3390/ijms19020347

41. Vergne I, Chua J, Lee HH, Lucas M, Belisle J, Deretic V. Mechanism of phagolysosome biogenesis block by viable Mycobacterium tuberculosis. *Proc Natl Acad Sci U S A* (2005) 102(11):4033–8. doi: 10.1073/pnas.0409716102

42. Groschel MI, Sayes F, Simeone R, Majlessi L, Brosch R. ESX secretion systems: mycobacterial evolution to counter host immunity. *Nat Rev Microbiol* (2016) 14 (11):677–91. doi: 10.1038/nrmicro.2016.131

43. Kurtz S, McKinnon KP, Runge MS, Ting JP, Braunstein M. The SecA2 secretion factor of Mycobacterium tuberculosis promotes growth in macrophages and inhibits the host immune response. *Infect Immun* (2006) 74(12):6855–64. doi: 10.1128/IAI.01022-06

44. Daffe M, Crick DC, Jackson M. Genetics of capsular polysaccharides and cell envelope (Glyco)lipids. *Microbiol Spectr* (2014) 2(4):MGM2-0021-2013. doi: 10.1128/9781555818845.ch28

45. Hussell T, Bell TJ. Alveolar macrophages: plasticity in a tissue-specific context. *Nat Rev Immunol* (2014) 14(2):81–93. doi: 10.1038/nri3600

46. Kawasaki T, Ikegawa M, Kawai T. Antigen presentation in the lung. *Front Immunol* (2022) 13:860915. doi: 10.3389/fimmu.2022.860915

47. Hou F, Xiao K, Tang L, Xie L. Diversity of macrophages in lung homeostasis and diseases. *Front Immunol* (2021) 12:753940. doi: 10.3389/fimmu.2021.753940

48. Mosser DM. The many faces of macrophage activation. *J Leukoc Biol* (2003) 73 (2):209–12. doi: 10.1189/jlb.0602325

49. Lambrecht BN. Alveolar macrophage in the driver's seat. *Immunity* (2006) 24 (4):366–8. doi: 10.1016/j.immuni.2006.03.008

50. Rajaram MV, Brooks MN, Morris JD, Torrelles JB, Azad AK, Schlesinger LS. Mycobacterium tuberculosis activates human macrophage peroxisome proliferator-activated receptor gamma linking mannose receptor recognition to regulation of immune responses. *J Immunol* (2010) 185(2):929–42. doi: 10.4049/jimmunol.1000866

51. Hoidal JR SD, Peterson PK. Phagocytosis, bacterial killing, and metabolism by purified human lung phagocytes. *J Infect Diseases* (1981) 144:61–71. doi: 10.1093/infdis/144.1.61

52. Greening AP LD. Extracellular release of hydrogen peroxide by human alveolar macrophages: the relationship to cigarette smoking and lower respiratory tract infections. *Ckin Sci (Lond)* (1983) 65:661–4. doi: 10.1042/cs0650661

53. Lyons CR BE, Toews GB, Weissler JC, Stastny P, Lipscomb MF. Inability of human alveolar macrophages to stimulate resting T cells correlates with decreased antigen-specific T cell-macrophage binding. *J Immunol* (1986) 137:1173–80. doi: 10.4049/jimmunol.137.4.1173

54. Kleinnijenhuis J, Oosting M, Joosten LA, Netea MG, Van Crevel R. Innate immune recognition of Mycobacterium tuberculosis. *Clin Dev Immunol* (2011) 2011:405310. doi: 10.1155/2011/405310

55. Holt PG, Oliver J, Bilyk N, McMenamin C, McMenamin PG, Kraal G, et al. Downregulation of the antigen presenting cell function(s) of pulmonary dendritic cells *in vivo* by resident alveolar macrophages. *J Exp Med* (1993) 177(2):397–407. doi: 10.1084/jem.177.2.397

56. Roth MD, Golub SH. Human pulmonary macrophages utilize prostaglandins and transforming growth factor beta 1 to suppress lymphocyte activation. *J Leukoc Biol* (1993) 53(4):366–71. doi: 10.1002/jlb.53.4.366

57. Yoshie O, Imai T, Nomiyama H. Chemokines in immunity. *Adv Immunol* (2001) 78:57–110. doi: 10.1016/S0065-2776(01)78002-9

58. Ansel KM, Harris RB, Cyster JG. CXCL13 is required for B1 cell homing, natural antibody production, and body cavity immunity. *Immunity* (2002) 16(1):67–76. doi: 10.1016/S1074-7613(01)00257-6

59. LeBlanc HN, Ashkenazi A. Apo2L/TRAIL and its death and decoy receptors. *Cell Death Differ* (2003) 10(1):66–75. doi: 10.1038/sj.cdd.4401187

60. Metzemaekers M, Vanheule V, Janssens R, Struyf S, Proost P. Overview of the mechanisms that may contribute to the non-redundant activities of interferon-inducible CXC chemokine receptor 3 ligands. *Front Immunol* (2017) 8:1970. doi: 10.3389/fimmu.2017.01970

61. Mosser DM, Zhang X. Interleukin-10: new perspectives on an old cytokine. *Immunol Rev* (2008) 226:205–18. doi: 10.1111/j.1600-065X.2008.00706.x

62. Pu W, Zhao C, Wazir J, Su Z, Niu M, Song S, et al. Comparative transcriptomic analysis of THP-1-derived macrophages infected with Mycobacterium tuberculosis H37Rv, H37Ra and BCG. *J Cell Mol Med* (2021) 25(22):10504–20. doi: 10.1111/jcmm.16980

63. Mantovani A, Sica A, Sozzani S, Allavena P, Vecchi A, Locati M. The chemokine system in diverse forms of macrophage activation and polarization. *Trends Immunol* (2004) 25(12):677–86. doi: 10.1016/j.it.2004.09.015

64. Gordon S, Martinez FO. Alternative activation of macrophages: mechanism and functions. *Immunity* (2010) 32(5):593–604. doi: 10.1016/j.immuni.2010.05.007

65. Martinez FO, Gordon S. The M1 and M2 paradigm of macrophage activation: time for reassessment. *F1000Prime Rep* (2014) 6:13. doi: 10.12703/P6-13

66. Lafourcade C, Sobo K, Kieffer-Jaquinod S, Garin J, van der Goot FG. Regulation of the V-ATPase along the endocytic pathway occurs through reversible subunit association and membrane localization. *PloS One* (2008) 3(7):e2758. doi: 10.1371/journal.pone.0002758

67. Zehner M, Marschall AL, Bos E, Schloetel JG, Kreer C, Fehrenschild D, et al. The translocon protein Sec61 mediates antigen transport from endosomes in the cytosol for cross-presentation to CD8(+) T cells. *Immunity* (2015) 42(5):850–63. doi: 10.1016/j.immuni.2015.04.008

68. Harding CV, Boom WH. Regulation of antigen presentation by Mycobacterium tuberculosis: a role for Toll-like receptors. *Nat Rev Microbiol* (2010) 8(4):296–307. doi: 10.1038/nrmicro2321

69. Walburger A, Koul A, Ferrari G, Nguyen L, Prescianotto-Baschong C, Huygen K, et al. Protein kinase G from pathogenic mycobacteria promotes survival within macrophages. *Science* (2004) 304(5678):1800–4. doi: 10.1126/science.1099384

70. Sturgill-Koszycki S, Schlesinger PH, Chakraborty P, Haddix PL, Collins HL, Fok AK, et al. Lack of acidification in Mycobacterium phagosomes produced by exclusion of the vesicular proton-ATPase. *Science* (1994) 263(5147):678–81. doi: 10.1126/science.8303277

71. Schnell DJ, Hebert DN. Protein translocons: multifunctional mediators of protein translocation across membranes. *Cell* (2003) 112(4):491–505. doi: 10.1016/S0092-8674(03)00110-7

72. Grotzke JE, Harriff MJ, Siler AC, Nolt D, Delepine J, Lewinsohn DA, et al. The Mycobacterium tuberculosis phagosome is a HLA-I processing competent organelle. *PloS Pathog* (2009) 5(4):e1000374. doi: 10.1371/journal.ppat.1000374

73. Harriff MJ, Burgdorf S, Kurts C, Wiertz EJ, Lewinsohn DA, Lewinsohn DM. TAP mediates import of Mycobacterium tuberculosis-derived peptides into phagosomes and facilitates loading onto HLA-I. *PloS One* (2013) 8(11):e79571. doi: 10.1371/journal.pone.0079571

74. Ravesloot-Chavez MM, Van Dis E, Stanley SA. The innate immune response to mycobacterium tuberculosis infection. *Annu Rev Immunol* (2021) 39:611–37. doi: 10.1146/annurev-immunol-093019-010426

75. Reiling N, Holscher C, Fehrenbach A, Kroger S, Kirschning CJ, Goyert S, et al. Cutting edge: Toll-like receptor (TLR)2- and TLR4-mediated pathogen recognition in resistance to airborne infection with Mycobacterium tuberculosis. *J Immunol* (2002) 169(7):3480–4. doi: 10.4049/jimmunol.169.7.3480

76. Sugawara I, Yamada H, Li C, Mizuno S, Takeuchi O, Akira S. Mycobacterial infection in TLR2 and TLR6 knockout mice. *Microbiol Immunol* (2003) 47(5):327–36. doi: 10.1111/j.1348-0421.2003.tb03404.x

77. Feng CG, Scanga CA, Collazo-Custodio CM, Cheever AW, Hieny S, Caspar P, et al. Mice lacking myeloid differentiation factor 88 display profound defects in host resistance and immune responses to Mycobacterium avium infection not exhibited by Toll-like receptor 2 (TLR2)- and TLR4-deficient animals. *J Immunol* (2003) 171(9):4758–64. doi: 10.4049/jimmunol.171.9.4758

78. Bafica A, Scanga CA, Feng CG, Leifer C, Cheever A, Sher A. TLR9 regulates Th1 responses and cooperates with TLR2 in mediating optimal resistance to Mycobacterium tuberculosis. *J Exp Med* (2005) 202(12):1715–24. doi: 10.1084/jem.20051782

79. Baumann CL, Aspalter IM, Sharif O, Pichlmair A, Bluml S, Grebien F, et al. CD14 is a coreceptor of Toll-like receptors 7 and 9. *J Exp Med* (2010) 207(12):2689–701. doi: 10.1084/jem.20101111

80. Maeda N, Nigou J, Herrmann JL, Jackson M, Amara A, Lagrange PH, et al. The cell surface receptor DC-SIGN discriminates between Mycobacterium species through selective recognition of the mannose caps on lipoarabinOmannan. *J Biol Chem* (2003) 278(8):5513–6. doi: 10.1074/jbc.C200586200

81. Kang PB, Azad AK, Torrelles JB, Kaufman TM, Beharka A, Tibesar E, et al. The human macrophage mannose receptor directs Mycobacterium tuberculosis lipoarabinOmannan-mediated phagosome biogenesis. *J Exp Med* (2005) 202(7):987–99. doi: 10.1084/jem.20051239

82. Doz E, Rose S, Nigou J, Gilleron M, Puzo G, Erard F, et al. Acylation determines the toll-like receptor (TLR)-dependent positive versus TLR2-, mannose receptor-, and SIGNR1-independent negative regulation of pro-inflammatory cytokines by mycobacterial lipOmannan. *J Biol Chem* (2007) 282(36):26014–25. doi: 10.1074/jbc.M702690200

83. Yonekawa A, Saijo S, Hoshino Y, Miyake Y, Ishikawa E, Suzukawa M, et al. Dectin-2 is a direct receptor for mannose-capped lipoarabinOmannan of mycobacteria. *Immunity* (2014) 41(3):402–13. doi: 10.1016/j.immuni.2014.08.005

84. Twigg MW, Freestone K, Homer-Vanniasinkam S, Ponnambalam S. The LOX-1 scavenger receptor and its implications in the treatment of vascular disease. *Cardiol Res Pract* (2012) 2012:632408. doi: 10.1155/2012/632408

85. Palanisamy GS, Kirk NM, Ackart DF, Obregon-Henao A, Shanley CA, Orme IM, et al. Uptake and accumulation of oxidized low-density lipoprotein during Mycobacterium tuberculosis infection in Guinea pigs. *PloS One* (2012) 7(3):e34148. doi: 10.1371/journal.pone.0034148

86. Marcais A, Coupet CA, Walzer T, Tomkowiak M, Ghittoni R, Marvel J. Cell-autonomous CCL5 transcription by memory CD8 T cells is regulated by IL-4. *J Immunol* (2006) 177(7):4451–7. doi: 10.4049/jimmunol.177.7.4451

87. Appay V, Rowland-Jones SL. RANTES: a versatile and controversial chemokine. *Trends Immunol* (2001) 22(2):83–7. doi: 10.1016/S1471-4906(00)01812-3

88. Du P, Sohaskey CD, Shi L. Transcriptional and Physiological Changes during Mycobacterium tuberculosis Reactivation from Non-replicating Persistence. *Front Microbiol* (2016) 7:1346. doi: 10.3389/fmicb.2016.01346

89. Minnikin DE, Kremer L, Dover LG, Besra GS. The methyl-branched fortifications of Mycobacterium tuberculosis. *Chem Biol* (2002) 9(5):545–53. doi: 10.1016/S1074-5521(02)00142-4

90. Zimmermann M, Kogadeeva M, Gengenbacher M, McEwen G, Mollenkopf HJ, Zamboni N, et al. Integration of Metabolomics and Transcriptomics Reveals a Complex Diet of Mycobacterium tuberculosis during Early Macrophage Infection. *mSystems* (2017) 2(4):e00057-17. doi: 10.1128/mSystems.00057-17

91. Lopez-Agudelo VA, Baena A, Barrera V, Cabarcas F, Alzate JF, Beste DJV, et al. Dual RNA sequencing of mycobacterium tuberculosis-infected human splenic macrophages reveals a strain-dependent host-pathogen response to infection. *Int J Mol Sci* (2022) 23(3):1803. doi: 10.3390/ijms23031803

92. Rienksma RA, Suarez-Diez M, Mollenkopf HJ, Dolganov GM, Dorhoi A, Schoolnik GK, et al. Comprehensive insights into transcriptional adaptation of intracellular mycobacteria by microbe-enriched dual RNA sequencing. *BMC Genomics* (2015) 16(1):34. doi: 10.1186/s12864-014-1197-2

93. Medley J, Goff A, Bettencourt PJG, Dare M, Cole L, Cantillon D, et al. Dissecting the mycobacterium bovis BCG response to macrophage infection to help prioritize targets for anti-tuberculosis drug and vaccine discovery. *Vaccines (Basel)* (2022) 10(1):113. doi: 10.3390/vaccines10010113

94. Vilcheze C, Yan B, Casey R, Hingley-Wilson S, Ettwiller L, Jacobs WR Jr. Commonalities of mycobacterium tuberculosis transcriptomes in response to defined persisting macrophage stresses. *Front Immunol* (2022) 13:909904. doi: 10.3389/fimmu.2022.909904

95. Li H, Li Q, Yu Z, Zhou M, Xie J. Mycobacterium tuberculosis PE13 (Rv1195) manipulates the host cell fate via p38-ERK-NF-kappaB axis and apoptosis. *Apoptosis* (2016) 21(7):795–808. doi: 10.1007/s10495-016-1249-y

96. Adhikary A, Biswal S, Chatterjee D, Ghosh AS. A NiCoT family metal transporter of Mycobacterium tuberculosis (Rv2856/NicT) behaves as a drug efflux pump that facilitates cross-resistance to antibiotics. *Microbiol (Reading)* (2022) 168(10). doi: 10.1099/mic.0.001260

97. Healy C, Golby P, MacHugh DE, Gordon SV. The MarR family transcription factor Rv1404 coordinates adaptation of Mycobacterium tuberculosis to acid stress via controlled expression of Rv1405c, a virulence-associated methyltransferase. *Tuberculosis (Edinb)* (2016) 97:154–62. doi: 10.1016/j.tube.2015.10.003

98. Pisu D, Huang L, Narang V, Theriault M, Le-Bury G, Lee B, et al. Single cell analysis of M. tuberculosis phenotype and macrophage lineages in the infected lung. *J Exp Med* (2021) 218(9):e20210615.

99. Voskuil MI, Bartek IL, Visconti K, Schoolnik GK. The response of mycobacterium tuberculosis to reactive oxygen and nitrogen species. *Front Microbiol* (2011) 2:105. doi: 10.3389/fmicb.2011.00105

100. Manganelli R. Sigma factors: key molecules in mycobacterium tuberculosis physiology and virulence. *Microbiol Spectr* (2014) 2(1):MGM2–0007-2013. doi: 10.1128/9781555818845.ch7

101. Ehebauer MT, Zimmermann M, Jakobi AJ, Noens EE, Laubitz D, Cichocki B, et al. Characterization of the mycobacterial acyl-CoA carboxylase holo complexes reveals their functional expansion into amino acid catabolism. *PloS Pathog* (2015) 11 (2):e1004623. doi: 10.1371/journal.ppat.1004623

102. Meng L, Tong J, Wang H, Tao C, Wang Q, Niu C, et al. PPE38 protein of mycobacterium tuberculosis inhibits macrophage MHC class I expression and dampens CD8(+) T cell responses. *Front Cell Infect Microbiol* (2017) 7:68. doi: 10.3389/fcimb.2017.00068

103. Jiang J, Natarajan K, Margulies DH. MHC molecules, T cell receptors, natural killer cell receptors, and viral immunoevasins-key elements of adaptive and innate immunity. *Adv Exp Med Biol* (2019) 1172:21–62. doi: 10.1007/978-981-13-9367-9_2

104. Uzhachenko RV, Shanker A. CD8(+) T lymphocyte and NK cell network: circuitry in the cytotoxic domain of immunity. *Front Immunol* (2019) 10:1906. doi: 10.3389/fimmu.2019.01906

105. Leddon SA, Sant AJ. Generation of MHC class II-peptide ligands for CD4 T-cell allorecognition of MHC class II molecules. *Curr Opin Organ Transplant* (2010) 15 (4):505–11. doi: 10.1097/MOT.0b013e32833bfc5c

frontiers | Frontiers in Immunology

TYPE Original Research
PUBLISHED 19 September 2023
DOI 10.3389/fimmu.2023.1199092

OPEN ACCESS

EDITED BY
Zhidong Hu,
Fudan University, China

REVIEWED BY
Suraj P. Parihar,
University of Cape Town, South Africa
Amandine Hauer,
University of Gdansk, Poland

*CORRESPONDENCE
Bappaditya Dey
bdey@niab.org.in

RECEIVED 02 April 2023
ACCEPTED 29 August 2023
PUBLISHED 19 September 2023

CITATION
Kumar R, Gandham S, Rana A, Maity HK, Sarkar U and Dey B (2023) Divergent proinflammatory immune responses associated with the differential susceptibility of cattle breeds to tuberculosis.
Front. Immunol. 14:1199092.
doi: 10.3389/fimmu.2023.1199092

Divergent proinflammatory immune responses associated with the differential susceptibility of cattle breeds to tuberculosis

Rishi Kumar[1,2], Sripratyusha Gandham[1,2], Avi Rana[1], Hemanta Kumar Maity[3], Uttam Sarkar[4] and Bappaditya Dey[1,2]*

[1]National Institute of Animal Biotechnology, Hyderabad, Telangana, India, [2]Regional Centre for Biotechnology, Faridabad, Haryana, India, [3]Department of Avian Sciences, West Bengal University of Animal and Fishery Sciences, Kolkata, West Bengal, India, [4]Department of Animal Genetics and Breeding, West Bengal University of Animal and Fishery Sciences, Kolkata, West Bengal, India

Tuberculosis (TB) in the bovine is one of the most predominant chronic debilitating infectious diseases primarily caused by *Mycobacterium bovis*. Besides, the incidence of TB in humans due to *M. bovis*, and that in bovines (bovine TB, bTB) due to *M. tuberculosis*- indicates cattle as a major reservoir of zoonotic TB. While India accounts for the highest global burden of both TB and multidrug-resistant TB in humans, systematic evaluation of bTB prevalence in India is largely lacking. Recent reports emphasized markedly greater bTB prevalence in exotic and crossbred cattle compared to indigenous cattle breeds that represent more than one-third of the total cattle population in India, which is the largest globally. This study aimed at elucidating the immune responses underlying the differential bTB incidence in prominent indigenous (Sahiwal), and crossbred (Sahiwal x Holstein Friesian) cattle reared in India. Employing the standard Single Intradermal Tuberculin Test (SITT), and mycobacterial gene-targeting single as well as multiplex-PCR-based screening revealed higher incidences of bovine tuberculin reactors as well as *Mycobacterium tuberculosis* Complex specific PCR positivity amongst the crossbred cattle. Further, *ex vivo* mycobacterial infection in cultures of bovine peripheral blood mononuclear cells (PBMC) from SITT, and myco-PCR negative healthy cattle exhibited significantly higher intracellular growth of *M. bovis* BCG, and *M. tuberculosis* H37Ra in the crossbred cattle PBMCs compared to native cattle. In addition, native cattle PBMCs induced higher pro-inflammatory cytokines and signaling pathways, such as interferon-gamma (IFN-γ), interleukin-17 (IL-17), tank binding kinase-1 (TBK-1), and nitric oxide (NO) upon exposure to live mycobacterial infection in comparison to PBMCs from crossbred cattle that exhibited higher expression of IL-1β transcripts. Together, these findings highlight that differences in the innate immune responses of these cattle breeds might be contributing to the differential susceptibility to bTB infection, and the resultant disparity in bTB incidence amongst indigenous, and crossbred cattle.

KEYWORDS

tuberculosis, bovine tuberculosis, *Mycobacterium tuberculosis*, *Mycobacterium bovis*, BCG

Introduction

Bovine tuberculosis (bTB) is a globally prevalent chronic debilitating infectious disease of cattle with a considerable impact on the public health and farm economy. Of the 188 countries and territories globally reporting their bovine TB (bTB) situation to the World Organisation of Animal Health (OIE), 82 countries (44%) reported bTB prevalence (1). Notably, while 97.6% of the affected countries reported bTB prevalence in livestock, 35.4% of countries documented bTB presence in both livestock and wildlife animals (1). In addition, the incidence of TB in humans and bovines due to either the human or bovine tubercle bacilli signifies the impact of bTB on livestock farming, and highlights its transmission between cattle and humans (2–4). Since, about 54.6% of the total workforce in India is engaged in agriculture and animal husbandry, and livestock provides livelihood to two third of the rural community, therefore, bTB exerts a hugely adverse effect on public health (3, 5).

Bovine TB has been largely controlled in many high-income countries due to strict implementation of bTB control programs and policies, whereas in lower, and lower-middle-income countries, control of bTB still poses a major challenge (6, 7). This is largely because of unhygienic farm management practices, lack of regular surveillance, and lack of strict prevention, and control policies. While a meta-analysis of published literature on bTB reported prevalence rates of 2-50% in cattle in India, the true incidence of bTB in India remains ambiguous in the absence of routine national bTB surveillance (8). Seminal findings in the past showed lower incidences of bTB in the indigenous Indian zebu cattle (*Bos indicus*) compared to exotic European cattle (*Bos taurus*) (9–14). Susceptibility to bTB has also been estimated to be influenced by various factors such as herd size, nutritional requirement, age, sex, and dairy farm management practices (9, 15, 16). A recent study reported significantly higher bTB prevalence in exotic and crossbred cattle than in indigenous cattle breeds (17). A plethora of studies in the mouse model as well as in humans has indicated that the genetic makeup of a host substantially influences the intracellular survival of mycobacteria by inducing differential immune responses (18–23). However, a systematic study to compare the underlying immune responses amongst indigenous Indian cattle, and crossbred cattle has not been reported. We hypothesized that higher incidences of bTB in the crossbred cattle might be arising due to inadequate immune response to bTB infection compared to the native cattle breeds. To compare the innate cellular responses, first, we segregated the healthy, single intradermal tuberculin test (SITT) negative, and myco-PCR [PCR targeting *M. tuberculosis, M. bovis*, *M. orygis*, Mycobacterium tuberculosis complex (MTC)] and Non-Tuberculous Mycobacteria (NTM) negative cattle from two prominent breeds- indigenous breed Sahiwal, and crossbred- Sahiwal x Holstein Friesian (SHF). Subsequently, we performed a comparative mycobacterial growth assay in the PBMCs isolated from these healthy mycobacterium-naive cattle. Concurrently, we compared the innate immune cytokine responses induced by the PBMCs upon mycobacterial infection and antigenic stimulation. We identified considerable differences in key pro-inflammatory cytokine responses between these breeds that potentially contribute to the differential susceptibility to mycobacterial infection and varied incidence of bTB in these breeds of cattle in India.

Results

Higher incidence of tuberculin reactors and myco-PCR positivity in crossbred cattle

To identify, and segregate bTB-negative animals we performed standard SITT, and myco-PCR-based screening of both indigenous Sahiwal breed, and SHF crossbred cattle from a dairy herd (Figure 1). Comparison of SITT response to bovine tuberculin was performed on 24 Sahiwal, and 26 SHF cattle. A total of 9 animals were found to be bovine tuberculin reactors equating to SITT positivity of 18% (9/50) (Figure 1A). Estimation of the breed-specific tuberculin reactors revealed 8.33% (2/24) positivity among Sahiwal cattle, whereas 26.92% (7/26) positivity in the case of crossbred SHF cattle. Concurrently, our myco-PCR methodology that involves a

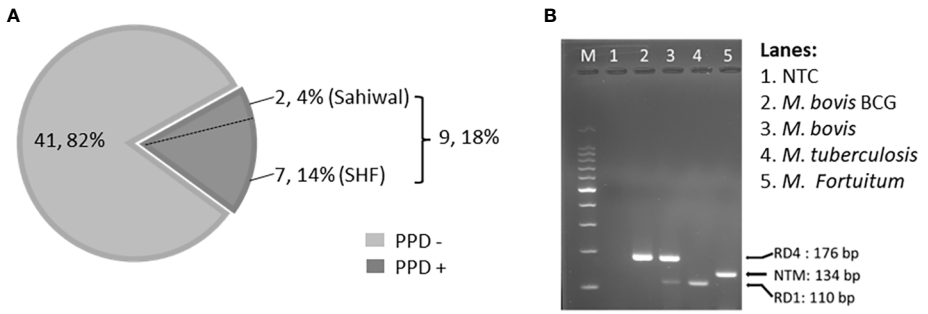

FIGURE 1
Single Intradermal Tuberculin Test, and PCR-based detection of mycobacterial DNA. **(A)** The pie chart depicts the incidence of SITT positivity in cattle. A total of 50 cattle were analyzed by SITT. Out of 50 cattle, 9 (18%) were tuberculin reactors. Out of 9 SITT+ cattle, 7 cattle (14%) belonged to Cross Breed and the remaining 2 (4%) were Sahiwal cattle. **(B)** Agarose gel electrophoresis image of the multiplex PCR using a combination of, - a primer pair targeting specific DNA sequence of the Region of Difference-1 (RD-1) that detects both *M. bovis*, and *M. tuberculosis* but not BCG, or NTMs, - a primer pair targeting the upstream and downstream sequences of the RD-4 region specifically detecting BCG, and *M. bovis* DNA but not *M. tuberculosis* or NTMs, and – a primer pair that detects the presence of pan NTMs DNA. NTC, no treatment control.

combination of singlet PCRs using previously published primers that detect *M. bovis, M. tuberculosis, M. orygis, MTC*, and pan non-tuberculous mycobacterial (NTM) DNA including the *Mycobacterium avium* complex (MAC) (Supplementary Figure S1), and an in-house assembled multiplex-PCR that simultaneously detects and differentiate *M. bovis, M. bovis* BCG, *M. tuberculosis* and pan NTM DNA in the cattle milk and urine samples (Figure 1B) revealed presences of 4% of *M. bovis* positivity (2/50, RD1+, RD4+), 6% *M. tuberculosis* positivity (3/50, RD1+, RD4-), 14% MTC positivity (7/50), and 32% NTM positivity (16/50) (Table 1) (24–27). Altogether, a considerably higher number of crossbred cattle was found to be myco-PCR positive (8/26) compared to the native Sahiwal breed (1/24). Supplementary Table S1 depicts the detailed distribution of SITT and myco-PCR assay results among all the animals. The primers targeting different mycobacteria are listed in Supplementary Table S2. We have excluded animals showing SITT positivity, or PCR positivity to any of the mycobacterial species screened in this study for the subsequent evaluation of mycobacterial growth, host cellular responses to mycobacterial infection, and antigenic stimulation (Table 1 and Supplementary Table S1). These SITT-negative and Mycobacterial-PCR-negative cattle were considered mycobacteria-naïve animals that are expected to show primary immune responses when exposed to mycobacterial infection of antigenic stimulation.

Crossbred cattle PBMCs are conducive to mycobacterial replication

For a comparative evaluation of the permissiveness of the two breeds of cattle to mycobacterial infection, a bovine PBMC-mycobacteria *in vitro* infection assay was established. First, we generated reporter strains of *M. bovis* BCG, and *M. tuberculosis H37Ra* expressing mCherry and tdTomato via episomal plasmids *pMSP12::mCherry* and *pTEC27-Hyg*, respectively (Supplementary Table S3) (28). The correlation of the fluorescence of the reporter mycobacterial strains to the CFU was evaluated both in the 7H9 broth culture (Supplementary Figures S2A, B), as well as in the bovine macrophage cells (BOMAC) (Supplementary Figures S2C, D) (29, 30). The association of the reporter mycobacterial number to total fluorescence was found to be in strong agreement, and a bacterial number-dependent increase in the total fluorescence was observed over five days in both broth culture and BOMAC cell culture (Supplementary Figure S2). A pre-calibrated MOI of 1:10 (Cell: Bacteria) was used for a 5 days-long bovine PBMC culture along with fluorescence measurement at an interval of 24 hours following infection to evaluate the comparative mycobacterial growth in two breeds of cattle (Figure 2). The mean fluorescence of *M. bovis BCG* in the SHF derived PBMC exhibited increasing trend compared to the PBMCs derived from Sahiwal breed of cattle, and at day-5 post-infection the bacterial fluorescence was found to be significantly higher in the former group compared to the later (Figure 2A). Further, PBMCs from Sahiwal breed showed a considerably lower fluorescence for *M. tuberculosis* H37Ra over the course of infection which is significantly lower at day-4 and day-5 post-infection highlighting restricted growth of the bacteria in comparison to the PBMCs from the crossbred SHF cattle (Figure 2B). These observations clearly indicate that indigenous Sahiwal breed of cattle possess significantly greater control over the growth of *M. bovis*, and *M. tuberculosis* strains in comparison to the crossbred SHF cattle.

Higher IFN-γ production by PBMCs from indigenous cattle breed upon mycobacterial infection, and antigenic stimulation

IFN-γ is an important cytokine that regulates innate as well as acquired cell-mediated and humoral immunity to infection by eliciting a number of biological responses in several cell types (31, 32). IFN-γ plays a pivotal role in exerting the host's protective immunity against Mycobacterial infection (33, 34). Evaluation of the protein level of IFN-γ by ELISA in the bPBMC culture media at 24-hour post-infection with *M. bovis BCG, and M. tuberculosis H37Ra* revealed a significant difference between Sahiwal and SHF cattle (Figure 3). In the first set of experiments, PBMCs from Sahiwal cattle showed a higher production of IFN-γ than SHF cattle when exposed to *M. bovis BCG, and M. tuberculosis H37Ra* infection (Figure 3A), while LPS stimulation resulted in a comparable level of IFN-γ production by PBMCs from both the sources. This observation was reconfirmed by subsequent experiments wherein in addition to *M. bovis BCG, M. tuberculosis H37Ra* infection, bPBMC were also stimulated with bovine PPD (PPD-B), avium PPD (PPD-A), *M. tuberculosis*- whole cell lysate (WCL), cell wall (CW), and lipoarabinomannan (LAM). We observed that the IFN-γ levels at 24-hour post-infection were significantly higher in PBMCs from Sahiwal cattle than SHF cattle in the case of *M. bovis BCG*, and *M. tuberculosis H37Ra* infection, and PPD-B stimulation (Figure 3B). For the rest of the stimulant groups no considerable difference was observed. These observations indicate higher induction of IFN-γ by PBMC from indigenous Sahiwal cattle during infection might contribute to the restriction of mycobacterial growth and the resultant lower incidence of bTB in this breed of cattle.

TABLE 1 Distribution of SITT and myco-PCR positivity across all the cattle.

Categories	RD1+	RD4+	RD1+ RD4+	MTC+	NTM+	SITT+	SITT+ RD1/ RD4/ MTC+	SITT+ or RD1/ RD4/ MTC +	SITT+ RD1/ RD4/ MTC -	SITT- RD1/ RD4/ MTC +	Any positive
No. of cattle	5	2	2	7	16	9	5	15	4	6	20

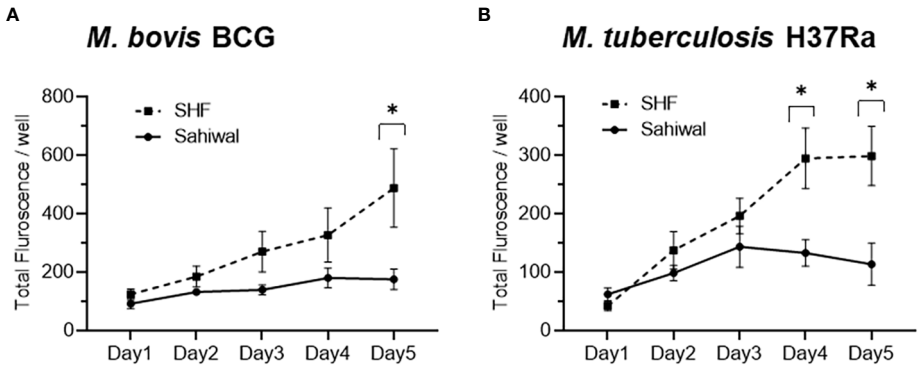

FIGURE 2
Growth of mycobacteria in bovine PBMC. PBMC from Sahiwal and SHF cattle were infected with fluorescence reporter **(A)** *M. bovis BCG-mCherry;* λ_{ex}:587nm and λ_{em}:610nm, and **(B)** *M. tuberculosis H37Ra-tdTomato;* λ_{ex}:554nm and λ_{em}:583nm at an MOI of 1:10 (cell: bacteria). The fluorescence intensity of reporter mycobacteria strains was monitored every 24 hours for 5 days post-infection, and data is depicted as line plots by adjoining the mean ± SEM fluorescence/well measured every day for each mycobacterial strain. n = 6, *,p<0.05 (t-test). The data is representative of two experiments.

Transcriptional induction of pro-inflammatory immuno-signature by indigenous cattle PBMCs

Pathogenesis of pulmonary TB largely depends on the orchestration of the players of the cellular immune system and a synchronized interaction of various pro- and anti-inflammatory cytokines at the site of infection (18, 31, 33). A fine-tuning of multiple cytokines is essential to an effective clearance of the pathogen (35–37). RNA extracted from the PBMCs from the above experiment at 24 hours post-infection were analyzed for several major cytokines, and signaling molecules by real-time RT-PCR using gene-specific primers (Supplementary Table S4). These includes IFN-γ, IL-17, TNF-α, IFN-β, IL-1β, IL-6, IL-10, cGAS, STING, TBK1, IRF3, and IRF7. Figure 4 depicts the relative expression of relevant immune-response genes in bar diagrams. Of these various immunological mediators, significantly higher transcriptional induction of IFN-γ was observed in case of PBMCs from Sahiwal cattle than crossbred cattle when infected with *M. bovis BCG* and *M. tuberculosis H37Ra*, (Figure 4A). In addition, a similar pattern of significantly higher induction was observed in case of IL-17 gene expression by PBMCs from Sahiwal

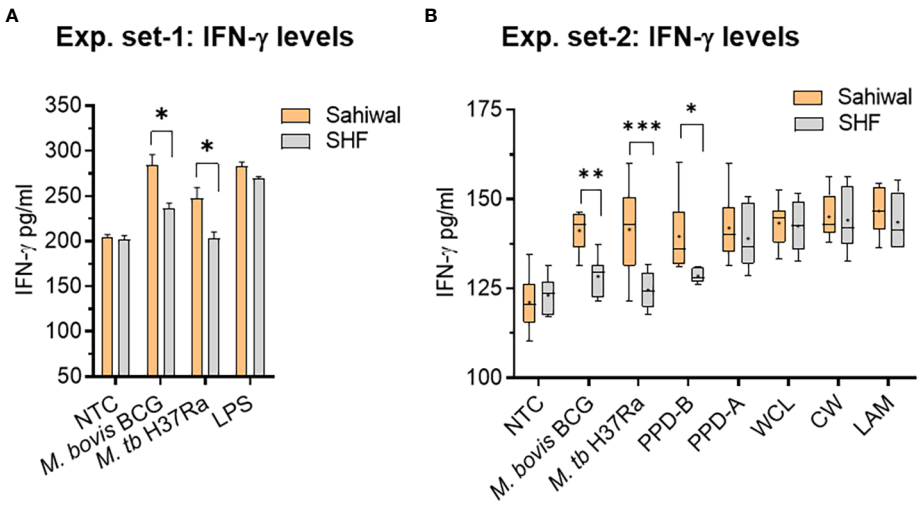

FIGURE 3
IFN-γ response of bovine PBMC to mycobacterial infection and antigenic stimulation. Two separate sets of experiments were performed at an interval of six months using freshly prepared PBMCs from same cohort of cattle. In the first set of experiment, **(A)** the PBMCs obtained from SITT and myco-PCR negative Sahiwal and SHF cattle were infected with *M. bovis* BCG or *M. tuberculosis* H37Ra at an MOI of 1:10 (cell: bacteria) or stimulated with Lipopolysaccharide (LPS, 5ug/ml). The bar graph represents IFN-γ level in the culture supernatant (pg/ml). Data is mean ± SEM, n=3 animals per group, *, p<0.05. In the second set of experiment, **(B)** PBMC were either infected with *M. bovis* BCG or *M. tuberculosis* H37Ra at an MOI of 1:10 (cell: bacteria) or stimulated with bovine PPD (PPD-B, 300 IU/ml), Avian PPD (PPD-A, 250 IU/ml), *M. tuberculosis* whole cell lysate (WCL, 5 ug/ml), cell wall (CW, 5 ug/ml) and lipoarabinomannan (LAM, 5ug/ml). IFN-γ level was measured at 24 hours post-infection and graphically represented by a box plot, wherein median values are denoted by the horizontal line, the mean is represented by '+', the interquartile range by boxes, and the maximum and minimum values by whiskers. n=6 animals per group. *, P < 0.05; **, P < 0.01; ***, P < 0.001 (t-test). The data is representative of two experiments. NTC, no treatment control.

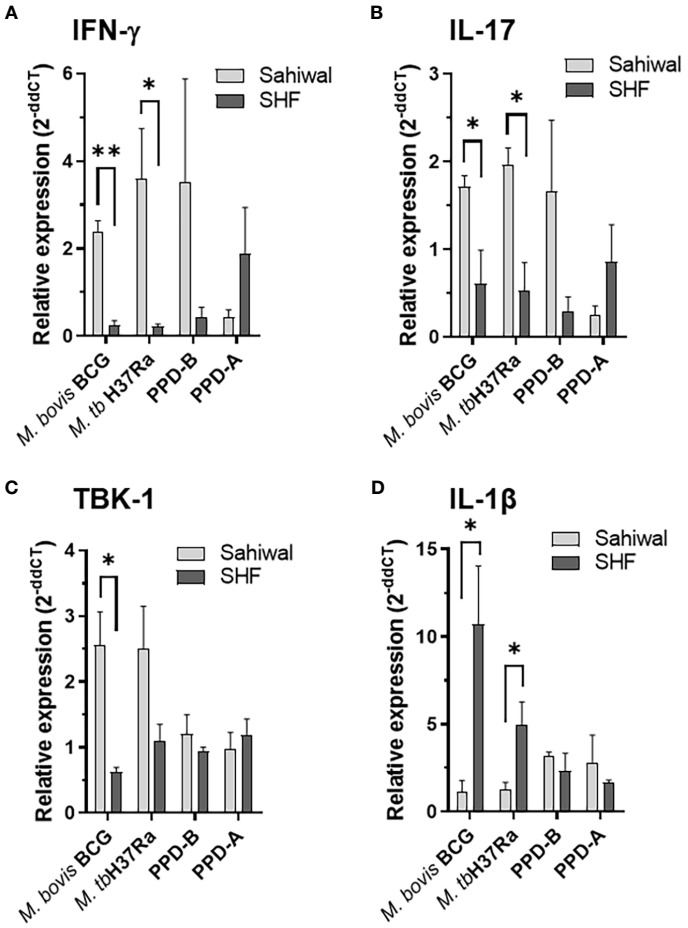

FIGURE 4
Modulation of host gene expression in bovine PBMC by mycobacterial infection and antigenic stimulation. Expression of various cytokines and immunity-related genes were measured on the RNA extracted from PBMC infected with *M. bovis* BCG or *M. tuberculosis* H37Ra at an MOI of 1:10 (cell: bacteria) or stimulated with bovine PPD (PPD-B, 300 IU/ml) and Avium PPD (PPD-A, 250 IU/ml at 24-hour post-infection by semi-quantitative real-time RT-PCR using gene-specific primers. **(A)** IFN-γ, **(B)** IL-17, **(C)** TBK-1 and **(D)** IL-1β. The data were normalized to RPLP0 expression levels and then normalized to the values of uninfected/unstimulated cells to obtain ddCT values. Data is represented as a bar diagram of mean ± SEM of 2^{-ddCT} values as relative expression, n=3, *, p<0.05 (t-test); **, p<0.01.

cattle compared to the PBMCs from crossbred SHF cattle when exposed to *M. bovis BCG* and *M. tuberculosis H37Ra* infection (Figure 4B). The serine/threonine kinase TBK-1, which is known for its involvement in the innate immune response to infection by mediating the cGAS-STING-IFN-β axis of cytosolic surveillance pathway, was also found to be significantly upregulated following *M. bovis* BCG infection of the PBMCs from Sahiwal cattle in comparison to the PBMCs from crossbred cattle (Figure 4C). In contrast, IL-1β expression was significantly higher in crossbred cattle PBMCs upon infection with both *M. bovis BCG* and *M. tuberculosis H37Ra.* (Figure 4D). Rest of the genes analyzed in this study exhibited a comparable expression pattern in case of both the breeds of cattle (Supplementary Figure S3). Stimulation with PPD-B, PPD-A, WCL, CW, and LAM did not exhibit a considerable difference in gene expression between the two breeds of cattle (data not shown). Our findings from quantitative real-time PCR indicates differential transcriptional regulation of important cytokines and signaling pathway such as IFN-γ, IL-17, IL-1β, and TBK-1 upon mycobacterial infection may contribute to the differential permissiveness of the two breeds of cattle to bTB infection.

Higher nitric oxide production by PBMCs from indigenous cattle

Production of NO by macrophages represents an important defense mechanism against *M. tuberculosis* and contributes to the host's ability to control and combat the infection (38, 39). We measured nitrite levels in the PBMC culture supernatants, which is an indirect measure of NO production. As shown in Figure 5, PBMCs from the Sahiwal cattle produced relatively higher levels of NO over the crossbred cattle PBMCs upon *Mycobacterial* infection or antigenic stimulation. Notably, a statistically significant difference was observed in the case of *M. tuberculosis* H37Ra infection and PPD-A stimulation.

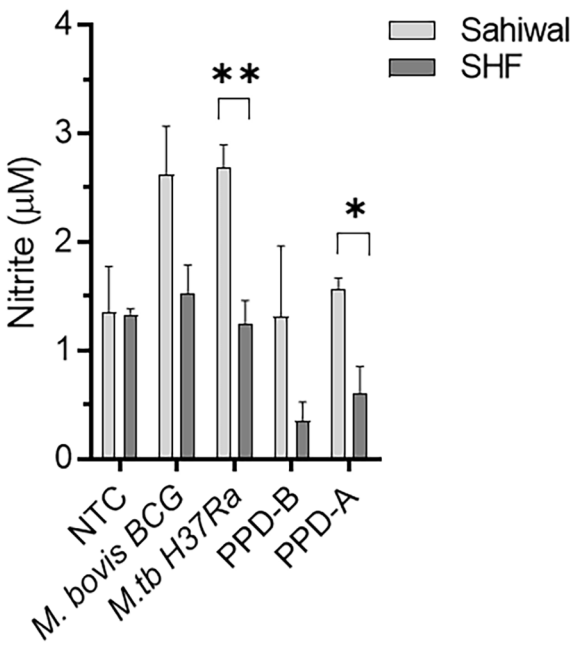

FIGURE 5
Nitric Oxide production by bovine PBMCs upon Mycobacterial infection and antigenic stimulation. PBMC were either infected with *M. bovis* BCG or *M. tuberculosis* H37Ra at an MOI of 1:10 (cell: bacteria) or stimulated with bovine PPD (PPD-B, 300 IU/ml), Avian PPD (PPD-A, 250 IU/ml). Culture supernatant was separated at 24 hours post-infection and subjected to Griess assay for nitrite, a stable metabolite of NO. The bar diagram depicts the Mean ± SEM of Nitrite levels in the culture media. n=3 animals per group. *, P < 0.05, **, P < 0.01, (t-test). NTC, No treatment control. The data are representative of two similar experiments.

Discussion

The susceptibility and/or resistance of a host to TB is influenced by multiple factors which include: the nutritional status of the host, age, sex, underlying diseases, host genetic traits, and interaction between the host and the environment (16). Numerous studies have indicated that genetic diversity among organisms contributes immensely to the differential immune response (21, 22). A number of studies reported that bTB was more prevalent in crossbred cattle compared to the indigenous cattle breeds in India (17, 40). Thakur and colleagues investigated the prevalence of bTB in an organized farm, and a cow shelter in northern India and reported higher bTB positivity in Jersey crossbreds (40). Das and colleagues reported markedly higher incidences of bTB in exotic and crossbred cattle (34.6%) compared to indigenous cattle (10.5%) in India (17). A higher incidence and severity of pathology of bTB in the Holsteins breed compared to Zebu breeds was reported in a study conducted in central Ethiopia (10). As it is apparent that indigenous breeds of cattle have a markedly lower incidence of bTB compared to the exotic and crossbred cattle, a comparison of immune responses to bTB infection in these cattle may discern the clue of protective immune signature to bTB in cattle.

India is home to the largest cattle population in the world with an array of indigenous, and crossbred varieties with enormous genetic variability. Cross-breeding practices remained a preferred approach to enhance the milk yield of indigenous dairy breeds of cattle for more than half a century in India (41). Especially, the use of European donor breeds such as Holstein Friesian, Jersey, Brown Swiss, Red Dane, etc. for improving non-descript Indian cattle as well as pure-breed indigenous cattle, and the impact of cross-breeding on milk production, reproductive performance, and sustainability in Indian agro-climatic conditions were thoroughly studied via a number of cattle development programs. Exotic inheritance of 1/2 and 5/8 was found to be superior in milk production and sustainability parameters in the majority of the studies compared to other genetic grades (41, 42). Lower or higher exotic inheritance than the above-mentioned grades did not result in any economic benefit from such cross-breeding practices but rather resulted in unsustainable breed quality in the Indian agro-climatic conditions. As per the last livestock census, crossbred cattle represent more than one-third of India's total cattle population and contribute to nearly 48% of total cow milk (43). However, how cross-breeding has influenced the susceptibility and/or resistance trait to different infectious diseases, and the underlying genetic and immunological mechanisms are rarely evaluated systematically.

Here, we studied two of the most prominent dairy breeds of cattle in India, indigenous Sahiwal and crossbred SHF. The crossbred SHF animals included in this study possess 50%-62.5% exotic inheritance. Using myco-PCR alone, and a combination of both standard SITT assay and myco-PCR, we found a significantly ($p<.05$ and $p<.01$, respectively) higher incidence of tuberculin reactors-cum-PCR positivity in SHF cattle compared to Sahiwal cattle (Table 2). Our findings are in accordance with the previous studies where a higher percentage of tuberculin reactors was seen in exotic/crossbred cattle than in native cattle (10, 15, 44, 45). Further, the Mycobacterial-PCR assays enabled us to detect the presence of MTC and NTM genomic DNA in the milk and urine samples isolated from cattle. The presence of NTM may interfere not only with the SITT readout but also may affect the cellular immune responses of PBMCs isolated from the cattle. Application of such PCR assays provides a cost-effective method to detect not only the species of the infecting mycobacteria in the clinical settings but also allowed us to identify mycobacterial infection-free cattle to be included in the subsequent *ex vivo* PBMC-based experiments.

IFN-γ is the key cytokine indispensable in defence against TB. IFN-γ activated macrophages enhance the microbicidal activity of macrophages by allowing the formation of phagolysosomes wherein the mycobacteria are deprived of essential nutrients such as iron, and exposed to anti-microbial peptides, and reactive oxygen or nitrogen intermediates (46–48). Lower production of IFN-γ indicates a reduced activity of macrophages which promotes mycobacterial growth (32, 37). The findings from ELISA and real-time RT-PCR indicated a significantly higher induction of IFN-γ response by PBMCs from Sahiwal cattle compared to crossbreed cattle PBMCs indicating induction of superior anti-TB immune responses in the native Sahiwal cattle (Figures 3, 4). This observation was supported by the lower growth of both *M. bovis BCG* and *M. tuberculosis H37Ra* strains in the PBMC cultures of Sahiwal cattle compared to the crossbred SHF cattle (Figure 2). Notably, only live *Mycobacterial* infection and PPD-B stimulation resulted in differences in IFN-γ levels, whereas neither LPS

10.3389/fimmu.2023.1199092

TABLE 2 Influence of breed variation on the incidence of bTB in cattle.

Distribution of number of cattle showing positive and negative test results									
Breed	SITT			Myco-PCR			Combined SITT and Myco-PCR		
	+	-	Total	+	-	Total	+	-	Total
Sahiwal	2	22	24	1	23	24	2	22	24
Sahiwal x HF	7	19	26	8	18	26	13	13	26
Total	9	41	50	9	41	50	15	35	50

Statistical significance of difference of bTB incidence between breeds			
	Level of significance (*p value*)		
Types of Significance tests	SITT	Myco-PCR	Combined SITT and Myco-PCR
Pearson Chi-square	0.087	0.014*	0.001**
Fisher's Exact Test	0.089	0.016*	0.001**
Phi-coefficient	0.087	0.014*	0.001**
Cramer's V	0.087	0.014*	0.001**

*$p < 0.05$, **$p < 0.01$, Statistical package SPSS Vr.25 was used for the analysis.

stimulation nor stimulation with other *M. tuberculosis* derived antigen complexes such as LAM, CW, and WCL showed any differences between the breeds. This may be due to the upregulation and secretion of immunodominant antigens during live bacilli infection, and the dominant presence of such antigens in PPD-B, resulting in differential immune activation by PBMCs from the two cattle breeds through a mechanism that is yet to be identified. Additionally, comparable immune responses to LPS suggest the presence of similar TLR-4 mediated responses by PBMCs from both cattle breeds.

Although IFN-γ plays a key role in the defence against TB, this cytokine alone can't generate the necessary immune response to provide protection against TB. The TB disease progression is controlled by a coordinated network of several different cytokines, chemokines, and signaling molecules. We analyzed the mRNA levels of a number of pro-inflammatory, anti-inflammatory, and immuno-regulatory mediators in addition to IFN-γ such as IL-17, TNF-α, IFN-β, IL-1β, IL-10, cGAS, STING, TBK1, IL-6, IRF3, and IRF7. While IL-17, IL-1β, and TBK1 exhibited considerable differential regulation in the mRNA levels, a comparable level of expression was observed for the rest of the immune mediators (Figure 4). A significantly higher induction of IL-17 was exhibited by PBMCs from Sahiwal cattle compared to crossbreed cattle PBMCs (Figure 4B). IL-17 is another key cytokine involved in exhibiting protective immunity against *M. tuberculosis* infection. It plays a major role in combating the growth of the tubercle bacilli by promoting a Th1-biased immune response (49). The differentiation of Th17 cells occurs as a result of an increase in the level of pro-inflammatory cytokines such as IL-6, IL-23, IL-1β, and TNF-α (36, 49–51). IL-17 induces the recruitment of neutrophils, macrophages, and Th1 cells to the site of inflammation. IL-17 also restricts the growth of Mycobacteria by inducing the expression of various chemokines, and by recruiting IFN-γ-producing cells (35). In contrast, IL-1β expression was significantly higher in crossbred cattle PBMCs upon mycobacterial infection (Figure 4D). While IFN-γ and IL-17 primarily promote macrophage activation, granuloma formation, and clearance of intracellular tubercle bacilli, IL-1β has been implicated in aggravated inflammation (52). Further, phosphorylation of TBK-1 is involved in a plethora of intracellular signaling events including the cGAS-STING-IFN-β axis of the cytosolic surveillance pathway of the host to respond to invading infectious agents including regulation of cell proliferation, autophagy, and apoptosis (53, 54). While the role of TBK-1 in antiviral response is well documented, divergent views on the anti-bacterial effect especially anti-mycobacterial responses are linked to this cytosolic kinase (55–58). Several studies reported the essentiality of the TBK-1 phosphorylation-mediated activation of the IRF-1 pathway for mycobacterial clearance, while others associated it with higher immunopathology (56, 57). These observations indicate the necessity of tightly regulated TBK-1-mediated signaling for a host-favored immune response.

During *M. tuberculosis* infection, the association of increased IFN-γ and with increased NO production by macrophages plays a critical role in host defense against the pathogen (38, 39). IFN-γ is a pro-inflammatory cytokine produced by activated T cells and natural killer cells, and it stimulates macrophages to enhance their antimicrobial activities (46). When macrophages encounter *M. tuberculosis*, the production of IFN-γ is triggered, leading to the activation of macrophages. Activated macrophages then produce increased levels of NO through the inducible nitric oxide synthase pathway, which serves as a potent bactericidal agent against *M. tuberculosis*. Thus, increased IFN-γ levels coupled with enhanced NO production by PBMCs from Sahiwal cattle represents a crucial immune response that aids in the control of the *Mycobacterial* growth.

In some, our study elucidated the association of important mediators of immune responses with the differential bTB susceptibility phenotype of the indigenous Sahiwal cattle and the

crossbred SHF cattle by employing *ex vivo* bovine PBMC-mycobacterial infection model using *M. bovis* BCG vaccine strain, and *M. tuberculosis* H37Ra strain. Especially, our study highlighted that divergence in the expression of host factors such as IFN-γ, IL-17, IL-1β, and TBK-1 potentially play a major role in determining the degree of susceptibility to mycobacterial infection in cattle. In addition, heightened activation of macrophages as evident from increased IFN-γ, and NO levels in the Sahiwal cattle might be contributing to a greater control of *Mycobacterial* growth. However, it is important to acknowledge certain limitations to this study that require further investigation. Based on our use of BSL2 grade mycobacteria- *M. bovis* BCG and *M. tuberculosis* H37Ra, this study primarily serves as a proof-of-principle that susceptibility to bTB is higher in crossbred SHF cattle compared to native Sahiwal cattle. Further studies with virulent human and bovine tubercle bacilli, a greater number of indigenous and crossbred cattle, and application of genomic, transcriptomic and proteomic approaches would elucidate the association of the global immune response signature to bTB susceptibility and/or resistance in cattle.

Our study also highlighted the importance of the use of PCR-based mycobacterial DNA detection and differentiation of mycobacteria species in studies that allow the identification of mycobacterial infection-naïve cattle to evaluate the innate immune response of PBMCs to mycobacterial stimulation or infection. Further, a highly sensitive multiplex-PCR-based assay would be immensely useful for screening cattle herds as well as human clinical TB cases that would aid in the epidemiological characterization of causative mycobacterial species and devising appropriate treatment strategies.

Finally, this study is an important step forward toward identifying the association of bTB susceptibility to the underlying innate immune responses in indigenous and crossbred cattle in India. This study addresses an extremely important yet untouched aspect of the bTB scenario in Indian cattle which is identifying host factors conferring susceptibility and/or resistance to bTB that remained one of the biggest public health problems for centuries. Our results not only provide proof-of-concept data for the hypothesis that genetic variability of bovine due to breed variation influences bTB susceptibility and resistance but also provide a reason for adopting an appropriate crossbreeding policy that balances production and disease resistance traits for sustainable livestock farming.

Materials and methods

Bacteria, plasmids, and generation of reporter mycobacterial strains

The mycobacterial strains and plasmids used in the study are listed in Supplementary Table S1. *M. bovis* BCG (Danish 1331 sub-strain), and *M. tuberculosis* H37Ra strain was kindly provided by Prof. S. Banerjee, University of Hyderabad, India. Non-Tuberculous Mycobacteria (NTM) *M. fortuitum* was procured form MTCC, CSIR-IMTECH, Chandigarh, India. Mycobacterial strains were grown to mid-log phase in Middle Brook (MB) 7H9 media and glycerol stocks were prepared and stored at -80°C as described earlier (59). For *in vitro* infection, fresh bacterial cultures were grown to the mid-log phase, and bacterial cells were washed thoroughly with 1XPBS, and finally resuspended in cell-culture media following pre-calibrated dilutions, as described previously (56). For generating Mycobacterial reporter strains first, electrocompetent cells of *M. bovis* BCG and *M. tuberculosis* were prepared as described previously (56), and transformed with pMSP12::mCherry (was a gift from Lalita Ramakrishnan, Addgene plasmid # 30169; http://n2t.net/addgene:30169), and pTEC27-Hyg (was a gift from Lalita Ramakrishnan, Addgene plasmid # 30182; http://n2t.net/addgene:30182) (28). Briefly, 100µl of competent Mycobacterial cells were mixed with 100ng of plasmid DNA, and transferred to a Micro Pulser Electroporation cuvette (Biorad # 1652086 with 0.2 cm gap) and pulsed at 2500V, 25uF capacitance, and 1000 Ω resistance using an electroporator (Gene Pulser Xcell Microbial System #1652662, Bio-Rad). The cells were immediately aspirated and inoculated in 2ml of MB-7H9 broth without any selective antibiotics and incubated at 37°C under shaking conditions for 48 hours. Subsequently, bacterial cells are plated onto MB-7H11 agar containing selective antibiotics- 25 µg/ml of Kanamycin, and 150 µg/ml of Hygromycin, respectively, and incubated at 37°C for 4 weeks. Transformed bacterial clones grown on the selective plates were detected by colored colonies, and also confirmed for the presence of plasmid by colony PCR, and subsequently confirmed by fluorescence microscopy. Glycerol stocks of the reporter mycobacterial strains were prepared, and stored for future use. All the mycobacterial strains used in this study were of the BSL-2 category, and these are cultured in a BSL-2 laboratory.

Genomic DNA extraction from mycobacteria

Standard methodology was followed for genomic DNA extraction from various mycobacteria as described previously (60). Briefly, the bacterial culture was incubated with 1% glycine in a 37°C shaker for 24 hours. After incubation, the cells were harvested by centrifuging the bacteria at 8000 rpm for 10 minutes. The cells were resuspended in 5ml of TEG (Tris 25mM pH 8.0, EDTA 10mM pH 8.0, Glucose 50 mM) solution and mixed gently. 500µ of lysozyme (10mg/ml) was added to this suspension and incubated overnight at 37°C a shaker incubator. Later, 1 ml of 10% SDS and 500µl of Proteinase K (20mg/ml) were added to the cell lysate and incubated at 55°C for 40 minutes. Subsequently, a solution comprising 2ml of 5M NaCl and 1.6ml of pre-warmed 10% CTAB was added to the cell lysate which was later incubated at 65°C for 10 minutes. The suspension was then centrifuged at 12000 rpm for 30 minutes at room temperature. The supernatant was subjected to phenol-chloroform extraction twice, and genomic DNA was precipitated by the addition of isopropanol. The DNA pellet was washed twice with 70% ethanol, air dried, and resuspended in autoclaved distilled water and stored at -20°C. The genomic DNA was used as a template for PCR experiments. Genomic DNA from *Mycobacterium bovis* BCG, *M. tuberculosis*

H37Ra, and *M. fortuitum* were extracted by the above method. Genomic DNA extracted from *Mycobacterium bovis* irradiated whole cells (#NR-31210), and purified Genomic DNA of *M. tuberculosis* H37Rv strain (#NR-13648) procured from BEI resources, USA was used as PCR templates.

Animals

For this study, we selected cattle herds from two neighboring organized dairy farms in the Nadia district of West Bengal, India. Both farms follow similar feeding and management practices, and both raise a mixed population of Sahiwal and SHF crossbred cattle. We selected cattle (cows) that were over two years old, not pregnant during the study period, and had not undergone any tuberculin testing in the previous one year. Based on these criteria, a total of 50 cattle were included in the study, consisting of 24 Sahiwal and 26 SHF cattle.

DNA extraction from cow milk and urine

Genomic DNA was isolated from cow milk and urine samples as described previously (2). Briefly, milk samples were centrifuged at 12,000 x g for 20 minutes at room temperature. A sterile cotton swab was used to remove the fat layer, and the supernatant was discarded. The pellet was vortexed and subsequently resuspended in 500µl of IRS [Inhibitory Removing Solution with pH (7.4) containing 25M guanidium isothiocyanate, 0.025M EDTA, 0.05M Tris, 0.5% Sarkosyl and 0.186M β-mercaptoethanol]. Later the samples were incubated at 37°C for 60 minutes. After incubation, the samples were again centrifuged at 12,000 x g for 10 minutes and the supernatant was discarded. The pellet was washed with water once and resuspended in 100µl of lysis buffer (10% Chelex 100, 0.3% tween 20, 0.03% Triton X100). The samples were then incubated at 90°C for 40 minutes and subjected to another round of centrifugation at 10,000 x g for 10 minutes at room temperature. The supernatant was collected and used as template DNA for PCR reactions, or stored at -20°C for future use.

Single and multiplex- PCR assay for mycobacterial DNA detection

PCR assays were carried out targeting the genomic DNA of single mycobacterial species as well as multiple species in a single reaction. We observed higher sensitivity of single species/gene-specific PCR compared to the multiplex-PCR assay. Comparative genomics has revealed that based on the presence or absence of regions of difference (RD) mycobacterial species or strains can be differentiated. In this study, a combination of previously published primers targeting specific sequences of RD1, RD4, RD12, and *rpoB* gene was used to develop the single and multiplex- PCR to detect and differentiate *M. tuberculosis*, *M. bovis*, *M. bovis BCG*, *M. orygis, pan-MTC* and pan-*NTM (*including MACs*)* in the cattle samples (Supplementary Figure S1). Supplementary Table S1 shows the list of mycobacterial genomic region-specific primers used in this study. The PCR protocol was executed using the Sapphire PCR master mix (TAKARA) following manufacturer protocol. Subsequently, PCR amplicons were analyzed by agarose gel electrophoresis and visualized using a UV trans-illuminator. The expected size of amplicons with RD1, RD4, RD12-*M. orygis*, MTC, and NTM primers are 110bp, 176bp, 264bp, 235bp, and 134bp, respectively (Supplementary Figure S1). While the multiplex-PCR could detect mycobacteria in 0.1ng of template DNA, the single species PCR could detect mycobacteria in 0.01ng of total genomic DNA extracted from cattle milk or urine.

Single intradermal tuberculin test

Fifty cows from two adjacent herds were subjected to the single intradermal tuberculin test. The neck region of the animals was shaved and the thickness of the skin was measured with the use of a caliper before injecting bPPD. One hundred microliters (0.1ml) of bovine PPD (2,000 U/animal of bPPD) (obtained from Indian Veterinary Research Institute, Izatnagar, India; 1mg protein/ml) was injected into the skin of the cervical region. Seventy-two-hour post bPPD injection skin induration was evaluated by measuring the skin thickness with a caliper. The result was graded as bPPD positive reactor when differences in the skin thickness at the injection sites are at least 5 mm or greater.

In vitro bovine macrophage cell culture and mycobacterial growth assay

Bovine macrophage cell line- BOMAC was used for calibrating the infection dose (MOI), and evaluating the association of fluorescence measurements of the reporter mycobacterial strains with the number of bacteria over the period of infection (29, 30). BOMAC cells were maintained in DMEM supplemented with 10% heat-inactivated Fetal Bovine Serum (FBS). BOMAC cells were infected with the reporter strains of *M. tuberculosis H37Ra-tdTomato*, and *M. bovis BCG*-mCherry at different MOIs. The cells were infected for 3 hours, subsequently, the cells were washed thoroughly, and incubated in a TC incubator in fresh media. The fluorescence intensity was measured at λex/λem 554/581nm (*M. tuberculosis H37Ra-pTEC27*), and 587/610nm (*M. bovis BCG*-mCherry) respectively at an interval of 24 hours daily for 5 days using a fluorescence multimode plate reader (Biorad). An MOI of 1: 10 was considered for *ex vivo* mycobacterial growth in the bPBMC.

Ex vivo bovine PBMC culture and mycobacterial growth assay

Blood samples were collected from clinically healthy, SITT-negative, and myco-PCR-negative cattle. Five ml of blood was collected from the jugular vein of each animal, and bPBMC was isolated using Histopaque®-1077 (Sigma) following manufacturer

recommendations. Briefly, blood was diluted with DPBS at a ratio of 1:1. The sample was layered slowly on top of the Ficoll density gradient buffer (5 ml diluted Blood on 3 ml Ficoll) and centrifuged at 400 x g for 30 minutes. The monocyte layer was carefully separated and washed twice with DPBS at 200 x g for 10 minutes. Contaminating RBCs were removed from the cell suspension by adding RBC lysis buffer (Sigma-Aldrich) and following manufacturer protocol. Purified bPBMC were then finally suspended in 5ml of DMEM complete media containing antibiotics, and added to an ultra-low attachment 6-well plate. The cells were incubated in a TC incubator for 24 hours. For mycobacterial growth assay, bPBMC were seeded on to 96-well TC plate at a density of $5X10^4$ cells/well. The cells were infected with mid-log phase cultures of reporter mycobacteria (*M. tuberculosis H37Ra-pTEC27* and *M. bovis BCG-mCherry)* at a pre-calibrated MOI of 1:10 and were incubated in a TC incubator. The fluorescence intensity was measured at λex/λem 554/581nm (*M. tuberculosis H37Ra-pTEC27*), and 587/610nm (*M. bovis BCG*-mCherry) respectively at an interval of 24 hours daily for 5 days using a fluorescence multimode plate reader.

Infection and antigenic stimulation of bovine PBMC for evaluation of innate immune responses

For the evaluation of innate immune responses, bPBMC were seeded onto 24-well TC plates at a density of $2X10^5$ cells/well, and infected with either of the mycobacteria (*M. tuberculosis H37Ra, or M. bovis BCG*) at a pre-calibrated MOI of 1:10, or cells were stimulated with LPS (1μg/ml), PPD-B (300 IU/ml), PPD-A (250 IU/ml), *M. tuberculosis* H37Rv Whole Cell Lysate (WCL, 5 μg/ml), cell wall (CW, 5 μg/ml) and purified Lipoarabinomannan (LAM, 5μg/ml). Twenty-four hours post-infection cell culture supernatants were separated for measurement of IFN-γ protein levels, and total RNA was extracted from bPBMC for measurement of the mRNA transcripts levels of major cytokines, chemokines, and innate immune-signaling mediators.

RNA extraction, and real-time RT-PCR

Total RNA was extracted from bPBMC using RNeasy Plus Kit (Qiagen Inc, CA, USA) following manufacturer protocol. Contaminating genomic DNA was removed by additional treatment with RNase-free DNase (Qiagen Inc, CA, USA). The quality and quantity of RNA were analyzed using a NanoDrop Spectrophotometer (Thermo Scientific). cDNA was synthesized from RNA using the Prime script 1st-strand cDNA synthesis kit (Takara) as per the manufacturer's instructions and using a mixture of random hexamer and oligo dT primers. Primers were designed for bovine gene targets (IFN-γ, IL-17, TNF-α, IFN-β, IL-1β, IL-6, IL-10, cGAS, STING, TBK1, IRF3, and IRF7) (Supplementary Table S4) using Primer-BLAST (NCBI) and real-time PCR was performed using a CFX96 Touch System (Biorad). Real-time PCR protocol started with an initial denaturation and enzyme activation at 95°C for 2 minutes followed by 40 cycles of denaturation at 95°C for 15 seconds, annealing and extension were carried out for 1 minute at a temperature ranging from 55°C to 65°C (based on the target gene). Melt curve analysis was performed by heating the samples from 65° C to 95°C with an increment of 0.5 and fluorescence was recorded. Relative gene expression of the target genes was calculated using the $2^{-\Delta\Delta CT}$ method with RPLP0 as an internal control.

Bovine cytokine enzyme-linked immunosorbent assay

Twenty-four hours post-infection cell culture supernatants were separated, filtered through 0.2 μ membrane plate filters, and subjected to ELISA for the measurement of IFN-γ protein levels using bovine IFN-γ specific sandwich ELISA kit as per the manufacturer protocol (K04-0002, Krishgen Biosystems). The absolute concentrations were estimated by referring to a standard curve and expressed as picogram per millilitre.

Nitric oxide measurement by Griess assay

The NO levels were determined using Griess reagent (# 35657, Sisco Research Laboratories Pvt. Ltd.) according to the method described previously (61). Briefly, the assay was performed in 96-well microtiter plate format using cell culture supernatants collected 24 hours post-infection and filtered through 0.2 μ membrane plate filters. 100μl of the culture supernatants were mixed with 100μl of Griess Reagent (0.1% naphthylethylene diamine dihydrochloric acid and 1% sulphanilamide in 5% phosphoric acid) and added to each well in technical duplicates. The samples were incubated at room temperature (25-30°C) for 10 minutes, and optical density was measured with a spectrophotometer at 546nm and the nitrite levels (as an indirect measure of NO) in the samples were quantified according to the standard graph for sodium nitrite.

Statistical analysis

GraphPad Prism 9 was used to perform the statistical analysis and preparation of the graphs. For comparison of group means Student's t-tests were performed, and differences were considered significant when $p<0.05$. All the results are shown as the mean ± SEM unless otherwise described in the figure legends. For comparison of SITT, Myco-PCR, and combined tests data, SPSS vr.25 software was used for performing statistical significance tests.

Data availability statement

The original contributions presented in the study are included in the article/Supplementary Material. Further inquiries can be directed to the corresponding author.

Ethics statement

The animal study was approved by Animal Ethics Committee of the West Bengal University of Animal and Fishery Sciences, Kolkata, India (Approval No. IAEC/22 (B), CPCSEA Reg. No.763/GO/Re/SL/03/CPCSEA, Committee for the Purpose of Control and Supervision on Experiments on Animals, India). The study was conducted in accordance with the local legislation and institutional requirements.

Author contributions

Conceived and designed the experiments: BD. Performed the experiments: RK, SG, AR, HM, US, and BD. Analyzed the data: RK, SG, US, and BD. Contributed reagents/materials/analysis tools/facility: BD and US. Wrote the paper: RK, SG, US, and BD. Provided overall supervision throughout the study: BD. All authors contributed to the article and approved the submitted version.

Funding

Financial support from the NIAB intramural grant, and the Department of Biotechnology (DBT), Govt. of India (Grant No. BT/PR31378/AAQ/1/745/2019) are thankfully acknowledged. Support by DBT for providing Junior Research Fellowship to RK and AR; Department of Science and Technology (DST), Govt. of India for providing the Inspire fellowship (JRF) to SG.

Acknowledgments

Prof. Sharmistha Banerjee, University of Hyderabad, India is thankfully acknowledged for providing *the M. tuberculosis* H37Ra strain.

Conflict of interest

The authors declare that the research was conducted in the absence of any commercial or financial relationships that could be construed as a potential conflict of interest.

Publisher's note

Supplementary material

The Supplementary Material for this article can be found online at: https://www.frontiersin.org/articles/10.3389/fimmu.2023.1199092/full#supplementary-material

References

1. Murai K, Tizzani P, Awada L, Wall L, Mapitse NJ, Cceres P. Panorama 2019-1: Bovine tuberculosis: global distribution and implementation of prevention and control measures according to WAHIS data. In: *Panorama 2019-1: Controlling bovine tuberculosis: a One Health challenge.* (2019) OIE Bulletin. p1:3. doi: 10.20506/bull.2019.1.2912

2. Mishra A, Singhal A, Chauhan DS, Katoch VM, Srivastava K, Thakral SS, et al. Direct detection and identification of Mycobacterium tuberculosis and Mycobacterium bovis in bovine samples by a novel nested PCR assay: correlation with conventional techniques. *J Clin Microbiol* (2005) 43(11):5670–8. doi: 10.1128/JCM.43.11.5670-5678.2005

3. Prasad HK, Singhal A, Mishra A, Shah NP, Katoch VM, Thakral SS, et al. Bovine tuberculosis in India: potential basis for zoonosis. *Tuberculosis (Edinb)* (2005) 85(5-6):421–8. doi: 10.1016/j.tube.2005.08.005

4. Muller B, Durr S, Alonso S, Hattendorf J, Laisse CJ, Parsons SD, et al. Zoonotic Mycobacterium bovis-induced tuberculosis in humans. *Emerg Infect Dis* (2013) 19 (6):899–908. doi: 10.3201/eid1906.120543

5. *Annual Report: 2020-2021, Department of Agriculture, Cooperation & Farmers' Welfare, Ministry of Agriculture & Farmers Welfare, Government of INDIA*. New Delhi: Government of India (2021). p. 295.

6. Ramanujam H, Palaniyandi K. Bovine tuberculosis in India: The need for One Health approach and the way forward. *One Health* (2023) 16:100495. doi: 10.1016/j.onehlt.2023.100495

7. Refaya AK, Bhargavi G, Mathew NC, Rajendran A, Krishnamoorthy R, Swaminathan S, et al. A review on bovine tuberculosis in India. *Tuberculosis (Edinb)* (2020) 122:101923. doi: 10.1016/j.tube.2020.101923

8. Srinivasan S, Easterling L, Rimal B, Niu XM, Conlan AJK, Dudas P, et al. Prevalence of Bovine Tuberculosis in India: A systematic review and meta-analysis. *Transbound Emerg Dis* (2018) 65(6):1627–40. doi: 10.1111/tbed.12915

9. Allen AR, Minozzi G, Glass EJ, Skuce RA, McDowell SW, Woolliams JA, et al. Bovine tuberculosis: the genetic basis of host susceptibility. *Proc Biol Sci* (2010) 277 (1695):2737–45. doi: 10.1098/rspb.2010.0830

10. Ameni G, Aseffa A, Engers H, Young D, Gordon S, Hewinson G, et al. High prevalence and increased severity of pathology of bovine tuberculosis in Holsteins compared to zebu breeds under field cattle husbandry in central Ethiopia. *Clin Vaccine Immunol* (2007) 14(10):1356–61. doi: 10.1128/CVI.00205-07

11. Firdessa R, Tschopp R, Wubete A, Sombo M, Hailu E, Erenso G, et al. High prevalence of bovine tuberculosis in dairy cattle in central Ethiopia: implications for the dairy industry and public health. *PloS One* (2012) 7(12):e52851. doi: 10.1371/journal.pone.0052851

12. Vordermeier M, Ameni G, Berg S, Bishop R, Robertson BD, Aseffa A, et al. The influence of cattle breed on susceptibility to bovine tuberculosis in Ethiopia. *Comp Immunol Microbiol Infect Dis* (2012) 35(3):227–32. doi: 10.1016/j.cimid.2012.01.003

13. Driscoll EE, Hoffman JI, Green LE, Medley GF, Amos W. A preliminary study of genetic factors that influence susceptibility to bovine tuberculosis in the British cattle herd. *PloS One* (2011) 6(4):e18806. doi: 10.1371/journal.pone.0018806

14. Brotherstone S, White IM, Coffey M, Downs SH, Mitchell AP, Clifton-Hadley RS, et al. Evidence of genetic resistance of cattle to infection with Mycobacterium bovis. *J Dairy Sci* (2010) 93(3):1234–42. doi: 10.3168/jds.2009-2609

15. Islam SKS, Rumi TB, Kabir SML, van der Zanden AGM, Kapur V, Rahman A, et al. Bovine tuberculosis prevalence and risk factors in selected districts of Bangladesh. *PloS One* (2020) 15(11):e0241717. doi: 10.1371/journal.pone.0241717

16. Humblet MF, Boschiroli ML, Saegerman C. Classification of worldwide bovine tuberculosis risk factors in cattle: a stratified approach. *Vet Res* (2009) 40(5):50. doi: 10.1051/vetres/2009033

17. Das RD, Dandapat P, Chakrabarty A, Nanda PK, Bandyopadhyay S, Bandyopadhyay S. A cross-sectional study on prevalence of bovine tuberculosis in Indian and crossbred cattle in Gangetic delta region of West Bengal, India. *Int J One Health* (2018) 4:7. doi: 10.14202/IJOH.2018.1-7

18. Dey B, Bishai WR. Crosstalk between Mycobacterium tuberculosis and the host cell. *Semin Immunol* (2014) 26(6):486–96. doi: 10.1016/j.smim.2014.09.002

19. Kramnik I, Dietrich WF, Demant P, Bloom BR. Genetic control of resistance to experimental infection with virulent Mycobacterium tuberculosis. *Proc Natl Acad Sci USA* (2000) 97(15):8560–5. doi: 10.1073/pnas.150227197

20. North RJ, LaCourse R, Ryan L, Gros P. Consequence of Nramp1 deletion to Mycobacterium tuberculosis infection in mice. *Infect Immun* (1999) 67(11):5811–4. doi: 10.1128/IAI.67.11.5811-5814.1999

21. Aravindan PP. Host genetics and tuberculosis: Theory of genetic polymorphism and tuberculosis. *Lung India* (2019) 36(3):244–52. doi: 10.4103/lungindia.lungindia_146_15

22. Moller M, Kinnear CJ, Orlova M, Kroon EE, van Helden PD, Schurr E, et al. Genetic resistance to Mycobacterium tuberculosis infection and disease. *Front Immunol* (2018) 9:2219. doi: 10.3389/fimmu.2018.02219

23. Naranbhai V. The role of host genetics (and genomics) in tuberculosis. *Microbiol Spectr* (2016) 4(5):p1–36. doi: 10.1128/microbiolspec.TBTB2-0011-2016

24. Kim BJ, Hong SK, Lee KH, Yun YJ, Kim EC, Park YG, et al. Differential identification of Mycobacterium tuberculosis complex and nontuberculous mycobacteria by duplex PCR assay using the RNA polymerase gene (rpoB). *J Clin Microbiol* (2004) 42(3):1308–12. doi: 10.1128/JCM.42.3.1308-1312.2004

25. Duffy SC, Srinivasan S, Schilling MA, Stuber T, Danchuk SN, Michael JS, et al. Reconsidering Mycobacterium bovis as a proxy for zoonotic tuberculosis: a molecular epidemiological surveillance study. *Lancet Microbe* (2020) 1(2):e66–73. doi: 10.1016/S2666-5247(20)30038-0

26. Taylor GM, Worth DR, Palmer S, Jahans K, Hewinson RG. Rapid detection of Mycobacterium bovis DNA in cattle lymph nodes with visible lesions using PCR. *BMC Vet Res* (2007) 3:12. doi: 10.1186/1746-6148-3-12

27. Halse TA, Escuyer VE, Musser KA. Evaluation of a single-tube multiplex real-time PCR for differentiation of members of the Mycobacterium tuberculosis complex in clinical specimens. *J Clin Microbiol* (2011) 49(7):2562–7. doi: 10.1128/JCM.00467-11

28. Takaki K, Davis JM, Winglee K, Ramakrishnan L. Evaluation of the pathogenesis and treatment of Mycobacterium marinum infection in zebrafish. *Nat Protoc* (2013) 8(6):1114–24. doi: 10.1038/nprot.2013.068

29. Donofrio G, van Santen VL. A bovine macrophage cell line supports bovine herpesvirus-4 persistent infection. *J Gen Virol* (2001) 82(Pt 5):1181–5. doi: 10.1099/0022-1317-82-5-1181

30. Stabel JR, Stabel TJ. Immortalization and characterization of bovine peritoneal macrophages transfected with SV40 plasmid DNA. *Vet Immunol Immunopathol* (1995) 45(3-4):211–20. doi: 10.1016/0165-2427(94)05348-V

31. Cooper AM, Khader SA. The role of cytokines in the initiation, expansion, and control of cellular immunity to tuberculosis. *Immunol Rev* (2008) 226:191–204. doi: 10.1111/j.1600-065X.2008.00702.x

32. Khan TA, Mazhar H, Saleha S, Tipu HN, Muhammad N, Abbas MN. Interferon-Gamma Improves Macrophages Function against M. tuberculosis in Multidrug-Resistant Tuberculosis Patients. *Chemother Res Pract* (2016) 2016:7295390. doi: 10.1155/2016/7295390

33. Lalvani A, Millington KA. T cells and tuberculosis: beyond interferon-gamma. *J Infect Dis* (2008) 197(7):941–3. doi: 10.1086/529049

34. Flynn JL, Chan J, Triebold KJ, Dalton DK, Stewart TA, Bloom BR. An essential role for interferon gamma in resistance to Mycobacterium tuberculosis infection. *J Exp Med* (1993) 178(6):2249–54. doi: 10.1084/jem.178.6.2249

35. Khader SA, Bell GK, Pearl JE, Fountain JJ, Rangel-Moreno J, Cilley GE, et al. IL-23 and IL-17 in the establishment of protective pulmonary CD4+ T cell responses after vaccination and during Mycobacterium tuberculosis challenge. *Nat Immunol* (2007) 8(4):369–77. doi: 10.1038/ni1449

36. Happel KI, Dubin PJ, Zheng M, Ghilardi N, Lockhart C, Quinton LJ, et al. Divergent roles of IL-23 and IL-12 in host defense against Klebsiella pneumoniae. *J Exp Med* (2005) 202(6):761–9. doi: 10.1084/jem.20050193

37. Cavalcanti YV, Brelaz MC, Neves JK, Ferraz JC, Pereira VR. Role of TNF-alpha, IFN-gamma, and IL-10 in the development of pulmonary tuberculosis. *Pulm Med* (2012) 2012:745483. doi: 10.1155/2012/745483

38. MacMicking JD, North RJ, LaCourse R, Mudgett JS, Shah SK, Nathan CF. Identification of nitric oxide synthase as a protective locus against tuberculosis. *Proc Natl Acad Sci USA* (1997) 94(10):5243–8. doi: 10.1073/pnas.94.10.5243

39. Nathan C, Shiloh MU. Reactive oxygen and nitrogen intermediates in the relationship between mammalian hosts and microbial pathogens. *Proc Natl Acad Sci USA* (2000) 97(16):8841–8. doi: 10.1073/pnas.97.16.8841

40. Thakur AS, Mandeep S, Katoch V, Dhar P, Katoch RC. A study on the prevalence of Bovine Tuberculosis in farmed dairy cattle in Himachal Pradesh. *Vet World* (2010) 3(9):6. doi: 10.5455/vetworld.2010.408-413

41. Singh CV. Cross-breeding in cattle for milk production: achievements, challenges and opportunities in India-A review. *Adv Dairy Res* (2016) 4(3):14. doi: 10.4172/2329-888X.1000158

42. Dhillon JS, Jain AK. Comparison of Sahiwal and different grades of Holstein Friesian × Sahiwal crossbreds for efficiency of milk production. *Indian J Dairy Sci (India)* (1977) 30(3):4.

43. Ministry of Fisheries, A.H.D., Govt. of India and 20th Livestock Census. *All Q25 INDIA Report*. Ministry of Fisheries, Animal Husbandry & Dairying, Govt. of India, New Delhi. p. 1–55.

44. Almaw G, Conlan AJK, Ameni G, Gumi B, Alemu A, Guta S, et al. The variable prevalence of bovine tuberculosis among dairy herds in Central Ethiopia provides opportunities for targeted intervention. *PloS One* (2021) 16(7):e0254091. doi: 10.1371/journal.pone.0254091

45. Ambaw M, Gelalcha BD, Bayissa B, Worku A, Yohannis A, Zewude A, et al. Pathology of bovine tuberculosis in three breeds of dairy cattle and spoligotyping of the causative mycobacteria in Ethiopia. *Front Vet Sci* (2021) 8:715598. doi: 10.3389/fvets.2021.715598

46. Koul A, Herget T, Klebl B, Ullrich A. Interplay between mycobacteria and host signalling pathways. *Nat Rev Microbiol* (2004) 2(3):189–202. doi: 10.1038/nrmicro840

47. Purdy GE, Russell DG. Lysosomal ubiquitin and the demise of Mycobacterium tuberculosis. *Cell Microbiol* (2007) 9(12):2768–74. doi: 10.1111/j.1462-5822.2007.01039.x

48. Gutierrez MG, Master SS, Singh SB, Taylor GA, Colombo MI, Deretic V. Autophagy is a defense mechanism inhibiting BCG and Mycobacterium tuberculosis survival in infected macrophages. *Cell* (2004) 119(6):753–66. doi: 10.1016/j.cell.2004.11.038

49. Aujla SJ, Dubin PJ, Kolls JK. Th17 cells and mucosal host defense. *Semin Immunol* (2007) 19(6):377–82. doi: 10.1016/j.smim.2007.10.009

50. van Beelen AJ, Zelinkova Z, Taanman-Kueter EW, Muller FJ, Hommes DW, Zaat SA, et al. Stimulation of the intracellular bacterial sensor NOD2 programs dendritic cells to promote interleukin-17 production in human memory T cells. *Immunity* (2007) 27(4):660–9. doi: 10.1016/j.immuni.2007.08.013

51. Gerosa F, Baldani-Guerra B, Lyakh LA, Batoni G, Esin S, Winkler-Pickett RT, et al. Differential regulation of interleukin 12 and interleukin 23 production in human dendritic cells. *J Exp Med* (2008) 205(6):1447–61. doi: 10.1084/jem.20071450

52. Ling WL, Wang LJ, Pong JC, Lau AS, Li JC. A role for interleukin-17A in modulating intracellular survival of Mycobacterium bovis bacillus Calmette-Guerin in murine macrophages. *Immunology* (2013) 140(3):323–34. doi: 10.1111/imm.12140

53. Pilli M, Arko-Mensah J, Ponpuak M, Roberts E, Master S, Mandell MA. TBK-1 promotes autophagy-mediated antimicrobial defense by controlling autophagosome maturation. *Immunity* (2012) 37(2):223–34. doi: 10.1016/j.immuni.2012.04.015

54. Decout A, Katz JD, Venkatraman S, Ablasser A. The cGAS-STING pathway as a therapeutic target in inflammatory diseases. *Nat Rev Immunol* (2021) 21(9):548–69. doi: 10.1038/s41577-021-00524-z

55. Guo B, Cheng G. Modulation of the interferon antiviral response by the TBK1/IKKi adaptor protein TANK. *J Biol Chem* (2007) 282(16):11817–26. doi: 10.1074/jbc.M700017200

56. Dey B, Dey RJ, Cheung LS, Pokkali S, Guo H, Lee JH, et al. A bacterial cyclic dinucleotide activates the cytosolic surveillance pathway and mediates innate resistance to tuberculosis. *Nat Med* (2015) 21(4):401–6. doi: 10.1038/nm.3813

57. Wassermann R, Gulen MF, Sala C, Perin SG, Lou Y, Rybniker J, et al. Mycobacterium tuberculosis Differentially Activates cGAS- and Inflammasome-Dependent Intracellular Immune Responses through ESX-1. *Cell Host Microbe* (2015) 17(6):799–810. doi: 10.1016/j.chom.2015.05.003

58. Watson RO, Bell SL, MacDuff DA, Kimmey JM, Diner EJ, Olivas J, et al. The Cytosolic Sensor cGAS Detects Mycobacterium tuberculosis DNA to Induce Type I Interferons and Activate Autophagy. *Cell Host Microbe* (2015) 17(6):811–9. doi: 10.1016/j.chom.2015.05.004

59. Jain R, Dey B, Dhar N, Rao V, Singh R, Gupta UD, et al. Enhanced and enduring protection against tuberculosis by recombinant BCG-Ag85C and its association with modulation of cytokine profile in lung. *PloS One* (2008) 3(12):e3869. doi: 10.1371/journal.pone.0003869

60. De Almeida IN, Da Silva Carvalho W, Rossetti ML, Costa ER, De Miranda SS. Evaluation of six different DNA extraction methods for detection of Mycobacterium tuberculosis by means of PCR-IS6110: preliminary study. *BMC Res Notes* (2013) 6:561. doi: 10.1186/1756-0500-6-561

61. Green LC, Wagner DA, Glogowski J, Skipper PL, Wishnok JS, Tannenbaum SR. Analysis of nitrate, nitrite, and [15N]nitrate in biological fluids. *Anal Biochem* (1982) 126(1):131–8. doi: 10.1016/0003-2697(82)90118-X

frontiers | Frontiers in Immunology

TYPE Review
PUBLISHED 27 September 2023
DOI 10.3389/fimmu.2023.1255920

OPEN ACCESS

EDITED BY
Zhidong Hu,
Fudan University, China

REVIEWED BY
Resmi Ravindran,
University of California, Davis, United States
Abhishek Mishra,
Houston Methodist Research Institute,
United States

*CORRESPONDENCE
Hongtao Wang
hongtaowang@bbmc.edu.cn
Tao Xu
taoxu@bbmc.edu.cn

RECEIVED 10 July 2023
ACCEPTED 25 August 2023
PUBLISHED 27 September 2023

CITATION
Guo F, Wei J, Song Y, Li B, Qian Z, Wang X, Wang H and Xu T (2023) Immunological effects of the PE/PPE family proteins of *Mycobacterium tuberculosis* and related vaccines.
Front. Immunol. 14:1255920.
doi: 10.3389/fimmu.2023.1255920

Immunological effects of the PE/PPE family proteins of *Mycobacterium tuberculosis* and related vaccines

Fangzheng Guo[1,2], Jing Wei[1,2], Yamin Song[1,2], Baiqing Li[1,2,3], Zhongqing Qian[1,2,3], Xiaojing Wang[4], Hongtao Wang[1,2,3]* and Tao Xu[1,2,5]*

[1]Research Center of Laboratory, Bengbu Medical College, Bengbu, China, [2]Anhui Province Key Laboratory of Immunology in Chronic Diseases , Bengbu Medical College, Bengbu, China, [3]Department of Immunology, School of Laboratory, Bengbu Medical College, Bengbu, China, [4]Anhui Province Key Laboratory of Clinical and Preclinical Research in Respiratory Disease, Bengbu Medical College, Bengbu, China, [5]Department of Clinical Laboratory, School of Laboratory, Bengbu Medical College, Bengbu, China

Tuberculosis (TB) is a chronic infectious disease caused by *Mycobacterium tuberculosis* (*Mtb*), and its incidence and mortality are increasing. The BCG vaccine was developed in the early 20th century. As the most widely administered vaccine in the world, approximately 100 million newborns are vaccinated with BCG every year, which has saved tens of millions of lives. However, due to differences in region and race, the average protective rate of BCG in preventing tuberculosis in children is still not high in some areas. Moreover, because the immune memory induced by BCG will weaken with the increase of age, it is slightly inferior in preventing adult tuberculosis, and BCG revaccination cannot reduce the incidence of tuberculosis again. Research on the mechanism of *Mtb* and the development of new vaccines against TB are the main strategies for preventing and treating TB. In recent years, Pro-Glu motif-containing (PE) and Pro-Pro-Glu motif-containing (PPE) family proteins have been found to have an increasingly important role in the pathogenesis and chronic protracted infection observed in TB. The development and clinical trials of vaccines based on *Mtb* antigens are in progress. Herein, we review the immunological effects of PE/PPE proteins and the development of common PE/PPE vaccines.

KEYWORDS

***Mycobacterium tubercolosis*, PE/PPE family, vaccine, tuberculosis, immunology**

1 Introduction

Tuberculosis (TB), also known as "phthisis" and "white plague," is a chronic infectious disease caused by *Mycobacterium tuberculosis* (*Mtb*), which endangers human health. According to the Global Tuberculosis Report by the World Health Organization (WHO) in 2022 (1), TB is the second most deadly single infectious disease after coronavirus disease 2019, with 10.6 million new cases of TB worldwide recorded in 2021 and 1.6 million deaths due to TB. Multidrug-resistant tuberculosis (MDR-TB), extensively drug-resistant tuberculosis (XDR-TB), and tuberculosis combined with human immunodeficiency virus (HIV)

infection have further increased the global economic burden. Hence, the prevention and control of TB is a major public health issue.

Genomics studies on *Mtb* have shown that the Pro-Glu motif-containing (PE) and Pro-Pro-Glu motif-containing (PPE) gene family is present in pathogenic *Mtb*. Also, 99 PE genes and 69 PPE genes (accounting for ~10% of the coding sequence, encoding 168 proteins in total) are closely related to bacterial virulence (2, 3). The N-terminal sequence of this protein family is relatively conserved, and the C-terminal sequence is highly polymorphic. According to the difference in the C-terminal motif, this protein family can be divided into PPE-PPW (contains the PxxPxxW sequence), PPE-SVP (contains the Gxx-SVPxxW sequence), PPE-MPTR (major polymorphic tandem repeat), and PE-PGRS (polymorphic GC-rich-sequence). The variable C-terminal sequence may be the molecular basis of mutations of the PE-PPE gene or how *Mtb* evades immune attack by the host. In contrast, PGRS or MPTR is absent in rapidly growing non-pathogenic mycobacteria such as *Mycolicibacterium smegmatis* (*Ms*) (4, 5).

Most PE/PPE family proteins are localized in the cell wall and can inhibit macrophage apoptosis (6). This location indirectly enables bacteria to survive and spread in pulmonary macrophages, which is important in immune escape and interaction between the pathogen and host immune cells. Compared with *Mtb* grown *in vitro*, PE11, PE34, PE-PGRS14, PE-PGRS33, PE-PGRS57, and PE-PGRS62 are more abundant in the granuloma tissues of patients with pulmonary TB, and the upregulation trend is statistically significant (7). This observation supports the notion that some PE/PPE proteins enhance the ability of pathogens to survive in the host under unfavorable environmental conditions. PE-PGRS3 mediates adhesion to the type 2 pneumocytes through a unique arginine-rich C-terminal motif. This interaction of PE-PGRS3 with type 2 pneumocytes allows *Mtb* to acquire cardiolipin and phosphatidylinositol for integration into *Mtb* as a source of raw material for phosphate synthesis if phosphate is lacking in the environment in which *Mtb* grows (8). The ability of the protein to capture materials essential for growth and development from the host during crucial processes in TB pathogenesis is thought to be why *Mtb* can survive for a long time in caseous granulomas and foamy macrophages (8).

The Bacillus Calmette–Guerin (BCG) vaccine has been unable to curb the spread of TB in some underdeveloped countries or regions (9). BCG can help stop children from contracting TB, but not adults (10). With the increase in MDR-TB and XDR-TB cases, new TB vaccines with stronger and wider immunity are needed to prevent TB. This review summarizes the role of PE/PPE family proteins and the research progress of related vaccines against TB to provide a reference for further research on PE/PPE family proteins and related vaccines.

2 PE/PPE family proteins regulate the immune function of host cells

2.1 Regulation of *Mtb* virulence

Secretion of PE/PPE proteins is dependent upon the early secreted antigenic target 6 kDa (ESAT-6) secretion system (ESX) (11). Mutations in PPE38 can block the secretion of the two major ESX-5 substrates, PPE-MPTR and PE-PGRS, thereby increasing the virulence of bacteria and promoting the transmission of hypervirulent strains. Hence, the substrate of ESX-5 appears to be indispensable for attenuating bacterial virulence (12). The highly pathogenic Beijing strain has defective expression of PPE38 and a lack of secretion of the ESX-5 substrate. Knockout of Rv2352c expression can increase the virulence of moderately virulent *Mtb* and manifests as active bacterial growth and apparent inflammatory damage (13). Some studies have found that the ability of PE-PGRS33 knockout mutant (MtbΔ33 strain) to invade macrophages is decreased. Nevertheless, the ability of intracellular replication and immune regulation of this strain has not been observed in a mouse model of TB. The MtbΔ33 strain has shown increased virulence and pathogenicity by aggravating lung tissue damage during chronic infection. PPE27 was expressed in non-pathogenic *Ms* to form Ms-PPE27. Ms-PPE27 and Ms-Vec were injected into mice in a single-cell suspension, respectively, and the colony-forming units (CFUs) in different tissues of the two groups were compared on days 3, 6, and 9. Ms-PPE27 increased the number of bacteria in the lungs, spleen, and liver of mice significantly, and the clearance rate was slow, which prolonged the survival time of Ms *in vivo* (14). The release of lactate dehydrogenase from the supernatant of ANA-1 macrophages infected with PPE27 at 24 h and 48 h was significantly higher than that of Ms-Vec and negative controls. Those results suggest that PPE27 may induce macrophage necrosis, thereby contributing to disease progression (15). *Ms* with overexpression of PE-PGRS19 has a higher tolerance to isoniazid *in vitro*. The former can accelerate the growth rate and survival ability of Ms-Vc and increase the invasion ability and infection rate of Ms-PGRS-19 to macrophages significantly. Those observations indicate that PE-PGRS19 can aggravate bacterial damage to the host and cause toxicity in infected cells (16). In addition, Rv0256c (PPE2) contains a DNA-binding site on the leucine zipper and a functional monopartite nuclear localization signal (NLS) at 473–481 amino acids in the C-terminus of the protein. With the help of the latter, PPE2 can target the nucleus and bind to the gene-regulatory region of the host to manipulate gene transcription, thereby reducing its immune defense function and helping *Mtb* to establish a stable infection *in vivo* (17). As a second messenger, nitric oxide (NO) can stabilize the structure and function of hypoxia-inducible factor (Hif)-1α so that interferon (IFN)-γ can exert an optimal anti-inflammatory effect. If the function of Hif-1α is impaired, even if IFN-γ is maintained at a high level, Hif-1α-deficient macrophages cannot exert a normal killing effect against *Mtb*. PPE2 can block the release of inducible nitric oxide synthase (iNOS) and NO and inhibit the physiological function of Hif-1α competitively because it contains two unique structures and acts as an analog of host transcription factors (18). Meanwhile, PPE2 can also interact with the p67 subunit of reduced nicotinamide adenine dinucleotide phosphate (NADPH) to weaken the activity of the NADPH oxidase system and reduce the content of reactive oxygen species (ROS). These actions are conducive to the continuous growth and reproduction of *Mtb*, leading to higher bacterial load in macrophages and long-term survival of *Mtb* (16, 19).

2.2 Interaction with essential trace elements in the body, such as iron and calcium

As a second messenger, calcium [in the form of calcium ions (Ca^{2+})] plays a key part in cellular signal transduction and maintenance of homeostasis and is also indispensable for the development and acidification of phagosomes. *Mtb* can inhibit the maturation of phagosomes by chelating intracellular Ca^{2+} (20). Calmodulin (CAM) is a calcium-binding protein that has an important adaptor role in Ca^{2+}-mediated signaling pathways in various cellular responses. In bacteria, calmodulin-like proteins (CAMLPs) have a high degree of domain homology with eukaryotic CAM. The protein encoded by Rv1211 is a phosphodiesterase and NAD-kinase CAMLP. During *Mtb* infection, CAMLP can inhibit the fusion of phagosomes and lysosomes by binding Ca^{2+} and reducing the concentration of free Ca^{2+} in macrophages, thereby weakening the pernicious effect of immune cells on pathogens and promoting the intracellular survival of *Mtb* indirectly (21, 22). Rv1818c (PE-PGRS33) and Rv3653 (PE-PGRS61) also have Ca^{2+}-binding properties. The CFU of THP-1 cells infected with *Ms* expressing Rv1818c and Rv3653 was shown to be significantly higher than that of Ms-Vc at 24 h, 48 h, or 72 h. Increased counts at each time point correlated with the downregulation of iNOS expression (a key determinant of intracellular load in the host). Interleukin (IL)-10 is an anti-inflammatory inhibitory factor that negatively regulates the defense function of immune cells (23), the IL-10 content in the supernatant of THP-1 cells infected with the two strains was increased significantly. After Ca^{2+} depletion with the chelator ethylene glycol-bis (β-aminoethyl ether)-*N,N,N′,N′*-tetraacetic acid, this response was abolished completely (22). Those results indicate that Ms-1818c and Ms-3653 increase IL-10 content in a Ca^{2+}-dependent manner to improve their viability (22).

Iron ions are essential trace elements for the human body. Studies have found that cluster of differentiation (CD)4^+ T cells increase iron demand significantly after activation, while iron deficiency impairs the epigenetic regulation of T-helper (Th)17 cells and hinders the proliferation and differentiation of $CD4^+$ T cells and $CD8^+$ T cells (24). *Mtb* competes with host cells to uptake iron from the environment through siderophore-mediated iron acquisition (SMIA) and heme iron acquisition (HIA). SMIA captures iron from lactoferrin and transferrin. HIA can obtain iron ions from hemoglobin (which is also closely related to the pathogenic process of *Mtb*). Normal *Mtb* utilizes the low concentration of heme in the medium efficiently, and if siderophore synthesis was blocked or dysfunctional, bacteria grew poorly or stopped growing in an iron-rich 7H9 medium and returned to average growth after the addition of extra siderophore-like molecules (25, 26). Deleting PPE37 resulted in a Mtb△PPE37-deficient strain, which grew poorly in the original medium with almost unchanged concentrations of heme and iron. Approximately 200 times the heme concentration in the original medium was required to achieve similar growth to that of parental *Mtb*. BCG is a PPE37 mutant strain, and survival in a low-iron environment was consistent with that of wild-type (WT) *Mtb* only if the gene encoding functional PPE37 was added to BCG. Those results suggest that PPE37 is crucial in the pathological process of iron interception through HIA, which may be related to the reduced permeability of bacterial cell walls to heme, but the specific mechanism warrants further exploration (26).

2.3 Regulation of apoptosis, pyroptosis, and autophagy in the host

During *Mtb* infection, PE/PPE family proteins can regulate various cell death pathways, such as apoptosis and pyroptosis (27). The mitochondria are important organelles involved in apoptosis, so proteins targeting the mitochondria of host cells may play a part in regulating infection immunity and apoptotic pathways (28). The C-terminal sequence of PE6 (Rv0335c) contains two homology domains similar to BH3 in the proapoptotic protein B-cell lymphoma-2 (Bcl-2). Apoptosis-related proteins activate each other through BH3 to promote apoptosis on the one hand, and PE6 can enhance TLR4 expression and upregulate the level of tumor necrosis factor (TNF)-α on the other hand, because PE6 contains a BH3-like domain at its C-terminus, and it can also take advantage of the mitochondrial processing peptidase activity of this domain to target the mitochondria to cleave its signal peptide sequence, resulting in increasing cytosolic levels of cytochrome C (CytC) and intracellular Ca^{2+} loading, inducing caspase-mediated apoptosis of macrophages and promoting the long-term survival of *Mtb*. However, no obvious Ca^{2+} influx was observed in Rv0335cΔC-ter-infected cells, compared with intact PE6, and the content of caspase-3/7/9 and the proportion of apoptotic cells were significantly decreased in Rv0335cΔC-ter-infected cells (29). Sharma et al. treated RAW264.7 cells with PE6 (5 μg/mL, 7.5 μg/mL, or 10 μg/mL) for 24 h and detected apoptosis by flow cytometry. They found that PE6 at 5 μg/mL could promote macrophage apoptosis in a concentration-dependent manner. Meanwhile, protein assays showed that PE6 increased the secretion of proapoptotic proteins Bax and CytC and activated caspase-3. Higher levels of unfolded proteins (UPs) such as C/EBP homologous protein (CHOP), p-protein kinase R (PKR)-like endoplasmic reticulum kinase (PERK), and phosphorylated (p)-eukaryotic initiation factor-2α (eIF2α) were also detected, indicating that PE6 induces the production of a large number of proteins of ER stress-related responses in macrophages, thereby causing macrophage apoptosis (30). After THP-1 cells had been infected with PPE10 (Rv0442c) for 6 h or 24 h, the expression of caspase-3, 7, and 8 in the host cells was decreased. Reverse transcription-polymerase chain reaction showed that Bax transcription was decreased significantly, suggesting that apoptosis was reduced and that PPE10 could inhibit the apoptosis of host cells and promote *Mtb* survival indirectly (31). Persistent ER stress can trigger a regulation cascade to initiate apoptosis signals (32). PE-PGRS1 downregulates the expression of the ER stress-induced markers C/EBP homologous protein (CHOP), phosphorylated (p)-eukaryotic initiation factor-2α (eIF2α), and

p-protein kinase R (PKR)-like endoplasmic reticulum kinase (PERK), thereby inhibiting the intracellular stress of THP-1 cells induced by *Ms*. These actions reduce the content of caspase-3/9 and permit alternative splicing of Bax to inhibit apoptosis, which is conducive to the survival, reproduction, and pathogenesis of bacteria in macrophages (33).

Apoptosis is considered to be a relatively "safe" form of cell death. Simultaneously, pyroptosis is accompanied by a strong inflammatory response, which is caused by the expansion and rupture of the plasma membrane due to intracellular and extracellular pathogens or toxins, and results in the release of many cytokines and bacteria (34). Therefore, it has been speculated that pyroptosis promotes the dissemination of *Mtb in vivo* to a certain extent, leading to the chronic trend of TB. Peroxisome proliferator-activated receptor (PPAR)γ binds competitively to the p65/p50 subunit of nuclear factor-kappa B (NF-κB) to inhibit the function of mononuclear macrophages and expression of proinflammatory factors. In one study, PPARγ transcription in Ms-PPE60-infected cells was inhibited, whereas the expression of the proinflammatory cytokines IL-1β, IL-6, and IL-12 was upregulated. Mitochondrial fusion protein (Mfn)2 is located in the outer membrane of the mitochondria and has anti-apoptotic activity. Quantitative detection of Mfn2 showed that PPE60 did not change the Mfn2 level, indicating that the integrity of the mitochondrial membrane was unaffected. However, messenger (m)RNA expression of important pyroptosis molecules such as caspase-1/4, NOD-, LRR-, and pyrin domain-containing protein 3 (NLRP3) and gasdermin D (GSDMD) was increased significantly, suggesting that PPE60 induced macrophage pyroptosis to a greater extent in this form of cell death (35). Compared with Ms-Vec, Ms-PPE13 enhanced IL-1β secretion and cleaved GSDMD into more GSDMD-NT (p30) by activating NLRP3 and caspase-1, which translocated to the cell membrane to form a pore (10–15 nm) and led to leakage from the plasma membrane. Finally, progression to GSDMD-mediated pyroptosis was observed. Interestingly, Ms-Vec induced 10 times more GSDMD expression than Ms-PPE13 after 48 h of culture, but the amount of IL-1β in the supernatant that seeped through GSDMD wells in the Ms-PPE13 group was higher than that in Ms-Vec group. Those results suggest that PPE13 may also cleave other members of the gasdermin family (e.g., GSDMA, GSDMB, GSDME), which are involved in cell membrane pore formation and pyroptosis (36). In addition, PE-PGRS19 is a novel agonist of the non-canonical pyroptosis pathway (caspase-11-GSDMD-Il-1β/18) in *Mtb*, which leads to pyroptosis by activating caspase-11 and inducing GSDMD cleavage to the p25 fragment (15).

Autophagy is a process of cellular self-degradation. Autophagy is essential to innate immunity and adaptive immunity. It plays a vital part in the resistance to bacterial infection and the clearance of intracellular pathogens (37). High-throughput screening of a transposable sequence mutation library of *Mtb* for loss of function revealed that *Mtb* contained 16 inhibitory autophagy-related genes, of which six encoded PE-PPE family proteins (Rv1068c, Rv1087, Rv1651c, Rv2471, Rv2770c, Rv3136) (38). PE-PGRS47 has been reported to prevent the acidification and maturation of phagosomes and the association of autophagosomes with lysosomes, thereby increasing the virulence and resistance to the adverse intracellular environment of *Mtb*. p62 expression in WT *Mtb*-infected cells was shown to be higher than that in △PE-PGRS47 mutant cells, which could be restored to the same level as that in WT *Mtb*-infected cells (39). Strong et al. demonstrated that PE-PGRS20 and PE-PGRS47 inhibited the transition of the Unc-51-like kinase (ULK1) complex to autophagosomes by interacting with the Rab1A protein, resulting in reduced phosphorylation of ULK1 at the mammalian target of rapamycin (mTOR)C1 and negative autophagy. Compared with *Mtb* infection in WT cells, RAW264.7 cells infected with △PE-PGRS20 or △PE-PGRS47 had increased autophagy-related gene 5 (Atg5) content and decreased p62 content, indicating that autophagy was increased in cells infected with mutant strains. However, PE-PGRS expression inhibited the activation of the autophagy pathway and intracellular anti-infective efficacy against *Mtb* (40).

2.4 Regulation of cellular immunity

Cellular immunity plays a significant part in the protective immunity against *Mtb*. PE/PPE proteins can induce T cells to produce cellular immunity. The crucial prerequisite for this immune response is the activation of antigen-presenting cells (APCs) and the effective presentation of antigenic peptides. Dendritic cells (DCs) are crucial for antigen presentation. Initiation of the Th1-type immune response is essential for controlling *Mtb* replication within the host cells. Choi et al. isolated PPE39 from a virulent Beijing strain of *Mtb*. They treated DCs with PPE39 and found that expression of the major histocompatibility complex (MHC) type-I/II molecules CD80 and CD86 on the surface of DCs was enhanced. Those data indicated that PPE39 could induce DC maturation and that DCs treated with PPE39 could promote the proliferation of $CD4^+$ T cells. Meanwhile, the expression of the Th1-related transcription factor T-bet was increased, but the contents of Th2-related molecules and proteins were not increased (41). TLRs are the only known host cell receptors for PE/PPE proteins (42). Their interaction regulates the release of proinflammatory/anti-inflammatory cytokines by activating NF-κB and c-Jun N-terminal kinase-mitogen-activated protein kinase (JNK-MAPK) signaling pathways. Some studies have found that PE-PGRS11 (Rv0754) and PE-PGRS17 (Rv0978c) can induce the maturation and activation of human DCs and stimulate the secretion of proinflammatory cytokines by recognizing TLR2 (43). PE-PGRS33 and its PE domain were found to promote IFN-γ secretion and the proliferation of $CD4^+$ T cells and $CD8^+$ T cells in BALB/c mice and latent *Mtb* infection (44). PE31 induced the expression of the anti-inflammatory cytokine IL-10 by activating the downstream pathway of NF-κB. At 48 h after infection, IL-10 expression was increased significantly, whereas transcription of IL-6 and IL-12 was decreased significantly, and the presentation of activated caspase-3 protein fell. Those data suggest that PE31 may reduce macrophage apoptosis (45). IL-10 expression has been found to be increased in macrophages infected with Ms-PE-PGRS41, and regulation of IL-6 is similar to that by PE31 (46). It has been found

that IL-10 inhibits phagosome maturation in *Mtb*-infected human macrophages, leading to a reduction in the amount of proinflammatory cytokines (47). This observation suggests that specific PE/PPE family proteins can enhance *Mtb* resistance within the host cells by inhibiting the release of proinflammatory cytokines. PPE65 can trigger signaling pathways that secrete proinflammatory factors by binding to the leucine-rich repeats (LRR) domain of TLR2, such as the interleukin-1 receptor-associated kinase 3 (IRAK3) cascade, to stimulate NO release and upregulate the expression of IL-6 and TNF-α (48). As an agonist of TLR4, PPE39 can also activate MAPK and NF-κB pathways to trigger DCs (49), induce the maturation and activation of DCs, promote the polarization of Th1 cells, and control the growth of intracellular *Mtb*. In conclusion, PE/PPE family proteins regulate *Mtb* survival in host cells by binding to TLRs to activate cell signaling pathways and regulate the secretion of inflammatory factors. PPE7 can prolong the survival of *Mtb* in macrophages by activating MAPK and NF-κB signaling pathways and regulating the extracellular signal-regulated kinase (ERK)–p38–NF-κB axis. In one study, the expression of TNF-α, IL-6, and IL-1β in THP-1 cells was increased significantly within 48 h after infection, whereas secretion of the anti-inflammatory factor IL-10 was inhibited. Due to the release of proinflammatory factors, the colony load of Ms-PPE7 in the organs of infected mice was increased significantly, and they all showed severe tissue damage caused by a rapid inflammatory response. Microscopy revealed thickening of the alveolar septum with exudation of red blood cells, infiltration by many inflammatory cells in the lungs and spleen, and punctate necrosis in the liver. In addition, Ms-PPE7 could also resist the threats of a high concentration of lysozyme (2.5 g/mL) and a more acidic medium (pH = 3) (50). After combining with herpesvirus-associated ubiquitin-specific protease (HAUSP), PE-PGRS38 could regulate cytokine levels in mouse bone marrow-derived macrophages (BMDMs) by inhibiting the deubiquitination of tumor necrosis factor receptor-associated factor (TRAF) 6 by HAUSP. Through downregulating the expression of TNF-α, IL-1β, IL-6, and IL-10, the inflammatory response *in vivo* could be balanced to a suitable environment for *Mtb* survival, thereby increasing the duration of intracellular survival and potency of bacteria. Interestingly, PE-PGRS38 was also observed to reduce the hyperinflammation caused by a high bacterial load, which seems to be a "beneficial" phenomenon for the host (51). The Figures 1 and 2 briefly shows the immunological mechanism of PE/PPE proteins. We summarize the subcellular localization of the different PE/PPE proteins and their mechanisms of action with the host in Table 1.

2.5 Involvement in humoral immunity

B cells are important components of tuberculous granulomas and regulate the inflammatory process by secreting antibodies and IL-10 (79). However, *Mtb* is an intracellular pathogen, so the classical view is that $CD4^+$ T cells and Th1-type cytokines are mainly responsible for the components that have an anti-TB effect *in vivo*. Hence, few reports have focused on the changes in B cells during *Mtb* infection (80). This lack of research has led to a long underestimated contribution of humoral immunity to the control of *Mtb* infection.

Some studies have found that PPE18 participates in cellular immunity but also limits humoral immunity to a certain extent, which provides survival advantages for *Mtb*. PPE18 interferes with the uptake and processing of antigens by APCs in a dose-dependent manner, which affects the formation of MHC–antigen peptide complexes, resulting in impaired activation of $CD4^+$ T cells and significant reduction in the IL-2 level. If peripheral blood mononuclear cells (PBMCs) are treated with PPE18, the response of lymphocytes to purified protein derivative (PPD) is weak. Three days after infecting mice with Ms-PPE18, flow cytometric analysis showed that compared with Ms-pVV16 infection, PPE18 increased the percentage of immature B cells in mice (26.14%) and that the dark zone/light zone (DZ/LZ) ratio at the germinal center increased. The number of B cells in the bright area was low, suggesting that B-cell activation had been impaired. Continued infection of mice revealed low levels of mouse-specific immunoglobulin (Ig)G and IgM antibodies on days 11 and 21. Those results indicate that PPE18 interferes with the humoral immune response by inhibiting the maturation and activation of B cells and antibody production (81). B cells play an important role in regulating host response and curbing *M. tuberculosis* infection. Impairment of B cells enhances the susceptibility of mice to tuberculosis, and B lymphocyte-deficient mice challenged with *Mtb* exhibit higher visceral bacterial loads (82).

3 Novel vaccines based on PE/PPE family proteins against TB

BCG is one of the most widely administered vaccines worldwide, with approximately 100 million newborns receiving BCG each year (83). BCG vaccination within 1 week of birth can protect 73% of newborns against tuberculous meningitis and 77% against miliary TB (84). BCG also improves the innate immune response to pathogenic microorganisms other than *Mtb*, such as *Candida albicans* and *Staphylococcus aureus*, indicating that BCG could induce non-specific cross-protection against pathogens unrelated to *Mtb* in young children (85). The novel coronavirus infection that began in late 2019 was a catastrophic event for global public health, which has worsened the TB prevention and control situation. *Mtb* infection could increase host susceptibility to severe acute respiratory syndrome coronavirus 2 (SARS-CoV-2) infections (86). Coronavirus disease 2019 (COVID-19) co-infection with TB can cause a large number of inflammatory cell infiltration in the lung; further enhance the immune response of the injured site; produce excessive cytokines like IL-1, IL-6, IL-10, IL-18, and IFN-α; and promote cytokine storms that lead to multiple organ dysfunction, resulting in a higher risk of death than a single pathogen (87, 88). However, it is surprising that some studies have shown that BCG has a certain degree of non-specific cross-protection against SARS-CoV-2. Previous studies have shown that BCG vaccination protects against tuberculosis, herpes, and influenza virus infections and reduces their morbidity and mortality (89). This may be due to heterologous immunity by antigen-independent activation of B and T cells and

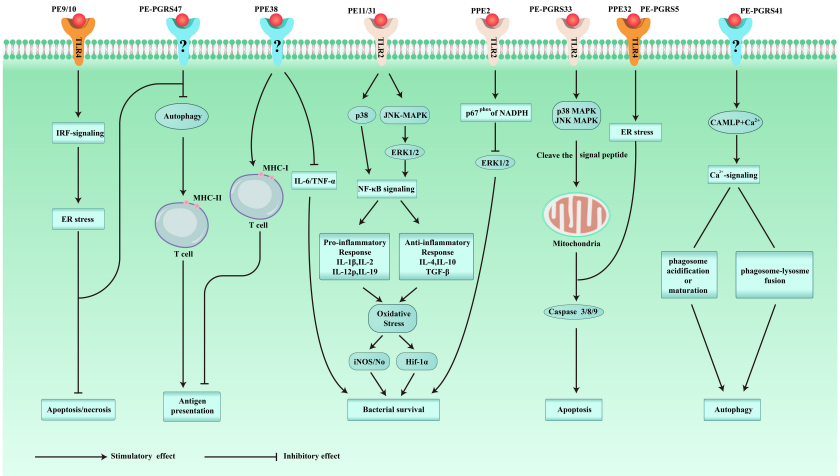

FIGURE 1
Schematic representation of some of the immunomodulatory roles played by PE/PPE proteins.

reprogramming of innate immune cells—the effect exerted by training immunity (90). BCG can regulate the response of lymphocytes to secondary infection by stimulating $CD4^+$ and $CD8^+$ T cells against untargeted antigens, thereby increasing the resistance of non-specific proinflammatory cytokines IL-1β and IL-6 to pathogens (85) and promoting the immune response of innate immune cells including monocytes, natural killer cells, and alveolar macrophages, leading to increasing the host resistance to infection with a variety of pathogens, especially SARS-CoV-2 (86, 91), so BCG can prevent or reduce SARS-CoV-2 infection, inhibit virus replication, reduce viral load, and further alleviate inflammatory damage and clinical symptoms, especially in children vaccinated with BCG (92, 93). Counoupas et al. (94) proposed the use of an interesting combination of BCG and a trimeric SARS-CoV-2 spike protein antigen (BCG : CoVac), which induces the generation of specific T cells in mice that promote the production of Th1-type cytokines and high-titer IgG neutralizing antibodies. A single dose of BCG : CoVac completely eliminated the symptoms and significantly reduced inflammation in challenged animals. Surprisingly, no viral load was detected in the lungs of any of these challenged animals. A randomized, double-blind, placebo-controlled trial conducted in the USA showed that multi-dose BCG vaccine was effective in preventing and reducing the severity of infection in patients with type 1 diabetes—a high-risk factor for SARS-CoV-2 infection—who had not previously received either BCG or COVID-19 vaccines (95). In another phase III, multicenter,

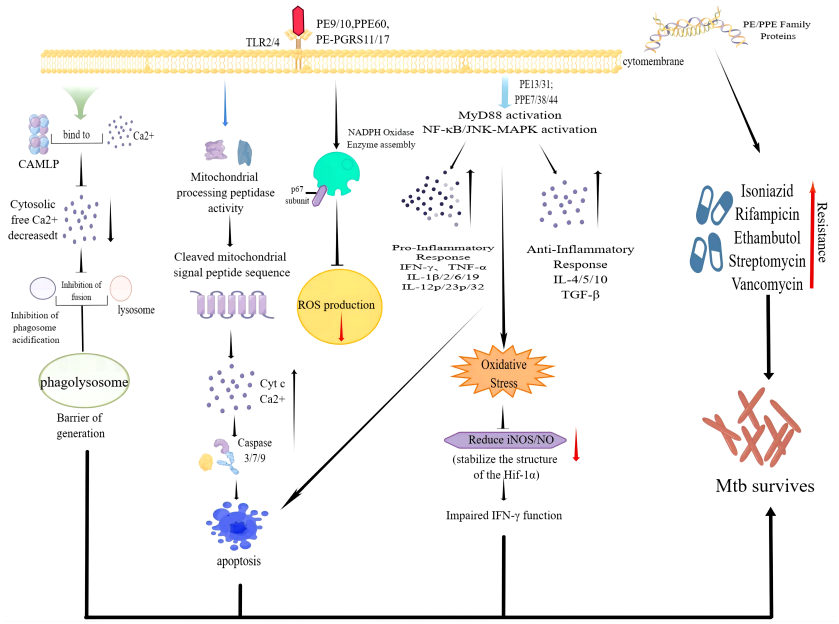

FIGURE 2
Some PE/PPE family proteins function intracellular to promote the survival of Mtb.

TABLE 1 Subcellular localization and mechanism of action of PE/PPE family proteins in *Mycobacterium tuberculosis*.

Protein	Subcellular localization	Effect on immune response	References
PE4	Cytomembrane	Expresses at the chronic stages and enhances *Mtb* survival during hypoxia	(52)
PE9/PE10	Cytomembrane	Interacts with TLR4 and induces apoptosis via IRF3 signaling	(53)
PE11	Cytoderm	Involvement in bacterial cell wall remodeling by modifying fatty acids	(54, 55)
PE13	Cytomembrane	Inhibits apoptosis and enhances stress resistance capacity of *Mtb*	(52)
PE16	Cytomembrane	Regulates intracellular triglyceride levels	(56)
PE20	Cytomembrane	Involved in magnesium ion transport in *Mycobacterium tuberculosis*; promotes cell division and metabolism	(57)
PE25/ PE41	Cytomembrane	Induces macrophage necrosis to facilitate the dissemination of pathogens	(58)
PE27	Cytomembrane	Activates DC and the expression of co-stimulatory molecules and upregulates the production of proinflammatory cytokines via MAPK–NF-κB signaling	(59)
PE31	Cytomembrane	Attenuates host cell apoptosis; Up-regulates production of anti-inflammatory cytokines and down-regulates production of proinflammatory cytokine	(45)
PPE2	Cytomembrane	Inhibits NO production by downregulating the expression of the iNOS gene; contains SH3 domain which enables its binding to p67phox and downregulates ROS levels	(19, 60)
PPE13	Cytomembrane	Activates NLRP3 inflammasome and induces cleavage of caspase-1 and secretion of IL-1β	(36)
PPE18	Cytoderm	Upregulation of IL-10 and inhibition of IL-12/TNF-α production in macrophages; prolongs the survival time of bacteria in macrophages	(81)
PPE25	Cytomembrane	Up-regulates production of proinflammatory cytokines via p38-MAPK-ERK-NF-κB signaling and induces host cell necrosis	(61)
PPE26	Cytomembrane	Interacts with TLR2 and enhances the expression of co-stimulatory molecules along with CXCR3 and CD4 T-cell responses; upregulates the production of proinflammatory cytokines via p38–MAPK–ERK–NF-κB signaling and induces host cell necrosis	(61, 62)
PPE32	Cytoderm	Promotes ER stress-mediated apoptosis involving caspase 3/9 activation	(63)
PPE36	Cytomembrane	Involved in heme transport across the membrane	(64)
PPE37	Cytomembrane	Encodes siderophore associated with iron uptake; reduces the content of IL-6/TNF-α	(26)
PPE38	Cytomembrane	Induces macrophages to secrete IL-6/TNF-α; downregulates MHC-I antigen presentation	(65)
PPE57	Cytomembrane	Interacts with TLR2 and enhances the expression of co-stimulatory molecules and establishes cross-talk with p38–ERK–NF-κB signaling	(66)
PPE60	Cytoderm	Interacts with TLR2 and activates maturation of DC and expression of co-stimulatory molecules (CD80, CD86, MHC-I/II); upregulates the production of proinflammatory cytokines; induces pyroptosis via NF-κB signaling; enhances the stress resistance capacity of *Mtb*	(35, 67)
PPE62	Cytomembrane	Heme-iron acquisition and growth of pathogen	(64)
PPE68	Cytomembrane/ cytoderm	Regulates antigen release ESX-1 gating channel; promotes bacterial survival in the host; induces IFN-γ secreting $CD4^+$ T cells and host cell necrosis	(68, 69)
PE-PGRS3	Cytoderm	Promotes adhesion to macrophages and alveolar epithelial cells; increases persistence in host tissues	(8, 70)
PE-PGRS5	Cytoderm	Induces caspase-3/8/9-mediated apoptosis and is UPR/TLR4-dependent	(71)
PE-PGRS11	Cytomembrane	Encodes functional phosphoglycerate mutase; enhances resistance to H_2O_2-induced oxidative stresses thanks to the anti-apoptotic signals triggered by the TLR2-dependent activation of COX-2/Bcl-2 expression	(72)
PE-PGRS17	Cytoderm	Interacts with TLR2 and activates maturation of DC and stimulation of co-stimulatory molecules and upregulates the production of proinflammatory cytokines via MAPK-NF-κB pathway; induces host cell death with secretion of TNF-α via the Erk kinase pathway	(43, 73)
PE-PGRS18	Cytoderm	Promotes cell apoptosis; induces IL-12 and inhibits IL-6, IL-1β, and IL-10	(74)

(Continued)

TABLE 1 Continued

Protein	Subcellular localization	Effect on immune response	References
PE-PGRS30	Cytoderm	Blocks phagosome maturation to enhance *Mtb* intracellular survival	(75, 76)
PE-PGRS33	Cytoderm	Induces necrosis and apoptosis; increases IL-10 and decreases IL-12/TNF-α in macrophage; induces inflammation in a TLR2-dependent mechanism; promotes entry in macrophages via the TLR2/CR-3 inside-out signaling pathway	(14, 77)
PE-PGRS41	Cytoderm	Promotes anti-inflammatory response; inhibits host cell apoptosis and autophagy	(78)
PE-PGRS47	Cytoderm	Blocks autophagy and phagosome acidification; inhibits MHC-II antigen presentation which suppresses *Mtb*-specific $CD4^+$ T-cell responses	(39)
PE-PGRS61	Cytoderm	Binding of calcium to PE-PGRS61 increases affinity toward TLR2 and upregulates anti-inflammatory cytokine IL-10	(22)
PE-PGRS62	Cytoderm	Inhibits phagosome–lysosome maturation; reduces the production of NO in macrophages	(6)

double-blind trial in which 301 volunteers aged >50 were randomized (1:1) to BCG or placebo, approximately 5% of the participants in the BCG group had positive antibodies against SARS-CoV-2, with a 68% lower risk for COVID-19, compared with the placebo group (96). Although the WHO has not recommended the use of BCG as a means to prevent or treat COVID-19, it is anticipated that BCG will be considered an ideal measure to fight COVID-19 for developing and underdeveloped countries that lack treatment. However, the efficacy of BCG vaccination in adults is not high. The individual variation in the efficacy of BCG against TB in adults has been reported to range from 0% to 80% (97). Because of regional and ethnic differences, the average percentage protection of BCG against TB in children in some areas is only 52% (98). In addition, BCG is a live attenuated vaccine, so it is unsuitable for people who are immunosuppressed or immunodeficient. BCG vaccination in HIV-infected patients is prone to strain mutation or BCG-disseminated disease (99). Therefore, there is an urgent need to develop safer and more efficacious new vaccines to prevent and treat *Mtb* infection.

The PE/PPE vaccine of *Mtb* is a component vaccine. It is made by screening and purifying the immunogenic PE/PPE protein, combining it with other types of antigens, and aligning it with adjuvants or carriers. This type of vaccine has stability and safety and can fuse various protective antigens selectively to aid expression, thereby improving its specificity and the level of immune response *in vivo*. Most PE/PPE vaccines are used as booster vaccines. They are designed to enhance the immune response and prolong the duration of resistant protection after vaccination with a primary vaccine such as BCG. The section below reviews recent vaccines against TB based on PE/PPE family proteins as antigen targets. Table 2 presents the immunoprotective effects of fusion proteins or vaccines incorporating members of the PE/PPE family proteins.

3.1 PPE15-related vaccines

PPE15 is involved in the lipid accumulation of latent *Mtb* and plays an important part in stabilizing the lipid synthesis, metabolism, and stress state of *Mtb* (100). Four types of vector vaccines containing PE/PPE proteins have been prepared by expressing PE3, PE12, PPE15, and PPE51 on chimpanzee adenovirus vector ChAdOx1, respectively. Mice were given a single intranasal vaccination. Four weeks later, mice were challenged with an *Mtb*-containing aerosol. The CFU count showed that the vaccine expressing PPE15 and PPE51 could reduce the bacterial load in the lungs and spleen significantly. The degree of inhibition of the PPE15 vaccine was similar to that of BCG, but the two other vaccines (PE3 and PE12) did not control the growth or reproduction of bacteria in organs. Among the vaccines stated above, only the vaccine expressing PPE15 could improve the protective efficacy of BCG in primary immunization, promote the proliferation of $CD4^+$ T cells and $CD8^+$ T cells induced by BCG, and enhance the clearance ability of BCG against *Mtb* and its protective effect in mice. However, this effect was statistically significant only in C57BL/6 mice, and not in BALB/c mice, and the combination of the four vaccines did not produce an additive protective effect (101). Recently, Xu et al. purified PPE15 and found that it had strong antigenicity and could react specifically with the serum of patients suffering from TB but not with the serum of patients with pneumonia or healthy adults (102). Although few studies have been done on PPE15, those results suggest that PPE15 is a promising antigen target for developing vaccine candidates against TB, but the specific immune mechanism merits further exploration.

3.2 PPE18-related vaccines

3.2.1 M72:AS01

Among the vaccines designed to target PPE18, the most advanced is M72:AS01. M72 is a vaccine based on recombinant protein subunits consisting of Mtb39A (Rv0125) and PPE18 (Rv1196). PPE18 is associated with the cell wall of *Mtb* and is an important virulence factor. The MtBΔ18 recombinant strain can protect mice from *Mtb* infection, reduce inflammatory damage, and increase the number of infected mice who survive (103). AS01 is a liposome vaccine adjuvant containing two immunostimulants: lipid monophosphoryl A (MPL) and saponin QS-21 (104). M72:

AS01 could generate a comprehensive and robust immune response, resulting in the elicitation of strong IFN-γ and Ab responses and a strong CD8 response directed against the Mtb32 epitope. The protective effect of M72 was better than that of BCG in aerosol-challenged mice and guinea pigs by observing the signs and surviving numbers of mice and guinea pigs challenged with virulent *Mtb* strains at different time periods (0–70 weeks), and the survival time of mice and guinea pigs injected with M72 vaccine is 1 year longer than that of BCG alone (105). Surprisingly, M72 delivered by the coadministration with BCG vaccination significantly improved the survival of these animals compared with BCG alone, with some animals still alive and healthy in their appearance at >100 weeks post-aerosol challenge in the more stringent guinea pig disease model. M72 can improve the ability of BCG to reconstruct the airway and limit the progression of pulmonary consolidation caused by *M. tuberculosis* and promote the regression of lung tissue lesions (106). The cynomolgus monkey is an ideal non-human primate model for tuberculosis vaccine research (107). In another study, it was confirmed that M72 had good safety in cymophagus monkeys, with no body weight loss or abnormal inflammatory indicators such as erythrocyte sedimentation rate before challenge. The combined use of BCG and M72 induced a potent anti-tuberculosis cytokine profile in cynomolgus monkeys, mainly IFN-γ, TNF-α, IL-2, and IL-6, which enabled the challenge animals to achieve long-term survival and reverse the outcome of tuberculosis progression (108). Two doses of the vaccine could induce solid and durable immune responses, with a high frequency of M72-specific $CD4^+$ T cells and significant secretion of Th1 cell-related factors. The main adverse reactions appear to be redness and swelling at the vaccination site, but severe safety events have not been observed (109). Phase II clinical trials conducted in India have shown that M72 is well tolerated and immunogenic in HIV-positive populations (110). Compared with several common subunit vaccines that have entered clinical trials (H1, H56, ID93, MVA85, eras-402), M72:AS01 elicited the highest levels of Th1 cytokines and memory $CD4^+$ T-cell responses (111), which also highlights the advantages of M72 as a novel vaccine against TB. Analyses of a more extensive phase IIb randomized placebo-controlled trial evaluating M72:AS01 in 3,573 adult volunteers recruited in South Africa, Zambi, nd Kenya found that M72:AS01 protected progression to active pulmonary TB for 3 years in HIV-negative patients with latent tuberculosis infection (LTBI). The percent protection was ~54%, and there were no apparent safety problems, which met the requirements of WHO for new vaccines against TB (112). However, due to regional and ethnic differences, larger and longer trials in broader populations are needed to confirm those results. In addition, the C-terminal domain of PPE18 has many gene polymorphisms and has a high frequency of mutation that changes the polypeptide sequence of the corresponding epitope region. The mutation types are mostly single-nucleotide polymorphisms and frameshifts, which may reduce the immune protection induced by M72 to varying degrees (113). This should attract the attention of vaccine designers.

3.2.2 ACP vaccine

ACP vaccine comprises Ag85B, CFP21, and PPE18 proteins. Recent studies have demonstrated the safety of this vaccine in animal models. The amount and titer of specific antibodies in mice were increased significantly after immunization. The vaccine increased the number of $CD4^+$ T cells and secretion of the Th1-type cytokines IL-2 and IFN-γ significantly. The bacterial load in mouse lungs was decreased, and the pathological damage tended to be alleviated (114). Those effects may have been due to the absence of appropriate adjuvants in the vaccine or the route and frequency of vaccination needed to be improved to improve immunogenicity.

3.2.3 INP-0288-1196-0125

The INP-0288-1196-0125 recombinant vector vaccine was constructed by a "mosaic" ice nucleation protein (INP) on the surface of *Escherichia coli*, and then Rv0288, Rv1196 (PPE18), and Rv0125 were expressed on INP. Without eliciting adverse reactions, this vaccine induced strong humoral immunity and $CD4^+$ T-cell immune responses in mice. High levels of specific IgG could be detected after the first immunization. With an increase in immunization times, the number of $CD4^+$ T cells and $CD8^+$ T cells also increased, and the IL-4 level increased most significantly (115). ACP and INP vector vaccines show good tolerance and immunogenicity in mice and can induce a high level of immune response *in vivo*. In the next step, different suitable animal models can be found to test the characteristics of the vaccines multiple times to shorten the time required for the vaccines to enter clinical trials. A study on PPE18 suggests that analyses of the variability of protein–subunit sequences in vaccine candidates should not be neglected to improve the potential of vaccine-induced protective immune responses.

3.3 PPE42-related vaccines

3.3.1 ID93:GLA-SE

PPE42 is also a valuable candidate protein for vaccines. PPE42 is involved in the construction of various vaccines, of which the most advanced is ID93:GLA-SE. ID93 is composed of Rv1813, Rv2608 (PPE42), Rv3619, and Rv3620. GLA-SE is an adjuvant containing the TLR4 agonist glucopyranosyl lipid A (GLA) and emulsifying stabilizer SE (116). This vaccine can enhance BCG immune outcomes and enhance drug efficacy as first-line treatment in patients with *Mtb* infection (117). ID93 showed immunogenicity in a variety of animal models (mice, guinea pigs, rhesus monkeys) and induced a multifunctional $CD4^+$ Th1 cell response characterized by IFN-γ, TNF-α, and IL-2, which reduced the number of bacteria in the lungs of drug-resistant *Mtb* strains that attacked the lungs of the animals, and effectively lowered the mortality rate of tuberculosis in experimental animals (118). In phase I trials, the vaccine induced high-titer specific IgG (predominantly lgG1 and lgG3 (119), as demonstrated in dose-escalation trials) and Th1-cell responses *in vivo* in healthy BCG-naive adults, and vaccine-

TABLE 2 Comparison of PE/PPE family protein-associated TB vaccines.

Vaccine	Composition	Advantage	Deficiency
ChAdOx1-PPE15	PPE15, chimpanzee adenovirus vector	It can effectively clear *Mtb* and enhance the immune efficacy of BCG	The results varied depending on the mouse lineage.
M72:AS01	Fusion protein of PPE18-Rv0125, AS01 adjuvant. It is currently in phase IIb clinical trials.	The Th1 response is strong and prevents LTBI from progressing to the active stage. The protective effect of M72 was better than that of BCG and significantly prolonged the survival time of the challenged animals. Combined treatment with BCG could reverse the lung injury caused by tuberculosis.	The bacterial load in the lungs of infected animals could not be significantly reduced. There are regional and ethnic differences, which need to be further verified by clinical trials.
ACP	Fusion protein of Ag85B-CFP21-PPE18	The specific antibody increased significantly and reduced the CFU and inflammatory damage in the lung.	It did not improve the immune effect of BCG.
INP-0288-1196-0125	The fusion protein Rv0288-Rv1196 (PPE18)-Rv0125 was expressed on INP.	The effect within a certain range increased with the increase in immunization times.	The experimental animals were single.
ID93:GLA-SE	The fusion protein of Rv1813-Rv3620-Rv3629-PPE42, GLA-SE adjuvant. It is currently in phase IIa clinical trials.	Various immune pathways can improve the protective efficacy of BCG, improve drug efficacy, and prevent *Mtb* recurrence. It can effectively reduce the mortality of tuberculosis in experimental animals.	It is necessary to further compare the differences between different vaccination methods to find the best immunization route.
rBCG::Ag85B-EAST-6-PPE42	The fusion protein of Ag85B-EAST-6-PPE42 was expressed in BCG.	A stronger specific response was induced than that of BCG.	Duration and immune memory are unknown.
Tri-Fu64	The fusion protein of PPE42-Rv1793-Rv2628	It can significantly reduce the bacterial load in the body and improve the ability of anti-*Mtb* infection.	The protective effect was single, and the combination with MPL or DDA could reduce the body weight of mice.
HPERC	The fusion protein of Rv2031c-EAST-6-PPE44, resiquimod adjuvant	$CD4^+$ T-cell response and humoral immunity are obvious while limiting inflammatory damage caused by hyperimmunity.	No corresponding clinical human trial data were available.
Tetrafu56	The fusion protein of Esp-C-TB10.4-PPE57-Hsp-X	A multiphase therapeutic vaccine that produces significant immunity against active pulmonary tuberculosis infection *in vitro*	*In-vivo* experiments have not been carried out. It was not effective in preventing *Mtb* in healthy adults.
A3-len	The fusion protein of Ag85B-PPE57 was expressed in the lentivirus vector.	It reduced the number of bacteria in the lung and spleen, attenuated lung lesions, protected against *Mtb* damage, and restored the body weight of the infected mice.	$CD8^+$ T cells were decreased.
A39	Rv2029c was added to A3-len.	It promoted T-cell polarization to Th1 and inhibited bacterial reproduction in the organs.	A variety of animal models are needed for further verification.
rBCG::PPE68	PPE68 was expressed in BCG.	Th1 response was superior to BCG and maintained a high level of humoral immunity.	It still needs to be verified by repeated experiments.
rLmMtb9Ag	Nine antigens including PPE68 were fused in the *Listeria* vector.	Hypervirulent *Mtb* infection can be antagonized in guinea pigs without BCG primary vaccination.	The immunodominant epitope P9 peptide of PPE68 requires further purification.
rBCG::PE-MPT64	The fusion protein of the MPT64-PE segment of PE-PGRS33 was expressed in BCG.	The PE segment targets the delivery of antigenic peptides, and the PE-PGRS antibody inhibits *Mtb* entry into macrophages with better protective efficiency than BCG and can be used for LTBI.	The experiment is still in the preliminary stage and needs further study.

related serious adverse events were not observed (120). In a phase IIa trial in Cape Town (South Africa) involving adults with a history of TB, ID93 was shown to be safe and efficacious in improving treatment outcomes and preventing TB recurrence (121). ID93 has also been shown to reduce the bacterial load in the lungs of *Mtb*-infected mice effectively (122). Sixteen weeks after challenge with a hypervirulent Beijing strain of *Mtb* in BCG-immunized mice, ID93 could induce robust and sustained $CD4^+$ T-cell responses and provide long-term, high-level protection against *Mtb* infection (123). Recently, researchers administered a dry-powder vaccine via intranasal and intralung routes in *Mtb*-infected mice. They found that ID93:GLA-SE could control inflammation progression, and detected a significant increase in the number of T cells and related cytokines. The immunogenicity and protective effect of ID93:GLA-SE were similar to those after intramuscular injection (124).

3.3.2 Ag85B-EAST-6-PPE42 (rBCG)

The more studied vaccine target proteins Ag85B and ESAT-6 can also be fused with PPE42 to form a new recombinant BCG vaccine (rBCG) called Ag85b-ESAT-6-PPE42. rBCG can induce a stronger Th1-type cellular immune response and antigen-specific humoral immune response in an animal model compared with BCG. This vaccine has been shown to promote the proliferation of $CD4^+$ T cells/$CD8^+$ T cells, increase the level of IL-2/TNF-α significantly, and inhibit the secretion of the Th2-type cytokine IL-10. Meanwhile, an increase in IgG titer and IgG2b/IgG1 ratio has been observed (125).

3.3.3 Tri-Fu64

Some researchers have recombined PPE42 with the *Mtb*-related virulence factor Rv1793 and latent antigen Rv2628 into a Tri-Fu64 vaccine. The latter can reduce the number of bacteria in the lungs of aerosol *Mtb*-infected mice and induce a certain degree of protective immunity. However, although Tri-Fu64 combined with the adjuvants MPL or dimethyl dioctadecyl ammonium bromide (DDA) can also improve the anti-infection ability of mice, different degrees of body weight loss were found in mice (126). This observation is a reminder that, in evaluating a vaccine, the focus should be not only on the immunogenicity of the vaccine and that attention should be paid to the possible rare types of adverse reactions. In addition, how to use the vaccine with the appropriate adjuvant should also be considered.

3.4 PPE44-related vaccines

PPE44 has multiple immunodominant T-cell epitopes and is involved in T-cell activation. The artificially prepared recombinant PPE44 protein (rPPE44) is a protective antigen that can stimulate cellular solid and humoral immunity in mice and induce similar protection to that seen with BCG (127). Among the vaccines developed using PPE44 as a candidate protein, research has focused on HPE. HPE comprises Rv2031c with the properties of heat shock protein X (HspX), the ESAT-6 family member Esx-V, and PPE44. This vaccine has been shown to enhance the primary immune response induced by BCG, and in addition to the increase in the IFN-γ level, the secretion of IL-12 and TGF-β in a suspension of spleen cells increased significantly. The application of the pDNA-HspX-PPE44-EsxV vaccine was safe, and no intolerance was observed in the injected mice throughout the experiment. Those results indicate that HPE can activate Th1 cells effectively and has advantages in maintaining the cellular immunity of T cells for a long time (128). To enhance the immunogenicity of HPE, HPE was combined with the TLR7/8 agonist resiquimod as an adjuvant and conjugated to chitosan nanoparticles to form the HPERC vaccine. Resiquimod is a potent, safe, and simple vaccine adjuvant. It can induce a powerful immune response, exhibiting effective antitumor effects in a murine melanoma model. It is considered to have great potential not only in tumor immunotherapy but also in infectious diseases caused by intracellular pathogens (129). This vaccine was injected (s.c.) into mice immunized with BCG at 1 and 2 weeks. High levels of specific cytokines, such as IFN-γ, IL-4, and IL-17, and significant humoral immune responses were observed, among which IgG2a content and titer increased the most (130). Although the level of the inhibitory factor IL-4 was also increased, this may be a mechanism to regulate the immune response to limit excessive inflammatory damage. A combination of HPE and the lipid adjuvants DDA and trehalose 6,6-dibehenate (TDB) could also enhance the protective efficacy of BCG and induce strong anti-*Mtb* cellular immune responses (131, 132). There is no doubt about the safety of DDA and TDB. In the tuberculosis vaccine currently in phase II clinical trials, H1 is combined with CAF01 adjuvant composed of DDA and TDB, and phase I clinical trials have confirmed that the vaccine containing DDA and TDB has excellent safety (133) and can improve the humoral immune response in AIDS patients (134). In conclusion, the HPE vaccine with PPE44 as a component showed good safety and immunogenicity in mice, could be used as a BCG booster vaccine, and could be improved further for clinical trials.

3.5 PPE57-related vaccines

PPE57 (Rv3425) is also a PE/PPE family member with strong immunogenicity and specificity. Immunization of mice with PPE57 protein was shown to increase IFN-γ production significantly and induce a strong IgG1 antibody response, leading to Th1- and Th2-type responses (135). Studies have shown that the degree of specific lgG response induced by artificially recombinant rPPE57 was higher than that induced by ESAT-6 and identical to that caused by CFP-10. Hence, PPE57 could be a vaccine candidate (136).

3.5.1 Tetrafu56

The fusion peptide tetrafu56 was constructed by combining Rv3615c, TB10.4, PPE57, and HspX (a protein with high expression in the latent phase of *Mtb*). These four antigens contain a small number of specific T-cell epitopes. Their construction into a fusion protein can enable interaction with T cells and amplify the immune effect. This vaccine has been shown to induce high levels of protective IFN-γ (average = 397 pg/mL) from the PBMCs of patients with active pulmonary TB, but PBMCs from healthy adults were not sensitive to the vaccine and induced a low level of IFN-γ (average = 26.0 pg/mL) (137). Tetrafu56 (which incorporates PPE57) is a multiphase vaccine against TB composed of antigens from the active replication and resting stages of *Mtb*. Although it does not have a preventive effect, tetrafu56 has been shown *in vitro* to be more effective in interacting with PBMCs exposed to *Mtb* antigens, achieving adequate protection in patients with TB in a genetically heterogeneous population. In the next step, appropriate animal models can be selected to verify the immunological characteristics of the vaccine *in vivo*.

3.5.2 A3 vaccine

The enhancement effect of PPE57 (Rv3425) is greater than that of Ag85B. The former can help maintain the body weight of mice after *Mtb* infection and has a longer-lasting protective effect on

intravenously challenged mice (138). This fusion protein (whether carrying a virus or DNA vector) can increase the defensive efficacy of BCG (139). The Ag85B-Rv3425 (A3-lentivirus, abbreviated as "A3-len") vaccine is constructed by the lentivirus vector. A single dose of A3-len has been shown to stimulate the proliferation of $CD4^+$ T cells and reduce the number of $CD8^+$ T cells, as well as induce high levels of IFN-γ, IL-2, TNF-α, and A3-specific IgG. The CFU count and pathological examination showed that the vaccine could reduce the bacterial population in the lungs and spleen by inhibiting the growth and reproduction of *Mtb in vivo*. A3-len can reduce the severity of lung tissue lesions, increase the body weight of mice with active TB gradually, fight against the injury wrought by acute *Mtb* infection, and provide immune protection for mice (140, 141). Based on the A3 platform, Su et al. added the latent period protein Rv2029c to it to form the A39 vaccine. Rv2029c and PPE57 are the same as the crucial components of this vaccine. The former can increase the antigen presentation ability of $CD4^+$ T cells, stimulate macrophages to activate T cells so that they secrete large amounts of IFN-γ and IL-2 to maintain immune memory, and help T cells to polarize to Th1 cells (142). The most important feature of A39 is that it can control bacterial replication in organs, and the inhibitory effect of A39 on bacterial load reactivation is higher than that of drugs used for TB therapy. Several studies have shown the advantages of A3 in mice. A3 could be used as a "platform" to screen and add safer and highly immunogenic antigen-modified vaccines and improve efficacy.

3.6 PPE68-related vaccines

PPE68 (Rv3873) is one of the proteins encoded by the region of differences (RD) 1 region of the H37Rv strain. As an immunodominant antigen, it is involved in antigen diversity and immune escape of *Mtb* but is unrelated to the virulence of the RD1 region.

3.6.1 PPE68-rBCG

PPE68 expression in BCG without an RD1-related protein constitutes a safe PPE68-rBCG which can induce a higher Th1 response than that elicited by BCG alone. The levels of IFN-γ, IL-12, and IgG2a and the splenic $CD4^+$ T-cell count were increased significantly as measured by enzyme-linked immunosorbent assays, and the ratio of $CD4^+$ T cells/$CD8^+$ T cells decreased (143). Insertion of the fusion proteins PPE68, CFP-10, and ESAT-6 into the plasmid vector was shown to stimulate a large amount of IFN-γ release in the blood of patients with active pulmonary TB *in vitro*. Murine experiments also showed that the fusion protein could increase the titers of IFN-γ and lgG and maintain a long duration of humoral immunity (144).

3.6.2 rLmMtb9Ag

This recombinant vaccine is composed of *Listeria monocytogenes* and nine antigens (including PPE68). The safety and immunogenicity of rLmMtb9Ag were evaluated in mice and guinea pigs without primary vaccination using BCG. This multi-antigen vaccine induced the proliferation of antigen-specific $CD4^+$ T cells and $CD8^+$ T cells, reduced the CFU count of *Mtb* in the lungs and spleen, and produced protective immunity in guinea pigs infected with an aerosol of the hypervirulent Erdman strain of *Mtb* (145). The high immunogenicity of PPE68 may be due to its P9 peptide composed of amino acids 121–145, which is highly conserved in pathogenic mycobacteria (146). P9 can be purified by genetic engineering and used as a candidate subunit of a vaccine against TB.

3.7 PE-PGRS33-related vaccines

PE family proteins are rich in PGRS, so they are expressed constitutively only in pathogenic mycobacteria and are essential for the basic functions of bacteria. The most well-studied protein is PE-PGRS33 (Rv1818c), which is associated with long-term latent infection with *Mtb*. The PE segment is inserted into the cell wall and is necessary for *Mtb* to transport and localize proteins through the cell wall (147, 148). PGRS are partially located in the extracellular domain, in which other antigens can be inserted into the "sandwich domain" PG II without affecting the stability of their structure (149). Therefore, the immunogenicity of the protein can be increased by modification such as insertion. Bioinformatics analysis has shown that PE-PGRS33 contains 27 B-cell- and four T-cell-dominant epitopes, thereby significantly stimulating a highly effective humoral immune response. Delogu and colleagues first isolated PE and PPE fragments and cloned the PE sequence. Inoculation of rPE into mice could stimulate the proliferation of mouse T cells and secrete IFN-γ, and specific antibodies could be obtained when the intact PE-PGRS33 was inoculated (150). The PE-PGRS33 antibody was conjugated onto the surface of *Mtb*, which could bind to TLR2 to inhibit *Mtb* entry into macrophages and its proinflammatory activity, block the pathogenic pathway of TB, and promote activation of macrophages as well as the effective uptake and killing of bacteria (151). The PE segment and MPT64 could be combined to form rBCG. Due to the transport function of the PE segment, MPT64 could be delivered to the cell surface, providing higher protection efficiency than BCG, reducing the number of bacteria in the lungs and spleen, and stimulating the proliferation of $CD4^+$ T cells and $CD8^+$ T cells and the release of IFN-γ (152). Subsequent experiments demonstrated that IFN-γ and specific antibodies against Rv1818c were also observed in patients with LTBI and healthy adults immunized with BCG (44). Those results suggest that the PE fragment can induce protective cellular immunity and that the development of a vaccine formulation associated with an anti-PE-PGRS33 antibody may help suppress inflammation and prevent TB progression.

4 Discussion

In recent years, the increasing incidence of TB worldwide has incited the need to prevent the disease. The research and development of vaccines against TB have been at the forefront of this strategy. PE/PPE is a multifunctional protein family of *Mtb* with a wide range of members and complex sequences. PE/PPE proteins are involved in the interaction between pathogens and macrophages and play essential roles in immune recognition,

immune escape, and pathogenicity of *Mtb*. The application of bioinformatics analysis has enabled the prediction and understanding of the biological structure of PE/PPE proteins as well as the crucial roles of PE/PPE in *Mtb* infection. Also, understanding the targets and processes of the interaction between PE/PPE proteins and immune cells will aid in the screening of antigens for the development of new vaccines against TB. PE/PPE-related vaccines are representative of subunit vaccines, and PE/PPE proteins are combined with adjuvants or other vectors, which have both stability and safety. It is designed to enhance the immune response after BCG vaccination and prolong the duration of protection. Due to the importance of PE/PPE family proteins in the pathogenesis of *Mtb*, more and more tuberculosis vaccines are designed to include PE/PPE family proteins to further improve the immune effect. Among the PE/PPE protein vaccines, M72 and ID93 have made rapid progress and are about to enter phase III clinical trials. Both vaccines are well tolerated in the subject population and can effectively control the progression of inflammation and the recurrence of tuberculosis. Other PE/PPE vaccines have also shown outstanding safety and immunogenicity in animal trials and have made remarkable achievements, with great hope to enter the clinical trial stage. 'Taking BCG as the "gold standard", the long-term safety and immunoprotective development of other vaccines against TB should be as good as that of BCG' is a recognized principle of the International Organization for the Prevention of Tuberculosis. The difficulty in developing a new vaccine against TB is that the pathogenesis of TB and the immune response to *Mtb* infection are incompletely understood. Further understanding of the mechanism of action of *Mtb* has profound importance for vaccine development. In addition, an appropriate adjuvant can increase the immunogenicity and optimize the targeted delivery of antigen based on reducing the antigen dose. Hence, choosing an appropriate adjuvant for use with the vaccine is also crucial.

The increasing incidence of TB has brought heavy political and economic burdens to developing countries. The international community and public welfare organizations should increase investment in the research and development of vaccines. In 2018, the WHO proposed a vaccine to prevent TB in adults that should achieve >50% protection (153). This requirement also increases the standard and difficulty of vaccine development. However, with the rapid development in immunology and molecular biology, we believe that, through in-depth research and optimization of vaccines against TB, eliminating TB by 2050 is achievable. In conclusion, we believe that the PE/PPE family will remain a highly active and promising area of research and that their potential as TB vaccine targets will continue to be exploited, with more exciting properties to be explored.

Author contributions

FG: Data curation, Formal Analysis, Investigation, Project administration, Writing – original draft. JW: Investigation, Formal Analysis, Methodology, Writing – original draft. YS: Investigation, Writing – original draft, Methodology. BL: Writing – review & editing. ZQ: Methodology, Supervision, Writing – review & editing. XW: Writing – review & editing, Supervision, Validation. HW: Funding acquisition, Resources, Supervision, Writing – review & editing. TX: Funding acquisition, Investigation, Resources, Supervision, Writing – review & editing.

Funding

This work was supported by the Anhui Provincial Natural Science Foundation (1908085MH252, 2008085QH405), Anhui Province Key Laboratory of Immunology in Chronic Diseases (KLICD-2022-Z3), Anhui Province Key Laboratory of Clinical and Preclinical Research in Respiratory Disease (HX2022Z02), and the 512 Talent Cultivation Plan of Bengbu Medical College (by51201309).

Acknowledgments

We thank Figdraw (www.figdraw.com) for the assistance in creating Figure 2 in this paper.

Conflict of interest

The authors declare that the research was conducted in the absence of any commercial or financial relationships that could be construed as a potential conflict of interest.

Publisher's note

All claims expressed in this article are solely those of the authors and do not necessarily represent those of their affiliated organizations, or those of the publisher, the editors and the reviewers. Any product that may be evaluated in this article, or claim that may be made by its manufacturer, is not guaranteed or endorsed by the publisher.

References

1. World Health Organization. *Global Tuberculosis report 2022* (2022). Available at: https://www.who.int/teams/global-tuberculosis-programme/tb-reports/global-tubeculosis-report-2022.

2. Cole ST, Brosch R, Parkhill J, Garnier T, Churcher C, Harris D, et al. Deciphering the biology of Mycobacterium tuberculosis from the complete genome sequence. *Nature* (1998) 393(6685):537–44. doi: 10.1038/31159

3. Medha, Sharma S, Sharma M. Proline-Glutamate/Proline-Proline-Glutamate (PE/PPE) proteins of Mycobacterium tuberculosis: The multifaceted immune-modulators. *Acta Trop* (2021) 222:106035. doi: 10.1016/j.actatropica.2021.106035

4. Yu X, Feng J, Huang L, Liu J, Bai S, Wu B, et al. Molecular basis underlying host immunity subversion by mycobacterium tuberculosis PE/PPE family molecules. *DNA Cell Biol* (2019) 38(11):1178–87. doi: 10.1089/dna.2019.4852

5. Ahmed A, Das A, Mukhopadhyay S. Immunoregulatory functions and expression patterns of PE/PPE family members: Roles in pathogenicity and impact on anti-tuberculosis vaccine and drug design. *IUBMB Life* (2015) 67(6):414–27. doi: 10.1002/iub.1387

6. Long Q, Xiang X, Yin Q, Li S, Yang W, Sun H, et al. PE_PGRS62 promotes the survival of Mycobacterium smegmatis within macrophages via disrupting ER stress-mediated apoptosis. *Cell Physiol* (2019) 234(11):19774–84. doi: 10.1002/jcp.28577

7. Sampson SL. Mycobacterial PE/PPE proteins at the host-pathogen interface. *Clin Dev Immunol* (2011) 2011:497203. doi: 10.1155/2011/497203

8. De Maio F, Salustri A, Battah B, Palucci I, Marchionni F, Bellesi S, et al. PE_PGRS3 ensures provision of the vital phospholipids cardiolipin and phosphatidylinositols by promoting the interaction between M. *tubercul Host Cells Virulence* (2021) 12(1):868–84. doi: 10.1080/21505594.2021.1897247

9. Cho T, KhatChadourian C, Nguyen H, Dara Y, Jung S, Venketaraman V. A review of the BCG vaccine and other approaches toward tuberculosis eradication. *Hum Vaccin Immunother* (2021) 17(8):2454–70. doi: 10.1080/21645515.2021.1885280

10. Fatima S, Kumari A, Das G, Dwivedi VP. Tuberculosis vaccine: A journey from BCG to present. *Life Sci* (2020) 25(2):1175–94. doi: 10.1016/j.lfs.2020.117594

11. Abdallah AM, Verboom T, Weerdenburg EM, Gey van Pittius NC, Mahasha PW, Jiménez C, et al. PPE and PE_PGRS proteins of Mycobacterium marinum are transported via the type VII secretion system ESX-5. *Mol Microbiol* (2009) 73(3):329–40. doi: 10.1111/j.1365-2958.2009.06783.x

12. Ates LS, Dippenaar A, Ummels R, Piersma SR, van der Woude AD, van der Kuij K, et al. Mutations in ppe38 block PE_PGRS secretion and increase virulence of Mycobacterium tuberculosis. *Nat Microbiol* (2018) 3(2):181–8. doi: 10.1038/s41564-017-0090-6

13. McEvoy CR, van Helden PD, Warren RM, Gey van Pittius NC. Evidence for a rapid rate of molecular evolution at the hypervariable and immunogenic Mycobacterium tuberculosis PPE38 gene region. *BMC Evol Biol* (2009) 9):23–7. doi: 10.1186/1471-2148-9-237

14. Camassa S, Palucci I, Iantomasi R, Cubeddu T, Minerva M, De Maio F, et al. Impact of pe_pgrs33 Gene Polymorphisms on Mycobacterium tuberculosis Infection and Pathogenesis. *Front Cell Infect Microbiol* (2017) 7:137. doi: 10.3389/fcimb.2017.00137

15. Yang G, Luo T, Sun C, Yuan J, Peng X, Zhang C, et al. PPE27 in mycobacterium smegmatis enhances mycobacterial survival and manipulates cytokine secretion in mouse macrophages. *Interferon Cytokine Res* (2017) 37(9):421–31. doi: 10.1089/jir.2016.0126

16. Qian J, Hu Y, Zhang X, Chi M, Xu S, Wang H, et al. Mycobacterium tuberculosis PE_PGRS19 Induces Pyroptosis through a Non-Classical Caspase-11/GSDMD Pathway in Macrophages. *Microorganisms* (2022) 10(12):2473. doi: 10.3390/microorganisms10122473

17. Pal R, Ghosh S, Mukhopadhyay S. Moonlighting by PPE2 protein: focus on mycobacterial virulence. *J Immunol* (2021) 207(10):2393–7. doi: 10.4049/jimmunol.2100212

18. Braverman J, Stanley SA. Nitric Oxide Modulates Macrophage Responses to Mycobacterium tuberculosis Infection through Activation of HIF-1α and Repression of NF-κB. *J Immunol* (2017) 199(5):1805–16. doi: 10.4049/jimmunol.1700515

19. Srivastava S, Battu MB, Khan MZ, Nandicoori VK, Mukhopadhyay S. Mycobacterium tuberculosis PPE2 Protein Interacts with p67phox and Inhibits Reactive Oxygen Species Production. *J Immunol* (2019) 203(5):1218–29. doi: 10.4049/jimmunol.1801143

20. Meena LS. Interrelation of Ca2+ and PE_PGRS proteins during Mycobacterium tuberculosis pathogenesis. *J Biosci* (2019) 44(1):24. doi: 10.1128/IAI.05249-11

21. Sharma S, Meena LS. Potential of ca2+ in mycobacterium tuberculosis H37Rv pathogenesis and survival. *Appl Biochem Biotechnol* (2017) 181(2):762–71. doi: 10.1007/s12010-016-2247-9

22. Yeruva VC, Kulkarni A, Khandelwal R, Sharma Y, Raghunand TR. The PE_PGRS proteins of mycobacterium tuberculosis are ca(2+) binding mediators of host-pathogen interaction. *Biochemistry* (2016) 55(33):4675–87. doi: 10.1021/acs.biochem.6b00289

23. Wong EA, Evans S, Kraus CR, Engelman KD, Maiello P, Flores WJ, et al. IL-10 Impairs Local Immune Response in Lung Granulomas and Lymph Nodes during Early Mycobacterium tuberculosis Infection. *J Immunol* (2020) 204(3):644–59. doi: 10.4049/jimmunol.1901211

24. Nairz M, Weiss G. Iron in infection and immunity. *Mol Aspects Med* (2020) 75:100864. doi: 10.1016/j.mam.2020.100864

25. Ratledge C. Iron, mycobacteria and tuberculosis. *Tuberculosis (Edinb)* (2004) 84 (1-2):110–30. doi: 10.1016/j.tube.2003.08.012

26. Tullius MV, Nava S, Horwitz MA. PPE37 Is Essential for Mycobacterium tuberculosis Heme-Iron Acquisition (HIA), and a Defective PPE37 in Mycobacterium bovis BCG Prevents HIA. *Infect Immun* (2019) 87(2):e00540–18. doi: 10.1128/IAI.00540-18

27. Liu CH, Liu H, Ge B. Innate immunity in tuberculosis: host defense vs pathogen evasion. *Cell Mol Immunol* (2017) 14(12):963–75. doi: 10.1038/cmi.2017.88

28. Vringer E, Tait SWG. Mitochondria and cell death-associated inflammation. *Cell Death Differ* (2023) 30(2):304–12. doi: 10.1038/s41418-022-01094-w

29. Medha, Priyanka, Bhatt P, Sharma S, Sharma M. Role of C-terminal domain of Mycobacterium tuberculosis PE6 (Rv0335c) protein in host mitochondrial stress and macrophage apoptosis. *Apoptosis* (2023) 28(1-2):136–65. doi: 10.1007/s10495-022-01778-1

30. Sharma N, Shariq M, Quadir N, Singh J, Sheikh JA, Hasnain SE, et al. Mycobacterium tuberculosis protein PE6 (Rv0335c), a novel TLR4 agonist, evokes an inflammatory response and modulates the cell death pathways in macrophages to enhance intracellular survival. *Front Immunol* (2021) 12:696491. doi: 10.3389/fimmu.2021.696491

31. Asaad M, Kaisar Ali M, Abo-Kadoum MA, Lambert N, Gong Z, Wang H, et al. Mycobacterium tuberculosis PPE10 (Rv0442c) alters host cell apoptosis and cytokine profile via linear ubiquitin chain assembly complex HOIP-NF-κB signaling axis. *Int Immunopharmacol* (2021) 94):1063–73. doi: 10.1016/j.intimp.2020.107363

32. Fu X, Cui J, Meng X, Jiang P, Zheng Q, Zhao W, et al. Endoplasmic reticulum stress, cell death and tumor: Association between endoplasmic reticulum stress and the apoptosis pathway in tumors (Review). *Oncol Rep* (2021) 45(3):801–8. doi: 10.3892/or.2021.7933

33. Yu X, Huang Y, Li Y, Li T, Yan S, Ai X, et al. Mycobacterium tuberculosis PE_PGRS1 promotes mycobacteria intracellular survival via reducing the concentration of intracellular free Ca2+ and suppressing endoplasmic reticulum stress. *Mol Immunol* (2023) 154:24–32. doi: 10.1016/j.molimm.2022.12.007

34. Yu P, Zhang X, Liu N, Tang L, Peng C, Chen X. Pyroptosis: mechanisms and diseases. *Signal Transduct Target Ther* (2021) 6(1):128. doi: 10.1038/s41392-021-00507-5

35. Gong Z, Kuang Z, Li H, Li C, Ali MK, Huang F, et al. Regulation of host cell pyroptosis and cytokines production by Mycobacterium tuberculosis effector PPE60 requires LUBAC mediated NF-κB signaling. *Cell Immunol* (2019) 335:41–50. doi: 10.1016/j.cellimm.2018.10.009

36. Yang Y, Xu P, He P, Shi F, Tang Y, Guan C, et al. Mycobacterial PPE13 activates inflammasome by interacting with the NATCH and LRR domains of NLRP3. *FASEB J* (2020) 34(9):12820–33. doi: 10.1096/fj.202000200RR

37. Xiao Y, Cai W. Autophagy and bacterial infection. *Adv Exp Med Biol* (2020) 1207:413–23. doi: 10.1007/978-981-15-4272-5_29

38. Strong EJ, Jurcic Smith KL, Saini NK, Ng TW, Porcelli SA, Lee S. Identification of autophagy-inhibiting factors of mycobacterium tuberculosis by high-throughput loss-of-function screening. *Infect Immun* (2020) 88(12):e00269–20. doi: 10.1128/IAI.00269-20

39. Saini NK, Baena A, Ng TW, Venkataswamy MM, Kennedy SC, Kunnath VS, et al. Suppression of autophagy and antigen presentation by Mycobacterium tuberculosis PE_PGRS47. *J Nat Microbiol* (2016) 1(9):16133. doi: 10.1038/nmicrobiol.2016.133

40. Strong EJ, Ng TW, Porcelli SA, Lee S. Mycobacterium tuberculosis PE_PGRS20 and PE_PGRS47 proteins inhibit autophagy by interaction with rab1A. *mSphere* (2021) 6(4):e0054921. doi: 10.1128/mSphere.00549-21

41. Choi HH, Kwon KW, Han SJ, Kang SM, Choi E, Kim A, et al. PPE39 of the Mycobacterium tuberculosis strain Beijing/K induces Th1-cell polarization through dendritic cell maturation. *Cell Sci* (2019) 132(17):jcs228700. doi: 10.1242/jcs.228700

42. Brennan MJ. The enigmatic PE/PPE multigene family of mycobacteria and tuberculosis vaccination. *Infect Immun* (2017) 85(6):e00969–16. doi: 10.1128/IAI.00969-16

43. Bansal K, Elluru SR, Narayana Y, Chaturvedi R, Patil SA, Kaveri SV, et al. PE_PGRS antigens of Mycobacterium tuberculosis induce maturation and activation of human dendritic cells. *Immunol* (2010) 184(7):3495–504. doi: 10.4049/jimmunol.0903299

44. Cohen I, Parada C, Acosta-Gío E, Espitia C. The PGRS domain from PE_PGRS33 of mycobacterium tuberculosis is target of humoral immune response in mice and humans. *Front Immunol* (2014) 5):236. doi: 10.3389/fimmu.2014.00236

45. Ali MK, Zhen G, Nzungize L, Stojkoska A, Duan X, Li C, et al. Mycobacterium tuberculosis PE31 (Rv3477) Attenuates Host Cell Apoptosis and Promotes Recombinant M. smegmatis Intracellular Survival via Up-regulating GTPase Guanylate Binding Protein-1. *Front Cell Infect Microbiol* (2020) 10:40. doi: 10.3389/fcimb.2020.00040

46. Deng W, Long Q, Zeng J, Li P, Yang W, Chen X, et al. Mycobacterium tuberculosis PE_PGRS41 Enhances the Intracellular Survival of M. smegmatis within Macrophages Via Blocking Innate Immunity and Inhibition of Host Defense. *Sci Rep* (2017) 7:46716. doi: 10.1038/srep46716

47. Park HS, Back YW, Jang IT, Lee KI, Son YJ, Choi HG, et al. Mycobacterium tuberculosis rv2145c promotes intracellular survival by STAT3 and IL-10 receptor signaling. *Front Immunol* (2021) 12:666293. doi: 10.3389/fimmu.2021.666293

48. Qureshi R, Rameshwaram NR, Battu MB, Mukhopadhyay S. PPE65 of M. tuberculosis regulate pro-inflammatory signalling through LRR domains of Toll like receptor-2. *Biochem Biophys Res Commun* (2019) 508(1):152–8. doi: 10.1016/j.bbrc.2018.11.094

49. Kim A, Hur YG, Gu S, Cho SN. Protective vaccine efficacy of the complete form of PPE39 protein from mycobacterium tuberculosis Beijing/K strain in mice. *Clin Vaccine Immunol* (2017) 24(11):e00219–17. doi: 10.1128/CVI.00219-17

50. Suo J, Wang X, Zhao R, Ma P, Ge L, Luo T. Mycobacterium tuberculosis PPE7 Enhances Intracellular Survival of Mycobacterium smegmatis and Manipulates Host Cell Cytokine Secretion Through Nuclear Factor Kappa B and Mitogen-Activated Protein Kinase Signaling. *J Interferon Cytokine Res* (2022) 42(10):525–35. doi: 10.1089/jir.2022.0062

51. Kim JS, Kim HK, Cho E, Mun SJ, Jang S, Jang J, et al. PE_PGRS38 interaction with HAUSP downregulates antimycobacterial host defense via TRAF6. *Front Immunol* (2022) 13:862628. doi: 10.3389/fimmu.2022.862628

52. Singh SK, Tripathi DK, Singh PK, Sharma S, Srivastava KK. Protective and survival efficacies of Rv0160c protein in murine model of Mycobacterium tuberculosis. *Appl Microbiol Biotechnol* (2013) 97(13):5825–37. doi: 10.1007/s00253-012-4493-2

53. Tiwari B, Ramakrishnan UM, Raghunand TR. The Mycobacterium tuberculosis protein pair PE9 (Rv1088)-PE10 (Rv1089) forms heterodimers and induces macrophage apoptosis through Toll-like receptor 4. *Cell Microbiol* (2015) 17 (11):1653–69. doi: 10.1111/cmi.12462

54. Singh P, Rao RN, Reddy JR, Prasad RB, Kotturu SK, Ghosh SR, et al. PE11, a PE/PPE family protein of Mycobacterium tuberculosis is involved in cell wall remodeling and virulence. *Sci Rep* (2016) 6:21624. doi: 10.1038/srep21624

55. Deng W, Zeng J, Xiang X, Li P, Xie J. PE11 (Rv1169c) selectively alters fatty acid components of Mycobacterium smegmatis and host cell interleukin-6 level accompanied with cell death. *Front Microbiol* (2015) 6:613. doi: 10.3389/fmicb.2015.00613

56. Sultana R, Vemula MH, Banerjee S, Guruprasad L. The PE16 (Rv1430) of Mycobacterium tuberculosis is an esterase belonging to serine hydrolase superfamily of proteins. *PloS One* (2013) 8(2):e55320. doi: 10.1371/journal.pone.0055320

57. Wang Q, Boshoff HIM, Harrison JR, Ray PC, Green SR, Wyatt PG, et al. PE/PPE proteins mediate nutrient transport across the outer membrane of Mycobacterium tuberculosis. *Science* (2020) 367(6482):1147–51. doi: 10.1126/science.aav5912

58. Tundup S, Mohareer K, Hasnain SE. Mycobacterium tuberculosis PE25/PPE41 protein complex induces necrosis in macrophages: Role in virulence and disease reactivation? *FEBS Open Bio* (2014) 4:822–8. doi: 10.1016/j.fob.2014.09.001

59. Kim WS, Kim JS, Cha SB, Kim SJ, Kim H, Kwon KW, et al. Mycobacterium tuberculosis PE27 activates dendritic cells and contributes to Th1-polarized memory immune responses during in *vivo* infection. *Immunobiology* (2016) 221(3):440–53. doi: 10.1016/j.imbio.2015.11.006

60. Bhat KH, Srivastava S, Kotturu SK, Ghosh S, Mukhopadhyay S. The PPE2 protein of Mycobacterium tuberculosis translocates to host nucleus and inhibits nitric oxide production. *Sci Rep* (2017) 7:39706. doi: 10.1038/srep39706

61. Mi Y, Bao L, Gu D, Luo T, Sun C, Yang G. Mycobacterium tuberculosis PPE25 and PPE26 proteins expressed in Mycobacterium smegmatis modulate cytokine secretion in mouse macrophages and enhance mycobacterial survival. *Res Microbiol* (2017) 168(3):234–43. doi: 10.1016/j.resmic.2016.06.004

62. Su H, Kong C, Zhu L, Huang Q, Luo L, Wang H, et al. PPE26 induces TLR2-dependent activation of macrophages and drives Th1-type T-cell immunity by triggering the cross-talk of multiple pathways involved in the host response. *Oncotarget* (2015) 6(36):38517–37. doi: 10.18632/oncotarget.5956

63. Deng W, Yang W, Zeng J, Abdalla AE, Xie J. Mycobacterium tuberculosis PPE32 promotes cytokines production and host cell apoptosis through caspase cascade accompanying with enhanced ER stress response. *Oncotarget* (2016) 7(41):67347–59. doi: 10.18632/oncotarget.12030

64. Mitra A, Ko YH, Cingolani G, Niederweis M. Heme and hemoglobin utilization by Mycobacterium tuberculosis. *Nat Commun* (2019) 10(1):4260. doi: 10.1038/s41467-019-12109-5

65. Dong D, Wang D, Li M, Wang H, Yu J, Wang C, et al. PPE38 modulates the innate immune response and is required for Mycobacterium marinum virulence. *Infect Immun* (2012) 80(1):43–54. doi: 10.1128/IAI.05249-11

66. Xu Y, Yang E, Huang Q, Ni W, Kong C, Liu G, et al. PPE57 induces activation of macrophages and drives Th1-type immune responses through TLR2. *J Mol Med (Berl)* (2015) 93(6):645–62. doi: 10.1007/s00109-014-1243-1

67. Su H, Zhang Z, Liu Z, Peng B, Kong C, Wang H, et al. Mycobacterium tuberculosis PPE60 antigen drives Th1/Th17 responses via Toll-like receptor 2-dependent maturation of dendritic cells. *J Biol Chem* (2018) 293(26):10287–302. doi: 10.1074/jbc.RA118.001696

68. Ahmad J, Khubaib M, Sheikh JA, Pancsa R, Kumar S, Srinivasan A, et al. Disorder-to-order transition in PE-PPE proteins of Mycobacterium tuberculosis augments the pro-pathogen immune response. *FEBS Open Bio* (2020) 10(1):70–85. doi: 10.1002/2211-5463.12749

69. Danelishvili L, Everman J, Bermudez LE. Mycobacterium tuberculosis PPE68 and Rv2626c genes contribute to the host cell necrosis and bacterial escape from macrophages. *Virulence* (2016) 7(1):23–32. doi: 10.1080/21505594.2015.1102832

70. De Maio F, Battah B, Palmieri V, Petrone L, Corrente F, Salustri A, et al. PE_PGRS3 of Mycobacterium tuberculosis is specifically expressed at low phosphate concentration, and its arginine-rich C-terminal domain mediates adhesion and persistence in host tissues when expressed in Mycobacterium smegmatis. *Cell Microbiol* (2018) 20(12):e12952. doi: 10.1111/cmi.12952

71. Grover S, Sharma T, Singh Y, Kohli S, Singh A, Semmler T, et al. The PGRS Domain of Mycobacterium tuberculosis PE_PGRS Protein Rv0297 Is Involved in Endoplasmic Reticulum Stress-Mediated Apoptosis through Toll-Like Receptor 4. *mBio* (2018) 9(3):e01017–18. doi: 10.1128/mBio.01017-18

72. Chaturvedi R, Bansal K, Narayana Y, Kapoor N, Sukumar N, Togarsimalemath SK, et al. The multifunctional PE_PGRS11 protein from Mycobacterium tuberculosis plays a role in regulating resistance to oxidative stress. *J Biol Chem* (2010) 285 (40):30389–403. doi: 10.1074/jbc.M110.135251

73. Chen T, Zhao Q, Li W, Xie J. Mycobacterium tuberculosis PE_PGRS17 promotes the death of host cell and cytokines secretion via Erk kinase accompanying with enhanced survival of recombinant Mycobacterium smegmatis. *J Interferon Cytokine Res* (2013) 33(8):452–8. doi: 10.1089/jir.2012.0083

74. Yang W, Deng W, Zeng J, Ren S, Ali MK, Gu Y, et al. Mycobacterium tuberculosis PE_PGRS18 enhances the intracellular survival of M. smegmatis via altering host macrophage cytokine profiling and attenuating the cell apoptosis. *Apoptosis* (2017) 22(4):502–9. doi: 10.1007/s10495-016-1336-0

75. Chatrath S, Gupta VK, Dixit A, Garg LC. PE_PGRS30 of Mycobacterium tuberculosis mediates suppression of proinflammatory immune response in macrophages through its PGRS and PE domains. *Microbes Infect* (2016) 18(9):536–42. doi: 10.1016/j.micinf.2016.04.004

76. Iantomasi R, Sali M, Cascioferro A, Palucci I, Zumbo A, Soldini S, et al. PE_PGRS30 is required for the full virulence of Mycobacterium tuberculosis. *Cell Microbiol* (2012) 14(3):356–67. doi: 10.1111/j.1462-5822.2011.01721.x

77. Palucci I, Camassa S, Cascioferro A, Sali M, Anoosheh S, Zumbo A, et al. PE_PGRS33 Contributes to Mycobacterium tuberculosis Entry in Macrophages through Interaction with TLR2. *PloS One* (2016) 11(3):e0150800. doi: 10.1371/journal.pone.0150800

78. Dheenadhayalan V, Delogu G, Brennan MJ. Expression of the PE_PGRS 33 protein in Mycobacterium smegmatis triggers necrosis in macrophages and enhanced mycobacterial survival. *Microbes Infect* (2006) 8(1):262–72. doi: 10.1016/j.micinf.2005.06.021

79. Rao M, Valentini D, Poiret T, Dodoo E, Parida S, Zumla A, et al. B in TB: B cells as mediators of clinically relevant immune responses in tuberculosis. *Clin Infect Dis* (2015) 61Suppl 3(Suppl 3):225–34. doi: 10.1093/cid/civ614

80. Scriba TJ, Coussens AK, Fletcher HA. Human immunology of tuberculosis. *Microbiol Spectr* (2017) 5(1):112–8. doi: 10.1128/microbiolspec.GPP3-0022-2018

81. Dolasia K, Nazar F, Mukhopadhyay S. Mycobacterium tuberculosis PPE18 protein inhibits MHC class II antigen presentation and B cell response in mice. *Eur J Immunol* (2021) 51(3):603–19. doi: 10.1002/eji.201848071

82. Maglione PJ, Xu J, Chan J. B cells moderate inflammatory progression and enhance bacterial containment upon pulmonary challenge with Mycobacterium tuberculosis. *J Immunol* (2007) 178(11):7222–34. doi: 10.4049/jimmunol.178.11.7222

83. Dye C. Making wider use of the world's most widely used vaccine: Bacille Calmette-Guerin revaccination reconsidered. *R Soc Interface* (2013) 10(87):e20130365. doi: 10.1098/rsif.2013.0365

84. Trunz BB, Fine P, Dye C. Effect of BCG vaccination on childhood tuberculous meningitis and miliary tuberculosis worldwide: a meta-analysis and assessment of cost-effectiveness. *Lancet* (2006) 367(9517):1173–80. doi: 10.1016/S0140-6736(06)68507-3

85. Covián C, Fernández-Fierro A, Retamal-Díaz A, Díaz FE, Vasquez AE, Lay MK, et al. BCG-induced cross-protection and development of trained immunity: implication for vaccine design. *Front Immunol* (2019) 2806:2806(10). doi: 10.3389/fimmu.2019.02806

86. Shah T, Shah Z, Yasmeen N, Baloch Z, Xia X. Pathogenesis of SARS-coV-2 and mycobacterium tuberculosis coinfection. *Front Immunol* (2022) 13:909011. doi: 10.3389/fimmu.2022.909011

87. Liu B, Li M, Zhou Z, Guan X, Xiang Y. Can we use interleukin-6 (IL-6) blockade for coronavirus disease 2019 (COVID-19)-induced cytokine release syndrome (CRS)? *J Autoimmun* (2020) 111:102452. doi: 10.1016/j.jaut.2020.102452

88. Tadolini M, Codecasa LR, García-García JM, Blanc FX, Borisov S, Alffenaar JW, et al. Active tuberculosis, sequelae and COVID-19 co-infection: first cohort of 49 cases. *Eur Respir J* (2020) 56(1):2001398. doi: 10.1183/13993003.01398-2020

89. Moorlag SJCFM, Arts RJW, van Crevel R, Netea MG. Non-specific effects of BCG vaccine on viral infections. *Clin Microbiol Infect* (2019) 25(12):1473–8. doi: 10.1016/j.cmi.2019.04.020

90. Goodridge HS, Ahmed SS, Curtis N, Kollmann TR, Levy O, Netea MG, et al. Harnessing the beneficial heterologous effects of vaccination. *Nat Rev Immunol* (2016) 16(6):392–400. doi: 10.1038/nri.2016.43

91. Kleinnijenhuis J, Quintin J, Preijers F, Benn CS, Joosten LA, Jacobs C, et al. Long-lasting effects of BCG vaccination on both heterologous Th1/Th17 responses and innate trained immunity. *J Innate Immun* (2014) 6(2):152–8. doi: 10.1159/000355628

92. O'Neill LAJ, Netea MG. BCG-induced trained immunity: can it offer protection against COVID-19? *Nat Rev Immunol* (2020) 20(6):335–7. doi: 10.1038/s41577-020-0337-y

93. Urashima M, Otani K, Hasegawa Y, Akutsu T. BCG vaccination and mortality of COVID-19 across 173 countries: an ecological study. *Int J Environ Res Public Health* (2020) 17(15):5589. doi: 10.3390/ijerph17155589

94. Counoupas C, Johansen MD, Stella AO, Nguyen DH, Ferguson AL, Aggarwal A, et al. A single dose, BCG-adjuvanted COVID-19 vaccine provides sterilising immunity against SARS-CoV-2 infection. *NPJ Vaccines* (2021) 6(1):143. doi: 10.1038/s41541-021-00406-4

95. Faustman DL, Lee A, Hostetter ER, Aristarkhova A, Ng NC, Shpilsky GF, et al. Multiple BCG vaccinations for the prevention of COVID-19 and other infectious diseases in type 1 diabetes. *Cell Rep Med* (2022) 3(9):100728. doi: 10.1016/j.xcrm.2022.100728

96. Tsilika M, Taks E, Dolianitis K, Kotsaki A, Leventogiannis K, Damoulari C, et al. ACTIVATE-2: A double-blind randomized trial of BCG vaccination against COVID-

19 in individuals at risk. *Front Immunol* (2022) 13:873067. doi: 10.3389/fimmu.2022.873067

97. Subbian S, Singh P, Kolloli A, Nemes E, Scriba T, Hanekom WA, et al. BCG vaccination of infants confers mycobacterium tuberculosis strain-specific immune responses by leukocytes. *J.ACS Infect Dis* (2020) 6(12):3141–6. doi: 10.1021/acsinfecdis.0c00696

98. Bonifachich E, Chort M, Astigarraga A, Diaz N, Brunet B, Pezzotto SM, et al. Protective effect of Bacillus Calmette-Guerin (BCG) vaccination in children with extra-pulmonary tuberculosis, but not the pulmonary disease: a case-control study in Rosario, Argentina. *Vaccine* (2006) 2006(24):2894–9. doi: 10.1016/j.vaccine.2005.12.044

99. Hesseling AC, Marais BJ, Gie RP, Schaaf HS, Fine PE, Godfrey-Faussett P, et al. The risk of disseminated Bacille Calmette-Guerin (BCG) disease in HIV-infected children. *Vaccine* (2007) 25(1):14–8. doi: 10.1016/j.vaccine.2006.07.020

100. Daniel J, Kapoor N, Sirakova T, Sinha R, Kolattukudy P. The perilipin-like PPE15 protein in Mycobacterium tuberculosis is required for triacylglycerol accumulation under dormancy-inducing conditions. *Mol Microbiol* (2016) 101 (5):784–94. doi: 10.1111/mmi.13422

101. Stylianou E, Harrington-Kandt R, Beglov J, Bull N, Pinpathomrat N, Swarbrick GM, et al. Identification and evaluation of novel protective antigens for the development of a candidate tuberculosis subunit vaccine. *Infect Immun* (2018) 86(7): e00014–18. doi: 10.1128/IAI.00014-18

102. Xu T, Li M, Wang C, Chang X, Qian Z, Li B, et al. [Prokaryotic expression and identification of PPE15 protein from Mycobacterium tuberculosis and preparation of rabbit polyclonal antibodies]. *Xi Bao Yu Fen Zi Mian Yi Xue Za Zhi* (2022) 38(1):78–83. doi: 10.13423/j.cnki.cjcmi.009311

103. Bhat KH, Ahmed A, Kumar S, Sharma P, Mukhopadhyay S. Role of PPE18 protein in intracellular survival and pathogenicity of Mycobacterium tuberculosis in mice. *PloS One* (2012) 7(12):e52601. doi: 10.1371/journal.pone.0052601

104. Didierlaurent AM, Laupèze B, Di Pasquale A, Hergli N, Collignon C, Garçon N. Adjuvant system AS01: helping to overcome the challenges of modern vaccines. *Expert Rev Vaccines* (2017) 16(1):55–63. doi: 10.1080/14760584.2016.1213632

105. Skeiky Y, lderson MR, Ovendale PJ, Guderian JA, Brandt L, Dillon DC, et al. Differential immune responses and protective efficacy induced by components of a tuberculosis polyprotein vaccine, Mtb72F, delivered as naked DNA or recombinant protein. *J Immunol* (2004) 172(12):7618–28. doi: 10.4049/jimmunol.172.12.7618

106. Brandt L, Skeiky Y, lderson MR, Lobet Y, Dalemans W, Turner OC, et al. The protective effect of the Mycobacterium bovis BCG vaccine is increased by coadministration with the Mycobacterium tuberculosis 72-kilodalton fusion polyprotein Mtb72F in M. tuberculosis-infected Guinea pigs. *Infect Immun* (2004) 72(11):6622–32. doi: 10.1128/IAI.72.11.6622-6632.2004

107. Peña JC, Ho WZ. Monkey models of tuberculosis: lessons learned. *Infect Immun* (2015) 83(3):852–62. doi: 10.1128/IAI.02850-14

108. Reed SG, Coler RN, Dalemans W, Tan EV, DeLa Cruz EC, Basaraba RJ, et al. Defined tuberculosis vaccine, Mtb72F/AS02A, evidence of protection in cynomolgus monkeys. *Proc Natl Acad Sci U S A.* (2009) 106(7):2301–6. doi: 10.1073/pnas.0712077106

109. Penn-Nicholson A, Geldenhuys H, Burny W, van der Most R, Day CL, Jongert E, et al. Safety and immunogenicity of candidate vaccine M72/AS01E in adolescents in a TB endemic setting. *Vaccine* (2015) 33(32):4025–34. doi: 10.1016/j.vaccine.2015.05.088

110. Kumarasamy N, Poongulali S, Bollaerts A, Moris P, Beulah FE, Ayuk LN, et al. A randomized, controlled safety, and immunogenicity trial of the M72/AS01 candidate tuberculosis vaccine in HIV-positive Indian adults. *Med (Baltimore)* (2016) 95(3): e2459. doi: 10.1097/MD.0000000000002459

111. Rodo MJ, Rozot V, Nemes E, Dintwe O, Hatherill M, Little F, et al. A comparison of antigen-specific T cell responses induced by six novel tuberculosis vaccine candidates. *PloS Pathog* (2019) 15(3):e1007643. doi: 10.1371/journal.ppat.1007643

112. Tait DR, Hatherill M, van der Meeren O, Ginsberg AM, Van Brakel E, Salaun B, et al. Final analysis of a trial of M72/AS01E vaccine to prevent tuberculosis. *N Engl J Med* (2019) 381(25):2429–39. doi: 10.1056/NEJMoa1909953

113. Su W. *Study on gene polymorphism of antigen PPE18 and pepA in clinical isolates of children with tuberculosis*. Chongqing Medical University, China (2016).

114. Gong W, Liang Y, Mi J, Xue Y, Wang J, Wang L, et al. A peptide-based vaccine ACP derived from antigens of Mycobacterium tuberculosis induced Th1 response but failed to enhance the protective efficacy of BCG in mice. *Indian J Tuberc* (2022) 69 (4):482–95. doi: 10.1016/j.ijtb.2021.08.016

115. Liu SY. *The surface of Escherichia coli showing the PepA, PPE18 and EsxH proteins of Mycobacterium tuberculosis and their immunogenicity*. Chinese Academy of Agricultural Sciences, Beijing, China (2016).

116. Schneider-Ohrum K, Cayatte C, Bennett AS, Rajani GM, McTamney P, Nacel K, et al. Immunization with low doses of recombinant postfusion or prefusion respiratory syncytial virus F primes for vaccine-enhanced disease in the cotton rat model independently of the presence of a th1-biasing (GLA-SE) or th2-biasing (Alum) adjuvant. *Virol* (2017) 91(8):e02180–16. doi: 10.1128/JVI.02180-16

117. Baldwin SL, Reese VA, Larsen SE, Pecor T, Brown BP, Granger B, et al. Therapeutic efficacy against Mycobacterium tuberculosis using ID93 and liposomal adjuvant formulations. *Front Microbiol* (2022) 13):e935444. doi: 10.3389/fmicb.2022.935444

118. Bertholet S, Ireton GC, Ordway DJ, Windish HP, Pine SO, Kahn M, et al. A defined tuberculosis vaccine candidate boosts BCG and protects against multidrug-resistant Mycobacterium tuberculosis. *Sci Transl Med* (2010) 2(53):53ra74. doi: 10.1126/scitranslmed.3001094

119. Coler RN, Day TA, Ellis R, Piazza FM, Beckmann AM, Vergara J, et al. The TLR-4 agonist adjuvant, GLA-SE, improves magnitude and quality of immune responses elicited by the ID93 tuberculosis vaccine: first-in-human trial. *NPJ Vaccines* (2018) 3(34). doi: 10.1038/s41541-018-0057-5

120. Penn-Nicholson A, Tameris M, Smit E, Day TA, Musvosvi M, Jayashankar L, et al. Safety and immunogenicity of the novel tuberculosis vaccine ID93 + GLA-SE in BCG-vaccinated healthy adults in South Africa: a randomised, double-blind, placebo-controlled phase 1 trial. *Lancet Respir Med* (2018) 6(4):287–98. doi: 10.1016/S2213-2600(18)30077-8

121. Day TA, Penn-Nicholson A, Luabeya AKK, Fiore-Gartland A, Du Plessis N, Loxton AG, et al. Safety and immunogenicity of the adjunct therapeutic vaccine ID93 + GLA-SE in adults who have completed treatment for tuberculosis: a randomised, double-blind, placebo-controlled, phase 2a trial. *Lancet Respir Med* (2021) 9(4):373–86. doi: 10.1016/S2213-2600(20)30319-2

122. Baldwin SL, Reese VA, Larsen SE, Beebe E, Guderian J, Orr MT, et al. Prophylactic efficacy against Mycobacterium tuberculosis using ID93 and lipid-based adjuvant formulations in the mouse model. *PloS One* (2021) 16(3):e0247990. doi: 10.1371/journal.pone.0247990

123. Kwon KW, Lee A, Larsen SE, Baldwin SL, Coler RN, Reed SG, et al. Long-term protective efficacy with a BCG-prime ID93/GLA-SE boost regimen against the hyper-virulent Mycobacterium tuberculosis strain K in a mouse model. *Sci Rep* (2019) 9 (1):155–60. doi: 10.1038/s41598-019-52146-0

124. Gomez M, Ahmed M, Das S, McCollum J, Mellett L, Swanson R, et al. Development and testing of a spray-dried tuberculosis vaccine candidate in a mouse model. *Front Pharmacol* (2022) 12):e799034. doi: 10.3389/fphar.2021.799034

125. Lu Y, Xu Y, Yang E, Wang C, Wang H, Shen H. Novel recombinant BCG coexpressing Ag85B, ESAT-6 and Rv2608 elicits significantly enhanced cellular immune and antibody responses in C57BL/6 mice. *Scand J Immunol* (2012) 76 (3):271–77. doi: 10.1111/j.1365-3083.2012.02726.x

126. Sulman S, Savidge BO, Alqaseer K, Das MK, Nezam Abadi N, Pearl JE, et al. Balance between protection and pathogenic response to aerosol challenge with mycobacterium tuberculosis (Mtb) in mice vaccinated with triFu64, a fusion consisting of three mtb antigens. *Vaccines (Basel)* (2021) 9(5):51–9. doi: 10.3390/vaccines9050519

127. Romano M, Rindi L, Korf H, Bonanni D, Adnet PY, Jurion F, et al. Immunogenicity and protective efficacy of tuberculosis subunit vaccines expressing PPE44 (Rv2770c). *Vaccine* (2008) 26(48):6053–63. doi: 10.1016/j.vaccine.2008.09.025

128. Moradi B, Sankian M, Amini Y, Gholoobi A, Meshkat Z. A new DNA vaccine expressing HspX-PPE44-EsxV fusion antigens of Mycobacterium tuberculosis induced strong immune responses. *Iran J Basic Med Sci* (2020) 23(7):909–14. doi: 10.22038/ijbms.2020.38521.9171

129. Igartua M, Pedraz JL. Topical resiquimod: a promising adjuvant for vaccine development? *Expert Rev Vaccines* (2010) 9(1):23–7. doi: 10.1586/erv.09.135

130. Hoseinpur R, Hasani A, Baradaran B, Abdolalizadeh J, Amini Y, Salehi R, et al. Chitosan nanoparticles containing fusion protein (Hspx-PPE44-EsxV) and resiquimod adjuvant (HPERC) as a novel booster vaccine for Mycobacterium tuberculosis. *Biomater Appl* (2022) 37(1):40–7. doi: 10.1177/08853282221079105

131. Mansury D, Ghazvini K, Amel Jamehdar S, Badiee A, Tafaghodi M, Nikpoor AR, et al. Enhancement of the effect of BCG vaccine against tuberculosis using DDA/TDB liposomes containing a fusion protein of HspX, PPE44, and EsxV. *Artif Cells Nanomed Biotechnol* (2019) 47(1):370–7. doi: 10.1080/21691401.2018.1557674

132. Mansury D, Ghazvini K, Amel Jamehdar S, Badiee A, Tafaghodi M, Nikpoor AR, et al. Increasing cellular immune response in liposomal formulations of DOTAP encapsulated by fusion protein hspx, PPE44, and esxv, as a potential tuberculosis vaccine candidate. *Rep Biochem Mol Biol* (2019) 7(2):156–66.

133. van Dissel JT, Joosten SA, Hoff ST, Soonawala D, Prins C, Hokey DA, et al. A novel liposomal adjuvant system, CAF01, promotes long-lived Mycobacterium tuberculosis-specific T-cell responses in human. *Vaccine* (2014) 32(52):7098–107. doi: 10.1016/j.vaccine.2014.10.036

134. Klessing S, Temchura V, Tannig P, Peter AS, Christensen D, Lang R, et al. CD4 + T cells induced by tuberculosis subunit vaccine H1 can improve the HIV-1 env humoral response by intrastructural help. *Vaccines (Basel)* (2020) 8(4):604. doi: 10.3390/vaccines8040604

135. Wang J, Qie Y, Zhang H, Zhu B, Xu Y, Liu W, et al. PPE protein (Rv3425) from DNA segment RD11 of Mycobacterium tuberculosis: a novel immunodominant antigen of Mycobacterium tuberculosis induces humoral and cellular immune responses in mice. *Microbiol Immunol* (2008) 52(4):224–30. doi: 10.1111/j.1348-0421.2008.00029.x

136. Zhang H, Wang J, Lei J, Zhang M, Yang Y, Chen Y, et al. PPE protein (Rv3425) from DNA segment RD11 of Mycobacterium tuberculosis: a potential B-cell antigen used for serological diagnosis to distinguish vaccinated controls from tuberculosis patients. *Clin Microbiol Infect* (2007) 13(2):139–45. doi: 10.1111/j.1469-0691.2006.01561.x

137. Arif S, Akhter M, Khaliq A, Akhtar MW. Fusion peptide constructs from antigens of M. tuberculosis producing high T-cell mediated immune response. *PloS One* (2022) 17(9):e0271126. doi: 10.1371/journal.pone.0271126

138. Yang E, Gu J, Wang F, Wang H, Shen H, Chen ZW. Recombinant BCG prime and PPE protein boost provides potent protection against acute Mycobacterium tuberculosis infection in mice. *Microb Pathog* (2016) 93):1–7. doi: 10.1016/j.micpath.2016.01.006

139. Xu Y, Yang E, Wang J, Li R, Li G, Liu G, et al. Prime-boost bacillus Calmette-Guérin vaccination with lentivirus-vectored and DNA-based vaccines expressing antigens Ag85B and Rv3425 improves protective efficacy against Mycobacterium tuberculosis in mice. *Immunology* (2014) 143(2):277–86. doi: 10.1111/imm.12308

140. Huang H, Wang F, Yang E, Wang H, Gao P, Shen H. Assessment of recombinant plasmid expressing fusion antigen Ag85B-Rv3425 in management of acute tuberculosis infection in mice. *Exp Ther Med* (2018) 15(3):3034–39. doi: 10.3892/etm.2018.5785

141. Yang E, Wang F, Xu Y, Wang H, Hu Y, Shen H, et al. A lentiviral vector-based therapeutic vaccine encoding Ag85B-Rv3425 potently increases resistance to acute tuberculosis infection in mice. *Acta Biochim Biophys Sin (Shanghai)* (2015) 47(8):588–96. doi: 10.1093/abbs/gmv059

142. Su H, Zhu S, Zhu L, Kong C, Huang Q, Zhang Z, et al. Mycobacterium tuberculosis Latent Antigen Rv2029c from the Multistage DNA Vaccine A39 Drives TH1 Responses via TLR-mediated Macrophage Activation. *Front Microbiol* (2017) 11:2266(17). doi: 10.3389/fmicb.2017.02266

143. Dong Z, Xu L, Yang J, He Y, She Q, Wang J, et al. Primary application of PPE68 of Mycobacterium tuberculosis. *Hum Immunol* (2014) 75(5):428–32. doi: 10.1016/j.humimm.2014.02.017

144. Xu JN, Chen JP, Chen DL. Serodiagnosis efficacy and immunogenicity of the fusion protein of Mycobacterium tuberculosis composed of the 10-kilodalton culture filtrate protein, ESAT-6, and the extracellular domain fragment of PPE68. *Clin Vaccine Immunol* (2012) 19(4):536–44. doi: 10.1128/CVI.05708-11

145. Jia Q, Masleša-Galić S, Nava S, Horwitz MA. Listeria-vectored multi-antigenic tuberculosis vaccine protects C57BL/6 and BALB/c mice and Guinea pigs against Mycobacterium tuberculosis challenge. *Commun Biol* (2022) 5(1):1388. doi: 10.1038/s42003-022-04345-1

146. Mustafa AS. Characterization of a cross-reactive, immunodominant and HLA-promiscuous epitope of Mycobacterium tuberculosis-specific major antigenic protein PPE68. *PloS One* (2014) 9(8):e103679. doi: 10.1371/journal.pone.0103679

147. Fan B. *Preliminary study on immunogenicity of some protein polypeptides of PE and PPE families of Mycobacterium tuberculosis*. Beijing Institute of Tuberculosis and Chest Cancer, Beijing, China. (2010).

148. Shang QY, Sun HL, Liang LJ, Ju XH. Research progress on PE_PGRS family proteins of Mycobacterium tuberculosis. *Chin J Zoonotic Dis* (2022) 30(04):222–8. doi: 10.19958/j.cnki.cn31-2031/s.2022.04.016

149. Kramarska E, Squeglia F, De Maio F, Delogu G, Berisio R. PE_PGRS33, an important virulence factor of mycobacterium tuberculosis and potential target of host humoral immune response. *Cells* (2021) 10(1):161. doi: 10.3390/cells10010161

150. Delogu G, Brennan MJ. Comparative immune response to PE and PE_PGRS antigens of Mycobacterium tuberculosis. *Infect Immun* (2001) 69(9):5606–11. doi: 10.1128/IAI.69.9.5606-5611.2001

151. Minerva M, De Maio F, Camassa S, Battah B, Ivana P, Manganelli R, et al. Evaluation of PE_PGRS33 as a potential surface target for humoral responses against Mycobacterium tuberculosis. *Pathog Dis* (2017) 75(8):1093–100. doi: 10.1093/femspd/ftx100

152. Sali M, Di Sante G, Cascioferro A, Zumbo A, Nicolò C, Donà V, et al. Surface expression of MPT64 as a fusion with the PE domain of PE_PGRS33 enhances Mycobacterium bovis BCG protective activity against Mycobacterium tuberculosis in mice. *Infect Immun* (2010) 78(12):5202–13. doi: 10.1128/IAI.00267-10

153. Schrager LK, Chandrasekaran P, Fritzell BH, Hatherill M, Lambert PH, McShane H, et al. WHO preferred product characteristics for new vaccines against tuberculosis. *Lancet Infect Dis* (2018) 18(8):828–9. doi: 10.1016/S1473-3099(18)30421-3

frontiers | Frontiers in Immunology

TYPE Review
PUBLISHED 18 October 2023
DOI 10.3389/fimmu.2023.1254347

OPEN ACCESS

EDITED BY
Zhidong Hu,
Fudan University, China

REVIEWED BY
Hanwei Cui,
Shenzhen Samii Medical Center, China
Ping Xu,
Fifth People's Hospital of Suzhou, China
Dharmendra Kumar Soni,
Uniformed Services University of the Health Sciences, United States

*CORRESPONDENCE
Jianjun Wang
wangjianjun0520@163.com

†These authors have contributed equally to this work

RECEIVED 07 July 2023
ACCEPTED 02 October 2023
PUBLISHED 18 October 2023

CITATION
Wang N, Yao Y, Qian Y, Qiu D, Cao H, Xiang H and Wang J (2023) Cargoes of exosomes function as potential biomarkers for *Mycobacterium tuberculosis* infection. *Front. Immunol.* 14:1254347.
doi: 10.3389/fimmu.2023.1254347

Cargoes of exosomes function as potential biomarkers for *Mycobacterium tuberculosis* infection

Nan Wang[1†], Yongliang Yao[1†], Yingfen Qian[2†], Dewen Qiu[3†], Hui Cao[4†], Huayuan Xiang[1] and Jianjun Wang[1*]

[1]Department of Clinical Laboratory, Kunshan Hospital Affiliated to Jiangsu University, Suzhou, Jiangsu, China, [2]Department of Clinical Laboratory, Kunshan Fourth People's Hospital, Suzhou, Jiangsu, China, [3]Department of Clinical Laboratory, Jiangxi Maternal and Child Health Hospital Maternal and Child Heath Hospital of Nanchang College, Nanchang, China, [4]Department of Food and Nutrition Safety, Jiangsu Provincial Center for Disease Control and Prevention, Nanjing, Jiangsu, China

Exosomes as double-membrane vesicles contain various contents of lipids, proteins, mRNAs and non-coding RNAs, and involve in multiple physiological processes, for instance intercellular communication and immunomodulation. Currently, numerous studies found that the components of exosomal proteins, nucleic acids or lipids released from host cells are altered following infection with *Mycobacterium tuberculosis*. Exosomal contents provide excellent biomarkers for the auxiliary diagnosis, efficacy evaluation, and prognosis of tuberculosis. This study aimed to review the current literatures detailing the functions of exosomes in the procedure of *M. tuberculosis* infection, and determine the potential values of exosomes as biomarkers to assist in the diagnosis and monitoring of tuberculosis.

KEYWORDS
exosomes, mycobacterium tuberculosis, biomarkers, diagnosis, tuberculosis

1 Introduction

Tuberculosis (TB) is a bacterial infectious disease which causes a serious threat to the health and hygiene of human (1). According to the report of World Health Organization (WHO), ~25% of the worldwide population suffers from TB, and 1.6 million TB-related deaths occurred in 2021 (2). Notably, the incidence of TB among adolescents aged 10 to 24 years has increased in recent years (3). TB is transmitted via droplets of *Mycobacterium tuberculosis* (*M. tuberculosis*) complex when the body exhibits low levels of immunity (4). *M. tuberculosis* may infect various parts of the human, with the majority of bacteria colonizing the lungs (5). However, not all cases of *M. tuberculosis* infections will progress to TB, and the majority of infected individuals do not present with notable symptoms; a condition known as latent TB infection (LTBI) (6). Moreover, 5~10% of patients with LTBI

develop active TB (ATB) during their whole lifetime; thus, presenting as novel sources of TB infection (7). This condition leads to complexities in the global prevention and control of TB.

M. tuberculosis enters the respiratory system, and is subsequently encapsulated by native immune cells, containing dendritic cells (DCs) and macrophages (8). Innate immune cells use membrane surface pattern recognition receptors (PRRs) to recognize the pathogen-associated molecular pattern (PAMP) or damage-associated molecular pattern (DAMP) of *M. tuberculosis*, and these trigger a signaling cascade within innate immune cells to induce the downstream immune response (9). Alveolar macrophages (AMs) are the primary targets of *M. tuberculosis* early infection (10). Phagocytosis of AMs is activated by the recognition of complement, Fcγ receptors, mannose receptor (11) or scavenger receptors (12), and rely on an intact surface sphingomyelin biosynthetic pathway to uptake *M. tuberculosis* into the cytoplasm to form phagosomes (13). During phagosome maturation, the pH value inside the phagosome decreases (14). Phagosomes bind to lysosomes to form phagolysosomes, which are further acidified, leading to *M. tuberculosis* inhibition or death (15). This process is known as LC3-associated phagocytosis (LAP). Macrophages also actively metabolize 1, 25-dihydroxy vitamin D (1, 25D) in response to the invasion of *M. tuberculosis*. 1, 25D participated in immune regulating responses through binding to the receptor of vitamin D, and regulating the expression of NOD2, antimicrobial proteins (CAMP and β-defensin 2) and inflammatory factors (IL-1β and IL-8). However, *M. tuberculosis* escapes the immune response via resisting the natural immunity of immune cells, and inhibiting apoptosis (16). Following the appearance of drug-resistant and multi-drug resistant *M. tuberculosis*, the diagnosis and therapy of TB have increased in complexity.

Therefore, the development of biomarkers with high specificity and sensitivity is particularly important for TB diagnosis. However, traditional methods for the etiologic diagnosis of TB, including sputum smears and culturing for *M. tuberculosis* exhibit limitations. *M. tuberculosis* cannot be distinguished from other acid-fast bacilli using sputum smears, and this method exhibits low levels of sensitivity. This limits the positive detection rate of patients with TB. Although culturing for *M. tuberculosis* is the common standard for ATB diagnosis, this method exhibits notable disadvantages. For example, *M. tuberculosis* culturing exhibits low positivity rates and prolonged culture times, which are not conducive to early diagnosis. X-ray imaging of the chest may aid in the detection of pulmonary TB; however, this process cannot be used to identify LTBI (17). Immunological strategies for TB diagnosis include tuberculin skin tests and INF-γ releasing assays. Notably, the aforementioned immunological tools are recommended for the diagnosis of *M. tuberculosis* infection; however, these are not currently recommended for ATB diagnosis (17, 18). Rapid molecular biology diagnostic techniques for TB, such as GeneXpert MTB/RIF and DNA sequencing, require high levels of instrumentation and specific expertise, and these techniques may lead to false negatives or false positives (19). At present, various studies is focused on the application of exosomes as biomarkers or vaccines for TB. Exosomes are stable structures with low invasiveness, which carry high levels of specific biomolecular information. The present article aimed to review the current literature detailing the immunomodulatory roles, diagnostic marker application of exosomes in the infection course of *M. tuberculosis*, and the challenges of exosomes as diagnostic markers for TB (Figure 1). The present review could provide a novel theoretical foundation for the role of exosomes as novel diagnostic markers of TB.

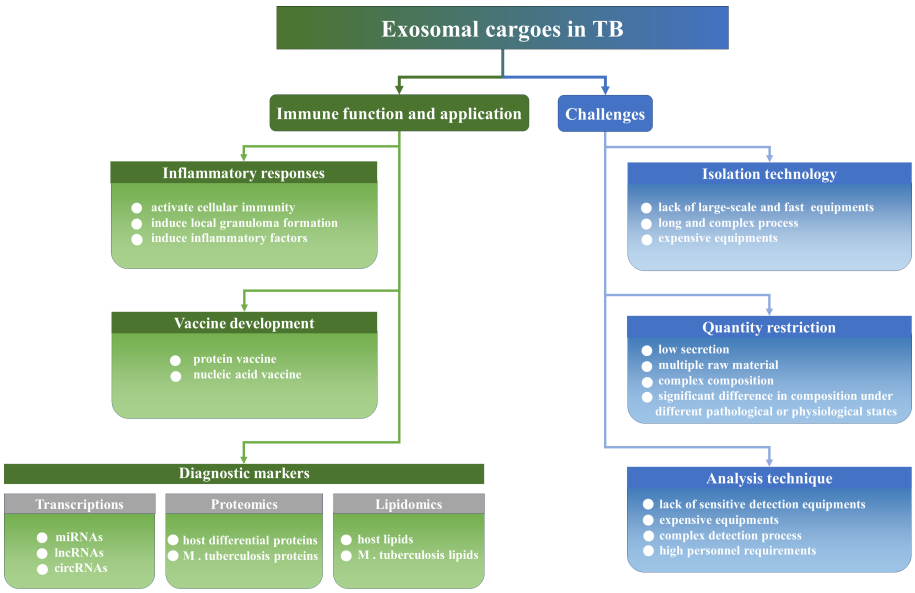

FIGURE 1
The immune function, the application and challenges of exosomes in TB. Exosomes regulate inflammatory responses and could be developed as vaccines and diagnostic biomarkers. Of course, exosomes still face a series of challenges to become a convenient diagnostic marker in clinical practice, such as isolation technologies, quantity limitations, and equipment and personnel limitations.

2 The biogenesis and functions of exosomes

Exosomes are nanovesicles that are with the diameter about 30~150 nm, and could be secreted into the extracellular matrix via numerous different cell types (20, 21). Exosomes form cup-shaped vesicles through endocytosis (20, 22, 23), including extracellular proteins and other components, and cell membrane receptors (23). These are known as early endosomes. The maturation of early endosomes into late endosomes [also known as multivesicular bodies (MVBs)] is accompanied by the sorting and enrichment of cargo molecules on early endosomal membranes, and the formation of intraluminal vesicles (ILVs) via membrane invagination (24). The mechanisms underlying MVB formation are categorized into endosomal sorting complexes required for transport (ESCRT)-dependent or independent pathways (25–27). Generated MVBs may fuse with lysosomes, and are degraded via lysosomal acid and proteolysis. MVBs may also fuse with the plasma membrane and secrete ILVs that are released to extracellular, or these directly bud through the cytoplasmic membrane to form exosomes (23–26). Notably, the inhibition of exosomes secretion leads to increased degradation of MVBs via lysosomes (26). The release of exosomes and their fusion with receptor cells is associated with the Ras superfamily. Rab proteins, including Rab 2B, 5A, 7, 9A, 11, 27 and 35 are molecular switches for the transport of MVBs, and these play critical functions in the process of vesicle transport (25, 27). Moreover, RalA/B GTPases promote the secretion of exosomes via the regulation of various effector proteins and lipids, such as phospholipase D1, which plays a role in the homeostasis of MVBs (28, 29), and PLD2, which is involved in the budding of exosomes cargoes (27). Rab GTPase facilitates the folding of membrane-bound soluble N-ethylmaleimide-sensitive factor attachment protein receptors into tetrameric coiled-coil complexes at exosomal and receptor cell membranes (30). This process is carried out via the recruitment of tethering proteins; thus, the two membranes remain in close proximity (31). Additionally, there are numerous other proteins in exosomes, such as the transmembrane 4 superfamily proteins (CD63, CD81 and CD9), flotillin, Alix and TSG101, which are also involved in exosomes biogenesis (27). The complex biogenesis, selection and transfer mechanisms contribute to the high heterogeneity of exosomes.

3 The functions of exosomes in *M. tuberculosis* infected hosts

Exosomes possess a wide range of various cargo molecules, including nucleic acids (miRNA, lncRNA, mRNA and DNA), proteins, lipids and metabolites (27, 32). Notably, exosomes are involved in intercellular messaging, maintenance of cellular homeostasis and immune regulatory processes. Results of previous studies demonstrated that the immune response induced by the interaction of exosomes with *M. tuberculosis* exerts an important impact on the development of TB (33). Intracellular *M. tuberculosis* uses SecA2 (34) and ESX-1 secretion systems to mediate cell membrane cleavage, and the *M. tuberculosis* genome, proteins and other components are transferred between cells via exosomes (35). Exosomes are recognized by PRRs as carriers of PAMP, which activate the inflammasome, LAP (34) and initiate an innate immune response for *M. tuberculosis* clearance (36). Exosomes released from *M. tuberculosis*-infected mesenchymal stem cells (MSCs) induce macrophages to produce TNF-α, C-C Motif Ligand-5 and iNOS. These factors promote inflammatory responses and immunoreaction through the signaling pathway synergistically mediated by Toll-like receptor 2/4 (TLR2/4) and MyD88 (37). Exosomes released from *M. tuberculosis*-infected macrophages induce the differentiation of naïve monocytes, and also activate MK-2 and NF-κb to produce functionally active macrophages (38). Following the stimulation of LPS and IFN-γ, exosomes released from macrophages bind to their secreted endoplasmic reticulum aminopeptidase 1 to enhance macrophage phagocytosis and NO synthesis activity (39). Necroptotic exosomes are phagocytosed by macrophages to induce the increased production of inflammatory cytokines, TNF-α, IL-6, and chemokine CCL2 (40). APCs secrete exosomes containing MHC-I/II that present antigenic information to T lymphocytes to activate specific immune responses (41, 42). Activated T cells stimulate DCs to increase the release of miR155-containing exosomes, further inducing specific T cell activation (43). Notably, T helper 1 (Th1) cells receive let-7b-containing exosomes released from Treg cells, and the inhibition of Th1 cell proliferation and IFN-γ secretion prevents excessive inflammatory injury (44). Exosomes released from activated T lymphocytes deliver genomic and mitochondrial DNA to DCs, which, in turn, trigger an innate immune response against *M. tuberculosis* infection (45), as the mitochondrial component is the main source of DAMPs (46). Exosomes may also stimulate autophagy and *M. tuberculosis* clearance (47). Exosomes derived from *M. tuberculosis*-infected neutrophils stimulate macrophage to produce O2- and induce autophagy, facilitating intracellular *M. tuberculosis* clearance (48).

Although exosomes secreted by infected immune cells enhance the ability of uninfected immune cells to defend against *M. tuberculosis*, exosomes also aid *M. tuberculosis* immune evasion, providing a favorable environment for survival. Modified exosomes carry components of *M. tuberculosis* that affect the capacity of the host to eliminate them. Infected macrophages release exosomes containing miR-18a, which promotes *M. tuberculosis* survival in macrophages via inhibition of the autophagic process. This is carried out via regulation of the ATM-AMPK autophagic pathway (49). Exosomes derived from macrophages also inhibit CD4+ T cell antigen receptor signaling and IL-2 production (50), and downregulated IFN-γ induces the expression of CD64 or MHC-II in macrophages (51). Exosomes may exhibit a dual role in regulating the immune response. Exosomes come from a variety of tissues and cells, and with the rapid changes in new detection technologies, it has become possible for exosomes to become diagnostic biomarkers for TB (Figure 2).

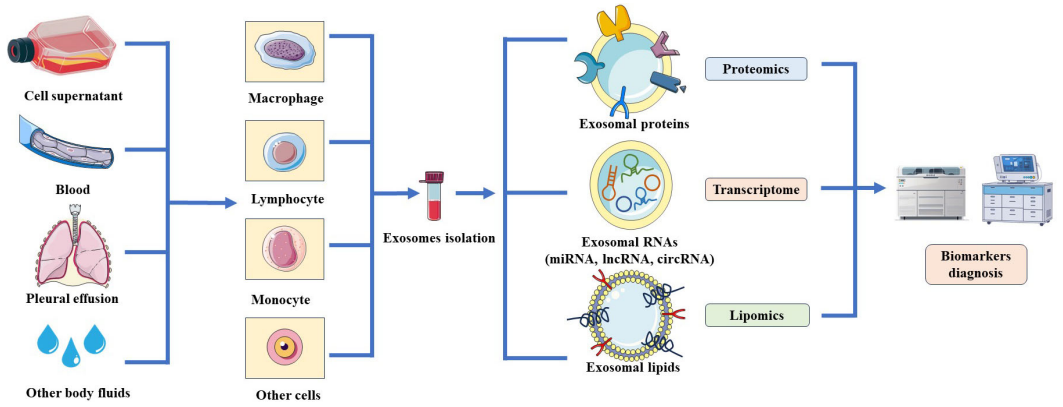

FIGURE 2
Schematic of the resources and analyzed technologies of exosomes. Exosomes are released by various cells such as macrophages, lymphocytes, monocytes and could purified from cell culture supernatant or body fluids. Exosomal contents could be screened through proteomics, transcriptomics and lipomics to identify potential biomarkers for the diagnosis of TB.

4 Potential of exosomal miRNAs as biomarkers

4.1 The synthesis and function of miRNAs

MiRNAs are endogenous non-coding single-stranded RNA molecules that are 18-24 nucleotides in length, and are highly conserved during evolution (52). MiRNAs participate in regulating various fundamental biological functions, for instance cell proliferation, differentiation, migration (53), apoptosis (54) and autophagy (55), through binding to the 3'-untranslated region of target gene mRNAs (56, 57). The biosynthetic pathways of miRNAs could be classified into canonical and noncanonical pathways (56, 58). The canonical pathway is the dominant pathway for miRNA generation (57). The majority of miRNA genes are transcribed through RNA polymerase II in the nucleus to form pri-miRNAs containing hairpin structures (59). Subsequently, pri-miRNA is cleaved into pre-miRNA with stem-loop structures by the Drosha complex, which includes Drosha, RNase III, the double-stranded RNA-binding protein, DiGeorge syndrome critical region 8, and partner proteins (60). Thus, pre-miRNA is delivered into the cytoplasm via Exportin-5, and subsequently treated with RNase III endonuclease, Dicer, to produce double-stranded miRNAs (61). Double-stranded miRNAs and argonaute protein bind into the miRNA-induced silencing complex, where one strand is selected as the mature miRNA and the other strand is degraded (56, 61). Mature miRNAs may be packaged in exosomes and transferred between cells. As miRNAs are protected by the exosomal lipid bilayer, they may be protected from RNase degradation (Figure 3). Therefore, exosomal miRNAs remain highly stable, and remain in the blood and other bodily fluids for prolonged periods. Thus, these are considered as promising candidate biomarkers for TB.

4.2 The functions of exosomal miRNAs in *M. tuberculosis* infected subjects

Exosomal miRNAs released by macrophages infected with *M. tuberculosis* are stored in the supernatant, providing a theoretical basis for studying the potential of exosomal miRNAs as biomarkers for the diagnosis of *M. tuberculosis* infection. Zhang et al. showed that miR-20b-5p was expressed in exosomes from *M. tuberculosis*-infected macrophages, but not in exosomes from non-infected macrophages (62). Zhan et al. used high-throughput sequencing to detect miRNAs in exosomes secreted from *Mycobacterium bovis*-infected macrophages, and the results demonstrated that 20 exosomal miRNAs were increased, and 7 exosomal miRNAs were decreased in the infected group, compared with the non-infected group (63). Moreover, expression levels of let-7c-5p, miR-27-3p, miR-25-3p, let-7a-5p, miR-98-5p and miR-30a-3p were increased in the infected group, while the expression levels of miR-5110 and miR-194-5p were decreased (63). Results of a previous study suggested that the expression levels of exosomal miR-106a, miR-20a, miR-20b, miR-17 and miR-93 were downregulated in infected macrophages, as well as in the lungs, spleens and lymph nodes of mice infected with *M. tuberculosis* (64). The different exosomal miRNAs expression profiles of *M. tuberculosis*-infected patients were exhibited in body fluids. These miRNAs hold promise as potential biomarkers for the rapid and noninvasive diagnosis of TB. Kaushik et al. revealed that miR-185-5p in plasma exosomes were increased significantly in TB patients, compared with healthy controls (HCs), with a sensitivity and specificity of 50 and 93.75%, respectively. Moreover, Kaushik et al. suggested that the use of miR-185-5p in combination with other biomarkers may exhibit potential in TB diagnosis (65). Tu et al. confirmed that exosomal miR-423-5p is increased in the plasma of TB patients (66). The area under the curve (AUC) of the TB diagnostic model was 0.908 and the 10-fold cross validation demonstrated a prediction accuracy of 78.18%, which indicated that the model exhibited clinical value in differentiating ATB patients from HCs (65, 66). Lyu et al. demonstrated that miRNAs were differentially expressed in the serum of exosomes from HCs, LTBI patients and ATB patients, suggesting that miRNA cargo is selectively packaged into exosomes at different stages of *M. tuberculosis* infection (67). Notably, miR-450a-5p, let-7e-5p, miR-140-5p and let-7d-5p were only increased in the serum exosomes from LTBI patients, whereas

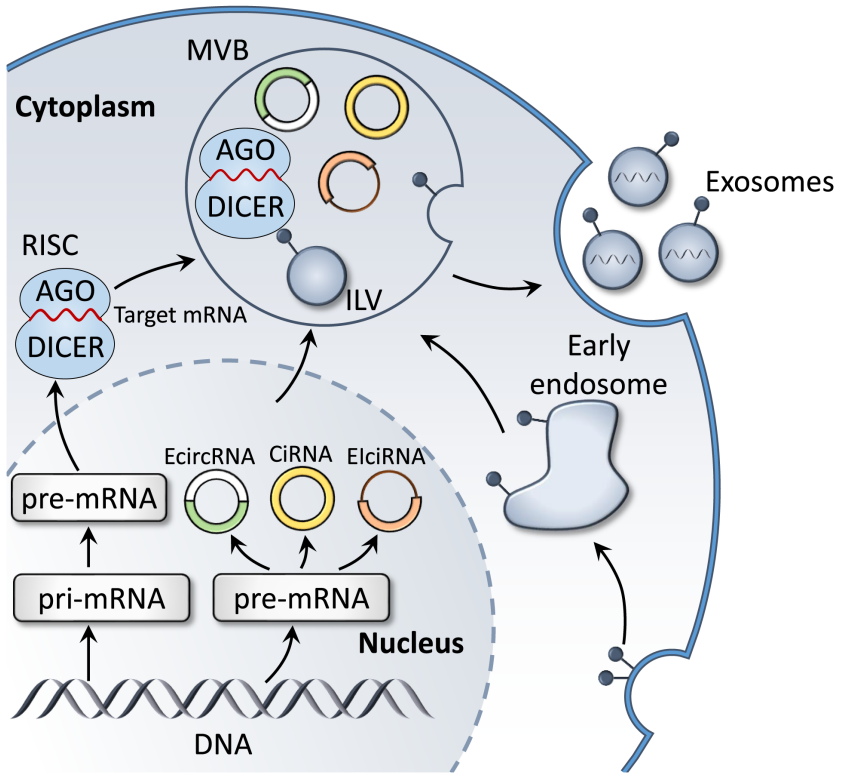

FIGURE 3
Biogenesis of exosomal miRNAs and circRNAs. In the cytoplasm, miRNA genes are transcribed into pri-miRNA, which is further processed to form pre-miRNA. Mature target miRNAs are integrated into RISC and fuse with MVBs, prior to releasing miRNA-containing exosomes. In addition, the main product of circRNA gene transcription, pre-mRNA, is processed to form three subclasses: ecircRNAs, ElciRNAs and circRNAs. These also fuse with MVB to form exosomes that are released into the extracellular environment.

miR-370-3p, miR-1246, miR-193b-5p, miR-2110 and miR-28-3p were only increased in the serum exosomes from patients with ATB (67). Moreover, miR-26a-5p was upexpressed in LTBI serum exosomes, but decreased in ATB (67). Results of further studies demonstrated that miR-140-3p, miR-423-3p and miR-3184-5p were sequentially increased in HCs, LTBI and ATB patients, and this differentiation may exhibit potential in determining the infectious stages of *M. tuberculosis* (67). In addition, Alipoor et al. demonstrated that the expression of miR-96, miR-484 and miR-425 were significantly increased in serum exosomes of TB patients, and the combined testing with sputum smears improved the detection rate of TB (68).

Exosomal miRNAs may also be used to differentiate TB from other lung-related diseases. Wang et al. verified the differential expression profiles of exosomal miRNAs in pleural effusions from adenocarcinoma of the lung (ADC), TB and other benign lesions using quantitative PCR (qPCR). Notably, the expression levels of miR-205-5p, miR-429, miR-483-5p, miR-375, miR-200b-3p and miR-200c-3p were higher in ADC-derived exosomes, compared with TB or other benign lesions (69). In addition, miR-148a-3p and miR-150-5p were upexpressed in TB-derived exosomes, and downexpressed in other benign lesion-derived exosomes. Interestingly, the opposite results were observed for the expression levels of miR-451a (69). Zhang et al. compared the expression profiles of exosomal miRNAs in TB pleural effusion and malignant pleural effusion. The results demonstrated that miR-3614-5p and miR-150-5p were decreased in malignant pleural effusion, and miR-629-5p, miR-200b-3p and miR-182-5p were increased in TB pleural effusion (70). Guio et al. carried out sRNA sequencing to analyze exosomes that were extracted from blood samples obtained from patients with LTBI, ATB or ADC. The results demonstrated that miR-210-3p and miR-143-3p were downregulated in the serum exosomes from patients with LTBI, and miR-20a-5p was upregulated in the serum exosomes from patients with LTBI (71). MiR-23b, miR-17 and miR-181b-5p were only downregulated in the serum exosomes from patients with ATB, and miR-584 was only upregulated in the serum exosomes from patients with ATB. A total of 15 miRNAs, including miR-320a, miR-185-5p, miR-144-3p, let-7f-5p and miR-199b-3p, were only downregulated in the serum exosomes of patients with ADC (71).

The diagnosis and treatment of drug-resistant TB (DR-TB) and multidrug-resistant TB (MDR-TB) are important for the prevention and control of TB. Notably, exosomal miRNAs exhibit potential as biomarkers in the early diagnosis and prognosis of DR-TB and MDR-TB. Carranza et al. analyzed the expression profiles of exosomal miRNAs in the serum of MDR-TB patients before and after 12 months of treatment, and revealed that the expression of

exosomal miR-328-3p, miR-20a-3p and miR-195-5p and was decreased in the serum following treatment (72). Moreover, let-7e-5p and miR-197-3p were increased in post-treatment serum. Excluding patients with type 2 diabetes mellitus, results of the previous study demonstrated that the expression of let-7e-5p in the serum exosomes of patients with MDR-TB were upexpressed following treatment progression. Compared with HCs, miR-197-3p and miR-223-3p were decreased in the serum of DR-TB patients, while let7e-5p was increased in the serum of DR-TB patients (72). These results implied that the differential expression of exosomal miRNAs in the serum of MDR-TB patients with prolonged treatment may act as a biomarker for monitoring MDR-TB therapy, and that the differential expression in the serum of DR-TB and HCs may exhibit potential as a biomarker for determining drug-sensitive and drug-resistant TB.

In short, the differential expression profiles of miRNAs in TB patients may provide a novel perspective for the diagnosis and differential diagnosis of TB (Table 1). However, further investigations are still required to illustrate the mechanisms by which exosomal miRNAs contribute to the pathogenesis of TB, thus assisting in the development of biomarkers for the diagnosis and therapy of TB. The role of exosomal miRNAs in predicting the success of anti-TB therapy has also been highlighted in previous studies (73). Unfortunately, there is currently a limited amount of research focusing on the involvement of exosomes in TB prognosis, and additional investigations are needed to explore and understand the potential implications of exosomal miRNAs in TB prognosis.

5 Exosomal circRNAs used as a biomarkers

5.1 The biogenesis and roles of circRNAs

Circular RNAs (circRNAs) are endogenous non-coding single stranded RNAs present in all eukaryotic cells (74), and are characterized by a covalently closed loop structure without a 5' terminal cap and a 3' terminal poly (A) tail (75). CircRNAs are grouped into intronic RNAs (ciRNAs), exonic circRNAs (ecircRNAs) and exon-intron circRNAs (elciRNAs) (76), displaying critical biological roles through playing as transcriptional regulators, ceRNA or miRNA sponges and protein templates (Figure 3) (77). Importantly, several studies have showed that the expression levels of circRNAs are dysregulated during *M. tuberculosis* infection (Table 2). CircRNAs are resistant to degradation by ribonucleases and RNA nucleic acid exonucleases due to their unique structure, and are highly conserved and detectable in various body fluids, such as plasma, saliva and urine. Additionally, circRNAs exhibit tissue specificity (84, 85); thus, are optimal candidates for the development of diagnostic biomarkers for clinical diseases.

TABLE 1 Summary of exosomal miRNAs from *M. tuberculosis* infected subjects.

Number	Exosomal miRNAs	Exosomes sources	Method screening	Expression pattern	Refs
1	miR-20b-5p	Supernatant of macrophage infected with *M. tuberculosis*	RT-PCR	decrease	(62)
2	miR-27-3p, let-7a-5p, let-7c-5p, miR-25-3p, miR-98-5p, miR-30a-3p, etc.	Supernatant of macrophage infected with *M. tuberculosis*	RNA sequencing	increase	(63)
3	miR-194-5p, miR-5110	Supernatant of macrophage infected with *M. bovis*	RNA sequencing	decrease	(63)
4	miR-185-5p	Plasma of TB patient	RNA sequencing	increase	(65)
5	miR-423-5p, miR-17-5p, miR-20b-5p	Serum of TB patient	RNA sequencing	increase	(66)
6	let-7e-5p, let-7d-5p, miR-450a-5p, miR-140-5p	Serum of LTBI patient	RNA sequencing	increase	(67)
7	miR-1246, miR-2110, miR-370-3p, miR -28-3p, miR-193b-5p, etc.	Serum of TB patient	RNA sequencing	increase	(67)
8	miR-26a-5p	Serum of ATB patient	RNA sequencing	decrease	(67)
9	miR-484, miR-425, miR-96, etc.	Serum of TB patient	qRT-PCR	increase	(68)
10	miR-205-5p, miR-200c-3p, miR-141-3p, etc.	Pleural effusion of TB patient	RNA sequencing	increase	(69)
11	miR-483-5p, miR-375	Pleural effusion of TB patient	RNA sequencing	decrease	(69)
12	miR-33a-3p, miR-153-3, miR-373-5p, etc.	Pleural effusion of TB patient	RNA sequencing	increase	(70)
13	miR-3120-5p, miR-489-3p, -miR-4669-5p, etc.	Pleural effusion of LTBI patient	sRNA sequencing	decrease	(70)
14	miR-143-3p, miR-210-3p, miR-20a-5p, etc.	Serum of LTBI patient	sRNA sequencing	increase	(71)
15	miR-23b, miR-17, miR-584, etc.	Serum of ATB patient	sRNA sequencing	increase	(71)

TABLE 2 Summary of exosomal circRNAs in *M. tuberculosis* infected subjects.

Number	Exosomal circRNAs	Exosomes sources	Method screening	Expression pattern	Refs
1	circRNA_0001380	Plasma of ATB patient	qRT-PCR	decrease	(78)
2	circRNA_059914, circRNA_103017, circRNA_101128, etc.	Plasma of ATB patient	RNA sequencing	increase	(79)
3	circRNA_062400	Plasma of ATB patient	RNA sequencing	decrease	(79)
4	circRNA_103571, circRNA_091692, circRNA_102296, etc.	Plasma of ATB patient	circRNA microarrays	increase	(80)
5	circRNA_103571, circRNA_406755	Plasma of ATB patient	circRNA microarrays	decrease	(80)
6	circRNA_0009024, circRNA_0001953, circRNA_0008297, etc.	Plasma of ATB patient	RNA sequencing	increase	(81)
7	circRNA_0001204, circRNA_0001747	Plasma of ATB patient	RNA sequencing	decrease	(82)
8	circRNA_051239, circRNA_029965, circRNA_404022, etc.	Serum of ATB patient	RNA sequencing	increase	(83)

5.2 The functional analysis of exosomal circRNAs in samples of TB patients

Yuan et al. used bioinformatics to screen three central genes related to the development of TB, including circRNA_0002419 and circRNA_0007919 (86). The aforementioned genes were upregulated in TB tissues, and circRNA_0005521 was decreased in TB tissues (86). Moreover, Yi et al. confirmed that both miR-223-3p and miR-448 were decreased in the plasma of patients with TB, and also concluded that the mRNA-miRNA-circRNA interaction chain may function significant roles in *M. tuberculosis* infection (87). In addition, SAMD8_circRNA_994 and TWF1_circRNA_9897 may act as novel diagnostic biomarkers for TB (87). Zhang et al. carried out qPCR and demonstrated that circRNA_0028883 expression levels were upexpressed in PBMCs from ATB patients (88). Moreover, Zhang et al. performed ROC curve analysis and determined an AUC value of 0.773 (88). These foundings suggested that circRNA_0028883 could serve as a novel biomarker for ATB diagnosis. Further studies demonstrated that compared with HCs, circRNA_0001380 was decreased significantly in PBMCs from ATB patients (78), and circRNA_0009128 or circ_0005836 were also downexpressed in PBMCs of ATB patients (89). CircRNA_101128, circRNA_059914 and circRNA_103017 were expressed at higher levels in PMBCs from ATB patients, while circRNA_062400 expression was significantly lower in ATB samples than in HCs (79). The expression of circRNA_103571 decreased in the plasma of ATB patients, and this study demonstrated an interaction between circRNA_103571 and ATB-associated miRNAs (miR-29a and miR-16) (80). Thus, the selective expression of exosomal circRNA in TB demonstrates that exosomes exhibit potential as non-invasive diagnostic tools.

Huang et al. reported that circRNA_001937, circRNA_005086 and circRNA_009024 increased significantly, but circRNA_102101, circRNA_104296and circRNA_104964 decreased obviously in PBMCs of ATB patients, compared with HCs (90). In addition, circRNA_001937 expression levels were markedly increased in PBMCs of ATB patients, compared with patients with pneumonia, lung cancer and chronic obstructive pulmonary disease. Interestingly, circRNA_001937 could be increased following ATB treatment (90). Results of this study further demonstrated that circRNA_0003528, circRNA_0009024, circRNA_0001953, circRNA_0003524, circRNA_0008297 and circRNA_0015879 in plasma were increased markedly in ATB patients. However, the expression levels of circRNA_0001747and circRNA_0001204 were notably decreased in the plasma of ATB patients, compared with those of HCs (81). Reports also show that circRNA_0009024 and circRNA_0001953 in plasma were associated with the severity of ATB disease. Moreover, the AUC value of the ROC curve of ATB patients was increased to 0.928 with the combined detection of circRNA_0001747 and circRNA_0001204, and in ATB patients, the expression levels of circRNA_0001747and circRNA_0001204 returned to baseline in the plasma following treatment (82). Huang et al. also reported that monocyte derived macrophages from ATB patients exhibited significantly higher levels of circRNA_0043497 compared with HCs, with an AUC value of 0.860 (91). In addition, circRNA_0043497 levels decreased and returned to baseline following anti-TB therapy (91). Therefore, circRNAs may be used for the differential diagnosis of TB and associated diseases, and for the assessment of TB severity and prognosis. The combined detection of multiple circRNAs exhibited greater diagnostic value for patients with TB. CircRNA may also aid in distinguishing patients with DR-TB from patients with pan-sensitive TB. Liu et al. revealed that circRNA_051239, circRNA_404022 and circRNA_029965 were increased in the sera of ATB patients, and circRNA_051239 was decreased significantly in the sera of patients with DR-TB (83).

CircRNAs are highly enriched in exosomes compared with production cells. The regulation of relevant miRNAs in donor cells causes to changes in the composition of exosomal circRNAs and may transmit molecular information to recipient cells (92). In this process, various RNA binding proteins act as key factors that facilitate the propagation of circRNAs in donor cells (93). Results of a previous study demonstrated that exosomal circRNAs of host cells exhibit distinct expression patterns following *M. tuberculosis* infection (65). This provides evidence for the potential of exosomal circRNAs as biomarkers for the diagnosis of TB. But there is still a need for large-scale screening of blood samples, and

further investigation based on existing research is required to explore the potential role of exosomal circRNAs as biomarkers for early diagnosis and prognosis of TB.

6 Exosomal proteins act as biomarkers of TB

At present, studies is focused on the protein content of exosomes. Previous studies have demonstrated which exosomes from *M. tuberculosis*-infected macrophages are present with highly antigenic mycobacterial proteins, such as KatG (Rv1908c), GroES (Rv3418c), GlnA (Rv2220), MPT63 (Rv1926c), ESAT-6 (Rv3875), 19 KDa lipoprotein/LpqH (Rv3763), CFP-10, Ag85 complex (Rv3804c, Rv1886c, Rv0129c) and SodA (Rv3846) (94). Lee et al. performed proteomic analysis of *M. tuberculosis* extracellular vehicles (EVs) and identified a total of 287 vesicular proteins (95). Among them, SodB, PstS1, EsxN, KatG, LppX, Apa, LpqH, FadA3, GlnA1, AcpM, FbpA, Mtc28 and Fba were abundant proteins in EVs of *M. tuberculosis*. Proteins such as SodB, FbpA, LpqH, FbpC, FbpB, and PstS1 were associated with *M. tuberculosis* virulence (95). The aforementioned *M. tuberculosis* proteins carried by exosomes may impact the innate or adaptive immune response (96), and may play important functions in the development of TB.

The composition of exosomal proteins released by cells infected with *M. tuberculosis* is altered (Table 3), thus the differential expression profiles of proteins in TB patients may provide a novel perspective for the diagnosis of *M. tuberculosis* infection (Figure 4). Diaz et al. evaluated differences in exosomal proteins between *M. tuberculosis*-infected and -uninfected macrophages using tandem mass spectrometry. Results of study demonstrated that a total of 41 proteins were significantly upregulated in the exosomes of *M. tuberculosis*-infected cells (97). Notably, some of the aforementioned proteins were confirmed via western blot analysis, including moesin, HSP90, vimentin and Coronin 1C (97). Kruh-Garcia et al. highlighted bacterial-derived biomarkers in the serum exosomes of TB patients, including multiple peptides from 8 proteins (Antigen85B, Antigen85C, Apa, HspX, BfrB, Mpt64, GlcB and KatG). Of these, 29 peptides from 17 proteins were unique to ATB patients, such as AcpM, Ald, Ag85a, DnaK, Mpt51, GroES, Mpt63, Mpt53 and MrsA (98). Among 41 patients with TB, biomarker candidates consisting of seven peptides were used to correctly diagnose 83% of TB cases, and at least one peptide was present in 81% of TB patients, and 90% of patients with extrapulmonary TB (98). The combined testing of two peptides increased the diagnosis of patients with intrapulmonary or extrapulmonary TB to 90%. Obviously, human immunodeficiency virus infection does not affect the number of peptides observed in the plasma of TB patients (98). These results demonstrated that exosomal proteins may be used as biomarkers for TB diagnosis, and that the simultaneous detection of multiple peptides may substantially improve the accuracy of TB diagnosis. Through proteomic analysis, Zhang et al. indicated 123 differential proteins in serum exosomes from HCs and ATB patients, including 40 upregulated proteins and 83 downregulated proteins (99). Notably, lipopolysaccharide binding protein expression was increased in the serum exosomes of ATB patients, while CD36 and MHC-I expression levels were decreased (99). The aforementioned three proteins were identified as potential biomarkers for ATB diagnosis with ROC analysis. In addition, Mehaffy et al. characterized peptides from *M. tuberculosis* proteins involved in nitrogen metabolism, and these included GarA (Rv1827), peptide FLL and SVF belonging to glutamine synthetase GlnA1 (Rv2220) (100). Heat shock chaperone proteins, including GroES and DnaK (Rv0350) were also characterized in the serum EVs of patients with LTBI (100). Among them, a single peptide in glutamine synthetase

TABLE 3 Summary of exosomal proteins and lipids from *M. tuberculosis* infected subjects.

Number	Exosomal proteins	Exosomal lipids	Exosomes sources	Method screening	Expression pattern	Refs
1	HSP90, vimentin, Coronin 1 C, moesin, etc	—	Supernatant of macrophage infected with *M. tuberculosis*	Tandem mass spectrometry	increase	(97)
2	AcpM, Ag85a, Ald, DnaK, GroES, Mpt51, Mpt53, Mpt63, MrsA, etc	—	Serum of ATB patient	MRM-MS	increase	(98)
3	LBP	—	Serum of ATB patient	ELISA	increase	(99)
4	CD36, MHC-I	—	Serum of ATB patient	ELISA	decrease	(99)
5	Rv1827, Rv2220, Rv0350, etc.	—	Serum of LTBI patient	MRM-MS	increase	(100)
6	Hsp16.3		Plasma of ATB patient	Western blot	increase	(101)
7	HP, PRG4, STOM, CD151, ICAM2, ORM1, SAA1, SLC2A3, etc.	—	Plasma of TB patient	Tandem mass Tag-labeled (TMT)	increase	(102)
8	C1R, GRIP1	—	Plasma of TB patient	TMT	increase	(102)
9	—	PS	Supernatant of macrophage infected with *M. tuberculosis*	Western blotting	increase	(103)
10	—	LAM, CFP-10	Urine of TB patient	I-PCR	increase	(104)
11	—	TAG, CEs	Plasma of TB patient	ESI-MS	increase	(102)

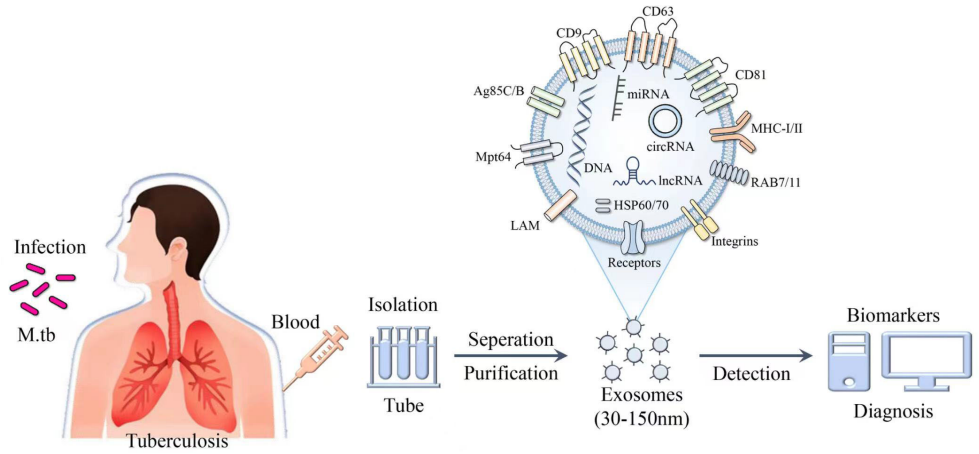

FIGURE 4
Schematic of the composition and identification of exosomes. Exosomes purified from the blood of patients with *M. tuberculosis* contain a variety of derivatives, such as nucleic acids, proteins and lipids, and exhibit potential as biomarkers in the diagnosis of TB.

(GlnA1) enzyme was present in the serum of 82% of LTBI patients, indicating that peptides from *M. tuberculosis* proteins involved in nitrogen metabolism may act as candidate biomarkers for the detection of LTBI pathogen specificity (100). Exosomal proteins may be used to distinguish ATB from other associated diseases. Results of previous studies demonstrated that Hsp16.3 protein levels were detected in exosomes extracted from the plasma of ATB patients; however, Hsp16.3 was not detected in the plasma exosomes of LTBI patients (101). Biadglegne et al. demonstrated that haptoglobin (HP), proteoglycan 4, CD151, stomatin, ICAM-2, alpha-1-acid glycoprotein 1, solute carrier family 2A3 and serum amyloid A-1 protein were abundant in plasma exosomes from TB patients, compared with HCs (102). In addition, immunoglobulins, glutamate receptor-interacting protein 1 and complement component 1r were enriched in TB patients' lymphadenitis (102). Thus, the specific expression levels of exosomal proteins in TB and TB lymphadenitis may exhibit potential for diagnosis and differential diagnosis.

Exosomal proteins exhibit potential in determining the prognosis of TB patients. Du et al. confirmed that S100A9 and C4BPA in plasma exosomes of LTBI patients were differentially decreased following therapy, and the area under the ROC curve was 0.73 and 0.69, respectively (105). Biadglegne et al. reported that plasma exosomes myosin-9, IG chain IGHV4-28 and GRIP1 were increased markedly in TB patients following anti-TB treatment, while HP, ficolin 3, transmembrane protein 215, serum amyloid A-4 protein and apolipoprotein B-100 were decreased following anti-TB treatment (102).

Due to their small size, exosomes pass freely across the tissue barriers of the body. Exosomes protect proteins from free protease hydrolysis using their lipid bilayer membrane structure (106). The composition of exosomal proteins from infected *M. tuberculosis* reflects the exosomal proteomic profile more directly than that of nucleic acids (106, 107). In conclusion, exosomal proteins may exhibit potential as novel biomarkers of TB, and could be used for the development of new diagnostic methods. In addition, lipids and lipid metabolism are currently a research hotspot, and exosomes lipids are also potential diagnostic biomarkers for tuberculosis.

7 Exosomal lipids function as biomarkers of TB

The lipid components of the host is closely associated with the pathogenic mechanisms of *M. tuberculosis*. When macrophages consume glucose, *M. tuberculosis* could utilize host lipids as the main source of energy (108). *M. tuberculosis* may also produce a variety of unique lipids that act as inflammatory regulators, and these are implicated in preventing phagosome maturation (109). A previous study revealed that lipids produced by *M. tuberculosis* are glycolipids, including atrehalose-6, 6'-dimycolate, lipomannan, lipoarabinomannan (LAM) and phosphatidylinositol mannosides (PIMs), the sugar fraction of which is recognized by PRRs that stimulate the innate immune response of the organism during infection (110). In summary, *M. tuberculosis* lipids take a multifaceted approach to disrupt the antimicrobial response of host cells to ensure their survival and proliferation in host cells, and also act important roles in the immune process as immunomodulators.

Existing studies have shown that exosomes in the peripheral blood of TB patients contain rich lipids, with various sources and components. These liposomes can be used to assess TB infection and may serve as biomarkers for TB diagnosis (Table 3). Garcia-Martinez et al., discovered that phosphatidylserine (PS) was more abundant in extracellular vesicles released from macrophages of *M. tuberculosis*-infected mouse compared to those of normal mouse (103). Dahiya et al. detected LAM and CFP-10, using immunopolymerase chain reaction in urine EVs from patients with pulmonary and extrapulmonary TB (104). Apparently, the sensitivity of LAM detection in the urine EVs of patients with pulmonary and extrapulmonary TB was 74.3 and 67.9%, respectively, and the specificity was 91.5-92.8% (104). The presence of large amounts of triacylglycerols and cholesterylesters

(CEs) in plasma exosomes of patients infected with *M. tuberculosis* has also been reported, while CEs are difficult to detect in HCs (102). The accumulation of CEs facilitates the survival and multiplication of *M. tuberculosis*, and promotes the dissemination of *M. tuberculosis* following cytolytic disintegration (102). Han et al. revealed that plasma CEs may act as novel biomarkers in TB diagnosis with optimal accuracy (AUC, 0.863; specificity, 83.5%; sensitivity, 79.4%) (111). Thus, certain differentially expressed lipid components in exosomes may also play a role in TB diagnosis. However, there is currently relatively little research on this topic, and there are also relatively few lipids found to have diagnostic value.

8 Future perspective

Exosomes have vast clinical potential in the diagnosis of TB and the differential diagnosis of related diseases (112, 113). However, the current research on exosomes in the prognosis and therapeutic evaluation of TB is relatively limited. In order to fully explore the potential of exosomes as biomarkers for TB (114), it is necessary to collect more clinical samples, conduct large-scale clinical trials, and utilize highly sensitive and specific techniques to analyze and identify the changes in exosomal components after *M. tuberculosis* infection (115). Unfortunately, obtaining highly pure exosomes remains technical challenges for large-scale clinical diagnostic applications due to the lack of standardized isolation and purification protocols and the high heterogeneity of exosomes (116). Therefore, it is necessary to conduct in-depth research to innovate and improve exosomes extraction techniques, in order to provide more accurate and reliable methods for the diagnosis, treatment, and monitoring of TB in the future.

Author contributions

NW: Conceptualization, Writing – original draft. YY: Conceptualization, Visualization, Writing – review & editing. YQ: Investigation,Visualization, Validation, Writing– review & editing. DQ: Formal Analysis, Investigation, Methodology, Resources, Validation, Writing – review & editing. HC: Formal Analysis, Investigation, Methodology, Resources, Writing – review & editing. HX: Data curation, Investigation, Resources, Writing – review & editing. JW: Conceptualization, Funding acquisition, Project administration, Validation, Writing – review & editing.

Funding

This project was supported by the National Natural Science Foundation of China (grant no. 82002111) and the Suzhou Science and Technology Development Plan Project (grant no. SKY2022078).

Acknowledgments

The authors thank members of the laboratory for helpful discussions and critiques.

Conflict of interest

The authors declare that the research was conducted in the absence of any commercial or financial relationships that could be construed as a potential conflict of interest.

Publisher's note

References

1. Drain PK, Bajema KL, Dowdy D, Dheda K, Naidoo K, Schumacher SG, et al. Incipient and subclinical tuberculosis: a clinical review of early stages and progression of infection. *Clin Microbiol Rev* (2018) 31(4):e00021–18. doi: 10.1128/CMR.00021-18

2. Bagcchi S. WHO's global tuberculosis report 2022. *Lancet Microbe* (2023) 4(1): e20. doi: 10.1016/S2666-5247(22)00359-7

3. Snow KJ, Cruz AT, Seddon JA, Ferrand RA, Chiang SS, Hughes JA, et al. Adolescent tuberculosis. *Lancet Child Adolesc Health* (2020) 4(1):68–79. doi: 10.1016/S2352-4642(19)30337-2

4. Moule MG, Cirillo JD. *Mycobacterium tuberculosis* dissemination plays a critical role in pathogenesis. *Front Cell Infect Microbio* (2020) 10:65. doi: 10.3389/fcimb.2020.00065

5. Suárez I, Fünger SM, Kröger S, Rademacher J, Fätkenheuer G, Rybniker J. The diagnosis and treatment of tuberculosis. *Dtsch Arztebl Int* (2019) 116(43):729–35. doi: 10.3238/arztebl.2019.0729

6. Carranza C, Pedraza-Sanchez S, de Oyarzabal-Mendez E, Torres M. Diagnosis for latent tuberculosis infection: new alternatives. *Front Immunol* (2020) 11:2006. doi: 10.3389/fimmu.2020.02006

7. Ferluga J, Yasmin H, Al-Ahdal MN, Bhakta S, Kishore U. Natural and trained innate immunity against Mycobacterium tuberculosis. *Immunobiology* (2020) 225 (3):151951. doi: 10.1016/j.imbio.2020.151951

8. Sia JK, Rengarajan J. Immunology of mycobacterium tuberculosis infections. *Microbiol Spectr* (2019) 7(4):10. doi: 10.1128/microbiolspec.GPP3-0022-2018

9. Boom WH, Schaible UE, Achkar JM. The knowns and unknowns of latent *Mycobacterium tuberculosis* infection. *J Clin Invest* (2021) 131(3):e136222. doi: 10.1172/JCI136222

10. Cohen SB, Gern BH, Delahaye JL, Adams KN, Plumlee CR, Winkler JK, et al. Alveolar macrophages provide an early *mycobacterium tuberculosis* niche and initiate dissemination. *Cell Host Microbe* (2018) 24(3):439–446.e4. doi: 10.1016/j.chom.2018.08.001

11. Choudhuri S, Chowdhury IH, Garg NJ. Mitochondrial regulation of macrophage response against pathogens. *Front Immunol* (2021) 11:622602. doi: 10.3389/fimmu.2020.622602

12. Linares-Alcántara E, Mendlovic F. Scavenger receptor A1 signaling pathways affecting macrophage functions in innate and adaptive immunity. *Immunol Invest* (2022) 51(6):1725–55. doi: 10.1080/08820139.2021.2020812

13. Niekamp P, Guzman G, Leier HC, Rashidfarrokhi A, RiChina V, Pott F, et al. Sphingomyelin Biosynthesis Is Essential for Phagocytic Signaling during *Mycobacterium tuberculosis* Host Cell Entry. *mBio* (2021) 12(1):e03141–20. doi: 10.1128/mBio.03141-20

14. Rai R, Singh V, Mathew BJ, Singh AK, Chaurasiya SK. Mycobacterial response to an acidic environment: protective mechanisms. *Pathog Dis* (2022) 80(1):ftac032. doi: 10.1093/femspd/ftac032

15. Weiss G, Schaible UE. Macrophage defense mechanisms against intracellular bacteria. *Immunol Rev* (2015) 264(1):182–203. doi: 10.1111/imr.12266

16. Wang J, Wang Y, Tang L, Garcia RC. Extracellular vesicles in mycobacterial infections: Their potential as molecule transfer vectors. *Front Immunol* (2019) 10:1929. doi: 10.3389/fimmu.2019.01929

17. Acharya B, Acharya A, Gautam S, Ghimire SP, Mishra G, Parajuli N, et al. Advances in diagnosis of Tuberculosis: an update into molecular diagnosis of Mycobacterium tuberculosis. *Mol Biol Rep* (2020) 47(5):4065–75. doi: 10.1007/s11033-020-05413-7

18. Halliday A, Masonou T, Tolosa-Wright M, Mandagere V, Lalvani A. Immunodiagnosis of active tuberculosis. *Expert Rev Respir Med* (2019) 13(6):521–32. doi: 10.1080/17476348.2019.1615888

19. MacLean E, Kohli M, Weber SF, Suresh A, Schumacher SG, Denkinger CM, et al. Advances in molecular diagnosis of tuberculosis. *J Clin Microbiol* (2020) 58(10): e01582–19. doi: 10.1128/JCM.01582-19

20. Kang T, Atukorala I, Mathivanan S. Biogenesis of extracellular vesicles. *Subcell Biochem* (2021) 97:19–43. doi: 10.1007/978-3-030-67171-6_2

21. Li YJ, Wu JY, Wang JM, Hu XB, Xiang DX. Emerging strategies for labeling and tracking of extracellular vesicles. *J Control Release* (2020) 328:141–59. doi: 10.1016/j.jconrel.2020.08.056

22. Dreyer F, Baur A. Biogenesis and functions of exosomes and extracellular vesicles. *Methods Mol Biol* (2016) 1448:201–16. doi: 10.1007/978-1-4939-3753-0_15

23. Kalluri R, LeBleu VS. The biology, function, and biomedical applications of exosomes. *Science* (2020) 367(6478):eaau6977. doi: 10.1126/science.aau6977

24. Kita S, Shimomura I. Extracellular vesicles as an endocrine mechanism connecting distant cells. *Mol Cells* (2022) 45(11):771–80. doi: 10.14348/molcells.2022.0110

25. Rayamajhi S, Aryal S. Surface functionalization strategies of extracellular vesicles. *J Mater Chem B* (2020) 8(21):4552–69. doi: 10.1039/D0TB00744G

26. Eitan E, Suire C, Zhang S, Mattson MP. Impact of lysosome status on extracellular vesicle content and release. *Ageing Res Rev* (2016) 32:65–74. doi: 10.1016/j.arr.2016.05.001

27. Gurunathan S, Kang MH, Kim JH. A comprehensive review on factors influences biogenesis, functions, therapeutic and clinical implications of exosomes. *Int J Nanomed* (2021) 16:1281–312. doi: 10.2147/IJN.S291956

28. Zago G, Biondini M, Camonis J, Parrini MC. A family affair: A Ral-exocyst-centered network links Ras, Rac, Rho signaling to control cell migration. *Small GTPases* (2019) 10(5):323–30. doi: 10.1080/21541248.2017.1310649

29. Ghoroghi S, Mary B, Larnicol A, Asokan N, Klein A, Osmani N, et al. Ral GTPases promote breast cancer metastasis by controlling biogenesis and organ targeting of exosomes. *Elife* (2021) 10:e61539. doi: 10.7554/eLife.61539

30. Wickner W, Rizo J. A cascade of multiple proteins and lipids catalyzes membrane fusion. *Mol Biol Cell* (2017) 28(6):707–11. doi: 10.1091/mbc.e16-07-0517

31. Borchers AC, Langemeyer L, Ungermann C. Who's in control? Principles of Rab GTPase activation in endolysosomal membrane trafficking and beyond. *J Cell Biol* (2021) 220(9):e202105120. doi: 10.1083/jcb.202105120

32. Kugeratski FG, Hodge K, Lilla S, McAndrews KM, Zhou X, Hwang RF, et al. Quantitative proteomics identifies the core proteome of exosomes with syntenin-1 as the highest abundant protein and a putative universal biomarker. *Nat Cell Biol* (2021) 23(6):631–41. doi: 10.1038/s41556-021-00693-y

33. Schorey JS, Bhatnagar S. Exosome function: from tumor immunology to pathogen biology. *Traffic* (2008) 9(6):871–81. doi: 10.1111/j.1600-0854.2008.00734.x

34. Cheng Y, Schorey JS. Extracellular vesicles deliver Mycobacterium RNA to promote host immunity and bacterial killing. *EMBO Rep* (2019) 20(3):e46613. doi: 10.15252/embr.201846613

35. Tiwari S, Casey R, Goulding CW, Hingley-Wilson S, Jacobs WR Jr. Infect and inject: how *mycobacterium tuberculosis* exploits its major virulence-associated type VII secretion system, ESX-1. *Microbiol Spectr* (2019) 7(3):10. doi: 10.1128/microbiolspec.BAI-0024-2019

36. Chen Z, Larregina AT, Morelli AE. Impact of extracellular vesicles on innate immunity. *Curr Opin Organ Transplan* (2019) 24(6):670–8. doi: 10.1097/MOT.0000000000000701

37. Liu M, Wang Z, Ren S, Zhao H. Exosomes derived from mycobacterium tuberculosis-infected MSCs induce a pro-inflammatory response of macrophages. *Aging (Albany NY)* (2021) 13(8):11595–609. doi: 10.18632/aging.202854

38. Singh A, Das K, Banerjee S, Sen P. Elucidation of the signalling pathways for enhanced exosome release from *Mycobacterium*-infected macrophages and subsequent induction of differentiation. *Immunology* (2023) 168(1):63–82. doi: 10.1111/imm.13561

39. Goto Y, Ogawa Y, Tsumoto H, Miura Y, Nakamura TJ, Ogawa K. Contribution of the exosome-associated form of secreted endoplasmic reticulum aminopeptidase 1 to exosome-mediated macrophage activation. *Biochim Biophys Acta Mol Cell Res* (2018) 1865(6):874–88. doi: 10.1016/j.bbamcr.2018.03.009

40. Shlomovitz I, Erlich Z, Arad G, Edry-Botzer L, Zargarian S, Cohen H, et al. Proteomic analysis of necroptotic extracellular vesicles. *Cell Death Dis* (2021) 12 (11):1059. doi: 10.1038/s41419-021-04317-z

41. André F, Chaput N, Schartz NE, Flament C, Aubert N, Bernard J, et al. Exosomes as potent cell-free peptide-based vaccine. I. Dendritic cell-derived exosomes transfer functional MHC class I/peptide complexes to dendritic cells. *Immunol* (2004) 172 (4):2126–36. doi: 10.4049/jimmunol.172.4.2126

42. Ramachandra L, Qu Y, Wang Y, Lewis CJ, Cobb BA, Takatsu K, et al. *Mycobacterium tuberculosis* synergizes with ATP to induce release of microvesicles and exosomes containing major histocompatibility complex class II molecules capable of antigen presentation. *Infect Immun* (2010) 78(12):5116–25. doi: 10.1128/IAI.01089-09

43. Okoye IS, Coomes SM, Pelly VS, Czieso S, Papayannopoulos V, Tolmachova T, et al. MicroRNA-containing T-regulatory-cell-derived exosomes suppress pathogenic T helper 1 cells. *Immunity* (2014) 41(1):89–103. doi: 10.1016/j.immuni.2014.05.019

44. Lindenbergh MFS, Koerhuis DGJ, Borg EGF, van 't Veld EM, Driedonks TAP, Wubbolts R, et al. Bystander T-cells support clonal T-cell activation by controlling the release of dendritic cell-derived immune-stimulatory extracellular vesicles. *Front Immunol* (2019) 10:448. doi: 10.3389/fimmu.2019.00448

45. Torralba D, Baixauli F, Villarroya-Beltri C, Fernández-Delgado I, Latorre-Pellicer A, Acín-Pérez R, et al. Priming of dendritic cells by DNA-containing extracellular vesicles from activated T cells through antigen-driven contacts. *Nat Commun* (2018) 9(1):2658. doi: 10.1038/s41467-018-05077-9

46. Koenig A, Buskiewicz-Koenig IA. Redox activation of mitochondrial DAMPs and the metabolic consequences for development of autoimmunity. *Antioxid Redox Signal* (2022) 36(7-9):441–61. doi: 10.1089/ars.2021.0073

47. Sun YF, Pi J, Xu JF. Emerging role of exosomes in tuberculosis: from immunity regulations to vaccine and immunotherapy. *Front Immunol* (2021) 12:628973. doi: 10.3389/fimmu.2021.628973

48. Alvarez-Jiménez VD, Leyva-Paredes K, García-Martínez M, Vázquez-Flores L, García-Paredes VG, Campillo-Navarro M, et al. Extracellular vesicles released from *mycobacterium tuberculosis*-infected neutrophils promote macrophage autophagy and decrease intracellular mycobacterial survival. *Front Immunol* (2018) 9:272. doi: 10.3389/fimmu.2018.00272

49. Yuan Q, Chen H, Yang Y, Fu Y, Yi Z. miR-18a promotes Mycobacterial survival in macrophages via inhibiting autophagy by down-regulation of ATM. *J Cell Mol Med* (2020) 24(2):2004–12. doi: 10.1111/jcmm.14899

50. Athman JJ, Sande OJ, Groft SG, Reba SM, Nagy N, Wearsch PA, et al. *Mycobacterium tuberculosis* membrane vesicles inhibit T cell activation. *J Immunol* (2017) 198(5):2028–37. doi: 10.4049/jimmunol.1601199

51. Singh PP, LeMaire C, Tan JC, Zeng E, Schorey JS. Exosomes released from M. tuberculosis infected cells can suppress IFN-γ mediated activation of naïve macrophages. *PloS One* (2011) 6(4):e18564. doi: 10.1371/journal.pone.0018564

52. Iacomino G. miRNAs: the road from bench to bedside. *Genes (Basel)* (2023) 14 (2):314. doi: 10.3390/genes14020314

53. Farina FM, Hall IF, Serio S, Zani S, Climent M, Salvarani N, et al. miR-128-3p is a novel regulator of vascular smooth muscle cell phenotypic switch and vascular diseases. *Circ Res* (2020) 126(12):e120–35. doi: 10.1161/CIRCRESAHA.120.316489

54. Song Y, Zhang C, Zhang J, Jiao Z, Dong N, Wang G, et al. Localized injection of miRNA-21-enriched extracellular vesicles effectively restores cardiac function after myocardial infarction. *Theranostics* (2019) 9(8):2346–60. doi: 10.7150/thno.29945

55. Zhu Q, Zhang Q, Gu M, Zhang K, Xia T, Zhang S, et al. MIR106A-5p upregulation suppresses autophagy and accelerates Malignant phenotype in nasopharyngeal carcinoma. *Autophagy* (2021) 17(7):1667–83. doi: 10.1080/15548627.2020.1781368

56. Riahi Rad Z, Riahi Rad Z, Goudarzi H, Goudarzi M, Mahmoudi M, Yasbolaghi Sharahi J, et al. MicroRNAs in the interaction between host-bacterial pathogens: A new perspective. *J Cell Physiol* (2021) 236(9):6249–70. doi: 10.1002/jcp.30333

57. Hill M, Tran N. miRNA:miRNA interactions: A novel mode of miRNA regulation and its effect on disease. *Adv Exp Med Biol* (2022) 1385:241–57. doi: 10.1007/978-3-031-08356-3_9

58. Sun Z, Shi K, Yang S, Liu J, Zhou Q, Wang G, et al. Effect of exosomal miRNA on cancer biology and clinical applications. *Mol Cancer* (2018) 17(1):147. doi: 10.1186/s12943-018-0897-7

59. Yu X, Odenthal M, Fries JW. Exosomes as miRNA carriers: formation-function-future. *Int J Mol Sci* (2016) 17(12):2028. doi: 10.3390/ijms17122028

60. Matsuyama H, Suzuki HI. Systems and synthetic microRNA biology: from biogenesis to disease pathogenesis. *Int J Mol Sci* (2019) 21(1):132. doi: 10.3390/ijms21010132

61. Kilikevicius A, Meister G, Corey DR. Reexamining assumptions about miRNA-guided gene silencing. *Nucleic Acids Res* (2022) 50(2):617–34. doi: 10.1093/nar/gkab1256

62. Zhang D, Yi Z, Fu Y. Downregulation of miR-20b-5p facilitates *Mycobacterium tuberculosis* survival in RAW 264.7 macrophages via attenuating the cell apoptosis by Mcl-1 upregulation. *J Cell Biochem* (2019) 120(4):5889–96. doi: 10.1002/jcb.27874

63. Zhan X, Yuan W, Zhou Y, Ma R, Ge Z. Small RNA sequencing and bioinformatics analysis of RAW264.7-derived exosomes after *Mycobacterium Bovis Bacillus Calmette-Guérin* infection. *BMC Genomics* (2022) 23(1):355. doi: 10.1186/s12864-022-08590-w

64. Kumar R, Sahu SK, Kumar M, Jana K, Gupta P, Gupta UD, et al. MicroRNA 17-5p regulates autophagy in *Mycobacterium tuberculosis*-infected macrophages by targeting Mcl-1 and STAT3. *Cell Microbiol* (2016) 18(5):679–91. doi: 10.1111/cmi.12540

65. Kaushik AC, Wu Q, Lin L. Exosomal ncRNAs profiling of mycobacterial infection identified miRNA-185-5p as a novel biomarker for tuberculosis. *Brief Bioinform* (2021) 22(6):bbab210. doi: 10.1093/bib/bbab210

66. Tu H, Yang S, Jiang T, Wei L, Shi L, Liu C, et al. Elevated pulmonary tuberculosis biomarker miR-423-5p plays critical role in the occurrence of active TB by inhibiting autophagosome-lysosome fusion. *Emerg Microbes Infect* (2019) 8(1):448–60. doi: 10.1080/22221751.2019.1590129

67. Lyu L, Zhang X, Li C, Yang T, Wang J, Pan L, et al. Small RNA profiles of serum exosomes derived from individuals with latent and active tuberculosis. *Front Microbiol* (2019) 10:1174. doi: 10.3389/fmicb.2019.01174

68. Alipoor SD, Tabarsi P, Varahram M, Movassaghi M, Dizaji MK, Folkerts G, et al. Serum exosomal miRNAs are associated with active pulmonary tuberculosis. *Dis Markers* (2019) 2019:1907426. doi: 10.1155/2019/1907426

69. Wang Y, Xu YM, Zou YQ, Lin J, Huang B, Liu J, et al. Identification of differential expressed PE exosomal miRNA in lung adenocarcinoma, tuberculosis, and other benign lesions. *Med (Baltimore)* (2017) 96(44):e8361. doi: 10.1097/MD.0000000000008361

70. Zhang X, Bao L, Yu G, Wang H. Exosomal miRNA-profiling of pleural effusion in lung adenocarcinoma and tuberculosis. *Front Surg* (2023) 9:1050242. doi: 10.3389/fsurg.2022.1050242

71. Guio H, Aliaga-Tobar V, Galarza M, Pellon-Cardenas O, Capristano S, Gomez HL, et al. Comparative profiling of circulating exosomal small RNAs derived from Peruvian patients with tuberculosis and pulmonary adenocarcinoma. *Front Cell Infect Microbiol* (2022) 12:909837. doi: 10.3389/fcimb.2022.909837

72. Carranza C, Herrera MT, Guzmán-Beltrán S, Salgado-Cantú MG, Salido-Guadarrama I, Santiago E, et al. A Dual Marker for Monitoring MDR-TB Treatment: Host-Derived miRNAs and M. tuberculosis-Derived RNA Sequences in Serum. *Front Immunol* (2021) 12:760468. doi: 10.3389/fimmu.2021.760468

73. Barry SE, Ellis M, Yang Y, Guan G, Wang X, Britton WJ, et al. Identification of a plasma microRNA profile in untreated pulmonary tuberculosis patients that is modulated by anti-mycobacterial therapy. *J Infect* (2018) 77(4):341–8. doi: 10.1016/j.jinf.2018.03.006

74. Patop IL, Wüst S, Kadener S. Past, present, and future of circRNAs. *EMBO J* (2019) 38(16):e100836. doi: 10.15252/embj.2018100836

75. Wang Y, Liu J, Ma J, Sun T, Zhou Q, Wang W, et al. Exosomal circRNAs: biogenesis, effect and application in human diseases. *Mol Cancer* (2019) 18(1):116. doi: 10.1186/s12943-019-1041-z

76. Kour B, Gupta S, Singh R, Sophiarani Y, Paul P. Interplay between circular RNA, microRNA, and human diseases. *Mol Genet Genomics* (2022) 297(2):277–86. doi: 10.1007/s00438-022-01856-8

77. Zhou WY, Cai ZR, Liu J, Wang DS, Ju HQ, Xu RH. Circular RNA: metabolism, functions and interactions with proteins. *Mol Cancer* (2020) 19(1):172. doi: 10.1186/s12943-020-01286-3

78. Luo HL, Peng Y, Luo H, Zhang JA, Liu GB, Xu H, et al. Circular RNA hsa_circ_0001380 in peripheral blood as a potential diagnostic biomarker for active pulmonary tuberculosis. *Mol Med Rep* (2020) 21(4):1890–6. doi: 10.3892/mmr.2020.10992

79. Wang J, Li Y, Wang N, Wu J, Ye X, Jiang Y, et al. Functions of exosomal non-coding RNAs to the infection with Mycobacterium tuberculosis. *Front Immunol* (2023) 14:1127214. doi: 10.3389/fimmu.2023.1127214

80. Yi Z, Gao K, Li R, Fu Y. Dysregulated circRNAs in plasma from active tuberculosis patients. *J Cell Mol Med* (2018) 22(9):4076–84. doi: 10.1111/jcmm.13684

81. Huang Z, Su R, Qing C, Peng Y, Luo Q, Li J. Plasma Circular RNAs hsa_circ_0001953 and hsa_circ_0009024 as Diagnostic Biomarkers for Active Tuberculosis. *Front Microbiol* (2018) 9:2010. doi: 10.3389/fmicb.2018.02010

82. Huang Z, Su R, Yao F, Peng Y, Luo Q, Li J. Circulating circular RNAs hsa_circ_0001204 and hsa_circ_0001747 act as diagnostic biomarkers for active tuberculosis detection. *Int J Clin Exp Pathol* (2018) 11(2):586–94.

83. Liu H, Lu G, Wang W, Jiang X, Gu S, Wang J, et al. A panel of circRNAs in the serum serves as biomarkers for *mycobacterium tuberculosis* infection. *Front Microbiol* (2020) 11:1215. doi: 10.3389/fmicb.2020.01215

84. Mumtaz PT, Taban Q, Dar MA, Mir S, Haq ZU, Zargar SM, et al. Deep Insights in Circular RNAs: from biogenesis to therapeutics. *Biol Proced Online* (2020) 22:10. doi: 10.1186/s12575-020-00122-8

85. Zhang Q, Wang W, Zhou Q, Chen C, Yuan W, Liu J, et al. Roles of circRNAs in the tumour microenvironment. *Mol Cancer* (2020) 19(1):14. doi: 10.1186/s12943-019-1125-9

86. Yuan Q, Wen Z, Yang K, Zhang S, Zhang N, Song Y, et al. Identification of key circRNAs related to pulmonary tuberculosis based on bioinformatics analysis. *BioMed Res Int* (2022) 2022:1717784. doi: 10.1155/2022/1717784

87. Yi XH, Zhang B, Fu YR, Yi ZJ. STAT1 and its related molecules as potential biomarkers in *Mycobacterium tuberculosis* infection. *J Cell Mol Med* (2020) 24(5):2866–78. doi: 10.1111/jcmm.14856

88. Zhang X, Zhang Q, Wu Q, Tang H, Ye L, Zhang Q, et al. Integrated analyses reveal hsa_circ_0028883 as a diagnostic biomarker in active tuberculosis. *Infect Genet Evol* (2020) 83:104323. doi: 10.1016/j.meegid.2020.104323

89. Zhuang ZG, Zhang JA, Luo HL, Liu GB, Lu YB, Ge NH, et al. The circular RNA of peripheral blood mononuclear cells: Hsa_circ_0005836 as a new diagnostic biomarker and therapeutic target of active pulmonary tuberculosis. *Mol Immunol* (2017) 90:264–72. doi: 10.1016/j.molimm.2017.08.008

90. Huang ZK, Yao FY, Xu JQ, Deng Z, Su RG, Peng YP, et al. Microarray expression profile of circular RNAs in peripheral blood mononuclear cells from active tuberculosis patients. *Cell Physiol Biochem* (2018) 45(3):1230–40. doi: 10.1159/000487454

91. Huang Z, Su R, Deng Z, Xu J, Peng Y, Luo Q, et al. Identification of differentially expressed circular RNAs in human monocyte derived macrophages response to *Mycobacterium tuberculosis* infection. *Sci Rep* (2017) 7(1):13673. doi: 10.1038/s41598-017-13885-0

92. Li Y, Zheng Q, Bao C, Li S, Guo W, Zhao J, et al. Circular RNA is enriched and stable in exosomes: a promising biomarker for cancer diagnosis. *Cell Res* (2015) 25(8):981–4. doi: 10.1038/cr.2015.82

93. Zang J, Lu D, Xu A. The interaction of circRNAs and RNA binding proteins: An important part of circRNA maintenance and function. *J Neurosci Res* (2020) 98(1):87–97. doi: 10.1002/jnr.24356

94. Giri PK, Kruh NA, Dobos KM, Schorey JS. Proteomic analysis identifies highly antigenic proteins in exosomes from M. tuberculosis-infected and culture filtrate protein-treated macrophages. *Proteomics* (2010) 10(17):3190–202. doi: 10.1002/pmic.200900840

95. Lee J, Kim SH, Choi DS, Lee JS, Kim DK, Go G, et al. Proteomic analysis of extracellular vesicles derived from Mycobacterium tuberculosis. *Proteomics* (2015) 15(19):3331–7. doi: 10.1002/pmic.201500037

96. Layre E. Trafficking of *mycobacterium tuberculosis* envelope components and release within extracellular vesicles: host-pathogen interactions beyond the wall. *Front Immunol* (2020) 11:1230. doi: 10.3389/fimmu.2020.01230

97. Diaz G, Wolfe LM, Kruh-Garcia NA, Dobos KM. Changes in the Membrane-Associated Proteins of Exosomes Released from Human Macrophages after *Mycobacterium tuberculosis* Infection. *Sci Rep* (2016) 6:37975. doi: 10.1038/srep37975

98. Kruh-Garcia NA, Wolfe LM, Chaisson LH, Worodria WO, Nahid P, Schorey JS, et al. Detection of *Mycobacterium tuberculosis* peptides in the exosomes of patients with active and latent M. tuberculosis infection using MRM-MS. *PloS One* (2014) 9(7):e103811. doi: 10.1371/journal.pone.0103811

99. Zhang M, Xie Y, Li S, Ye X, Jiang Y, Tang L, et al. Proteomics analysis of exosomes from patients with active tuberculosis reveals infection profiles and potential biomarkers. *Front Microbiol* (2022) 12:800807. doi: 10.3389/fmicb.2021.800807

100. Mehaffy C, Kruh-Garcia NA, Graham B, Jarlsberg LG, Willyerd CE, Borisov A, et al. Identification of *mycobacterium tuberculosis* peptides in serum extracellular vesicles from persons with latent tuberculosis infection. *J Clin Microbiol* (2020) 58(6):e00393–20. doi: 10.1128/JCM.00393-20

101. Huang C, Pan L, Shen X, Tian H, Guo L, Zhang Z, et al. Hsp16.3 of *mycobacterium tuberculosis* in exosomes as a biomarker of tuberculosis. *Eur J Clin Microbiol Infect Dis* (2021) 40(11):2427–30. doi: 10.1007/s10096-021-04246-x

102. Biadglegne F, Schmidt JR, Engel KM, Lehmann J, Lehmann RT, Reinert A, et al. *Mycobacterium tuberculosis* affects protein and lipid content of circulating exosomes in infected patients depending on tuberculosis disease state. *Biomedicines* (2022) 10(4):783. doi: 10.3390/biomedicines10040783

103. García-Martínez M, Vázquez-Flores L, Álvarez-Jiménez VD, Castañeda-Casimiro J, Ibáñez-Hernández M, Sánchez-Torres LE, et al. Extracellular vesicles released by J774A.1 macrophages reduce the bacterial load in macrophages and in an experimental mouse model of tuberculosis. *Int J Nanomed* (2019) 14:6707–19. doi: 10.2147/IJN.S203507

104. Dahiya B, Khan A, Mor P, Kamra E, Singh N, Gupta KB, et al. Detection of Mycobacterium tuberculosis lipoarabinomannan and CFP-10 (Rv3874) from urinary extracellular vesicles of tuberculosis patients by immuno-PCR. *Pathog Dis* (2019) 77(5):ftz049. doi: 10.1093/femspd/ftz049

105. Du Y, Xin H, Cao X, Liu Z, He Y, Zhang B, et al. Association between plasma exosomes S100A9/C4BPA and latent tuberculosis infection treatment: proteomic analysis based on a randomized controlled study. *Front Microbiol* (2022) 13:934716. doi: 10.3389/fmicb.2022.934716

106. Li W, Li C, Zhou T, Liu X, Liu X, Li X, et al. Role of exosomal proteins in cancer diagnosis. *Mol Cancer* (2017) 16(1):145. doi: 10.1186/s12943-017-0706-8

107. Hu C, Jiang W, Lv M, Fan S, Lu Y, Wu Q, et al. Potentiality of exosomal proteins as novel cancer biomarkers for liquid biopsy. *Front Immunol* (2022) 13:792046. doi: 10.3389/fimmu.2022.792046

108. Kiran D, Podell BK, Chambers M, Basaraba RJ. Host-directed therapy targeting the *Mycobacterium tuberculosis* granuloma: a review. *Semin Immunopathol* (2016) 38(2):167–83. doi: 10.1007/s00281-015-0537-x

109. Augenstreich J, Briken V. Host cell targets of released lipid and secreted protein effectors of mycobacterium tuberculosis. *Front Cell Infect Microbiol* (2020) 10:595029. doi: 10.3389/fcimb.2020.595029

110. Ishikawa E, Mori D, Yamasaki S. Recognition of mycobacterial lipids by immune receptors. *Trends Immunol* (2017) 38(1):66–76. doi: 10.1016/j.it.2016.10.009

111. Han YS, Chen JX, Li ZB, Chen J, Yi WJ, Huang H, et al. Identification of potential lipid biomarkers for active pulmonary tuberculosis using ultra-high-performance liquid chromatography-tandem mass spectrometry. *Exp Biol Med (Maywood)* (2021) 246(4):387–99. doi: 10.1177/1535370220968058

112. Wu M, Yang Q, Yang C, Han J, Lui H, Qiao L, et al. Characteristics of plasma exosomes in drug-resistant tuberculosis patients. *Tuberculosis (Edinb)* (2023) 141:102359.

113. Krug S, Parveen S, Bishai WR. Host-directed therapies: Modulating inflammation to treat tuberculosis. *Front Immunol* (2021) 12:660916. doi: 10.3389/fimmu.2021.660916

114. Zhang W, Jiang X, Bao J, Wang Y, Liu H, Tang L. Exosomes in pathogen infections: A bridge to deliver molecules and link functions. *Front Immunol* (2018) 9:90. doi: 10.3389/fimmu.2018.00090

115. Kim JS, Kim YR, Yang CS. Host-directed therapy in tuberculosis: Targeting host metabolism. *Front Immunol* (2020) 11:1790. doi: 10.3389/fimmu.2020.01790

116. Yu D, Li Y, Wang M, Gu J, Xu W, Cai H, et al. Exosomes as a new frontier of cancer liquid biopsy. *Mol Cancer* (2022) 21(1):56. doi: 10.1186/s12943-022-01509-9

frontiers | Frontiers in Immunology

TYPE Original Research
PUBLISHED 31 October 2023
DOI 10.3389/fimmu.2023.1210372

OPEN ACCESS

EDITED BY
Jianping Xie,
Southwest University, China

REVIEWED BY
Kayvan Zainabadi,
NewYork-Presbyterian, United States
Lanbo Shi,
Rutgers University, Newark, United States
Yifan Bao,
Johnson & Johnson, United States

*CORRESPONDENCE
Jae-Gook Shin
phshinjg@inje.ac.kr
Nguyen Phuoc Long
phuoclong@inje.ac.kr

RECEIVED 22 April 2023
ACCEPTED 18 October 2023
PUBLISHED 31 October 2023

CITATION
Phat NK, Tien NTN, Anh NK, Yen NTH, Lee YA, Trinh HKT, Le K-M, Ahn S, Cho Y-S, Park S, Kim D H, Long NP and Shin J-G (2023) Alterations of lipid-related genes during anti-tuberculosis treatment: insights into host immune responses and potential transcriptional biomarkers.
Front. Immunol. 14:1210372.
doi: 10.3389/fimmu.2023.1210372

Alterations of lipid-related genes during anti-tuberculosis treatment: insights into host immune responses and potential transcriptional biomarkers

Nguyen Ky Phat[1,2], Nguyen Tran Nam Tien[1,2], Nguyen Ky Anh[1,2], Nguyen Thi Hai Yen[1,2], Yoon Ah Lee[3], Hoang Kim Tu Trinh[4], Kieu-Minh Le[4], Sangzin Ahn[1,2], Yong-Soon Cho[1,2], Seongoh Park[3,5], Dong Hyun Kim[1], Nguyen Phuoc Long[1,2]* and Jae-Gook Shin[1,2]*

[1]Department of Pharmacology and PharmacoGenomics Research Center, Inje University College of Medicine, Busan, Republic of Korea, [2]Center for Personalized Precision Medicine of Tuberculosis, Inje University College of Medicine, Busan, Republic of Korea, [3]School of Mathematics, Statistics and Data Science, Sungshin Women's University, Seoul, Republic of Korea, [4]Center for Molecular Biomedicine, University of Medicine and Pharmacy at Ho Chi Minh, Ho Chi Minh, Vietnam, [5]Data Science Center, Sungshin Women's University, Seoul, Republic of Korea

Background: The optimal diagnosis and treatment of tuberculosis (TB) are challenging due to underdiagnosis and inadequate treatment monitoring. Lipid-related genes are crucial components of the host immune response in TB. However, their dynamic expression and potential usefulness for monitoring response to anti-TB treatment are unclear.

Methodology: In the present study, we used a targeted, knowledge-based approach to investigate the expression of lipid-related genes during anti-TB treatment and their potential use as biomarkers of treatment response.

Results and discussion: The expression levels of 10 genes (*ARPC5*, *ACSL4*, *PLD4*, *LIPA*, *CHMP2B*, *RAB5A*, *GABARAPL2*, *PLA2G4A*, *MBOAT2*, and *MBOAT1*) were significantly altered during standard anti-TB treatment. We evaluated the potential usefulness of this 10-lipid-gene signature for TB diagnosis and treatment monitoring in various clinical scenarios across multiple populations. We also compared this signature with other transcriptomic signatures. The 10-lipid-gene signature could distinguish patients with TB from those with latent tuberculosis infection and non-TB controls (area under the receiver operating characteristic curve > 0.7 for most cases); it could also be useful for monitoring response to anti-TB treatment. Although the performance of the new signature was not better than that of previous signatures (i.e., RISK6, Sambarey10, Long10), our results suggest the usefulness of metabolism-centric biomarkers

Conclusions: Lipid-related genes play significant roles in TB pathophysiology and host immune responses. Furthermore, transcriptomic signatures related to the immune response and lipid-related gene may be useful for TB diagnosis and treatment monitoring.

KEYWORDS

tuberculosis, lipid-related gene, transcriptomic biomarker, treatment monitoring, differential diagnosis

1 Introduction

Tuberculosis (TB) is a severe infectious disease that remains a global public health emergency. According to the World Health Organization (WHO), approximately 1.4 million people lost their lives due to TB in 2022 (1). Despite attempts to reduce the duration of TB treatment, the 6-month regimen is still widely used for drug-susceptible TB (2, 3). This prolonged duration can lead to poor treatment adherence (4, 5) and consequently lead to negative outcomes such as treatment failure, relapse, antibiotic resistance, and disease spread (6, 7). Furthermore, conventional TB diagnosis and treatment monitoring rely on sputum-based tests, which have low sensitivity and modest specificity. Additionally, the collection of sputum samples for assays is difficult (8, 9). Underdiagnosis and insufficient treatment monitoring hinder the timely and accurate treatment of TB, leading to poor outcomes. Over the past two decades, significant efforts have been made to develop novel non–sputum-based biomarkers that can be used to rapidly and accurately identify active TB infection and monitor the treatment response (10). Among these biomarkers, blood transcriptomic biosignatures, which reflect host immune responses during anti-TB treatment, are promising candidates (11).

Although multiple transcriptomic signatures for the diagnosis of TB have been proposed (12, 13), the dynamic responses of these biomarkers to TB treatment have not been the main focus in prior works. Only a few transcriptomic signatures have been evaluated for use in the monitoring of anti-TB treatment (9, 10, 14). These signatures have also been found to be useful for TB diagnosis, treatment monitoring, and risk prediction (9). A multi-national study validated the use of the six-gene RISK6 signature (*TRMT2A*, *SDR39U1*, *TUBGCP6*, *SERPING1*, *GBP2*, and *FCGR1B*) for TB diagnosis and treatment monitoring. This signature had a high performance for the differentiation of untreated patients with those who completed the intensive phase of treatment, at the end of treatment, and those who had completed treatment two months previously. Additionally, the RISK6 signature fulfills the WHO target product profile criteria for screening/triage tests for the diagnosis of TB (15). We previously developed the Long10 signature comprising 10 genes (*CD274*, *KIF1B*, *IL15*, *TLR1*, *TLR5*, *FCGR1A*, *GBP1*, *NOD2*, *GBP2*, *EGF*) that were consistently downregulated during TB treatment. The signature displayed comparable performance to other signatures for TB diagnosis, treatment monitoring, and risk assessment (16). The satisfactory performance of the RISK6 and Long10 signatures suggests that a combination of transcriptomic biosignatures can be useful for multiple aspects of TB management. Although the Sambarey10 signature (*FCGR1A*, *HK3*, *RAB13*, *RBBP8*, *IFI44L*, *TIMM10*, *BCL6*, *SMARCD3*, *CYP4F3*, *SLPI*) showed promising performance in TB diagnosis, it has not been evaluated for the monitoring of treatment responses (12, 13, 17). Furthermore, in an individual participant data meta-analysis, only the Sambarey10 and Sweeney3 signatures fulfilled the WHO target product profile criteria for TB triage tests, which requires 90% sensitivity and 70% specificity at the minimum (13, 18).

Despite significant advancements in recent decades, further efforts are needed to develop transcriptional biomarkers for use in TB management. In a prospective cohort study, none of the evaluated transcriptome-based biosignatures fulfilled the WHO target product profile criteria for blood-based confirmatory tests (9). The significant variations in host responses to TB among individuals, cohorts, and comorbidities make the development of a universal biosignature challenging (11). Additionally, the multi-step experimental process, statistical analysis pipelines for data with thousands of genes, and the nature of array- or next-generation sequencing-based technologies can lead to high false-positive rates (19–23). Thus, the reproducibility and robustness of biosignatures need to be improved.

Lipid signaling and immune responses are complex, interlinked processes. Lipoproteins, free fatty acids (FFAs), lipokines, interleukins, and other biological components modulate the complex interactions between these systems (24). In TB, proinflammatory lipid signaling cascades are associated with tricarboxylic acid cycle remodeling, increased interleukin-1β expression, and decreased granulocyte-macrophage colony-stimulating factor expression (25). Our previous study showed significant perturbations related to metabolism and immune response of the host signaling based on the alteration in plasma lipid profiles between TB patients and non-TB controls. Subsequently, dysregulated metabolic and signaling pathways were identified using gene enrichment analysis. Among the genes involved in these pathways, 162 non-overlapped lipid-related genes potentially associated with the pathophysiology of TB were extracted and validated in three datasets (26). Our other study of the plasma lipidome of patients with TB during the 6-month treatment regimen showed changes in pathways related to lipid metabolism and the host immune response (27). These findings suggest an association between systemic lipid alterations and TB

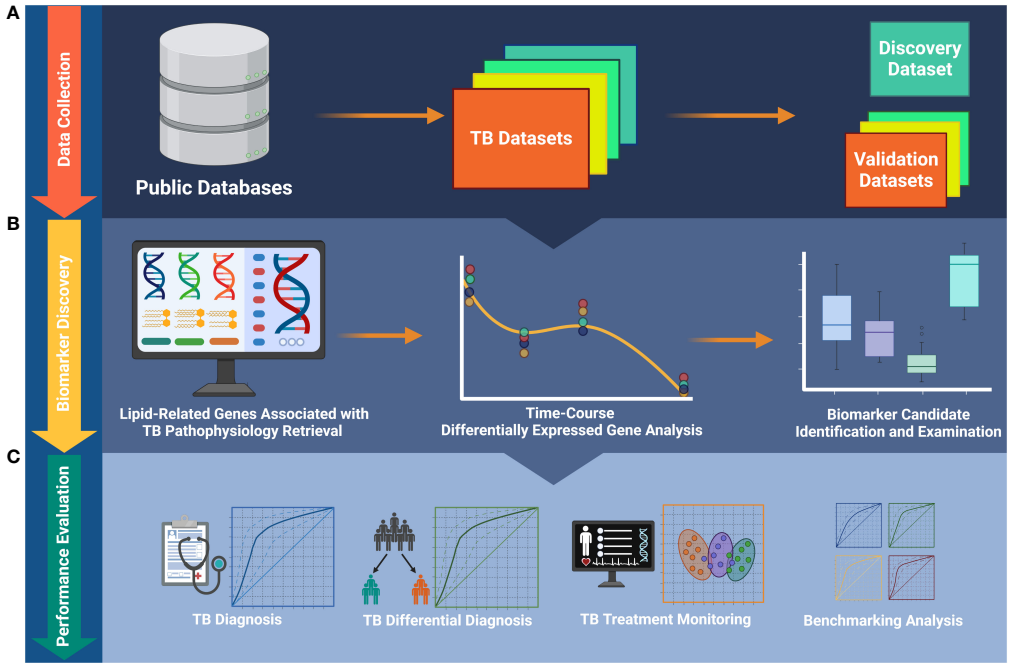

FIGURE 1
The workflow of the study. **(A)** Publicly available data collection. **(B)** Identification of biomarkers and foundation of biosignature. **(C)** Validation of the ability of the biosignature for TB diagnosis and treatment monitoring. TB, tuberculosis.

disease status. Thus, changes in lipid-related genes may serve as indicators of the response to TB treatment.

In the present study, we used a targeted, knowledge-based approach to select the most significant TB biomarker candidates from the 162 lipid-related genes previously found. The study workflow is described in Figure 1. We evaluated the potential usefulness of these genes for pulmonary TB diagnosis and treatment monitoring in multiple cohorts. Additionally, we conducted a benchmark analysis to compare the performance of the candidate biomarkers with that of publicly available signatures. We found that the performance of the lipid-related genes was not better than that of certain other biosignatures. Our results demonstrate that lipid metabolism is involved in the host immune response during TB treatment. Importantly, we provide more evidence that lipid metabolism and signaling researches can contribute to improve the management of TB.

2 Materials and methods

2.1 Published transcriptomics data acquisition

Transcriptomic datasets of pulmonary TB were collected from the Gene Expression Omnibus (GEO) and ArrayExpress databases. The search term was built as previously described and restricted to *Homo sapiens* species (16). For longitudinal datasets, drug susceptibility (DS)-TB cases with no known severe comorbidities were selected. Additionally, patients with known failure treatment outcomes were excluded. Three representative datasets [GSE31348 (28), GSE89403 (29), and GSE181143 (30)] were included for subsequent analyses to demonstrate the dynamic response of lipid-related genes during the TB treatment time course. These three longitudinal TB datasets were obtained from patients who underwent the standard six-month anti-TB treatment. GSE31348 was used as the identification cohort, while GSE89403 and GSE181143 were utilized for validation. Additional datasets were collected to demonstrate the potential of lipid-related genes in TB diagnosis. They covered different medical conditions with or without human immunodeficiency virus (HIV), including TB, latent TB infection (LTBI), non-TB, and other diseases (OD). Of note, the OD groups from the GSE37250 dataset consist of patients with multiple diseases that are common in the African population (e.g., pneumonia (PNA)/lower respiratory tract infection/ *Pneumocystis jirovecii* pneumonia; malignancy and other neoplasia other than Kaposi's sarcoma; pelvic inflammatory disease/urinary tract infection; bacterial, viral meningitis, or meningitis of uncertain origin; and hepatobiliary disease). Detailed information is available in the original study of the dataset (31). The collected datasets were also comprised of healthy control, active sarcoidosis (SARC), non-active SARC, lung cancer, and pneumonia individuals. Eight chosen datasets were E-MTAB-8290 (non-TB-non-HIV, non-TB-HIV, TB, TB-HIV) (32), GSE37250 (OD, OD-HIV, LTBI, LTBI-HIV, TB, and TB-HIV) (31), GSE107991 (healthy control, TB, LTBI) (33), GSE107994 (healthy control, TB, LTBI) (33), GSE101705 (TB, LTBI) (34), and a combined dataset from GSE42825, GSE42826, and GSE42830 (healthy control, active SARC, non-active SARC, lung cancer, PNA) (35). The information of all datasets included in this study is summarized in Supplementary Table 1.

2.2 Targeted lipid-related genes list and other available signatures

A list of 162 lipid-related genes associated with the biological pathways underlying TB pathophysiology was retrieved from our previous study (Supplementary Table 2) (26). This list was extracted from significantly enriched pathways of our reported lipid biomarkers for TB and non-TB control differentiation. Of note, all of these 162 genes are host genes and not derived from *Mycobacterium tuberculosis* (*Mtb*).

For comparison purposes, three other signatures were created by directly extracting the component genes of publicly available signatures, i.e., RISK6 (36), Sambarey10 (17), and Long10 (16).

2.3 Data processing and normalization

Microarray data were normalized using *affy* (version 1.74.0, Affymetrix) (37) and *lumi* (version 2.48.0, Illumina) (38) packages, respectively. The batch effects of microarray datasets with multi-site cohorts was corrected by the Combat method (39) using *sva* package (version 3.44.0) (40) after being examined with the *BatchQC* package (version 1.24.0) (41). Regarding RNA-seq data, the batch effect of datasets was inspected by *BatchQC* and corrected using Combat-seq (42). RNA-seq data were normalized using the median of ratio method combined with regularized logarithmic transformation. The pipeline was conducted by the *DESeq2* package (version 1.36.0) (43).

2.4 Single-sample scoring of gene signature

Gene set variation analysis (GSVA) was carried out using *GSVA* package (version 1.44.5) (44) to evaluate the treatment monitoring and diagnosis characteristics of gene signatures. GSVA transforms the transcriptome profile of an individual sample into a signature enrichment profile. The GSVA score of a signature characterizes the coordination in the regulation (either up or down) of its component genes and indicates its activity level.

2.5 Statistical analysis

The molecular profiles of the lipid-related genes of patients during TB treatment were examined using principal component analysis (PCA) and t-distributed stochastic neighbor embedding (t-SNE). The profiles were visualized using three-dimensional PCA and t-SNE score plots drawn by *plotly* package (version 4.10.1). *ComplexHeatmap* package (version 2.15.1) (45) was used to create heatmap visualization of GSVA score for obtained biosignature. A polynomial regression targeted to 162 lipid-relate genes was implemented by *maSigPro* package (version 1.68.0) (46) to identify differentially expressed genes (DEGs) during the TB treatment time course. In short, the algorithm built a profile model for time-course gene expression:

$$y_i = \beta_0 + \beta_1 T_i + \beta_1 T_i^2 + \ldots + \beta_d T_i^d + \eta_1 Z_{i1} + \ldots \eta_p Z_{ip} + \epsilon_i,$$

where y_i is the expression level for a gene and ϵ_i is the error term. The model consists of two parts: (1) polynomial of degree d in the time variable and (2) the linear regression explained by p explanatory variables. This is assumed to be the full model, but due to model complexity, the package considers a reduced model, which uses fewer variables than the full model but still has enough predictive power. The selection procedure is either forward or backward step-wise selection where each variable is sequentially tested if the addition or elimination of the variable improves the model. In our case, we did not include any explanatory variable and set the polynomial degree as 2. For testing the overall significance of the regression model, F-test was performed for each gene. Lipid-related genes with a false discovery rate (FDR) < 0.05 were selected as DEGs. The R^2 value was set to ≥ 0.3 for selecting the genes as biomarker candidates.

The Kruskal-Wallis test and the *post hoc* two-sided unpaired Wilcoxon rank sum test were performed for testing unpaired data. With paired data, the Friedman test followed by the *post hoc* paired Wilcoxon signed rank test was applied. For a single statistical testing, a raw P-value < 0.05 was considered statistically significant. For multiple comparisons, the FDR of 0.05 was established as the significant threshold. Statistical tests were conducted using *rstatix* package (version 0.7.1).

2.6 Gene signature performance evaluation

The potential of the signature to characterize different TB treatment states was evaluated by applying k-means clustering. In detail, the expression profile of each gene was considered a variable, and the sample at a specific time point was treated as an observation. The number of clusters was predetermined. As a result, the algorithm identified clusters of samples that exhibited similar expression profiles of the signature, regardless of their actual sampling time point. The data was Pareto scaled prior to the analysis. MetaboAnalyst 5.0 (47) was employed to conduct the classification model.

For TB diagnosis, the classification model was built using a logistic regression. Model validation was performed with a 10-fold nested cross-validation procedure where the outer loop is for splitting training and test data and the inner for searching the best tuning parameters. The *caret* package (version 6.0-93) (48) was used for model building and validation. Model performance was assessed by the area under the curve (AUC) value of the receiver operating characteristic (ROC) curve. All statistical analyses and presentations were implemented in R version 4.2.1. Besides the base R graphics, the *ggplot2* (version 3.4.0) and its extension *ggpubr* (version 0.5.0) were used for visualization unless stated otherwise.

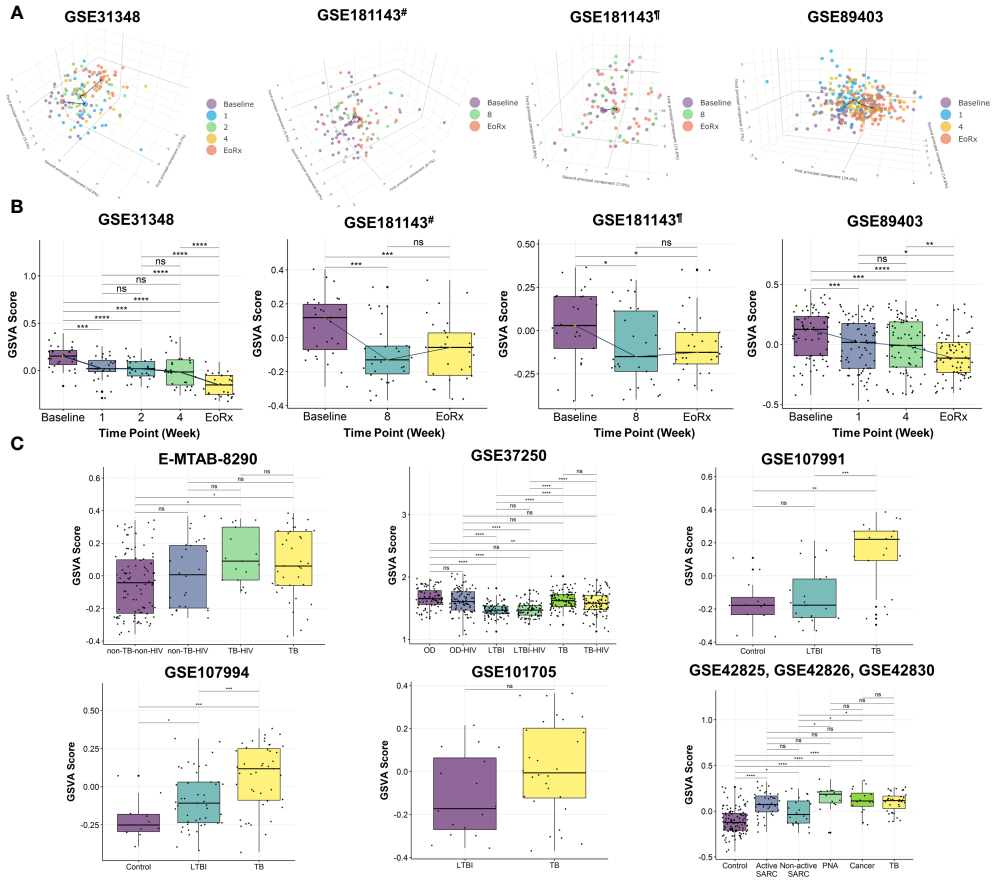

FIGURE 2
The potential of 162 lipid-related genes in TB treatment monitoring and diagnosis. **(A)** 3D principal component analysis scores plots represent the transcriptome profiles for 162 lipid-related genes during the TB treatment. **(B)** The GSVA score of 162 lipid-related genes across the TB treatment time course. The orange point represents the median GSVA score of the subject group and the box plot represent the correspondent interquartile range. **(C)** The GSVA score of 162 lipid-related genes in TB and its counterparts. GSVA, gene set variation analysis; 1, after one week; 2, after two weeks; 4, after four weeks; 8, after eight weeks; EoRx, treatment completion; TB, tuberculosis; LTBI, latent TB infection; OD, other diseases; HIV, human immunodeficiency virus; SARC, sarcoidosis; Cancer, lung cancer; PNA, pneumonia; #, subset from India of GSE181143 dataset; ¶, subset from Brazil of GSE181143 dataset; ns, not significant; *,<0.05; **,<0.01; ***,<0.001, ****,<0.0001; *two-sided paired Wilcoxon signed rank test* **(B)** and *two-sided Wilcoxon rank sum test* **(C)**.

3 Results

3.1 The association of 162 lipid-related genes with different TB treatment states and various disease conditions

PCA was performed to investigate the dynamic responses of the expression profiles of 162 lipid-related genes during TB treatment. The PCA scores plots showed clear separations between the transcriptomes at baseline and at treatment completion, but not after one, two, four, or eight weeks of treatment, in all datasets except the Brazilian population subset of GSE181143 (no clear separation was observed for this subset) (Figure 2A). Interestingly, t-SNE displayed three clusters of lipid-related gene transcriptomes (*i.e.*, baseline, mid-time points, and treatment completion) as observed with PCA, except GSE181143 cohort (Supplementary Figure 1). The lipid-related gene expression profiles generally formed three clusters corresponding to baseline, treatment completion, and other time points.

To further explore the associations between alterations in the gene expression of lipid-related genes and TB treatment states, we performed GSVA. The GSVA score declined significantly from baseline to treatment completion, reflecting that the lipid-related genes were less activated at the end of the treatment course (Figure 2B). Moreover, the Friedman test demonstrated significant differences in GSVA scores across various time points in GSE31348, GSE89403, and GSE181143 (Supplementary Table 3). Pairwise comparison showed that the GSVA score for the 162 lipid-related genes differed significantly between baseline, mid-treatment, and treatment completion, with no significant difference among mid-treatment time points. In GSE181143, no significant difference was observed between the mid-treatment (after eight weeks) time point and treatment completion. These findings were in line with the PCA results.

We also performed GSVA to investigate the association between the lipid-related genes and different disease conditions. The GSVA score was significantly higher for patients with TB than for those with other conditions (i.e., non-TB-non-HIV, LTBI, LTBI-HIV, healthy

control, non-active SARC) (Figure 2C) and differed significantly across patient groups. However, no significant differences were found between the TB group with OD, active SARC, lung cancer, and PNA groups (Figure 2C, Supplementary Table 4). Additionally, the GSVA score of the LTBI group differed significantly from those of other groups (GSE37250 and GSE107994). Notably, the GSVA score did not differ significantly between patients with and without HIV infection in the non-TB (E-MTAB-8290), OD, LTBI, or TB groups (GSE37250). Taken collectively, these results indicated the association between 162 lipid-related genes and TB treatment states. This suggested further investigation into the ability of 162 lipid-related genes for TB treatment monitoring and diagnosis.

3.2 The foundation of 10-lipid-gene transcriptional signature

To develop a clinically applicable biosignature, 162 genes were screened to identify the most promising candidate biomarkers. A time-course regression analysis targeted to 162 lipid-related genes was conducted on 135 samples with 5 different time points (GSE31348) to identify DEGs throughout TB treatment. The analysis identified 80 lipid-related genes that are differentially expressed during TB treatment, with most changes in the expression levels of these genes were subtle. Ten DEGs with $R^2 > 0.3$ were identified as the most potential biomarker candidates (Table 1). The ten lipid-related genes together formed the so-called "10-lipid-gene" signature.

GSVA was performed on the discovery dataset (i.e., GSE31348) to demonstrate the dynamic response of the 10-lipid-gene signature. Overall, the GSVA scores for the signature showed similar changes during treatment as did those for the 162 lipid-related genes (Figures 2B, 3A, Supplementary Table 5). GSVA scores for all 27 patients of the discovery dataset were visualized using heatmaps to examine the interindividual response variability in the 10-lipid-gene signature. Although some patients showed unusual patterns of change during the initial four weeks of treatment, most cases showed a significant reduction in the GSVA score at treatment completion (Figure 3B). The changes in individual gene expression of all 27 patients in the GSE31348 dataset were analyzed to determine the gene-specific variability. Two main trends were observed during TB treatment: chronological down-regulation and up-regulation (Figure 3C). In particular, the expression of nine genes (*ARPC5*, *ACSL4*, *LIPA*, *CHMP2B*, *RAB5A*, *GABARAPL2*, *PLA2G4A*, *MBOAT2*, and *MBOAT1*) was altered only slightly during the initial four weeks of treatment, but was down-regulated significantly at treatment completion. In contrast, the expression of *PLD4* increased during treatment.

TABLE 1 List of the most potential lipid-related gene candidates.

EntrezID	Gene Symbol	Gene Name	FDR*	R-squared*	Main Biological Function of Encoded Protein	Reference
10092	*ARPC5*	actin-related protein 2/3 complex subunit 5	5.23E-11	0.335	Regulate fatty acid synthesis. Involve in cup formation during phagocytosis Regulate the homeostasis of T cells	(49–51)
2182	*ACSL4*	acyl-coenzyme A synthetase long-chain family member 4	1.74E-11	0.349	Promote fatty acid oxidation and lipid biosynthesis Regulate ferroptosis	(52, 53)
122618	*PLD4*	phospholipase D family member 4	5.52E-13	0.396	Involve in macrophage activation and phagocytosis	(54, 55)
3988	*LIPA*	lipase A, lysosomal acid type	1.74E-11	0.348	Generate free fatty acids and free cholesterol Involves in the maturation and function of immune cells	(56)
25978	*CHMP2B*	charged multivesicular body protein 2B	5.45E-10	0.307	Participate in membrane remodeling and repair Involves in fatty acid trafficking to maintain lipid and energy homeostasis	(57, 58)
5868	*RAB5A*	RAB5A, member RAS oncogene family	1.74E-11	0.349	Encode a small GTPase that regulates endocytosis	(59, 60)
11345	*GABARAPL2*	gamma-aminobutyric acid receptor-associated protein-like 2	3.32E-10	0.315	Regulate lipid droplet biogenesis Facilitate autophagosome formation	(61, 62)
5321	*PLA2G4A*	phospholipase A2 group IVA	6.05E-10	0.305	Regulate lipid droplet biogenesis Participate in initial step of the arachidonic acid pathway	(63, 64)
129642	*MBOAT2*	membrane-bound O-acyltransferase domain containing 2	1.23E-11	0.360	Regulate the free arachidonic acid level through arachidonate recycling process	(65)
154141	*MBOAT1*	membrane-bound O-acyltransferase domain containing 1	4.68E-10	0.310	Regulate the free arachidonic acid level through arachidonate recycling process	(65)

FDR, False Discovery Rate.
*FDR and R-squared values were obtained from time series analysis using GSE31348.

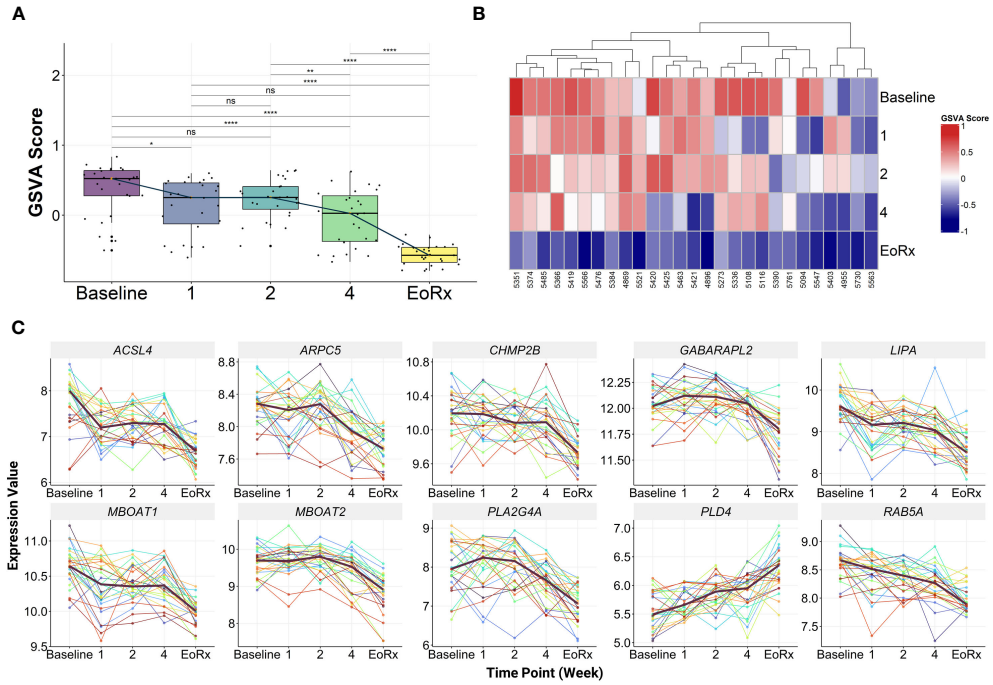

FIGURE 3
The characteristics of 10-lipid-gene biosignature. **(A)** The GSVA score of 10-lipid-gene signature during TB treatment (N = 27). The orange point represents the median GSVA score of the subject group and the box plot represent the correspondent interquartile range. **(B)** Heatmap represents the signature enrichment profiles of individual patients for 10-lipid-gene signature during TB treatment (N = 27). **(C)** The expression level of individual gene component of the signature across the TB treatment time course (N = 27). The dark mauve line indicates the median gene expression level. GSVA, gene set variation analysis; 1, after one week; 2, after two weeks; 4, after four weeks; EoRx, treatment completion; ns, not significant; *,<0.05; **,<0.01; ****,<0.0001; *two-sided paired Wilcoxon signed rank test.*

3.3 The ability of 10-lipid-gene transcriptional biosignature to reflect different TB treatment states

External validation was performed to evaluate the dynamic response of the 10-lipid-gene biosignature during TB treatment (Figure 4A). To enhance the reliability of the assessment, we also compared it with other priory-established signatures (i.e., Long10, RISK6, and Sambarey10). In the two subsets of GSE181143, the 10-lipid-gene signature was down-regulated from baseline to after eight weeks and remained stable until treatment completion (Supplementary Table 6). However, the GSVA scores for the other three signatures decreased consistently during the treatment course; this reduction was subtle for the RISK6 signature and significant at all-time points for the Long10 and Sambarey10 signatures (Figure 4A, Supplementary Table 6). In the Catalysis treatment response cohort (CTRC) (i.e., GSE89403), the GSVA scores for the 10-lipid-gene and RISK6 signatures decreased from baseline to after one week, remained stable after four weeks, and thereafter continued to decrease until treatment completion. Figure 4A shows the significant reduction of the GSVA scores for the Long10 and Sambarey10 signatures during treatment in the CTRC cohort. Notably, only the score for the Sambarey10 signature differed significantly between after one week and after four weeks of treatment.

We evaluated the ability of the 10-lipid-gene signature to differentiate among TB treatment states using k-means clustering. Three clusters were pre-determined to correspond to the distinct states of TB treatment (baseline, mid-time points, and treatment completion) that were previously observed. Overall, the three clusters showed a high degree of overlap in all datasets. In the subset from India of GSE181143, the 10-lipid-gene signature exhibited weak performance, with a cluster corresponding to the baseline but none corresponding to the other time points; the performance of 10-lipid-gene signature was not superior to other signatures (Figure 4B). In the cohort from Brazil of GSE181143, the grouping based on 10-lipid-gene signature was not in concordance with TB treatment states (Figure 4C). The RISK6 signature could cluster the samples at treatment completion and the Sambarey10 signature could cluster samples at baseline, although the tendency is unclear. Remarkably, the Long10 signature exhibited good concordance with the original labels in clustering the samples at baseline and at the end of treatment. In the CTRC cohort, the clusters based on the 10-lipid-gene signature and the treatment states were not concordant (Figure 4D). The other three signatures surpassed the 10-lipid-gene signature in clustering the samples into different TB treatment states, illustrated by better concordance between the original labels and pre-determined clusters. These findings are in line with the observation of subtle changes in the 10-lipid-gene signature during TB treatment. Collectively, the 10-

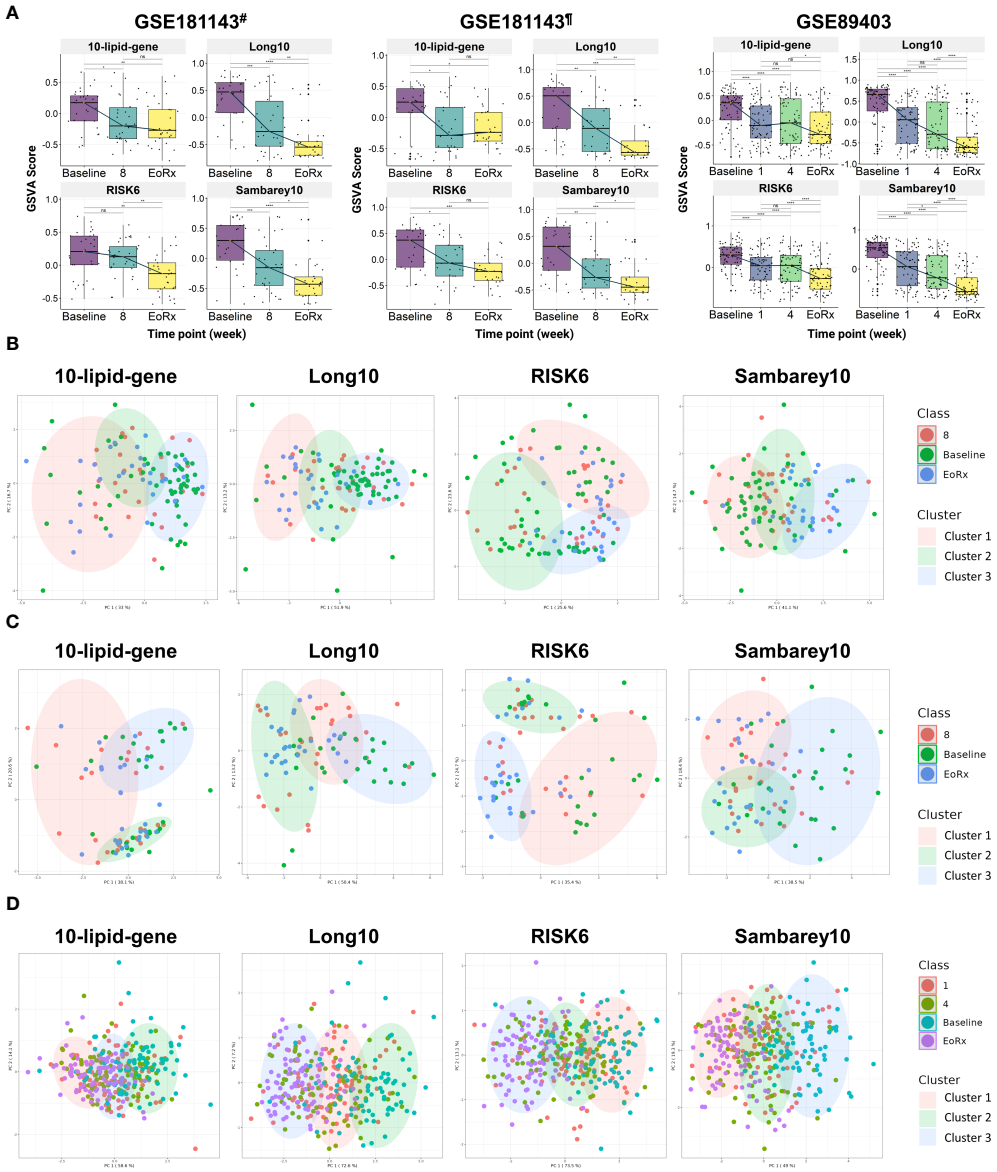

FIGURE 4
The potential 10-lipid-gene biosignature in TB treatment monitoring. **(A)** The GSVA score of 10-lipid-gene, Long10, RISK6, and Samberey10 biosignatures during the TB treatment time course. The orange point represents the median GSVA score of the subject group and the box plot represent the correspondent interquartile range **(B)** Classification of different TB treatment states based on the 10-lipid-gene signature for subset from India of the GSE181143 dataset. **(C)** Classification of different TB treatment states based on the 10-lipid-gene signature for subset from Brazil of the GSE181143 dataset. **(D)** Classification of different TB treatment states based on the 10-lipid-gene signature for the GSE89403 dataset. GSVA, gene set variation analysis; 1, after one week; 2, after two weeks; 4, after four weeks; 8, after eight weeks; EoRx, treatment completion; #, the subset of Indian samples from GSE181143 dataset; ¶, the subset of Brazilian samples from GSE181143 dataset. ns, not significant; *,<0.05; **,<0.01; ***, <0.001; ****,<0.0001; *two-sided paired Wilcoxon signed rank test*.

lipid-gene biosignature exhibited weak clustering ability and only partially reflected the TB treatment states.

3.4 The ability of 10-lipid-gene transcriptional biosignature for TB diagnosis and TB differential diagnosis

We investigated the relationships between the 10-lipid-gene signature and multiple subject groups in various clinical situations. Notably, GSVA scores for this signature were higher for patients with TB than for most other groups, irrespective of the HIV status, except in the GSE37250 and the combined GSE42825/GSE42826/GSE42830 dataset (Figures 5A–F, Supplementary Table 7). The GSVA score differed significantly across subject groups. In particular, the GSVA score for the 10-lipid-gene signature differed significantly between the TB groups and the other groups (excluding the OD groups in GSE37250 as well as cancer and PNA in GSE42825, GSE42826, and GSE42830) (Figures 5A–F). These findings are in line with those observed for the 162 lipid-related genes (Figures 2B, C). Interestingly, the simplified signature showed a better ability than the 162-gene set to differentiate

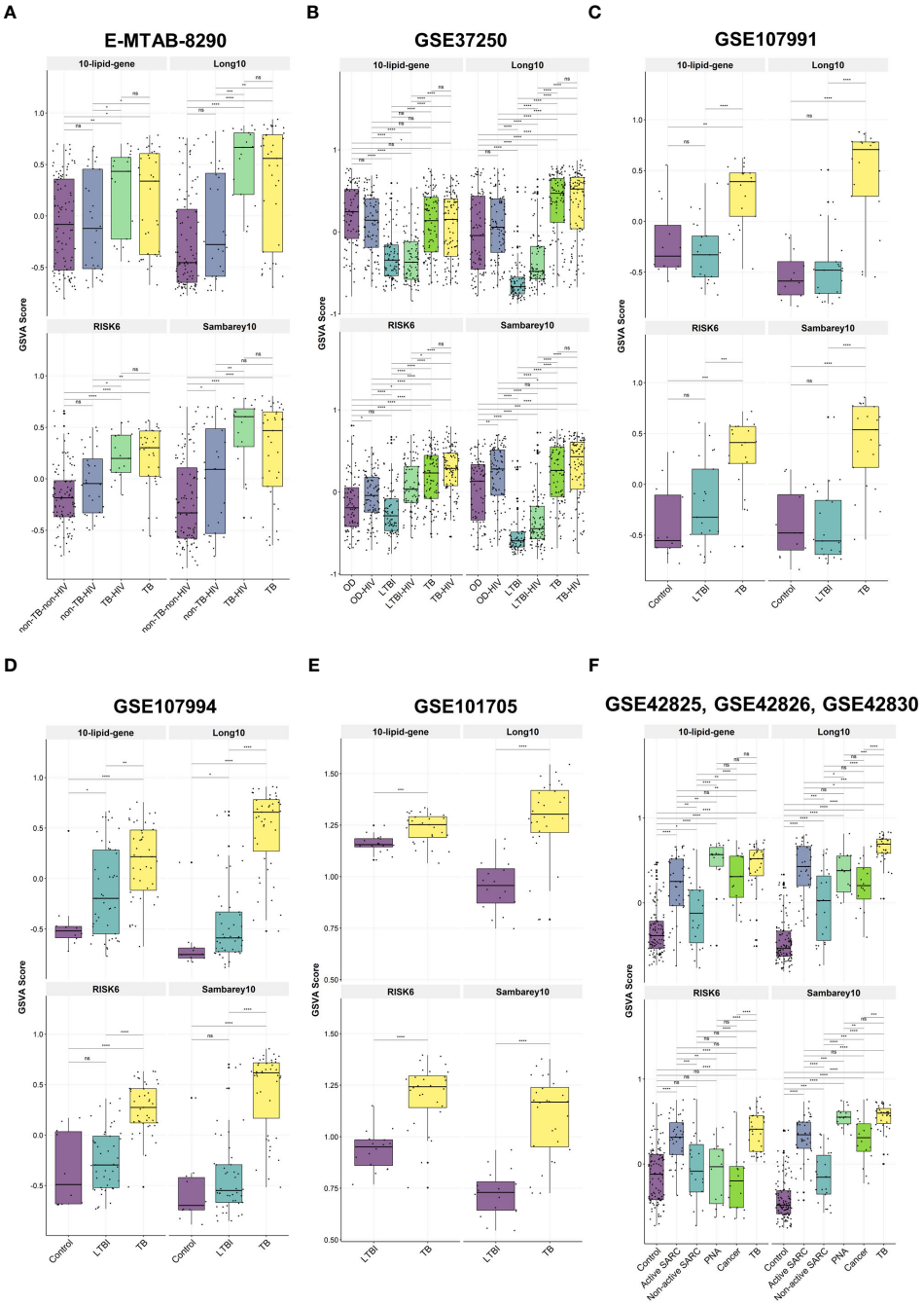

FIGURE 5
The GSVA score of 10-lipid-gene, Long10, RISK6, and Samberey10 biosignatures in TB and its counterparts. **(A)** E-MTAB-8290. The box plot represents the median and the interquartile range of the GSVA score for each subject group **(B)** GSE37250. **(C)** GSE107991. **(D)** GSE107994. **(E)** GSE101705. **(F)** GSE4285, GSE42826, GSE42830. GSVA, gene set variation analysis; TB, tuberculosis; LTBI, latent TB infection; OD, other diseases; HIV, human immunodeficiency virus; SARC, sarcoidosis; Cancer, lung cancer; PNA, pneumonia; ns: not significant; *,<0.05; **,<0.01; ***,<0.001; ****,<0.0001; *two-sided Wilcoxon rank sum test*.

between TB and non-TB-HIV, TB and active SARC, and TB-HIV and non-TB-HIV groups based on the GSVA score (Figures 2B, C, 5A, F). The GSVA score patterns for three other signatures were similar to that for the 10-lipid-gene signature in most datasets, except in the GSE37250 and the combined GSE42825/GSE42826/GSE42830 dataset. However, based on the GSVA scores, the other signatures showed comparable or better distinction among subject groups than the 10-lipid-gene signature. None of the tested signatures had a GSVA score that differed significantly between the TB and TB-HIV groups.

The differential diagnosis performance of the 10-lipid-signature was evaluated in multiple clinical cohorts (Figure 6, Table 2). A logistic regression classifier based on the 10-lipid-gene signature exhibited good performance when distinguishing TB-only patients from non-TB controls without HIV (AUC of ROC curve and standard deviation from the 10-fold nested cross-validation =

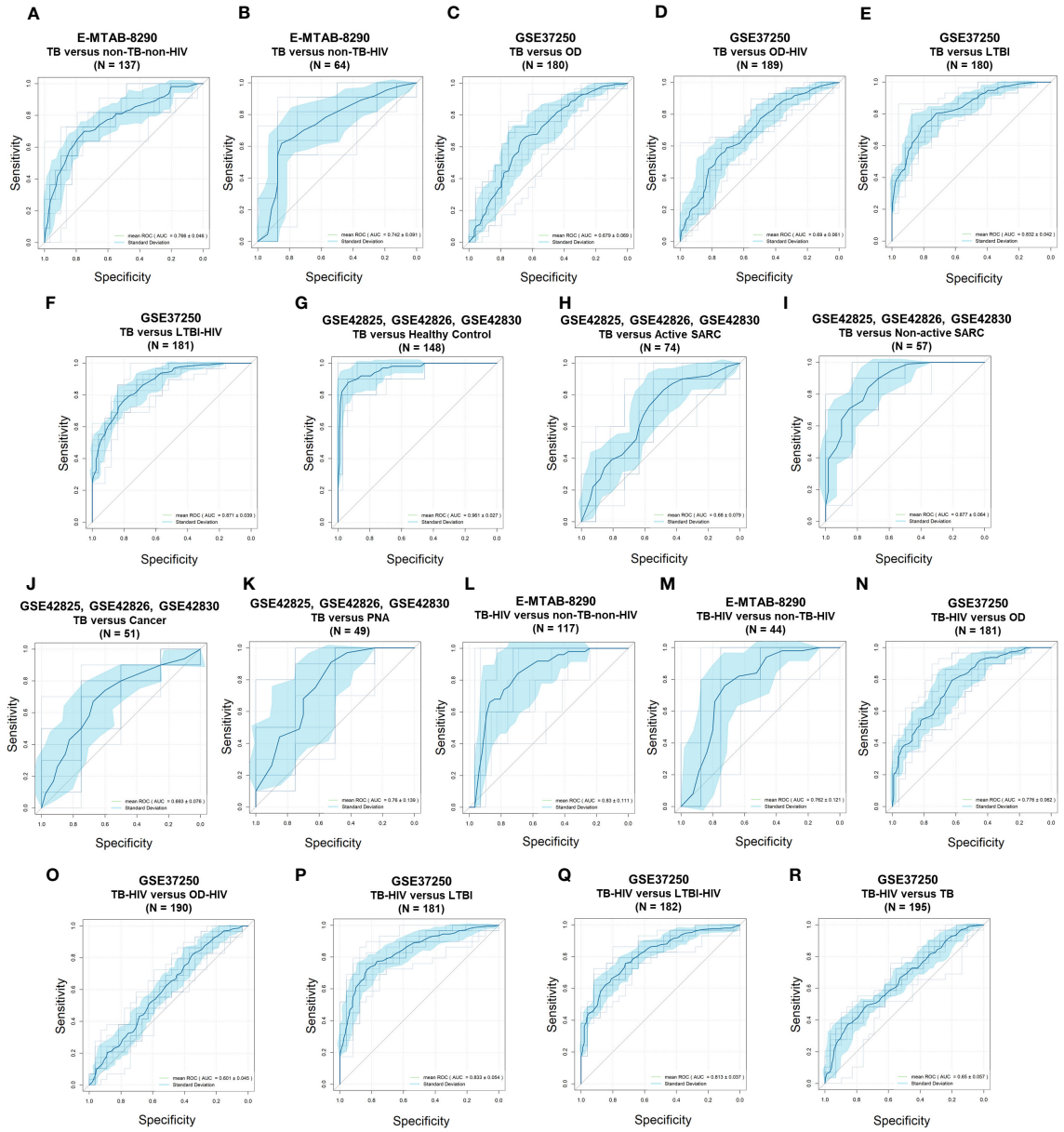

FIGURE 6
Receiver operating characteristic curves of the 10-lipid-gene signatures in TB diagnosis. **(A)** E-MTAB-8290, TB *versus* non-TB-non-HIV. **(B)** E-MTAB-8290, TB *versus* non-TB-HIV. **(C)** GSE37250, TB *versus* OD. **(D)** GSE37250, TB versus OD-HIV. **(E)** GSE37250, TB *versus* LTBI. **(F)** GSE37250, TB *versus* LTBI-HIV. **(G)** GSE42825; GSE42826; GSE42830, TB *versus* healthy control. **(H)** GSE42825; GSE42826; GSE42830, TB *versus* active SARC. **(I)** GSE42825; GSE42826; GSE42830; TB *versus* non-active SARC. **(J)** GSE42825; GSE42826; GSE42830, TB versus Cancer. **(K)** GSE42825; GSE42826; GSE42830, TB *versus* PNA, **(L)** E-MTAB-8290, TB-HIV *versus* non-TB-non-HIV. **(M)** E-MTAB-8290, TB-HIV *versus* non-TB-HIV. **(N)** GSE37250, TB-HIV versus OD. **(O)** GSE37250, TB-HIV versus OD-HIV. **(P)**, GSE37250, TB-HIV *versus* LTBI. **(Q)** GSE37250, TB-HIV versus LTBI-HIV. **(R)** GSE37250, TB-HIV versus TB. TB, tuberculosis; LTBI, latent TB infection; OD, other diseases; HIV, human immunodeficiency virus; SARC, sarcoidosis; Cancer, lung cancer; PNA, pneumonia.

0.766 ± 0.046) (Figure 6A). When differentiating between the TB-only group and non-TB controls with HIV, the classifier was not robustly against a random guess (the ROC crossed the diagonal line) (Figure 6B). The model showed an acceptable ability to differentiate the TB-only group from the OD (AUC = 0.679 ± 0.069) and OD-HIV (AUC = 0.690 ± 0.061) (Figures 6C, D). Additionally, the 10-lipid-gene signature showed excellent and good results in differentiating patients with TB from those with LTBI in GSE37250 (AUC = 0.832 ± 0.042) and in GSE107994 (AUC = 0.792 ± 0.067), respectively (Figure 6E, Table 2). Similarly, the 10-lipid-gene classifier distinguished the TB and LTBI-HIV groups with excellent performance (AUC = 0.871 ± 0.039) (Figure 6F). In the combined GSE42825/GSE42826/GSE42830 dataset, the 10-lipid-gene signature exhibited its best performance when distinguishing between patients with TB and healthy controls (AUC = 0.961 ± 0.027) (Figure 6G). Also, in this dataset, the 10-lipid-gene signature showed acceptable performance in distinguishing between TB and active SARC (AUC = 0.680 ±

TABLE 2 The performance of 10-lipid-gene signature for TB diagnosis in comparison with Long10, RISK6, and Sambarey10 signatures.

Dataset	Country	Comparison (number of patients)	AUC ± SD				FDR (Wilcoxon Rank Sum Test)		
			10-lipid-gene	Long10	RISK6	Sambarey10	Long10 *versus* 10-lipid-gene	RISK6 *versus* 10-lipid-gene	Sambarey10 *versus* 10-lipid-gene
E-MTAB-8290	South Africa	TB (37)/non-TB-non-HIV (100)	0.766 ± 0.046	0.851 ± 0.077	0.860 ± 0.068	0.877 ± 0.062	0.028	0.016	0.005
		TB (37)/non-TB-HIV (27)	0.742 ± 0.091	0.673 ± 0.072	0.748 ± 0.136	0.684 ± 0.16	0.148	1.000	0.590
		TB-HIV (17)/non-TB-non-HIV (100)	0.830 ± 0.111	0.949 ± 0.061	0.906 ± 0.083	0.925 ± 0.052	0.028	0.251	0.093
		TB-HIV (17)/non-TB-HIV (27)	0.762 ± 0.121	The SD was not sufficiently estimated	0.872 ± 0.115	0.790 ± 0.112	NA	0.157	0.622
		TB (37)/TB-HIV (17)	0.667 ± 0.142	0.591 ± 0.091	0.716 ± 0.130	0.596 ± 0.095	0.172	0.479	0.480
GSE37250*	Malawi, South Africa	TB (97)/OD (83)	0.679 ± 0.069	0.836 ± 0.045	0.798 ± 0.043	0.845 ± 0.055	4.90E-04	0.002	7.02E-04
		TB (97)/OD-HIV (92)	0.690 ± 0.061	0.812 ± 0.066	0.762 ± 0.052	0.907 ± 0.038	0.001	0.020	3.65E-04
		TB (97)/LTBI (83)	0.832 ± 0.042	0.955 ± 0.023	0.969 ± 0.018	0.942 ± 0.022	4.90E-04	6.39E-04	3.65E-04
		TB (97)/LTBI-HIV (84)	0.871 ± 0.039	0.939 ± 0.026	0.932 ± 0.033	0.954 ± 0.022	0.002	0.010	5.74E-04
		TB-HIV (98)/OD (83)	0.776 ± 0.062	0.912 ± 0.029	0.855 ± 0.048	0.917 ± 0.047	4.90E-04	0.002	6.80E-04
		TB-HIV (98)/OD-HIV (92)	0.601 ± 0.045	0.778 ± 0.044	0.861 ± 0.050	0.867 ± 0.036	4.90E-04	6.39E-04	3.65E-04
		TB-HIV (98)/LTBI (83)	0.833 ± 0.054	0.977 ± 0.010	0.975 ± 0.012	0.973 ± 0.011	4.90E-04	6.39E-04	3.65E-04
		TB-HIV (98)/LTBI-HIV (84)	0.813 ± 0.037	0.891 ± 0.036	0.866 ± 0.037	0.901 ± 0.066	0.001	0.006	0.008
		TB (97)/TB-HIV (98)	0.650 ± 0.057	0.780 ± 0.061	0.749 ± 0.041	0.837 ± 0.032	4.90E-04	0.002	3.65E-04
		LTBI (83)/OD (83)	0.814 ± 0.054	0.871 ± 0.054	0.869 ± 0.058	0.878 ± 0.039	0.025	0.048	0.008
		LTBI (83)/OD-HIV (92)	0.842 ± 0.050	0.924 ± 0.032	0.921 ± 0.024	0.947 ± 0.022	0.001	0.002	3.65E-04
		LTBI-HIV (84)/OD (83)	0.861 ± 0.060	0.913 ± 0.045	0.877 ± 0.057	0.905 ± 0.038	0.031	0.700	0.140
		LTBI-HIV (84)/OD-HIV (92)	0.868 ± 0.048	0.774 ± 0.039	0.875 ± 0.050	0.894 ± 0.034	0.001	0.791	0.257
		LTBI-HIV (84)/LTBI (83)	0.589 ± 0.072	0.873 ± 0.032	0.872 ± 0.039	0.873 ± 0.036	4.90E-04	6.39E-04	3.65E-04
GSE107991	United Kingdom	TB (21)/Control (12)	The SD was not sufficiently estimated	The SD was not sufficiently estimated	The SD was not sufficiently estimated	The SD was not sufficiently estimated	NA	NA	NA
		TB/LTBI (21)	The SD was not	The SD was not	0.850 ± 0.106	The SD was not	NA	NA	NA

(Continued)

TABLE 2 Continued

Dataset	Country	Comparison (number of patients)	AUC ± SD				FDR (Wilcoxon Rank Sum Test)		
			10-lipid-gene	Long10	RISK6	Sambarey10	Long10 *versus* 10-lipid-gene	RISK6 *versus* 10-lipid-gene	Sambarey10 *versus* 10-lipid-gene
			sufficiently estimated	sufficiently estimated		sufficiently estimated			
		LTBI (21)/ Control (12)	The SD was not sufficiently estimated	0.678 ± 0.128	0.756 ± 0.160	0.717 ± 0.149	NA	NA	NA
GSE107994	United Kingdom	TB (43)/ Control (10)	The SD was not sufficiently estimated	The SD was not sufficiently estimated	The SD was not sufficiently estimated	The SD was not sufficiently estimated	NA	NA	NA
		TB (43)/LTBI (45)	0.792 ± 0.067	0.904 ± 0.066	0.910 ± 0.066	0.912 ± 0.053	0.006	0.006	0.004
		LTBI (45)/ Control (10)	0.579 ± 0.091	0.697 ± 0.107	0.615 ± 0.088	0.636 ± 0.117	0.021	0.519	0.288
GSE101705	India	TB (28)/LTBI (16)	The SD was not sufficiently estimated	The SD was not sufficiently estimated	The SD was not sufficiently estimated	The SD was not sufficiently estimated	NA	NA	NA
GSE42825, GSE42826, GSE42830*¶#	United Kingdom, France	TB (35)/ Control (113)	0.961 ± 0.027	The SD was not sufficiently estimated	The SD was not sufficiently estimated	The SD was not sufficiently estimated	NA	NA	NA
		TB (35)/ Active SARC (39)	0.680 ± 0.079	0.803 ± 0.068	0.785 ± 0.076	0.859 ± 0.074	*0.004*	0.014	*9.95E-04*
		TB (35)/Non-active SARC (22)	0.877 ± 0.064	The SD was not sufficiently estimated	0.975 ± 0.024	The SD was not sufficiently estimated	NA	0.001	NA
		TB (35)/ Cancer (16)	0.693 ± 0.076	The SD was not sufficiently estimated	0.887 ± 0.144	The SD was not sufficiently estimated	NA	0.018	NA
		TB (35)/PNA (14)	0.760 ± 0.139	The SD was not sufficiently estimated	0.930 ± 0.057	The SD was not sufficiently estimated	NA	0.013	NA

AUC, Area under the receiver operating characteristic curve; SD, standard deviation calculated from the 10-fold nested cross-validation; FDR, False Discovery Rate; TB, Tuberculosis (without HIV); HIV, Human Immunodeficiency Virus; TB-HIV, Tuberculosis with HIV; LTBI, Latent tuberculosis infection (without HIV); LTBI-HIV, Latent tuberculosis infection with HIV; OD, Other diseases (without HIV); OD-HIV, Other diseases with HIV; SARC, Sarcoidosis (without HIV); Cancer, Lung cancer (without HIV); PNA, Pneumonia (without HIV).
Italic value: raw P-value was used instead of FDR.
*The Long10 signature could not be fully retrieved from this dataset.
¶The 10-lipid-gene signature could not be fully retrieved from this dataset.
The RISK6 signature could not be fully retrieved from this dataset.
NA, Not available.

0.079) and excellent performance in distinguishing between TB and non-active SARC (AUC = 0.877 ± 0.064) (Figures 6H, I). Other comparisons yielded acceptable accuracy (TB *versus* Cancer, AUC = 0.693 ± 0.076) or insignificant classification with a high variability (TB *versus* PNA, AUC = 0.760 ± 0.139) (Figures 6J, K).

The results from the comparison between TB-HIV and non-TB–non-HIV groups did not show strong evidence against a random guess (the ROC crossed the diagonal line) (Figure 6L). In contrast, the logistic regression classifier differentiated TB-HIV from non-TB-HIV with good accuracy (AUC = 0.762 ± 0.121) (Figure 6M). The performance of classifier in comparing the TB-HIV group with the OD (AUC = 0.776 ± 0.062), OD-HIV (AUC = 0.601 ± 0.045), LTBI (AUC = 0.833 ± 0.054), and LTBI-HIV (AUC = 0.813 ± 0.037) was comparable to that for the comparison of the TB-only group with these groups (Figures 6N–Q). Noticeably, the model could distinguish between TB and TB-HIV in GSE37250 with acceptable performance (AUC = 0.650 ± 0.057) (Figure 6R). Nevertheless, the results from the same comparison in E-MTAB-8290 were insignificant with a high variability (AUC = 0.667 ± 0.142) (Table 2). Additionally, the 10-lipid-gene signature exhibited an

excellent ability to differentiate LTBI with OD (AUC = 0.814 ± 0.054) and OD-HIV (AUC = 0.842 ± 0.050) in the GSE37250 cohort (Table 2). Similar results were observed for the comparisons of LTBI-HIV with OD (AUC = 0.861 ± 0.060) and OD-HIV (AUC = 0.868 ± 0.048) (Table 2). The classifications between LTBI and healthy control (AUC = 0.579 ± 0.091) as well as LTBI-HIV and LTBI (AUC = 0.589 ± 0.072) were insignificant due to their high variability.

Where applicable, the diagnostic performance of the 10-lipid-gene signature was compared with that of other signatures (Table 2). In brief, the performance of the 10-lipid-gene signature was significantly poorer than that of the other signatures in most datasets. Nevertheless, the performance of the 10-lipid-gene signature was comparable to that of the RISK6 and Sambery10 signatures for certain comparisons in E-MTAB-8290, GSE37250, and GSE107994. They were TB with or without HIV *versus* non-TB-HIV in E-MTAB-8290, LTBI-HIV versus OD with or without HIV in GSE37250, and LTBI versus healthy control in GSE107994. Taken together, our results demonstrate the potential usefulness of the 10-lipid-gene signature for TB diagnosis in certain scenarios.

4 Discussion

The implementation of the WHO End TB strategy requires concerted efforts from the global scientific community to end the TB epidemic. A key focus area is the development of new tools for TB diagnosis, treatment monitoring, vaccine development, and therapeutic discovery. In recent years, host-based transcriptomic biosignature for TB diagnosis and treatment monitoring has been endorsed by scientific communities (13, 32, 36, 66–68). TB entails a spectrum of pathophysiological processes from the infection to the treatment completion stage (36), including inflammatory, interferon, immune, and T- and B-cell pathways (28, 69, 70). These pathophysiological events and molecular abnormalities can be evaluated by transcriptomics (70). Furthermore, although the interindividual variability of host responses is high, transcriptome-based signatures may display stable patterns during TB treatment, making them potential for treatment monitoring (71). Focusing on genes with clear patterns of changes during anti-TB treatment would help to discover relevant biomarkers, which together may form a robust predictive signature (72). In the present study, we evaluated lipid-related genes because previous studies have demonstrated the host immunological responses and lipidome alterations in TB and during anti-TB treatment (26, 27). Additionally, a knowledge-based and targeted approach derived from functional interpretation and mechanistic understanding may overcome the challenges of an entirely data-driven approach (16). These challenges include limited sample sizes, differences in the design of available data sets, the high-dimensional nature of transcriptomics data, and the lack of validation of particular signatures (9).

We employed a workflow that combined data-driven and knowledge-based approaches to investigate the expression of lipid-related genes during anti-TB treatment and its potential application for TB diagnosis in diverse clinical settings. A 10-lipid-gene signature showing clear changes during anti-TB treatment was established using time-course regression analysis. The potential usefulness of this signature for treatment monitoring was compared with that of three other signatures (*i.e.*, RISK6, Sambarey10, and our previously reported Long10 signature) in three cohorts using GSVA. GSVA provides a direct way for a head-to-head comparison between different signatures. Wang et al. found that scores for signatures obtained with gene set enrichment methods could differentiate between active TB and other clinical conditions with equivalent or better accuracy than could conventional methods (73). The GSVA scores for all four signatures differed significantly in investigated cohorts, perhaps because of the inclusion of genes playing a critical role in TB immune-signaling pathways. The 10-lipid-gene signature generally showed poor results when classifying different TB treatment states. However, its performance was not far behind RISK6 and Sambarey10 signatures. Only the Long10 signature exhibited acceptable performance in all investigated datasets. It is worth noting that, among all longitudinal validating datasets, the shortest time point was after one week of treatment (GSE89403), and the minimum sample size was 29 TB patients with samples collected from three time points for each patient (GSE181143 – subset from Brazil). Among 10-lipid-gene signature, some genes are found on immune cells, such as monocytes (e.g., *ARPC5*), neutrophils (e.g., *MBOAT1*, *MBOAT2*), lymphocytes (e.g., *ARPC5*), dendritic cells (e.g., *PLD4*) (65, 74–77). The expression level of these genes on immune cells as well as the frequency of cell source population could lead to difference of performance between the investigated datasets. Overall, the benchmark analysis results highlighted the role of lipid-related genes in TB pathophysiology. Nevertheless, the 10-lipid-gene signature has certain limitations and may not be the optimal choice for accurate monitoring of the anti-TB treatment response. Our results reinforced the usefulness of gene signatures related to the immune response for anti-TB treatment monitoring.

The usefulness of the 10-lipid-gene signature for the differentiation of active TB and non-TB counterparts was investigated in multiple clinical cohorts. In multiple comparisons, GSVA scores for the 10-lipid-gene signature were higher in the TB group than in other groups, with a remarkable ability to differentiate the TB and LTBI groups in all tested cohorts. These also indicated the association between the activation of lipid-related genes with TB disease. However, the performance of the 10-lipid-gene signature was generally not as excellent as other signatures because the expression of lipid-related genes changed only subtly. The caution should also be made since the OD group consisted of multiple respiratory diseases, which might introduce bias into the analysis (31). Consistent with the GSVA scores, the logistic regression classifier based on the 10-lipid-gene signature performed well in differentiating patients with TB from non-TB controls and those with LTBI (with or without HIV), and non-active SARC. The 10-lipid-gene signature had the best results for distinguishing TB from healthy controls. Noticeably, the good performance of the 10-lipid-gene signature in differentiating between TB and non-TB controls,

healthy controls, LTBI, non-active SARC but not between TB and OD, active SARC, lung cancer, PNA indicates its limited capacity for TB differential diagnosis. The results are consistent with our previous investigations of lipid and lipid-related genes to diagnose active TB disease (26). Host lipids play a vital role in the immune response to TB infection. Our findings further confirm the role of lipid-related genes in the dysregulated host metabolism and immune signaling during TB activation relative to LTBI. Of note, the TB and TB-HIV groups could not be classified significantly across all cohorts, possibly due to heterogeneity among cohorts and relatively small sample sizes in the tested datasets. For instance, the status of antiretroviral therapy, which can alter the transcriptome of HIV patients (78), differs across cohorts and may partially contribute to variations in the performance of the signatures. Besides, similar shortcomings associated with small sample sizes for biomarker validation have been reported in other biomarker studies, such as RISK4 and RISK6 (36, 79). The 10-lipid-gene signature displayed unsatisfactory performance in differentiating patients with LTBI from healthy controls, concordant with the fact that metabolomes and lipidomes are similar between these groups (80). Overall, the 10-lipid-gene signature exhibited the potential to be used for further optimization of TB diagnosis.

At the current setup of biosignature, metabolism-centric biomarkers may not outperform other leading signatures. However, individual biomarkers reported in our work could be strong candidates to be considered when establishing a biosignature that takes into account the metabolic alterations during TB treatment. We provided proof-of-concept results regarding the potential of lipid biomarkers (27). These findings collectively demonstrate that metabolism-centric biomarkers could be a significant aspect to be explored further in addition to approaches targeting immunological processes.

The biological relevance of derived biosignature must be examined thoroughly due to its significance. The products encoded by the 10 candidate genes are involved in multiple immune processes (Table 1). For instance, subunit 5 of actin-related protein 2/3 complex, encoded by *ARPC5*, involves in the entry of *Mtb* into lung epithelial cells (81) as well as lymphocyte activation, adhesion, and migration, which are hallmarks of the TB pathophysiology (82–84). ACSL4 regulates ferroptosis by modulating the cellular lipidome (52). Furthermore, *ACSL4* was found to be overexpressed in anti-TB drug-induced liver injury, indicating ferroptosis induction during anti-TB treatment (85). *PLD4* is differentially expressed in patients with TB (27). Phospholipase D activation is associated closely with *Mtb* phagocytosis by macrophages (86). During the early stages of TB infection, *Mtb* inhibits phagosome maturation and acidification by various bacterial factors (87, 88). As the treatment progression with *Mtb* elimination, this inhibition is reduced. Additionally, the increase in the interferon-γ level during anti-TB treatment induces phagosome maturation in macrophages (89). The rise of phagocytosis could be associated with the elevation of *PLD4* gene expression during the TB treatment time course. Lysosomal acid lipase, encoded by *LIPA*, is involved in the maturation and function of immune cells via the regulation of FC and FFA levels (56). Interestingly, the rs1051338 and rs7922269 single-nucleotide polymorphisms of *LIPA* are associated with individual susceptibility to pulmonary TB (90). The CHMP2B protein is a subunit of the endosomal sorting complex required for transport III (ESCRT-III) (57). ESCRT-III is recruited and engaged with *Mtb* phagosomes, preventing *Mtb* release into the cytosol (91). *RAB5A* encodes a crucial small GTPase that regulates the fusion between bacteria-containing phagosomes (including *Mtb*) and cytoplasmic organelles (59), thereby influencing the ability of neutrophils to restrict pathogen spread (59, 60). Moreover, RAB5A is tightly involved in TB immune infiltration (92). The GABARAPL2 protein participates in the autophagy pathway an essential biological process that defends against intracellular microbes, including *Mtb* (61, 93). *Mtb*-dependent macrophage apoptosis requires phospholipase A2 group IVA, encoded by *PLA2G4A* (94). Phospholipase A2 group IVA is also responsible for the initial step in the arachidonic acid (AA) pathway, which involves the cleavage of AA from the sn-2 position of phospholipids in cell membranes (63). AA promotes the formation of eicosanoids, crucial inflammatory mediators (95). Interestingly, the two last components of our signature, MBOAT1 and MBOAT2, also regulate the free AA level through the arachidonate recycling process and relate to eicosanoids production (65, 95). AA-derived eicosanoids, including prostaglandins, leukotrienes, and lipoxins, can modulate the host response to *Mtb* infection (96, 97). Previous studies demonstrated the altered levels of eicosanoids in TB, TB with comorbid diabetes, and after TB treatment (98, 99). In general, the ten genes can be roughly categorized into three groups based on their associated immunological pathways. They are genes involved in apoptosis/phagocytosis/autophagy pathways (*CHMP2B*, *RAB5A*, *GABARAPL2*, *PLA2G4A*, *PLD4*), genes involved in AA/FFAs pathways (*PLA2G4A*, *MBOAT1*, *MBOAT2*, *LIPA*, *ACSL4*), and gene involves in lymphocyte migration (*ARPC5*). These findings suggest the existence of associations between lipid signaling and immune pathways.

This study has several limitations which should be assessed. Firstly, the biosignature was derived from a time-series analysis on a single cohort, which may limit the generalizability of the biosignature on diverse populations with heterogeneous backgrounds. We addressed the limitation by validating our signature in a cross-platform, multi-ethnic, multi-cohort scenario to demonstrate its applicability across diverse populations and settings. We further expanded the scope of our investigation beyond TB treatment monitoring to also include TB diagnostics, showcasing the flexibility of our signature. Furthermore, we conducted a head-to-head benchmarking analysis with other publicly available signatures to demonstrate the capacity of our signature. The second shortcoming is that we did not account for confounding factors during the time series analysis, which could potentially lead to false-positive signals. However, we mitigated this issue by adopting a targeted approach based on prior knowledge to minimize the number of false-positive findings. Thirdly, focusing on lipid-related genes, which exhibited subtle alteration between TB

and its counterparts (26), might limit the robustness of the signature. However, finding a signature with excellent performance is an aim but not the primary goal of this study. Our study was conducted to demonstrate the potential of lipid-related gene markers in TB management and suggest the direction for subsequent studies. Moreover, the identification of certain genes as potential candidates might be attributed to their high correlation with the "true" markers. Indeed, the partial overlap between signatures is frequently observed. The 10-lipid-gene biosignature also intersects one gene (*MBOAT2*) with the 558-gene signature representing the TB treatment response of Bloom et al. (35). However, to the best of our knowledge, the remaining nine genes were reported for the first time in our study. This finding implicates that there is still ample room for further research in discovering metabolism-centric biomarkers, particularly lipid-related genes. Last but not least, exploring the integration of lipid-related genes with other signatures to enhance their performance should be pursued in future investigations.

In the present study, we developed a biosignature based on key lipid-related genes that can be used to assist the management of TB. Our findings emphasize the crucial role of lipid metabolism in TB pathophysiology and treatment response. Additionally, the lipid-related genes have been implicated in the host immune response, highlighting the significant association between lipid metabolism and the immune system in TB. This association presents a promising target for the development of novel TB diagnostic and treatment monitoring strategies. It should be explored further to enhance our understanding and improve TB management.

Data availability statement

The original contributions presented in the study are included in the article/Supplementary Material. Further inquiries can be directed to the corresponding authors.

Author contributions

Conceptualization, SP, NL, DK, and J-GS; Investigation, NP and NL; Formal Analysis, NP, SP, NL, and NT; Writing – Original draft, NP, NA, NL, DK, and J-GS; Writing – Review & Editing, NP, NT, NA, NY, YL, HT, K-ML, SA, Y-SC, SP, NL, DK, and J-GS; Visualization, NP, NT, and NY, Data curation, NP, NT, NA, and NY; Methodology, NP, NT, NA, NY, YL, HT, K-ML, SA, Y-SC, SP, NL, DK, and J-GS; Validation, NP, NT, NA, NY, YL, HT, K-ML, SA, Y-SC, SP, NL, DK, and J-GS; Supervision, SP, NL, DK, and J-GS; Resources, J-GS; Funding acquisition, J-GS. All authors contributed to the article and approved the submitted version.

Funding

The National Research Foundation of Korea (NRF) grant funded by the Korean government (MSIT) (grant No. 2018R1A5A2021242) provided financial support for this study. The funders had no involvement in the study design, data collection, data analysis, interpretation, or development of the research content.

Acknowledgments

Figure 1 was created using biorender.com.

Conflict of interest

The authors declare that the research was conducted in the absence of any commercial or financial relationships that could be construed as a potential conflict of interest.

Publisher's note

All claims expressed in this article are solely those of the authors and do not necessarily represent those of their affiliated organizations, or those of the publisher, the editors and the reviewers. Any product that may be evaluated in this article, or claim that may be made by its manufacturer, is not guaranteed or endorsed by the publisher.

Supplementary material

The Supplementary Material for this article can be found online at: https://www.frontiersin.org/articles/10.3389/fimmu.2023.1210372/full#supplementary-material

References

1. World Health Organization. *Global tuberculosis report 2022*. Geneva, Switzerland: World Health Organization (2022).

2. Gill CM, Dolan L, Piggott LM, McLaughlin AM. New developments in tuberculosis diagnosis and treatment. *Breathe (Sheff)* (2022) 18(1):210149. doi: 10.1183/20734735.0149-2021

3. Lee A, Xie YL, Barry CE, Chen RY. Current and future treatments for tuberculosis. *BMJ* (2020) 368:m216. doi: 10.1136/bmj.m216

4. Sant´Anna FM, Araújo-Pereira M, Schmaltz CAS, Arriaga MB, de Oliveira RVC, Andrade BB, et al. Adverse drug reactions related to treatment of drug-susceptible tuberculosis in Brazil: A prospective cohort study. *Front Trop Dis* (2022) 2:748310. doi: 10.3389/fitd.2021.748310

5. Chung SJ, Byeon SJ, Choi JH. Analysis of adverse drug reactions to first-line anti-tuberculosis drugs using the Korea adverse event reporting system. *J Korean Med Sci* (2022) 37(16):e128. doi: 10.3346/jkms.2022.37.e128

6. van den Boogaard J, Kibiki GS, Kisanga ER, Boeree MJ, Aarnoutse RE. New drugs against tuberculosis: problems, progress, and evaluation of agents in clinical development. *Antimicrob Agents Chemother* (2009) 53(3):849–62. doi: 10.1128/AAC.00749-08

7. Volmink J, Garner P. Directly observed therapy for treating tuberculosis. *Cochrane Database Syst Rev* (2007) 4):CD003343. doi: 10.1002/14651858.CD003343.pub3

8. Horne DJ, Royce SE, Gooze L, Narita M, Hopewell PC, Nahid P, et al. Sputum monitoring during tuberculosis treatment for predicting outcome: systematic review and meta-analysis. *Lancet Infect Dis* (2010) 10(6):387–94. doi: 10.1016/S1473-3099(10)70071-2

9. Hamada Y, Penn-Nicholson A, Krishnan S, Cirillo DM, Matteelli A, Wyss R, et al. Are mRNA based transcriptomic signatures ready for diagnosing tuberculosis in the clinic? - A review of evidence and the technological landscape. *EBioMedicine* (2022) 82:104174. doi: 10.1016/j.ebiom.2022.104174

10. Zimmer AJ, Lainati F, Aguilera Vasquez N, Chedid C, McGrath S, Benedetti A, et al. Biomarkers that correlate with active pulmonary tuberculosis treatment response: a systematic review and meta-analysis. *J Clin Microbiol* (2022) 60(2):e0185921. doi: 10.1128/JCM.01859-21

11. Singhania A, Wilkinson RJ, Rodrigue M, Haldar P, O'Garra A. The value of transcriptomics in advancing knowledge of the immune response and diagnosis in tuberculosis. *Nat Immunol* (2018) 19(11):1159–68. doi: 10.1038/s41590-018-0225-9

12. Gupta RK, Turner CT, Venturini C, Esmail H, Rangaka MX, Copas A, et al. Concise whole blood transcriptional signatures for incipient tuberculosis: a systematic review and patient-level pooled meta-analysis. *Lancet Respir Med* (2020) 8(4):395–406. doi: 10.1016/S2213-2600(19)30282-6

13. Warsinske H, Vashisht R, Khatri P. Host-response-based gene signatures for tuberculosis diagnosis: A systematic comparison of 16 signatures. *PloS Med* (2019) 16(4):e1002786. doi: 10.1371/journal.pmed.1002786

14. MacLean E, Broger T, Yerlikaya S, Fernandez-Carballo BL, Pai M, Denkinger CM. A systematic review of biomarkers to detect active tuberculosis. *Nat Microbiol* (2019) 4(5):748–58. doi: 10.1038/s41564-019-0380-2

15. Bayaa R, Ndiaye MDB, Chedid C, Kokhreidze E, Tukvadze N, Banu S, et al. Multi-country evaluation of RISK6, a 6-gene blood transcriptomic signature, for tuberculosis diagnosis and treatment monitoring. *Sci Rep* (2021) 11(1):13646. doi: 10.1038/s41598-021-93059-1

16. Long NP, Phat NK, Yen NTH, Park S, Park Y, Cho YS, et al. A 10-gene biosignature of tuberculosis treatment monitoring and treatment outcome prediction. *Tuberculosis (Edinb)* (2021) 131:102138. doi: 10.1016/j.tube.2021.102138

17. Sambarey A, Devaprasad A, Mohan A, Ahmed A, Nayak S, Swaminathan S, et al. Unbiased identification of blood-based biomarkers for pulmonary tuberculosis by modeling and mining molecular interaction networks. *EBioMedicine* (2017) 15:112–26. doi: 10.1016/j.ebiom.2016.12.009

18. World Health Organization. *High priority target product profiles for new tuberculosis diagnostics: report of a consensus meeting, 28-29 April 2014*. Geneva, Switzerland: World Health Organization (2014).

19. Walsh CJ, Hu P, Batt J, Santos CCD. Microarray meta-analysis and cross-platform normalization: integrative genomics for robust biomarker discovery. *Microarrays (Basel)* (2015) 4(3):389–406. doi: 10.3390/microarrays4030389

20. Simon J, Evans, Akil H, Watson SJ. Analyzing gene expression in depression. *Am J Psychiatry* (2009) 166(9):961–3. doi: 10.1176/appi.ajp.2009.09060806

21. Dozmorov I, Lefkovits I. Internal standard-based analysis of microarray data. Part 1: analysis of differential gene expressions. *Nucleic Acids Res* (2009) 37(19):6323–39. doi: 10.1093/nar/gkp706%JNucleicAcidsResearch

22. Li Y, Ge X, Peng F, Li W, Li JJ. Exaggerated false positives by popular differential expression methods when analyzing human population samples. *Genome Biol* (2022) 23(1):79. doi: 10.1186/s13059-022-02648-4

23. Shi H, Zhou Y, Jia E, Pan M, Bai Y, Ge Q. Bias in RNA-seq library preparation: current challenges and solutions. *BioMed Res Int* (2021) 2021:6647597. doi: 10.1155/2021/6647597

24. Bernardi S, Marcuzzi A, Piscianz E, Tommasini A, Fabris B. The complex interplay between lipids, immune system and interleukins in cardio-metabolic diseases. *Int J Mol Sci* (2018) 19(12). doi: 10.3390/ijms19124058

25. Collins JM, Jones DP, Sharma A, Khadka M, Liu KH, Kempker RR, et al. TCA cycle remodeling drives proinflammatory signaling in humans with pulmonary tuberculosis. *PloS Pathog* (2021) 17(9):e1009941. doi: 10.1371/journal.ppat.1009941

26. Long NP, Anh NK, Yen NTH, Phat NK, Park S, Thu VTA, et al. Comprehensive lipid and lipid-related gene investigations of host immune responses to characterize metabolism-centric biomarkers for pulmonary tuberculosis. *Sci Rep* (2022) 12(1):13395. doi: 10.1038/s41598-022-17521-4

27. Anh NK, Phat NK, Yen NTH, Jayanti RP, Thu VTA, Park YJ, et al. Comprehensive lipid profiles investigation reveals host metabolic and immune alterations during anti-tuberculosis treatment: Implications for therapeutic monitoring. *BioMed Pharmacother* (2023) 158:114187. doi: 10.1016/j.biopha.2022.114187

28. Cliff JM, Lee JS, Constantinou N, Cho JE, Clark TG, Ronacher K, et al. Distinct phases of blood gene expression pattern through tuberculosis treatment reflect modulation of the humoral immune response. *J Infect Dis* (2013) 207(1):18–29. doi: 10.1093/infdis/jis499

29. Thompson EG, Du Y, Malherbe ST, Shankar S, Braun J, Valvo J, et al. Host blood RNA signatures predict the outcome of tuberculosis treatment. *Tuberculosis (Edinb)* (2017) 107:48–58. doi: 10.1016/j.tube.2017.08.004

30. Queiroz ATL, Vinhaes CL, Fukutani ER, Gupte AN, Kumar NP, Fukutani KF, et al. A multi-center, prospective cohort study of whole blood gene expression in the tuberculosis-diabetes interaction. *Sci Rep* (2023) 13(1):7769. doi: 10.1038/s41598-023-34847-9

31. Kaforou M, Wright VJ, Oni T, French N, Anderson ST, Bangani N, et al. Detection of tuberculosis in HIV-infected and -uninfected African adults using whole blood RNA expression signatures: a case-control study. *PloS Med* (2013) 10(10):e1001538. doi: 10.1371/journal.pmed.1001538

32. Turner CT, Gupta RK, Tsaliki E, Roe JK, Mondal P, Nyawo GR, et al. Blood transcriptional biomarkers for active pulmonary tuberculosis in a high-burden setting: a prospective, observational, diagnostic accuracy study. *Lancet Respir Med* (2020) 8(4):407–19. doi: 10.1016/S2213-2600(19)30469-2

33. Singhania A, Verma R, Graham CM, Lee J, Tran T, Richardson M, et al. A modular transcriptional signature identifies phenotypic heterogeneity of human tuberculosis infection. *Nat Commun* (2018) 9(1):2308. doi: 10.1038/s41467-018-04579-w

34. Leong S, Zhao Y, Joseph NM, Hochberg NS, Sarkar S, Pleskunas J, et al. Existing blood transcriptional classifiers accurately discriminate active tuberculosis from latent infection in individuals from south India. *Tuberculosis (Edinb)* (2018) 109:41–51. doi: 10.1016/j.tube.2018.01.002

35. Bloom CI, Graham CM, Berry MP, Rozakeas F, Redford PS, Wang Y, et al. Transcriptional blood signatures distinguish pulmonary tuberculosis, pulmonary sarcoidosis, pneumonias and lung cancers. *PloS One* (2013) 8(8):e70630. doi: 10.1371/journal.pone.0070630

36. Penn-Nicholson A, Mbandi SK, Thompson E, Mendelsohn SC, Suliman S, Chegou NN, et al. RISK6, a 6-gene transcriptomic signature of TB disease risk, diagnosis and treatment response. *Sci Rep* (2020) 10(1):8629. doi: 10.1038/s41598-020-65043-8

37. Gautier L, Cope L, Bolstad BM, Irizarry RA. affy–analysis of Affymetrix GeneChip data at the probe level. *Bioinformatics* (2004) 20(3):307–15. doi: 10.1093/bioinformatics/btg405

38. Du P, Kibbe WA, Lin SM. lumi: a pipeline for processing Illumina microarray. *Bioinformatics* (2008) 24(13):1547–8. doi: 10.1093/bioinformatics/btn224

39. Johnson WE, Li C, Rabinovic A. Adjusting batch effects in microarray expression data using empirical Bayes methods. *Biostatistics* (2007) 8(1):118–27. doi: 10.1093/biostatistics/kxj037

40. Leek JT, Johnson WE, Parker HS, Jaffe AE, Storey JD. The sva package for removing batch effects and other unwanted variation in high-throughput experiments. *Bioinformatics* (2012) 28(6):882–3. doi: 10.1093/bioinformatics/bts034

41. Manimaran S, Selby HM, Okrah K, Ruberman C, Leek JT, Quackenbush J, et al. BatchQC: interactive software for evaluating sample and batch effects in genomic data. *Bioinformatics* (2016) 32(24):3836–8. doi: 10.1093/bioinformatics/btw538

42. Zhang Y, Parmigiani G, Johnson WE. ComBat-seq: batch effect adjustment for RNA-seq count data. *NAR genom Bioinform* (2020) 2(3):lqaa078. doi: 10.1093/nargab/lqaa078

43. Love MI, Huber W, Anders S. Moderated estimation of fold change and dispersion for RNA-seq data with DESeq2. *Genome Biol* (2014) 15(12):550. doi: 10.1186/s13059-014-0550-8

44. Hänzelmann S, Castelo R, Guinney J. GSVA: gene set variation analysis for microarray and RNA-Seq data. *BMC Bioinf* (2013) 14(1):7. doi: 10.1186/1471-2105-14-7

45. Gu Z, Eils R, Schlesner M. Complex heatmaps reveal patterns and correlations in multidimensional genomic data. *Bioinformatics* (2016) 32(18):2847–9. doi: 10.1093/bioinformatics/btw313

46. Conesa A, Nueda MJ, Ferrer A, Talón M. maSigPro: a method to identify significantly differential expression profiles in time-course microarray experiments. *Bioinformatics* (2006) 22(9):1096–102. doi: 10.1093/bioinformatics/btl056

47. Pang Z, Chong J, Zhou G, de Lima Morais DA, Chang L, Barrette M, et al. MetaboAnalyst 5.0: narrowing the gap between raw spectra and functional insights. *Nucleic Acids Res* (2021) 49(W1):W388–W96. doi: 10.1093/nar/gkab382

48. Kuhn M. Building predictive models in R using the caret package. *J Stat Softw* (2008) 28(5):1–26. doi: 10.18637/jss.v028.i05

49. Zhao P, Han H, Wu X, Wu J, Ren Z. ARP2/3 regulates fatty acid synthesis by modulating lipid droplets' Motility. *Int J Mol Sci* (2022) 23(15). doi: 10.3390/ijms23158730

50. Herdoiza Padilla E, Crauwels P, Bergner T, Wiederspohn N, Förstner S, Rinas R, et al. mir-124-5p regulates phagocytosis of human macrophages by targeting the actin cytoskeleton *via* the ARP2/3 complex. *Front Immunol* (2019) 10:2210. doi: 10.3389/fimmu.2019.02210

51. Zhang Y, Shen H, Liu H, Feng H, Liu Y, Zhu X, et al. Arp2/3 complex controls T cell homeostasis by maintaining surface TCR levels *via* regulating TCR + endosome trafficking. *Sci Rep* (2017) 7(1):8952. doi: 10.1038/s41598-017-08357-4

52. Doll S, Proneth B, Tyurina YY, Panzilius E, Kobayashi S, Ingold I, et al. ACSL4 dictates ferroptosis sensitivity by shaping cellular lipid composition. *Nat Chem Biol* (2017) 13(1):91–8. doi: 10.1038/nchembio.2239

53. Padanad MS, Konstantinidou G, Venkateswaran N, Melegari M, Rindhe S, Mitsche M, et al. Fatty acid oxidation mediated by acyl-coA synthetase long chain 3 is required for mutant KRAS lung tumorigenesis. *Cell Rep* (2016) 16(6):1614–28. doi: 10.1016/j.celrep.2016.07.009

54. Gao L, Zhou Y, Zhou SX, Yu XJ, Xu JM, Zuo L, et al. PLD4 promotes M1 macrophages to perform antitumor effects in colon cancer cells. *Oncol Rep* (2017) 37 (1):408–16. doi: 10.3892/or.2016.5216

55. Otani Y, Yamaguchi Y, Sato Y, Furuichi T, Ikenaka K, Kitani H, et al. PLD4 is involved in phagocytosis of microglia: expression and localization changes of PLD4 are correlated with activation state of microglia. *PloS One* (2011) 6(11):e27544. doi: 10.1371/journal.pone.0027544

56. Gomaraschi M, Bonacina F, Norata GD. Lysosomal acid lipase: from cellular lipid handler to immunometabolic target. *Trends Pharmacol Sci* (2019) 40(2):104–15. doi: 10.1016/j.tips.2018.12.006

57. Alqabandi M, de Franceschi N, Maity S, Miguet N, Bally M, Roos WH, et al. The ESCRT-III isoforms CHMP2A and CHMP2B display different effects on membranes upon polymerization. *BMC Biol* (2021) 19(1):66. doi: 10.1186/s12915-021-00983-9

58. Jorgensen JR, Tei R, Baskin JM, Michel AH, Kornmann B, Emr SD. ESCRT-III and ER-PM contacts maintain lipid homeostasis. *Mol Biol Cell* (2020) 31(12):1302–13. doi: 10.1091/mbc.E20-01-0061

59. Weiss G, Schaible UE. Macrophage defense mechanisms against intracellular bacteria. *Immunol Rev* (2015) 264(1):182–203. doi: 10.1111/imr.12266

60. Alvarez-Dominguez C, Stahl PD. Increased expression of rab5a correlates directly with accelerated maturation of listeria monocytogenesPhagosomes*. *JBC* (1999) 274(17):11459–62. doi: 10.1074/jbc.274.17.11459

61. Xie Y, Li J, Kang R, Tang D. Interplay between lipid metabolism and autophagy. *Front Cell Dev Biol* (2020) 8:431. doi: 10.3389/fcell.2020.00431

62. Eck F, Phuyal S, Smith MD, Kaulich M, Wilkinson S, Farhan H, et al. ACSL3 is a novel GABARAPL2 interactor that links ufmylation and lipid droplet biogenesis. *J Cell Sci* (2020) 133(18). doi: 10.1242/jcs.243477

63. Grkovich A, Armando A, Quehenberger O, Dennis EA. TLR-4 mediated group IVA phospholipase A2 activation is phosphatidic acid phosphohydrolase 1 and protein kinase C dependent. *Biochim Biophys Acta Mol Cell Biol Lipids* (2009) 1791(10):975–82. doi: 10.1016/j.bbalip.2009.02.002

64. Gubern A, Casas J, Barcelo-Torns M, Barneda D, de la Rosa X, Masgrau R, et al. Group IVA phospholipase A2 is necessary for the biogenesis of lipid droplets. *J Biol Chem* (2008) 283(41):27369–82. doi: 10.1074/jbc.M800696200

65. Gijon MA, Riekhof WR, Zarini S, Murphy RC, Voelker DR. Lysophospholipid acyltransferases and arachidonate recycling in human neutrophils. *J Biol Chem* (2008) 283(44):30235–45. doi: 10.1074/jbc.M806194200

66. Heyckendorf J, Georghiou SB, Frahm N, Heinrich N, Kontsevaya I, Reimann M, et al. Tuberculosis treatment monitoring and outcome measures: new interest and new strategies. *Clin Microbiol Rev* (2022) 35(3):e0022721. doi: 10.1128/cmr.00227-21

67. Warsinske HC, Rao AM, Moreira FMF, Santos PCP, Liu AB, Scott M, et al. Assessment of validity of a blood-based 3-gene signature score for progression and diagnosis of tuberculosis, disease severity, and treatment response. *JAMA Netw Open* (2018) 1(6):e183779. doi: 10.1001/jamanetworkopen.2018.3779

68. Hoang LT, Jain P, Pillay TD, Tolosa-Wright M, Niazi U, Takwoingi Y, et al. Transcriptomic signatures for diagnosing tuberculosis in clinical practice: a prospective, multicentre cohort study. *Lancet Infect Dis* (2021) 21(3):366–75. doi: 10.1016/S1473-3099(20)30928-2

69. Cliff JM, Kaufmann SH, McShane H, van Helden P, O'Garra A. The human immune response to tuberculosis and its treatment: a view from the blood. *Immunol Rev* (2015) 264(1):88–102. doi: 10.1111/imr.12269

70. Maertzdorf J, Kaufmann SH, Weiner J 3rd. Toward a unified biosignature for tuberculosis. *Cold Spring Harb Perspect Med* (2014) 5(1):a018531. doi: 10.1101/cshperspect.a018531

71. Cadena AM, Fortune SM, Flynn JL. Heterogeneity in tuberculosis. *Nat Rev Immunol* (2017) 17(11):691–702. doi: 10.1038/nri.2017.69

72. Vargas R, Abbott L, Frahm N, Yu W-H. Common gene signature model discovery and systematic validation for TB prognosis and response to treatment. *bioRxiv* (2022) 2022:11.28.518302. doi: 10.1101/2022.11.28.518302

73. Wang X, VanValkenberg A, Odom-Mabey AR, Ellner JJ, Hochberg NS, Salgame P, et al. Comparison of gene set scoring methods for reproducible evaluation of multiple tuberculosis gene signatures. *bioRxiv* (2023) 2023:1.19.520627. doi: 10.1101/2023.01.19.520627

74. Gavin AL, Huang D, Huber C, Martensson A, Tardif V, Skog PD, et al. PLD3 and PLD4 are single-stranded acid exonucleases that regulate endosomal nucleic-acid sensing. *Nat Immunol* (2018) 19(9):942–53. doi: 10.1038/s41590-018-0179-y

75. Sadhu L, Tsopoulidis N, Hasanuzzaman M, Laketa V, Way M, Fackler OT. ARPC5 isoforms and their regulation by calcium-calmodulin-N-WASP drive distinct Arp2/3-dependent actin remodeling events in CD4 T cells. *Elife* (2023) 12. doi: 10.7554/eLife.82450

76. Ming Y, Luo C, Ji B, Cheng J. ARPC5 acts as a potential prognostic biomarker that is associated with cell proliferation, migration and immune infiltrate in gliomas. *BMC Cancer* (2023) 23(1):937. doi: 10.1186/s12885-023-11433-w

77. Huang S, Sun L, Hou P, Liu K, Wu J. A comprehensively prognostic and immunological analysis of actin-related protein 2/3 complex subunit 5 in pan-cancer and identification in hepatocellular carcinoma. *Front Immunol* (2022) 13:944898. doi: 10.3389/fimmu.2022.944898

78. Zhao F, Ma J, Huang L, Deng Y, Li L, Zhou Y, et al. Comparative transcriptome analysis of PBMC from HIV patients pre- and post-antiretroviral therapy. *Meta Gene* (2017) 12:50–61. doi: 10.1016/j.mgene.2017.01.004

79. Suliman S, Thompson EG, Sutherland J, Weiner J 3rd, Ota MOC, Shankar S, et al. Four-gene pan-African blood signature predicts progression to tuberculosis. *Am J Respir Crit Care Med* (2018) 197(9):1198–208. doi: 10.1164/rccm.201711-2340OC

80. Cho Y, Park Y, Sim B, Kim J, Lee H, Cho S-N, et al. Identification of serum biomarkers for active pulmonary tuberculosis using a targeted metabolomics approach. *Sci Rep* (2020) 10(1):3825. doi: 10.1038/s41598-020-60669-0

81. Wen D, Cui J, Li P, Xiong Q, Chen G, Wu C. Syndecan-4 assists Mycobacterium tuberculosis entry into lung epithelial cells by regulating the Cdc42, N-WASP, and Arp2/3 signaling pathways. *Microbes Infect* (2022) 24(4):104931. doi: 10.1016/j.micinf.2022.104931

82. Sun J, Zhong X, Fu X, Miller H, Lee P, Yu B, et al. The actin regulators involved in the function and related diseases of lymphocytes. *Front Immunol* (2022) 13:799309. doi: 10.3389/fimmu.2022.799309

83. Wu YE, Zhang SW, Peng WG, Li KS, Li K, Jiang JK, et al. Changes in lymphocyte subsets in the peripheral blood of patients with active pulmonary tuberculosis. *J Int Med Res* (2009) 37(6):1742–9. doi: 10.1177/147323000903700610

84. Feng L, Li L, Liu Y, Qiao D, Li Q, Fu X, et al. B lymphocytes that migrate to tuberculous pleural fluid *via* the SDF-1/CXCR4 axis actively respond to antigens specific for Mycobacterium tuberculosis. *Eur J Immunol* (2011) 41(11):3261–9. doi: 10.1002/eji.201141625

85. Pan Y, Tang P, Cao J, Song Q, Zhu L, Ma S, et al. Lipid peroxidation aggravates anti-tuberculosis drug-induced liver injury: Evidence of ferroptosis induction. *Biochem Biophys Res Commun* (2020) 533(4):1512–8. doi: 10.1016/j.bbrc.2020.09.140

86. Kusner DJ, Hall CF, Schlesinger LS. Activation of phospholipase D is tightly coupled to the phagocytosis of Mycobacterium tuberculosis or opsonized zymosan by human macrophages. *J Exp Med* (1996) 184(2):585–95. doi: 10.1084/jem.184.2.585

87. Carranza C, Chavez-Galan L. Several routes to the same destination: inhibition of phagosome-lysosome fusion by mycobacterium tuberculosis. *AJMS* (2019) 357 (3):184–94. doi: 10.1016/j.amjms.2018.12.003

88. Zhai W, Wu F, Zhang Y, Fu Y, Liu Z. The immune escape mechanisms of mycobacterium tuberculosis. *Int J Mol Sci* (2019) 20(2). doi: 10.3390/ijms20020340

89. Maphasa RE, Meyer M, Dube A. The macrophage response to mycobacterium tuberculosis and opportunities for autophagy inducing nanomedicines for tuberculosis therapy. *Front Cell Infect Microbiol* (2020) 10:618414. doi: 10.3389/fcimb.2020.618414

90. Kabuye D, Ndibalema A. Lysosomal acid lipase gene single nucleotide polymorphism and pulmonary tuberculosis susceptibility. *Indian J Tuberc* (2021) 68 (2):179–85. doi: 10.1016/j.ijtb.2020.07.030

91. Mittal E, Skowyra ML, Uwase G, Tinaztepe E, Mehra A, Koster S, et al. Mycobacterium tuberculosis type VII secretion system effectors differentially impact the ESCRT endomembrane damage response. *mBio* (2018) 9(6):e01765–18. doi: 10.1128/mBio.01765-18

92. Xiao S, Zhou T, Pan J, Ma X, Shi G, Jiang B, et al. Identifying autophagy-related genes as potential targets for immunotherapy in tuberculosis. *Int Immunopharmacol* (2023) 118:109956. doi: 10.1016/j.intimp.2023.109956

93. Deretic V. Autophagy in tuberculosis. *Cold Spring Harb Perspect Med* (2014) 4 (11):a018481. doi: 10.1101/cshperspect.a018481

94. Duan L, Gan H, Arm J, Remold HG. Cytosolic phospholipase A2 participates with TNF-alpha in the induction of apoptosis of human macrophages infected with Mycobacterium tuberculosis H37Ra. *J Immunol* (2001) 166(12):7469–76. doi: 10.4049/jimmunol.166.12.7469

95. Higgins AJ, Lees P. The acute inflammatory process, arachidonic acid metabolism and the mode of action of anti-inflammatory drugs. *Equine Vet J* (1984) 16(3):163–75. doi: 10.1111/j.2042-3306.1984.tb01893.x

96. Bafica A, Scanga CA, Serhan C, MaChado F, White S, Sher A, et al. Host control of Mycobacterium tuberculosis is regulated by 5-lipoxygenase-dependent lipoxin production. *J Clin Invest* (2005) 115(6):1601–6. doi: 10.1172/JCI23949

97. Tobin DM, Roca FJ, Oh SF, McFarland R, Vickery TW, Ray JP, et al. Host genotype-specific therapies can optimize the inflammatory response to mycobacterial infections. *Cell* (2012) 148(3):434–46. doi: 10.1016/j.cell.2011.12.023

98. Mayer-Barber KD, Andrade BB, Oland SD, Amaral EP, Barber DL, Gonzales J, et al. Host-directed therapy of tuberculosis based on interleukin-1 and type I interferon crosstalk. *Nature* (2014) 511(7507):99–103. doi: 10.1038/nature13489

99. Pavan Kumar N, Moideen K, Nancy A, Viswanathan V, Shruthi BS, Shanmugam S, et al. Plasma eicosanoid levels in tuberculosis and tuberculosis-diabetes co-morbidity are associated with lung pathology and bacterial burden. *Front Cell Infect Microbiol* (2019) 9:335. doi: 10.3389/fcimb.2019.00335

frontiers | Frontiers in Immunology

TYPE Original Research
PUBLISHED 06 December 2023
DOI 10.3389/fimmu.2023.1307429

OPEN ACCESS

EDITED BY
Zhidong Hu,
Fudan University, China

REVIEWED BY
Gurpreet Kaur,
Institute of Microbial Technology (CSIR), India
Mohammad Aqdas,
National Institutes of Health (NIH), United States

*CORRESPONDENCE
María García-Bengoa
Maria.Garcia.Bengoa@tiho-hannover.de

†These authors have contributed equally to this work

RECEIVED 04 October 2023
ACCEPTED 21 November 2023
PUBLISHED 06 December 2023

CITATION
García-Bengoa M, Vergara EJ, Tran AC, Bossi L, Cooper AM, Pearl JE, Mussá T, von Köckritz-Blickwede M, Singh M and Reljic R (2023) Immunogenicity of PE18, PE31, and PPE26 proteins from *Mycobacterium tuberculosis* in humans and mice.
Front. Immunol. 14:1307429.
doi: 10.3389/fimmu.2023.1307429

Immunogenicity of PE18, PE31, and PPE26 proteins from *Mycobacterium tuberculosis* in humans and mice

María García-Bengoa[1,2,3*†], Emil Joseph Vergara[4†], Andy C. Tran[4†], Lorenzo Bossi[5], Andrea M. Cooper[6], John E. Pearl[6], Tufária Mussá[7], Maren von Köckritz-Blickwede[1,2], Mahavir Singh[3] and Rajko Reljic[4]

[1]Institute of Biochemistry, University of Veterinary Medicine Hannover, Hannover, Germany, [2]Research Center for Emerging Infections and Zoonosis (RIZ), University of Veterinary Medicine Hannover, Hannover, Germany, [3]LIONEX Diagnostics and Therapeutics GmbH, Braunschweig, Germany, [4]Institute for Infection and Immunity, St. George's University of London, London, United Kingdom, [5]Immunxperts SA, a Q[2] Solutions Company, Gosselies, Belgium, [6]Department of Infection, Immunity and Inflammation, University of Leicester, Leicester, United Kingdom, [7]Department of Microbiology, Faculty of Medicine, Eduardo Mondlane University, Maputo, Mozambique

Introduction: The large family of PE and PPE proteins accounts for as much as 10% of the genome of *Mycobacterium tuberculosis*. In this study, we explored the immunogenicity of three proteins from this family, PE18, PE31, and PPE26, in humans and mice.

Methods: The investigation involved analyzing the immunoreactivity of the selected proteins using sera from TB patients, IGRA-positive household contacts, and IGRA-negative BCG vaccinated healthy donors from the TB endemic country Mozambique. Antigen-recall responses were examined in PBMC from these groups, including the evaluation of cellular responses in healthy unexposed individuals. Moreover, systemic priming and intranasal boosting with each protein, combined with the Quil-A adjuvant, were conducted in mice.

Results: We found that all three proteins are immunoreactive with sera from TB patients, IGRA-positive household contacts, and IGRA-negative BCG vaccinated healthy controls. Likewise, antigen-recall responses were induced in PBMC from all groups, and the proteins stimulated proliferation of peripheral blood mononuclear cells from healthy unexposed individuals. In mice, all three antigens induced IgG antibody responses in sera and predominantly IgG, rather than IgA, responses in bronchoalveolar lavage. Additionally, CD4+ and CD8+ effector memory T cell responses were observed in the spleen, with PE18 demonstrating the ability to induce tissue-resident memory T cells in the lungs.

Discussion: Having demonstrated immunogenicity in both humans and mice, the protective capacity of these antigens was evaluated by challenging immunized mice with low-dose aerosol of *Mycobacterium tuberculosis* H37Rv. The *in vitro* Mycobacterial Growth Inhibition Assay (MGIA) and assessment of viable bacteria in the lung did not demonstrate any ability of the vaccination protocol to reduce bacterial growth. We therefore concluded that these three specific PE/PPE proteins, while immunogenic in both humans and mice, were unable to confer protective immunity under these conditions.

KEYWORDS

tuberculosis, PE18, PE31, PPE26, antigens, vaccine, immunity

Introduction

Tuberculosis (TB) is a contagious infectious disease caused by *Mycobacterium tuberculosis* (Mtb). TB remains a significant public health issue globally, with nearly one-quarter of the world's population infected with Mtb, and around 10.6 million new cases with 1.6 million deaths in 2021 (1). The rise of drug-resistant strains of Mtb has further complicated treatment efforts. Additionally, the *Bacillus Calmette-Guérin* (BCG) vaccine, the only licensed TB vaccine, although providing partial protection against disseminated forms of TB in children, has limited efficacy in preventing pulmonary TB in adults (1–3). Furthermore, BCG appears to be less effective in areas of the world with higher prevalence of exposure to environmental mycobacteria also known as non-tuberculous mycobacteria (NTM), such as the South-East Asian and the African Regions. The working model is that since some of these bacteria share numerous antigens with Mtb, including the proteins from the distinctive Proline-glutamic (PE)/proline-proline-glutamic (PPE) family (4, 5), the exposure to NTM alters the immune response to these potentially cross-reactive proteins. These issues highlight the urgent need for novel vaccines that can provide better protection against TB.

PE and PPEs are unique to mycobacteria (4, 6, 7) and abundantly expressed by Mtb, making up to 10% of the total Mtb genome (6). In recent years, these proteins have garnered significant interest due to their unique characteristics, role in virulence, and antigenic potential (8–10). Specifically, two subunit vaccines containing PPE proteins in their composition, the M72/AS01E (GlaxoSmith-Kline) and the ID93-GLASE (IDRI) vaccines, which are in phase IIb and I human clinical trials respectively. The two vaccines elicit both humoral and cellular immune responses with M72/AS01E able to increase the frequency of antigen-specific CD4+ T cells in both HIV-positive and -negative adults in a phase II randomized controlled trial in India (10, 11), and the IDRI vaccine able to elicit specific humoral and cellular responses in 60 non-BCG vaccinated healthy individuals (12). Importantly, M72/AS01E also conferred about 50% protection from active TB in pre-exposed (latent) individuals for at least the first three years (11). These studies highlight the potential of PE/PPE proteins as immunogenic targets and their ability to be part of a vaccine capable of inducing protective immune responses to TB.

The ESX5 secretion system of Mtb is responsible for the transport and secretion of a subset of PE and PPE proteins (13). However, the precise roles of the majority of these proteins in the pathogenesis of Mtb, host-pathogen interactions, and immunity, are still being elucidated. One of these proteins, PPE26, binds to TLR2 in RAW264.7 macrophages, leading to the induction of Th1-type immune responses in C57BL/6 immunized mice. This was demonstrated by the polarization of naïve CD4+ T cells, resulting in increased CXCR3 expression and secretion of IFNγ and IL-2 (14). Further, immunization of C57BL/6 mice with rBCG::PPE26 induced proliferation of effector memory CD4+/CD8+ T cells (14). Other studies have shown some protection conferred by PPE26 in immunised mice (15, 16). Thus, there is evidence supporting the hypothesis that PPE26 is an attractive candidate for TB vaccine development.

The host immune response against Mtb infection is thought to be primarily driven by Th1 CD4+ and CD8+ mediated immunity (17, 18). PE proteins, like PE9 or PE_PGRS42, seem to be potential targets for CD8+ T cell responses, suggesting that PEs may influence cellular immune responses in Mtb infection (19). Previously, the immunogenic potential of PE18 has been suggested (20, 21). Furthermore, PE18 of Mtb shares ~90% homology with a PE protein from the NTM *Mycobacterium avium* (MaPE). MaPE induced increased levels of IFNγ by both CD4+ and CD8+ T cells, but no sera antibodies in a mouse model of TB (5). In addition, in the same study, immunization with a MaPE-DNA vaccine limited the replication of Mtb in the spleens and lungs from C57BL/6 mice challenged with a low-dose of Mtb Erdman, suggesting that mycobacteria express PE antigens with cross-protective T cell epitopes in TB (5). This suggests that PE18 could potentially elicit immune responses that cross-react with MaPE, or even with similar PE proteins of Mtb or other mycobacterial strains. Furthermore, the shared homology between MaPE and PE18 raises intriguing possibilities about the presence of analogous PE/PPE

Abbreviations: ATB, active tuberculosis; BCG, *Bacillus Calmette-Guérin*; IGRA, interferon gamma release assay; LTBI, latent tuberculosis infection; Mtb, *Mycobacterium tuberculosis*; NTM, non-tuberculous mycobacteria; PE, proline-glutamic; PPE, proline-proline-glutamic; TB, tuberculosis.

antigens, like PE18, in a range of mycobacterial species. This includes NTM as well as BCG strains. Importantly, the presence of *pe* and *ppe* genes can be variable across different BCG strains (22, 23). For instance, certain BCG strains might exhibit the absence or downregulation of genes such as those encoding proteins PPE26 and PE18, which contrasts with their overexpression in the BCG Tice strain (24). This overexpression can be attributed to the duplication of the ESX5 locus (24) within this specific BCG strain. Thus, a clear understanding of the presence of specific PE/PPE antigens across different mycobacterial species requires more comprehensive genomic and proteomic investigations. Similarly, Mtb PE31 is an important virulence factor (25), and exhibits potent immunogenic properties (26). Myllymäki et al. observed that PE31 from *Mycobacterium marinum* shares 89% homology with Mtb-PE31 (an ESX5-associated protein) (26). Notably, *M. marinum* PE31 was found to induce a protective response against a low dose mycobacterial challenge in that study (26). Furthermore, given the high homology between Mtb PE18 and PE31, it is plausible that these two *pe* genes could exert similar functions. Significantly, peptides of PPE26, PE31 and PE18, all present in both Mtb H37Rv and *M. bovis*, were shown to produce IFNγ responses in both TB patients and cattle infected with *M. bovis*, reflecting a similar immune recognition hierarchy independent of the stage of disease (27). Overall, the high sequence diversity and shared structural features observed among PE and PPE proteins suggest the possibility of general cross-reactivity, and this may also apply to PPE26, PE18 and PE31. Hence, these three antigens were selected for our study.

In this study, we analysed the immunogenic potential of PE18 (Rv1788), PPE26 (Rv1789), and PE31 (Rv3477) proteins of Mtb in humans and in immunised mice. To do so, respective proteins were produced in recombinant form as described before (28), and tested for immunoreactivity with sera and PBMC from TB patients, IGRA$^+$ household contacts, and IGRA$^-$ BCG vaccinated healthy controls from the TB endemic country, Mozambique. We then tested their immunogenicity and protective potential in C57BL/6 mice after aerosol challenge with a low dose of *Mycobacterium tuberculosis* H37Rv.

Materials and methods

Expression and purification of recombinant proteins

The purification of the recombinant proteins was carried out as described before (28). Briefly, the plasmids containing genes of interest fused to 6xHis-tags were transformed and expressed in *E. coli BL21(DE3)* strain and the recombinant proteins were later purified by metal ion affinity chromatography. The individual proteins PE18 (Rv1788), PE31 (Rv3478) and PPE26 (Rv1789) were purified by the on-column refolding method using an 8M Urea gradient. Purity was assessed by SDS-PAGE (>97% purity) and identity confirmed by Western blot. Molecular weight references for SDS-PAGE and Western blot were provided using PageRuler Unstained Protein Ladder (Thermofisher, 26614) and PageRuler Prestained Protein Ladder (Thermofisher, 26616), respectively. The concentration of the recombinant proteins was determined using the Lowry assay (BioRad Laboratories, Inc.) and the endotoxin content determined using Limulus amebocyte lysate (LAL) test (PYROTELL®-T Lysate).

Study population

Peripheral blood was obtained from a cohort of TB patients (EMI-TB Verification Cohort, Maputo Region, Mozambique) under the framework of the EMI-TB project. Briefly, patients with TB were confirmed by tuberculin skin test (TST) and/or the Quantiferon-TB-Gold test (QST), radiographic examination was used to discriminate between LTBI and ATB, and observation of acid-fast bacilli in sputum by Lowenstein-Jensen and Colletsos culture was used to confirm all TB-diagnosed patients. Exclusion criteria were age <18 years, co-infection with the human immunodeficiency virus (HIV) and any other immunosuppressive medical condition or concomitant use of immunosuppressive drugs. The participants in this study were originally part of the wider EMI-TB project. For the current study, we had access to a subset of serum samples and PBMCs. Sera and PBMC samples were collected after final diagnosis and before commencement of the anti-TB drug treatment. Study groups were formed as follows: ATB (n=16), LTBI (n=19) and Healthy Controls (HC, BCG vaccinated volunteers with no evidence of TB; n=17). The study was approved by the Mozambican National Bioethics committee (IRB:00002657; ID: 298/CNBS/15).

Animals

Female C57BL/6 mice at the age of 6–8 weeks were obtained from Charles River (UK) and bred in-house at University of Leicester Preclinical Research Facility. The mice were then divided in five groups (n=10 for PBS and BCG, n=9 for PE/PPE vaccinated), with 3 animals in each group assigned for immunogenicity analysis and the remaining for Mtb challenge. All animals were used with approval from University of Leicester Ethics Committee under an approved UK Home Office animal project license (Establishment License X1798C4D2) and used in accordance with the Animals (Scientific Procedures) Act 1986.

Immunization of C57BL/6 mice

C57BL/6 mice were immunized subcutaneously in the flank with 10μg of each PE/PPE protein and 1μg Quil-A (Invivogen) or a matched volume of saline solution (Sigma) as a control. Quil-A, known for inducing a robust adjuvant response, promotes Th1-biased immune responses and potentiates the response to mucosal antigens (29). A second subcutaneous immunization was administered three weeks later in the opposing flank, followed by a final intranasal boosting under isoflurane anaesthesia (using 0.1μg Quil-A per animal in this case) three weeks after. BCG vaccinated

mice were given 5×10^5 CFU BCG Pasteur in 0.1mL subcutaneously in the first week. Three weeks after the last immunization, mice from each group (n=3) were humanely sacrificed for immunogenicity analysis by overdose of pentobarbital given intraperitoneally, and death was verified by severing femoral artery. At the same time, remaining mice (n=6 from each group for PE/PPE and n=7 for PBS and BCG) were used for an Mtb challenge experiment. Further details of the immunization and dosing regimen are given in the corresponding figure legends.

Challenge with M. tuberculosis

The Mtb strain H37Rv was grown in Proskauer Beck medium containing 0.05% Tween-80 to mid-log phase and frozen in 1mL aliquots at -70°C. In containment level 3 facilities, mice were challenged with approximately 100 colony forming units (CFU) using a self-contained bespoke aerosol chamber (Walker Safety Cabinets Ltd., Glossop, UK) based on the "jet in air" venturi nebulizer. On day 1 (for determination of infectious dose) and three weeks after Mtb challenge, animals were euthanised by overdose of pentobarbital given intraperitoneally, and lungs were aseptically collected to evaluate mycobacterial burden.

Preparation of tissues from mice

Isolation of splenocytes

The spleens of immunised, uninfected mice were collected in 1mL of MACS Tissue preservation media (Miltenyi Biotec) and rinsed in PBS. Afterwards, spleens were mechanically disrupted through a 40µm Corning® cell strainer (Sigma-Aldrich) prewashed with 2mL of cold R10 media (RPMI, 10% FBS, 5mM L-Glutamine, 100units/ml penicillin, 100µg/ml streptomycin, 10mM HEPES and 50µM 2-β-mercaptoethanol) (Sigma) and the cells were further washed with 18mL R10. Cells were centrifuged at 250g for 5 minutes at room temperature and resultant pellets were lysed with ammonium–chloride–potassium (ACK) lysis buffer (Sigma-Aldrich) to remove red blood cells for additional 5 minutes after which the reaction was stopped by addition of R10 media. Cells were maintained in complete RPMI medium in a humidified incubator at 37°C and 5% CO_2. Spleens were processed for splenocyte re-stimulation assays to assess antigen-specific cell-mediated responses to PE/PPE antigens.

Isolation of lung cells

Lungs were collected in Petri dishes containing 1mL of MACS Tissue preservation media (Miltenyi Biotec) and rinsed in sterile PBS. Lungs were cut into 1mm sections and resuspended in 1mL D-PBS. Afterwards, cells were incubated for 40 minutes at 37°C with constant agitation with 1mL of 2x digestion buffer D-PBS with 1mg/mL collagenase and 0.15mg/mL DNaseI, and finally dissociated by slow pipetting. Cells were then passed through a 70µm cell strainer Corning®, after which R10 medium was added to quench the enzyme activity and cells were centrifuged at 250g for 5 minutes at room temperature, and lysed with ACK lysis buffer (Sigma-Aldrich) for 5 minutes. The lysis was stopped through the addition of R10 medium. Cells were centrifuged again at 250g for 5 minutes and resuspended in complete RPMI medium. The lung single cell suspensions were used to assess percentage of tissue resident memory T cells.

Preparation of sera from mice

Blood was withdrawn by cardiac puncture for serological analysis and allowed to clot at room temperature for 1h followed by centrifugation at 1000-2000g for 10 min at 4°C. Sera were stored at -20°C until analysis.

Collection of bronchoalveolar lavage fluid

Bronchoalveolar lavage was collected from lungs of vaccinated sacrificed animals by injecting 1mL of sterile PBS into the lungs via an incision in the trachea followed by three rounds of flushing. Afterwards, the washes were centrifuged at 1000g and supernatant was collected and stored at −20°C until further use.

Bacterial enumeration in mouse lungs

Bacterial burden from mouse organs was assessed by CFU enumeration. Lung homogenates were prepared by GentleMACS Dissociator (Myltenyi Biotec) in solution containing 0.1% Triton X-100. Homogenates were plated in technical duplicates on Middlebrooks 7H11 agar (BD Biosciences) supplemented with oleic acid-albumin-dextrose-catalase (OADC) (Millipore), glycerol and Selectab (Mast Diagnostics). CFUs were counted after 3–4 weeks incubation at 37°C.

Splenocyte re-stimulation with PE/PPE antigens and BCG whole cell lysates

Cells from splenocytes of unimmunized, BCG immunized, and PE/PPE-immunized mice were quantified using the TC20™ automated cell counter (BioRad Laboratories, Inc.).

For antigen-recall experiments, splenocytes were incubated with respective antigens or controls (PBS or BCG whole cell lysate) in 96-well flat-bottom plates in R10 medium for 96h at 37°C with 5% CO_2 in a humidified atmosphere. One million cells per well were used and samples were plated in duplicates. Eight hours before harvesting the cells, a combination of 50ng/mL PMA and 500ng/mL Ionomycin was added to respective wells as positive control. Between 5-6h before collecting the cells, 5µg/mL brefeldin A was added to each well for 4h to block cell trafficking. Cells were harvested and stained for surface and intracellular markers followed by flow cytometry analysis. Resultant supernatants were collected after centrifugation and stored at -80°C for cytokine ELISA.

ELISA analysis of cytokines from splenocyte re-stimulation assay

For the assessment of cytokine production, supernatants from the re-stimulation assay were collected and used for quantitative ELISA to measure concentrations of IFNγ (Invitrogen 88-7314-88),

TNF (Invitrogen 88-7324-88), IL-4 (Invitrogen 88-7044-88), IL-10 (Invitrogen 88-7105-88), and IL-17A (Invitrogen 88-7371-88), according to manufacturer's instructions. A 1:2 dilution was used for IFNγ and TNF, while a 1:3 dilution was used for IL-4, IL-10 and IL-17A. Cytokine concentrations in the supernatants were determined by interpolating from standard curves, and the data were plotted using GraphPad Prism V10.

Flow cytometry analysis of mouse cells

Single cell suspensions from 96h stimulated splenocytes were added to a 96-well U-bottom plate, washed in PBS and further incubated with Fc Block (Human TruStainFcX™/TruStain fcX™ (anti-mouse CD16/32) for 45 minutes at 4°C together with fluorochrome-conjugated mAb anti-CD3-APC/Cy7, CD4-PerCP-Cy5.5, CD8-AF700, CD44-FITC, CD62L-PE (BioLegend, San Diego, CA, USA) and fixable viability dye-BV510 (BD Biosciences). Afterwards, cells were washed twice in PBS, and subsequently fixed/permeabilized using a Fix/Perm kit according to manufacturer instructions (Thermofischer Scientific).

Cells were then washed twice with permeabilization buffer and expression levels of intracellular TNF, IFNγ and IL-2 (Panel A) or IL-17 and IL-2 (Panel B) were analysed by flow cytometry after 1h incubation at 4°C with specific anti-mouse antibodies (Panel A: TNF-APC, IFNγ-PE-Dazzle 594, IL-2-BV605 or Panel B: IL-17-PE-Cy7 and IL-2-BV605, respectively), diluted in permeabilization buffer.

Spleen cells were gated by forward and side scatter. T effector memory (Tem) cells were gated by expression of CD3, then CD4 or CD8, and finally CD44+ and CD62L-. Flow cytometry data was obtained on a Beckman Coulter CytoFLEX cytometer (BD Biosciences). The data were processed using FlowJoTM v10.8.1 (BD Biosciences, Ashland, OR, USA). Each T cell population was analysed individually for cell proliferation and activation. Fluorescence minus one (FMO) controls were used for each marker to set the appropriate gates and determine positive populations. Examples of gating strategies are shown in Supplementary Figure S1.

For detection of lung resident memory T cells (Trm), 4 million mononuclear cells were plated per well in a 96-well U-bottom plate for staining of surface markers. The same protocol that was used for the spleens was also applied for the lungs, in which cocktail of antibodies for surface staining contained CD44-FITC, CD4-PerCP/Cy5.5, CD3-APC, CD62L-PE, CD69-PE-Cy7, CD103-BV421, CD8-BV510 (BioLegend, San Diego, CA, USA) and Fixable Viability dye-BV510 (BD Biosciences). Gating strategy for lung-resident memory T cells is illustrated in Supplementary Figure S2.

Modified mycobacterial growth inhibition assay

A modified method of mycobacterial growth inhibition assay (MGIA) was used to assess the capacity of mouse splenocytes for *in vitro* killing of *M. tuberculosis* H37Rv-lux. Briefly, C57BL/6-M cells (Kerafast, ENH166-FP) were seeded onto 48 well plates (Corning, 3548) at a density of $5x10^5$ cells per well using antibiotic-free R10 (RPMI with 10% FBS, 5mM L-Glutamine and 10mM HEPES). Cells were then infected with H37Rv-lux using a multiplicity of infection (MOI) of 1:1. After 48 h, $3x10^6$ splenocytes were added on top of infected cells. Plates were incubated for an additional 120h in a humidified CO_2 incubator. Afterwards, media were aspirated from each well followed by cell lysis using 200µL of sterile distilled water. Luciferase assay was done to quantify viable bacteria in each well as previously described (30). Briefly, cell lysates were added to tubes (Greiner Bio-One, 115101) with 1mL of 0.1% n-decyl aldehyde (Sigma-Aldrich, W236217-SAMPLE-K). Bioluminescence was measured using a Junior LB Portable Luminometer (Berthold Technologies) set to collect data for 30 seconds. Data are expressed as relative light units (RLU).

Determination of PE/PPE-specific IgG and IgA isotypes by ELISA

ELISA assays were used to determine antigen-specific titres for IgG isotypes in serum and BAL of vaccinated mice, and IgA in the BAL of these animals. Microtiter 96-well plates (Nunc, Maxisorp) were coated with 5µg/mL of the respective PE/PPE protein in 0.1M $NaHCO_3$ pH 9.6, at 37°C for 2h, after which the coating solution was removed and the plates washed three times with distilled water. Plates were later blocked with 5% skimmed milk powder in PBS for another 2h at 37°C. The wells were washed three times with distilled water. Mice sera and BAL samples were added in 2-fold serial dilutions and plates incubated at 4°C overnight. The plates were then washed three times before the addition of goat anti-mouse immunoglobulin G (IgG) (Sigma, A2554), IgG1 (Southern Biotech, 1071-05), IgG2a (BD Pharmingen, 553391), IgA–horseradish peroxidase (HRP)-conjugated antibodies (Invitrogen, 62-6720) diluted 1:2000 in blocking buffer, except for the IgG2a antibody that was diluted 1:5000, at RT for 2h. Afterwards, plates were washed five times and the o-phenylenediamine dihydrochloride (OPD; SigmaFast OPD Peroxidase substrate. PCode 1003344899. Source SLCJ3691) substrate was added and incubated for 30 minutes at room temperature and the absorbance measured at 450nm in an ELISA plate reader (TECAN Sunrise). The data were expressed as endpoint titres calculated as double the background absorbance value.

IgG and IgM detection in sera from TB patients

For the detection of PE/PPE-specific IgG and IgM in human sera, a similar protocol that was used for the serology studies in mice was applied. Following coating and blocking, the plates were incubated with anti-human IgG–HRP (Jackson 109:053-008) or anti-human IgM-HRP (Abcam ab97205) diluted 1:2000 in assay diluent for 2h at room temperature. OPD Substrate Tablets (Sigma-Aldrich) were used for colour development, following the manufacturer's instructions. The OD at 450nm was measured after 15 minutes incubation at room temperature.

PBMC re-stimulation assay in a Mozambican cohort

Cryopreserved PBMC were revived in R10 with 150µg/mL DNase I (Roche, 10104159001). After two wash steps with R10+DNase, cell viability was determined using Trypan Blue exclusion method. Only samples with a cell viability of more than 70% were used for the assay. Cells ($5x10^5$ viable cells/well) were plated in U-bottom 96-well plates for each donor, having designated wells for unstimulated (media alone), positive control (PMA/ionomycin) and treatments (PE18, PE31 and PPE26). Antigen treated cells were stimulated with 5µg/mL of the respective antigen (PE18, PE31 or PPE26) for 18-24h. Six hours before cell harvest, positive control wells were stimulated with 10ng/mL PMA (Sigma, P1585) and 250ng/mL ionomycin (Sigma, I9657). Finally, all wells were treated with Brefeldin A (BioLegend, San Diego, CA, USA, 420601) (5µg/mL) 4h before FACS staining. Cells were washed with DPBS and stained with a master mix of 1:250 anti-human Fc receptor blocking antibodies (BioLegend, San Diego, CA, USA, 422302), 1:500 fixable viability dye eFluor 780TM (Invitrogen, 65-0865-14), 1:200 Brilliant Violet 421-conjugated anti-human CD3 (317344), 1:200 PerCP/Cy5.5-conjugated anti-human CD4 (357414) and 1:200 Brilliant Violet 510-conjugated anti-human CD8 (301048) (all from BioLegend, San Diego, CA, USA) for 45 minutes at 4°C. Cells were fixed and permeabilized for 15 minutes using IC Fixation buffer (Invitrogen, 00-822-49). Intracellular cytokine staining with 1:200 Alexa Fluor 700-conjugated anti-human IFN-γ (BD Biosciences, 557995), and 1:200 PE-Cyanine7-conjugated anti-human TNF (BioLegend, San Diego, CA, USA, 502930) was done with eBioscienceTM permeabilization buffer (Invitrogen, 00-8333-56). Stained samples were analysed within 24h after intracellular staining. Cell acquisition was performed using CytoFLEX S flow cytometer (Beckman-Coulter) and analysed using FlowJoTM v10.8.1 (BD Biosciences, Ashland, OR, USA). The frequencies of IFNγ+, TNF+ and IFNγ+TNF+ cells in total T cells, CD4 and CD8 T cells, were summed up and expressed as percentage of cytokine-positive cells. Gating strategy is shown in Supplementary Figure 4. Baseline values from unstimulated wells were deducted from stimulated wells to obtained proportion of stimulated cells.

Preparation of BCG lysates

Mycobacterium bovis BCG (strain Pasteur) was cultured in Middlebrook 7H9 broth supplemented with 10% OADC enrichment for three weeks. The bacterial cells were harvested, washed, and lysed using a sonication method (UP200ST ultrasonic processor, Hielscher), by five 30s pulses with intermittent cooling. The lysate was centrifuged, and the supernatant containing the soluble BCG proteins was filtered using a 22µm syringe driven filter unit (Millex) and collected. Protein concentration was determined by measuring absorbance at 260/280 using nanodrop (Thermo Scientific, Nanodrop 2000). BCG lysate stocks were prepared at 1mg/mL concentration and frozen until further use.

Western blotting for detection of antigen-specific antibodies against BCG

To determine the presence of PE/PPE antigens in the BCG Pasteur 1173P2 strain employed in this study, PE/PPEs (3µg) and BCG lysate (20µg) protein samples were separated by SDS-PAGE using 4-12% Bis-Tris polyacrylamide gels (Invitrogen) in MES running buffer (Invitrogen) for 1h at 100V 49mA. PE/PPEs were prepared in reducing and non-reducing conditions by addition of β-mercaptoethanol (Sigma) as reducing agent. The separated proteins were transferred onto PVDF membranes using a semi-dry transfer system. The membranes were blocked with 5% non-fat dry milk in Tris-buffered saline with Tween 20 (TBST) and then incubated with correspondent serum samples from immunized mice (1:500 dilution) overnight at 4°C. After washing with TBST the next day, the membranes were incubated with HRP-conjugated anti-mouse IgG secondary antibody (1:2000; Sigma). Protein-antibody complexes were visualized using an enhanced chemiluminescence detection system (Amersham ECL Prime).

Detection of BCG antigen-specific antibodies by ELISA

High-binding ELISA plates (Nunc) were coated with respective antigens or BCG (6 or 20µg/mL) diluted in carbonate buffer and incubated as described earlier. After blocking the plates, diluted mouse serum samples (1:500 dilution) were added to the wells and incubated for 2h at room temperature. Following washing, HRP-conjugated anti-mouse IgG secondary antibody was added, and the plates were incubated for 2h. Substrate solution containing 3,3',5,5'-tetramethylbenzidine (TMB) (Invitrogen) was added, and the reaction was stopped with 2N sulfuric acid after 25 minutes. Absorbance was measured at 450nm using a microplate reader.

Generation of human DC

Peripheral blood mononuclear cells (PBMCs) from human healthy donors were thawed from ImmunXperts SA (Belgium) biobank. Monocytes were isolated from PBMCs using a MACS magnetic separation column CD14 MicroBeads (Miltenyi) and purity was evaluated by CD14 FACS staining (Fortessa). Cells were then resuspended at a cellular density of 10^6 cells/mL and plated into a 24-well tissue culture microplate (1mL per well) in CellGenix DC medium (CellGenix, Cat.N° 20801-0500) added with Gentamycin, IL-4 (Miltenyi, 130-093-866) and GM-CSF (Miltenyi, 130-093-922) for 5 days. At day 5, cells were stained for FACS analysis with several DC activation markers to assess their immature dendritic cell (iDC) state: CD14-FITC (Miltenyi, 130-110-518), CD40-BV510 (BD Biosciences, 563456), CD80-BV421 (BD Biosciences, 564160), CD83-PE-Vio 770 (Miltenyi, 130-110-505), CD86-APC (Miltenyi, 130-116-161), CD209-PE (Miltenyi,

130-117-706), and HLA-DR-BUV395 (BD Biosciences, 564040). On the same day, respective antigens (10µg/mL) were added to the cell culture for 48h. At day 7, cells were stained for FACS analysis with same markers to assess their mature state. LPS (Sigma, L4391-1MG) (1µg/mL), and TNF (Miltenyi, 130-094-024) (800U/mL), with IL-1b (Miltenyi, 130-093-898) (150U/mL), were used as positive control.

Human non-exposed PBMC proliferation assay

Human PBMCs from five healthy donors were thawed from ImmunXperts biobank and incubated with respective PE/PPE candidates (10µg/mL) for 7 days at 37°C. PBMCs from same donors were incubated with CEF (Mabtech, 3616-1) (HLA class I control) and CEFTA (Mabtech, 3617-1) (HLA class II control) peptide pools, a positive control for T cell activation. On day 6 of culture, the cells were incubated with 5-ethynyl-2'-deoxyuridine (EdU) (Thermofisher) (1µM) for 16h for assessment of T cell proliferation. The day after, supernatants from human PBMC stimulation assays were collected and stored at−80°C for further cytokine analysis. Each cell culture included a set of untreated control wells. Cells were stained for flow cytometry analysis of T cell surface markers (CD4 and CD8), fixed/permeabilized, and the incorporated EdU was stained with a fluorescent azide to assess T cell proliferation by measuring EdU uptake using flow cytometry.

Human IFNγ ELISA

Cell supernatants were stored at −80°C and then analyzed for IFNγ expression with LEGEND MAX™ Human IFNγ Kit (BioLegend, San Diego, CA, USA) following the manufacturer's instructions. Cytokine levels were determined by ELISA and absorption was read by using a microplate reader (Thermofisher). Each sample was tested in duplicate. The detection limit of the kit was 15.6-1000 pg/mL.

Sample size and statistical analysis

Sample size for human cohorts was described above and was not based on power calculations but rather availability of samples from a previous exploratory study (EMI-TB project). Mouse groups for Mtb challenge experiment were based on power calculations and prior experience, where the minimal group size is six animals (seven were used, taking into account possible attrition). GraphPad Prism software, version V10 was used for determining the significant differences in the mean values between the samples when using parametric tests, or the mean rank of the data for non-parametric tests. For multiple group comparisons, one-way or two-way ANOVA tests with correspondent corrections were applied. In all, p-value of ≤0.05 was considered to be statistically significant.

Results

Antigen selection, expression and purification

In order to investigate the immunogenicity and protective capacity of mycobacterial proteins we needed to generate quantities of pure protein. To do this, mycobacteria specific genes encoding proteins PE18, PE31 and PPE26 were expressed and purified as described before (28). Protein expression was induced with 1mM IPTG resulting in accumulation of insoluble proteins, and purity and precision of protein production confirmed by weight, with SDS-PAGE showing an apparent molecular weight of 9.8kDa for the PEs and 38kDa for PPE26. His-tagged protein products were isolated, affinity purified under denaturing conditions, and examined on 15% SDS-PAGE. Endotoxins were removed during the purification process (<10EU/mL). SDS-PAGE and immunoblot analysis were performed for the three proteins and are shown in Figure 1.

PE18, PE31 and PPE26 are recognised by sera of TB, LTBI and HC (BCG) hosts

To evaluate the immunogenic potential of PE18, PE31 and PPE26, we first analysed their immunoreactivity using sera derived from TB patients (n=16), IGRA$^+$ close contacts (n=19), and IGRA$^-$ BCG vaccinated healthy controls (n=17) from Mozambique (Figure 2). All three antigens were recognised by sera from TB-exposed individuals as well as LTBI hosts, as shown by antigen-specific IgG levels. The three proteins were also immunoreactive with sera of healthy BCG-vaccinated controls. There were no significant differences in their immunoreactivity between the three population groups, except for PE31, which showed a trend toward higher immunoreactivity with BCG-vaccinated healthy individuals compared to patients with TB, although this difference was not statistically significant ($p=0.0863$) (Figure 2A). Furthermore, as shown in Figure 2B, a comparison of the immunoreactivity levels of each of the three proteins per population group revealed that PE31 was recognized to a higher specific IgG antibody titre in latent TB patients compared to both PE18 and PPE26, with a significant difference found for PE18 ($p=0.0343$). As for the BCG-vaccinated control and the ATB groups, differences were also found with individuals exhibiting a higher PE31 titre, although this did not reach statistical significance. Notably, not all individuals were equally responsive. This may reflect not all subjects being diagnosed at the same stage of infection. In addition, we further measured the titres of antigen-specific IgM antibodies for a representative pool of five individuals per group (Figure S3). Sera from TB patients, IGRA$^+$ household contacts, and IGRA$^-$ BCG vaccinated healthy controls all reacted to all three proteins; however, PPE26 induced a weak antigen-specific IgM antibody response in IGRA$^+$ household contacts (Figures S3B), while PE31 showed highest IgM antibody titres in this same group, resulting in significant differences ($p=0.0286$) when compared to PPE26 (Figures S3-B). PPE26 shows similar or higher proportion of antibody positivity in subjects from both the IGRA$^-$ BCG vaccinated healthy control and the TB groups, but without being statistically

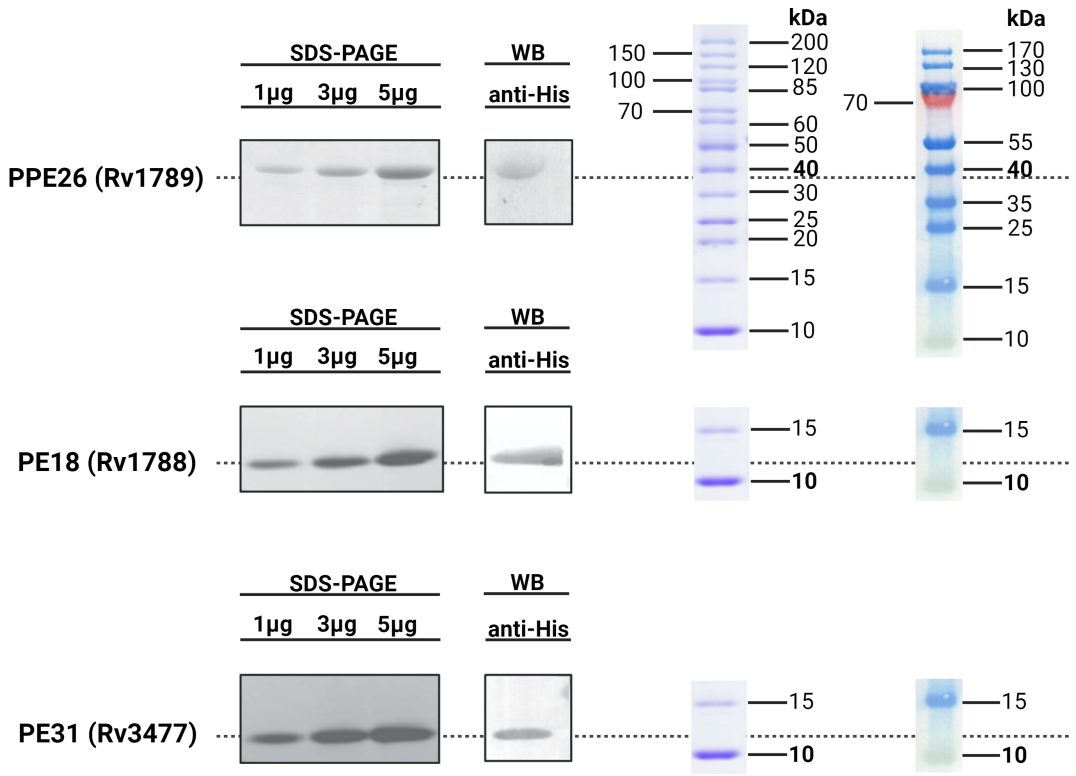

FIGURE 1
Immunoblot analysis of His-tagged recombinant Rv1789, Rv1788 and Rv3477. The purified recombinant proteins PPE26 (Rv1789), PE18 (Rv1788) and PE31 (Rv3477) of *Mycobacterium tuberculosis H37Rv* were separated by 15% SDS-PAGE and transferred to a PVDF membrane. These proteins were probed with polyclonal mouse anti-His antibody followed by goat anti-mouse IgG-HRP conjugated secondary antibody. Protein ladders for SDS-PAGE (left) and Western Blot (right) are included for molecular weight reference. All respective molecular weights with approximate expected sizes for proteins are highlighted in bold. Blots have been cropped for presentation purposes.

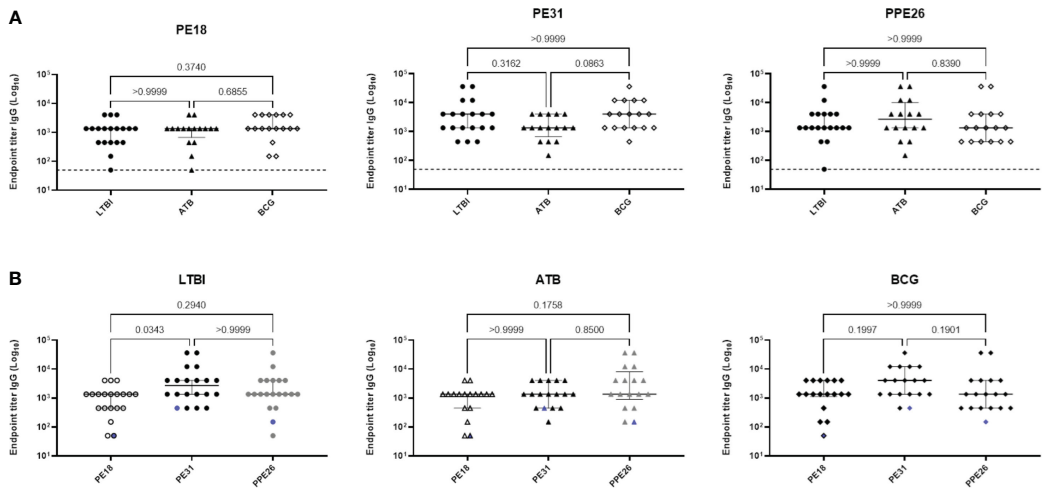

FIGURE 2
Human antibody response to Mtb proteins PE18, PE31 and PPE26. Serum derived from TB patients (n=16), IGRA-positive close contacts (n=19), and IGRA-negative BCG vaccinated healthy controls (n=17) from Mozambique were measured for antigen specific IgG antibodies **(A, B)**. The results are presented as individual values with median and interquartile range (IQR). For statistical analysis, non-parametric Kruskal-Wallis test was used. Multiple comparisons were corrected using the Dunn's test. The significance levels are indicated numerically. The dotted line in **(A)** and the blue pattern symbols in **(B)** represent background antibody response from a European healthy donor with no history of TB or previous BCG vaccination.

significant. Importantly, no reactivity was detected from a European healthy donor with no history of TB or previous BCG vaccination. Overall, all three PE/PPE proteins are immunoreactive with sera from TB patients, IGRA^{+} household contacts, and also IGRA^{-} BCG vaccinated healthy controls from the Mozambique cohort.

PE/PPE antigens are recognised by human PBMC and induce homeostatic-like T cell proliferation

While immunoglobulin responses indicate exposure to antigen, it is cellular responses that are considered critical for immunity to TB (31–33). To examine the potential for these antigens to induce cellular immunity, we measured proliferation and cytokine production in PBMC from individuals who have been exposed to either Mtb or BCG in response to our antigens of interest. Using a subset of participants from the Mozambique cohort, we observed Th1 (IFNγ and TNF) cytokine production by CD4+ T cells in LTBI, ATB, and BCG groups, with all three antigens (Figure 3A). We also observed a clear trend of highest production of these cytokines in PBMC from LTBI donors, though this did not reach statistical significance due to a small sample size (n=12). This trend was also observed when comparing all T cells producing IFNγ and TNF (Figure S5). In contrast, there were no differences in the CD8+ T cell subset, with all three cohort groups showing similar levels of cytokine producing cells (Figure 3B). When comparing the responses between the three PE/PPE antigens in each sub-cohort, again the highest frequencies were generally observed in LTBI individuals but there were no significant differences between the three antigens (Figures S6-A, C). This suggests that antigen-specific immune responses exist in all individuals exposed to mycobacteria, with LTBI hosts displaying a trend of higher antigen-specific CD4+ T cell frequencies than active patients or BCG-vaccinated controls.

The observation of broad stimulatory capacity of these antigens raised the question of how much of the response is antigen-specific T cell activation versus other non-specific stimuli. In a first analysis we measured the capacity of the proteins to alter the phenotype of human dendritic cells. Supplementary Figure 7 indicates that none of the three PE/PPE proteins were able to alter surface expression levels of DC-associated activation markers (CD40, CD80, CD83, CD86), or of the pathogen recognition receptors (CD209/DC-SIGN) or antigen presentation (HLA-DR) molecules. We then tested the capacity of these proteins to induce proliferation of T cells from PBMC of healthy (but unscreened in terms of mycobacterial exposure) blood donors (Figure S8). Surprisingly, PE18 and PPE26, but not PE31, induced some CD4+ and CD8+ T cell proliferation in seven-day cultures, expressed as stimulation indices (Figure S8). Supporting these results, IFNγ was also detected in culture supernatants by ELISA. However,

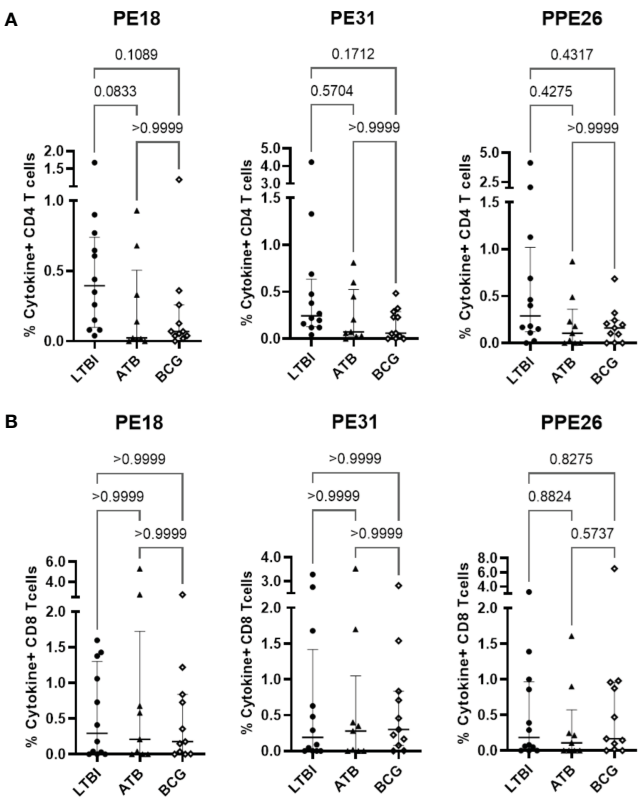

FIGURE 3
Antigen-specific T cell proliferation in PBMC from individuals exposed to Mtb or BCG. Human PBMC (n=12) from the Mozambique cohort that have been exposed to either Mtb (ATB or LTBI) or BCG were stimulated *in vitro* with each protein. For each antigen, the percentages of IFNγ and TNF positive antigen-specific CD4 **(A)** and CD8 **(B)** T cells in the LTBI, ATB, and BCG groups are depicted. The results are presented as median with IQR, showing the percentage of IFNγ+ TNF+ antigen-specific T cells. Statistical analysis was performed using the Kruskal-Wallis test followed by Dunn´s test correction.

none of the three proteins showed significant differences relative to unstimulated control. While prior mycobacterial exposure (whether BCG or Mtb) could not be eliminated, it is also possible that some of the PE/PPE antigens may induce homeostatic-like proliferation of circulating memory T cells.

Immunogenicity of proteins PE18, PE31 and PPE26 in C57BL/6 mice

To investigate the T and B cell responses induced by the three vaccine candidates, C57BL/6 mice (n=3 per group) were immunized three times (two subcutaneous and one intranasal) 3 weeks apart with each individual antigen, BCG or PBS medium alone. Antigen-specific antibody titres and cytokine responses were determined three weeks after the last boost (Figure 4A).

Immunogenicity was assessed by measuring levels of antigen-specific IgG including individual subtypes IgG1 and IgG2a, in sera from immunized mice (Figure 4B). Mucosal immunogenicity was also analysed by levels of antigen-specific IgG and IgA in BAL samples (Figure 4D). The three PE/PPE proteins induced mixed IgG1/IgG2a antibody responses in sera as shown in Figure 4B. However, groups immunized with PE31 or PPE26 included some

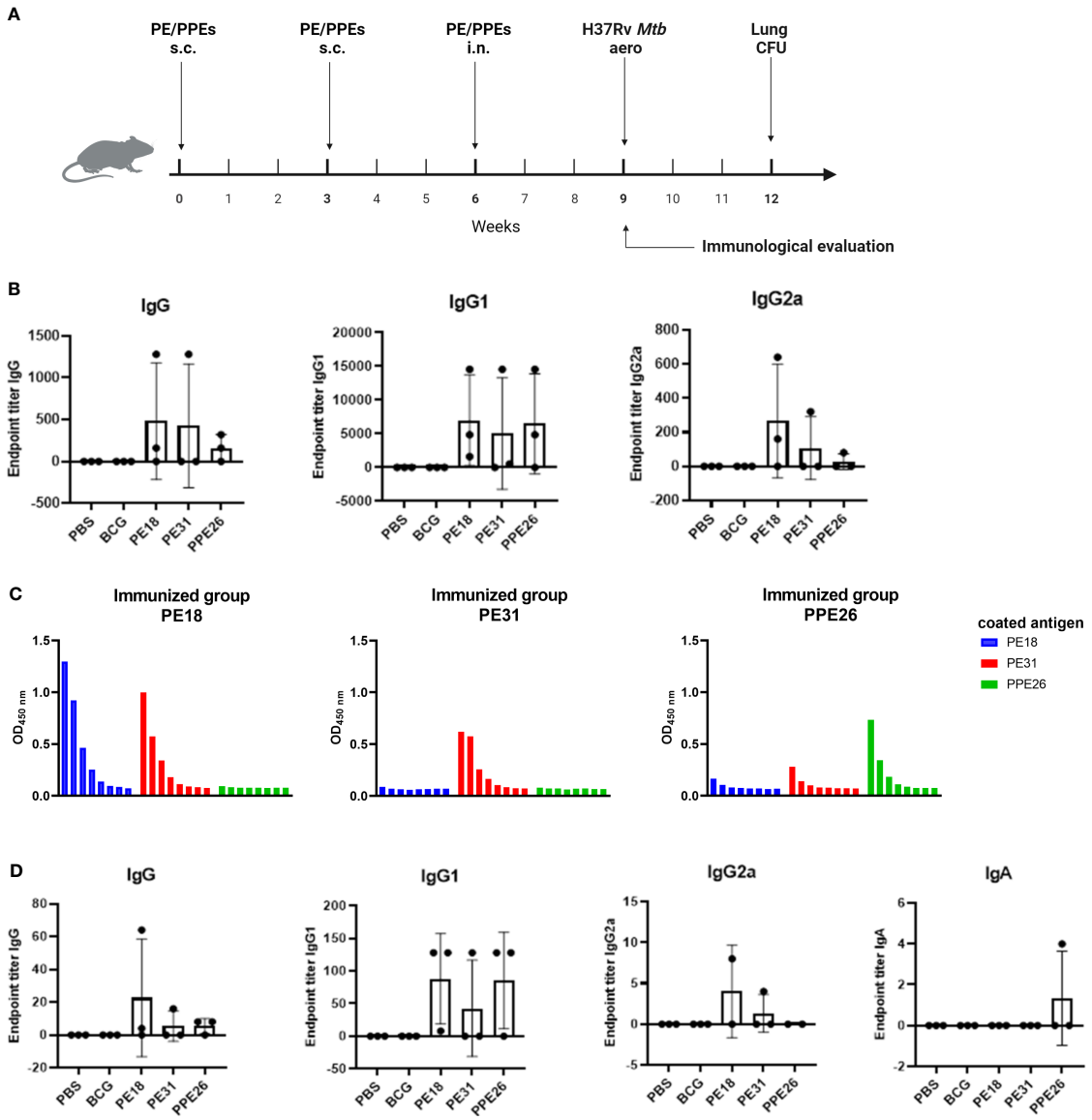

FIGURE 4
Antibody responses to Mtb recombinant antigens PE18, PE31 and PPE26 in immunized mice. **(A)** Mice were left unvaccinated (phosphate saline solution) or vaccinated either with BCG ($5x10^5$ CFU BCG Pasteur) or 10µg of recombinant individual protein PE18, PE31 or PPE26 in combination with 1µg of adjuvant Quil-A, with immunisation schedule and subsequent Mtb challenge as schematically indicated. **(B)** Serum samples after the final immunization were subjected to ELISA to measure antigen-specific IgG, IgG1, and IgG2a antibodies. The endpoint titers were determined by calculating double the background absorbance value. Results show mean of reciprocal dilution ± SD. **(C)** PE/PPE proteins cross-react in serum from vaccinated animals. Serum samples from immunized mice were assessed for reactivity against the three proteins used in this study. The reactivity was determined using serial 3-fold dilutions ELISA and the absorbance at 450nm was measured. **(D)** Levels of antigen-specific IgG, IgG1 and IgG2a subtypes, as well as IgA antibody, were assessed in BAL from immunized mice similar to serum samples.

animals which appear to be non-responders for unknown reason, most probably due to suboptimal delivery. Furthermore, IgG1 titres in serum from immunized mice appear to be higher compared to IgG2a and total IgG, probably due to quality/sensitivity of secondary reagents (Figure 4B). Interestingly, we identified cross-reactivity within the sera against the three proteins (Figure 4C). Thus, the PE18-immunized mice not only responded with PE18-specific IgG but also showed cross-reactivity with PE31, probably due to the high level of homology between these two proteins (~64%). However, only PE31-specific IgG antibodies were identified in the PE31-immunized group with no cross-reactivity to either of the two other proteins. Nevertheless, two animals within the PE31-immunized group were poor responders, making definitive conclusions not possible. Mice immunized with PPE26 responded specifically to PPE26, with some weak cross-reactivity to PE31. Groups immunized with PBS or BCG that served as controls did not show any response to any of the three proteins, further suggesting that none of them is present in the BCG Pasteur 1173P2 strain used in this study (Figures 4B, D). To measure mucosal responses induced by the proteins, antibody levels were assessed in bronchoalveolar lavage (Figure 4D). BAL collected three weeks after final boost from animals immunized with PE18, PE31 or PPE26 showed relatively high levels of IgG as well as the IgG1 and IgG2a subtypes, especially for PE18. However, no antigen-specific IgA was detected in BAL (Figure 4D). Our results indicate that PE18, PE31 and PPE26 elicited humoral and cellular immune responses in humans and mice, which might contribute to protection.

Absence of PPE26, PE18, and PE31 reactivity in BCG Pasteur suggests differential antigenic composition

To investigate the presence of PPE26 (Rv1789), PE18 (Rv1788) and PE31 (Rv3477) in the BCG Pasteur strain, mice were immunized with respective antigens, and their sera were collected for further analysis. ELISA and Western blotting were performed using the collected serum samples to evaluate reactivity of the three proteins to BCG (Figure S9). The findings demonstrated that immunized mice showed a strong immune response specifically directed at the respective antigens they were immunized with; however, no detectable reactivity was observed against BCG lysate in either of the mice that were immunized with the different antigens, as revealed by both ELISA (Figures S9-A) and Western blotting (Figures S9-B). Together, these results strongly suggest the absence of PPE26, PE18 and PE31 in the BCG Pasteur strain that we utilized in our study. However, other possibilities or alternative approaches like sequencing of the BCG Pasteur strain and potentially other BCG strains could provide definitive evidence whether the absence of these proteins is unique to the strain we used, or if it extends to other BCG strains as well.

Polyfunctional T cells in splenocytes from immunized mice

To assess the ability of the vaccine candidate to induce specific functional T cells we examined the CD4+ and CD8+ T cell response to recall antigens. We used expression of multiple cytokines and effector molecules in response to stimulation with the specific antigens at the single cell level by intracellular cytokine staining (ICS) and flow cytometry. Expression of IFNγ, TNF and IL-2 (Panel A) or IL-2 and IL-17 (Panel B) in CD4+ and CD8+ T cells was determined (Figures 5, 6A). Stimulation with PE18 as recall antigen led to an increased trend in the levels of IFNγ in both CD4+ and CD8 + T cell compartments in mice vaccinated with this specific antigen (Figures 5A, B), whereas in the case of PPE26-vaccinated mice, stimulation with PPE26 resulted in significantly higher levels of CD4+ T cells expressing TNF compared to the control group (Figure 5A). Additionally, there was an observed increased trend of CD8+ T cells expressing IFNγ alone in response to PPE26 (Figure 5B). The observed trends in increased levels of IFNγ and TNF in response to PE18 and PPE26, respectively, suggest a potential Th1 response in both instances. Furthermore, as shown in Figure 6A, splenocytes from PPE26 immunized animals resulted in a significant number of IL-17 cytokine producing CD4+ T cells (0.674%), suggesting a potential role for PPE26 in inducing a Th17 response. A similar trend was seen in CD8+ T cells, although it did not reach statistical significance, likely due to high variability in the saline control group (Figure 6A). Although there was an increase in the frequencies of CD4+ and CD8+ T cells showing IL-2+IL-17+ expression upon re-stimulation with each of the individual proteins as compared to the unstimulated control, these differences did not reach statistical significance (Figure 6A). We analyzed cytokine secretion in the supernatants from the re-stimulation assays using ELISA (Figure 7). Compared to the control, IFNγ levels were elevated for all three antigens, with significant differences found upon re-stimulation with PE31. Notably, significant differences in TNF secretion were detected for PE31 and PPE26 upon recall compared to the unstimulated control. Additionally, although not significant, elevated levels of IL-10 were observed in response to re-stimulation by all three antigens (Figure 7). Conversely, levels of IL-17A, although not statistically significant, were increased compared to the control, with PPE26 being the lowest inducer in comparison to the other two PE antigens. Finally, re-stimulation with each of the three antigens did not result in an increase of IL-4. Taken together, these results indicate that PE18, PE31 and PPE26 predominantly elicited Th1-type CD4+ and CD8+ effector T cell immune responses in C57BL/6 mice.

PE18 stimulates resident memory T cells (Trm) in the lungs

We investigated if there was evidence of T cell resident memory (Trm) in the lungs of mice immunized with PE18, PE31 and PPE26, and used flow cytometry to quantify these cells in the lung homogenates. As seen in Figure 6B, the total numbers of Trm as defined by the CD69+ CD103+ phenotype for both the CD4+ and CD8+ compartments, were very low for BCG immunized animals, probably due to the vaccine having been given subcutaneously, while naïve animals showed only background levels (Figure 6B). In contrast, there was an increase in Trm populations in the PE18-immunized group for both T cell compartments, though this did not reach statistical significance, possibly due to large variations

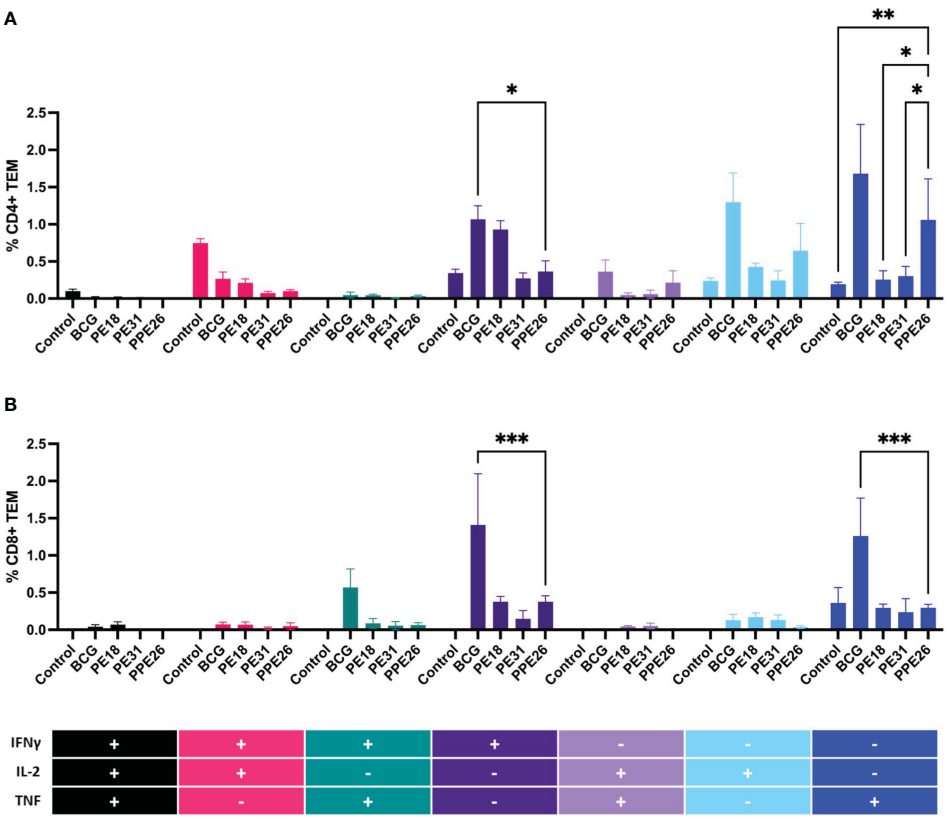

FIGURE 5
Antigen-specific CD4+ and CD8+ cell cytokine responses in vaccinated mice. Splenocytes from immunized mice were re-stimulated *in vitro* with respective proteins (10μg/mL) or BCG lysate, and stained for cell surface CD4 **(A)** and CD8 **(B)** molecules. Intracellular IFNγ, IL-2 and TNF were additionally stained. The percentage of cells expressing one cytokine or multiple cytokines IFNγ, TNF, and IL-2 was determined. The gating strategy for these experiments is shown in Supplementary Figure S1. The results represent mean values (n= 3 mice/group) for percentage of CD4+ or CD8+ T effector memory cells, with SEM. Asterisks denote significant differences according to a two-way ANOVA fit to a main effects only model. Dunnett test was applied for correction of multiple comparisons. The levels of significance are represented as follows: (*$p < 0.05$); (**$p < 0.01$); (***$p < 0.001$).

between the three animals. PE31 and PPE26 did not show the same trend of Trm increase, in either compartment. It should be noted though that our analysis was restricted to the total Trm population rather than antigen-specific Trm cells in the lungs.

Nevertheless, considering the experimental design where each group was immunized with a single antigen, and the mice were housed under controlled indoor conditions, it is reasonable to attribute any observed differences between groups to the respective vaccine candidates. While other possibilities exist, the consistent delivery of antigens suggests that intrinsic reasons for distinct mucosal responses are less likely. Finally, the fact that there was an increase in Trm populations within the PE18-immunized group for both CD4+ and CD8+ T cell compartments suggests that only immunization with PE18 might have triggered a localized immune response in the lungs.

PE18, PE31 and PPE26 proteins did not confer protection against Mtb

To address the capacity of the candidate proteins to induce protective effects, we first tested immunised mouse splenocytes for the ability to restrict mycobacterial growth *in vitro*, in a modified MGIA assay. Following 5 days co-culture with Mtb-LUX strain, we measured luminescence as a proxy for viable bacterial count. The results shown in Figure 8A indicate that splenocytes from BCG-immunised mice resulted in an approximate 0.5 log-fold reduction in bacterial count, compared to unimmunised mice. However, none of the PE/PPE proteins induced a significant effect on bacterial growth inhibition. To assess the ability of the vaccines to induce lung specific immunity we determined viable Mtb counts in lung homogenates from vaccinated mice, in a standard colony-forming unit (CFU) assay. The number of viable bacilli (CFU) in the lungs expressed as mean lung Log10 CFU was reduced from 5.2 in the unvaccinated group to 4.5 in BCG vaccinated mice. However, no reduction was observed as a result of vaccination with the PE/PPE proteins (Figure 8B), though unfortunately, due to technical issues, only three animals were assessed. Taken together, the MGIA assay and the bacterial plating suggest that none of the three PE/PPE proteins tested were protective in the mouse model of infection with Mtb.

Discussion

In this study, we investigated the immunogenicity of PPE26, PE18 and PE31 proteins of Mtb H37Rv in both humans exposed to Mtb, and in mice vaccinated with the proteins.

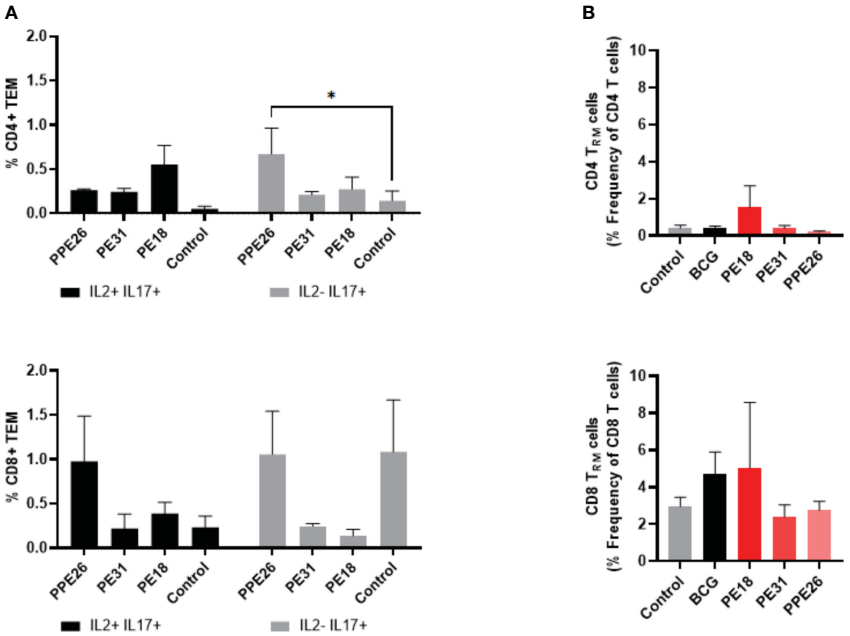

FIGURE 6
Antigen-specific CD4+ and CD8+ cytokine responses and tissue resident T cell populations in the lungs of immunized mice. **(A)** Antigen-specific CD4+ and CD8+ T cell cytokine responses in the spleens of immunized mice. The percentage of cells expressing IL-2, IL-17, or both cytokines was determined. The results represent mean values (n= 3 mice/group) with SEM for the percentage of CD4+ or CD8+ T effector memory cells, and were analyzed by a two-way ANOVA test followed by Dunnett correction test (*$p < 0.05$). **(B)** Total levels of CD4+ and CD8+ resident memory T cells were assessed in the lung tissue of vaccinated mice by flow cytometry, through staining of CD44+CD62L- and CD69+CD103+. The results show mean values (n= 3 mice/group) with SEM of percentage of CD4+ or CD8+ T resident memory cells. Statistical analysis was conducted using a one-way ANOVA test and a *post hoc* Tukey test.

In the quest for a successful TB vaccine, the research has been dedicated to identifying vaccine candidates that can trigger the generation of memory T cells exhibiting a Th1 phenotype. This involves the production of crucial cytokines such as IFNγ, TNF, and IL-2. These CD4+ Th1 lymphocytes and the IFNγ they produce are critical in controlling Mtb infection, as evidenced by susceptibility to mycobacterial disease in individuals with deficiencies affecting components of the IFNγ pathway (34). Notably, the secretion of IFNγ upon re-stimulation of cells exposed to the pathogen stands as a significant marker for cellular immune responses in Mtb infections (35). In the current investigation, we conducted *in vitro* re-stimulation assays to assess the proliferation and cytokine production, specifically IFNγ and TNF, by CD4+ and CD8+ T cells in response to PE18, PE31 and PPE26 proteins. These assays were performed using PBMCs from a cohort from the TB endemic region of Mozambique, which consisted of individuals with exposure to Mtb (both ATB and LTBI) as well as individuals who had received BCG vaccination (BCG-vaccinated healthy controls). Our results showed that the three antigens elicited Th1 cytokine (IFNγ+TNF+) production by CD4+ and CD8+ T cell subsets in individuals from the ATB, LTBI, and BCG-vaccinated groups. Notably, a trend towards higher cytokine production was observed in LTBI individuals, indicating the potential importance of these antigens in the context of latent infection. Although this trend did not reach statistical significance, it is consistent with previous findings indicating differential T cell responses in subjects with latent infection and active disease (36, 37). Latency-associated antigens, such as Rv1733c, have been reported to lead to higher numbers of T cells producing elevated levels of IL-2 in LTBI compared to ATB, supporting their potential for differential diagnosis (38). This suggests a potential association between the nature of the three PE/PPE proteins and latency. In our study, the lack of significant differences among the three groups may be influenced by various factors, including the prolonged exposure of LTBI individuals to the TB pathogen, potential immune compromise in active TB patients, and the specificity of T cell responses in BCG-vaccinated individuals. These findings indicate that the immune response to these proteins is not limited to active TB disease, but can be elicited in various TB or other mycobacterial exposure contexts. Additionally, the presence of antigen-specific antibodies against all three antigens in the sera of individuals across all three groups further supports these results. Importantly, we observed that not all individuals within the groups exhibited equal responsiveness, which could potentially be attributed to variations in the stage of infection at the time of diagnosis. Given the observation of broad T cell stimulatory capacity of these antigens, we also tested if the three antigens might have immunomodulatory properties in PBMC from non-exposed individuals. It has been shown previously that naive T lymphocytes can undergo heterogeneous proliferative responses (homeostatic proliferation) (39). Homeostatic proliferation, driven primarily by cytokines such as IL-7 and IL-15 rather than specific antigen recognition (40), is a gradual response. This slow nature could explain the observed lower levels of CD4 and CD8 T cells in PBMCs from non-exposed

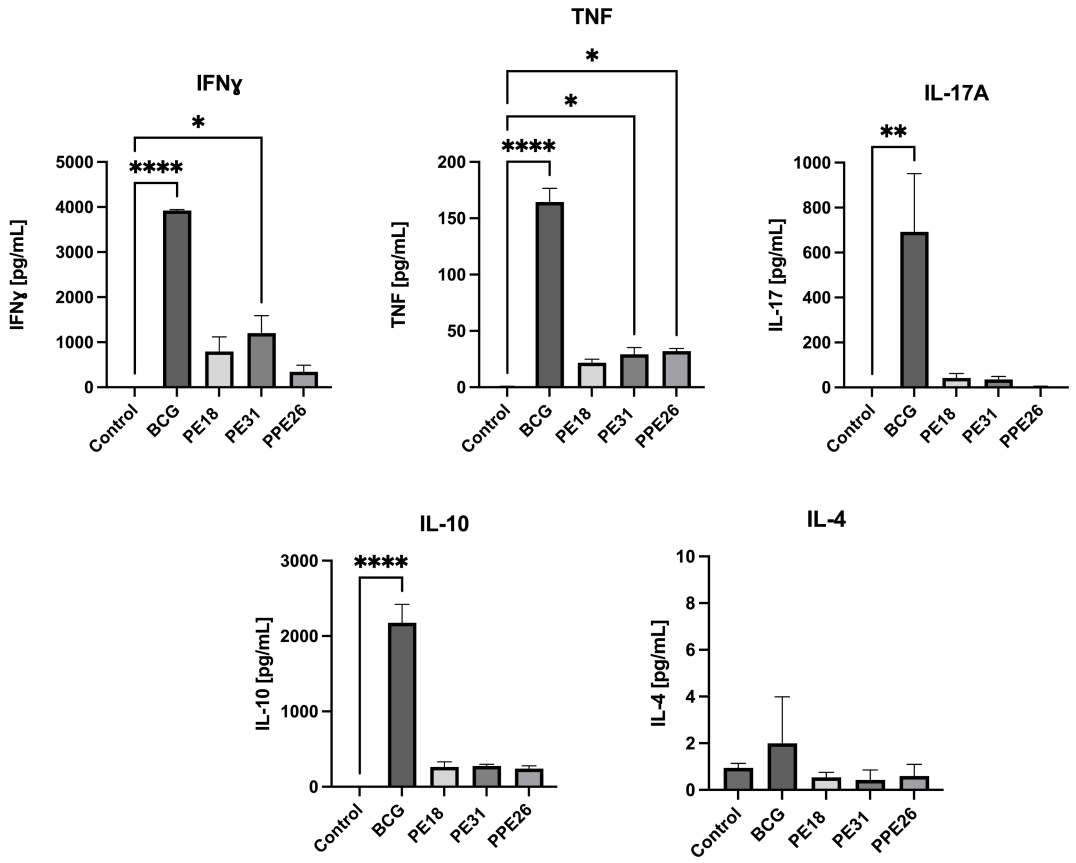

FIGURE 7
Cytokine production in splenocyte cultures supernatants. After re-stimulation with the respective antigens or with BCG lysate, cell culture supernatants were collected, and concentrations of IFNγ, TNF, IL-4, IL-10, and IL-17A were measured by quantitative ELISA. The data are presented as mean values with SEM. Statistical analysis was performed using one-way ANOVA followed by Dunnett test compared to control. (*p < 0.05, **p< 0.01, ****p < 0.0001).

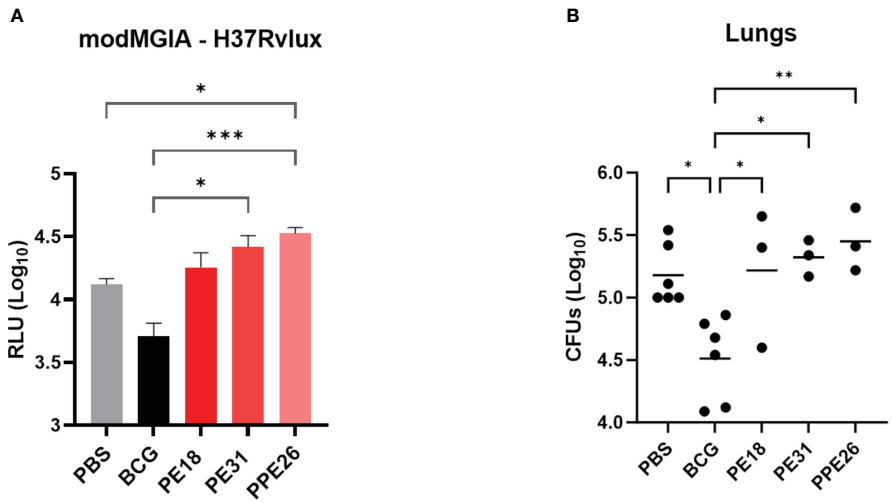

FIGURE 8
Assessment of protective efficacy by PE/PPE antigens in immunized mice. The figure depicts 2-fold evaluation of the protective response induced by PPE26, PE18 and PE31, as compared to negative and BCG control groups. **(A)** Splenocytes from immunized mice were evaluated for their ability to restrict mycobacterial growth *in vitro* using mycobacterial growth inhibition assay (MGIA). Splenocytes were subjected to a co-culture period with the Mtb-LUX strain, and luminescence measurements were employed as a surrogate for determining viable bacterial counts. Data are expressed as relative light units (RLU). **(B)** Lung homogenates were examined for colony-forming units (CFUs) after a 3–4-week incubation period. In both assays, one-way ANOVA with Tukey *post-hoc* test was performed. The data are presented as mean values with SEM. P-value of ≤0.05 was considered to be significant. (*p < 0.05, **p < 0.01, ***p < 0.001).

individuals in our study. This process needs of TCR interaction with MHC:peptide/antigen complexes and signals from cytokine receptors for T cell proliferation (41). Our findings suggest that these antigens may trigger a mechanism comparable to homeostatic T cell proliferation in PBMCs from individuals without prior exposure to Mtb or BCG. This response was observed upon stimulation with PE18 and PPE26, but not PE31. The observed proliferation of CD4+ and CD8+ T cells, along with increased levels of IFNγ upon stimulation with these proteins, suggest either some form of antigen cross-reactivity (such as environmental mycobacteria), or it could mean that they possess some inherent homeostatic properties, driving expansion of the general T cell memory populations in the absence of antigen presentation, a phenomenon that requires further investigation.

In this study, to delve deeper into the T and B cell responses prompted by the three vaccine candidates, C57BL/6 mice were immunized with the respective proteins and their potential to induce both humoral and cellular immune responses was evaluated. The choice of immunization routes, including two subcutaneous and one intranasal, was strategically planned to harness dual benefits. While intranasal immunization provides a localized defense at the site of initial infection (33, 42), subcutaneous immunization elicits a robust systemic immune response, capable of controlling the spread of the pathogen to other organs. First, we analysed reactivity to PE/PPE antigens in serum and BAL of immunized animals. Measured levels of antigen-specific IgG and IgA antibodies indicated a systemic rather than mucosal immune response. Furthermore, PE18 cross-reacts with PE31, and PPE26 has some degree of cross-reactivity with PE31, as showed by levels of antigen-specific IgG. The differential cross-reactivity observed between different PE/PPE proteins could be due to variations in antigenic similarity, with PE18 and PE31 sharing relatively high homology (~64%). Such cross-reactivity could be harnessed in vaccine development, as targeting multiple antigens with cross-reactive epitopes may enhance the breadth and potency of the immune response. Unlike our findings in humans, which demonstrated immunogenicity of PE/PPE antigens in individuals exposed to Mtb and BCG vaccination, mice immunized with BCG exhibited no response to any of the three proteins. This observation suggests that these antigens may be absent in the BCG Pasteur 1173P2 strain utilized in this investigation. To further confirm those results, we performed WB and ELISA analyses with sera from mice immunized with the respective antigens, and assessed their reactivity against the BCG Pasteur strain used in this study. Again, the absence of reactivity in BCG by either WB or ELISA conclusively indicates that the three proteins are not present or expressed in significant quantities in the BCG Pasteur strain. These contrasting observations in humans and mice raise the intriguing question about the nature of the immune response elicited to these antigens in the BCG cohort from Mozambique. The most likely explanation is the interference from NTM, which share numerous antigens with Mtb and BCG, including proteins from the distinctive PE/PPE family. Furthermore, the exact composition of PE/PPE proteins in BCG varies depending on the strain. As an example, Abdallah et al. found over-expressed levels of ESX5 locus genes *pe18* and *ppe26* exclusively in BCG Tice as a result of ESX5 locus duplication (24). Therefore, it is possible that the immune response observed in BCG-vaccinated individuals is a result of cross-reactivity with shared antigens or epitopes present in some NTM bacteria, rather than direct recognition of the proteins in the BCG vaccine strain. Nevertheless, further investigations are warranted to elucidate the specific antigenic components of BCG and their interactions with the host immune system, ultimately enhancing our understanding of BCG-mediated immunity and its potential for improved vaccine development strategies. Further, these findings raise important questions about the potential benefits of incorporating these antigens into BCG-based vaccine strategies. Based on these insights, the concept of using a BCG prime/protein boost strategy with these antigens becomes even more significant. This notion implies that incorporating these antigens into the vaccination scheme could address potential limitations in BCG's efficacy and amplify the immune reaction against tuberculosis.

We also evaluated T cellular proliferation and cytokine responses in immunized mice. In addition to antibody production, our results showed that the three proteins, especially PE18 and PPE26, were capable of inducing activation of both CD4+ and CD8+ T cell populations, accompanied by the secretion of Th1-associated cytokines such as IFNγ and TNF, upon re-stimulation with specific antigens. Furthermore, augmented levels of IL-2 and IL-17 were observed upon re-stimulation with all three proteins, in both the CD4+ and CD8+ compartments. Likewise, the increase in IFNγ and TNF secretion by all three antigens indicates their potential to elicit pro-inflammatory responses, which however appear self-limiting, due to also elevated trends of the regulatory cytokine IL-10. Additionally, in this study, none of the antigens led to the release of IL-4, as measured in the supernatants during antigen re-stimulation assays. This reinforces the idea that the immune response triggered by these antigens is favouring a Th1 profile rather than a Th2 response. In our study, we also observed a noticeable trend towards an increase in lung resident memory T cells among mice vaccinated with PE18, although the specificity to the antigen was not confirmed. The lack of a similar response in the other two groups could indicate antigen-specific variations in immune interactions. While the study's design has limitations, the controlled environment and consistent antigen delivery lend credibility to the idea that the observed differences are likely attributed to the antigenic stimuli themselves. Thus, the trend observed in the PE18-immunized group might indicate the potential presence of a mucosal immune response in the lungs of animals immunized with this specific antigen. Further investigation, including antigen-specific Trm analysis, could provide more precise insights into the impact of these antigens on lung-resident immunity.

Despite these promising immune characteristics, none of the tested PE/PPE proteins conferred protection in the mouse model of TB, as evidenced by the lack of reduction in the lung CFU counts. These findings suggest that while the PE/PPE proteins are capable of inducing broad immune responses, including antibody production and T cell memory, this does not translate into protective immunity against TB, at least in the mouse model of infection. However, several factors may contribute to this outcome. Firstly, the approach of using subunit vaccines, as employed in our

study with individual proteins and the Quil-A adjuvant, may not fully capture potential synergistic effects achievable by combining multiple proteins or even PE/PPE complexes. Additionally, the timing of infection and the assessment of immune responses can significantly impact the observed results. In our study, bacterial burdens in the lungs were assessed three weeks after Mtb challenge, a relatively short period. Contrasting studies (16) conducted assessments one to three months following aerosol infection, suggesting that longer evaluation periods might better capture protective effects or potential changes in immune responses over time. Furthermore, considering the observed levels of CFU counts and results from the MGIA assay, which indicated higher trends of bacterial loads in the PE/PPE-vaccinated animals compared to controls, particularly for antigen PPE26, raises the possibility that these proteins might not confer protection, but instead, could enhance bacterial burden. In this context, several Mtb proteins have been reported to evoke innate and adaptive immune responses, though many of these act as decoy antigens, mimicking host-pathogen effector components and misdirecting immune response pathways to favour the pathogen's survival (43, 44). Thus, PPE26 antigen may play a role in the bacterium's activation of immune evasion mechanisms or modulation of immune responses, interfering with the host's immune defence mechanisms and potentially creating a more favourable environment for bacterial growth. Future research could delve into the mechanisms by which these proteins may affect disease progression and explore modifications or combinations to mitigate any unintended consequences. In this regard, the combination of multiple antigens can elicit a more robust immune response compared to the individual proteins alone. This was shown, for example, when vaccination with adjuvanted individual Rv1789, Rv2220, or Rv3478 proteins conferred only partial protection against challenge with Mtb, but improved protection when the three were administered together (16). Similarly, Bertholet et al. investigated the protective efficacy of a combination of antigens (Rv2608, Rv1813, and Rv3620) against Mtb infection. Individually, these antigens provided partial protection; however, when administered as a combination, a marked increase in protection was observed, comparable to that achieved with BCG vaccination (15). These findings emphasize the potential benefits of combining multiple antigens to enhance the immune response by increasing the production of antigen-specific antibodies, activation of T cells, and release of cytokines involved in immune regulation and pathogen clearance. Furthermore, PE/PPE complexes are of particular interest due to their unique immunomodulatory properties (45). While individual antigens like PE35 and PPE68 are immunogenic individually, their corresponding complex, PE35/PPE68, exhibited significantly higher antibody response in mice (46). Similarly, the PE25/PPE41 complex elicits stronger immune responses compared to individually expressed PE25 or PPE41 proteins in TB patients as well as in a TB mouse model (47). It could therefore be argued that PE18 and PPE26 antigens that can form a potential PE/PPE complex (28, 48), could be more immunogenic and protective if used together, as opposed individually, as performed in this study. Moreover, the possibility of improving overall protection and expanding immune coverage by combining PE/PPE-based vaccines with established TB vaccines like BCG offers an interesting path for further investigation. Finally, additional factors beyond Th1 responses (32) might be important in controlling the Mtb infection in these mice. These results are consistent with previous findings from other studies and underscore the complex and diverse nature of immune responses in the fight against tuberculosis (49, 50).

In conclusion, our study highlights the immunogenicity of PPE26, PE18 and PE31 from Mtb and their ability to elicit broad antibody and T cell responses. However, the lack of protective efficacy observed underscores the need for a comprehensive understanding of the underlying mechanisms and potential synergistic interactions among different PE/PPE proteins. Further research in this area could lead to the development of new TB vaccine strategies that incorporate members of the PE/PPE protein family into their formulation.

Data availability statement

The original contributions presented in the study are included in the article/Supplementary Material. Further inquiries can be directed to the corresponding author.

Ethics statement

The studies involving humans were approved by the Mozambican National Bioethics committee (IRB:00002657; ID: 298/CNBS/15). The studies were conducted in accordance with the local legislation and institutional requirements. The participants provided their written informed consent to participate in this study. The animal study was approved by the University of Leicester Ethics Committee under an approved UK Home Office animal project license (Establishment License X1798C4D2) and in accordance with the Animals (Scientific Procedures) Act 1986. The study was conducted in accordance with the local legislation and institutional requirements.

Author contributions

MG-B: Conceptualization, Data curation, Formal analysis, Funding acquisition, Investigation, Methodology, Project administration, Resources, Software, Visualization, Writing – original draft, Writing – review & editing. EV: Conceptualization, Data curation, Formal analysis, Funding acquisition, Investigation, Methodology, Project administration, Resources, Software, Visualization, Writing – review & editing. AT: Conceptualization, Data curation, Formal analysis, Funding acquisition, Investigation, Methodology, Project administration, Resources, Software, Visualization, Writing – review & editing. LB: Data curation, Formal analysis, Methodology, Software, Writing – review & editing. AC: Conceptualization, Data curation, Formal analysis, Investigation, Methodology, Validation, Visualization, Writing – review & editing. JP: Conceptualization, Data curation, Formal

analysis, Investigation, Methodology, Validation, Visualization, Writing – review & editing. TM: Resources, Writing – review & editing. Mv: Formal analysis, Supervision, Writing – review & editing. MS: Funding acquisition, Project administration, Resources, Supervision, Writing – review & editing. RR: Conceptualization, Formal analysis, Funding acquisition, Project administration, Resources, Supervision, Writing – review & editing.

Funding

The author(s) declare financial support was received for the research, authorship, and/or publication of this article. MG-B and EV were supported by the EU PhD training grant through Marie Sklodowska-Curie Actions (BactiVax project, Ref N° 860325). Further funding support for this study was obtained from the H2020 EC project grant EMI-TB (Ref N° 643558), the VALIDATE Network award (Ref N° P062), and the VALIDATE Network which was funded by the Bill and Melinda Gates Foundation (INV-031830).

Acknowledgments

MG-B and EV were supported by the EU PhD training grant through Marie Sklodowska-Curie Actions (BactiVax project, Ref N° 860325). Further funding support for this study was obtained from the H2020 EC project grant EMI-TB (Ref N° 643558), the VALIDATE Network award (Ref N° P062), and the VALIDATE Network which was funded by the Bill and Melinda Gates Foundation (INV-031830). The artwork was created with BioRender.

Conflict of interest

Authors MG-B and MS were employed by LIONEX GmbH, and author LB was employed by ImmunXperts SA.

The remaining authors declare that the research was conducted in the absence of any commercial or financial relationships that could be construed as a potential conflict of interest.

Publisher's note

Supplementary material

The Supplementary Material for this article can be found online at: https://www.frontiersin.org/articles/10.3389/fimmu.2023.1307429/full#supplementary-material

References

1. World Health Organization. *Global Tuberculosis Report 2022* (2022). Available at: https://www.who.int/teams/global-tuberculosis-programme/tb-reports/global-tuberculosis-report-2022.

2. Colditz GA. Efficacy of BCG vaccine in the prevention of tuberculosis. *JAMA* (1994) 271(9):698. doi: 10.1001/jama.1994.03510330076038

3. Martinez L, Cords O, Liu Q, Acuna-Villaorduna C, Bonnet M, Fox GJ, et al. Infant BCG vaccination and risk of pulmonary and extrapulmonary tuberculosis throughout the life course: A systematic review and individual participant data meta-analysis. *Lancet Global Health* (2022) 10(9):e1307–16. doi: 10.1016/S2214-109X(22)00283-2

4. Brosch R, Gordon SV, Pym A, Eiglmeier K, Garnier T, Cole ST. Comparative genomics of the mycobacteria. *Int J Med Microbiol* (2000) 290(2):143–525. doi: 10.1016/S1438-4221(00)80083-1

5. Parra M, Cadieux N, Pickett T, Dheenadhayalan V, Brennan MJ. A PE protein expressed by mycobacterium avium is an effective T-cell immunogen. *Infection Immun* (2006) 74(1):786–895. doi: 10.1128/IAI.74.1.786-789.2006

6. Cole ST, Brosch R, Parkhill J, Garnier T, Churcher C, Harris D, et al. Deciphering the biology of mycobacterium tuberculosis from the complete genome sequence. *Nature* (1998) 393(6685):537–44. doi: 10.1038/31159

7. Gey Van Pittius NC, Sampson SL, Lee H, Kim Y, Van Helden PD, Warren RM. Evolution and expansion of the mycobacterium tuberculosis PE and PPE multigene families and their association with the duplication of the ESAT-6 (Esx) gene cluster regions. *BMC Evolutionary Biol* (2006) 6(1):1–315. doi: 10.1186/1471-2148-6-95/FIGURES/11

8. Palucci I, Camassa S, Cascioferro A, Sali M, Anoosheh S, Zumbo A, et al. PE_PGRS33 contributes to mycobacterium tuberculosis entry in macrophages through interaction with TLR2. *PLoS One* (2016) 11(3):e0150800. doi: 10.1371/journal.pone.0150800

9. Sayes F, Pawlik A, Frigui W, Gröschel MI, Crommelynck S, Fayolle C, et al. CD4+ T Cells Recognizing PE/PPE Antigens Directly or via Cross Reactivity Are Protective against Pulmonary Mycobacterium Tuberculosis Infection. *PLoS Pathog* (2016) 12(7): e1005770. doi: 10.1371/journal.ppat.1005770

10. Kumarasamy N, Poongulali S, Beulah FE, Akite EJ, Ayuk LN, Bollaerts A, et al. Long-term safety and immunogenicity of the M72/AS01E candidate tuberculosis vaccine in HIV-positive and -negative Indian adults. *Medicine* (2018) 97(45): e131205. doi: 10.1097/MD.0000000000013120

11. Tait DR, Hatherill M, Meeren Ovd, Ginsberg AM, Brakel EV, Salaun B, et al. Final analysis of a trial of M72/AS01 E vaccine to prevent tuberculosis. *New Engl J Med* (2019) 381(25):2429–39. doi: 10.1056/NEJMoa1909953

12. Coler RN, Day TA, Ellis R, Piazza FM, Beckmann AM, Vergara J, et al. The TLR-4 agonist adjuvant, GLA-SE, improves magnitude and quality of immune responses elicited by the ID93 tuberculosis vaccine: first-in-human trial. *NPJ Vaccines* (2018) 3 (1):34. doi: 10.1038/s41541-018-0057-5

13. Abdallah AM, Verboom T, Weerdenburg EM, Gey van Pittius NC, Mahasha PW, Jiménez C, et al. PPE and PE_PGRS proteins of mycobacterium marinum are transported via the type VII secretion system ESX-5. *Mol Microbiol* (2009) 73(3):329–40. doi: 10.1111/j.1365-2958.2009.06783.x

14. Su H, Kong C, Zhu L, Huang Qi, Luo L, Wang H, et al. PPE26 induces TLR2-dependent activation of macrophages and drives th1-type T-cell immunity by triggering the cross-talk of multiple pathways involved in the host response. *Oncotarget* (2015) 6(36):38517–375. doi: 10.18632/oncotarget.5956

15. Bertholet S, Ireton GC, Kahn M, Guderian J, Mohamath R, Stride N, et al. Identification of human T cell antigens for the development of vaccines against mycobacterium tuberculosis. *J Immunol* (2008) 181(11):7948–57. doi: 10.4049/jimmunol.181.11.7948

16. Derrick SC, Yabe IM, Yang A, Kolibab K, Hollingsworth B, Kurtz SL, et al. Immunogenicity and protective efficacy of novel mycobacterium tuberculosis antigens. *Vaccine* (2013) 31(41):4641–465. doi: 10.1016/j.vaccine.2013.07.032

17. Day CL, Abrahams DA, Lerumo L, Rensburg EJv, Stone L, O'rie T, et al. Functional capacity of mycobacterium tuberculosis -specific T cell responses in humans

is associated with mycobacterial load. *J Immunol* (2011) 187(5):2222–32. doi: 10.4049/jimmunol.1101122

18. Perdomo C, Zedler U, Kühl AA, Lozza L, Saikali P, Sander LE, et al. Mucosal BCG vaccination induces protective lung-resident memory T cell populations against tuberculosis. *MBio* (2016) 7(6). doi: 10.1128/mBio.01686-16

19. Lewinsohn DM, Swarbrick GM, Cansler ME, Null MD, Rajaraman V, Frieder MM, et al. Human mycobacterium tuberculosis CD8 T cell antigens/epitopes identified by a proteomic peptide library Edited by homayoun shams. *PLoS One* (2013) 8(6): e670165. doi: 10.1371/journal.pone.0067016

20. Bottai D, Luca MDi, Majlessi L, Frigui W, Simeone R, Sayes F, et al. Disruption of the ESX-5 system of mycobacterium tuberculosis causes loss of PPE protein secretion, reduction of cell wall integrity and strong attenuation. *Mol Microbiol* (2012) 83 (6):1195–209. doi: 10.1111/j.1365-2958.2012.08001.x

21. Sayes F, Sun L, Di Luca M, Simeone R, Degaiffier N, Fiette L, et al. Strong immunogenicity and cross-reactivity of mycobacterium tuberculosis ESX-5 type VII secretion -encoded PE-PPE proteins predicts vaccine potential. *Cell Host Microbe* (2012) 11(4):352–63. doi: 10.1016/j.chom.2012.03.003

22. Borgers K, Ou J-Y, Zheng P-X, Tiels P, Hecke AV, Plets E, et al. Reference genome and comparative genome analysis for the WHO reference strain for mycobacterium bovis BCG danish, the present tuberculosis vaccine. *BMC Genomics* (2019) 20(1):5615. doi: 10.1186/s12864-019-5909-5

23. Asadian M, Hassanzadeh SM, Safarchi A, Douraghi M. Genomic characteristics of two most widely used BCG vaccine strains: danish 1331 and pasteur 1173P2. *BMC Genomics* (2022) 23(1):6095. doi: 10.1186/s12864-022-08826-9

24. Abdallah AM, Hill-Cawthorne GA, Otto TD, Coll F, Guerra-Assunção JoséA, Gao Ge, et al. Genomic expression catalogue of a global collection of BCG vaccine strains show evidence for highly diverged metabolic and cell-wall adaptations. *Sci Rep* (2015) 5(1):15443. doi: 10.1038/srep15443

25. Ali MdK, Zhen G, Nzungize L, Stojkoska A, Duan X, Li C, et al. Mycobacterium tuberculosis PE31 (Rv3477) attenuates host cell apoptosis and promotes recombinant M. Smegmatis intracellular survival via up-regulating GTPase guanylate binding protein-1. *Front Cell Infection Microbiol* (2020) 10:40(February). doi: 10.3389/fcimb.2020.00040

26. Myllymäki H, Niskanen M, Oksanen KE, Sherwood E, Ahava M, Parikka M, et al. "Identification of novel antigen candidates for a tuberculosis vaccine in the adult zebrafish (Danio rerio)." Edited by pere-joan cardona. *PLoS One* (2017) 12(7): e01819425. doi: 10.1371/journal.pone.0181942

27. Vordermeier HM, Hewinson RG, Wilkinson RJ, Wilkinson KA, Gideon HP, Young DB, et al. Conserved immune recognition hierarchy of mycobacterial PE/PPE proteins during infection in natural hosts. *PLoS One* (2012) 7(8):e408905. doi: 10.1371/journal.pone.0040890

28. García-Bengoa María, Meurer M, Stehr M, Elamin AA, Singh M, Oehlmann W, et al. Mycobacterium tuberculosis PE/PPE proteins enhance the production of reactive oxygen species and formation of neutrophil extracellular traps. *Front Immunol* (2023) 14:1206529(August). doi: 10.3389/fimmu.2023.1206529

29. Chen K, Wang N, Zhang X, Wang M, Liu Y, Shi Y. Potentials of saponins-based adjuvants for nasal vaccines. *Front Immunol* (2023) 14:1153042(March). doi: 10.3389/fimmu.2023.1153042

30. Snewin VA, Gares M-P, ÓGaora P, Hasan Z, Brown IN, Young DB. Assessment of immunity to mycobacterial infection with luciferase reporter constructs. *Infection Immun* (1999) 67(9):4586–935. doi: 10.1128/IAI.67.9.4586-4593.1999

31. Cooper AM. Cell-mediated immune responses in tuberculosis. *Annu Rev Immunol* (2009) 27(1):393–422. doi: 10.1146/annurev.immunol.021908.132703

32. Lewinsohn DA, Lewinsohn DM, Scriba TJ. Polyfunctional CD4+ T cells as targets for tuberculosis vaccination. *Front Immunol* (2017) 8:1262(OCT). doi: 10.3389/fimmu.2017.01262

33. Li J, Zhao J, Shen J, Wu C, Liu J. Intranasal immunization with mycobacterium tuberculosis rv3615c induces sustained adaptive CD4+ T-cell and antibody responses in the respiratory tract. *J Cell Mol Med* (2019) 23(1):596–6095. doi: 10.1111/jcmm.13965

34. Boisson-Dupuis Stéphanie, Bustamante J, El-Baghdadi J, Camcioglu Y, Parvaneh N, Azbaoui SEl, et al. Inherited and acquired immunodeficiencies underlying tuberculosis in childhood. *Immunol Rev* (2015) 264(1):103–20. doi: 10.1111/imr.12272

35. Sable SB, Kalra M, Verma I, Khuller GK. Tuberculosis subunit vaccine design: the conflict of antigenicity and immunogenicity. *Clin Immunol* (2007) 122(3):239–515. doi: 10.1016/j.clim.2006.10.010

36. Sutherland JS, Adetifa IM, Hill PC, Adegbola RA, Ota MOC. Pattern and diversity of cytokine production differentiates between mycobacterium tuberculosis infection and disease. *Eur J Immunol* (2009) 39(3):723–295. doi: 10.1002/eji.200838693

37. Harari A, Rozot V, Enders FB, Perreau M, Stalder JM, Nicod LP, et al. Dominant TNF-A+ Mycobacterium tuberculosis–specific CD4+ T cell responses discriminate between latent infection and active disease. *Nat Med* (2011) 17(3):372–76. doi: 10.1038/nm.2299

38. Zhang L, Ma H, Wan S, Zhang Y, Gao M, Liu X. Mycobacterium tuberculosis latency-associated antigen rv1733c SLP improves the accuracy of differential diagnosis of active tuberculosis and latent tuberculosis infection. *Chin Med J* (2022) 135(1):63–695. doi: 10.1097/CM9.0000000000001858

39. Bell EB, Sparshott SM. The peripheral T-cell pool: regulation by non-antigen induced proliferation? *Semin Immunol* (1997) 9(6):347–535. doi: 10.1006/smim.1997.0092

40. Tan JT, Ernst B, Kieper WC, LeRoy E, Sprent J, Surh CD. Interleukin (IL)-15 and IL-7 jointly regulate homeostatic proliferation of memory phenotype CD8+ Cells but are not required for memory phenotype CD4+ Cells. *J Exp Med* (2002) 195(12):1523–325. doi: 10.1084/jem.20020066

41. Min B. Spontaneous T cell proliferation: A physiologic process to create and maintain homeostatic balance and diversity of the immune system. *Front Immunol* (2018) 9:547(MAR). doi: 10.3389/fimmu.2018.00547

42. Giri PK, Sable SB, Verma I, Khuller GK. Comparative evaluation of intranasal and subcutaneous route of immunization for development of mucosal vaccine against experimental tuberculosis. *FEMS Immunol Med Microbiol* (2005) 45(1):87–935. doi: 10.1016/j.femsim.2005.02.009

43. Goldberg MF, Saini NK, Porcelli SA. Evasion of innate and adaptive immunity by mycobacterium tuberculosis. *Mol Genet Mycobacteria* (2015) 2:747–72. doi: 10.1128/9781555818845.ch36

44. Khubaib M, Sheikh JA, Pandey S, Srikanth B, Bhuwan M, Khan N, et al. Mycobacterium tuberculosis co-operonic PE32/PPE65 proteins alter host immune responses by hampering th1 response. *Front Microbiol* (2016) 7:719(May). doi: 10.3389/fmicb.2016.00719

45. Strong M, Sawaya MR, Wang S, Phillips M, Cascio D, Eisenberg D. Toward the structural genomics of complexes: crystal structure of a PE/PPE protein complex from mycobacterium tuberculosis. *Proc Natl Acad Sci* (2006) 103(21):8060–655. doi: 10.1073/pnas.0602606103

46. Ahmad J, Khubaib M, Sheikh JA, Pancsa R, Kumar S, Srinivasan A, et al. Disorder-to-order transition in PE–PPE proteins of mycobacterium tuberculosis augments the pro-pathogen immune response. *FEBS Open Bio* (2020) 10(1):70–855. doi: 10.1002/2211-5463.12749

47. Tundup S, Pathak N, Ramanadham M, Mukhopadhyay S, Murthy KJR, Ehtesham NZ, et al. The co-operonic PE25/PPE41 protein complex of mycobacterium tuberculosis elicits increased humoral and cell mediated immune response. *PLoS One* (2008) 3(10):e35865. doi: 10.1371/journal.pone.0003586

48. Riley R, Pellegrini M, Eisenberg D. Identifying cognate binding pairs among a large set of paralogs: the case of PE/PPE proteins of mycobacterium tuberculosis;. *PLoS Comput Biol* (2008) 4(9):e10001745. doi: 10.1371/journal.pcbi.1000174

49. Cowley SiobhánC, Elkins KL. "CD4+ T cells mediate IFN-γ-independent control of mycobacterium tuberculosis infection both. *In Vitro In Vivo." J Immunol* (2003) 171 (9):4689–995. doi: 10.4049/jimmunol.171.9.4689

50. Majlessi L, Simsova M, Jarvis Z, Brodin P, Rojas Marie-Jésus, Bauche Cécile, et al. An increase in antimycobacterial th1-cell responses by prime-boost protocols of immunization does not enhance protection against tuberculosis. *Infection Immun* (2006) 74(4):2128–37. doi: 10.1128/IAI.74.4.2128-2137.2006

frontiers | Frontiers in Immunology

TYPE Original Research
PUBLISHED 12 December 2023
DOI 10.3389/fimmu.2023.1296501

OPEN ACCESS

EDITED BY
Jianping Xie,
Southwest University, China

REVIEWED BY
Sadiya Parveen,
Johns Hopkins University, United States
Hong Yien Tan,
Xiamen University, Malaysia

*CORRESPONDENCE
Susanna Brighenti
susanna.brighenti@ki.se

†These authors have contributed equally to this work

RECEIVED 18 September 2023
ACCEPTED 28 November 2023
PUBLISHED 12 December 2023

CITATION
Ashenafi S, Loreti MG, Bekele A, Aseffa G, Amogne W, Kassa E, Aderaye G and Brighenti S (2023) Inflammatory immune profiles associated with disease severity in pulmonary tuberculosis patients with moderate to severe clinical TB or anemia. *Front. Immunol.* 14:1296501. doi: 10.3389/fimmu.2023.1296501

Inflammatory immune profiles associated with disease severity in pulmonary tuberculosis patients with moderate to severe clinical TB or anemia

Senait Ashenafi[1,2†], Marco Giulio Loreti[2†], Amsalu Bekele[3], Getachew Aseffa[4], Wondwossen Amogne[3], Endale Kassa[3], Getachew Aderaye[3] and Susanna Brighenti[2*]

[1]Department of Pathology, School of Medicine, College of Health Sciences, Tikur Anbessa Specialized Hospital and Addis Ababa University, Addis Ababa, Ethiopia, [2]Department of Medicine Huddinge, Center for Infectious Medicine (CIM), ANA Futura, Karolinska Institutet, Stockholm, Sweden, [3]Department of Internal Medicine, School of Medicine, College of Health Sciences, Tikur Anbessa Specialized Hospital and Addis Ababa University, Addis Ababa, Ethiopia, [4]Department of Radiology, School of Medicine, College of Health Sciences, Tikur Anbessa Specialized Hospital and Addis Ababa University, Addis Ababa, Ethiopia

Background: Immune control of *Mycobacterium tuberculosis* (Mtb) infection is largely influenced by the extensive disease heterogeneity that is typical for tuberculosis (TB). In this study, the peripheral inflammatory immune profile of different sub-groups of pulmonary TB patients was explored based on clinical disease severity, anemia of chronic disease, or the radiological extent of lung disease.

Methods: Plasma samples were obtained from n=107 patients with active pulmonary TB at the time of diagnosis and after start of standard chemotherapy. A composite clinical TB symptoms score, blood hemoglobin status and chest X-ray imaging were used to sub-group TB patients into 1.) mild and moderate-severe clinical TB, 2.) anemic and non-anemic TB, or 3.) limited and extensive lung involvement. Plasma levels of biomarkers associated with inflammation pathways were assessed using a Bio-Plex Magpix 37-multiplex assay. In parallel, Th1/Th2 cytokines were quantified with a 27-multiplex in matched plasma and cell culture supernatants from whole blood stimulated with *M. tuberculosis*-antigens using the QuantiFERON-TB Gold assay.

Results: Clinical TB disease severity correlated with low blood hemoglobin levels and anemia but not with radiological findings in this study cohort. Multiplex protein analyses revealed that distinct clusters of inflammation markers and cytokines separated the different TB disease sub-groups with variable efficacy. Several top-ranked markers overlapped, while other markers were unique with regards to their importance to differentiate the TB disease severity groups. A distinct immune response profile defined by elevated levels of BAFF, LIGHT, sTNF-R1 and 2, IP-10, osteopontin, chitinase-3-like protein 1, and IFNα2 and IL-8, were most effective in separating TB patients with different clinical disease severity and were also promising candidates for treatment monitoring. TB

patients with mild disease displayed immune polarization towards mixed Th1/Th2 responses, while pro-inflammatory and B cell stimulating cytokines as well as immunomodulatory mediators predominated in moderate-severe TB disease and anemia of TB.

Conclusions: Our data demonstrated that clinical disease severity in TB is associated with anemia and distinct inflammatory immune profiles. These results contribute to the understanding of immunopathology in pulmonary TB and define top-ranked inflammatory mediators as biomarkers of disease severity and treatment prognosis.

KEYWORDS

tuberculosis, inflammation, cytokines, chemokines, disease severity, clinical symptoms, anemia, lung involvement

1 Introduction

Infection with *Mycobacterium tuberculosis* (Mtb) results in a broad spectrum of clinical presentations and tuberculosis (TB) disease outcomes (1). It is well known that Mtb infection initiates a cascade of both pro-inflammatory and anti-inflammatory mediators in the human host that can both promote and limit bacterial dissemination (2, 3). Consequently, immune control in TB is dictated by a range of soluble factors including cytokines, chemokines, and other inflammatory molecules that can influence disease progression (4). Clinical heterogeneity and disease severity of pulmonary TB are multifactorial but have been described to depend on the extent of clinical TB symptoms including anemia and the level of lung involvement such as fibrosis and cavitation (5). This complexity of TB complicates diagnosis, disease prognosis and treatment decision-making and follow up.

It is well-established that cell-mediated Th1 immunity coordinated by IFN-γ and TNF-α, is required to kill Mtb inside macrophages at the site of infection in the lung (6, 7). Instead, the role of Th2 responses including humoral B cell immunity is more controversial (8) but may be less effective to achieve immune control of TB disease. Th1 cytokines typically activate macrophages and cytolytic T cells to kill intracellular Mtb via induction of reactive oxygen and nitrogen species, antimicrobial peptides, and autophagy (6, 9). Conversely, Th2 cytokines including IL-4, IL-13 and IL-10 promote anti-inflammatory responses that are necessary to prevent pathological inflammation but also reduce the capacity of macrophages and T cells to effectively clear Mtb (10). Instead, Th2 cytokines promote the development of B cells into antibody-producing plasma cells (11) that may inactivate bacteria that are released in the extracellular microenvironment but are likely less operative in Mtb infection control (12). Besides pro-inflammatory cytokines such as IL-6, IL-1β, IL-8, and the classical Th1/Th2 polarization of immune cells, there are many different inflammatory mediators and immunomodulatory proteins that could contribute to immunopathogenic responses in TB. Less explored are for example the IL-20 subfamily of cytokines including IL-19, IL-20, IL-22, and IL-24, that have been shown to contribute to tissue healing processes upon chronic infections and inflammation in the lung by mainly targeting the epithelial barrier at mucosal sites (13). But the IL-20 sub-family have also been shown to down-modulate antigen-specific Th1 and Th17 responses in TB (14). Likewise, IL-11 (15), type I and III interferons (IFN) (16, 17), and acute phase proteins including pentraxin, diverse chemoattractants such as RANTES and MIP-1α and β, or eotaxin (3), as well as proteins that are involved in Mtb-driven tissue remodeling and lung matrix destruction, primarily matrix metalloproteinases (MMPs) (18) or ostepontin (19), have been linked to both protective as well as dysfunctional responses in the regulation of inflammation and development of lung pathology in TB and other diseases.

Recently, we described that anemia of chronic TB disease was associated with more severe clinical disease and elevated levels of pro-inflammatory IL-6 but a suppressed IFN-γ response (20). While it is clear that anemia of chronic diseases such as TB is characterized by systemic inflammation (21, 22), it has not been well described what type of signaling pathways or mediators are involved and how these contribute to immunopathology of Mtb. Now, we extend these findings by assessment of inflammatory mediators and cytokines in different sub-groups of pulmonary TB patients based on clinical disease severity, anemia or radiological findings. Plasma levels of biomarkers associated with inflammation pathways including pro-inflammatory and the IL-10 family of cytokines, type I/II/III IFN, TNF ligands and receptors as well as Th1/Th2 and immunomodulatory cytokines and proteins involved in tissue-remodeling and wound-healing were assessed using 37- and 27-multiplex assays, respectively. While these results add to the pipeline of studies using a proteomics approach to improve TB diagnosis and prognosis, we anticipate that these data will also contribute to the understanding of pathophysiology in TB by assessing the inflammatory profile in different TB patient subgroups.

2 Materials and methods

2.1 Study cohort

HIV-negative patients >18 years, with newly diagnosed active pulmonary TB (n=107) and healthy controls (n=19) were recruited at the Chest Unit, Department of Internal Medicine, Tikur Anbessa Specialized University Hospital in Addis Ababa, Ethiopia after written and signed informed consent. The study subjects were enrolled in a previously conducted clinical trial (23) that was approved by the ethical review boards in Ethiopia and Sweden, and registered at www.clinicaltrials.gov, NCT01698476, prior to inclusion of the first patient. Secondary endpoint measures including multiplex protein assays were conducted on one third (107/345; 31%) of the enrolled TB patients in the intervention (n=53) and placebo (n=54) treatment groups, respectively. A confirmed TB diagnosis was based on a positive sputum microscopy or Mtb-culture, and/or clinical symptoms and chest X-ray findings consistent with TB, i.e., clinical TB defined according to WHO criteria. HIV-infection, multidrug-resistant TB (MDR-TB) or extrapulmonary TB, anti-TB treatment in the past 2 years, pregnant women, patients with kidney or liver disease, cancer or autoimmune diseases were excluded from the study. Healthy controls (n=19) were also included to assess baseline levels of inflammatory mediators.

2.2 Clinical measurements

A previously validated clinical TB score (23–25) was used to assess clinical disease severity. This is a numerical composite TB score (2-point scale: symptom absent (0p) or present (1p), max 13p) that included self-reported clinical symptoms (cough, night sweats, and chest pain), as well as different variables documented upon clinical examination including conjunctival pallor, hemoptysis, dyspnea, tachycardia, positive findings at lung auscultation, fever, low BMI (<18 and/or <16), and low mid-upper arm circumference (MUAC) (<22 and/or <20 cm). Weight and height were measured to determine BMI (weight/(height^2)) while a measuring tape was used to assess MUAC. BMI was defined as underweight ≤ 18.5 Kg/m^2 or normal weight > 18.5 Kg/m^2), while MUAC was defined as underweight ≤ 21cm or normal weight > 21cm. Patients were sub-grouped into mild (TB score 0-6) or moderate-severe (TB score 7-13) clinical TB disease based on the average TB score obtained among n=107 included TB patients (Table 1). In addition to the TB score, patients were sub-grouped in anemic and non-anemic TB disease based on the normal reference blood Hb values for males (<13.5 g/dl) and females (<12 g/dl) (26).

An experienced radiologist examined standard full-size posteroanterior chest X-rays and graded pathological lung involvement at the time of diagnosis using the diagnostic standards and classifications of TB described by the American Thoracic Society and as previously reported (23, 27). Pulmonary pathologies included infiltrates, consolidations or opacifications, lesions such as nodules and granulomas, fibrosis, and cavitation. Radiological findings were graded as normal (grade 0): no lung involvement; mild/minimal (grade 1): non-confluent uni- or bilateral lung involvement confined to the apical segment with no visible cavitation; moderately advanced (grade 2): disseminated uni- or bilateral lung involvement in the absence or presence of cavitation (cavity size < 4 cm); or far advanced (grade 3): disseminated uni- or bilateral lung involvement with cavitation (cavity size > 4 cm). For mild TB, the extent of lung involvement did not exceed the volume of the lung on one side above the second costochondral junction or the 4th or 5th vertebrae. For moderately and far advanced TB, the extent of lung involvement comprised disseminated lesions of slight to moderate density that covered the total volume of one lung or equivalent volumes in both lungs, or dense and confluent lesion(s) that were limited to one third of the volume of one lung lobe. The study cohort of n=100 subjects (no available chest X-ray data from n=7) was sub-grouped into patients with more limited (grade 0-2) or extensive (grade 3) lung involvement.

2.3 Laboratory measurements

Peripheral blood was obtained at the time of inclusion and at week 4, 8 and 16 after start of standard chemotherapy from a sub-group of subjects including equal numbers of patients with mild (n=36), moderate (n=36), or severe (n=35) TB disease, determined using a composite clinical TB score described above (24). Blood analyses and chest X-ray were used to further sub-group TB patients into anemic and non-anemic patients or extensive and limited lung involvement using Hb values and imaging data, respectively. Whole blood samples were used for blood chemistry analyses and for Mtb-specific restimulation of blood cells *in vitro* using QuantiFERON-TB Gold in-Tube (Cellestis; Statens Serum Institut, Denmark), according to the manufacturer´s instructions. Plasma samples were isolated from Lymphoprep (Alere technologies, Norway) centrifugation (2000 rpm, 20-30 min at room temperature) of blood in Leucosep tubes (Greiner Bio-One, Austria). Plasma aliquots were stored at -80°C until multiplex analyses. Blood hemoglobin, white blood cell count (WBC) (Abbott, Il, USA), erythrocyte sedimentation rate (ESR), CD4 and CD8 T cell counts (BD Biosciences, NJ, USA) were assessed at the International Clinical Laboratory (ICL) in Addis Ababa, Ethiopia.

2.4 Multiplex assays

Plasma levels of inflammation-associated mediators were assessed using a Bio-Plex Pro Human Inflammation 37-Plex Panel 1, in 96-well plate format for the detection of 37 inflammation biomarkers (171AL001M; Bio-Rad, Hercules, CA). In parallel, secreted proteins in plasma and matched cell culture supernatants (n=79) obtained from whole blood stimulated with Mtb-antigens using the QuantiFERON-TB test, were quantified using a Bio-Plex Pro Human Cytokine 27-Plex Panel, in 96-well plate format for the detection of 27 Th1/Th2 cytokines and chemokines (M500KCAF0Y, Bio-Rad, Hercules, CA). Samples were analyzed using a Bio-Plex® MAGPIX™ Multiplex Reader and the Bio-Plex Manager software (Bio-Rad, Hercules, CA).

TABLE 1 Baseline characteristics of study subjects.

	Human inflammation 37-plex		Human cytokine 27-plex	
Variables[a]	Pulmonary TB (n=107)	Controls (n=12)	Pulmonary TB (n=60)	Controls (n=19)
Age in years (range)	25 (18-63)	30 (18-57)	24.5 (18-70)	29 (18-57)
Gender (M/F)	58/49	4/8	30/30	5/14
Sputum-smear pos/neg (no)	94/13	nd	54/6	nd
TB score (0-13p)	6	nd	6	nd
Mild/Mod-sev TB (no)[b]	58/49	nd	28/32	nd
Hemoglobin (g/dL) (M/F)	12.7 (13/12.4)	nd	13 (13/12.6)	nd
Non-anemic/Anemic TB (no)[c]	50/57	nd	28/32	nd
Chest X-ray grade (0-3p)[d]	3	nd	3	nd
Limited/extensive involvement (no)[e]	41/59	nd	25/29	nd
BMI (kg/m2)	17.75	21.7****	17.8	22.6****
Underweight ≤18.5/Normal weight >18.5	76/31	0/11	42/18	2/16
MUAC (cm)	21.5	25.75****	21.5	27****
ESR (mm/hour)	50	nd	50	nd
WBC counts (10^9 cells/L)	7.8	nd	7.6	nd
CD4 T cell counts (cells/mm^3)	419.5	665.5***	397.5	631***
CD8 T cell counts (cells/mm^3)	327.5	403	300	407*
QuantiFERON (IU/ml)[f]	2.71	1.29	2.79*	0.71

[a]Data are presented as numbers (no) or median.
[b]According to numerical TB score (0–6 p = mild TB, >6 = moderate-severe TB).
[c]According to normal blood Hb reference value for males (<13.5 g/dL) and females (<12 g/dL). Blood Hb was not determined for the healthy controls.
[d]According to radiological chest X-ray grading (0-2 = limited lung involvement, 3 = extensive lung involvement).
[e]n=7 patients did not have chest X-ray data.
[f]Determined using the QuantiFERON TB Gold In-Tube (QFTG) assay.
Statistical difference between TB patients and healthy controls was determined using a Mann-Whitney U test, except for blood Hb comparing the difference between males and females. *p≤0.05, ***p≤0.001, and ****p≤0.0001.
mod-sev TB, moderate-severe TB; BMI, body mass index; MUAC, mid-upper arm circumference; WBC, white blood cell count; ESR, erythrocyte sedimentation rate; nd, not determined.

Blood samples can be used to assess both cells and soluble factors that leak into the peripheral circulation from the site of infection. Inflammatory mediators are produced by diverse cell types including both innate and adaptive immune cells as well as epithelial cells, while specific Th1/Th2 cytokines are mostly produced by activated T cells. In a small pilot experiment, the inflammatory markers in the 37-plex were readily detectable in ex vivo collected plasma samples, while cytokines and chemokines in the 27-plex were expressed at very low levels. To enhance the detection levels of the 27-plex markers, the QuantiFERON-TB assay was used to re-stimulate Mtb-specific T cells in whole blood samples to promote accumulation of cytokines in cell culture supernatants.

2.5 Statistical analysis

Unsupervised analyses of acquired 37-plex and 27-plex data were performed in R programming language (R) version 4.2.2 (R Core Team, 2022) within the RStudio integrated development environment version 2023.03.1 + 446. These methods included random forest (RF) for classification and ranking of the most important mediators and principal component analysis (PCA) for dimensionality reduction and clusters analyses. Principal component 1 (PC1) and 2 (PC2), were presented in box plot graphs showing interquartile range and median. The normality of the data was tested using Shapiro–Wilk normality test. A non-parametric Mann-Whitney test or Kruskal-Wallis and Dunn's post-test as well as Holm's multiple correction test was used for comparison of two or multiple unpaired groups. A p-value < 0.05 was considered significant. Statistical analysis and box plot graphs were generated via the package 'ggstatsplot' (28).

Manual analyses of data were performed in GraphPad Prism 9.0, using an unpaired t-test for normally distributed data, while data that did not pass a normality test was analyzed using the Mann–Whitney test. Box and whiskers plots show data as median and 10-90 percentile, while violin plots shown median and range. Bar graphs show mean and 95% confidence interval (CI) or standard error (SE). Correlation was determined using Spearman´s correlation test. A repeated measurements ANOVA

and Sidak post-test was used for comparison of longitudinal data presented in bar graphs as mean and standard error at week 0, 4, 8 and 16. A p-value < 0.05 was considered significant.

3 Results

3.1 Clinical and laboratory characteristics of TB patient sub-groups

Baseline data from TB patients and controls is presented in Table 1. Enrolled TB patients were young, median 25 years, and around 70% of the TB subjects were underweight and accordingly both BMI and MUAC were significantly lower (p<0.0001) in the TB patients compared to healthy controls. Peripheral CD4 T cell counts have been shown to be associated with disease severity in HIV-negative TB patients (29) and were also significantly reduced (p<0.001) in the TB patients compared to the controls. In the subjects used in the 27-plex assay, CD8 T cell counts were higher (p<0.05) in the controls while IFN-γ levels detected by the QuantiFERON test were significantly higher (p<0.05) in the TB patients.

Chronic inflammation was mapped in four sub-groups of study subjects including 1.) pulmonary TB patients (n=107) vs healthy controls (HC) (n=12/19), 2.) patients with mild (n=58) vs moderate-severe (mod-sev) (n=49) clinical TB, 3.) anemic (n=57) vs non-anemic (n=50) patients and 4.) patients with limited (n=41) vs extensive (n=59) lung involvement. The proportion of cavitary TB in the cohort was high, around 84% (data not shown). As expected, the composite clinical TB score was significantly higher in patients with moderate/severe TB (p<0.0001) and in patients with anemia (p=0.0003) (Figures 1A, B). There was no difference in the TB score comparing extensive versus limited TB disease (Figure 1C), despite a higher radiological score in TB patients with extensive lung involvement (Figure 1F). Contrary, chest X-ray grading was similar in mild versus mod-sev TB and anemic versus non-anemic TB (Figures 1D, E). Blood Hb was naturally lower in anemic TB patients (p<0.0001) but also in patients with mod-sev TB (p=0.0001) (Figures 1G, H). As an indicator of inflammation severity (30), serum albumin levels were found to be significantly lower in mod-sev TB (p=0.0007) and anemic TB patients (p=0.001) (Figures 1J, K), and there was a positive correlation (r=0.38; p<0.0001) between blood Hb and serum albumin levels in all TB patients (Figure 1M). Serum albumin was similar in TB patients with extensive and limited chest X-ray findings (Figure 1L).

3.2 Longitudinal changes of soluble mediators demonstrate a normalization of inflammation in response to anti-TB treatment

The protein concentrations in plasma for the 37-plex and in plasma and QuantiFERON supernatants for the 27-plex are summarized in Supplementary Tables 1, 2A, B, 3, respectively. All marker abbreviations are listed in a footnote (Table S1, S2A, B). First, unsupervised analysis was exploited to provide an unbiased view of the inflammatory immune profile in the different study sub-groups. Random forest (RF) analyses ranked the importance of the markers in each multiplex assay to better discriminate between the different study sub-groups. Principal component analyses (PCA) were used to reduce data dimensionality when comparing different TB disease groups and to enable clusters generation. It was apparent that the magnitude of the detected 27-plex cytokine responses was clearly lower in plasma with many data points below the detection levels. Therefore, data obtained with restimulated whole blood samples were used for the unsupervised analyses.

In the first part of the analyses, baseline (week 0) and longitudinal treatment responses (week 4, 8 and 16) detected in the TB patients were plotted together with the control group (Figures 2A-H). For the 37-plex and 27-plex, 9 inflammation markers and 7 cytokines were ranked according to the order of importance based on a minimum of 50% variance in the PCA analyses (Figures 2A, B, E, F, Supplementary Figure 1). For the 37-plex, these included the TNF superfamily members (TNFSF) LIGHT/TNFSF14 and B cell activating factor (BAFF)/TNFSF13B, MMP-1 and 2, Osteocalcin, soluble TNF receptor (sTNF-R) 1 as well as sIL-6R-β (gp130), pentraxin-3, and the IL-6 family member IL-11 (Figures 2A, B). While these top-ranked 9 inflammation markers created diverse clusters at week 0, 4, and 8, the week 16 clusters overlapped to a great extent with the healthy controls (Figure 2B), which confirmed that the majority of the inflammatory markers (PC1: 38.64%) were normalized upon successful anti-TB treatment (week 0 vs week 16: p<0.0001) (Figure 2C). In addition, some markers (PC2: 15.86%) differed significantly comparing baseline data to week 4, 8 and 16 (p<0.01 – <0.0001), but this variability was gradually reduced from week 0 to week 16 (p<0.0001) (Figure 2D).

The 7 top-ranked markers in the corresponding 27-plex analyses were mostly chemokines including monocyte chemoattractant protein (MCP-1), IP-10 (CXCL10), RANTES (CCL5), IL-1 receptor antagonist (RA), TNF-α, eotaxin and IL-4 (Figures 2E, F). However, these markers did not discriminate the baseline and different follow up time-points to the same extent as the 37-plex data (Figure 2F). The PC1 (38.86%) analyses showed that the cluster of ranked cytokines did not differ from baseline to week 16 or compared to the control group (Figure 2G), while the PC2 (17.62%) variance between week 0, 4 or 8 and the controls was significant (week 0 vs HC: p=0.002, week 4 vs HC: p=0.007; week 8 vs HC: p=0.01) (Figure 2H).

3.3 Distinct sets of inflammation markers separate different TB disease severity groups

Next, the inflammatory response at baseline in TB patients with mild or mod-sev disease was analyzed together with (Figures 3A-D) and without (Figures 3E-H) the healthy control group. When the control group was included, the markers with highest discriminatory importance included BAFF, sTNF-R1 and 2,

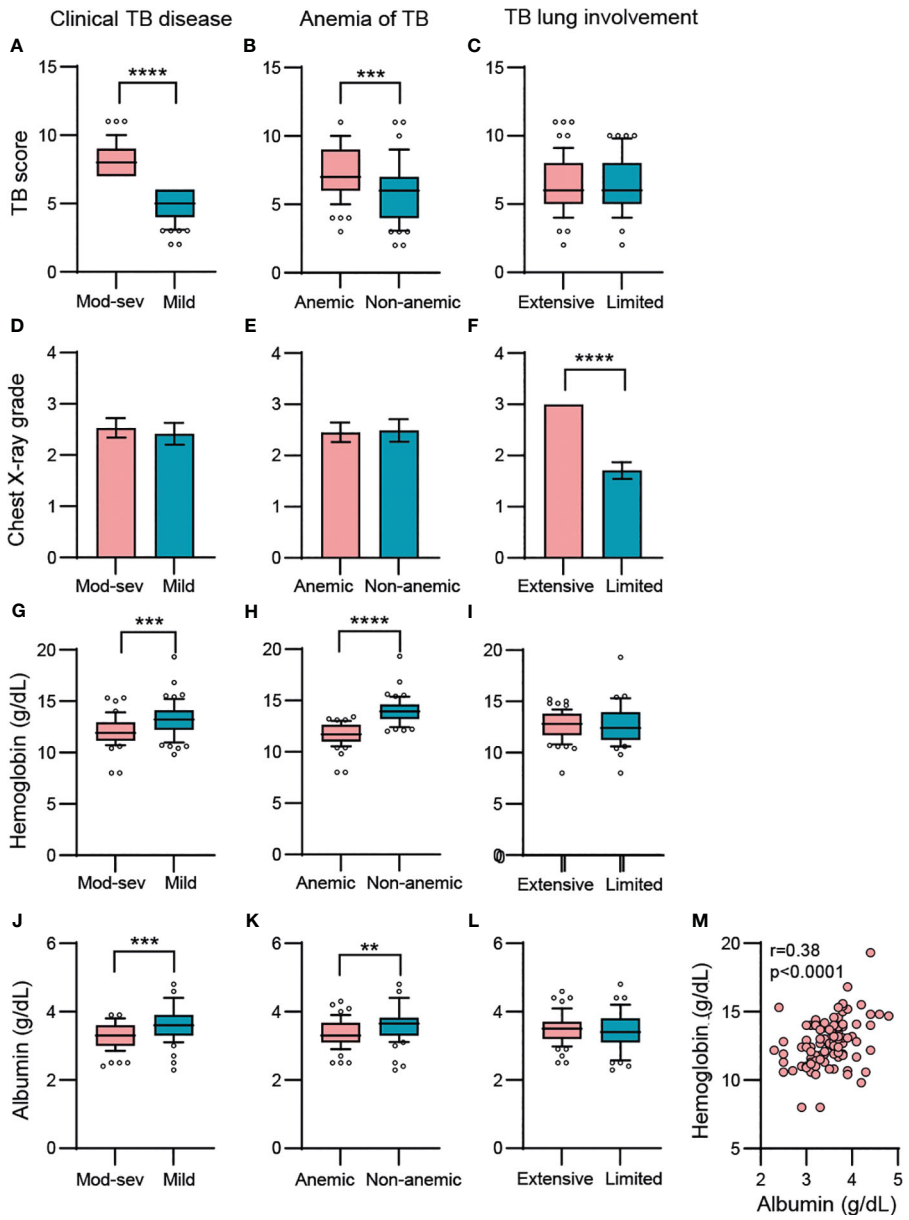

FIGURE 1
Baseline variables in clinical TB disease (mod-sev vs mild TB), anemia of TB (anemic vs non-anemic TB) and TB lung involvement (extensive vs limited TB). **(A-C)** Clinical TB score, **(D-F)** chest X-ray grade, **(G-I)** blood Hb, **(J-L)** serum albumin levels. **(M)** Correlation analysis between blood Hb and serum albumin including all TB patients was determined using Spearman´s correlation test. Data is presented in box and whiskers plots (median and 10-90 percentile) or bar graphs (mean and 95% CI) and was analyzed using a Mann-Whitney *U* test or an unpaired t-test. **p≤0.01, ***p≤0.001, and ****p≤0.0001.

MMP-2, sCD30, Osteopontin (or ETA-1, early T lymphocyte activation), Chitinase-3-like protein 1 (CHI3L1), sCD163 and MMP-3 (Figures 3A, B). Compared to the longitudinal treatment analyses for all TB patients (Figures 2A, B), only three markers overlapped with baseline analyses of clinical TB disease severity, including BAFF, sTNF-R1 and MMP2 (Figures 3A, B) that were all ranked to be of high importance in the respective RF analyses. For clinical TB disease severity, PC1 (44.97%) analyses demonstrated a significant difference between mod-sev TB versus mild TB (p=0.0003) and compared to the healthy control (mod-sev TB vs HC, p<0.0001; mild TB vs HC, p=0.0009) (Figure 3C). There was also a difference in PC2 (14.22%) comparing the clinical disease groups to controls (mod-sev TB or mild TB vs HC, p=0.000008), but no difference comparing mod-sev and mild TB (Figure 3D). Six of the top-ranked 9 markers remained listed in the RF plot when mild TB was compared to mod-sev TB in the absence of the controls (Figure 3E). Instead of MMP-2, 3, and CHI3L1, the acute phase protein, pentraxin-3, was ranked together with IL-19 and IL-8 (Figures 3E, F). PC1 (43.96%) analysis confirmed significant differences in mod-sev compared to mild TB (p=0.00005), while no difference in PC2 (12.02%) was detected (Figures 3G, H).

Thereafter, we continued to explore the inflammatory baseline profile comparing anemic to non-anemic TB patients (Figures 3I-L) as well as patients with extensive compared to limited lung

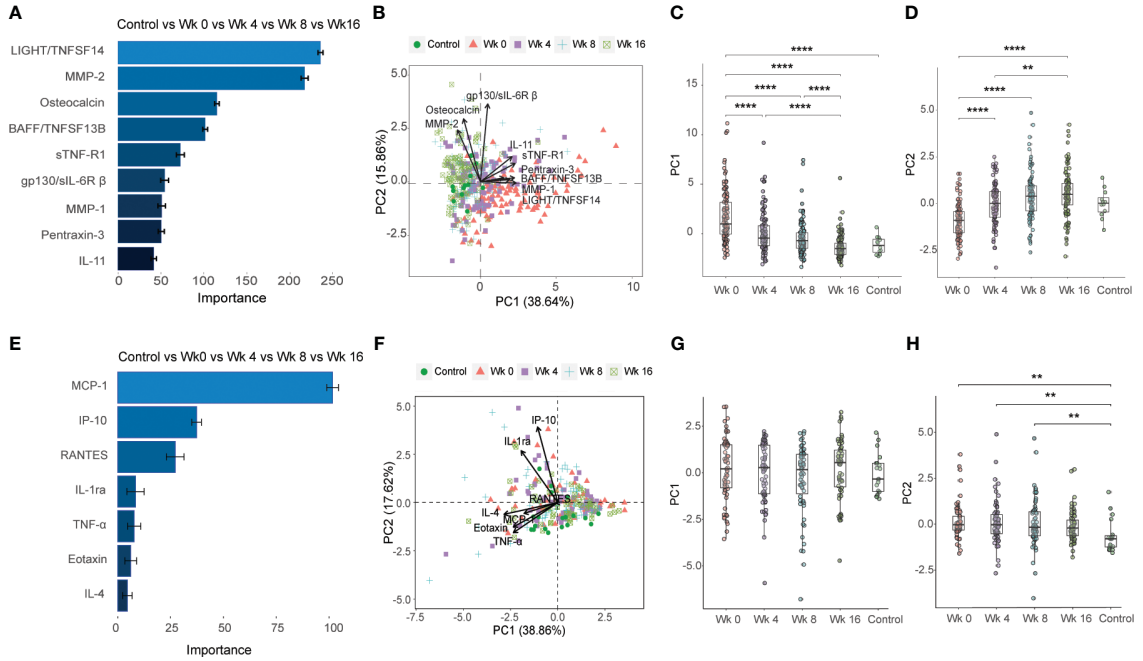

FIGURE 2
Importance ranking and dimensionality reduction facilitate cluster generation of multiplex data from longitudinal samples obtained from TB patients and healthy controls. **(A)** Random forest (RF) analyses of acquired 37-plex inflammation panel obtained at week 0, 4, 8 and 16 from TB patients and healthy controls. **(B)** Principal component analysis (PCA) showing the longitudinal response in all TB patients and controls including top-9 inflammation markers ranked by RF analyses. Scatter box plots of **(C)** PC1 and **(D)** PC2. **(E)** RF of acquired 27-plex cytokine panel obtained at week 0, 4, 8 and 16 from TB patients and healthy controls. **(F)** PCA showing the longitudinal response all TB patients and controls including top-7 cytokines ranked by RF analyses. Scatter box plots of PC1 **(G)** and PC2 **(H)**. Multiplex data in **(A-D)** were obtained from plasma samples, while multiplex data in **(E-H)** were obtained from QuantiFERON supernatants from whole blood samples. Data is presented as mean and standard error and all principal components were assessed using Kruskal-Wallis and Dunn´s post-test with multiple comparisons corrected by Holm–Bonferroni method. **p≤0.01, ***p≤0.001, and ****p≤0.0001.

involvement (Figures 3M-P). Five of the top-ranked 9 markers comparing mod-sev to mild TB (Figures 3E, F) were also listed comparing anemic to non-anemic TB patients, while 4 markers were unique, a proliferation-inducing ligand (APRIL/TNFSF13), IL-11, thymic stromal lymphopoietin (TSLP) and MMP-1, in discrimination of anemic and non-anemic TB patients (Figures 3I, J). Like clinical TB disease severity, PC1 (56.84%) analysis demonstrated significant differences comparing anemic to non-anemic TB patients (p=0.0002), with no difference in PC2 (11.40%) variance (Figures 3K, L). Contrary, three (sCD163, pentraxin-3 and IL-8) of the top-ranked 9 markers for clinical disease severity (Figures 3E, F) overlapped with the RF analyses comparing extensive with limited lung disease (Figures 3M, N), suggesting that there may be differences in inflammatory mediators involved in clinical and radiological disease severity. The variance in both PC1 (36.54%) and PC2 (12.95%), were significantly different in patients with extensive compared to limited lung disease (p=0.002 and p=0.005, respectively) (Figures 3O, P).

3.4 Diverse cytokine and chemokines profile separate different TB disease severity groups

The baseline inflammatory response was further explored using the Th1/Th2 cytokine 27-plex in patients with mod-sev and mild clinical TB in the presence (Figures 4A-D) or absence (Figures 4E-H) of the healthy control group. Four out of 7 markers overlapped among the top-ranked cytokines used to discriminate mod-sev TB from mild TB in the presence or absence of the controls (Figures 4A–H). While macrophage inflammatory protein (MIP-1β or CCL4), IL-17A and IL-1β were classified to be of high importance to separate the different groups, IFN-γ-induced protein 10 (IP-10 or CXCL10) and eotaxin were more related to separation of TB patients and controls (Figures 4A, B), whereas IL-7 was ranked of high importance to discriminate between mod-sev and mild TB (Figures 4E, F). PCA showed a low discriminatory power of PC1 (32.59%), while PC2 (19.04%) analysis showed that mod-sev TB was significantly different compared to both mild TB (p=0.04) and the healthy control (p=0.0003) (Figures 4C, D). Exclusion of the controls did not alter the relationship notably, but there was no difference between the disease severity groups detected for PC1 (46.96%) but significant differences (p=0.002) comparing these groups in PC2 (19.30%) (Figures 4G, H).

Comparison of anemic to non-anemic TB patients (Figures 4I-L) disclosed only one overlapping cytokine, IL-7, that was ranked as a top-classifier to separate both mod-sev from mild TB and anemic from non-anemic TB disease. Other markers ranked to separate anemia from non-anemia included IL-2, IL-1 receptor antagonist (RA), IL-13, IFN-γ, RANTES (CCL5) and IP-10 (Figures 4I, J). Based on these cytokines and chemokines, the PC1

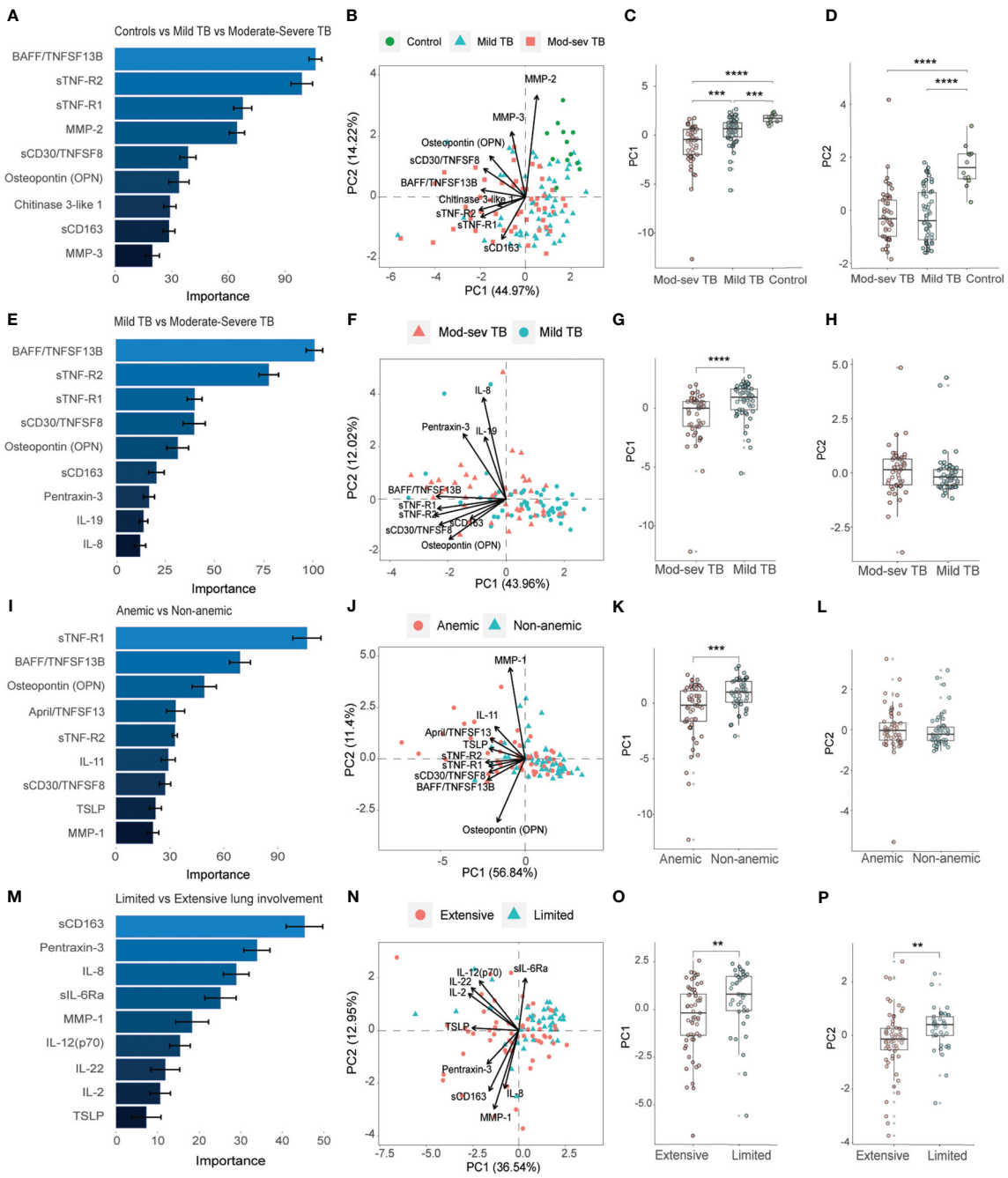

FIGURE 3
Importance ranking and dimensionality reduction facilitate clusters generation of multiplex inflammation data from different sub-groups of TB patients and healthy controls. **(A)** Random forest (RF) analyses of acquired 37-plex inflammation panel from patients with mild and mod-sev TB disease and healthy controls. **(B)** Principal component analysis (PCA) showing the baseline response in patients with mod-sev and mild TB as well as controls including top-9 inflammation markers ranked by RF analyses. Scatter box plots of **(C)** PC1 and **(D)** PC2. **(E)** RF analyses of acquired 37-plex inflammation panel from patients with mild and mod-sev TB disease. **(F)** PCA showing the baseline response in patients with mod-sev and mild TB including top-9 inflammation markers ranked by RF analyses. Scatter box plots of **(G)** PC1 and **(H)** PC2. **(I)** RF analyses of acquired 37-plex inflammation panel from patients with and without anemic TB disease. **(J)** PCA showing the baseline response in patients with mod-sev and mild TB including top-9 inflammation markers ranked by RF analyses. Scatter box plots of **(K)** PC1 and **(L)** PC2. **(M)** RF analyses of acquired 37-plex inflammation panel from TB patients with limited or extensive lung involvement. **(N)** PCA showing the baseline response in patients with extensive and limited lung involvement including top-9 inflammation markers ranked by RF analyses. Scatter box plots of **(O)** PC1 and **(P)** PC2. All multiplex data were obtained from plasma samples. Data is presented as mean and standard error and all principal components were assessed using Kruskal-Wallis and Dunn´s post-test with multiple comparisons corrected by Holm–Bonferroni method or Mann-Whitney *U* test. **$p \leq 0.01$, ***$p \leq 0.001$, and ****$p \leq 0.0001$.

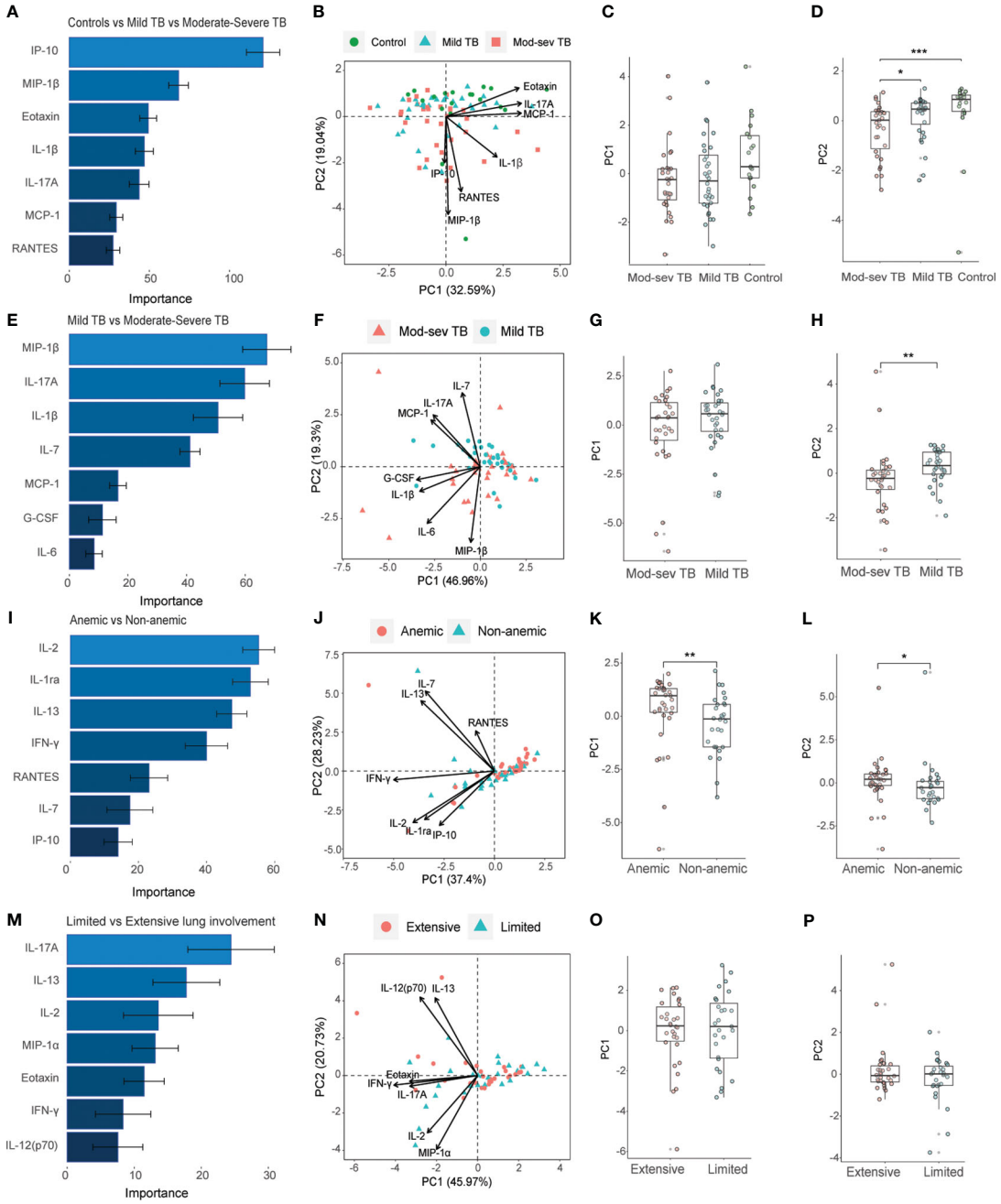

FIGURE 4
Importance ranking and dimensionality reduction facilitate clusters generation of multiplex cytokine data from different sub-groups of TB patients and healthy controls. **(A)** Random forest (RF) analyses of acquired 27-plex cytokine panel from patients with mild and mod-sev TB disease and healthy controls. **(B)** Principal component analysis (PCA) showing the baseline response in patients with mod-sev and mild TB as well as controls including top-7 cytokines ranked by RF analyses. Scatter box plots of **(C)** PC1 and **(D)** PC2. **(E)** RF analyses of acquired 27-plex cytokine panel from patients with mild and mod-sev TB disease. **(F)** PCA showing the baseline response in patients with mod-sev and mild TB including top-7 cytokines ranked by RF analyses. Scatter box plots of **(G)** PC1 and **(H)** PC2. **(I)** RF analyses of acquired 27-plex cytokine panel from patients with and without anemic TB disease. **(J)** PCA showing the baseline response in patients with mod-sev and mild TB including top-7 cytokines ranked by RF analyses. Scatter box plots of **(K)** PC1 and **(L)** PC2. **(M)** RF analyses of acquired 27-plex cytokine panel from TB patients with limited or extensive lung involvement. **(N)** PCA showing the baseline response in patients with extensive and limited lung involvement including top-7 cytokines ranked by RF analyses. Scatter box plots of **(O)** PC1 and **(P)** PC2. All multiplex data were obtained from QuantiFERON supernatants from whole blood samples. Data is presented as mean and standard error and all principal components were assessed using Kruskal-Wallis and Dunn´s post-test with multiple comparisons corrected by Holm–Bonferroni method or Mann-Whitney *U* test. *$p \leq 0.05$, **$p \leq 0.01$, and ***$p \leq 0.001$.

(37.4%) and PC2 (26.3%) analyses revealed significant discrepancies between the anemic and non-anemic TB groups (p=0.008 and p=0.02, respectively) (Figures 4K, L). Finally, the top-7 ranked markers to separate extensive from limited lung involvement partly overlapped with the set of cytokines determined to separate mod-sev and mild TB (IL-17A, eotaxin) as well as anemic and non-anemic TB patients (IL-2, IL-13, IFNγ), while unique cytokines included MIP-1α (CCL3) and IL-12

(Figures 4M, N). However, this cytokine module did not separate extensive from limited lung disease in either PC1 (45.97%) or PC2 (20.73%) (Figures 4O, P).

3.5 Inflammation profiles that associate with TB disease severity or immune control

To explore possible findings that were not uncovered by the unsupervised methods, manual analysis of the multiplex data was performed in more detail. About 25% of the inflammation markers and cytokines in the multiplex assays tested were significantly higher in TB disease compared to the healthy controls, while only five mediators, the type IV collagenases, MMP2 and 3, the bone matrix protein, osteocalcin, and the chemokines, eotaxin and MCP-1, were higher in the controls (Table S1, S2A, B). Most, but not all markers upregulated in TB patients were also related to disease severity. Overall, 8 out of 17 inflammation markers that were up-regulated in TB patients were also significantly ($p<0.03$ - <0.0001) elevated in mod-sev TB as well as anemic TB patients, generating an inflammation response module consisting of BAFF, LIGHT, sTNF-R1 and 2, IP-10, osteopontin, CHI3L1 and IFNα2 (Figures 5A-F; Table S1). APRIL demonstrated a very similar expression profile compared to BAFF (Table S1). Majority of these markers were significantly down-regulated upon successful chemotherapy (Figures 5A-E, right panel). Eotaxin levels were not restored during the first months of treatment (Figure 5F), but other markers that were down-modulated in the TB patients such as osteocalcin and MMP-2 were significantly up-regulated after 16 weeks chemotherapy (data not shown). Another 5 markers were only related to clinical disease severity and anemia including sCD30, IL-8, IL-20, IL-29/IFNδ1 and TNF-α (Table S1, S2A, B). Notably, CHI3L1 and IL-8 were the only markers significantly up-regulated in mod-sev TB, anemic TB as well as patients with extensive lung involvement (data not shown). BAFF and APRIL were also relatively higher in extensive compared to limited lung disease (data not shown).

Finally, to obtain an overview of markers related with potential protective or harmful effects, we mapped the immune markers associated with clinical TB disease severity and anemia (Figures 6A-T). While pro-inflammatory IL-6 ($p<0.009$) was elevated in the mod-sev TB group, Th1 cytokines such as IFN-γ ($p<0.002$) and TNF-α ($p<0.009$) but also IL-7 ($p<0.05$), IL-17A ($p<0.05$) and RANTES ($p<0.009$), were all significantly higher in mild TB disease (Figures 6A-F). Interestingly, both IP-10 ($p<0.02$), sTNF-R1 ($p<0.03$) and sTNF-R2 ($p<0.0001$) (Figures 5C, D, G, H), were inversely expressed as compared to IFN-γ and TNF-α (Figures 6B, C). Likewise, sCD30 ($p<0.0005$), IL-8 ($p<0.005$), CHI3L1 ($p<0.04$) and IL-20 ($p<0.03$) were significantly higher in mod-sev TB disease, while anti-inflammatory cytokines G-CSF ($p<0.007$), IL-4 ($p<0.003$) and IL-10 ($p<0.005$) were clearly higher in mild TB disease (Figures 6I-O). In support of the results in mod-sev TB, findings comparing anemic to non-anemic TB patients suggested that the immunomodulatory cytokines IL-11 ($p<0.03$) and IL-19 ($p<0.04$) were higher in TB patients with anemia, and IL-2 ($p<0.006$), MCP-1 ($p<0.03$) as well as IL-13 ($p<0.009$) were elevated in non-anemic disease (Figures 6P-T). Overall, these results implicate a mixed Th1/Th2 response in TB patients with mild disease, whereas inflammatory mediators and cytokines that are involved in pathological inflammation were more prevalent in mod-sev TB disease.

4 Discussion

4.1 Summary of current findings

This study intended to explore the peripheral inflammation profile in sub-groups of TB patients based on clinical disease severity, presence of anemia, or the radiological extent of lung disease. Multiplex protein analyses in plasma samples and QuantiFERON cell culture supernatants from TB patients and healthy controls demonstrated that distinct clusters of inflammation markers and cytokines separated the different TB disease sub-groups with variable efficacy. The sets of top-ranked markers changed to a variable degree depending on the inclusion of the healthy controls. Accordingly, a distinct set of markers may be effective to discriminate between TB patients and controls, while other markers may be effective to separate different disease severity groups or to follow treatment response over time. While several markers overlapped upon comparison of different TB patient sub-groups, other markers were unique with regards to their importance to differentiate the TB disease severity groups. The clinical disease and anemia sub-groups were generally more coherent compared to TB patients grouped based on the extent of lung involvement. Clearly, an immune response profile defined by up-regulated levels of BAFF, LIGHT, sTNF-R1 and 2, IP-10, osteopontin, CHI3L1 and IFNα2 and IL-8, were effective in separating TB patients with different disease clinical severity and were also rapidly down-regulated after start of anti-TB treatment. In addition, TB patients with mild disease displayed immune polarization towards mixed Th1/Th2 responses, while IL-6, IL-8, and the IL-20 subfamily of cytokines were more predominant in mod-sev TB disease and anemia of TB. Altogether, these results contribute to the understanding of the pathophysiology in TB and how to define peripheral immune response profiles to assess disease severity and to follow treatment prognosis and outcome of TB disease.

4.2 Discrepancy between clinical TB scores and radiological findings

A strength of this study is the sub-group comparisons that allowed us to view immunomodulation and the extent of inflammation in TB disease more carefully. For this purpose, we used a well-characterized patient cohort where clinical disease severity was determined using numerical scoring of typical TB symptoms according to a previously validated method (23–25). Many patients were malnourished and anemic and had low peripheral CD4 T cells counts and low albumin levels, consistent

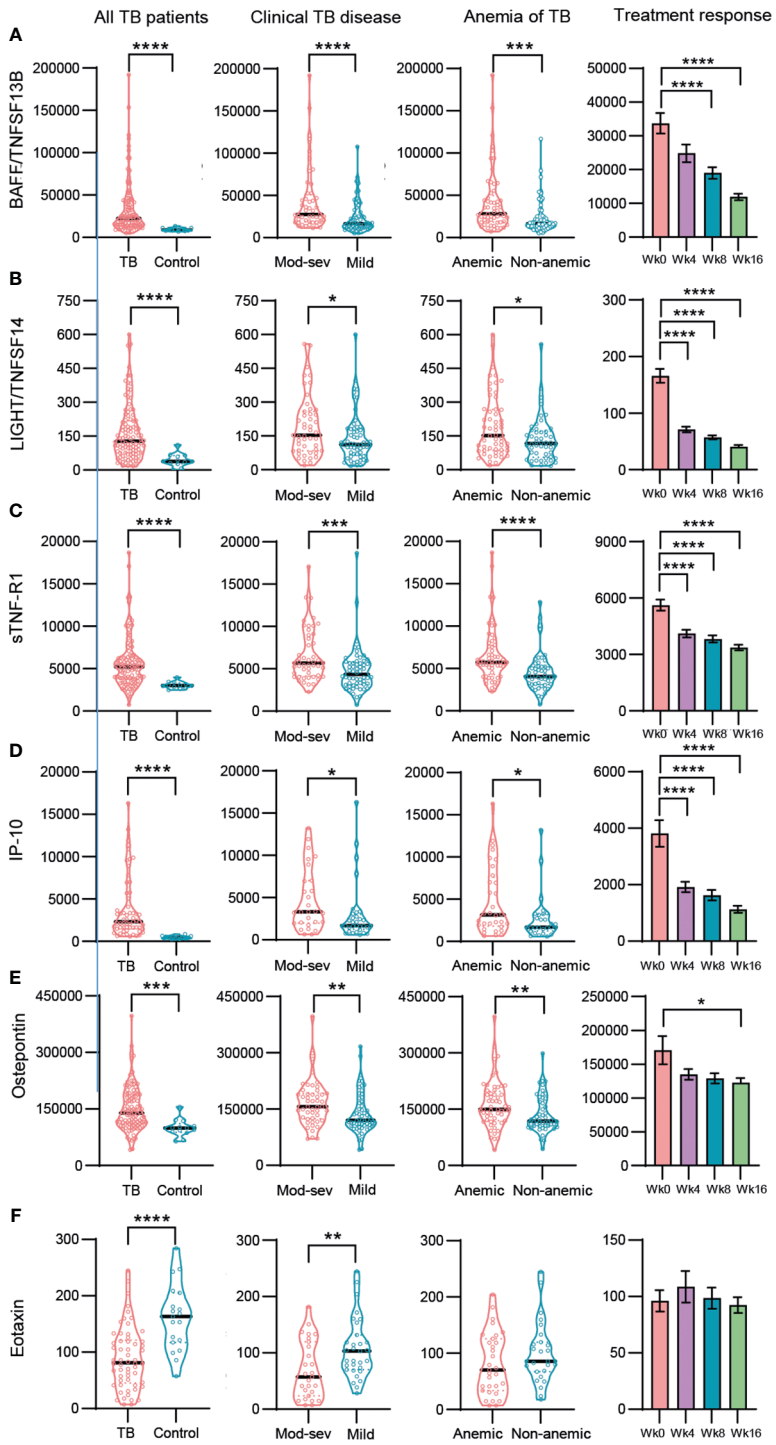

FIGURE 5
Baseline and longitudinal responses of selected top-ranked inflammation mediators and cytokines in different sub-groups of TB patients and healthy controls. **(A)** BAFF/TNFSF13B, **(B)** LIGHT/TNFSF14, **(C)** sTNF-R-1, **(D)** IP-10, **(E)** Osteopontin, **(F)** Eotaxin. Biomarker levels (pg/ml) is shown in all TB patients (TB patients vs controls), clinical TB disease (mod-sev vs mild TB), anemia of TB (anemic vs non-anemic TB) and treatment response (week 0, 4, 8 and 16). Data is presented in violin plots (median and range) or bar graphs (mean and SE) and was analyzed using a Mann-Whitney *U* test or a repeated measurements ANOVA and Sidak post-test. *$p \leq 0.05$, **$p \leq 0.01$, ***$p \leq 0.001$, and ****$p \leq 0.0001$.

with progressive TB disease. However, clinical TB disease and anemia did not correlate with the extent of pulmonary involvement as determined with chest X-ray. Radiological manifestations in TB are heterogeneous, and it is not clear how clinical symptoms are associated to the extent of lung involvement at the time of diagnosis. Although, it is evident that cavitary TB is related to a poor prognosis including unfavorable treatment outcomes, treatment relapse, higher transmission rates, and

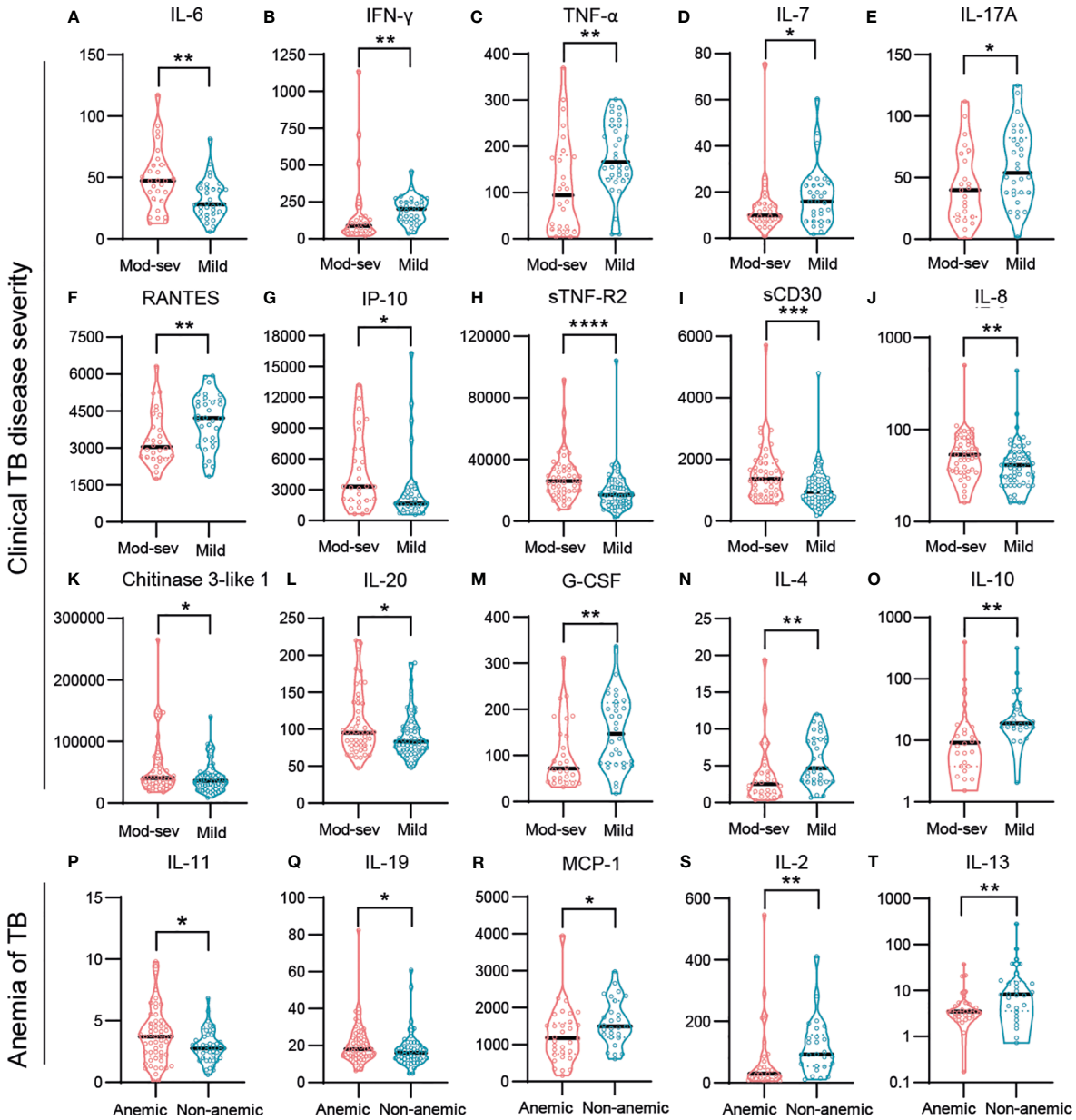

FIGURE 6
Baseline responses of selected inflammation mediators and cytokines in TB patients with different disease severity. **(A)** IL-6, **(B)** INF-γ, **(C)** TNF-α, **(D)** IL-7, **(E)** IL-17A, **(F)** RANTES, **(G)** IP-10, **(H)** sTNF-R2, **(I)** sCD30, **(J)** IL-8, **(K)** Chitinase 3-like 1, **(L)** IL-20, **(M)** G-CSF, **(N)** IL-4 **(O)** IL-10, **(P)** IL-11, **(Q)** IL-19, **(R)** MCP-1, **(S)** IL-2, **(T)** IL-13. Biomarker levels (pg/ml) are shown in patients with mod-sev TB compared to mild TB disease **(A-O)**, and in anemic TB patients compared to non-anemic TB patients **(P-T)**. Data is presented in violin plots (median and range) and was analyzed using a Mann-Whitney *U* test or an unpaired t-test. *p≤0.05, **p≤0.01, ***p≤0.001, and ****p≤0.0001.

development of drug resistance (31). The data from this study demonstrated that chronic inflammation in anemic TB patients was a highly associated to more severe clinical TB disease, which support the notion that anemia is a better predictor of disease severity compared to chest X-ray findings such as cavitation in TB. A previous study comparing pulmonary TB patients with and without diabetes (DM) demonstrated that a clinical score was not different comparing TB to TBDM patients, while radiological data revealed that cavitation was significantly more common in TBDM patients (32). Therefore, clinical disease severity and the extent of lung involvement may not be entirely consistent. In addition, it was found that TB and TBDM patient groups displayed similar cure rates with anti-TB therapy, despite a higher presence of cavitary TB among DM patients (32). Various methods and scoring systems to assess and quantify radiological changes in the lung have been reported that include different parameters such as cavitation, numbers and types of lesions, location, size, and coverage (33–35). PET-CT likely provides a more accurate image of the pathological involvement, but is not available at all health care facilities, especially not in developing countries.

4.3 Use of multiplex assays to explore immune biomarkers in TB infection and disease

To our knowledge, this is the first investigation to map a larger number of inflammatory mediators and cytokines based on clinical TB disease severity and anemia. Numerous studies have been conducted to investigate the diagnostic and prognostic potential of cytokines and chemokines in TB as compared to healthy controls and/or individuals with latent TB (36–40) and as biomarkers of TB disease severity and outcome (41, 42). A recent study compared a 14-plex cytokine assay in patients with drug-susceptible or multidrug-resistant (MDR)-TB as well as individuals with latent TB and uninfected controls and reported a mixed Th1/Th17/Th2 response in the MDR-TB patients with cytokine levels significantly higher compared to the other groups (40). This was proposed as a signature of hyperinflammation and disease severity that could discriminate different stages of Mtb infection (40). However, no significant differences in clinical symptoms were identified in the enrolled MDR-TB patients compared to patients with drug-susceptible TB (40), which suggests that clinical disease severity was not different in these groups. A similar study proposed that CXCL9 and IP-10 could be used as biomarkers to differentiate drug-susceptible TB from MDR-TB (43). The regulation of chemokines and chemokine receptor expression controls the recruitment of imperative effector cells that participate in granuloma formation and bacterial control, while other subsets of inflammatory cells promote pathological processes (7). Several cytokines and chemokines including IFNγ, TNFα, IL-17A, IL-1β (44) and MIP-1α and IP-10, have been described to be associated with bilateral lung involvement and cavitary TB (41). Furthermore, combinations of MIP-1α, IL-8, and IP-10, were proposed as novel biomarkers for predicting adverse treatment outcomes in pulmonary TB patients (41). Consistent with the results from our study, a clinical trial previously described that the majority of 69 biomarkers tested decreased with anti-TB treatment of pulmonary TB patients, except for osteocalcin, MCP-1 and MCP-4, which were significantly increased (42). While the role of osteocalcin in TB is unknown, a cohort study demonstrated an increased risk of osteoporosis in patients with active TB that is likely caused by persistent inflammation (45). MCP-1 levels in plasma have previously been reported to increase in pulmonary TB patients upon successful chemotherapy, similar to eotaxin levels that were shown to be lower in TB patients compared to the controls (36).

4.4 Diverse peripheral cytokine profiles representative of different TB endotypes

It is a common notion that lost immune control in TB is characterized by excess production of pro-inflammatory cytokines together with Th1 and Th17 cytokines, which result in neutrophil infiltration and bystander action of T cells that promote pathological inflammation and tissue destruction at the site of infection in the lung (46, 47). While this is true in many aspects, poor immune control in TB has also been shown to be dictated by premature expansion of anti-inflammatory macrophages or myeloid-derived suppressor cells (MDSC) as well as regulatory B and T cells (Breg and Treg) that emerge as a result of chronic inflammation (10, 48, 49). This is particularly evident in granulomatous lesions at the site of Mtb infection, where numerous recent reports from humans and non-human primates demonstrate that dysfunctional Th1/Th17 CD4+ and cytolytic CD8+ T cells responses correlate with bacterial growth and disease progression, while type 2 immunity as well as FoxP3+ Tregs and MDSCs expressing inhibitory molecules and mediators are associated with bacterial persistence (50–56). These data are all supportive of an immunosuppressive environment in the TB lesions that are driven by a hyperinflammatory response. Single-cell sequencing of Mtb granulomas in zebra fish and non-human primates, suggested that spatial organization of granulomas involving a mix of robust Th1 (IFN-γ, IL-12, IL1-β) but also counteracting Th2 (Il-4 and IL-13) responses, were associated with macrophage epithelialization and bacterial control (57). This is in line with our findings that support a mixed Th1/Th17/Th2 response in non-anemic TB patients and patients with mild TB disease. Perhaps some of the discrepancies among different reports can be explained by the fact that heterogeneity in clinical TB disease can be classified into different disease endotypes, characterized by multiple distinct molecular traits and disease mechanisms such as either immunodeficiency or pathologic excessive inflammation (58, 59).

4.5 TNF superfamily members regulate T cell and macrophage responses in TB

A large group of inflammatory mediators that were differentially regulated in mild compared to mod-sev TB disease belonged to the TNF superfamily. Here, LIGHT has been shown to contribute to the activation of both CD4+ and CD8+ T cells, but not to late control of Mtb infection (60), while CD30 is required for T cell activation and organization in TB granulomas. Soluble CD30 was one of the markers that did not differ between TB patients and controls but were strongly elevated in patients with mod-sev TB disease and anemia. Interestingly, children with active TB, low weight, and low blood Hb levels, had high sCD30 levels in plasma that also correlated to disease severity (61). *In vivo*, blockade of CD30-CD30L interactions on activated T cells has been shown to promote abnormal inflammation in mycobacteria-infected mice including decreased Th1 and Th17 responses (62). Thus, it is likely that excess levels of sCD30 in the circulation could bind to membrane-bound CD30L and prevent co-stimulatory interaction with CD30, which may impair essential Th1 responses and promote mycobacterial growth (63). Similarly, sTNFR-1 has been shown to be up-regulated in active TB patient's along with IL-8 and CXCL9 (64), while virulent Mtb can inactivate TNF-α and TNF-induced apoptosis of infected cells by release of sTNF-R2 (65). The soluble forms of TNFR are induced by TNF-α itself and act as a feed-back mechanism to prevent the pathological effects of TNF-α. As an

example, serum levels of sTNF-R1and 2 increased markedly after intervention of myocardial infarction and primarily sTNF-R1 appeared as an independent predictor of clinical outcomes in patients (66).

4.6 BAFF and APRIL signaling promote B cell responses in TB and other diseases

Our multiplex analyses demonstrated that BAFF and the related molecule APRIL, were among the top-ranked classifiers used to separate mild from mod-sev TB or non-anemic patients from anemia of TB. The BAFF/APRIL signaling pathways are known to be of crucial importance for B cell development and have a clinical relevance for development of autoimmune diseases but also infections (67, 68). Interestingly, BAFF expression is increased by IFN-α signaling (69, 70) and excess BAFF promotes inflammation in autoimmune diseases by increasing B cell numbers and antibody titers. Accordingly, neutrophils have been shown to produce BAFF that highly accelerated plasma cell generation and antigen-specific antibody production (71). It has also been reported that elevated levels of BAFF may activate class switching of B cells to enhance humoral immune responses in patients with TB pleuritis (72). A role of BAFF/APRIL on T cell function and survival has also been proposed (73) and increased levels of BAFF and APRIL mRNA were previously found in peripheral CD4+ T cells isolated from patients with active TB (74). These studies suggest that BAFF and APRIL correlate with enhanced Th1 responses and elevated survival of inflammatory CD4+ T cells (74, 75). Plasma levels of BAFF in our study correlated strongly with IL-6 ($r=0.52$, $p<0.0001$) but not with TNF-α or IFN-γ (data not shown). Moreover, while most CD19+ B cells express the BAFF-receptor, only a few percent of CD4+ and <1% of CD8+ T cells express this receptor, and majority of the BAFF-R expression was found on the surface of CD4+CD25+ Treg cells (76). These studies emphasize that the importance of elevated BAFF and APRIL levels in Mtb pathogenesis has not yet been properly addressed, but the overall relevance of B cells and humoral immunity in TB remains controversial. We have previous shown that enhanced plasmablast responses in pulmonary TB patients including antigen-specific IgG levels were associated with impaired peripheral Th1 cell responses and progressive TB disease (77). Likewise, bacterial persistence in granulomas has been shown to be related to enrichment of plasma cells, coordinated via Th2 signaling pathways (52). Possibly, B cells and antibodies may dictate Mtb-specific immune responses toward protection or pathogenesis depending on the stage of infection as well as the TB-specific endotype.

4.7 Immunoregulatory cytokines prevent proper activation of CD4+ T cells in a diverse spectrum of diseases including TB

Several cytokines in the multiplex assays tested exhibited anti-inflammatory and/or immunomodulatory effects. Comparisons of patients with mild TB and mod-sev disease or anemia, demonstrated that Th1 (IL-2, IFN-γ, and TNF-α) as well as Th2 (IL-4, IL-13, and IL-10) and Th17 responses were higher in mild TB disease. Instead, mod-sev TB disease presented higher levels of Osteopontin, CHI3L1, IL-11, IL-19 and IL-20. It has previously been shown that the profibrogenic molecule, Osteopontin, is elevated in TB patients (78) and that this could be considered as a potential biomarker for TB surveillance and severity assessment (19). CHI3L1 is a another profibrogenic factor that has been strongly associated with diseases including asthma, arthritis, sepsis, diabetes, liver fibrosis, and is also involved in cancer cell growth and proliferation including activation of tumor-associated macrophages, and Th2 polarization of CD4+ T cells (79). Likewise, G-CSF stimulation of PBMCs *in vitro*, alters the T cell function and promotes a Th2 type with an increase of IL-4 and decrease of IFN-α production (80). Accordingly, skewing towards a Th2 response in patients with cystic fibrosis and *P. aeruginosa* infection, correlated with elevated serum levels of G-CSF (81). In the human lung, IL-11 upregulation has been associated with a range of fibroinflammatory diseases, and fibroblast-specific IL-11 signaling drives chronic inflammation in fibrotic lung disease in mice (15). As such, a pathogenic role of IL-11 in TB infection has been proposed to involve early lung inflammation including pro-inflammatory cytokines and neutrophilic infiltration (82). The IL-20 family of cytokines are mainly expressed by lung epithelial cells that may dampen inflammatory responses during chronic inflammation. While the role of IL-20 cytokines in TB is poorly investigated, one report demonstrated that IL-19 and IL-24 are elevated in pulmonary TB patients and *in vitro* neutralization of these cytokines resulted in an enhanced CD4+ Th1/Th17 responses (14). Moreover, it has been found that IL-19, IL-20 and IL-24 promoted cutaneous infection with *S. aureus* in mice by down-regulation of IL-1β and IL-17A-dependent pathways (83). Inhibition of these IL-20 cytokines also improved bacterial clearance of *S. pneumoniae* and decreased pro-inflammatory cytokines and recruitment of neutrophils and dendritic cells in the lung (84). Perhaps these different immunomodulatory mediators contribute to inappropriate activation and poor recruitment of imperative immune cell subsets to the site of infection in the TB granuloma.

4.8 Soluble immune biomarkers as prognostic tools of TB disease and outcome

Even though the main aim with this study was to obtain new knowledge that could increase the understanding of the host immune response to Mtb, these results also add to the current literature related to discovery of biomarkers or immune response modules that could function as correlates of immune protection or progressive TB disease (85). TB disease severity is often assessed on the basis of chest X-ray or bacteriological results including sputum-positivity or numbers of acid-fast bacilli in sputum (86). In clinical trials, time to sputum conversion at 2 months is a common hard endpoint but is practically demanding to coordinate in an effective manner (87). Therefore, suitable surrogate markers in peripheral

blood could improve and facilitate qualitative and large-scale assessment of TB disease status and treatment outcome (88). A recent meta-analysis on biomarkers in active TB, identified a total of 81 markers with the potential to be used in treatment monitoring (89). This review highlighted the barriers created by heterogeneity in study design patient cohorts and data reporting (89), which are difficult to overcome comparing many small sized studies. Even so, multi-omics studies on proteins in circulation also enables a comprehensive understanding of the interaction of the immune system and the bacteria and facilitates identification of immune pathways that contribute to disease development. Importantly, immune biomarkers may not only benefit routine clinical management but also assessment of randomized trials, especially in a time when research on host-directed therapies comprise great future potential as adjunct treatment options for diverse groups of TB patients (90, 91).

Data availability statement

The original contributions presented in the study are included in the article/Supplementary Material. Further inquiries can be directed to the corresponding author.

Ethics statement

The studies involving humans were approved by the regional ethical review boards in Addis Ababa, Ethiopia and Stockholm, Sweden (EPN, dnr 2011/1014-31/1). The studies were conducted in accordance with the local legislation and institutional requirements. The participants provided their written informed consent to participate in this study.

Author contributions

SA: Conceptualization, Data curation, Formal analysis, Investigation, Methodology, Project administration, Software, Validation, Visualization, Writing – original draft. ML: Conceptualization, Data curation, Formal analysis, Investigation, Software, Visualization, Writing – original draft. AB: Conceptualization, Investigation, Methodology, Project administration, Resources, Writing – review & editing. GAs: Conceptualization, Investigation, Methodology, Writing – review & editing, Formal analysis. WA: Conceptualization, Investigation, Methodology, Writing – review & editing. EK: Conceptualization, Investigation, Methodology, Writing – review & editing. GAd: Conceptualization, Investigation, Methodology, Writing – review & editing, Project administration, Supervision. SB: Conceptualization, Investigation, Methodology, Project administration, Supervision, Data curation, Formal analysis, Funding acquisition, Resources, Software, Validation, Visualization, Writing – original draft.

Funding

The author(s) declare financial support was received for the research, authorship, and/or publication of this article. This project was funded by grants from the Swedish Heart and Lung Foundation (Hjärt-Lungfonden, HLF) (2019-0299/2019-0302 and 2022-0484 to SB) and the Swedish Research Council (Vetenskapsrådet, VR) (2019-01744/2022-00970 and 2019-04720/2022-03174 to SB). KID funding for doctoral student ML was provided by Karolinska Institutet. SB has ongoing research grants from HLF and VR (2023–2025). The APC was funded by VR.

Acknowledgments

Bioinformatics support was kindly provided by Assoc. Prof. Carsten Daub at the Center for Bioinformatics and Biostatistics (CBB), Anirudra Parajuli, Dept. of Medicine Huddinge (MedH), and Alen Lovric, Dept. of Laboratory Medicine (LABMED) at Karolinska Institutet in Stockholm, Sweden. We thank the local study team at the Tikur Anbessa Specialized University Hospital and the Armauer Hansen Research Institute (AHRI) in Addis Ababa, Ethiopia, coordinated by Nebiat Gebreselassie. We also thank all the nurses and administrative staff at the collaborative health centers in Addis Ababa. Finally, we are sincerely grateful to all the patients and healthy controls who participated in this study.

Conflict of interest

The authors declare that the research was conducted in the absence of any commercial or financial relationships that could be construed as a potential conflict of interest.

The author(s) declared that they were an editorial board member of Frontiers, at the time of submission. This had no impact on the peer review process and the final decision.

Publisher's note

All claims expressed in this article are solely those of the authors and do not necessarily represent those of their affiliated organizations, or those of the publisher, the editors and the reviewers. Any product that may be evaluated in this article, or claim that may be made by its manufacturer, is not guaranteed or endorsed by the publisher.

Supplementary material

The Supplementary Material for this article can be found online at: https://www.frontiersin.org/articles/10.3389/fimmu.2023.1296501/full#supplementary-material

References

1. Cadena AM, Fortune SM, Flynn JL. Heterogeneity in tuberculosis. *Nat Rev Immunol* (2017) 17(11):691–702. doi: 10.1038/nri.2017.69

2. Sasindran SJ, Torrelles JB. Mycobacterium tuberculosis infection and inflammation: what is beneficial for the host and for the bacterium? *Front Microbiol* (2011) 2:2. doi: 10.3389/fmicb.2011.00002

3. Domingo-Gonzalez R, Prince O, Cooper A, Khader SA. Cytokines and chemokines in mycobacterium tuberculosis infection. *Microbiol Spectr* (2016) 4(5):1–37. doi: 10.1128/microbiolspec.TBTB2-0018-2016

4. Tiwari D, Martineau AR. Inflammation-mediated tissue damage in pulmonary tuberculosis and host-directed therapeutic strategies. *Semin Immunol* (2023) 65:101672. doi: 10.1016/j.smim.2022.101672

5. Luies L, du Preez I. The echo of pulmonary tuberculosis: mechanisms of clinical symptoms and other disease-induced systemic complications. *Clin Microbiol Rev* (2020) 33(4):1–19. doi: 10.1128/CMR.00036-20

6. O'Garra A, Redford PS, McNab FW, Bloom CI, Wilkinson RJ, Berry MP. The immune response in tuberculosis. *Annu Rev Immunol* (2013) 31:475–527. doi: 10.1146/annurev-immunol-032712-095939

7. Saunders BM, Britton WJ. Life and death in the granuloma: immunopathology of tuberculosis. *Immunol Cell Biol* (2007) 85(2):103–11. doi: 10.1038/sj.icb.7100027

8. van Rensburg IC, Wagman C, Stanley K, Beltran C, Ronacher K, Walzl G, et al. Successful TB treatment induces B-cells expressing FASL and IL5RA mRNA. *Oncotarget* (2017) 8(2):2037–43. doi: 10.18632/oncotarget.12184

9. Arranz-Trullen J, Lu L, Pulido D, Bhakta S, Boix E. Host antimicrobial peptides: the promise of new treatment strategies against tuberculosis. *Front Immunol* (2017) 8:1499. doi: 10.3389/fimmu.2017.01499

10. Brighenti S, Joosten SA. Friends and foes of tuberculosis: modulation of protective immunity. *J Intern Med* (2018) 10:125–44. doi: 10.1111/joim.12778

11. Vazquez MI, Catalan-Dibene J, Zlotnik A. B cells responses and cytokine production are regulated by their immune microenvironment. *Cytokine* (2015) 74 (2):318–26. doi: 10.1016/j.cyto.2015.02.007

12. Lu LL, Chung AW, Rosebrock TR, Ghebremichael M, Yu WH, Grace PS, et al. A functional role for antibodies in tuberculosis. *Cell* (2016) 167(2):433–43 e14. doi: 10.1016/j.cell.2016.08.072

13. Rutz S, Wang X, Ouyang W. The IL-20 subfamily of cytokines–from host defence to tissue homeostasis. *Nat Rev Immunol* (2014) 14(12):783–95. doi: 10.1038/nri3766

14. Kumar NP, Moideen K, Banurekha VV, Nair D, Babu S. Modulation of Th1/Tc1 and Th17/Tc17 responses in pulmonary tuberculosis by IL-20 subfamily of cytokines. *Cytokine* (2018) 108:190–6. doi: 10.1016/j.cyto.2018.04.005

15. Ng B, Cook SA, Schafer S. Interleukin-11 signaling underlies fibrosis, parenchymal dysfunction, and chronic inflammation of the airway. *Exp Mol Med* (2020) 52(12):1871–8. doi: 10.1038/s12276-020-00531-5

16. Boxx GM, Cheng G. The roles of type I interferon in bacterial infection. *Cell Host Microbe* (2016) 19(6):760–9. doi: 10.1016/j.chom.2016.05.016

17. Odendall C, Voak AA, Kagan JC. Type III IFNs are commonly induced by bacteria-sensing TLRs and reinforce epithelial barriers during infection. *J Immunol* (2017) 199(9):3270–9. doi: 10.4049/jimmunol.1700250

18. Rohlwink UK, Walker NF, Ordonez AA, Li YJ, Tucker EW, Elkington PT, et al. Matrix metalloproteinases in pulmonary and central nervous system tuberculosis-A review. *Int J Mol Sci* (2019) 20(6):1–35. doi: 10.3390/ijms20061350

19. Wang D, Tong X, Wang L, Zhang S, Huang J, Zhang L, et al. The association between osteopontin and tuberculosis: A systematic review and meta-analysis. *PloS One* (2020) 15(12):e0242702. doi: 10.1371/journal.pone.0242702

20. Ashenafi S, Bekele A, Aseffa G, Amogne W, Kassa E, Aderaye G, et al. Anemia is a strong predictor of wasting, disease severity, and progression, in clinical tuberculosis (TB). *Nutrients* (2022) 14(16):1–14. doi: 10.3390/nu14163318

21. Ganz T. Anemia of inflammation. *N Engl J Med* (2019) 381(12):1148–57. doi: 10.1056/NEJMra1804281

22. Dasaradhan T, Koneti J, Kalluru R, Gadde S, Cherukuri SP, Chikatimalla R. Tuberculosis-associated anemia: A narrative review. *Cureus* (2022) 14(8):e27746. doi: 10.7759/cureus.27746

23. Bekele A, Gebreselassie N, Ashenafi S, Kassa E, Aseffa G, Amogne W, et al. Daily adjunctive therapy with vitamin D(3) and phenylbutyrate supports clinical recovery from pulmonary tuberculosis: a randomized controlled trial in Ethiopia. *J Intern Med* (2018) 284(3):292–306. doi: 10.1111/joim.12767

24. Wejse C, Gustafson P, Nielsen J, Gomes VF, Aaby P, Andersen PL, et al. TBscore: Signs and symptoms from tuberculosis patients in a low-resource setting have predictive value and may be used to assess clinical course. *Scand J Infect Dis* (2008) 40(2):111–20. doi: 10.1080/00365540701558698

25. Wejse C, Gomes VF, Rabna P, Gustafson P, Aaby P, Lisse IM, et al. Vitamin D as supplementary treatment for tuberculosis: a double-blind, randomized, placebo-controlled trial. *Am J Respir Crit Care Med* (2009) 179(9):843–50. doi: 10.1164/rccm.200804-567OC

26. Nicoll D, Mark LC, McPhee SJ. *Guide to diagnostic tests* (2017). Columbus, OH, USA: McGraw Hill. Available at: https://accessmedicine.mhmedical.com/content.aspx?bookid=2032&sectionid=151444058 (Accessed 15 October 2021).

27. Aderaye G, Bruchfeld J, Assefa G, Feleke D, Kallenius G, Baat M, et al. The relationship between disease pattern and disease burden by chest radiography, M. tuberculosis Load, and HIV status in patients with pulmonary tuberculosis in Addis Ababa. *Infection* (2004) 32(6):333–8. doi: 10.1007/s15010-004-3089-x

28. Patil I. Visualizations with statistical details: The 'ggstatsplot' approach. *J Open Source Software* (2021) 6(61):3167. doi: 10.21105/joss.03167

29. Jones BE, Oo MM, Taikwel EK, Qian D, Kumar A, Maslow ER, et al. CD4 cell counts in human immunodeficiency virus-negative patients with tuberculosis. *Clin Infect Dis* (1997) 24(5):988–91. doi: 10.1093/clinids/24.5.988

30. Murthy SE, Chatterjee F, Crook A, Dawson R, Mendel C, Murphy ME, et al. Pretreatment chest x-ray severity and its relation to bacterial burden in smear positive pulmonary tuberculosis. *BMC Med* (2018) 16(1):73. doi: 10.1186/s12916-018-1053-3

31. Urbanowski ME, Ordonez AA, Ruiz-Bedoya CA, Jain SK, Bishai WR. Cavitary tuberculosis: the gateway of disease transmission. *Lancet Infect Dis* (2020) 20(6):e117–e28. doi: 10.1016/S1473-3099(20)30148-1

32. Gil-Santana L, Almeida-Junior JL, Oliveira CA, Hickson LS, Daltro C, Castro S, et al. Diabetes is associated with worse clinical presentation in tuberculosis patients from Brazil: A retrospective cohort study. *PloS One* (2016) 11(1):e0146876. doi: 10.1371/journal.pone.0146876

33. Kriel M, Lotz JW, Kidd M, Walzl G. Evaluation of a radiological severity score to predict treatment outcome in adults with pulmonary tuberculosis. *Int J Tuberc Lung Dis* (2015) 19(11):1354–60. doi: 10.5588/ijtld.15.0098

34. Chakraborthy A, Shivananjaiah AJ, Ramaswamy S, Chikkavenkatappa N. Chest X ray score (Timika score): an useful adjunct to predict treatment outcome in tuberculosis. *Adv Respir Med* (2018) 86(5):205–10. doi: 10.5603/ARM.2018.0032

35. Ralph AP, Ardian M, Wiguna A, Maguire GP, Becker NG, Drogumuller G, et al. A simple, valid, numerical score for grading chest x-ray severity in adult smear-positive pulmonary tuberculosis. *Thorax* (2010) 65(10):863–9. doi: 10.1136/thx.2010.136242

36. Djoba Siawaya JF, Beyers N, van Helden P, Walzl G. Differential cytokine secretion and early treatment response in patients with pulmonary tuberculosis. *Clin Exp Immunol* (2009) 156(1):69–77. doi: 10.1111/j.1365-2249.2009.03875.x

37. Mihret A, Bekele Y, Bobosha K, Kidd M, Aseffa A, Howe R, et al. Plasma cytokines and chemokines differentiate between active disease and non-active tuberculosis infection. *J Infect* (2013) 66(4):357–65. doi: 10.1016/j.jinf.2012.11.005

38. Zhao Y, Yang X, Zhang X, Yu Q, Zhao P, Wang J, et al. IP-10 and RANTES as biomarkers for pulmonary tuberculosis diagnosis and monitoring. *Tuberculosis (Edinb)* (2018) 111:45–53. doi: 10.1016/j.tube.2018.05.004

39. Moideen K, Kumar NP, Bethunaickan R, Banurekha VV, Nair D, Babu S. Heightened systemic levels of anti-inflammatory cytokines in pulmonary tuberculosis and alterations following anti-tuberculosis treatment. *Cytokine* (2020) 127:154929. doi: 10.1016/j.cyto.2019.154929

40. Sampath P, Rajamanickam A, Thiruvengadam K, Natarajan AP, Hissar S, Dhanapal M, et al. Cytokine upsurge among drug-resistant tuberculosis endorse the signatures of hyper inflammation and disease severity. *Sci Rep* (2023) 13(1):785. doi: 10.1038/s41598-023-27895-8

41. Kumar NP, Moideen K, Nancy A, Viswanathan V, Thiruvengadam K, Nair D, et al. Plasma chemokines are baseline predictors of unfavorable treatment outcomes in pulmonary tuberculosis. *Clin Infect Dis* (2021) 73(9):e3419–e27. doi: 10.1093/cid/ciaa1104

42. Sigal GB, Segal MR, Mathew A, Jarlsberg L, Wang M, Barbero S, et al. Biomarkers of tuberculosis severity and treatment effect: A directed screen of 70 host markers in a randomized clinical trial. *EBioMedicine* (2017) 25:112–21. doi: 10.1016/j.ebiom.2017.10.018

43. Sampath P, Rajamanickam A, Thiruvengadam K, Natarajan AP, Hissar S, Dhanapal M, et al. Plasma chemokines CXCL10 and CXCL9 as potential diagnostic markers of drug-sensitive and drug-resistant tuberculosis. *Sci Rep* (2023) 13(1):7404. doi: 10.1038/s41598-023-34530-z

44. Kumar NP, Moideen K, Banurekha VV, Nair D, Babu S. Plasma proinflammatory cytokines are markers of disease severity and bacterial burden in pulmonary tuberculosis. *Open Forum Infect Dis* (2019) 6(7):ofz257. doi: 10.1093/ofid/ofz257

45. Feng JY, Chen YY, Yen YF, Pan SW, Su WJ. Active tuberculosis increases the risk of incident osteoporosis- A nation-wide population based cohort study. *Eur Respir J* (2016) 48:OA4823. doi: 10.1183/13993003.congress-2016.OA4823

46. Kaufmann SH, Dorhoi A. Inflammation in tuberculosis: interactions, imbalances and interventions. *Curr Opin Immunol* (2013) 25(4):441–9. doi: 10.1016/j.coi.2013.05.005

47. Muefong CN, Sutherland JS. Neutrophils in tuberculosis-associated inflammation and lung pathology. *Front Immunol* (2020) 11:962. doi: 10.3389/fimmu.2020.00962

48. Shaw JA, Malherbe ST, Walzl G, du Plessis N. Suppressive myeloid cells in SARS-CoV-2 and Mycobacterium tuberculosis co-infection. *Front Immunol* (2023) 14:1222911. doi: 10.3389/fimmu.2023.1222911

49. Ashenafi S, Brighenti S. Reinventing the human tuberculosis (TB) granuloma: Learning from the cancer field. *Front Immunol* (2022) 13:1059725. doi: 10.3389/fimmu.2022.1059725

50. McCaffrey EF, Donato M, Keren L, Chen Z, Delmastro A, Fitzpatrick MB, et al. The immunoregulatory landscape of human tuberculosis granulomas. *Nat Immunol* (2022) 23(2):318–29. doi: 10.1038/s41590-021-01121-x

51. Singh B, Singh DK, Ganatra SR, Escobedo RA, Khader S, Schlesinger LS, et al. Myeloid-derived suppressor cells mediate T cell dysfunction in nonhuman primate TB granulomas. *mBio* (2021) 12(6):e0318921. doi: 10.1128/mbio.03189-21

52. Gideon HP, Hughes TK, Tzouanas CN, Wadsworth MH 2nd, Tu AA, Gierahn TM, et al. Multimodal profiling of lung granulomas in macaques reveals cellular correlates of tuberculosis control. *Immunity* (2022) 55(5):827–46 e10. doi: 10.1016/j.immuni.2022.04.004

53. Esaulova E, Das S, Singh DK, Choreno-Parra JA, Swain A, Arthur L, et al. The immune landscape in tuberculosis reveals populations linked to disease and latency. *Cell Host Microbe* (2021) 29(2):165–78 e8. doi: 10.1016/j.chom.2020.11.013

54. Rahman S, Gudetta B, Fink J, Granath A, Ashenafi S, Aseffa A, et al. Compartmentalization of immune responses in human tuberculosis: few CD8+ effector T cells but elevated levels of FoxP3+ regulatory t cells in the granulomatous lesions. *Am J Pathol* (2009) 174(6):2211–24. doi: 10.2353/ajpath.2009.080941

55. Carow B, Hauling T, Qian X, Kramnik I, Nilsson M, Rottenberg ME. Spatial and temporal localization of immune transcripts defines hallmarks and diversity in the tuberculosis granuloma. *Nat Commun* (2019) 10(1):1823. doi: 10.1038/s41467-019-09816-4

56. Ashenafi S, Muvva JR, Mily A, Snall J, Zewdie M, Chanyalew M, et al. Immunosuppressive features of the microenvironment in lymph nodes granulomas from tuberculosis and HIV-co-infected patients. *Am J Pathol* (2022) 192(4):653–70. doi: 10.1016/j.ajpath.2021.12.013

57. Cronan MR, Hughes EJ, Brewer WJ, Viswanathan G, Hunt EG, Singh B, et al. A non-canonical type 2 immune response coordinates tuberculous granuloma formation and epithelialization. *Cell* (2021) 184(7):1757–74 e14. doi: 10.1016/j.cell.2021.02.046

58. DiNardo AR, Gandhi T, Heyckendorf J, Grimm SL, Rajapakshe K, Nishiguchi T, et al. Gene expression signatures identify biologically and clinically distinct tuberculosis endotypes. *Eur Respir J* (2022) 60(3):1–15. doi: 10.1183/13993003.02263-2021

59. DiNardo AR, Nishiguchi T, Grimm SL, Schlesinger LS, Graviss EA, Cirillo JD, et al. Tuberculosis endotypes to guide stratified host-directed therapy. *Med* (2021) 2(3):217–32. doi: 10.1016/j.medj.2020.11.003

60. Musicki K, Briscoe H, Britton WJ, Saunders BM. LIGHT contributes to early but not late control of Mycobacterium tuberculosis infection. *Int Immunol* (2010) 22(5):353–8. doi: 10.1093/intimm/dxq013

61. Hanekom WA, Hussey GD, Hughes EJ, Potgieter S, Yogev R, Check IJ. Plasma-soluble CD30 in childhood tuberculosis: effects of disease severity, nutritional status, and vitamin A therapy. *Clin Diagn Lab Immunol* (1999) 6(2):204–8. doi: 10.1128/CDLI.6.2.204-208.1999

62. Marin ND, Garcia LF. The role of CD30 and CD153 (CD30L) in the anti-mycobacterial immune response. *Tuberculosis (Edinb)* (2017) 102:8–15. doi: 10.1016/j.tube.2016.10.006

63. Tang C, Yamada H, Shibata K, Muta H, Wajjwalku W, Podack ER, et al. A novel role of CD30L/CD30 signaling by T-T cell interaction in Th1 response against mycobacterial infection. *J Immunol* (2008) 181(9):6316–27. doi: 10.4049/jimmunol.181.9.6316

64. Alessandri AL, Souza AL, Oliveira SC, Macedo GC, Teixeira MM, Teixeira AL. Concentrations of CXCL8, CXCL9 and sTNFR1 in plasma of patients with pulmonary tuberculosis undergoing treatment. *Inflammation Res* (2006) 55(12):528–33. doi: 10.1007/s00011-006-5136-9

65. Balcewicz-Sablinska MK, Keane J, Kornfeld H, Remold HG. Pathogenic Mycobacterium tuberculosis evades apoptosis of host macrophages by release of TNF-R2, resulting in inactivation of TNF-alpha. *J Immunol* (1998) 161(5):2636–41. doi: 10.4049/jimmunol.161.5.2636

66. Paccalet A, Crola Da Silva C, Mechtouff L, Amaz C, Varillon Y, de Bourguignon C, et al. Serum soluble tumor necrosis factor receptors 1 and 2 are early prognosis markers after ST-segment elevation myocardial infarction. *Front Pharmacol* (2021) 12:656928. doi: 10.3389/fphar.2021.656928

67. Vincent FB, Saulep-Easton D, Figgett WA, Fairfax KA, Mackay F. The BAFF/APRIL system: emerging functions beyond B cell biology and autoimmunity. *Cytokine Growth Factor Rev* (2013) 24(3):203–15. doi: 10.1016/j.cytogfr.2013.04.003

68. Sakai J, Akkoyunlu M. The role of BAFF system molecules in host response to pathogens. *Clin Microbiol Rev* (2017) 30(4):991–1014. doi: 10.1128/CMR.00046-17

69. Panchanathan R, Choubey D. Murine BAFF expression is up-regulated by estrogen and interferons: implications for sex bias in the development of autoimmunity. *Mol Immunol* (2013) 53(1-2):15–23. doi: 10.1016/j.molimm.2012.06.013

70. Mourik BC, Lubberts E, de Steenwinkel JEM, Ottenhoff THM, Leenen PJM. Interactions between type 1 interferons and the th17 response in tuberculosis: lessons learned from autoimmune diseases. *Front Immunol* (2017) 8:294. doi: 10.3389/fimmu.2017.00294

71. Parsa R, Lund H, Georgoudaki AM, Zhang XM, Ortlieb Guerreiro-Cacais A, Grommisch D, et al. BAFF-secreting neutrophils drive plasma cell responses during emergency granulopoiesis. *J Exp Med* (2016) 213(8):1537–53. doi: 10.1084/jem.20150577

72. Wang X, Liang KD, Zhang JA, Liu GB, Chen Z, Chen C, et al. Increased B cell activating factor is associated with B cell class switching in patients with tuberculous pleural effusion. *Mol Med Rep* (2018) 18(2):1704–9. doi: 10.3892/mmr.2018.9073

73. Mackay F, Leung H. The role of the BAFF/APRIL system on T cell function. *Semin Immunol* (2006) 18(5):284–9. doi: 10.1016/j.smim.2006.04.005

74. Liu K, Zhang Y, Hu S, Yu Y, Yang Q, Jin D, et al. Increased levels of BAFF and APRIL related to human active pulmonary tuberculosis. *PloS One* (2012) 7(6):e38429. doi: 10.1371/journal.pone.0038429

75. Sutherland AP, Ng LG, Fletcher CA, Shum B, Newton RA, Grey ST, et al. BAFF augments certain Th1-associated inflammatory responses. *J Immunol* (2005) 174(9):5537–44. doi: 10.4049/jimmunol.174.9.5537

76. Ye Q, Wang L, Wells AD, Tao R, Han R, Davidson A, et al. BAFF binding to T cell-expressed BAFF-R costimulates T cell proliferation and alloresponses. *Eur J Immunol* (2004) 34(10):2750–9. doi: 10.1002/eji.200425198

77. Ashenafi S, Aderaye G, Zewdie M, Raqib R, Bekele A, Magalhaes I, et al. BCG-specific IgG-secreting peripheral plasmablasts as a potential biomarker of active tuberculosis in HIV negative and HIV positive patients. *Thorax* (2013) 68(3):269–76. doi: 10.1136/thoraxjnl-2012-201817

78. Nau GJ, Guilfoile P, Chupp GL, Berman JS, Kim SJ, Kornfeld H, et al. A chemoattractant cytokine associated with granulomas in tuberculosis and silicosis. *Proc Natl Acad Sci U S A*. (1997) 94(12):6414–9. doi: 10.1073/pnas.94.12.6414

79. Zhao T, Su Z, Li Y, Zhang X, You Q. Chitinase-3 like-protein-1 function and its role in diseases. *Signal Transduct Target Ther* (2020) 5(1):201. doi: 10.1038/s41392-020-00303-7

80. Sloand EM, Kim S, Maciejewski JP, Van Rhee F, Chaudhuri A, Barrett J, et al. Pharmacologic doses of granulocyte colony-stimulating factor affect cytokine production by lymphocytes in *vitro* and in vivo. *Blood* (2000) 95(7):2269–74. doi: 10.1182/blood.V95.7.2269

81. Moser C, Jensen PO, Pressler T, Frederiksen B, Lanng S, Kharazmi A, et al. Serum concentrations of GM-CSF and G-CSF correlate with the Th1/Th2 cytokine response in cystic fibrosis patients with chronic Pseudomonas aeruginosa lung infection. *APMIS* (2005) 113(6):400–9. doi: 10.1111/j.1600-0463.2005.apm_142.x

82. Kapina MA, Shepelkova GS, Avdeenko VG, Guseva AN, Kondratieva TK, Evstifeev VV, et al. Interleukin-11 drives early lung inflammation during Mycobacterium tuberculosis infection in genetically susceptible mice. *PloS One* (2011) 6(7):e21878. doi: 10.1371/journal.pone.0021878

83. Myles IA, Fontecilla NM, Valdez PA, Vithayathil PJ, Naik S, Belkaid Y, et al. Signaling via the IL-20 receptor inhibits cutaneous production of IL-1beta and IL-17A to promote infection with methicillin-resistant Staphylococcus aureus. *Nat Immunol* (2013) 14(8):804–11. doi: 10.1038/ni.2637

84. Madouri F, Barada O, Kervoaze G, Trottein F, Pichavant M, Gosset P. Production of Interleukin-20 cytokines limits bacterial clearance and lung inflammation during infection by Streptococcus pneumoniae. *EBioMedicine* (2018) 37:417–27. doi: 10.1016/j.ebiom.2018.10.031

85. Walzl G, Ronacher K, Hanekom W, Scriba TJ, Zumla A. Immunological biomarkers of tuberculosis. *Nat Rev Immunol* (2011) 11(5):343–54. doi: 10.1038/nri2960

86. Babu S. Biomarkers for treatment monitoring in tuberculosis: A new hope. *EBioMedicine* (2017) 26:13–4. doi: 10.1016/j.ebiom.2017.11.002

87. Rockwood N, du Bruyn E, Morris T, Wilkinson RJ. Assessment of treatment response in tuberculosis. *Expert Rev Respir Med* (2016) 10(6):643–54. doi: 10.1586/17476348.2016.1166960

88. Nahid P, Saukkonen J, Mac Kenzie WR, Johnson JL, Phillips PP, Andersen J, et al. CDC/NIH Workshop. Tuberculosis biomarker and surrogate endpoint research roadmap. *Am J Respir Crit Care Med* (2011) 184(8):972–9. doi: 10.1164/rccm.201105-0827WS

89. Zimmer AJ, Lainati F, Aguilera Vasquez N, Chedid C, McGrath S, Benedetti A, et al. Biomarkers that correlate with active pulmonary tuberculosis treatment response: a systematic review and meta-analysis. *J Clin Microbiol* (2022) 60(2):e0185921. doi: 10.1128/jcm.01859-21

90. Wallis RS, Maeurer M, Mwaba P, Chakaya J, Rustomjee R, Migliori GB, et al. Tuberculosis–advances in development of new drugs, treatment regimens, host-directed therapies, and biomarkers. *Lancet Infect Dis* (2016) 16(4):e34–46. doi: 10.1016/S1473-3099(16)00070-0

91. Guler R, Ozturk M, Sabeel S, Motaung B, Parihar SP, Thienemann F, et al. Targeting molecular inflammatory pathways in granuloma as host-directed therapies for tuberculosis. *Front Immunol* (2021) 12:733853. doi: 10.3389/fimmu.2021.733853

frontiers | Frontiers in Immunology

TYPE Original Research
PUBLISHED 15 January 2024
DOI 10.3389/fimmu.2023.1256558

OPEN ACCESS

EDITED BY
Jianping Xie,
Southwest University, China

REVIEWED BY
Hridesh Mishra,
Rutgers University, Newark, United States
Adrian G. Rosas-Taraco,
Autonomous University of Nuevo León, Mexico
Mario César Salinas-Carmona,
Autonomous University of Nuevo León, Mexico

*CORRESPONDENCE
Luciana Silva Rodrigues
lrodrigues.uerj@gmail.com

†Deceased

RECEIVED 11 July 2023
ACCEPTED 18 December 2023
PUBLISHED 15 January 2024

CITATION
Corrêa RdS, Leal-Calvo T, Mafort TT, Santos AP, Leung J, Pinheiro RO, Rufino R, Moraes MO and Rodrigues LS (2024) Reanalysis and validation of the transcriptional pleural fluid signature in pleural tuberculosis. *Front. Immunol.* 14:1256558. doi: 10.3389/fimmu.2023.1256558

Reanalysis and validation of the transcriptional pleural fluid signature in pleural tuberculosis

Raquel da Silva Corrêa[1], Thyago Leal-Calvo[2], Thiago Thomaz Mafort[3], Ana Paula Santos[3], Janaína Leung[3], Roberta Olmo Pinheiro[2], Rogério Rufino[3], Milton Ozório Moraes[2†] and Luciana Silva Rodrigues[1*]

[1]Laboratory of Immunopathology, Medical Sciences Faculty, Rio de Janeiro State University (FCM/UERJ), Rio de Janeiro, Brazil, [2]Laboratory of Leprosy, Oswaldo Cruz Institute, Oswaldo Cruz Foundation (IOC/FIOCRUZ), Rio de Janeiro, Brazil, [3]Department of Pulmonary Care, Pedro Ernesto University Hospital, Rio de Janeiro State University (HUPE/UERJ), Rio de Janeiro, Brazil

Introduction: Pleural tuberculosis (PlTB), the most common site of extrapulmonary TB, is characterized by a paucibacillary nature and a compartmentalized inflammatory response in the pleural cavity, both of which make diagnosis and management extremely challenging. Although transcriptional signatures for pulmonary TB have already been described, data obtained by using this approach for extrapulmonary tuberculosis and, specifically, for pleural tuberculosis are scarce and heterogeneous. In the present study, a set of candidate genes previously described in pulmonary TB was evaluated to identify and validate a transcriptional signature in clinical samples from a Brazilian cohort of PlTB patients and those with other exudative causes of pleural effusion.

Methods: As a first step, target genes were selected by a random forest algorithm with recursive feature elimination (RFE) from public microarray datasets. Then, peripheral blood (PB) and pleural fluid (PF) samples from recruited patients presenting exudative pleural effusion were collected during the thoracentesis procedure. Transcriptional analysis of the selected top 10 genes was performed by quantitative RT-PCR (RT-qPCR).

Results: Reanalysis of the public datasets identified a set of candidate genes (*CARD17, BHLHE40, FCGR1A, BATF2, STAT1, BTN3A1, ANKRD22, C1QB, GBP2*, and *SEPTIN4*) that demonstrated a global accuracy of 89.5% in discriminating pulmonary TB cases from other respiratory diseases. Our validation cohort consisted of PlTB (n = 35) patients and non-TB (n = 34) ones. The gene expressions of *CARD17*, *GBP2*, and *C1QB* in PF at diagnosis were significantly different between the two (PlTB and non-TB) groups ($p < 0.0001$). It was observed that the gene expressions of *CARD17* and *GBP2* were higher in PlTB PF than in non-TB patients. *C1QB* showed the opposite behavior, being higher in the non-TB PF. After anti-TB therapy, however, *GBP2* gene expression was significantly reduced in PlTB patients ($p < 0.001$). Finally, the accuracy of the three above-cited highlighted genes in the PF was analyzed, showing AUCs of 91%, 90%, and 85%, respectively. *GBP2* was above 80% (sensitivity = 0.89/specificity = 0.81), and *CARD17* showed significant specificity (Se = 0.69/Sp = 0.95) in its capacity to discriminate the groups.

Conclusion: *CARD17*, *GBP2*, and *C1QB* showed promise in discriminating PlTB from other causes of exudative pleural effusion by providing accurate diagnoses, thus accelerating the initiation of anti-TB therapy.

KEYWORDS

tuberculosis, pleural tuberculosis, exudative effusion, gene expression, *Mycobacterium tuberculosis*

1 Introduction

It is estimated that, per annum, there are roughly 10 million people with active tuberculosis (TB), and 1.3 million subsequent deaths from TB worldwide, being the world's second leading cause of death from a single infectious agent after coronavirus disease (COVID-19) (1). Brazil is among the 30 countries with the highest TB rates, registering an annual estimated 80,000 new cases at an incidence of 36.3 cases/100,000 inhabitants and nearly 4,500 deaths (2). In 2021, the State of Rio de Janeiro, where this study was conducted, showed a disease incidence rate of 67.4/100,000 inhabitants, occupying the second position in Brazil (3).

Tuberculosis diagnosis and management remain a challenge due to the enormously complex and intricated immunopathology involved in combating *Mycobacterium tuberculosis* (Mtb), specifically in the extrapulmonary manifestations of the disease such as pleural TB (PlTB)—the most common site of extrapulmonary TB. PlTB is typically characterized by unilateral pleural effusion, pleuritic chest pain, persistent coughing, fever, nocturnal sweats, dyspnea, and weight loss (4, 5). The laboratory diagnosis of PlTB may be facilitated by the thoracentesis procedure by providing highly valuable clinical samples such as of exudative pleural fluid (PF), whose microbiological, biochemical, and immunological aspects can be analyzed. The compartmentalized immune response against Mtb in the pleural cavity seems to be paucibacillary, being enriched by a cytokine milieu that favors a lymphocytic dominant T-helper 1 (Th1), which is responsible for producing high levels of interferon-gamma (IFN-γ) and other Th1 cytokines (6–9). In addition, histological examination of pleural biopsies identifying caseating granulomas or visualization of acid-fast bacilli in the tissue and/or high levels of adenosine deaminase (ADA) in PF are also relevant guides toward a tuberculosis diagnosis (4). A fuller understanding of this compartmentalized and dynamic immune response may lead to a better comprehension of the varied antimycobacterial responses at different TB infection sites as well as contribute to a more timely and accurate diagnosis.

Among the *omics* approaches, whole-blood transcriptomics analysis has particularly contributed to gene profile identification in pulmonary TB and to a broader understanding of the mechanisms involved in the immune response and pathogenesis of many infectious diseases (10–12) in its ability to discriminate between active versus latent TB and compare characteristics of healthy uninfected individuals to those with pulmonary diseases (13–17). Altogether, these transcriptomic studies revealed a differential gene expression mainly represented by interferon-inducible pathways and pathogen/antigen recognition receptor-blood signatures. Subsequent works have evaluated the cytokine gene expression profile in samples from the pleural effusion of patients diagnosed with TB and diseases of other etiologies using blood (18, 19) and PF (20, 21). However, the transcriptomic analyses of extrapulmonary TB, particularly in PlTB, that use PF are scarce and provide limited heterogeneous data since most only utilize blood.

In the present study, signature genes that are differentially expressed in patients with pleural TB compared to other exudative etiologies that lead to pleural effusion were investigated. For this purpose, a preliminary reanalysis of public transcriptional datasets relative to pulmonary TB from Bloom et al. (2013) (22) was conducted. The top 10 candidate genes were identified and validated in paired PF and whole-blood samples collected at diagnosis and after anti-TB therapy. It is our hope that the data obtained in the present study contributes to the identification of new diagnostic and therapeutic procedures aiming to profoundly impact the management of PlTB patients.

2 Materials and methods

2.1 Clinical cohort and ethics statement

A longitudinal study was conducted with both male and female patients over the age of 18 suspected of pleural effusion, for whom an indication for thoracentesis was warranted, in attendance between June 2015 and February 2020 at the Pulmonary and Tisiology Service—a tertiary care center in the City of Rio de Janeiro, RJ, Brazil—in the Pedro Ernesto University Hospital of the Rio de Janeiro State University (HUPE/UERJ). The patients who were under 18, pregnant, or refused consent were not recruited. Among the 98 recruited patients, 29 were excluded: 14 had transudative pleural effusion (cardiac or renal failure), 7 had an

undefined diagnosis, 3 were HIV seropositive, and 5 had an insufficient RNA sample (Figure 1A). PF and peripheral blood (PB) samples were collected before treatment. Only PlTB patients had a new blood collection at the end of their anti-TB treatment.

The study protocol was approved by the HUPE/UERJ Ethics Committee (approval number 1,100,772), closely following the recommendations of the Helsinki Declaration. Participants were properly informed about the study objectives, and all voluntarily signed the written informed consent form prior to enrollment and sample collection. Medical information was obtained from electronic records and additional survey questionnaires.

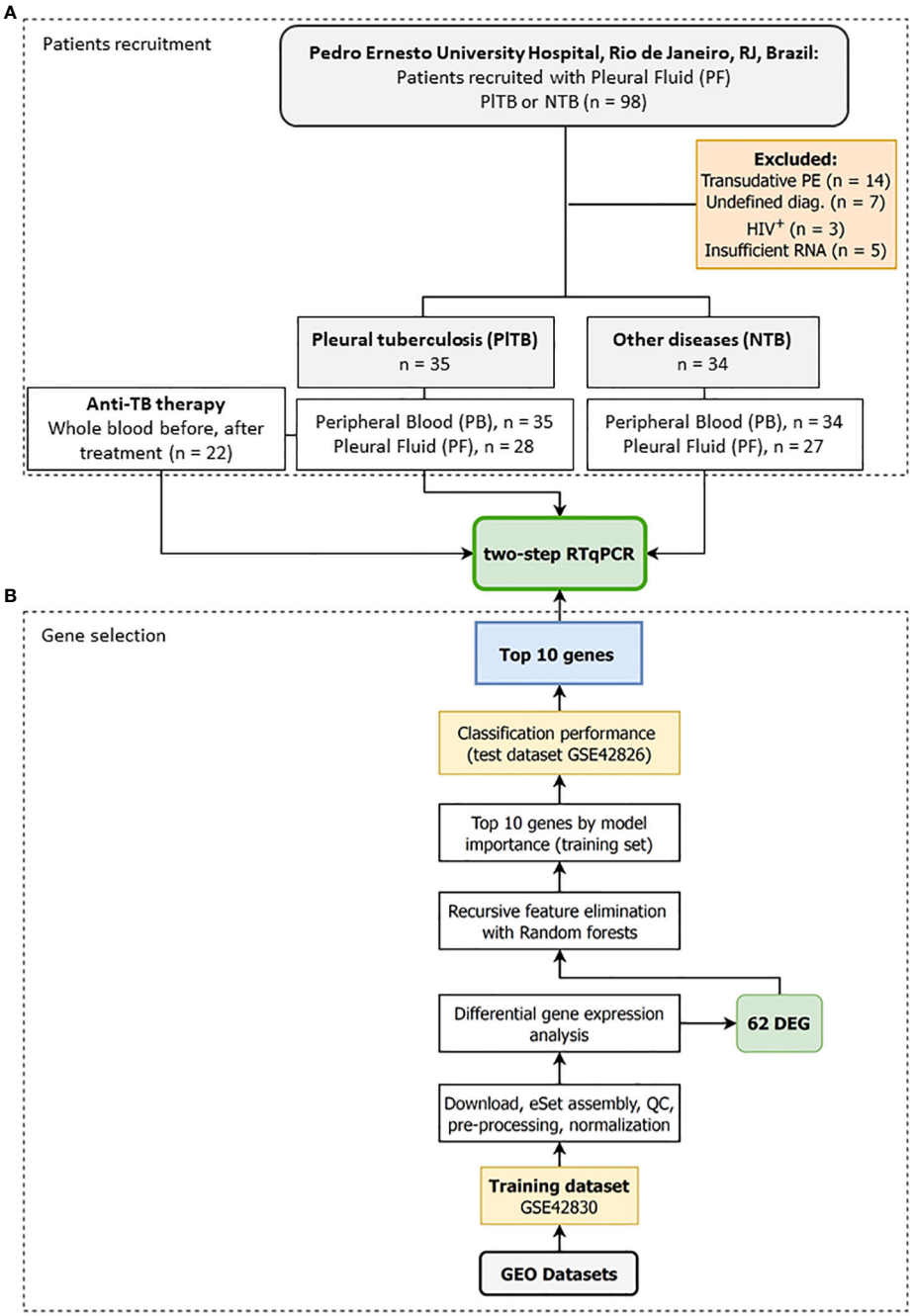

FIGURE 1
Study design to identify a transcriptomic signature associated with pleural tuberculosis. The study was divided into two stages: **(A)** Step A—Patients recruitment: Pleural fluid and whole blood were collected from patients showing pleural effusion with an indication for thoracentesis followed by grouping the participants into either pleural tuberculosis (PlTB) or non-tuberculosis (non-TB). A new whole-blood sample was collected from PlTB patients after anti-TB treatment. **(B)** Step B—Gene selection: *In silico* analysis was performed to define the top 10 genes differentially expressed in the whole blood from pulmonary tuberculosis patients based on the aforementioned study by Bloom et al. (22), and applied to the pleural effusion validation cohort by reverse transcription quantitative PCR (RT-qPCR).

2.2 Reanalysis and definition of candidate genes from public datasets

Because there are no available transcriptomic datasets of pleural effusion from tuberculosis, we reanalyzed two blood datasets published by Bloom et al. (2013) (22) and available in GEO (GSE42830 and GSE42826) to select genes that classify pulmonary TB from lung cancer, a common differential diagnosis (Figure 1B). The background-subtracted data were downloaded from GEO and quantile normalized using routines from the preprocessCore package v.1.56.0. Microarray probes were reannotated using the illuminaHumanv4.db annotation v.1.26 and AnnotationDbi packages v.1.56.2. Duplicated ENTREZIDs were removed while maintaining the probe with the greatest average expression across all samples. Differential gene expression analysis was then performed by fitting gene-wise linear models via limma v.3.50.0, making adjustments for biological sex and ethnic categorical variables (23), and comparatively testing tuberculosis (n = 16) vs. lung cancer (n = 8). After selecting the differentially expressed genes, they were ranked by model importance using Recursive feature elimination (RFE) with the random forests algorithm implemented in the caret package v.6.0-90. Briefly, the normalized $\log_2$ gene expression matrix from GSE42830 was adjusted to remove the estimated effects of sex and ethnicity using limma's RemoveBatchEffect function. Then, only the differentially expressed genes $|\log_2 FC| \geq 1$ and FDR ≤ 0.01 were used for feature selection. RFE with random forests was set to retain 2-to-20 genes by way of repeated 10-fold cross-validation with 50 repetitions by maximizing the area under the curve (AUC) metric. The variable importance output was used to rank and extract the top 16 genes from the RFE. Finally, the accuracy of these 16 genes was tested using a subset of GSE42826, the second independent test dataset, and analyzed as previously described. The variable importance of the RFE on the training dataset and the AUC together with their sensitivity (Se) and specificity (Sp) on the test set (TB, n = 11; lung cancer, n = 8) was used to select the final 10 gene list for RT-qPCR replication with our cohort from Rio de Janeiro, RJ, Brazil (Figure 1).

2.3 Diagnostic criteria

The diagnoses were made by specialized physicians from the Pulmonology and Tisiology Service at HUPE/UERJ through the analysis of radiological, tomographic, cytological, histological, and microbiological exams (bacilloscopy together with PF and pleural biopsy cultures), and clinical epidemiological data. *PlTB* was defined as a result of a detailed physical examination and the existence of at least one diagnostic criterion: (i) Ziehl–Neelsen stain positivity, or isolation of Mtb in the respiratory specimen, PF, or pleural tissue. Other characteristics included the (ii) identification of granuloma formation in the histopathological analysis, (iii) clinical manifestations of PlTB (fever, pleuritic pain, dyspnea, coughing, nocturnal sweats, hyporexia, and/or weight loss), and (iv) lymphocytic and exudative pleural effusion in combination with an ADA dosage above 40 IU/L, showing full recovery after at least 6 months of anti-tuberculous treatment. *Non-tuberculosis (NTB)* cases were defined as those with pleural or pleuropulmonary diseases other than TB in which the diagnoses were based on clinical, laboratory, radiological, microbiological, and cytopathological/histopathological features. Patients who did not fit the criteria used for the PlTB diagnosis as described above and with unknown causes of pleural effusion were categorized as having undefined pleural effusion and were considered *non-TB*, as previously described by Lisboa and colleagues (6).

2.4 Sample collection and processing

Whole-blood and PF (2.5 mL) samples were collected into PAXGene tubes (QIAGEN, Germany) and stored at −20°C after stabilization at room temperature for 2 h. RNA was isolated using the PAXgene Blood RNA Kit (QIAGEN) and DNAse-treated as per instructions of the manufacturer. RNA was eluted into a final volume of 40 µL and stored at −80°C until further use. RNA quality was assessed by NanoDrop spectrophotometer and non-denaturing agarose gel electrophoresis. Non-degraded RNA was reverse transcribed into cDNA using the SuperScript III (Thermo-Fisher Scientific, USA) according to the instructions of the manufacturer. Finally, cDNA was diluted to a working concentration of 5 ng/µL with Tris-EDTA buffer (10 mM Tris, EDTA 0.1 mM) and kept at −20°C.

2.5 Reverse transcription quantitative PCR

Gene expression experiments were done using the Fast SYBR Green Master Mix (Thermo-Fisher Scientific, USA) in line with the instructions of the manufacturer. Briefly, a 10-µL final reaction contained 10 ng of cDNA, 300 nM of each primer (Thermo-Fisher Scientific, USA) (Supplementary Table 1), and 5 µL of SYBR Green Master Mix. Reactions were performed in duplicate in a Viia7 (Applied BioSystems, USA) machine using the default thermal cycling program that included the melting curve. Raw data were exported in an RDML format using QuantStudio v.1.3 software after assessing primer specificity from the melting curves. Then, efficiency-adjusted N_0 values were obtained using LinRegPCR v.2021.2 with default parameters (24, 25). The N_0 values for genes of interest were normalized by calculating the ratio to the geometric average of N_0 values for two reference genes (*RPLP2* and *POLR2A*), followed by a $\log_2$ transformation. These logarithmized relative expression values were used for visualization and statistical inference.

2.6 Statistical analyses

Descriptive analyses of the study population, according to its sociodemographic and clinical characteristics among PlTB and NTB patients, were determined by the nonparametric Mann–Whitney test for continuous variables or Fisher's exact test for

comparison of the relative frequencies of categorical variables. Relative gene expression in log2 was used for comparing means between groups. Statistical analyses were done by fitting gene-wise linear mixed models with lme4 v.1.1.2 in R 4.1. Briefly, two models were used. The first estimated the effects between disease groups (TB, NTB) and tissues (PB, PF), i.e., both between- and within-subject effects, respectively. For this model, the mixed model (RML criterion) included three categorical variables such as fixed effects ("batch", "diagnosis", and "tissue") and "patient id" as a random intercept. The second model included only the "period" variable (categorical within-patient) as fixed effects and "patient id" as a random intercept. Outliers were removed during model fitting by excluding observations with absolute-scaled Pearson standardized residuals greater than 2.5. Next, the estimated marginal means and specific contrasts were obtained using emmeans v.1.7.2. *p*-values and 95% confidence intervals for the TB-NTB × PB-PF contrasts (four estimates) were adjusted within genes via the Sidak method. Model estimates were plotted over the normalized data alongside confidence intervals. To estimate the effect of demographic and laboratory variables in gene expression, each variable was separately included in the model as a fixed effect, both as an additive or interaction term. Continuous laboratory variables were $\log_{10} + 1$ transformed before any analysis. Then, *p*- values for the coefficients of these covariates were extracted and adjusted according to the Benjamini–Hochberg (1995) (26) procedure to simultaneously control the false discovery rate across all genes simultaneously. This was done to limit the type I error rate due to the large number of estimated coefficients. Any covariate with an adjusted *p*-value ≤ 0.1 was further investigated by Spearman correlation analyses and graphs. ROC curves and AUC were obtained with the pROC package v.1.18.0, and the best threshold was chosen by Youden's *J* statistic (1950) (27) and Delong's 95% confidence interval. Heatmaps were drawn using ComplexHeatmap v.2.10.0 from the gene-wise scaled $\log_2$ data, and genes were clustered using Spearman's *rho* as the distance metric.

3 Results

3.1 Bioinformatics reanalysis of a public microarray datasets from pulmonary tuberculosis patients

For the test dataset, GSE42830, the differentially expressed genes (DEGs) from tuberculosis vs. neoplasia were used in the recursive feature elimination (RFE) algorithm to select candidate genes from Bloom et al. (2013) (22). In this comparison, we found 120 DEGs with an adjusted *p*-value of (FDR) ≤ 0.01 e $|\log_2| \geq 1$. These genes were then subjected to RFE analysis via the random forest algorithm. The top 16 genes were subsequently tested for their classification potential in the GER42826 test data set and ranked according to the importance of these genes in the classification of tuberculosis vs. neoplasia in these samples (Supplementary Table 2 shows the 10 genes with their importance values). In this test dataset, these 10 genes showed an AUC of 89.5% to distinguish tuberculosis vs. neoplasia. Finally, the top 10 genes were selected from this ranking for independent validation by RT-qPCR in samples from a population in Rio de Janeiro, RJ, Brazil (Supplementary Figure 1). Supplementary Table 2 lists the 10 best genes according to their importance: *CARD17, BHLHE40, FCGR1A, BATF2, BTN3A1, C1QB, ANKRD22, GBP2, STAT1*, and *SEPTIN4*, in addition to their AUC, specificity, and sensitivity rates.

3.2 Characterization of the pleural effusion cohort

Among the 69 eligible patients in the present study, 41 (59.4%) were men and 28 (40.6%), were women, ranging in age from 18 to 92. In the PlTB group, the mean age was 40.7 and 60.9 in the non-TB group. Furthermore, 35 (50.7%) were diagnosed with PlTB (33 pleural tuberculosis, 2 pleuropulmonary) while 34 (49.3%) were classified as non-TB. At the beginning of the study, that is, prior to treatment and during diagnostic investigation, clinical samples (blood and PF) were collected at the moment of thoracentesis guided by transthoracic ultrasound. At another moment of the study, rather, at the end of anti-TB therapy, approximately 6 months later, PB samples were also collected solely from PlTB patients to evaluate the behavior of the genes of interest (Figure 1A). After treatment, as expected, pleural effusion disappeared and, as such, sample analysis from the pleural cavity was not possible.

Table 1 shows the demographic, clinical, and biochemical characteristics of the PB and PF samples of the 69 patients with a confirmed diagnosis (PlTB = 35; NTB = 34). For the most part, the non-TB group consisted of patients with cancer, corresponding to more than 75% of the total [the main cancer types were adenocarcinoma (59.09%), lymphoma (4.5%), squamous carcinoma (4.5%), metastatic (9.09%), and undefined (22.72%)], followed by 11.8% with undefined diagnoses, 8.8% with non-tuberculous empyema, and 2.9% with systemic lupus erythematosus (SLE). In the PlTB group, more than 94% corresponded to cases affecting only the pleura; and 5.3% affected both the pleura and the lungs. All volunteers had respiratory symptoms (coughing and/or dyspnea and/or fatigue) and their chest x-rays, computed tomography, and/or ultrasonography findings show unilateral or bilateral pleural effusion associated or not with lung parenchymal changes. Among the pleural TB group, 71.4% of cases showed high and/or moderate pleural effusion complexity as ascertained by the pleural ultrasound results, in comparison to 41.2% of the NTB group, demonstrating a significant difference between the groups (*p*-value = 0.0155; Table 1).

Table 1 also depicts laboratory characteristics. ADA measurement was 71.4% positive (≥40 U/L) in PlTB patients compared to 7.7% in the non-TB ones ($p < 0.001$). Mononuclear cells were significantly higher in the PlTB group ($p = 0.0076$) while polymorphonuclear cells increased in the non-TB group ($p = 0.0089$). The negativity percentages in the Mtb and AFB culture tests in the PlTB group were very high, 77.2% and 82.8%, respectively. Lastly, in

TABLE 1 Characteristics of the study population.

Characteristics/ Groups	Non-TB (n = 34)	Pleural TB (n = 35)	p-value
Age, mean (SD)	60.9 (16.8)	40.7 (18.9)	<0.001
Female (%)	16 (47.1%)	12 (34.3%)	0.332
Male (%)	18 (52.9%)	23 (65.7%)	
Diagnosis, n (%)			
Cancer	26 (76.5%)	0 (0%)	<0.001
Undefined diagnoses	4 (11.8%)	0 (0%)	
Non-tuberculous empyema	3 (8.8%)	0 (0%)	
Systemic lupus erythematosus	1 (2.9%)	0 (0%)	
Pleural TB	0 (0%)	33 (94.3%)	
Pleuropulmonary TB	0 (0%)	2 (5.3%)	
Pleural fluid categories by pleural cavity ultrasound, n (%)			
Low complexity	20 (58.8%)	10 (28.6%)	0.0155
Moderate/ high complexity	14 (41.2%)	25 (71.4%)	
ADA, U/L			
Mean (SD)	19.6 (26.3)	55.4 (26.8)	<0.001
Positive ≥ 40 (%)	8.8%	71.4%	
Mononuclear cells, %			
Mean (SD)	77.8 (21.1)	89.3 (16.6)	0.0076
Polymorphonuclear cells, %			
Mean (SD)	22.2 (21.1)	12.6 (22.5)	0.00899
LDH, IU/L			
Mean (SD)	832 (1,650)	442 (490)	0.84
Mycobacteria culture			
Negative, %	100%	77.2%	0.229
AFB			
Negative, %	100%	82.8%	1
Pleural histopathology, %			
Granuloma with necrosis	0%	14.3%	<0.001
Granuloma without necrosis	0%	14.3%	
Nonspecific inflammatory infiltrate	32.4%	20%	
Malignant identification	35.2%	0%	
Missing	32.4%	51.4%	

ADA, adenosine deaminase; AFB, acid-fast bacillus; LDH, lactate dehydrogenase; SD, standard deviation; TB, tuberculosis. Pleural effusion categories were classified as either "low complexity" (homogeneous and/or anechoic) or "moderate/high complexity" (nonloculated, or complex loculated pleural effusion, respectively) by pleural cavity ultrasound.
Demographic, clinical, and biochemical characteristics of the pleural fluid of non-TB (n = 34) and TB patients (n = 35).

the histopathological examination, the presence of granuloma with necrosis was revealed to cover 14.3% of all PlTB cases.

3.3 Validation of the top 10 candidate genes in clinical samples from the pleural effusion cohort

The previously defined top 10 genes as a result of *in silico* analysis were validated by RT-qPCR assays in whole-blood and PF clinical samples taken from our Brazilian cohort. The *SEPTIN4* gene did not obtain detectable levels of messenger RNA (data not shown). The following nine genes were then analyzed by RT-qPCR assays: *CARD17*, *BHLHE40*, *FCGR1A*, *BATF2*, *BTN3A1*, *C1QB*, *ANKRD22*, *GBP2*, and *STAT1*.

Transcriptional profiles of PlTB (red) and other non-TB (blue) etiologies of pleural effusion at diagnosis were clustered by whole blood (purple) and PF (yellow) in the heatmap plots and boxplots shown in Figure 2. The Z score demonstrated the behavior of each gene of interest regarding its up-or-down expression (from a bluish to a reddish color) in both groups as evidenced in the analyzed sample. In Figure 2B (boxplots), there are the same genes of interest with gene expression values normalized in log2. There was a significant difference among the gene expressions observed in the PlTB patients in comparison to the non-TB ones: *ANKRD22*, *BTN3A1*, *CARD17*, *GBP2*, and STAT1, all of which had p-values < 0.001. The *C1QB* gene, on the other hand, obtained a significantly higher gene expression in the PF in the non-TB group when compared to the PlTB one. The genes that showed a significant difference between groups, with higher values in the PB samples within the P1TB group, were *ANKRD22* ($p < 0.001$), *BATF2* ($p < 0.001$), *GBP2* ($p = 0.003$), and *STAT1* ($p = 0.016$). The expression of mRNA in the latter two genes (*GBP2* and *STAT1*) in both clinical samples was higher in the PlTB group. However, it is noteworthy that the distinction between the groups was more pronounced in the PF. As for the *ANKR22* gene, in both samples, there was a distinction between the groups (p-value < 0.001).

3.4 Expression of genes of interest after treatment with anti-TB therapy

The longitudinal variation of gene expression in the PlTB patients (n = 12) after treatment with anti-TB therapy (Figure 3) was subsequently investigated. The heatmap graphs (Figure 3A) and the dot graph (Figure 3B), both representing two moments of the study with the blood-paired samples, were used. Figure 3B shows a gray, continuous line linking the expression of a given gene before (red color) and after treatment (blue color) for better understanding. Significant p-values are shown in the graphs, comparing the biological samples at these two moments of collection. Genes that had significant p-values with reduced post-treatment gene expression were *ANKRD22* ($p < 0.001$), *BATF2* ($p < 0.001$), *GBP2* ($p < 0.001$), and *STAT1* ($p < 0.001$). The genes that showed significant p-values with increased gene expression after treatment were *BHLHE40* ($p < 0.001$) and *FCGR1A* ($p = 0.03$) (Figure 3B).

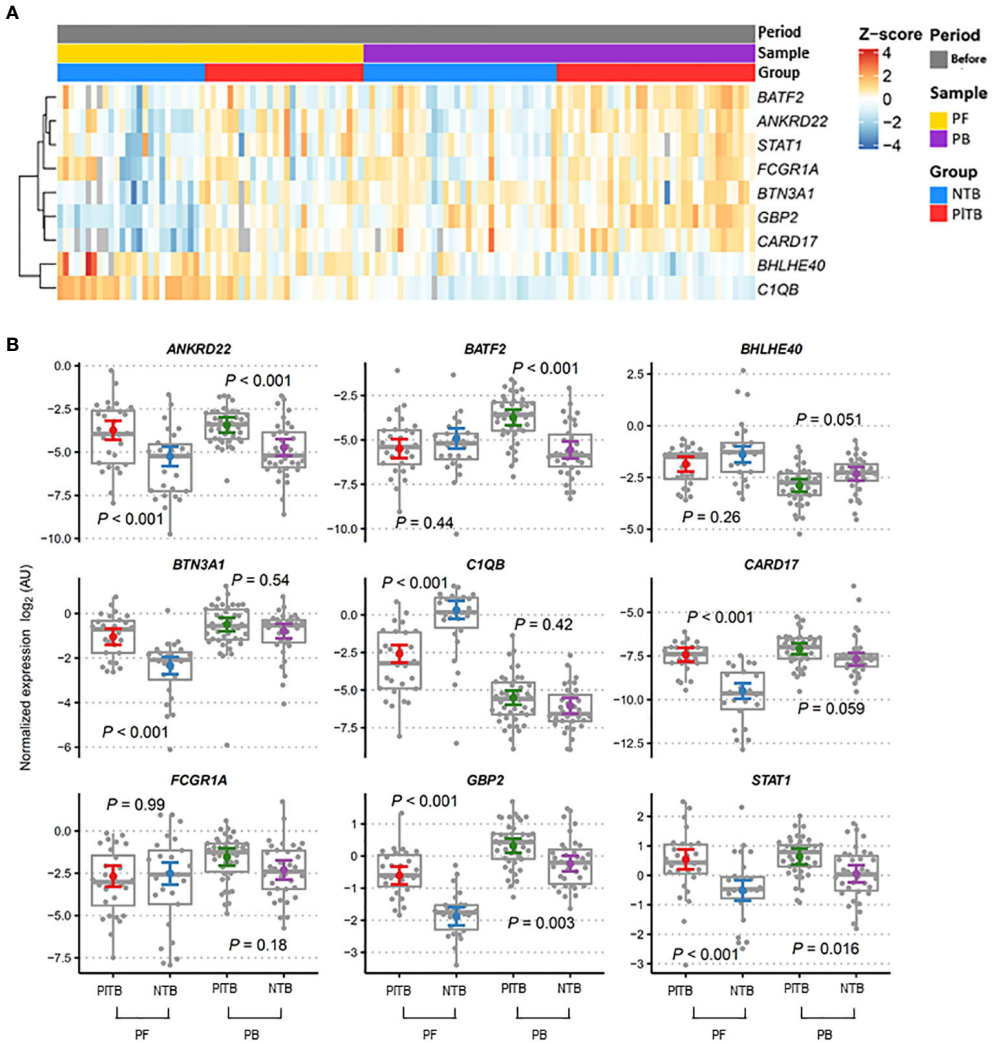

FIGURE 2
Blood and pleural fluid transcriptional signature associated with pleural tuberculosis. **(A)** Heatmap showing the relative expression of the pre-selected top 10 genes was analyzed by RT-qPCR from the study groups (red—PlTB, pleural tuberculosis; blue—NTB, non-tuberculosis) and samples (yellow—PF, pleural fluid; purple—PB, peripheral blood) were obtained before anti-TB therapy (gray). Genes in rows were clustered using the Pearson correlation coefficient distance and the complete agglomeration method. **(B)** Gene expression profiles in the peripheral blood (PB) and pleural fluid (PF) of pleural tuberculosis (PlTB) and non-tuberculosis patients (NTB) were analyzed. The Tukey box graphs and dots showed normalized gene expression values while the colored dot and error bar displayed the linear model point estimates and their 95% confidence intervals, respectively. *p*-values were calculated from the mixed linear models for specifically planned comparisons and adjusted via the Sidak method per gene. AU, arbitrary units.

3.5 Performance of the top 10 tuberculosis signature genes in the blood and pleural fluid

The receiver operating characteristic (ROC) analysis of the candidate genes in the RT-qPCR validation dataset (Figure 4) revealed the three most prominent genes in the PF sample: *CARD17, C1QB*, and *GBP2* (Figure 4A). Conversely, in the whole-blood samples, high values of sensitivity and specificity were not observed (Figure 4B). It is possible to better visualize these highlights in the PF samples of the sensitivity, specificity, and accuracy values in Table 2. In the PF, the *CARD17* gene had AUC, sensitivity, and specificity values of 0.91, 0.70, and 0.95, respectively; the *C1QB* gene had AUC, sensitivity, and specificity values of 0.84, 0.93 and 0.74, respectively. The *GBP2* gene had AUC, sensitivity, and specificity values of 0.90, 0.89, and 0.81, respectively (Table 2).

4 Discussion

Pleural tuberculosis is the main extrapulmonary clinical form of tuberculosis in which a reliable diagnosis can be reached by obtaining clinical samples by way of invasive procedures. In this context, a PlTB diagnosis remains a significant challenge, mainly due to the low bacillary load at the infectious site and the compartmentalized immune response (28, 29). The identification

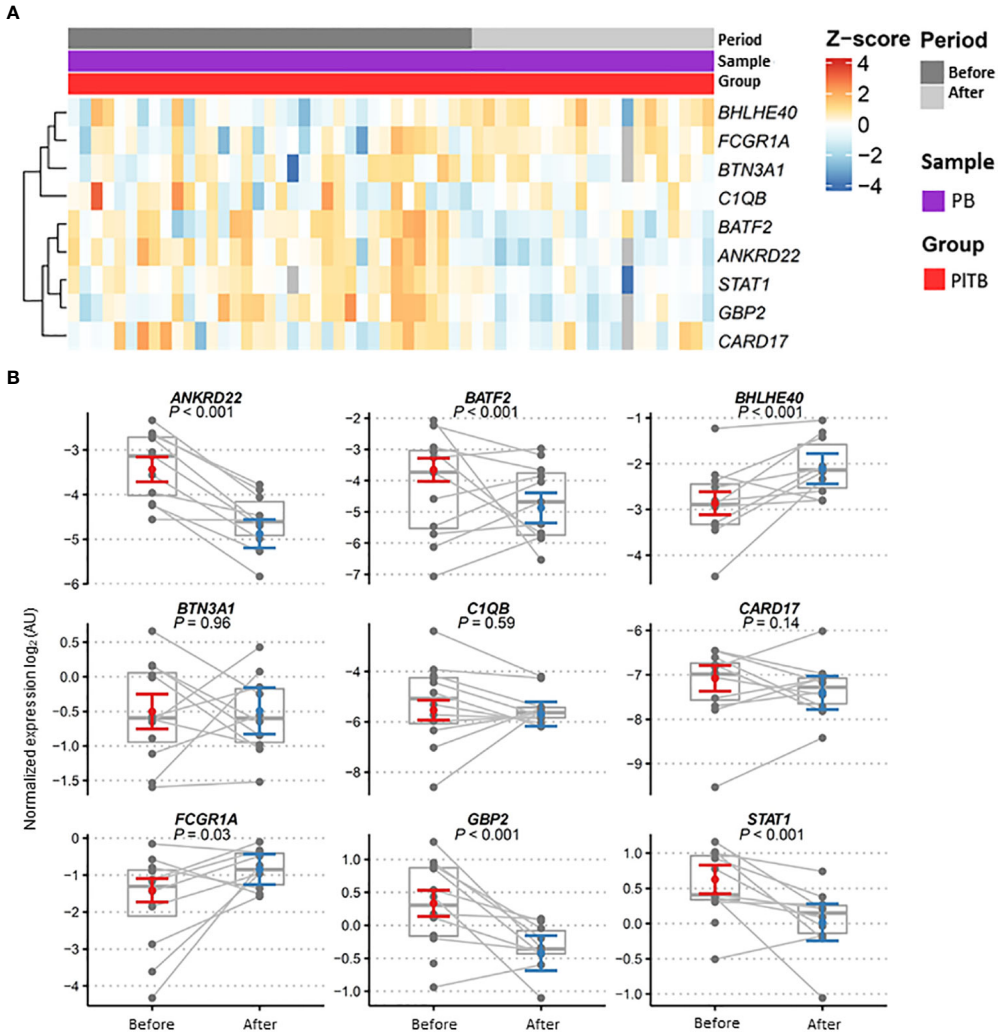

FIGURE 3
Gene expression profiles in patient blood after anti-TB therapy. **(A)** Heatmap showing the relative expression of the pre-selected top 10 genes analyzed by RT-qPCR from the pleural tuberculosis patients (PlTB, in red) and in the peripheral blood samples (PB, in purple) obtained before (dark gray) and after (light gray) anti-TB therapy. Genes in rows were clustered using the Pearson correlation coefficient distance and complete agglomeration methods. **(B)** Gene expression profiles in the blood of pleural tuberculosis patients before and after anti-TB therapy. Dots for these same patients are connected across periods. Model estimates and confidence intervals were obtained from linear mixed models after removing outliers (see Methods). Data are shown as normalized gene expressions (gray dots and box) and estimates based on linear mixed models (colored dot = marginal mean, error bars = 95% CI). AU, arbitrary units.

of new biomarkers associated with active disease may represent a paradigm shift in the clinical routine toward an early, quick, and accurate diagnosis. In the present study, we performed a bioinformatics reanalysis of previously published transcriptomic public datasets on pulmonary tuberculosis to validate the signature genes that are differentially expressed in PlTB patients when compared to other etiologies of exudative pleural effusion (lung neoplasms, pneumonia, autoimmune diseases, and non-tuberculous empyema). Our data revealed three genes—*CARD17*, *GBP2*, and *C1QB*—that demonstrated high accuracy in discriminating the PlTB from the non-TB patient groups.

Notable advances have been made in the development of the so-called "*omics*" sciences, namely, genomics, transcriptomics, proteomics, lipidomics, and metabolomics. Transcriptomic analysis in tuberculosis provided information regarding lung disease, contributing to the identification of transcriptional signatures, facilitating the ability to discriminate active from latent TB besides monitoring the treatment of the Mtb infection biomarkers in the development of active disease (30–33). However, it was our observation that data pertaining to the extrapulmonary forms were still scarce and heterogeneous. When beginning the present endeavor, a study by Bloom et al. (2013) (22) was selected from the published material in the literature to perform a reanalysis of the data using bioinformatics due to the common cellular immune pathways associated with both pulmonary tuberculosis and PlTB. Among the principal characteristics of the study by

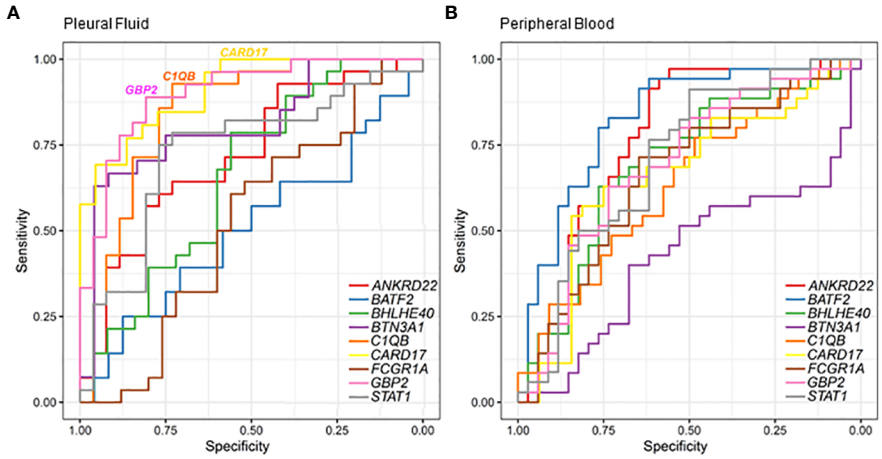

FIGURE 4
Classification of pleural tuberculosis using the top 10 gene expression profiles in the blood and pleural fluid along with the receiver operating characteristic (ROC) analysis of candidate genes validated by RT-qPCR to discriminate pleural tuberculosis from non-tuberculosis patients using pleural fluid **(A)** and peripheral blood **(B)**.

Bloom (22), it was clear that its experimental design was closer to our intentions regarding our cohort of patients in comparing pulmonary tuberculosis to other etiologies (pulmonary sarcoidosis, pneumonias, autoimmune diseases, and lung neoplasms).

The majority of transcriptomic studies have tracked transcriptional signatures in pulmonary tuberculosis while maintaining a systemic view in analyzing only whole-blood samples. Since PlTB, a disease with an immune and inflammatory response that is compartmentalized in the pleural space, was the focus of the present study, the site of infection is mandatory for this kind of exploration. In the study conducted by Bloom and colleagues (2013) (22), a small quantity of blood was obtained, similar to our samples. The importance of using a reduced volume is linked to greater short-term viability in the development of new point-of-care diagnostic tests (POCTs), which would be cost-effective and facilitate the rapid detection of diseases requiring immediate treatment (34–36).

In the present patient cohort, it was found that tuberculosis patients tended to be younger adults than those with other diseases ($p < 0.001$). The proportion of female and male patients was balanced in the non-TB group; (16/18) but, in the pleural TB group, there were almost twice as many men than women (12/23); data were also confirmed in other studies and detected by the World Health Organization (2, 37, 38). Moreover, the negativity in AFB and mycobacterial culture tests in PlTB was approximately 82% and 77%, respectively, reflecting the paucibacillary nature of PlTB (29, 39, 40). Granuloma with necrosis in the pleural TB group was present in only 14.3% of the samples, a percentage point below the value described in the literature of between 63% and 84% (40). In the end, the malignancy aspect in the non-TB group was found in 35.2% of the samples.

CARD17 and *GBP2* were increased in the PlTB patient samples whereas *C1QB* was higher in the non-TB samples. These two identified genes could act as TB biomarkers. Hence, further research on their use should be encouraged. *CARD17* is a gene associated with mycobacterial infection. *CARD17*, upregulated in blood from resistant (MDR/RR)-TB when compared to the susceptible/mono-resistant TB drug (41), is part of a molecular gene signature that can discriminate active from latent TB (30).

Furthermore, *CARD17* is associated with the cellular response to the components of the bacterial wall and in the negative regulation of IL-1β. Caspase recruitment domain (CARD)-17 inhibits the release of IL-1β in response to LPS by monocytes. The assembly of inflammasomes is initiated upon activation of cytosolic pattern recognition receptors (PRRs), followed by polymerization of the pyrin domain (PYN)-containing and caspase recruitment domain (CARD)-containing proteins. CARD17 displayed crucial CARD interactions between caspase 1 protein through competitive binding and the amelioration of uric acid crystal-mediated NLRP3 inflammasome activation and inflammatory disease (42).

Guanylate-binding proteins (GBPs) are effector molecules involved in the important autonomic responses induced by pro-inflammatory stimuli, mainly IFNs (43). *GBP2*, induced by IFN-γ (44, 45), has been linked to a myriad of different cancer types as an oncogenic gene. In the present study, it was seen that *GBP2* expression was significantly higher in the PF of the tuberculosis compared to the non-tuberculosis group, as also found by Zak et al. (17). This response profile suggests that the high expression of this gene may play a role in combating Mtb infection (31, 46). *GBP2* also participated in the cellular response to TNF. Marinho et al. (2020) (43) observed that mice deficient in GBP (GBP−/−) were more susceptible to Mtb infection, exhibiting a decreased expression of genes related to autophagy in the lungs in addition to a reduction in the production of pro inflammatory cytokines. TNF is also crucial in the formation and maintenance of granulomas. Changes in these cytokine levels have the ability to compromise the integrity of these structures, causing the reactivation of tuberculosis (47). In this context, it was concluded that *GBP2* is an important gene in stimulating cellular immunity and controlling mycobacterial

10.3389/fimmu.2023.1256558

TABLE 2 Receiver operating characteristic (ROC) comparison of selected genes in discriminating pleural TB from non-TB diagnoses.

Sample	Gene	AUC [95% CI]	Specificity	Sensitivity	LR+	LR-
PF	*CARD17*	0.91 [0.83–0.99]	0.956522	0.703704	16.19	0.31
PF	*BATF2*	0.51 [0.35–0.67]	0.88	0.241379	2.01	0.86
PF	*STAT1*	0.73 [0.59–0.87]	0.740741	0.758621	2.93	0.33
PF	*BTN3A1*	0.81 [0.68–0.93]	0.92	0.678571	8.48	0.35
PF	*FCGR1A*	0.52 [0.36–0.69]	0.423077	0.724138	1.26	0.65
PF	*C1QB*	0.85 [0.74–0.96]	0.740741	0.931034	3.59	0.09
PF	*GBP2*	0.9 [0.82–0.98]	0.814815	0.892857	4.82	0.13
PF	*BHLHE40*	0.66 [0.51–0.81]	0.576923	0.793103	1.87	0.36
PF	*ANKRD22*	0.72 [0.58–0.86]	0.777778	0.586207	2.64	0.53
PB	*CARD17*	0.66 [0.52–0.8]	0.727273	0.657895	2.41	0.47
PB	*BATF2*	0.83 [0.73–0.93]	0.628571	0.921053	2.48	0.13
PB	*STAT1*	0.71 [0.58–0.83]	0.485714	0.864865	1.68	0.28
PB	*BTN3A1*	0.43 [0.29–0.57]	0.685714	0.421053	1.34	0.84
PB	*FCGR1A*	0.66 [0.53–0.8]	0.628571	0.684211	1.84	0.50
PB	*C1QB*	0.64 [0.5–0.77]	0.5	0.789474	1.58	0.42
PB	*GBP2*	0.69 [0.57–0.82]	0.714286	0.578947	2.03	0.59
PB	*BHLHE40*	0.69 [0.57–0.82]	0.771429	0.631579	2.76	0.48
PB	*ANKRD22*	0.77 [0.65–0.89]	0.628571	0.894737	2.41	0.17

Pleural fluid (PF), peripheral blood (PB), Gene performance (AUC sensitivity, specificity, and likelihood ratio). Highlighted in gray is the performance of the CARD17, C1QB, and GBP2 genes in pleural fluid samples. AUC, area under the curve; C, confidence interval; PB, peripheral blood; and PF, pleural fluid; LR+, likelihood positive ratio; LR–, negative likelihood ratio.

infection (43). *GBP2* has also been associated with treatment monitoring (33) and its ability to discriminate active from latent TB (31).

As a final remark, the *C1QB* gene is involved in the regulation and activation pathways of the complement system, whose proteins participate in an innate and acquired defense mechanism by opsonizing pathogens and inducing inflammatory responses that help fight infections (36, 48). The high expression of this gene was also verified in the whole blood of patients with active tuberculosis in the Sambarey et al. study (2017) (49). However, in the present results, the *C1QB* gene obtained a significantly higher value of gene expression in the fluid of the non-TB group compared to the pleural tuberculosis group. In summary, the present results were similar to those described in a number of other works found in the literature (36, 48, 50).

When the CARD17, GBP2, and C1QB (Figure 3B) gene expressions in the blood of the non-TB group of patients following anti-tuberculosis therapy were checked, a reduction in the expression of all three genes was found. Activation of the *CARD17* gene triggers the activation of the innate immunity of the host during the inflammatory process as a result of its association with the inflammasome pathway during Mtb infection. The decline in the expression of this gene is indicative of patient cure and improvement in the inflammatory clinical picture, a finding corroborated by Natarajan et al. (2022) (30), demonstrating that the expression of *CARD17* in latent TB patients was significantly lower than in patients with active tuberculosis. The decrease in *GBP2* gene expression in the present cohort also suggests recovery of these tuberculous patients after treatment, as likewise observed in the works of Sambarey et al. (2017) (49) and Long et al. (2021) (33). As to the other genes, *C1QB* also showed a reduction in expression after tuberculosis treatment (49). Nonetheless, no significant *p*-value was observed in relation to the non-TB group.

Among the more favorable aspects of the present research, we highlight the following: (i) The originality of the study design. The investigation of the signature genes involved in the clinical form of PlTB, starting from previously established genes in the study of pulmonary tuberculosis, alludes to the greater reliability and discriminatory stability of these genes, making it possible to carry out gene expression assays by RT-qPCR, and thus, achieve our ultimate research objective. Moreover, until the completion of this work, we were not aware of the use of the same study design for the same purpose in the literature. (ii) The well-characterized study population in conformity with several standardized parameters provided by a tertiary care center in a highly TB-burdened country. Although any given study requires the meticulous application of the required eligibility criteria, our research was fundamentally based on two other previous PlTB studies performed by the present authors (5, 6). (iii) The relatively good sample size of our patient cohort suffering from this particular TB clinical form despite having to exclude samples from the volunteers who did not meet our eligibility and quality control criteria; and (iv) the ability to analyze paired samples in the post-treatment phase. At

the same time, it is important to mention some of the major limitations of the present study such as a potential bias due to having to use transcriptomic datasets from pulmonary TB patients and not from a pleural tuberculosis cohort, which could have enriched the list of candidate genes related to a systemic or circulating (blood) response to the detriment of the genes that could have been expressed more explicitly at the infection site. However, our choice was justified by the absence of previously published transcriptomic datasets in pleural effusion samples.

In summary, we reanalyzed a previously published transcriptomic signature in pulmonary TB to identify candidate genes, which were measured and shown to discriminate PlTB from other causes of pleural effusion by using whole blood and PF. Among the top 10 genes, *CARD-17*, *GBP2*, and *C1QB* expressed in PF showed an above 80% accuracy rate in discriminating PlTB from other causes of pleural effusion.

5 Conclusion

Altogether, our findings presented new strategies in identifying diagnostic biomarkers in PlTB by using the previously known "*omics*" approaches, which, it is conjectured, could lead to a more accurate diagnosis and timely initiation of anti-TB therapy. Based on a reanalytical methodology by bioinformatics that utilizes a previously published transcriptomic public dataset in pulmonary tuberculosis, we succeeded in validating a total of three candidates, *CARD17, GBP2*, and *C1QB* genes, in clinical specimens. They distinguished themselves by showing promise in accurately discriminating PlTB from other causes of exudative pleural effusion, making it possible to reach a more reliable diagnosis and timely initiation of anti-tuberculosis therapy. In addition, in our view, our data provided a better understanding of the pathophysiological mechanisms of the disease, thereby making a decisive contribution to the development of new therapeutic methods and strategies in this important field.

Data availability statement

The datasets presented in this study can be found in online repositories. The names of the repository/repositories and accession number(s) can be found in the article/Supplementary Material.

Ethics statement

The studies involving humans were approved by Pedro Ernesto University Hospital (HUPE), Rio de Janeiro State University (UERJ). The studies were conducted in accordance with the local legislation and institutional requirements. The participants provided their written informed consent to participate in this study.

Author contributions

RC: Formal Analysis, Investigation, Writing – original draft, Writing – review & editing, Data curation, Methodology, Validation, Visualization. TL-C: Data curation, Investigation, Methodology, Writing – original draft. TM: Investigation, Writing – original draft, Resources. AS: Investigation, Writing – original draft. JL: Investigation, Writing – original draft. RP: Writing – original draft, Writing – review & editing. RR: Writing – original draft, Formal Analysis, Visualization. MM: Conceptualization, Data curation, Formal Analysis, Writing – original draft. LR: Writing – original draft, Writing – review & editing, Conceptualization, Formal Analysis, Funding acquisition, Investigation, Project administration, Resources, Supervision.

Funding

The author(s) declare financial support was received for the research, authorship, and/or publication of this article. This study was funded in part by the Fundação Carlos Chagas Filho de Amparo à Pesquisa do Estado do Rio de Janeiro (FAPERJ - E-26/110.179/2014) and RC was supported by a doctoral scholarship from the Coordenação de Aperfeiçoamento de Pessoal de Nível Superior (CAPES).

Acknowledgments

We wish to acknowledge all the patients, nurses, medical and supporting staff from the Pleural Diseases and Tuberculosis Outpatient Clinics of HUPE/UERJ. We are particularly grateful to the Molecular Biology Platform at the Oswaldo Cruz Institute and the coauthors Dr. Milton Ozório Moraes (*In memoriam*) and TL-C for their collaboration and support in performing the RT-qPCR experiments. We also want to thank the funding institutions FAPERJ and CAPES as well as Judy Grevan for editing the text.

Conflict of interest

The authors declare that the research was conducted in the absence of any commercial or financial relationships that could be construed as a potential conflict of interest.

Publisher's note

All claims expressed in this article are solely those of the authors and do not necessarily represent those of their affiliated organizations, or those of the publisher, the editors and the reviewers. Any product that may be evaluated in this article, or claim that may be made by its manufacturer, is not guaranteed or endorsed by the publisher.

Supplementary material

The Supplementary Material for this article can be found online at: https://www.frontiersin.org/articles/10.3389/fimmu.2023.1256558/full#supplementary-material

References

1. *Global tuberculosis report 2023* (2023). Available at: https://iris.who.int/.

2. *Global Tuberculosis reporT 2022* (2022). Available at: http://apps.who.int/bookorders.

3. Governo do Estado do Rio de Janeiro (Brasil). *Boletim Epidemiológico de Tuberculose*. Secretaria de Saúde (2022). Available at: https://pesquisa.bvsalud.org/portal/resource/pt/biblio-1418663.

4. Shaw JA, Diacon AH, Koegelenberg CFN. Tuberculous pleural effusion. *Vol 24 Respirology Blackwell Publishing;* (2019) p:962–71. doi: 10.1111/resp.13673

5. Santos AP, da Silva Corrêa R, Ribeiro-Alves M, da Silva ACOS, Mafort TT, Leung J, et al. Application of Venn's diagram in the diagnosis of pleural tuberculosis using IFN-γ, IP-10 and adenosine deaminase. *PloS One* (2018) 13(8):e0202481. doi: 10.1371/journal.pone.0202481

6. da Cunha Lisboa V, Ribeiro-Alves M, da Silva Corrêa R, Ramos Lopes I, Mafort TT, Santos AP, et al. Predominance of th1 immune response in pleural effusion of patients with tuberculosis among other exudative etiologies. *J Clin Microbiol* (2019) 58 (1):e00927–19. doi: 10.1128/JCM.00927-19

7. Sharma SK, Mitra DK, Balamurugan A, Pandey RM, Mehra NK. Cytokine polarization in miliary and pleural tuberculosis. *J Clin Immunol* (2002) 22(6):345–52. doi: 10.1023/a:1020604331886

8. Mitra DK, Sharma SK, Dinda AK, Bindra MS, Madan B, Ghosh B. Polarized helper T cells in tubercular pleural effusion: Phenotypic identity and selective recruitment. *Eur J Immunol* (2005) 35(8):2367–75. doi: 10.1002/eji.200525977

9. Rossi GA, Balbi B, Manca F. Tuberculous Pleural Effusions Evidence for selective Presence of PPD-Specific T-Lymphocytes at Site of Inflammation in the Early Phase of the Infection. *Am Rev Respir Dis* (1987) 136(3):575–9. doi: 10.1164/ajrccm/136.3.575

10. Ramilo O, Allman W, Chung W, Mejias A, Ardura M, Glaser C, et al. Gene expression patterns in blood leukocytes discriminate patients with acute infections. *Blood* (2007) 109:2066–77. doi: 10.1182/blood-2006-02-002477

11. Ardura MI, Banchereau R, Mejias A, Di Pucchio T, Glaser C, Allantaz F, et al. Enhanced monocyte response and decreased central memory T cells in children with invasive Staphylococcus aureus infections. *PloS One* (2009) 4(5):e5446. doi: 10.1371/journal.pone.0005446

12. Guerreiro LTA, Robottom-Ferreira AB, Ribeiro-Alves M, Toledo-Pinto TG, Rosa Brito T, Rosa PS, et al. Gene expression profiling specifies chemokine, mitochondrial and lipid metabolism signatures in leprosy. *PloS One* (2013) 8(6): e64748. doi: 10.1371/journal.pone.0064748

13. Berry MPR, Graham CM, McNab FW, Xu Z, Bloch SAA, Oni T, et al. An interferon-inducible neutrophil-driven blood transcriptional signature in human tuberculosis. *Nat* (2010) 466(7309):973–7. doi: 10.1038/nature09247

14. Lesho E, Forestiero FJ, Hirata MH, Hirata RD, Cecon L, Melo FF, et al. Transcriptional responses of host peripheral blood cells to tuberculosis infection. *Tuberculosis* (2011) 91(5):390–9. doi: 10.1016/j.tube.2011.07.002

15. Maertzdorf J, Weiner J, Mollenkopf HJ, Network T, Bauer T, Prasse A, et al. Common patterns and disease-related signatures in tuberculosis and sarcoidosis. *Proc Natl Acad Sci U S A* (2012) 109(20):7853–8. doi: 10.1073/pnas.1121072109

16. Ottenhoff THM, Dass RH, Yang N, Zhang MM, Wong HEE, Sahiratmadja E, et al. Genome-wide expression profiling identifies type 1 interferon response pathways in active tuberculosis. *PloS One* (2012) 7(9):e45839. doi: 10.1371/journal.pone.0045839

17. Zak DE, Penn-Nicholson A, Scriba TJ, Thompson E, Suliman S, Amon LM, et al. A blood RNA signature for tuberculosis disease risk: a prospective cohort study. *Lancet* (2016) 387(10035):2312–22. doi: 10.1016/S0140-6736(15)01316-1

18. Blankley S, Graham CM, Turner J, Berry MPR, Bloom CI, Xu Z, et al. The transcriptional signature of active tuberculosis reflects symptom status in extra-pulmonary and pulmonary tuberculosis. *PloS One* (2016) 11(10):e0162220. doi: 10.1371/journal.pone.0162220

19. Roe JK, Thomas N, Gil E, Best K, Tsaliki E, MorrisJones S, et al. Blood transcriptomic diagnosis of pulmonary and extrapulmonary tuberculosis. *JCI Insight* (2016) 1(16):e87238. doi: 10.1172/jci.insight.87238

20. D'Attilio L, Díaz A, Santucci N, Bongiovanni B, Gardeñez W, Marchesini M, et al. Levels of inflammatory cytokines, adrenal steroids, and mRNA for GRα, GRβ and 11βHSD1 in TB pleurisy. *Tuberculosis* (2013) 93(6):635–41. doi: 10.1016/j.tube.2013.07.008

21. Espósito DLA, Bollela VR, Feitosa ALP, da Fonseca BAL. Expression profiles of cytokine mRNAs in the pleural fluid reveal differences among tuberculosis, Malignancies, and pneumonia-exudative pleural effusions. *Lung* (2015) 193(6):1001–7. doi: 10.1007/s00408-015-9809-4

22. Bloom CI, Graham CM, Berry MPR, Rozakeas F, Redford PS, Wang Y, et al. Transcriptional blood signatures distinguish pulmonary tuberculosis, pulmonary sarcoidosis, pneumonias and lung cancers. *PloS One* (2013) 8(8):e70630. doi: 10.1371/annotation/7d9ec449-aee0-48fe-8111-0c110850c0c1

23. Smyth GK. Linear models and empirical bayes methods for assessing differential expression in microarray experiments. *Stat Appl Genet Mol Biol* (2004) 3(1):article3. doi: 10.2202/1544-6115.1027

24. Ramakers C, Ruijter JM, Lekanne Deprez RH, Moorman AFM. Assumption-free analysis of quantitative real-time polymerase chain reaction (PCR) data. *Neurosci Lett* (2003) 339(1):62–6. doi: 10.1016/S0304-3940(02)01423-4

25. Ruijter JM, Ramakers C, Hoogaars WMH, Karlen Y, Bakker O, van den hoff MJB, et al. Amplification efficiency: Linking baseline and bias in the analysis of quantitative PCR data. *Nucleic Acids Res* (2009) 37(6):e45. doi: 10.1093/nar/gkp045

26. Benjaminit Y, Hochberg Y. Controlling the false discovery rate: a practical and powerful approach to multiple testing. *J R Statist Soc B* (1995) 57(1):289–300. doi: 10.1111/j.2517-6161.1995.tb02031.x

27. Youden WJ. Index for rating diagnostic tests. *Cancer* (1950) 3(1):32–5. doi: 10.1002/1097-0142(1950)3:1<32:aid-cncr2820030106>3.0.co;2-3

28. Seiscento M, Conde MB, Dalcolmo MMP. Tuberculous pleural effusions. *J Bras Pneumol.* (2006) 32(4):S174–81. doi: 10.1590/S1806-37132006000900003

29. Zumla A, Raviglione M, Hafner R, Fordham von Reyn C. Tuberculosis. *New Engl J Med* (2013) 368(8):745–55. doi: 10.1056/NEJMra1200894

30. Natarajan S, Ranganathan M, Hanna LE, Tripathy S. Transcriptional profiling and deriving a seven-gene signature that discriminates active and latent tuberculosis: an integrative bioinformatics approach. *Genes (Basel)* (2022) 13(4):616. doi: 10.3390/genes13040616

31. Perumal P, Abdullatif MB, Garlant HN, Honeyborne I, Lipman M, McHugh TD, et al. Validation of differentially expressed immune biomarkers in latent and active tuberculosis by real-time PCR. *Front Immunol* (2021) 11:612564. doi: 10.3389/fimmu.2020.612564

32. Nogueira BMF, Krishnan S, Barreto-Duarte B, Araújo-Pereira M, Queiroz ATL, Ellner JJ, et al. Diagnostic biomarkers for active tuberculosis: progress and challenges. *EMBO Mol Med* (2022) 14(12):e14088. doi: 10.15252/emmm.202114088

33. Long NP, Phat NK, Yen NTH, Park S, Park Y, Cho YS, et al. A 10-gene biosignature of tuberculosis treatment monitoring and treatment outcome prediction. *Tuberculosis* (2021) 131:102138. doi: 10.1016/j.tube.2021.102138

34. Kozel TR, Burnham-Marusich AR. Point-of-care testing for infectious diseases: past, present, and future. *J Clin Microbiol* (2017) 55(8):2313–20. doi: 10.1128/JCM.00476-17

35. Acharya B, Acharya A, Gautam S, Ghimire SP, Mishra G, Parajuli N, et al. Advances in diagnosis of Tuberculosis: an update into molecular diagnosis of Mycobacterium tuberculosis. *Mol Biol Rep* (2020) 47(5):4065–75. doi: 10.1007/s11033-020-05413-7

36. Chen LH, Liu JF, Lu Y, He XY, Zhang C, Zhou HH. Complement C1q (C1qA, C1qB, and C1qC) may be a potential prognostic factor and an index of tumor microenvironment remodeling in osteosarcoma. *Front Oncol* (2021) 11. doi: 10.3389/fonc.2021.642144

37. Zhai K, Lu Y, Shi HZ. Tuberculous pleural effusion. *J Thorac Dis* (2016), E486–94. doi: 10.21037/jtd.2016.05.87

38. Hertz D, Schneider B. Sex differences in tuberculosis. *Semin Immunopathol* (2019) 41:225–37. doi: 10.1007/s00281-018-0725-6

39. (2016). junior cts.

40. Silva DR, Rabahi MF, Sant'Anna CC, Da Silva-Junior JLR, Capone D, Bombarda S, et al. Diagnosis of tuberculosis: a consensus statement from the Brazilian Thoracic Association. *Jornal Brasileiro Pneumologia* (2021) 47(2):e20210054. doi: 10.36416/1806-3756/e20210054

41. Madamarandawala P, Rajapakse S, Gunasena B, Madegedara D, Magana-Arachchi D. A host blood transcriptional signature differentiates multi-drug/rifampin-resistant tuberculosis (MDR/RR-TB) from drug susceptible tuberculosis: a pilot study. *Mol Biol Rep* (2023) 50(4):3935–43. doi: 10.1007/s11033-023-08307-6

42. Huang Y, Xu W, Zhou R. NLRP3 inflammasome activation and cell death. *Cell Mol Immunol* (2021) 18(9):2114–27. doi: 10.1038/s41423-021-00740-6

43. Marinho FV, Fahel JS, de Araujo ACVSC, Diniz LTS, Gomes MTR, Resende DP, et al. Guanylate binding proteins contained in the murine chromosome 3 are important to control mycobacterial infection. *J Leukoc Biol* (2020) 108(4):1279–91. doi: 10.1002/JLB.4MA0620-526RR

44. Bocchino M, Bellofiore B, Matarese A, Galati D, Sanduzzi A. IFN-γ release assays in tuberculosis management in selected high-risk populations. *Expert Rev Mol Diagnostics* (2009) 9:165–77. doi: 10.1586/14737159.9.2.165

45. Li Q, Li J, Tian J, Zhu B, Zhang Y, Yang K, et al. IL-17 and IFN-γ production in peripheral blood following BCG vaccination and Mycobacterium tuberculosis infection in human. *Eur Rev Med Pharmacol Sci* (2012) 16(14):2029–36.

46. Shi T, Huang L, Zhou Y, Tian J. Role of GBP1 in innate immunity and potential as a tuberculosis biomarker. *Sci Rep* (2022) 12(1):11097. doi: 10.1038/s41598-022-15482-2

47. Godfrey MS, Friedman LN. Tuberculosis and biologic therapies: anti-tumor necrosis factor-α and beyond. *Clinics Chest Med* (2019) 40:721–39. doi: 10.1016/j.ccm.2019.07.003

48. Yang H, Che D, Gu Y, Cao D. Prognostic and immune-related value of complement C1Q (C1QA, C1QB, and C1QC) in skin cutaneous melanoma. *Front Genet* (2022) 13. doi: 10.3389/fgene.2022.940306

49. Sambarey A, Devaprasad A, Baloni P, Mishra M, Mohan A, Tyagi P, et al. Meta-analysis of host response networks identifies a common core in tuberculosis. *NPJ Syst Biol Appl* (2017) 3(4). doi: 10.1038/s41540-017-0005-4

50. Kemp SB, Steele NG, Carpenter ES, Donahue KL, Bushnell GG, Morris AH, et al. Pancreatic cancer is marked by complement-high blood monocytes and tumor-associated macrophages. *Life Sci Alliance* (2021) 4(6):1–17. doi: 10.26508/lsa.202000935

Frontiers in Immunology

Explores novel approaches and diagnoses to treat immune disorders.

The official journal of the International Union of Immunological Societies (IUIS) and the most cited in its field, leading the way for research across basic, translational and clinical immunology.

Discover the latest Research Topics

See more →

Frontiers

Avenue du Tribunal-Fédéral 34
1005 Lausanne, Switzerland
frontiersin.org

Contact us

+41 (0)21 510 17 00
frontiersin.org/about/contact